Quantum Physics in One Dimension

THIERRY GIAMARCHI

University of Geneva
and
Paris XI University

CLARENDON PRESS • OXFORD
2003

OXFORD
UNIVERSITY PRESS

Great Clarendon Street, Oxford OX2 6DP

Oxford University Press is a department of the University of Oxford.
It furthers the University's objective of excellence in research, scholarship,
and education by publishing worldwide in

Oxford New York

Auckland Bangkok Buenos Aires Cape Town Chennai
Dar es Salaam Delhi Hong Kong Istanbul Karachi Kolkata
Kuala Lumpur Madrid Melbourne Mexico City Mumbai Nairobi
São Paulo Shanghai Taipei Tokyo Toronto

Oxford is a registered trade mark of Oxford University Press
in the UK and in certain other countries

Published in the United States
by Oxford University Press Inc., New York

© Oxford University Press, 2003

The moral rights of the author have been asserted

Database right Oxford University Press (maker)

First published 2003

All rights reserved. No part of this publication may be reproduced,
stored in a retrieval system, or transmitted, in any form or by any means,
without the prior permission in writing of Oxford University Press,
or as expressly permitted by law, or under terms agreed with the appropriate
reprographics rights organization. Enquiries concerning reproduction
outside the scope of the above should be sent to the Rights Department,
Oxford University Press, at the address above

You must not circulate this book in any other binding or cover
and you must impose this same condition on any acquirer

A catalogue record for this title is available from the British Library

Library of Congress Cataloging in Publication Data
(Data available)

ISBN 0 19 852500 1

10 9 8 7 6 5 4 3 2 1

Typeset by the author in LaTeX

Printed in Great Britain
on acid-free paper by
Biddles Ltd, Guildford & King's Lynn

To Heinz

PREFACE

The best way to predict the future is to invent it.

Alan Kay

As a reader I always hated prefaces in books, finding them a loss of time and energy and preventing you to reach the interesting material inside the book and always skipped them. So now that I have to write one, I am in a fix, since I do not really know what to put in it.

After all if you have this book in hand and bother to read this, it is certainly because you already have some feeling that one-dimensional systems are quite fascinating, and that you want to know more about them. But just in case you are a reader who is able to browse leisurely through books,[1] let me just tell you briefly what this book is about.

One-dimensional systems of interacting particles have fascinated theorists for more than 50 years now. They are wonderful systems in which interactions play a very special role and whose physics is drastically different from the 'normal' physics of interacting particles, that is, the one known in higher dimensions. From the theoretical point of view, here again they are quite unique. The one-dimensional character makes the problem simple enough so that some rather complete solutions could be obtained using specific methods, and yet complex enough to lead to incredibly rich physics. Crucial theoretical progress were made and new theoretical tools developed in the 1970's which culminated in the 1980's with a new concept of interacting one-dimensional particles, analogous to the Fermi liquid for interacting electrons in three dimensions: the Luttinger liquid. From an experimental point of view, one-dimensional systems were mostly at the beginning a theorist's toy. Experimental realizations started to appear in the 1970's with polymers and organic compounds. But in the last 20 years or so we have seen a real explosion of realization of one-dimensional systems. The progress in material research made it possible to realize bulk materials with one-dimensional structures inside. The most famous ones are the organic superconductors, the ladder compounds, and the spin compounds. At the same time, the tremendous progress in nanotechnology allowed to obtain realizations of isolated one-dimensional systems such as quantum wires, Josephson junction arrays, edge states in quantum hall systems, and nanotubes. Last but not least, the recent progress in Bose condensation in optical traps offer great promises for the future in realizing one-dimensional systems of fermions or bosons with unique properties. These experimental developments have of course triggered a

[1] I am afraid that this is an endangered species, but I certainly hope it will never disappear!

corresponding burst of theoretical activity and our understanding of such systems has considerably progressed during this period. New theoretical tools have been developed and new concepts have emerged.

The book is intended to present this fascinating one-dimensional physics. On the theoretical side, some of the tools used to treat one-dimensional systems are quite specific and are thus not part of the standard package of many-body physics that is usually taught. The first part of the book thus gives a step-by-step introduction to the techniques and concepts in the field, while pushing it to the frontier of today's research. Given the amount of material it was of course impossible to be exhaustive. I thus preferred to make a selection of techniques, choosing the ones I knew best and that I used extensively for one-dimensional systems. I apologize in advance to those whose pet subject or technique I could not include in this book. To enjoy the technical sections, and although some brief summary is given in the book, some basic knowledge of many-body physics is suitable (corresponding roughly to the first three chapters of Mahan, 1981). For some of the one-dimensional techniques (e.g. Bethe-ansatz or conformal invariance) only a basic introduction is given in this book. For the readers who want to go further than what is given in this book, many references to review papers or more specialized books have been given in the corresponding chapters. Finally, some quite sophisticated or specialized techniques (e.g. non-abelian bosonization, Ising and WZWN models) are not treated in this book. Given the space constraints, and my quite limited knowledge of these methods, I felt it was impossible for me to make a decent pedagogical introduction to them. I thus chose to skip them completely and to focus on the others, which I could hopefully explain better. For the reader who wants to know more on these I recommend the very nice book by Gogolin, Nersesyan and Tsvelik (Gogolin *et al.*, 1999) where these techniques are explained in detail. The second part of the book is devoted to a study of the various physical realizations of one-dimensional systems. Most of the technicalities have been removed in these sections to directly focus on the physics. Given the multiplicity and importance of experimental realizations of one-dimensional systems I have tried to cover, however briefly, all main realizations.

Although I have tried to make every effort to eradicate minus sign problems and other factors of two in the formulas, I am sure that many mistakes remain in this book. I will thus maintain on my web page[2] a list of errors. This should avoid a few number of persons, including me, many useless sleepless nights.

That's all folks! Now just fasten your seat belts, turn the page and enjoy your trip in the one-dimensional world.

[2]Located on the Web site: dpmc.unige.ch

How to read this book

Let me tell briefly what each chapter contains to help the reader find his/her way in this one-dimensional maze.[3] This book can be read 'a la carte'. Depending on your knowledge of theory, and on what you expect to find in this book, the chapters should not be read in the same order.

All (most of) the technology is concentrated in the first five chapters and in the appendices. These parts do not focus on any specific physical system but give the tools needed to tackle any[4] one-dimensional problem. I have tried as much as possible not to assume any previous theoretical knowledge from the reader and to explain in a detailed and hopefully physical way the various theoretical techniques used. These chapters are thus intended to teach the techniques at a slow pace. Here are the contents in greater detail:

- Chapter 1: An introduction to the basic ideas of interacting electrons and the peculiarities of one dimension. The first and second parts of the chapter are simple and should be read since the basic ideas explained here (without any fancy techniques) recur in the rest of the book. The third part explains the fermionic techniques used to tackle one dimension. It is there for the professional[5] of standard many-body physics. If you do not known the book by Mahan (1981) by heart, just *skip this part*. You will not need it for the rest of the book, and it could seriously impair your love of one-dimensional systems. If you *do know* diagrammatic theory then read it since it contains very interesting solutions and will help you make the link with the rest of the book.
- Chapter 2: Explains the very technique of bosonization that will be used repeatedly in the rest of the book. It is a systematic, but step by step, introduction to the technique. If you want to become a professional in the field and use the technique, roll up your sleeves, take a deep breath, and go through the chapter. If not read the next chapter first, which is less systematic but explains the same ideas in a much more physical way. You will then come back to this chapter when you feel ready.
- Chapter 3: This chapter explains using very low level techniques the concept of Luttinger liquid. It is a must to have an idea of the physics of one-dimensional systems. If you do not want to know the technique in detail but simply the physical ideas, this chapter is enough. If you want more you will find it in Chapter 2.
- Chapter 4: This chapter discusses more sophisticated technical and physical situations. It also presents a certain number of pitfalls into which the

[3] Which proves that a one-dimensional world can also be a maze.

[4] Well, most of them anyway...

[5] You know, Feynman diagrams and all that.

bosonization beginners[6] can fall. You can read this chapter at your leisure or when you encounter the corresponding situation in one of the physical systems you are interested in.

- Chapter 5: This chapter presents the various microscopic methods used to tackle one-dimensional systems: the famous Bethe-ansatz and numerical techniques. Only for theorists or for long winter nights.

The remaining chapters deal with specific class of systems and discuss some experimental materials. They contain little technique and use the results of the previous technical chapters for the main formulas. You can thus read them directly if you do not care how the results were obtained (I still recommend reading the beginning of Chapter 1 and of Chapter 3 though). These chapters need not be read in sequence since they are independent of each other (with some correlations). You can probe the ones that are relevant to your own interests.

- Chapter 6: All about spin systems. Chains, frustration, spin-Peierls transition, ladders, and quasi-one-dimensional systems, and the corresponding experimental realizations.
- Chapter 7: Single chain fermionic systems. Mostly models: Hubbard, t–J, extended Hubbard. The corresponding experimental systems are discussed in Chapter 8. A discussion on transport in fermionic systems and the Mott transition.
- Chapter 8: Coupled fermionic chains and quasi-one-dimensional fermionic systems. Application to ladders (telephone number compounds) and to organic conductors.
- Chapter 9: Effects of disorder in fermionic systems. Introduction to replicas. Anderson localization in interacting fermionic systems. Application to quantum wires.
- Chapter 10: Boundaries, isolated impurities, and constrictions. Discusses mostly the mesoscopic realizations of Luttinger liquids such as carbon nanotubes and edge states in the quantum hall effect, for which such problems are important.
- Chapter 11: Other examples of Luttinger liquids. A break from Fermi statistics: the life of the one-dimensional bosons. Discussion of Josephson junction arrays and Bose condensates. Applications of bosonization to the study of quantum impurities in three-dimensional Fermi liquids.[7] X-ray, Kondo, and multichannel Kondo problems.

[6] Also known as bozos.

[7] I do not know whether this moves up or down in dimension since this is in fact a zero-dimensional problem.

ACKNOWLEDGEMENTS

I would like to express my thanks to all who contributed during the years to my understanding of correlated quantum systems and Luttinger liquids through collaborations or discussions. This includes especially all my colleagues at the Laboratoire de Physique des Solides in Orsay, where most of my own research on one-dimensional systems was carried out in the 20-year span I worked there. The exceptional research environment of 'Building 510' made life quite exciting. Halfway through the writing of this book, I made a move to the DPMC at the University of Geneva: I wish to thank my new colleagues there for their warm welcome and for making the transition as smooth as possible. Their enthusiastic interest for correlated systems in general and low-dimensional systems in particular is a promise that life after dis-location will continue to be as exciting as ever. The material presented in this book has directly benefited from constant interactions with talented students and postdocs, with whom I had the lucky chance to collaborate in the field of one-dimensional systems. I want to thank them especially for these enjoyable interactions and discussions. Needless to say I also benefited immensely from incalculable contributions from many colleagues around the world. Although the list of those I would like to thank is too long to fit here, I will mention in particular N. Andrei, C. Bourbonnais, R. Chitra, L. Degiorgi, A. Georges, D. Jérome, P. Le Doussal, K. Le Hur, A.J. Millis, E. Orignac, R. Shankar, B.S. Shastry, A.M. Tsvelik, and C.M. Varma.

I also would like to thank the brave hearts who had the courage to work through the unfinished drafts of this book, to correct mistakes,[8] and to make invaluable suggestions improving both the shape and the contents of this book: C. Bolech, M.A. Cazalilla, C. Kollath, K. Le Hur, J.S. Meyer, E. Orignac, K. Schönhammer, G. Seelig, D. Senechal, and R. Shankar.

Before writing this book I wondered why authors thanked their family. Now that I think I know why, I would like to thank Marido and Gabriel for being so patient during the completion of this one.

Finally, there is one person who deserves a very special place in these acknowledgements: Heinz Schulz. Heinz first introduced me to the beauty of one dimension, and patiently taught me bosonization during my PhD. In addition to being an excellent advisor and later a very dear friend, he was a remarkable scientist, who made major contributions to the field, spelt in a truly impressive style made of a combination of physical arguments and elegant calculations. I would like to dedicate this book to him.

[8] I assume full responsibility for the remaining ones.

CONTENTS

1 Peculiarities of $d = 1$ 1
- 1.1 Crash course on Fermi liquids 1
- 1.2 One dimension: Failure of perturbation theory 5
- 1.3 How to solve 14
  - 1.3.1 Dzyaloshinskii–Larkin solution 15
  - 1.3.2 Renormalization solution 21

2 Bosonization 29
- 2.1 Spinless model; representation of excitations 29
- 2.2 Physical properties and correlation functions 37
  - 2.2.1 Thermodynamics 40
  - 2.2.2 Correlations 42
- 2.3 Model with spin; charge and spin excitations 50
  - 2.3.1 Physical observables 53
  - 2.3.2 Renormalization equations for sine-Gordon Hamiltonians 56
  - 2.3.3 Phase diagram 65

3 Luttinger liquids 70
- 3.1 Phenomenological bosonization 70
- 3.2 Semiclassical and physical interpretations 81
- 3.3 Links with 2D statistical mechanics 86
  - 3.3.1 Elastic systems 86
  - 3.3.2 Coulomb gas and XY model 91
- 3.4 Basics of conformal theory 94

4 Refinements 100
- 4.1 Long-range interactions 100
- 4.2 Mott transition 106
  - 4.2.1 Basic ingredients 106
  - 4.2.2 Commensurate case: Luther–Emery solution 111
  - 4.2.3 Doping; C–IC transition 115
- 4.3 Effects of magnetic field and magnetic anisotropy 121
  - 4.3.1 Magnetic field 121
  - 4.3.2 Magnetic anisotropies 124
- 4.4 Logarithmic corrections of correlation functions 131

5 Microscopic methods 137
- 5.1 Bethe-ansatz 137
  - 5.1.1 Spin chain 138
  - 5.1.2 One, two, three 139

5.1.3 Many; Bethe-ansatz 143
5.1.4 Bethe-ansatz and Luttinger liquids 146
5.1.5 Partial solution of the equations 148
5.2 A zest of numerics 153
5.2.1 Exact diagonalizations 154
5.2.2 Monte-Carlo 155
5.2.3 DMRG 157

6 Spin 1/2 chains 160
6.1 Physical properties of the spin 1/2 chain 160
6.1.1 Hamiltonian 160
6.1.2 Bosonization solution 163
6.1.3 Finite magnetic field 170
6.2 Extensions 175
6.2.1 Frustrated chains 175
6.2.2 Spin-Peierls 177
6.3 Experimental realization of spin chains 184
6.4 Coupled chains 188
6.4.1 Spin ladders 189
6.4.2 Infinite number of chains 196

7 Interacting fermions on a lattice 200
7.1 Microscopic models 200
7.1.1 Hubbard model 200
7.1.2 t–J model 212
7.1.3 U–V model and beyond 215
7.2 Transport 219
7.2.1 Conductance, conductivity 219
7.2.2 Clean case; persistent currents 223
7.2.3 Mott insulator 228

8 Coupled fermionic chains 238
8.1 Fermionic ladders 239
8.1.1 Spinless ladders 239
8.1.2 Ladders with spins 246
8.2 Physical realizations of Ladders 253
8.3 Infinite number of chains 254
8.3.1 Hopping between chains 255
8.3.2 Two-body hopping 258
8.4 Organic quasi-one-dimensional conductors 262

9 Disordered systems 270
9.1 Effect of disorder; Anderson localization 270
9.1.1 Generalities on disordered systems 270
9.1.2 Collective versus single individual pinning 275
9.2 Many impurities 276

9.2.1 Basics 276
9.2.2 Physical properties 285
9.2.3 Extensions and pitfalls 296
9.3 Quantum wires 299

10 Boundaries and isolated impurities 303
10.1 Effect of a boundary 303
10.2 Isolated impurities 307
10.2.1 Weak coupling 308
10.2.2 Strong coupling 310
10.2.3 More than one impurity 318
10.3 Nanotubes 325
10.4 Edge states in quantum Hall systems 328

11 Significant others 333
11.1 Interacting one-dimensional bosons 333
11.1.1 Commensurate bosons 337
11.1.2 Disorder: Bose glass 339
11.1.3 Experimental realizations 342
11.2 Impurities in Fermi liquids 346
11.2.1 X-ray edge problem 347
11.2.2 Kondo problem 355
11.2.3 Multichannel Kondo problem 364

A Basics of Many-body 370
A.1 Notations and formulas 370
A.2 Digest of many-body 371

B Not so important fine technical points 376
B.1 Explicit form of U operators 376
B.2 Completness of Hilbert space 377

C Correlation functions 380
C.1 Path integral 380
C.2 Basic correlations 381
C.3 Analytic continuation 387
C.4 Fourier transform of the retarded correlation function 389

D Bosonization dictionary 391
D.1 Spinless fermions 391
D.2 Spin chains 392
D.3 Fermions with spins 393
D.4 Averages 393
D.5 Babel tower 394

E Sine-Gordon 396
E.1 Renormalization 396

E.2 Variational calculation 400
E.3 Semiclassical approximations 402

F Numerical solution 404

References 408

Index 421

1

PECULIARITIES OF $D = 1$

'Toto, I have a feeling we're not in Kansas anymore'

Dorothy, 'The Wizard of Oz'

Interactions among particles are what endows the one-dimensional world with its special properties. Indeed, there are little differences between, for example, one-dimensional free electrons and their higher-dimensional counterparts (Ziman, 1972). Before we embark on our one-dimensional journey, let me briefly recall the effects of interactions in higher dimensions. This will allow to set the stage, present the basic concepts and ideas of Fermi liquids, and to understand very simply why one-dimensional systems are so different. This will serve as a useful reference when studying their physics.

1.1 Crash course on Fermi liquids

When looking at the order of magnitude of the Coulomb interaction in solids, one notices that for typical systems it is neither dominant nor negligible compared to the kinetic energy. This is what makes interactions so difficult to treat: strictly speaking one cannot really use any perturbation theory. Of course, to have a qualitative idea of the effects of interactions the theorist usually considers models for which the interactions can be seen as adjustable parameters. The effects of interactions in 'high'-dimensional systems[9] has been masterfully explained by Landau's Fermi liquid theory (Landau, 1957*a*; Landau, 1957*b*; Landau, 1958). This theory has been the cornerstone of our understanding of interacting Fermi systems for the last 50 years and has been explained in detail in many textbooks (Nozieres, 1961; Abrikosov *et al.*, 1963; Pines and Nozières, 1966; Mahan, 1981). I will thus give here only a caricature of this theory and refer the reader to the aforementioned textbooks for more details.

The important characteristics of the excitations of a free electron gas are as follows. At $T = 0$ all states up to the Fermi energy are occupied (see Fig. 1.1). So the occupation n_k of a state with momentum k has a *discontinuity* at the Fermi surface. For free electrons the amplitude of the discontinuity is 1. The excitations of the system, compared to the ground state, consist in adding particles with a well-defined momentum k. These excitations have a well-defined momentum k and energy $\epsilon(k)$. They have an infinite lifetime since they are eigenstates of the Hamiltonian. To characterize these excitations one can introduce the spectral function $A(k, \omega)$, which is the probability to find a state with a frequency ω and

[9] In this book anything above one will be high dimensional.

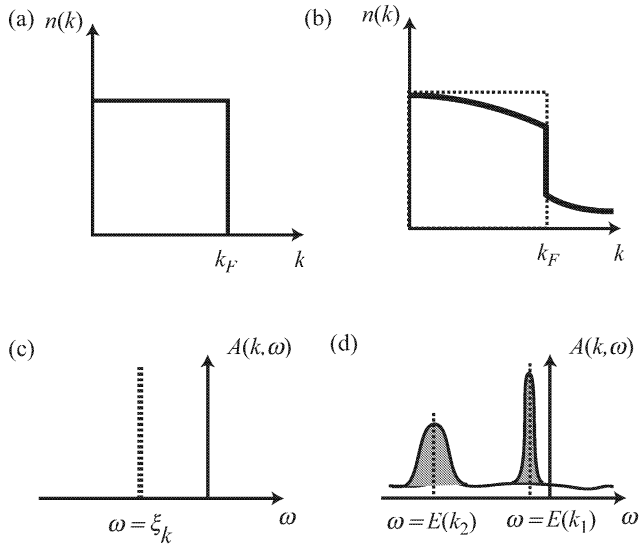

FIG. 1.1. (a) Free electrons: the occupation n_k has a discontinuity of amplitude 1 at the Fermi surface. The spectral function $A(k,\omega)$ (see text) is a delta function peak, showing excitations without damping and a well-defined frequency–momentum relation $\omega = \xi(k)$. The excitations are made of the individual particles of a given momentum. (b) Fermi liquid: it is *essentially* similar to a free electron gas, with some differences. The occupation n_k still has a discontinuity at the Fermi wavevector $k = k_F$, but with a reduced amplitude $Z < 1$. The excitations become sharper when they get closer to the Fermi surface. The total weight in these excitations (quasiparticles) is Z. The quasi-free excitations (quasiparticles) are electrons dressed by the particle–hole excitations of the electron gas.

a momentum k. For free electrons $A(k,\omega) = \delta(\omega - \xi(k))$, where $\xi(k)$ is the energy relative to the chemical potential $\xi(k) = \epsilon(k) - \mu$.

What remains of these nice properties when interactions are switched on in the system? The remarkable result of Fermi liquid theory is that not much changes and that the properties of the system remain *essentially* similar to those of *free* fermionic particles. The elementary particles are not the individual electrons anymore, but electrons dressed by the density fluctuations around them. Just as in electrodynamics an electron dresses by surrounding itself by a photon cloud, here the electrons surround themselves with particle–hole excitations of the ground state (see Fig. 1.1). Since these excitations are made of an electron plus density fluctuations they behave as fermions. These individual objects, called quasiparticles, can be considered as essentially free. Of course, this is only a caricature and the situation in a Fermi liquid is more complicated. Residual interactions exist between the quasiparticles, described by the so-called Landau

parameters, and they have an effect in some quantities like susceptibilities. But this caricature will be enough for our purposes. Thus, the occupation number n_k of a state with momentum k still has a *discontinuity* at the Fermi surface. The amplitude of this discontinuity is not 1 anymore but a number Z that represents the 'fraction' of the electron that remains in this quasiparticle state (I will give a more precise definition below). The more interacting the system is, the more scrambled it is and thus the smaller the discontinuity (see Fig. 1.1). The quasiparticles have a 'well-defined' relation between frequency ω and momentum $\omega = E(k)$, which simply reflects the fact that the wavefunction of a quasiparticle has a time dependence $e^{-iE(k)t}$. Of course, $E(k)$ is not the bare energy of an electron. Since one is close to the Fermi surface one can linearize the dispersion in powers of $k - k_F$

$$E(k) \simeq E(k_F) + \frac{k_F}{m^*}(k - k_F) \tag{1.1}$$

which defines the parameter m^*. For free electrons, $m^* = m$ is the mass of the electron. Close to the Fermi surface, changing the dispersion from $\epsilon(k)$ to $E(k)$ simply changes the mass of the excitation from m to a new mass m^*. This is the only change needed. The Fermi momentum is unchanged (for a spherical Fermi surface) thanks to a conservation law known as Luttinger theorem. This theorem states that although the shape of the Fermi surface can be affected by interactions the volume enclosed by the Fermi surface is an invariant (Nozieres, 1961; Abrikosov *et al.*, 1963; Pines and Nozières, 1966; Mahan, 1981). For a system invariant by rotation symmetry (spherical Fermi surface) this imposes that k_F cannot change.

Because they are not completely free the quasiparticle excitations also have a lifetime τ. Thus, the Fourier transform of the time dependence of the wavefunction of the excitation ($t > 0$)

$$e^{-iE(k)t}e^{-t/\tau} \tag{1.2}$$

is not just a delta function but a Lorentzian of width $1/\tau$ centered around $\omega = E(k)$ (see Fig. 1.1). When one looks at energies closer and closer to the Fermi level, $E(k)$, which measure the difference in energy relative to the Fermi level, goes to zero. If the lifetime was constant, the damping time τ would become smaller than the period $1/E(k)$ and thus the excitations would become overdamped. They could not be interpreted as particles similar to free electrons. Fortunately, the lifetime is due to the scattering between quasiparticles. Since close to the Fermi energy quasiparticles have less and less phase space to scatter, the lifetime *diverges* when one goes closer to the Fermi level. Landau remarkably has shown from simple phase space arguments that the lifetime diverges in $d = 3$ as $1/E(k)^2$. Thus, the lifetime is *always* larger than the period close the Fermi level. In fact, the excitations become better and better defined when one approaches the Fermi level. For most properties one can simply ignore the lifetime. It is only important when dealing with properties such as transport. Because it varies as $1/E(k)^2$ it naturally gives a resistivity proportional to T^2.

Having essentially free excitations is what makes Fermi liquid theory work and the concept of quasiparticle so useful. In condensed matter, one is very often for practical purposes 'close' to the Fermi level. The Fermi energy is about $10000K$ in normal metals and one works at temperatures of the order of 1–$100K$ which is very small compared to the Fermi energy. At these energies the quasiparticles are the correct well-defined and 'free' excitations, whereas the individual electrons themselves are strongly coupled. The spectral function $A(k, \omega)$ thus contains (Lorentzian) peaks centered at $\omega = E(k)$ that becomes sharper and sharper when k goes to k_F. The total weight of these peaks is Z and describes the part of the excitations that is in the quasiparticle state. The rest $1 - Z$ is in a continuous background that has no well-defined structure, but can be safely ignored, close to the Fermi surface compared to the well-defined peaks. Since only the sharp excitations have a reason to give a discontinuity in $n(k)$ at k_F (in a similar way than for free electrons), this explains why the jump in $n(k)$ at $k = k_F$ has an amplitude Z and not unity any more as for free electrons.

One can establish by doing perturbation in the interaction that these properties are indeed correct. But the great strength of Landau's theory resides in the fact that it is *not restricted to weak coupling.* The existence of quasiparticles, which have fermionic nature and the above properties, is extremely robust and relies only on a phase space argument. It can work even for extremely strong interactions. Self-consistent (Landau, 1958) and renormalization (Shankar, 1994) proofs of Fermi liquid theory have been given. To prevent the theory from applying one thus needs either exceedingly strong interactions or special conditions such that some other instability occurs (see, e.g. Varma *et al.*, 2002).

To complete our brief tour of Fermi liquid let us note two additional facts. First, in addition to these individual quasiparticle excitations, other types of excitations exist in an interacting system. One can define collective excitations that describe the response of the system to a disturbance of the density or the spin density. For example, for the charge, if only short-range interactions are present (as is, e.g. the case in helium) this collective excitation is called zero sound, and represents the way a density wave can propagate (with or without damping) in the electron gas. When long-range (Coulomb) interactions are present, this is the famous plasmon excitation (Abrikosov *et al.*, 1963; Pines and Nozières, 1966). The second point is more formal. One should note that the quasiparticle states are not the exact eigenstates of the interacting problem. Indeed, for an interacting system the number of eigenstates is exponentially large. For example, for a lattice system of fermions with spin the total number of states is 4^N where $N = L^d$ is the number of sites, L the linear dimensions of the system and d the spatial dimension. Since quasiparticles states have an energy $E_k = k_F(k - k_F)/m^*$ the distance between two such states is of the order of $1/L$ where L are the linear dimensions of the system. This is much larger than the exponentially small[10]

[10]This is for generic interacting systems. Of course, for the free electron gas, the level separation is $1/L$ and each energy level is highly degenerate. Interaction lifts in general this huge degeneracy between exact eigenstates.

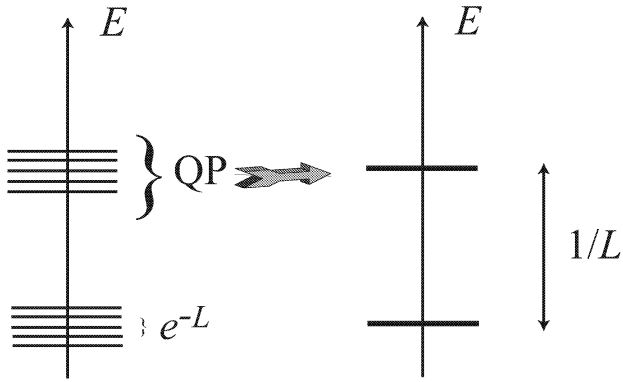

FIG. 1.2. A quasiparticle 'state' is in fact made of a very large number of *exact* eigenstates of the interacting system. The separation in energy of these states is exponentially small in the system size L and thus irrelevant physically, for reasonable systems. The cluster of all these states form the quasiparticle with its average energy and lifetime (inverse of the broadening in energy).

separation in energy between the *exact* eigenstates. As shown in Fig. 1.2, in a Fermi liquid, exact eigenstates thus cluster at given positions in energy. The ensemble of *all* these exact eigenstates form a quasiparticle with its lifetime.

I have purposefully used in this chapter handwaving descriptions. One can formalize the above concepts by introducing the standard many-body description of such systems. Since I will need this formalism later, Appendix A contains a brief summary of the many-body formalism that will be used in this book. I follow the notations of Mahan (1981). In particular, the spectral function is related to the single-particle Green's function by

$$A(k,\omega) = \frac{-1}{\pi}\mathrm{Im}\, G_{\mathrm{ret}}(k,\omega) \tag{1.3}$$

where Im denotes the imaginary part and $G_{\mathrm{ret}}(k,\omega)$ is the retarded Green's function.

1.2 One dimension: Failure of perturbation theory

How much of this beautiful Fermi liquid theory survives in one dimension? Without any calculations it is easy to see that interactions have drastic effects compared to higher dimension. Indeed, in high dimension nearly free quasiparticle excitations exist. In one dimension, as shown in Fig. 1.3, an electron that tries to propagate has to push its neighbors because of electron–electron interactions. No individual motion is possible. Any individual excitation has to become a collective one. This 'collectivization' of excitations is obviously a major difference between the one-dimensional world and higher dimensions. It clearly invalidates any possibility to have a Fermi liquid theory work. This proves that the physical

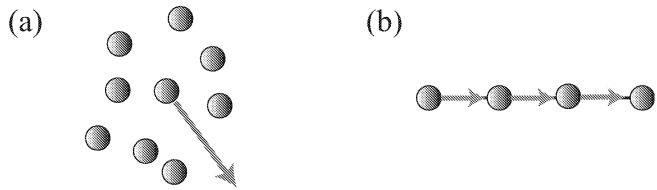

FIG. 1.3. (a) In high dimensions, nearly free quasiparticle excitations, that look nearly as individual particles are possible. (b) In a one-dimensional interacting system, an individual electron cannot move without pushing all the electrons. Thus, only *collective* excitations can exist.

properties of the one-dimensional electron gas are drastically different from the ones of a free electron gas. For fermions with spin this is even worse. Because only collective excitations can exists, it implies that a single fermionic excitation has to split into a collective excitation carrying charge (like a sound wave) and a collective excitation carrying spin (like a spin wave). These excitations have in general different velocities, so the electron has to 'break' into two elementary excitations. These properties, quite different from the ones of a Fermi liquid, will be the essence of the Luttinger liquid, examined in Chapter 3.

Let us be more formal. If some perturbation theory in interaction was attempted, some correlations such as the density–density correlation function would appear in the perturbation theory. Such correlation measures in linear response, the response $\langle \rho(x) \rangle$ of the electron gas to an applied external potential.

$$H_{\text{dens}} = \int d^d x \; V(x,t)\rho(x) \tag{1.4}$$

The susceptibility (see A.33) that measures this response is given by (Ziman, 1972; Mahan, 1981)

$$\chi(q,\omega) = \frac{1}{\Omega} \sum_k \frac{f_F(\xi_k) - f_F(\xi_{k+q})}{\omega + \xi(k) - \xi(k+q) + i\delta} \tag{1.5}$$

where $\delta = 0^+$. Generically, I denote by Ω the volume of the system. f_F is the Fermi factor (see Appendix A for notations). For a system in d dimensions with linear dimensions L, $\Omega = L^d$. Let us focus on the static susceptibility $\chi(q, \omega = 0)$. Normally, it is well behaved at all wavevectors and goes to a constant for $\omega = 0$. One recovers from (1.5) that $\chi(q \to 0, \omega = 0)$ is simply proportional to the density of states at the Fermi level (Ziman, 1972). The standard (positive) compressibility is defined with $V = -\mu$ compared to (1.4), so with our conventions χ is negative. For finite q its behavior is controlled by the way the energy $\xi(k)$ depends on k. When k is on the Fermi surface $\xi(k) = 0$, if one can find a wavevector Q such that both $\xi(k)$ and $\xi(k+Q)$ are zero this leads to singularities. In high dimensions, as shown in Fig 1.4, this occurs only for a very limited set of points. Because of the integration over k in (1.5) the singularity of the denominator is

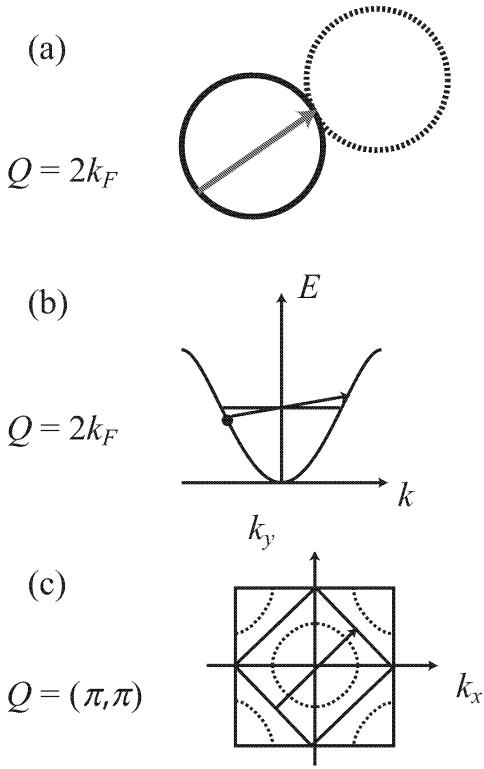

FIG. 1.4. Nesting properties of Fermi surfaces. In high dimensions, a normal Fermi surface leads to nesting only for a very limited set of points and thus to very weak singularities at $Q = 2k_F$ in the derivatives of the susceptibility (a). In one dimension, the Fermi surface consists of only two points and is thus totally nested. This leads to serious singularities at $Q = 2k_F$ (b). Nesting can also occur for special wavevectors Q in higher dimensions, for example, for a square Fermi surface in two dimensions (c).

smoothed out, and only surfaces as a singularity in the slope of $\chi(q)$. This is the root of such phenomena as the Friedel oscillations (Ziman, 1972) and is also known as Kohn anomaly. The only way to have a stronger singularity is for the Fermi surface to satisfy a nesting property, that is, there exists a wavevector Q such that for a finite domain of values of k the energy satisfies

$$\xi(k + Q) = -\xi(k) \tag{1.6}$$

In the domain for which the property (1.6) is satisfied, eqn (1.5) becomes

$$\mathrm{Re}\ \chi(Q, \omega = 0) = -\frac{1}{\Omega} \sum_k \frac{\tanh(\beta\xi(k)/2)}{2\xi(k)} \tag{1.7}$$

where Re denotes the real part and $\beta = 1/(k_B T)$ is the inverse of the temperature (see Appendix A for notations). This becomes, for an infinite volume

$$\mathrm{Re}\ \chi(Q, \omega = 0) = -\int d\xi\ N(\xi) \frac{\tanh(\beta\xi/2)}{2\xi} \tag{1.8}$$

where $N(\xi)$ is the density of states per unit volume. If the density of states is roughly a constant, as is usually the case close to the Fermi level, or if it does not vanish, (1.8) is dominated by a logarithmic singularity. In (1.8), this singularity is regularized by the temperature. A finite frequency leads to a similar regularization. Equation (1.8) behaves as

$$\chi(Q, \omega = 0) \sim -N(\xi = 0)\ \log(E/T) \tag{1.9}$$

where $E = v_F \Lambda$ is some ultraviolet cutoff, of the order of the range in energy over which the nesting property (1.6) holds and v_F the Fermi velocity.

In high dimensions, it is in general impossible to satisfy the nesting property (1.6), except on isolated points (see Fig. 1.4). Thus, χ itself cannot diverge, but its derivatives are in general singular. In one dimension, however, the nesting property is *always* satisfied. Indeed, close to the Fermi points one can linearize the dispersion relation, regardless of its precise nature

$$\begin{aligned} \xi(k) &\simeq v_F(k - k_F), \quad k \sim k_F \\ \xi(k) &\simeq v_F(-k - k_F), \quad k \sim -k_F \end{aligned} \tag{1.10}$$

because of the inversion properties of practically all systems, the Fermi velocity at k_F has to be the same as the one at $-k_F$. It is thus easy to see from (1.10) that

$$\xi(k + 2k_F) = -\xi(k) \tag{1.11}$$

This is shown in Fig. 1.4. Thus, in one dimension nesting is the rule rather than the exception, *regardless* of the precise dispersion relation. The nesting vector is $Q = 2k_F$. Since the susceptibility diverges at $Q = 2k_F$, one can expect any perturbation theory in the interaction to be singular at this wavevector. The fact that a perturbation theory diverges is an indication that the ground state of the interacting system is quite different from the one you started with (that is, the non-interacting one). We thus recover from this more formal argument that the physical properties of interacting electrons in one dimension, however weak the interaction, are drastically different from the free electron ones.

However, simply having a singularity in some susceptibility is usually not a major problem. A well-known example is the singularity that occurs in the particle pairing, leading to the Bardeen–Cooper–Schrieffer (BCS) superconducting instability. This susceptibility measures the response $\langle \psi^\dagger(x)\psi^\dagger(x')\rangle$ of the system to a potential that would like to create or destroy pairs

$$H_{\mathrm{pair}} = \int dx\ V(x,t)[\psi^\dagger(x)\psi^\dagger(x') + \mathrm{h.c.}] \tag{1.12}$$

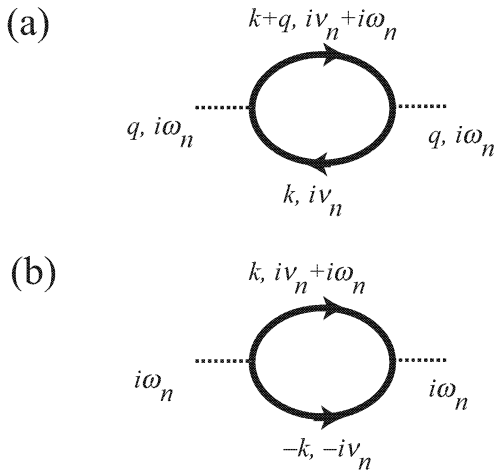

FIG. 1.5. (a) The particle–hole susceptibility (density fluctuations). (b) The particle–particle (pair fluctuations) of the electron gas (only shown for $q = 0$).

If the fermions have spin, one particle has spin up and the other spin down to have a singlet pair and $x' = x$. For spinless fermions, the term (1.12) is killed for $x = x'$ by the Pauli principle. Thus, in that case $x' = x+a$ where a is the smallest distance available on the system (typically the lattice spacing). I restrict here to the case for which the best momentum of the pair is $q = 0$ and show in Fig. 1.5 the corresponding susceptibility at $q = 0$. This is to be compared with (1.4). In that case the potential $V(x,t)$ creates a particle and a hole (the destruction of a particle), instead of creating two particles as in (1.12). In a diagrammatic representation these two susceptibilities are shown in Fig. 1.5. The corresponding susceptibility is given by

$$\begin{aligned} \chi_{\text{pair}}(q=0,\omega) &= \frac{1}{\Omega}\sum_k \frac{f(\xi_k)-f(-\xi_{-k})}{\omega-\xi(k)-\xi(-k)+i\delta} \\ \chi_{\text{pair}}(q=0,\omega=0) &\sim N(\xi=0)\ \log(E/T) \end{aligned} \tag{1.13}$$

In high dimension, the response to an external potential is usually treated in a self-consistent way. The susceptibility measures the response to the local potential seen by the electrons, which is the sum of the external one and of the response of the electron gas. If there is an interaction in the system one can treat the interaction in mean field, assuming some kind of order in the system. Typically, one considers order in the density (the so-called particle–hole channel) or order in the pair creation (the so-called particle–particle channel). Any fluctuation imposed by the external potential is thus modified by the presence of the interaction. Let us take an example with a local (Hubbard like, see Section 7.1.1) interaction:

$$H = U \int d^d x \; \rho_\uparrow(x)\rho_\downarrow(x) \tag{1.14}$$

where $\uparrow, \downarrow$ denotes the spin of the electron. If one expects some ordering of the density, the operator $\rho_\sigma(x)$ of the density of each spin species can be rewritten as

$$\rho_\sigma(x) = \langle \rho_\sigma(x) \rangle + (\rho_\sigma(x) - \langle \rho_\sigma(x) \rangle) \tag{1.15}$$

and one can consider that the fluctuations $\delta\rho_\sigma(x) = \rho_\sigma(x) - \langle \rho_\sigma(x) \rangle$ are small. The interaction (1.14) can thus be expanded to linear order in the fluctuations to give

$$\begin{aligned} H &\simeq U \int d^d x [\langle \rho_\uparrow(x) \rangle \langle \rho_\downarrow(x) \rangle + \langle \rho_\uparrow(x) \rangle \delta\rho_\downarrow(x) + \langle \rho_\downarrow(x) \rangle \delta\rho_\uparrow(x)] \\ &= U \int d^d x [\langle \rho_\uparrow(x) \rangle \rho_\downarrow(x) + \langle \rho_\downarrow(x) \rangle \rho_\uparrow(x) - \langle \rho_\uparrow(x) \rangle \langle \rho_\downarrow(x) \rangle] \end{aligned} \tag{1.16}$$

The last term in (1.16) is just a shift of the energy. The two first terms can be seen as an effective potential seen by the electrons of a given spin created by the electrons of the opposite spin via the interaction. For example, for the up electrons the potential is

$$V(x) = U \langle \rho_\downarrow(x) \rangle \tag{1.17}$$

This potential is dependent on the average density at a given point (here of the density of down electrons). In the absence of such interaction the response of the up electrons to an external potential V_{ext} would be

$$\langle \rho_\uparrow(q,\omega) \rangle = \chi^0(q,\omega) V^\uparrow_{\text{ext}}(q,\omega) \tag{1.18}$$

where χ^0 is the susceptibility of the free electron gas (1.5). In the presence of the interaction, one can consider that the linear response (1.18) gives the response to the effective potential. For the up electrons

$$\langle \rho_\uparrow(q,\omega) \rangle = \chi^0(q,\omega) V^\uparrow_{\text{eff}}(q,\omega) \tag{1.19}$$

where the effective potential is the sum of the external one and the one due to the interaction (1.17)

$$V^\uparrow_{\text{eff}}(q,\omega) = V^\uparrow_{\text{ext}}(q,\omega) + U \langle \rho_\downarrow(q,\omega) \rangle \tag{1.20}$$

Of course, the average of the density should be determined from (1.19) (the down electrons obey an identical equation). Putting the two equations together leads to (the argument (q,ω) is understood)

$$\begin{pmatrix} \rho_\uparrow \\ \rho_\downarrow \end{pmatrix} = \begin{pmatrix} 0 & U\chi^0 \\ U\chi^0 & 0 \end{pmatrix} \begin{pmatrix} \rho_\uparrow \\ \rho_\downarrow \end{pmatrix} + \begin{pmatrix} \chi^0 V^\uparrow_{\text{ext}} \\ \chi^0 V^\downarrow_{\text{ext}} \end{pmatrix} \tag{1.21}$$

Let us consider the response to a magnetic field $V^\uparrow_{\text{ext}} = -V^\downarrow_{\text{ext}}$ to probe the magnetic response. Using (1.21) the response to the external potential is

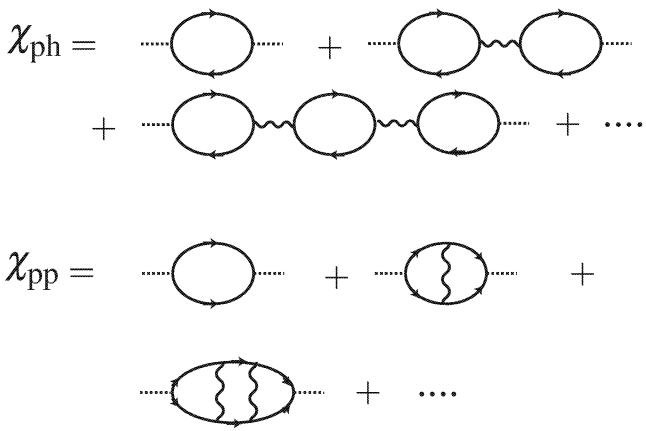

FIG. 1.6. In high dimension, the divergent susceptibilities either in the particle–hole channel (ph) or in the particle–particle one (pp) can be summed up individually, for example, in an RPA approximation, and lead to a finite temperature phase transition. The solid lines are the fermion propagators and the wiggly line is the interaction.

$$\langle \rho_\uparrow(q,\omega)\rangle = \frac{\chi^0(q,\omega)V^\uparrow_{\rm ext}(q,\omega)}{1+U\chi^0(q,\omega)} \tag{1.22}$$

In the presence of interaction, this calculation thus allows to obtain an approximation of the spin susceptibility, which is given by

$$\chi(q,\omega) = \frac{\chi^0(q,\omega)}{1+U\chi^0(q,\omega)} \tag{1.23}$$

This is the well-known RPA (random phase approximation) result that corresponds to summing bubbles or ladders as is shown on Fig. 1.6. A similar calculation can be done for the pairing susceptibility. Summing the diagrams shown in Fig. 1.6 leads to

$$\chi_{\rm pair}(q,\omega) = \frac{\chi^0_{\rm pair}(q,\omega)}{1+U\chi^0_{\rm pair}(q,\omega)} \tag{1.24}$$

If the denominator can be zero there is a finite temperature at which the response diverges. This is usually the signature of a phase transition to an ordered state. For the particle–hole channel, this is the transition to a phase where either the charge or spin density orders. This corresponds either to an antiferromagnetic state (spin order or spin density wave), or to a so-called charge density wave (charge order). The singularity corresponding to a divergence of the particle–particle susceptibility is of course the pairing or BCS superconducting transition. The BCS susceptibility is always divergent, irrespective of the shape of the Fermi surface. This results from the 'nesting' due to time reversal symmetry, that is,

$\epsilon(k) = \epsilon(-k)$. Thus, since χ^0_{pair} is positive, provided the interaction is negative there is always a transition at a given temperature. In the particle–hole channel in high dimension the susceptibility is not divergent (roughly the density of states), so one needs a finite and strongly repulsive (since χ^0 is negative) interaction to have a transition. This explains why the Fermi liquid state is generically so useful. Since the signs of χ^0_{pp} and χ^0_{ph} are opposite one sees that quite generally depending on the sign of the interaction no singularity exists at all in the other channel.

When there is nesting one has to face a special situation, since in that case the particle–hole susceptibility is also always divergent at the nesting wavevector. So there is always for repulsive interactions a transition towards an ordered state in (spin) density. However, as we saw, the particle–particle and particle–hole instabilities in general do not compete, the presence of one usually means that the others are completely killed. We can also expect the RPA to be roughly correct since we know that phase transitions towards ordered states are possible in high dimensions. One dimension is thus quite special. First, nesting always occurs. Second, and more importantly, the RPA result can only be incorrect, since we know that no finite temperature phase transition can exist, even for classical systems (Landau and Lifshitz, 1986). The presence of quantum fluctuations can only make things worse. At a technical level, it means that the simple ladder or bubble resummation of Fig. 1.6 is not enough. There are always two types of divergences, regardless of the shape of the Fermi surface, and *both* should be considered together. Taking into account both bubbles and ladder is known in the diagrammatic lingo as the parquet approximation. Needless to say, it is a nightmarish method, and we will discuss it in more details in Section 1.3. Since these instabilities compete and want to push the system towards different ordered states, they will partly cancel each other, and we can expect some state that will be on the verge of an instability, without ever being able to order completely. One can thus expect the behavior of one-dimensional systems to be close to the critical behavior of systems right at a critical temperature in higher dimension. I will come back to this point in Section 3.4.

Finally, after all these complications, let us note a final peculiarity of one dimension. This time, it will be a great help and in fact at the root of the solution discussed in the next two chapters. A crucial component of the excitations of the electron gas is the so-called particle–hole excitations where an electron is taken from below the Fermi level and promoted above. Since one destroys a particle with momentum k and creates some particle with momentum $k + q$ the momentum of the excitation is well fixed and equal to q. The energy of such an excitation, on the contrary, depends in general on *both* k and q. If one looks at the energy of the particle–hole excitations as a function of their momentum q, one has in general a continuum of energies. In high dimensions, for $q < 2k_F$ one can create particle–hole pairs of arbitrarily low-energy by killing a particle just below the Fermi surface at one point and recreating the particle just above the Fermi surface at another point, as shown in Fig. 1.7. The particle–hole excitations thus

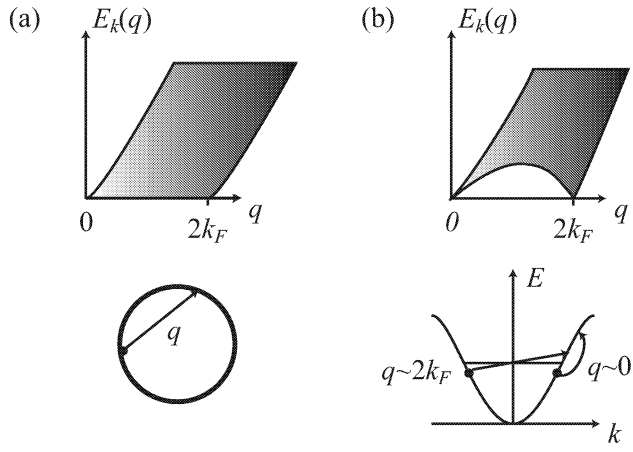

FIG. 1.7. Particle–hole spectrum for two- or three-dimensional systems (a) and for one-dimensional ones (b). In one dimension, contrary to higher dimensions, particle–hole excitations have both a well-defined momentum and energy, for small momentum q.

lead to a continuum extending to zero energy for all q vectors smaller than $2k_F$. In one dimension, the Fermi surface is reduced to two points and one cannot play with angles to increase the momentum q without moving away from the Fermi surface in energy. Since the only way to get a low-energy excitation is to destroy and recreate pairs close to the Fermi 'surface', the only places where the particle–hole energy can reach zero are for $q = 0$ and for $q = 2k_F$. The behavior of the particle–hole spectrum in one dimension is shown in Fig. 1.7. Note the difference with the one in $d \geq 2$. Let us focus on the behavior close to $q = 0$. If we look at excitations at small q the energy of a particle–hole excitation is

$$E_k(q) = \xi(k+q) - \xi(k) \tag{1.25}$$

where $\xi(k)$ should be occupied and $\xi(k+q)$ empty. Let us look at the possible values of $E_k(q)$ for the standard quadratic dispersion

$$\xi(k) = \frac{k^2 - k_F^2}{2m} \tag{1.26}$$

It is easy to check that for $k \in [k_F - q, k_F]$ the average value $E(q)$ of $E_k(q)$ and the dispersion $\delta E(q) = \max(E_k(q)) - \min(E_k(q))$ are

$$\begin{aligned} E(q) &= \frac{k_F q}{m} = v_F q \\ \delta E(q) &= \frac{q^2}{m} = \frac{E(q)^2}{m v_F^2} \end{aligned} \tag{1.27}$$

A similar calculation can be made by expanding the energy around k_F. If one writes

$$\xi(k) = v_F(k - k_F) + \frac{\lambda}{2}(k - k_F)^2 \tag{1.28}$$

Then it is obvious that

$$\begin{aligned} E(q) &= v_F q \\ \delta E(q) &= \lambda q^2 = \frac{\lambda}{v_F^2} E(q)^2 \end{aligned} \tag{1.29}$$

The results (1.27) or (1.29) are noteworthy. They show that regardless of the dispersion relation $\xi(k)$ provided it has a finite slope at the Fermi level: (i) the average energy of a particle–hole excitation is *only* dependent on its momentum q thus the particle–hole excitations are excitations with well-defined momentum q and energy $E(q)$; (ii) the dispersion in energy $\delta E(q)$ goes to zero much faster than the average energy. This is the same situation as the one we discussed for the Fermi liquid quasiparticles. It means that in one dimension the particle–hole excitations are well-defined 'particles' (that is, objects with well-defined momentum and energy), which become longer and longer lived when the energy tends to zero. Because these excitations are made of the destruction and creation of a fermion they are bosonic in nature. These bosonic quasiparticles will just be the key in solving our one-dimensional problem. This remark is at the root of the bosonization method that will be discussed in the next two chapters.

1.3 How to solve

As we have seen in the previous section, one can expect rather peculiar physics in one dimension. This is obvious from the various divergences that plague the perturbation theory in the interaction. These divergences are the way the perturbation theory can tell that the ground state of the interacting system is quite different from free fermions. The first attempt to solve the problem has been made directly in the fermion language. As I hinted in the previous section, this is extremely difficult since it implies the resummation of the various divergences in the perturbation theory. A much more clever method is to use the last remark in the previous section and to reformulate the Hamiltonian in a more convenient basis. This method, known as bosonization, exposed in detail in the next two chapters, will be the cornerstone of this book. However, before we embark on this bosonization solution, I want to expose very briefly in this chapter two of the methods that were put forward to tackle the problem directly in the fermion representation. The goal of this chapter is threefold: (i) A historical interest, since these were the first solutions of the problem and show how to deal with such divergences; (ii) Since these solutions are directly in the fermion representation they nicely complement the other methods. They can and have led to extensions to higher dimensions. (iii) They illustrate some general important concepts such as renormalization.

As you can guess, the rest of this chapter is not for the faint of heart.[11] It requires some knowledge of the many-body theory and diagrammatic techniques. This is the only section of this book with such requirement. Since this section is not necessary to read and understand the rest of the book it can be safely skipped if one wishes to.

1.3.1 *Dzyaloshinskii–Larkin solution*

I will first present a brute force but very elegant solution of the fermionic problem. This is a remarkable calculation (Dzyaloshinskii and Larkin, 1974), and historically a breakthrough in this complicated problem. It also illustrates some of the important properties of the one-dimensional electron gas. For simplicity, this section will deal only with spinless fermions even if the method can be used to treat fermions with spin as well.

If the interactions are much weaker than the bandwidth and if we want to retain the low-energy properties of the system, we want to deal with excitations close to the Fermi surface. In that case we can linearize the dispersion relation close to each Fermi points. We thus replace the original model by one on which the spectrum is purely linear, as shown in the next chapter in Fig. 2.1. This is nothing but the approximation that assumes a constant density of states. Since this approximation is crucial in most methods I will expose it in greater detail in the next chapter, which is supposed to be for a more general readership. I will just give here the main steps. The linearization of the spectrum forces us to introduce two species of fermions: right and left going fermions. The Hamiltonian of the system becomes (Tomonaga–Luttinger model)

$$H = \sum_{k;r=R,L} v_F(\epsilon_r k - k_F) c^\dagger_{r,k} c_{r,k} \tag{1.30}$$

where $\epsilon_R = +1$ for right going particles and $\epsilon_L = -1$ for left going particles. In order to avoid the notation ϵ_r in the following, I use the convention that $r = +1$ for $r = R$ and $r = -1$ for $r = L$ when used in mathematical expressions. What happens far from the Fermi surface is not really important for low-energy processes. Excitations way below the Fermi level are blocked by the Pauli principle and the ones too high in energy cannot be excited anyway. In fact, this is not totally true but I will come back to this point later. We can thus use an arbitrary cutoff procedure to cut the spectrum at large momentum: for example, only allow momentum between $[k_F - \Lambda, k_F + \Lambda]$ (and the same thing on the opposite Fermi point) to exist. Λ in that case can be used to mimic the original bandwidth.

We have the kinetic energy and now need to rewrite the interaction for our new model (1.30). For spinless fermions a typical interaction is

$$H_{\text{int}} = \int dx\, dx'\, V(x - x')\rho(x)\rho(x') \tag{1.31}$$

[11] The presentation of these methods fulfils thus another goal. Once you have seen them, you will realize how simple bosonization is!

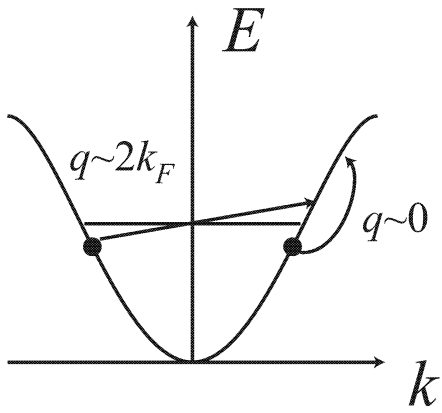

FIG. 1.8. Low-energy processes that the density operator is able to produce. The $q \sim 0$ component of this operator makes particle hole excitations on the same branch, whereas the $q \sim 2k_F$ one transports a particle from one side to the other of the Fermi surface. For the linearized spectrum these two processes correspond, respectively, to the $\psi_R^\dagger(x)\psi_R(x)$ and $\psi_R^\dagger(x)\psi_L(x)$ terms.

The density operator should be written using our left and right going fermions. The single-particle Fermion operator is

$$\begin{aligned}\psi(x) &= \frac{1}{\sqrt{\Omega}}\sum_k e^{ikx}c_k \simeq \frac{1}{\sqrt{\Omega}}\sum_{k\sim -k_F} e^{ikx}c_k + \frac{1}{\sqrt{\Omega}}\sum_{k\sim k_F} e^{ikx}c_k \\ &= \psi_L(x) + \psi_R(x) \end{aligned} \tag{1.32}$$

since only the part of the single-particle operator acting close to the Fermi surface is important for the low-energy properties. The expression (1.32) retains only these important parts. The density operator thus becomes

$$\begin{aligned}\rho(x) &= \psi^\dagger(x)\psi(x) \\ &= \psi_L^\dagger(x)\psi_L(x) + \psi_R^\dagger(x)\psi_R(x) + \psi_L^\dagger(x)\psi_R(x) + \psi_R^\dagger(x)\psi_L(x) \end{aligned} \tag{1.33}$$

The two first and two last terms in the density operators are the expression, using left and right going fermions of the low-energy processes produced by the density operator

$$\rho^\dagger(q) = \sum_k c_{k+q}^\dagger c_k \tag{1.34}$$

since both k and $k+q$ have to be close to one of the Fermi points. These processes are shown in Fig. 1.8.

The interaction (1.31) can be rewritten (see Appendix A)

$$H_{\text{int}} = \frac{1}{2\Omega} \sum_{k,k',q} V(q) c^\dagger_{k+q} c^\dagger_{k'-q} c_{k'} c_k \tag{1.35}$$

One has to keep in mind that the most efficient processes in the interaction are the ones that can act close to the Fermi surface. It means that all momenta in (1.35) have to be close to the Fermi points, that is, close to $-k_F$ or $+k_F$. The fact that in one dimension the Fermi surface is reduced to two points thus allows us to decompose the interaction in three different sectors. These three sectors are shown in Fig. 1.9. The first process g_4 in Fig. 1.9 only couples fermions on the same side of the Fermi surface. The second process g_2 couples fermions from one side of the Fermi surface with fermions on the other side. However, each species stays on the same side of the Fermi surface after the interaction (forward scattering). Finally, the last process g_1 corresponds to a $\sim 2k_F$ scattering (that is, to a backscattering) where fermions exchange sides. Note that for spinless fermions g_2 and g_1 processes are identical since one can exchange the outgoing particles (the particles are indiscernible). This is *not* the case if the fermions have a spin index since in that case one wants the spin to be conserved by the interaction and the processes g_2 and g_1 are different.

Let us now start with our solution. It only works if we do not have g_1 processes. For spinless fermions this is automatically achieved. For fermions with spin this would be a brutal approximation, but there are ways to rationalize this choice. The g_2 process corresponds to a small q matrix element of the interaction, whereas g_1 is clearly the $q \sim 2k_F$ component. For a local interaction the two processes are of the same value, since the Fourier transform of a delta function is a constant. But if the interaction is long-range, or at least non-local, the $q \sim 0$ component is usually much larger. One can thus expect, at least in this case, that keeping only g_2 is a reasonable approximation. The true reason, however, is the fact that the g_1 process is a pain in the neck to treat, as we will see in the next chapter, and one wants to start first with a soluble model. If one retains only the g_2 process then a wonderful simplification occurs. This simplification contains interesting physics that deserves to be discussed it detail. If only g_2 is present then the chirality (that is, the right or left character of the fermions) cannot be changed by an interaction line. Quite remarkably in that case only diagrams with fermion bubbles with *at most* two interaction lines contribute. All the other terms cancel! This is quite extraordinary in the fermion language, and the meaning of this miracle will only become transparent in Section 3.1 (see also Fig. 11.9). To prove this remarkable property, let us examine the two fermionic bubbles with three interaction lines shown in Fig. 1.10. Each time there is bubble (a) in a diagram one has a similar diagram with bubble (b). This would not be the case if there were only two interaction lines. In that case bubbles (a) and (b) would be identical and appear only once in the diagrammatic expansion. Let us evaluate bubble (a). Because the fermion cannot change chirality, the bubble is a product of Green's functions of, say, right going fermions.

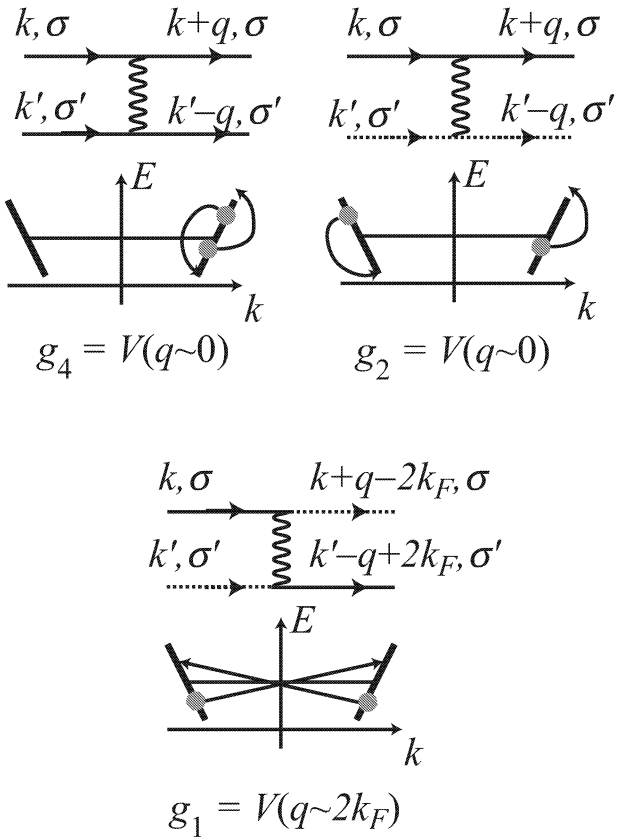

FIG. 1.9. The important low-energy processes of the interaction can be decomposed in three sectors. A full line is for a fermion with a momentum close to $+k_F$ (right going fermion) and a dashed line for a fermion with a momentum close to $-k_F$ (left going fermion). The notation g to designate the different processes is historical (the so-called g-ology). For fermions with spins each interaction can take two values $(g_\parallel, g_\perp)$ depending on whether the spin σ and σ' of each fermions are equal $(g_\parallel)$ or opposite $(g_\perp)$.

$$(a) \propto \sum_{\nu,k} \frac{1}{i\nu - v_F k} \frac{1}{i(\nu + \omega_a) - v_F(k + k_a)} \frac{1}{i(\nu + \omega_a + \omega_b) - v_F(k + k_a + k_b)} \tag{1.36}$$

Whereas bubble (b) is

$$(b) \propto \sum_{\nu,k} \frac{1}{i\nu - v_F k} \frac{1}{i(\nu + \omega_b) - v_F(k + k_b)} \frac{1}{i(\nu + \omega_a + \omega_b) - v_F(k + k_a + k_b)} \tag{1.37}$$

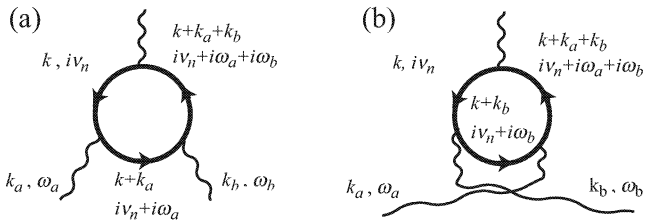

FIG. 1.10. Two fermionic bubbles with more than two interaction lines. These two contributions cancel exactly due to the strictly linear dispersion relation.

Thus, normally (1.36) and (1.37) are quite different. However, because the energy is strictly linear in the momentum and the chirality is conserved, one can rewrite (1.36) as

$$(a) = \frac{1}{i\omega_a - v_F k_a} \sum_{\nu,k} \left[\frac{1}{i\nu - v_F k} - \frac{1}{i(\nu+\omega_a) - v_F(k+k_a)} \right] \times \frac{1}{i(\nu+\omega_a+\omega_b) - v_F(k+k_a+k_b)} \tag{1.38}$$

performing the same operation for bubble (b) one gets

$$(b) = \frac{1}{i\omega_a - v_F k_a} \sum_{\nu,k} \frac{1}{i\nu - v_F k} \left[\frac{1}{i(\nu+\omega_b) - v_F(k+k_b)} - \frac{1}{i(\nu+\omega_a+\omega_b) - v_F(k+k_a+k_b)} \right] \tag{1.39}$$

The second term in (1.39) is obviously cancelled by the first term in (1.38). By shifting $\nu \to \nu + \omega_a$ and $k \to k + k_a$, which one can do unrestrictedly due to the perfectly linear dispersion relation, the remaining term cancels as well. This, of course, assumes that the cutoff Λ is essentially infinite. I will come back to that point in Section 11.2. Thus, bubbles (a) and (b), which are deduced one from the other by permuting two of the legs, cancel perfectly. If there are more than three-legs one can show by induction that the result still holds between the various crossings of the legs of the bubble. Note that when rewriting (1.36) as (1.38) one has one less Green's function depending on ν and k, thus it is similar to a diagram with one external leg less.

As a result, a given diagram can contain bubbles and series of bubbles only. It is as if RPA became exact. This is only true for the *interaction*. For a vertex other terms *do* appear. Let us write in Fig. 1.11 the equations for the effective interactions of the g_4 and g_2 type for our spinless fermions. For fermions with spin the solution is essentially the same (Sólyom, 1979). The equations are

$$\begin{aligned} \Gamma_4 &= g_4 - g_4 \Pi_R \Gamma_4 - g_2 \Pi_L \Gamma_2 \\ \Gamma_2 &= g_2 - g_2 \Pi_R \Gamma_4 - g_4 \Pi_L \Gamma_2 \end{aligned} \tag{1.40}$$

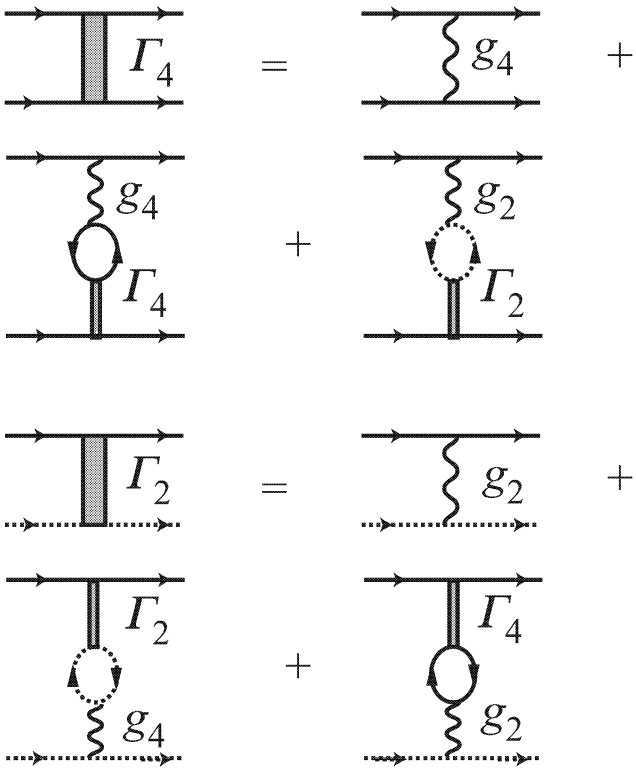

FIG. 1.11. Diagrammatic equations for the effective interactions Γ_4 and Γ_2. Only bubbles and string of bubbles can appear. The full line denotes a right going fermion and a doted line a left going one.

where $\Pi_{R,L}$ are the bubbles made of, respectively, right and left going fermions. For example,

$$\begin{aligned}
\Pi_R(i\nu, k) &= -\frac{1}{\beta\Omega}\sum_{\nu',k'}\frac{1}{i(\nu+\nu') - v_F(k+k')}\frac{1}{i\nu' - v_F k'} \\
&= -\frac{1}{\beta\Omega}\sum_{\nu',k'}\frac{1}{i\nu - v_F k}\Big[\frac{1}{i\nu' - v_F k'} - \frac{1}{i(\nu+\nu') - v_F(k+k')}\Big] \\
&= -\frac{1}{i\nu - v_F k}\frac{1}{\Omega}\sum_{k'}[f_F(v_F k') - f_F(v_F(k+k'))] \\
&= \frac{-k}{2\pi(i\nu - v_F k)} \qquad (1.41)
\end{aligned}$$

Similarly, one has

$$\Pi_L(i\nu, k) = \frac{k}{2\pi(i\nu + v_F k)} \qquad (1.42)$$

Equation (1.40) is easily solved giving Γ_4, Γ_2 as a function of the interaction constants g_4, g_2 and the $\Pi(i\nu_n, k)$. Let me give for simplicity the solution for $g_4 = 0$

$$\begin{aligned}\Gamma_2 &= \frac{g_2}{1 - g_2^2 \Pi_R(i\nu_n, k)\Pi_L(i\nu_n, k)} \\ &= \frac{g_2(\nu^2 + v_F^2 k^2)}{(\nu^2 + v_F^2 k^2) - \left(\frac{g_2}{2\pi v_F}\right)^2 (v_F k)^2}\end{aligned} \tag{1.43}$$

Note that there are now poles in the interaction for $i\nu = \pm uk$ where now the velocity is

$$u^2 = v_F^2 \left[1 - \left(\frac{g_2}{2\pi v_F}\right)^2\right] \tag{1.44}$$

This solution has two interesting features. First, contrary to the case of free electrons the interaction vertex has now poles for excitations with a well-defined energy–momentum relationship. Second, the velocity of these poles is not the free Fermi velocity but is renormalized by the interaction (compare with (2.43)). If one had kept the spin degrees of freedom *two* different velocities would have appeared, showing already that our beloved Fermi liquid is on shaky ground. Of course, (1.43) is only the effective interaction. In order to obtain the physics of the problem one needs to relate Γ_2 to some physical quantity. To determine such quantities one would need the exact vertex in addition to the exact interaction. Fortunately, the exact vertex can be extracted using a Ward identity (Dzyaloshinskii and Larkin, 1974; Sólyom, 1979), consequence of the conservation of particles of each chirality.

I stop here since the calculations become really intricate with little gain compared to the simpler methods of the next chapter. This remarkable method, which is purely fermionic, has the advantage to allow some extension to higher dimensions (Metzner *et al.*, 1998).

1.3.2 *Renormalization solution*

The Dzyaloshinskii–Larkin solution is a very nice exact solution of the model. It suffers, however, from many limitations. The most severe one is not to be able to be extended to fermions with spin because of the g_1 processes. I thus present another solution in the fermion representation (Anderson, 1970; Sólyom and Zawadowski, 1974; Sólyom, 1979). This solution is not exact, but its goal is to extract the main singularities from the perturbation theory and sum them. Although not exact such methods have the advantage of being very flexible since they are able to extract the dominant behavior while dropping all irrelevant details. They illustrate the important concept of the renormalization group for fermionic systems relatively simply.

As already pointed out, the perturbation theory in one dimension is plagued by divergences. A very transparent way to see these divergences is to look at

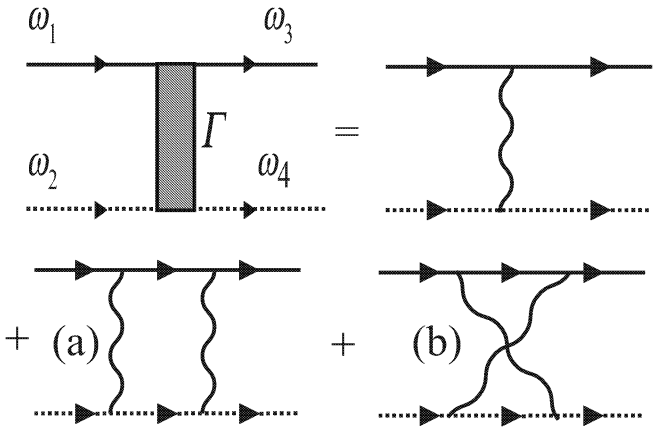

FIG. 1.12. Effective interaction Γ_2 up to second order for spinless fermions. A full line is a right going fermion and a dashed one a left going fermion. The wiggly line is the bare interaction g_2. All external momenta are on the Fermi surface. The second order terms (a) and (b) correspond respectively to the particle–particle and particle–hole channel.

the effective interaction between two particles, identical to the Γ of the previous subsection. Let us first discuss the case of spinless fermions, taking $g_4 = 0$ for simplicity. In that case only the diagrams of Fig. 1.12 exist, to second order. Both diagrams are logarithmically divergent. They can be computed by the standard diagrammatic method and give at $T = 0$ ((a) and (b) refer to the two diagrams in Fig. 1.12)

$$\begin{aligned}(a) &= \frac{1}{2\pi v_F}\log(\omega_{\rm pp}/E)\\ (b) &= \frac{-1}{2\pi v_F}\log(\omega_{\rm ph}/E)\end{aligned} \tag{1.45}$$

where $E = v_F\Lambda$ is the energy cutoff (the bandwidth). The frequency $\omega_{\rm pp} = \omega_1 + \omega_2$ for (a), and $\omega_{\rm ph} = \omega_1 - \omega_4$ for (b). We want the behavior when all these frequencies are small compared to E and of the same order of magnitude. Although one can perform the calculation for any frequency a simple trick is to choose $\omega_1 = 3\omega/2$, $\omega_2 = -\omega/2$, $\omega_3 = \omega_4 = \omega/2$. This satisfies the conservation of frequencies and ensures that $\omega_{\rm pp} = \omega_{\rm ph} = \omega$, which simplifies some expressions.

If only type (a) diagrams were present, they could be summed up by summing the ladder type diagrams. If only type (b) diagrams were present they could be summed by summing the bubbles. Since both diagrams are equally divergent they should be treated on an equal footing. One should thus keep in perturbation theory all higher-order terms where one line of interaction in (1.12) is replaced by one of the two diagrams of Fig. 1.12. Such an approximation, which goes

beyond the ladder and bubble summation, is known as the parquet approximation (Bychkov *et al.*, 1966). It is a way to sum these logarithmic divergences. Parquet leads to quite formidable integral equations. It is a pre-renormalization group technology that I will not explore further since it has been supplanted by a much more efficient method.

The idea of the renormalization group is quite simple and of course useful in a host of situations. All our troubles come from the fact that we are interested in the *low*-energy properties of the system. The effective interaction is of the form

$$\Gamma = g + g^2 \log(E/\omega) \tag{1.46}$$

where g is some bare coupling constant and ω the energy scale at which we are trying to compute. Because of the log in the perturbation theory, even if we start with a small coupling constant g, if we want the low-energy properties of the system $\log(E/\omega)$ is large and the second term (and a fortiori higher terms) in (1.46) becomes more important than the first term. If, however, we wanted to have *high*-energy properties of the system, that is, work at frequencies (or temperatures etc.) of the order of the cutoff, the $\log(E/\omega)$ would be a simple number of order one, and provided that the coupling constant be small the perturbation theory would be well behaved. This remark has led to the idea of the renormalization group. We start from a theory with some coupling constants g and a cutoff $E = v_F\Lambda$. If we could find another theory with the *same* low-energy properties but with new coupling constants g' and a *lower* cutoff $\Lambda' < \Lambda$, then this new theory would have a less divergent perturbation series (provided, of course, that the new coupling constants g' remain small) for a fixed ω. In doing so we have eliminated some unimportant degrees of freedom and thus have a new theory that is much closer to the one that describes the important degrees of freedom, that is, the low-energy ones. We can thus hope that the new Hamiltonian will be simpler to understand than the original Hamiltonian. This renormalization technique has been one of the most useful concepts in the study of phase transitions and condensed matter in the last 30 years. It is specially useful in condensed matter given the very large range in the typical cutoffs (a bandwidth, typically 1 eV or $12\,000K$) and the energies at which one observes the physical phenomena (typically the temperature, i.e. a few Kelvin). A common misconception is to believe that the renormalization group allows to solve problems. All it does is help to relate one problem to another, while keeping the low-energy physics of the two problems identical. The hope is that one of the related problems will be easily solvable. This can happen for various reasons: (i) One of the problems is exactly solvable. This is an incredible stroke of luck, but not so rare in one dimension. I will discuss examples of this situation in the next chapters. (ii) There is some approximate solution that becomes quite accurate on one of the Hamiltonians. For example, since the cutoff is reduced, if the coupling constants remain small, the perturbation theory is better and better behaved. It is thus possible to use straightforward perturbation theory. But other approxi-

mations are possible, and very often more easy to spot since in the renormalized Hamiltonian irrelevant degrees of freedom have been eliminated.

Let us now see how it works practically. For the spinless problem the effective interaction is

$$\Gamma_{\text{eff}} = g_2 + \frac{g_2^2}{2\pi v_F}\log(\omega_{\text{pp}}/E) - \frac{g_2^2}{2\pi v_F}\log(\omega_{\text{ph}}/E) \tag{1.47}$$

The effective interaction obviously controls all the low-energy properties of the system. Thus, we want to keep Γ_{eff} invariant while changing the cutoff. If we change $E \to E'$

$$\log(\omega_{\text{pp}}/E) = \log(\omega_{\text{pp}}/E') + \log(E'/E) \tag{1.48}$$

and thus

$$\Gamma_{\text{eff}} = g_2 + \frac{g_2^2}{2\pi v_F}\log(\omega_{\text{pp}}/E') - \frac{g_2^2}{2\pi v_F}\log(\omega_{\text{ph}}/E') \tag{1.49}$$

since the logarithmic contributions $\log(E'/E)$ cancel. Note that this is obvious if we use the special values of the frequencies that ensures $\omega_{\text{pp}} = \omega_{\text{ph}}$. Of course, as discussed before a different choice of frequencies will not affect the final RG equations. The new coupling constant is simply in that case

$$g_2(E') = g_2(E) \tag{1.50}$$

since all logs vanish. If we define the cutoff as $\Lambda(l) = \Lambda_0 e^{-l}$ (and a similar formula for $E = v_F\Lambda$) we can make the infinitesimal transformation $l \to l + \delta l$. With this variable (1.50) can be rewritten as

$$\frac{dg_2(l)}{dl} = 0 \tag{1.51}$$

We thus see that the forward scattering g_2 is not renormalized but stays the same at any lengthscale. This is consistent with the analysis of the previous section that g_2 drastically changes the properties compared to a free electron gas.

Before we analyze the physical consequences, and because of the simplicity of the method, let us seize the occasion to go one step further and write the interaction process for the system with spins. In that case because the density is

$$\rho(x) = \rho_\uparrow(x) + \rho_\downarrow(x) \tag{1.52}$$

one should rewrite the processes of Fig. 1.9, with a spin index on each fermion line. Thus, each process g can now be different depending on whether the spin on the two fermion lines are parallel $g_\parallel$ or antiparallel $g_\perp$. For interactions that respect spin rotation invariance $g_\parallel = g_\perp$, but one might want to consider more general processes. To illustrate the method I set $g_4 = 0$ for simplicity. We will examine in detail the effects of such processes in the next two chapters. We are thus left with the g_2 and g_1 processes. Since we have spin, we cannot transform the $g_{1\perp}$ process into a g_2 one. However, a $g_{1\parallel}$ is identical by permutation of two

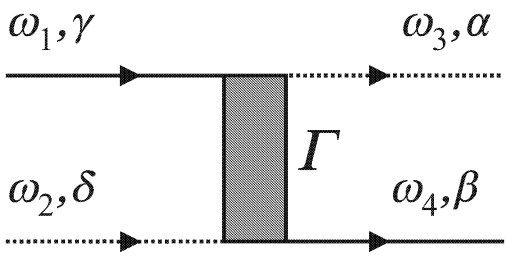

FIG. 1.13. The effective interaction. α, β, γ, δ are the spin indices of the four legs. To ensure that the frequency transfers in the particle–particle and the particle–hole channels are identical, which simplifies expressions, one can take $\omega_1 = 3\omega/2$, $\omega_2 = -\omega/2$, $\omega_3 = \omega_4 = \omega/2$.

fermion lines to a $g_{2\|}$ process. Thus, in defining the effective interaction we have to find a way to separate these two processes. One possible way is to define the effective interaction as

$$\Gamma_{\alpha\beta\delta\gamma} = \Gamma_{1\|}\delta_{\alpha\gamma}\delta_{\beta\delta}\delta_{\alpha\beta} + \Gamma_{1\perp}\delta_{\alpha\gamma}\delta_{\beta\delta}\delta_{\alpha,-\beta} - \Gamma_2\delta_{\alpha\delta}\delta_{\beta\gamma} \tag{1.53}$$

where $\alpha, \beta, \gamma, \delta$ denote the spins on the four fermion lines as shown in Fig. 1.13. This definition fixes all g_2 processes to be isotropic and to put all the difference between $g_{2\|}$ and $g_{2\perp}$ as a $g_{1\|}$ process. It is easy to check that the spinless fermion case is recovered by taking all perpendicular interactions to zero (the two spin species do not talk to each other). This gives $g_2 = 0$ (since g_2 should be isotropic) and $g_{1\perp} = 0$. $g_{1\|}$ plays in that case the role of $-g_2$ in the previous analysis.

With this prescription it is possible to identify each term in the perturbation series. At second order in the interaction the effective interaction is given by the diagrams of Fig. 1.14. Let us write the equation for $g_{1\|}$

$$\Gamma_{1\|} = g_{1\|} - \frac{2g_{1\perp}^2}{2\pi v_F}\log(E/\omega) \tag{1.54}$$

and thus upon a change of the cutoff

$$\Gamma_{1\|} = g_{1\|} - \frac{g_{1\perp}^2}{\pi v_F}\log(E/E') - \frac{g_{1\perp}^2}{\pi v_F}\log(E'/\omega) \tag{1.55}$$

To keep the effective vertex invariant one has thus to change the interaction $g_{1\|}$ as

$$g_{1\|}(E') = g_{1\|}(E) - \frac{g_{1\perp}^2(E)}{\pi v_F}\log(E/E') \tag{1.56}$$

A similar equation for $g_{1\perp}$ gives

$$g_{1\perp}(E') = g_{1\perp}(E) - \frac{g_{1\perp}(E)g_{1\|}(E)}{\pi v_F}\log(E/E') \tag{1.57}$$

	$\Gamma_{1\parallel}-\Gamma_2$	$\Gamma_{1\perp}$	$-\Gamma_2$
	$-(g_{1\parallel}-g_2)^2$	$-2g_{1\perp}(-g_2)$	$-g_{1\perp}{}^2$
	$(g_{1\parallel}-g_2)^2+g_{1\perp}{}^2$	$2(g_{1\parallel}-g_2)g_{1\perp}$	0

FIG. 1.14. Diagrams entering, up to second order, into the effective interaction between two particles. To obtain the value of the diagram one should multiply the value given in the above table by $A = -\frac{1}{2\pi v_F}\log(E/\omega)$.

Introducing the dimensionless variables $y = g/(\pi v_F)$, the full set of equations for fermions with spins is thus

$$\begin{aligned}\frac{dy_2(l)}{dl} &= -\frac{y_{1\perp}^2(l)}{2}\\ \frac{dy_{1\parallel}(l)}{dl} &= -y_{1\perp}^2(l)\\ \frac{dy_{1\perp}(l)}{dl} &= -y_{1\parallel}(l)y_{1\perp}(l)\end{aligned} \tag{1.58}$$

These equation will be analyzed in great detail in the next chapter. I thus investigate here some simple consequences only.

As is obvious from (1.58), the combination $y_\rho = y_{1\parallel} - 2y_2$ is invariant under renormalization. This combination is the equivalent of (1.51) for spinless fermions. As we will see in the following chapters this is the combination of interactions that controls the charge sector of the system (see (2.105)). The interactions $y_{1\parallel}$ and $y_{1\perp}$ control the spin sector, and have non-trivial renormalization. As expected, for a system with spin rotation invariance $y_\parallel = y_\perp$, the spin rotation invariance is preserved under renormalization. For a system with such spin rotation invariance, the equation for $y_1 = y_{1\parallel} = y_{1\perp}$ is

$$\frac{dy_1(l)}{dl} = -y_1^2(l) \tag{1.59}$$

whose solution is obviously

$$y_1(l) = \frac{y_1(l=0)}{1 + y_1(l=0)l} \tag{1.60}$$

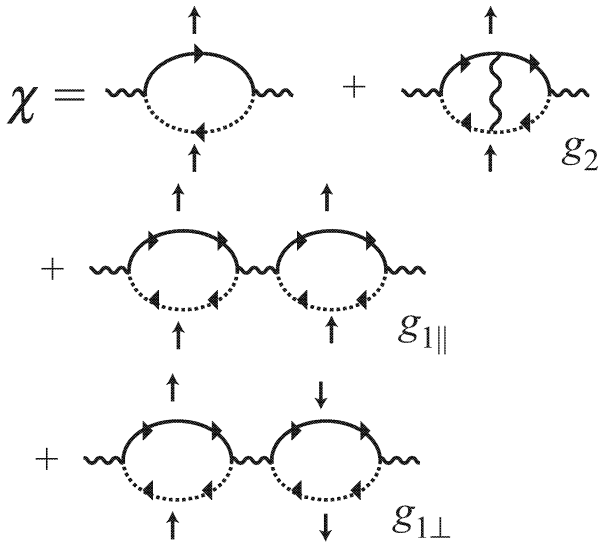

FIG. 1.15. Charge susceptibility, up to first-order in the interaction. One should add to the diagrams shown in the figure the equivalent diagrams where all spins are reversed to get the full χ.

We thus see that if we start from an arbitrary interaction, which gives rise to g_2 and g_1 terms, as we focus on the low-energy properties of the system, y_ρ stays unchanged, whereas the backward scattering renormalizes to zero. The low-energy properties of a physical system will thus be similar to the one of a system with *only* forward scattering. We know how to solve such systems, for example by using the Dzyaloshinskii–Larkin method. This is an example where the RG allows us to simplify the original model and realize that the low-energy properties are in fact equivalent to the ones of a simpler model that we know how to solve.

Let us see how one can extract the physical properties of the system directly from the RG itself. Let us compute, for example, the charge susceptibility $\chi(q = 2k_F, \omega)$, which we argued should be singular for the interacting system. It is given by the diagrams of Fig. 1.15. It gives up to first-order in the interaction

$$\chi(Q = 2k_F, \omega) = \frac{1}{\pi v_F} \log(\omega/E)[1 + \frac{1}{2\pi v_F}(g_{1\parallel} + g_{1\perp} - g_2) \log(\omega/E)] \quad (1.61)$$

As we will see in Section 4.4, $\chi(Q = 2k_F, \omega)$ does not obey a simple RG equation. The correct quantity to renormalize is (Sólyom, 1973; Sólyom, 1979)

$$\overline{\chi}(\omega) = \pi v_F \frac{d\chi(Q = 2k_F, \omega)}{d\log(\omega)} \quad (1.62)$$

Thus, $\overline{\chi}(\omega)$ obeys an equation of the form

$$\overline{\chi}(\omega) = 1 + 2y \log(\omega/E) \tag{1.63}$$

where y stands for the various dimensionless coupling constants $g/(\pi v_F)$. Changing the cutoff from $E = E_0 e^{-l}$ to $E' = E_0 e^{-(l+dl)}$ allows us to write the RG equations for $\log(\overline{\chi})$ at first-order in the coupling constants

$$\frac{d \log \overline{\chi}(l)}{dl} = y_{1\|}(l) + y_{1\perp}(l) - y_2(l) \tag{1.64}$$

Let us consider the spin isotropic case. In that case we could just substitute the solution (1.60) in (1.64) and integrate. Let us here brutally simplify the equation by setting $y_{1\|} = y_{1\perp} = 0$. A more refined treatment will be seen in Section 4.4. Since y_2 is independent of l the remaining equation can be easily solved

$$\log(\overline{\chi}(l)/\overline{\chi}(l = 0)) = -y_2 l \tag{1.65}$$

We want to obtain $\overline{\chi}(l = 0)$, that is, the correlation function for the original cutoff. We should just find an l such that we can compute $\overline{\chi}(l)$. This is easily achieved when the renormalized cutoff is of the order of ω, that is, for

$$l^* = \log(E_0/\omega) \tag{1.66}$$

in that case $\overline{\chi}(l)$ can straightforwardly be computed from the perturbation formula (1.63) and $\overline{\chi}(l^*) \sim 1$. Thus,

$$\overline{\chi}(\omega) = e^{y_2 l^*} = \left(\frac{E_0}{\omega}\right)^{y_2} \tag{1.67}$$

Integrating one last time, using (1.62) and the fact that for $\omega = E_0$, $\chi(\omega) = 0$ (see (1.61)) one gets

$$\chi(Q = 2k_F, \omega) \simeq \frac{1}{\pi v_F y_2} \left[1 - \left(\frac{E_0}{\omega}\right)^{y_2}\right] \tag{1.68}$$

It is easy to see that an expansion in powers of y_2 reproduces the perturbative result (1.61) as it should. However, we now see that if one looks at the low-energy properties $\omega \to 0$, the correlation function diverges as a *power law*, with *non-universal* exponents depending on the interactions. This is in marked contrast with a Fermi liquid behavior, where $\chi(Q = 2k_F, \omega) \sim \log(\omega/E)$. We will, of course, discuss the physics in detail in the next chapter, after having rederived this result by more convenient methods.

It is possible to push the expansion to higher-order and thus to obtain the exponents in (1.68) in a systematic expansion in the interaction y_2. I refer the reader to (Sólyom, 1979; Chitov and Bourbonnais, 2002) for more on this point.

2

BOSONIZATION

A child of five would understand this. Send someone to fetch a child of five.

Groucho Marx

Let us now look at a way to describe the low-energy properties of one-dimensional systems. The method I will present is known as bosonization and is one of the most useful tools in one dimension. To introduce this method I will proceed in two steps. In this chapter, I present a model on which this method is essentially exact. This allows to derive precise formulas that can be used for other models as well. This chapter is thus mostly technical. In the next chapter, I present a more phenomenological derivation that allows to show the universality of the model and to make contact with a host of other systems. A physical interpretation of the bosonization formulas will also be presented in the next chapter. So it is best to start with the following chapter if you are more interesting by the spirit of the method than by the method itself, and to come back to this chapter afterwards.

2.1 Spinless model; representation of excitations

So let us start with the formal derivation. Description of this technique has been the subject of many reviews (Emery, 1979; Sólyom, 1979; Schulz, 1995; Voit, 1995; von Delft and Schoeller, 1998; Gogolin *et al.*, 1999; Schönhammer, 2002; Senechal, 2003). To build the method we start with spinless fermions. As we saw in Fig. 1.7, the particle–hole excitations of the system have a nearly linear spectrum, and are essentially well-defined excitations, with a well-defined energy and momentum. In order to make this relation perfect we replace the original model by one on which the spectrum is purely linear (Tomonaga–Luttinger model), as shown in Fig. 2.1. To get a total independence of the energy of the particle–hole pair on the initial momentum for all q it is also necessary to extend the energy spectrum down to $-\infty$ (see (1.25)). This forces to introduce two species of fermions: right and left going fermions. The Hamiltonian of the system becomes

$$H = \sum_{k;r=R,L} v_F(\epsilon_r k - k_F) c^\dagger_{r,k} c_{r,k} \tag{2.1}$$

where $\epsilon_R = +1$ for right going particles and $\epsilon_L = -1$ for left going particles. In order to avoid the notation ϵ_r in the following,[12] I will use the convention that $r = +1$ for $r = R$ and $r = -1$ for $r = L$ when used in mathematical expressions. (2.1) is the one-dimensional equivalent of a Dirac Hamiltonian. Similarly, the

[12] ϵ is used already for so many things in physics in general and in this book in particular.

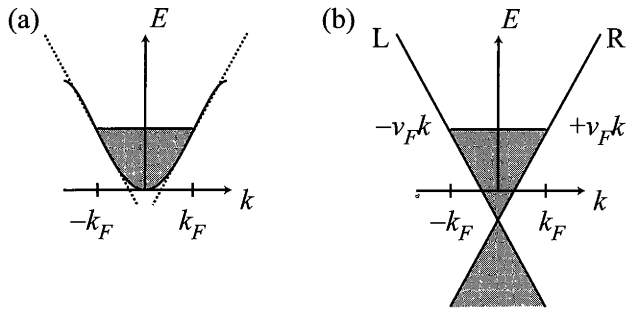

FIG. 2.1. The original model of fermions with band curvature (a) is replaced by a model of fermions with a linear spectrum (b). This forces to introduce two species of fermions (right (R) and left (L) going fermions). The spectrum is now extended to all values of k, leading to an infinite number of negative energy states. A cutoff on the momentum might be needed to make the model well-defined.

Fermi sea where all states below the chemical potential ($\xi_k < 0$) are filled is replaced here by a 'Dirac' sea where the infinite number of states with negative energy ($\xi_{r,k} < 0$) are filled.

Although the two systems of Fig. 2.1 are different for large momentum, their low-energy physics is similar. Note also that taking a linear spectrum is simply equivalent to taking a constant density of states, a quite common approximation for fermions. I will come back to this point in the next chapter. For the moment let us just try to solve our new free model (2.1). The particle–hole excitations of this model are now given by (e.g. for right going particles)

$$E_{R,k}(q) = v_F(k+q) - v_F k = v_F q \tag{2.2}$$

and are thus totally independent on k. The particle–hole excitations are thus well-defined excitations. They have a well-defined momentum q and a well-defined energy $E = v_F q$. This leads to the particle–hole excitation spectrum of Fig. 2.2. Since the particle–hole excitations of the system are well-defined excitations, let us try to rewrite (2.1) in this basis. Why is such a basis so useful? First, as we saw in Section 1.2, only collective excitations can remain in one dimension. Density fluctuations are thus a very natural basis to use. Indeed, the density fluctuations are essentially a superposition of particle–hole excitations (see Appendix A)

$$\rho^\dagger(q) = \sum_k c^\dagger_{k+q} c_k \tag{2.3}$$

If we can show that the density fluctuation of momentum q is a well-defined excitation, with a well-defined energy, it means that we can quantize it. Since it is made of a product of two fermion operators it is of bosonic nature. Thus, we have $\rho(q) \sim b_q$ or $\rho(q) \sim b_q^\dagger$ (or some linear combination). What makes

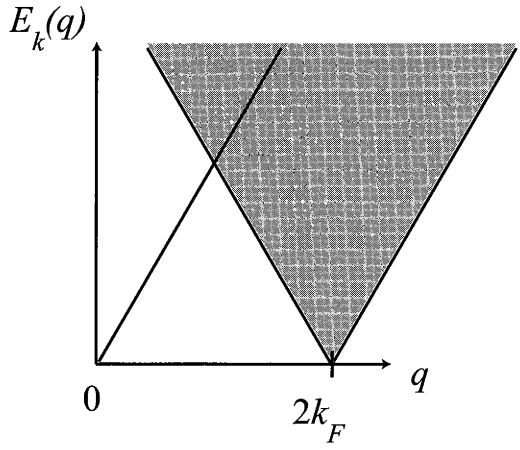

FIG. 2.2. Particle–hole excitation spectrum for the linearized model (2.1). For small q particle–hole excitations are sharp excitations with well defined energy and momentum.

interaction so difficult to treat is the fact that it is a product of four fermion operators and we do not know how to diagonalize such terms. However, in terms of the boson basis the interaction would simply become (A.23) (since in one dimension $\Omega = L$, I will use indifferently both notations in the following)

$$\begin{aligned} H_{\text{int}} &= \frac{1}{2\Omega}\sum_q V(q)\rho(q)\rho(-q) \\ &= \frac{1}{2\Omega}\sum_q V(q)(\cdots b_q + \cdots b_q^\dagger)^2 \end{aligned} \tag{2.4}$$

The interaction Hamiltonian thus remains *quadratic* in the boson basis and is thus trivial to diagonalize.

Let us now be more precise. Because we have introduced an infinite number of occupied states in (2.1) (see Fig. 2.1), one needs to be careful in defining the density operator to avoid infinities. To do so one introduces the normal ordering of a product of operators $:ABC:$. In a normal ordered product the destruction operators (with respect to a given vacuum) are put on the right and creation operators on the left. For two operators A and B that are linear combinations of creation and destruction operators it is easy to check that normal ordering the operators is equivalent to subtracting the average value in the vacuum (this is all we need to know about normal ordering)

$$:AB: = AB - \langle 0|AB|0\rangle \tag{2.5}$$

The normal ordered density, for example, is thus defined as

$$: \rho_r(x) := : \psi_r^\dagger(x)\psi_r(x) : \tag{2.6}$$

where I have used the notation $\psi_r^\dagger(x)$ for the operator creating a right ($r = R$) or left ($r = L$) moving particle at point x. The Fourier component $\rho_r^\dagger(p)$ of the density is defined by

$$: \rho_r(x) := \frac{1}{\Omega}\sum_p : \rho_r(p) : e^{ipx} \tag{2.7}$$

It is given by

$$\begin{aligned} : \rho_r^\dagger(p) : &= \sum_k c_{r,k+p}^\dagger c_{r,k}, \quad (p \neq 0) \\ &= N_r = \sum_k [c_{r,k}^\dagger c_{r,k} - \langle 0|c_{r,k}^\dagger c_{r,k}|0\rangle], \quad (p = 0) \end{aligned} \tag{2.8}$$

which defines the operator N_r. As usual $\rho^\dagger(p) = \rho(-p)$ since $\rho(x)$ is real. $|0\rangle$ is the ground state of (2.1). It is the Dirac sea where all the negative energy states are occupied. The subtraction of the average value (that is, the normal ordering) in (2.8) ensures that the matrix elements of the density operator are finite, despite the infinite number of occupied states.

Let us now look at the commutator of the density operators. It is obviously zero between two different species

$$[\rho_R^\dagger(p), \rho_L^\dagger(p')] = 0 \tag{2.9}$$

For identical species

$$\begin{aligned} [\rho_r^\dagger(p), \rho_r^\dagger(-p')] &= \sum_{k1,k2} [c_{r,k1+p}^\dagger c_{r,k1}, c_{r,k2-p'}^\dagger c_{r,k2}] \\ &= \sum_{k1,k2} (c_{r,k1+p}^\dagger c_{r,k2}\delta_{k1,k2-p'} - c_{r,k2-p'}^\dagger c_{r,k1}\delta_{k1+p,k2}) \\ &= \sum_{k2} (c_{r,k2+p-p'}^\dagger c_{r,k2} - c_{r,k2-p'}^\dagger c_{r,k2-p}) \end{aligned} \tag{2.10}$$

Naively one would just perform a change of variables in the second term of (2.10) and find that the commutator is zero. However, because of the infinite number of occupied states the bare density operators contain infinity and (2.10) is in fact the subtraction of two such infinities. One can only make a change of variable in the normal ordered densities

$$\begin{aligned} [\rho_r^\dagger(p), \rho_r^\dagger(-p')] &= \sum_{k2} (: c_{r,k2+p-p'}^\dagger c_{r,k2} : - : c_{r,k2-p'}^\dagger c_{r,k2-p} :) \\ &\quad + \sum_{k2} (\langle 0|c_{r,k2+p-p'}^\dagger c_{r,k2}|0\rangle - \langle 0|c_{r,k2-p'}^\dagger c_{r,k2-p}|0\rangle) \\ &= \sum_{k2} (\langle 0|c_{r,k2+p-p'}^\dagger c_{r,k2}|0\rangle - \langle 0|c_{r,k2-p'}^\dagger c_{r,k2-p}|0\rangle) \end{aligned} \tag{2.11}$$

since in the normal ordered products the change of variable can be performed safely (all matrix elements are finite). The last term is easily evaluated to give

$$[\rho_r^\dagger(p), \rho_r^\dagger(-p')] = \delta_{p,p'} \sum_{k2} (\langle 0|c_{r,k2}^\dagger c_{r,k2}|0\rangle - \langle 0|c_{r,k2-p}^\dagger c_{r,k2-p}|0\rangle) \quad (2.12)$$

The momentum k is quantized. Let us take, for example, periodic boundary conditions, then one has $k = 2\pi n/L$. $\langle 0|c_{r,k2}^\dagger c_{r,k2}|0\rangle = 1$ if the state is occupied and zero otherwise. This leads to

$$[\rho_r^\dagger(p), \rho_{r'}^\dagger(-p')] = -\delta_{r,r'}\delta_{p,p'} \frac{rpL}{2\pi} \quad (2.13)$$

The result (2.13) is crucial. It shows that because of the large (infinite in the model we considered) number of occupied states, the density operators have commutation relations similar, up to a normalization factor to *boson operators.* One thus recovers from this formal calculation the intuitive result that density fluctuations should behave as boson creation and destruction operators. Note that for the Luttinger model (2.1) this is an *exact* result. Since in addition

$$\begin{aligned} \rho_L^\dagger(p > 0)|0\rangle &= 0 \\ \rho_R^\dagger(p < 0)|0\rangle &= 0 \end{aligned} \quad (2.14)$$

these density operators can be identified with the destruction operators for bosons. This allows to define the boson creation and destruction operators as

$$\begin{aligned} b_p^\dagger &= \left(\frac{2\pi}{L|p|}\right)^{1/2} \sum_r Y(rp)\rho_r^\dagger(p) \\ b_p &= \left(\frac{2\pi}{L|p|}\right)^{1/2} \sum_r Y(rp)\rho_r^\dagger(-p) \end{aligned} \quad (2.15)$$

where Y is the step function (see Appendix A). Note the bosons operators are only defined for $p \neq 0$.

For these boson operators to be useful we need to show that all fermionic operators can be expressed in the new basis, and of course that this new basis is a complete one. Let us start with the Hamiltonian itself. One can again compute the commutator of the Hamiltonian with the boson operators using the fermionic (anti) commutation rules (let us assume, e.g. that $p_0 > 0$)

$$
\begin{aligned}
[b_{p_0}, H] &= \left(\frac{2\pi}{L|p_0|}\right)^{1/2} \sum_{r,k} [\rho_R^\dagger(-p_0), v_F(rk - k_F) c_{r,k}^\dagger c_{r,k}] \\
&= \left(\frac{2\pi}{L|p_0|}\right)^{1/2} \sum_{k,k_1} v_F(k - k_F)(c_{R,k_1-p_0}^\dagger c_{R,k} \delta_{k_1,k} - c_{R,k}^\dagger c_{R,k_1} \delta_{k_1-p_0,k}) \\
&= \left(\frac{2\pi}{L|p_0|}\right)^{1/2} \sum_{k} v_F p_0 c_{R,k-p_0}^\dagger c_{R,k} \\
&= v_F p_0 b_{p_0}
\end{aligned}
\tag{2.16}
$$

Similar results can be obtained with $p_0 < 0$ or by commuting with $b_{p_0}^\dagger$. If we assume for the moment that the basis generated by the operators b is complete, then the results (2.16) define completely the Hamiltonian in the boson basis. It is easy to check, from the boson commutation relations, that the operator that would satisfy the commutation rules (2.16) is

$$
H \simeq \sum_{p \neq 0} v_F |p| b_p^\dagger b_p \tag{2.17}
$$

This formula is quite remarkable. It shows that the kinetic energy, that is, normally *quadratic* in fermions operators, can also be expressed by (2.17), which is a *quartic* term in fermion operators. This formula is crucial to be able to use this boson representation, since it shows that contrary to the naive expectations the kinetic energy is *quadratic* in terms of the boson operators. Thus, adding the interaction will keep the Hamiltonian quadratic and thus allows to solve the problem in a remarkably simple way.

Single-particle creation operators can be determined by the same method. First, one should introduce an operator for each species of fermions. Let us call $\psi_R(x)$ (resp. $\psi_L(x)$) the operator destroying a right (resp. left) going fermion at point x. It satisfies

$$
\begin{aligned}
[\rho_r^\dagger(p), \psi_r(x)] &= \frac{1}{\sqrt{\Omega}} \sum_{k,k_1} e^{ik_1 x} [c_{r,k+p}^\dagger c_{r,k}, c_{r,k_1}] \\
&= -e^{ipx} \psi_r(x)
\end{aligned}
\tag{2.18}
$$

Thus, an operator written directly in terms of boson operators and that would produce the same commutation relations is

$$
\psi_r(x) \simeq e^{\sum_p e^{ipx} \rho_r^\dagger(-p) \left(\frac{2\pi r}{pL}\right)} \tag{2.19}
$$

Formulas (2.15), (2.17) and (2.19) would thus be a dictionary relating the fermionic representation to the bosonic one. This is a mere change of basis, although of course this change is highly non-trivial. The hope is that the new basis is better adapted to diagonalize the problem, as we already discussed. Since (2.19) gives

the single-particle operator, any fermionic operator can now be written in the boson language.

The above formulas are essentially physically correct and embed the right physics. Unfortunately, it is easy to see that (2.17) and (2.19) cannot be exact. $\psi_r(x)$ changes the total number of fermion of species r by one. On the other hand, b and $b^\dagger$ conserve the number of fermions of each species since they are simple density fluctuations (2.15). To reproduce all possible states of the original fermionic Fock space, it is thus necessary to introduce two additional operators (one for each species) that change the *total* number of fermions. Such operators are also known in the field theory language as 'Klein factors'. Let us thus introduce U_r such that U_r commutes with the boson operators and $U_r^\dagger$ adds one fermion of species r. A more correct expression for (2.19) would be

$$\psi_r(x) = U_r e^{\sum_p e^{ipx}\rho_r^\dagger(-p)\left(\frac{2\pi r}{pL}\right)} \tag{2.20}$$

In (2.20), the operator U_r suppresses a charge uniformly whereas the factors in the exponential ensure that the charge will be moved, that is, added at some points in space and removed at some others, to ensure that the charge is only destroyed at point x. So only the exponential is important to compute the space–time dependence of correlation functions. I will come back to this physical interpretation later. Introducing the operators U allows to make the mapping between the fermion basis and the boson one rigorous (Heidenreich *et al.*, 1980; Haldane, 1981*a*). Constructing the operators U_r and making the mapping rigorous is a little bit tedious and brings in the end little additional physics, beside the important fact that now one has an *exact* operator identity. So this construction as well as a proof that the bosonic space plus the operators U is a complete Hilbert space is given in Appendices B.1 and B.2.

Rather than to work directly in terms of the boson operators it is convenient to introduce the two fields $\phi(x)$ and $\theta(x)$ defined by

$$\phi(x), \theta(x) = \mp(N_R \pm N_L)\frac{\pi x}{L} \mp \frac{i\pi}{L}\sum_{p\neq 0}\frac{1}{p}e^{-\alpha|p|/2-ipx}(\rho_R^\dagger(p) \pm \rho_L^\dagger(p)) \tag{2.21}$$

where the upper signs are for ϕ. Using these fields (or the boson operators) the *exact* expressions for the Hamiltonian and the single-particle operator are

$$\begin{aligned} H &= \sum_{p\neq 0} v_F|p|b_p^\dagger b_p + \frac{\pi v_F}{L}\sum_r N_r^2 \\ \psi_r(x) &= U_r \lim_{\alpha\to 0}\frac{1}{\sqrt{2\pi\alpha}}e^{ir(k_F-\pi/L)x}e^{-i(r\phi(x)-\theta(x))} \end{aligned} \tag{2.22}$$

where compared to Appendix B.1 the cutoff is $\pi\alpha = \epsilon L$. The terms containing N can be viewed as the $p \to 0$ limit of the boson terms. One can get an intuitive feeling of this by expanding the e^{-ipx} in (2.21) and comparing with (2.8). α is an arbitrary cutoff that regularizes the theory and mimics a finite bandwidth since

it prevents the momentum from becoming too large (roughly the bandwidth is $\Lambda \sim 1/\alpha$). Using (2.15), (2.21) can be rewritten in terms of the bosons

$$\begin{aligned}\phi(x) &= -(N_R + N_L)\frac{\pi x}{L} - \frac{i\pi}{L}\sum_p \left(\frac{L|p|}{2\pi}\right)^{1/2} \frac{1}{p} e^{-\alpha|p|/2 - ipx}(b_p^\dagger + b_{-p}) \\ \theta(x) &= (N_R - N_L)\frac{\pi x}{L} + \frac{i\pi}{L}\sum_p \left(\frac{L|p|}{2\pi}\right)^{1/2} \frac{1}{|p|} e^{-\alpha|p|/2 - ipx}(b_p^\dagger - b_{-p})\end{aligned} \tag{2.23}$$

Strictly speaking, one should take the limit $\alpha \to 0$. However, as we will see, keeping α finite is a good way to artificially reintroduce a finite bandwidth in this model. The fields ϕ and θ satisfy simple commutation rules. Using the commutation rules for bosons one easily gets from (2.23)

$$\begin{aligned}[\phi(x_1), \theta(x_2)] &= \sum_{p\neq 0} \frac{\pi}{Lp} e^{ip(x_2 - x_1) - \alpha|p|} \\ &\to i\int_0^\infty \frac{dp}{p} \sin(p(x_2 - x_1)) e^{-\alpha|p|} \\ &= i\frac{\pi}{2}\mathrm{Sign}(x_2 - x_1)\end{aligned} \tag{2.24}$$

the last two lines being in the limit $L \to \infty$ and then $\alpha \to 0$. Similarly

$$\begin{aligned}[\phi(x_1), \nabla\theta(x_2)] &= i\int_0^\infty dp\ \cos(p(x_2 - x_1)) e^{-\alpha|p|} \\ &= i\pi\delta(x_2 - x_1)\end{aligned} \tag{2.25}$$

(2.25) shows that the conjugate momentum $\Pi(x)$ to the field $\phi(x)$ is simply given by

$$\Pi(x) = \frac{1}{\pi}\nabla\theta(x) \tag{2.26}$$

which gives using (2.23)

$$\Pi(x) = \frac{(N_R - N_L)}{L} + \frac{1}{L}\sum_{p\neq 0}\left(\frac{L|p|}{2\pi}\right)^{1/2} \mathrm{Sign}(p) e^{-\alpha|p|/2 - ipx}(b_p^\dagger - b_{-p}) \tag{2.27}$$

Using (2.21) one obtains (for $L \to \infty$)

$$\begin{aligned}\nabla\phi(x) &= -\pi[\rho_R(x) + \rho_L(x)] \\ \nabla\theta(x) &= \pi[\rho_R(x) - \rho_L(x)]\end{aligned} \tag{2.28}$$

$\nabla\phi$ is thus the $q \sim 0$ part of the density fluctuations at point x. $\nabla\theta(x)$ counts the difference between right and left goers and is thus simply the current operator in this one-dimensional world. I will come back in a more rigorous way on the

current in Section 7.2. Hamiltonian (2.22) can be rewritten in terms of these new fields

$$H = \frac{1}{2\pi} \int dx\, v_F[(\pi\Pi(x))^2 + (\nabla\phi(x))^2] \tag{2.29}$$

Since the operators N are normal ordered and thus have finite matrix elements, the corresponding terms vanish when one takes the limit $L \to \infty$, giving back essentially the naive formulas (2.15), (2.17), and (2.19). From now on I will often drop the parts that vanish in the thermodynamic limit $L \to \infty$ and consider only the boson part. Similarly, the single particle operator becomes after having dropped $1/L$ quantities

$$\psi_r(x) = e^{irk_F x}\tilde{\psi}_r(x) = \frac{U_r}{\sqrt{2\pi\alpha}} e^{irk_F x} e^{-i[r\phi(x)-\theta(x)]} \tag{2.30}$$

The field $\tilde{\psi}(x)$ varies slowly at the scale of k_F^{-1}, so all rapidly oscillating factors are in the $e^{ik_F x}$ term. This will be used in simplifying some expressions in the continuum limit. Once again in (2.30) the limit $\alpha \to 0$ should be taken in principle.

The fields ϕ and θ have simple physical interpretations that we will examine in detail in the next chapter. They also allow a nice field theory description as shown in Appendix C. The above formulas are the complete mapping between the bosons and the fermions. A summary of this mapping is given in Appendix D.

2.2 Physical properties and correlation functions

Since we have now a mapping between the fermions and the bosons we can look at the effect of the interactions. For the continuum model with right and left going fermions the allowed interactions are classified in Fig. 1.9. For those who skipped[13] the previous chapter let me briefly recall the idea. The interaction is of the form

$$H = \int dx\, V(x - x')\rho(x)\rho(x') \tag{2.31}$$

Because we have now left and right movers we have first to define what we call density. In fact, if we look back at the original fermionic operator we can write it as

$$\psi(x) = \frac{1}{\sqrt{\Omega}} \sum_k e^{ikx} c_k \tag{2.32}$$

If we confine ourselves close to the Fermi surface we can decompose the sum into momenta close to $+k_F$ and momenta close to $-k_F$:

$$\psi(x) \simeq \frac{1}{\sqrt{\Omega}} \left[\sum_{-\Lambda<k-k_F<\Lambda} e^{ikx} c_k + \sum_{-\Lambda<k+k_F<\Lambda} e^{ikx} c_k \right] \tag{2.33}$$

[13]Now might be a time to go back and have a look; after all this is a useful chapter too ...

where Λ is a momentum cutoff such that $v_F\Lambda$ is of the order of the bandwidth. In the continuum model, the first term would correspond to right movers only and the second one to left movers only (see Fig. 2.1). Thus, one has

$$\psi(x) = \psi_R(x) + \psi_L(x) \tag{2.34}$$

The density thus becomes

$$\psi^\dagger(x)\psi(x) = \psi_R^\dagger(x)\psi_R(x) + \psi_L^\dagger(x)\psi_L(x) + [\psi_R^\dagger(x)\psi_L(x) + \text{h.c.}] \tag{2.35}$$

In fermion language we can think of the density operator as

$$\rho(x) = \frac{1}{\Omega}\sum_{k,q} e^{-iqx} c_{k+q}^\dagger c_k \tag{2.36}$$

The first two terms in (2.35) correspond to the $q \sim 0$ part of the density, where particles are excited on the same side of the Fermi surface. The last two terms are the $q \sim \pm 2k_F$ excitations where a particle gets transferred from one side of the Fermi surface to the other (see Fig. 1.8). In the continuum model, these are the only two low-lying excitations (see Fig. 2.2). Using the expression for the density (2.35) for the continuum model one has different interaction processes depending on whether the incoming or outgoing fermions are right or left movers. These processes have been classified in Fig. 1.9. Since the density contains two fermion operators at the same point one has to take some care in some cases. This will be discussed in more details in Section 7.1.1.

For spinless fermions we have only to worry about g_4 and g_2 processes. The g_4 process can be written in the boson language as

$$\begin{aligned}\frac{g_4}{2}\psi_R^\dagger(x)\psi_R(x)\psi_R^\dagger(x)\psi_R(x) &= \frac{g_4}{2}\rho_R(x)\rho_R(x) \\ &= \frac{g_4}{2}\frac{1}{(2\pi)^2}(\nabla\phi - \nabla\theta)^2\end{aligned} \tag{2.37}$$

and a similar term for the left movers (with $R \to L$ and $\phi - \theta \to \phi + \theta$). The sum of the two processes leads for the g_4 interaction to

$$\frac{g_4}{(2\pi)^2}\int dx[(\nabla\phi)^2 + (\nabla\theta)^2] \tag{2.38}$$

When added to Hamiltonian (2.29) one sees that the g_4 process only renormalizes the velocity of excitations, which becomes

$$u = v_F\left(1 + \frac{g_4}{\pi v_F}\right) \tag{2.39}$$

In a similar way, the g_2 process becomes

$$\begin{aligned} g_2\psi_R^\dagger(x)\psi_R(x)\psi_L^\dagger(x)\psi_L(x) &= g_2\rho_R(x)\rho_L(x) \\ &= \frac{g_2}{(2\pi)^2}(\nabla\phi - \nabla\theta)(\nabla\phi + \nabla\theta) \\ &= \frac{g_2}{(2\pi)^2}[(\nabla\phi)^2 - (\nabla\theta)^2] \end{aligned} \tag{2.40}$$

Note that for the moment we consider q independent interaction processes, that is, a δ function interaction in real space. In fact, since we are interested in the low-energy properties of the system we can take the limit $g(q \to 0)$ if the interaction constants have a q dependence. As long as the limit $g(q \to 0)$ is finite the physics we describe asymptotically holds. Taking q dependent interaction is not much more complicated and will be examined in detail in Section 4.1 for long-range interactions.

Thus, we see that the Hamiltonian remains *quadratic* even in the presence of interactions. As discussed before this is one of the main interests of the bosonization method. Solving the interacting problem is not more complicated than obtaining the free Hamiltonian.[14] Contrary to the g_4 process that only modifies the velocity, the g_2 interaction changes the relative weights of the $\nabla\phi$ and $\nabla\theta$ terms in the Hamiltonian. The net effect can be absorbed in *two* parameters. If we rewrite the quadratic Hamiltonian as

$$H = \frac{1}{2\pi}\int dx[uK(\pi\Pi(x))^2 + \frac{u}{K}(\nabla\phi(x))^2] \tag{2.41}$$

where u has the dimensions of a velocity, and K is a dimensionless parameter. We thus have

$$\begin{aligned} uK &= v_F\left(1 + \frac{g_4}{2\pi v_F} - \frac{g_2}{2\pi v_F}\right) \\ \frac{u}{K} &= \left(1 + \frac{g_4}{2\pi v_F} + \frac{g_2}{2\pi v_F}\right)v_F \end{aligned} \tag{2.42}$$

which can be solved as

$$\begin{aligned} u &= v_F[(1 + y_4/2)^2 - (y_2/2)^2]^{1/2} \\ K &= \left(\frac{1 + y_4/2 - y_2/2}{1 + y_4/2 + y_2/2}\right)^{1/2} \end{aligned} \tag{2.43}$$

where $y = g/(\pi v_F)$ is a dimensionless coupling constant. Note that quite generally $K < 1$ for repulsive interactions ($y_2 > 0$) and $K > 1$ for attractive ones ($y_2 < 0$). Note the wonder of the thing: for spinless fermions we have effortlessly solved *any*[15] interacting one-dimensional Hamiltonian! The physics of such an interacting system is described by free bosonic excitations. Let us now examine the various consequences.

[14] Now you know why I like one-dimensional systems!

[15] Well, practically any. There are of course some (physically interesting) complications such as the presence of a lattice, which we will examine later.

2.2.1 *Thermodynamics*

The interacting system is still described by *free* bosons. This means that the spectrum is still of the form

$$\epsilon(p) = u|p| = u\frac{2\pi|n|}{L} \tag{2.44}$$

and this has some practical consequences that we will explore in more details in Section 3.4. The simplest physical quantity that can be computed from the energy is the specific heat

$$C_V = \frac{dE}{dT} = \frac{d}{dT}\sum_{p\neq 0}\epsilon(p) f_B(\epsilon(p)) \tag{2.45}$$

The only effect of the interaction is to change the energy from $\epsilon(p) = v_F|p|$ into $\epsilon(p) = u|p|$. The specific heat is thus

$$\begin{aligned} C_V &= \beta^2 \sum_{p\neq 0}\epsilon(p)^2 \frac{e^{\beta\epsilon(p)}}{(e^{\beta\epsilon(p)}-1)^2} \\ &= \frac{u^2}{4T^2}\sum_{p\neq 0}\frac{p^2}{\sinh^2(\beta up/2)} \\ &= \frac{u^2}{4T^2}\frac{L}{2\pi}\left[\frac{\pi^2 8}{3(\beta u)^3}\right] = \frac{T}{u}\left(\frac{L\pi}{3}\right) \end{aligned} \tag{2.46}$$

The specific heat can also be computed for the free fermion system. The energy of a fermionic system is

$$E = 2\sum_p \epsilon_p^F f_F(\epsilon_p^F) \tag{2.47}$$

where $\epsilon_p^F = v_F p$ is the energy of the free right moving fermions. The factor 2 in (2.47) comes from the sum over the right and left movers. Using (2.47) leads for the specific heat

$$\begin{aligned} C_V &= \frac{L}{\pi v_F}\beta^2 \int_{-\infty}^{+\infty} d\epsilon \frac{\epsilon^2}{4\cosh^2(\beta\epsilon/2)} \\ &= \frac{T}{v_F}\left(\frac{L\pi}{3}\right) \end{aligned} \tag{2.48}$$

This is exactly (for non-interacting fermions $u = v_F$) the same result as (2.46) obtained in the boson language. This is a strong indication that we have not

missed part of the Hilbert space in going from the fermion to the boson representation. Even in the presence of interactions the specific heat remains *linear* in temperature, but with a renormalization factor

$$C_V/C_V^0 = v_F/u \tag{2.49}$$

The compressibility of the system can be computed in a similar way. The usual compressibility measures the relative change of volume Ω with a change of pressure P

$$\kappa_{\text{true}} = -\frac{1}{\Omega}\frac{\partial\Omega}{\partial P} = \frac{1}{\rho^2}\frac{\partial\rho}{\partial\mu} \tag{2.50}$$

It is thus directly related to the change of density as a function of the chemical potential. In the rest of this book, I define the compressibility that way, that is,

$$\kappa = \frac{\partial\rho}{\partial\mu} \tag{2.51}$$

A uniform chemical potential adds a term in the Hamiltonian

$$-\mu\int dx\ \rho(x) \tag{2.52}$$

The density should be expressed in terms of the right and left going fermions using (2.35). The density contains two kind of terms. The terms

$$\psi_R^\dagger(x)\psi_R(x) + \psi_L^\dagger(x)\psi_L(x) = \tilde{\psi}_R^\dagger(x)\tilde{\psi}_R(x) + \tilde{\psi}_L^\dagger(x)\tilde{\psi}_L(x) \tag{2.53}$$

which contain only slowly varying fields. The k_F terms have completely disappeared. This contribution corresponds to the $q \sim 0$ terms in the original density operators. These terms thus survive the integration over x in (2.52). On the other hand, the terms of the form

$$\psi_R^\dagger(x)\psi_L(x) = e^{-2ik_F x}\tilde{\psi}_R^\dagger(x)\tilde{\psi}_L(x) \tag{2.54}$$

contain a rapidly (at a lengthscale of $\sim k_F^{-1}$) oscillating component, multiplied by slowly varying fields. These terms correspond to the $2k_F$ components of the original density operators. Upon integration, the oscillating factor makes the integral vanish. One can thus safely drop these terms in the continuum limit in (2.52). This procedure of keeping only slowly varying terms to get the relevant operators in the continuum limit will be used repeatedly. Using

$$\rho(x) = \rho_R(x) + \rho_L(x) = -\frac{1}{\pi}\nabla\phi(x) \tag{2.55}$$

the density is simply given by

$$\frac{1}{L}\int dx\langle\rho(x)\rangle = \langle\rho_R(x_0) + \rho_L(x_0)\rangle = -\frac{1}{\pi}\langle\nabla\phi(x_0)\rangle \tag{2.56}$$

since the oscillating terms in the density vanish and the average is independent of the point x_0. Equation (2.52) becomes in boson representation

$$\frac{\mu}{\pi}\int dx\ \nabla\phi(x) \tag{2.57}$$

One can absorb this term in the Hamiltonian (2.41) by shifting the field ϕ

$$\tilde{\phi}(x) = \phi + \mu\frac{K}{u}x \tag{2.58}$$

The compressibility is thus

$$\kappa = \frac{d\langle\rho(x_0)\rangle}{d\mu} = \frac{-1}{\pi}\frac{d\langle\nabla\phi(x_0)\rangle}{d\mu} = \frac{K}{u\pi} \tag{2.59}$$

since the average of $\nabla\tilde{\phi}$ is zero. The parameter u/K is thus directly related to the *exact* compressibility of the system. We will see in Chapter 5 how to turn this trick into a very efficient method to compute these parameters. Compared to the compressibility of a free electron gas κ_0, it is renormalized by

$$\kappa/\kappa_0 = v_F\frac{K}{u} \tag{2.60}$$

Another way to get the compressibility is to compute the density–density correlation function (the linear response is exact for a quadratic Hamiltonian). It is given by (see Appendix C)

$$\langle\delta\rho(k,\omega_n)\delta\rho(-k,-\omega_n)\rangle = \frac{k^2}{\pi^2}\langle\phi(k,\omega_n)\phi(-k,-\omega_n)\rangle = \frac{k^2K}{\pi(\omega_n^2/u + uk^2)} \tag{2.61}$$

The compressibility is given by taking first $\omega_n = 0$ (static chemical potential to get a thermodynamic response) and then $k \to 0$ (uniform potential) in the above expression. This of course leads back to the value (2.59).

The thermodynamic quantities thus look very much like those of a Fermi liquid. Except for a renormalization of the coefficients, the interactions still leave a specific heat linear in T and a constant compressibility. If we want to see 'real' effects of the interactions we will have to look at the $2k_F$ part of the correlation functions. This can be guessed from the perturbative analysis of Chapter 1 that showed singularities for these correlation functions.

2.2.2 *Correlations*

Let us start with the density–density correlation function. Using the continuum expression (2.35) the density can be rewritten in terms of the bosons

$$\rho(r) = -\frac{1}{\pi}\nabla\phi(r) + \frac{1}{2\pi\alpha}[e^{i2k_Fx}e^{-i2\phi(r)} + \text{h.c.}] \tag{2.62}$$

The density–density correlation thus becomes in real space:

$$\langle\rho(r)\rho(0)\rangle = \frac{1}{\pi^2}\langle\nabla\phi(r)\nabla\phi(0)\rangle + \frac{1}{(2\pi\alpha)^2}[e^{-i2k_F x}\langle e^{i(2\phi(r)-2\phi(0))}\rangle + \text{h.c.}] \quad (2.63)$$

where $r = (x, u\tau)$ (see Appendix A). The average $\langle\cdots\rangle$ of any operator is to be understood from now on as the (imaginary) time-ordered average. Other correlation functions (retarded, etc.) will be written explicitly (see Appendix A). Compared with (2.30), I have dropped the operators U. As we discussed before, they do not contain any space and time dependence and thus cannot contribute to the correlation functions. However, since they are fermion operators and thus anticommute they can lead to *global* minus signs. This complication can be important for some correlation functions and I will come back to that point in Section 4.3.2. The various correlations are evaluated in Appendix C. They give

$$\begin{aligned}\langle[\phi(r)-\phi(0)]^2\rangle &= KF_1(r)\\ \langle[\theta(r)-\theta(0)]^2\rangle &= K^{-1}F_1(r)\\ \langle[\phi(r)\theta(0)]\rangle &= \frac{1}{2}F_2(r)\end{aligned} \quad (2.64)$$

where for $T = 0$ (see Appendix C)

$$\begin{aligned}F_1(r) &= \frac{1}{2}\log\left[\frac{x^2+(u|\tau|+\alpha)^2}{\alpha^2}\right]\\ F_2(r) &= -i\ \mathrm{Arg}(y_\alpha + ix)\end{aligned} \quad (2.65)$$

where $y_\alpha = u\tau + \alpha\ \mathrm{Sign}(\tau)$, and Arg is the argument of the complex number $y_\alpha + ix$ (see Appendix C). The argument function Arg has a cut on the negative real axis (that is, for $a < 0$, $\mathrm{Arg}(a \pm i\epsilon) = \pm\pi$). For example, for $x > 0$ and $\tau > 0$

$$F_2(r) = -i\ \arctan\left(\frac{x}{u\tau+\alpha}\right) \quad (2.66)$$

In addition, for a quadratic Hamiltonian one has for any number A_j and B_j

$$\left\langle e^{i\sum_j(A_j\phi(r_j)+B_j\theta(r_j))}\right\rangle = e^{-\frac{1}{2}\left\langle\left(\sum_j A_j\phi(r_j)+B_j\theta(r_j)\right)^2\right\rangle} \quad (2.67)$$

This identity is easy to prove using the functional integral (see Appendix C). It can also be proven directly (but more lengthly) by replacing the ϕ and θ by their expressions in terms of the bosons b and $b^\dagger$ and using the quadratic form of the Hamiltonian (see, e.g. Emery 1979). This allows to compute all correlation functions. This is explained in detail in Appendix C using functional integral and in the next chapter using the operator representation. I thus just give the results here.

The density–density correlation function is (for $r \gg \alpha$)

$$R_0(r) = \langle \rho(r)\rho(0)\rangle = \frac{K}{2\pi^2}\frac{y_\alpha^2 - x^2}{(x^2+y_\alpha^2)^2} + \frac{2}{(2\pi\alpha)^2}\cos(2k_F x)\left(\frac{\alpha}{r}\right)^{2K} \tag{2.68}$$

Note that the action (see (C.17)) corresponding to (2.41) is Lorentz invariant (forgetting the cutoff), thus in correlation functions that contain only ϕ or θ, only the combination $\sqrt{x^2+(u\tau)^2}$ appears (see (2.64)). The $q \sim 0$ part of the correlation is again Fermi liquid like. It decays, just as a free fermion correlation would do, as $1/x^2$. Only the amplitude is renormalized by the interactions. The Fourier transform of this part would give back the compressibility. The $2k_F x$ part, however, is highly unusual. It behaves as a *non-universal* power law, with an exponent dependent on the interactions. Such a behavior is drastically different from the one of a Fermi liquid where the decay of the $2k_F x$ part should have remained $1/r^2$. Technically, this power law is the resummation of the logarithmic singularities that were already manifest at the lowest order in the perturbation theory, as we discussed in the previous chapter. The competition between the particle–particle and particle–hole channel prevents the correlation to have a singularity at a finite energy scale. This would mean a finite temperature phase transition, which is impossible in one dimension. Instead, these two instabilities compete to give a critical like (power law) behavior of the correlation functions at zero temperatures. The one-dimensional electron gas is thus always at the verge of an instability without being able to order. A system with these correlations is referred to as a Luttinger liquid.

Note that in the above expressions we have kept α finite. Strictly speaking, one should take the limit $\alpha \to 0$ to recover the original fermionic model. It is clear that letting $\alpha \to 0$ would lead to divergences. This is due to the fact that in our model, where we have taken a point like interaction, there is no other scale that can play the role of a lattice spacing (that is, of an ultraviolet cutoff). Let us see what happens if we have an interaction of finite range ξ. We can take for the interaction $g(x-x') = ge^{-(x-x')^2/\xi^2}$ or any rapidly decaying correlation function. In momentum space this gives a p dependent interaction

$$\frac{1}{\Omega}\sum_p g(p)\rho_R(p)\rho_L(-p) \tag{2.69}$$

for the g_2 process (let us forget the g_4 process for this example). One gets the same correlation functions than before, with a p dependent K and u as can be seen from (2.43). Let me take for simplicity $K(p) = K(p=0)$ if $p < 1/\xi$ and $K(p) = 1$ otherwise. This leads to the correlation (see Appendix C)

$$\frac{1}{(2\pi\alpha)^2}\langle e^{i2\phi(x)}e^{-i2\phi(0)}\rangle = \frac{1}{(2\pi\alpha)^2}e^{-2\int_0^\infty \frac{dp}{p}\, e^{-\alpha|p|}(1-\cos(px))K(p)} \tag{2.70}$$

we can crudely estimate the role of the cutoff α in the integral by cutting the integration at $1/\alpha$. In addition, if x is large we can consider that terms containing

$\cos(px)$ are negligible for $p > 1/\xi$ because such terms oscillate rapidly. This gives for the correlation function

$$\begin{aligned}\frac{1}{(2\pi\alpha)^2}\langle e^{i2\phi(r)}e^{-i2\phi(0)}\rangle &= \frac{1}{(2\pi\alpha)^2}e^{-2\int_0^{1/\alpha}\frac{dp}{p}(1-\cos(px))K(p)}\\ &\simeq \frac{1}{(2\pi\alpha)^2}e^{-2\int_0^{1/\xi}\frac{dp}{p}(1-\cos(px))K(p=0)-2\log(\xi/\alpha)}\\ &= \frac{1}{(2\pi\xi)^2}e^{-2\int_0^{1/\xi}\frac{dp}{p}(1-\cos(px))K(p=0)}\\ &= \frac{1}{(2\pi\xi)^2}e^{-2K(p=0)\log(x/\xi)} \qquad (2.71)\end{aligned}$$

We see that if we have an interaction of finite range ξ we can safely take the limit $\alpha \to 0$ and still have finite correlation functions (Haldane, 1981*a*). The interaction range replaces the cutoff in the final expressions. It is natural that in our continuum model were there is no natural lengthscale associated with a lattice spacing (or alternatively a bandwidth) one needs some parameter with the dimension of a length to play this role. Since the range of the interaction merely replaces the original cutoff α in the final expressions, it is in fact much simpler to let the range of the interaction go to zero, thereby taking an expression for the interaction that is rigorously q independent and keep α fixed of the order of the lattice spacing of the original model. This is the procedure that I will follow from now on.

Other correlations can be easily obtained from the boson representation. The operator

$$O_{\mathrm{SU}}(r) = \psi^\dagger(r)\psi^\dagger(r+a) \qquad (2.72)$$

describes the tendency to pairing. One should create the two fermions on neighboring sites since for spinless fermions the Pauli principle prevents from creating the two fermions on the same site. In the continuum limit this becomes

$$O_{\mathrm{SU}}(r) = \psi_R^\dagger(r)\psi_R^\dagger(r+a)+\psi_L^\dagger(r)\psi_L^\dagger(r+a)+[\psi_R^\dagger(r)\psi_L^\dagger(r+a)+\psi_L^\dagger(r)\psi_R^\dagger(r+a)] \qquad (2.73)$$

One can easily see that in the limit $a \to 0$ the first two terms will be strongly suppressed by the Pauli principle. One can expect the dominant contribution to come from the last two terms. They can be written

$$\begin{aligned}&[\psi_R^\dagger(r)\psi_L^\dagger(r+a)+\psi_L^\dagger(r)\psi_R^\dagger(r+a)]\\ &\quad= \tilde{\psi}_R^\dagger(r)\tilde{\psi}_L^\dagger(r+a)e^{ik_Fa}-\tilde{\psi}_R^\dagger(r+a)\tilde{\psi}_L^\dagger(r)e^{-ik_Fa}\\ &\quad= \tilde{\psi}_R^\dagger(r)\tilde{\psi}_L^\dagger(r)2i\ \sin(k_Fa) \qquad (2.74)\end{aligned}$$

since the $\tilde{\psi}$ are slowly varying at the scale of the lattice. The pairing is thus essentially given by the correlation

$$\tilde{\psi}_R^\dagger(r)\tilde{\psi}_L^\dagger(r) \qquad (2.75)$$

Note that this corresponds indeed to a pair with zero total momentum. Performing the same operation with the two first terms in (2.73), one can approximate the pairing operator by

$$O_{\mathrm{SU}}(r) \to \frac{2}{2\pi\alpha}[e^{-i2\theta(r)}\cos(2\phi(r) - 2k_F x) + e^{-i2\theta(r)}] \tag{2.76}$$

The last term in the above formula corresponds to (2.75). Since each correlation of an exponential of a field leads to a power law decay, the first term that piles up more operators decays faster as a function of distance or time, in agreement with our intuitive argument. Thus, the superconducting correlation functions are dominated by $\psi_R^\dagger(r)\psi_L^\dagger(r)$ leading to

$$O_{\mathrm{SU}}(r) \simeq \frac{e^{-i2\theta(r)}}{\pi\alpha} \tag{2.77}$$

This gives the decay for superconducting correlations

$$R_{\mathrm{SU}}(r) = \langle O_{\mathrm{SU}}(r) O_{\mathrm{SU}}^\dagger(0)\rangle = \frac{1}{(\pi\alpha)^2}\left(\frac{\alpha}{r}\right)^{1/(2K)} \tag{2.78}$$

Note that the superconducting correlations are also decaying very slowly, as a power law with a non-universal exponent. The tendency of the system to have superconducting fluctuations is stronger when the decay of the correlation function is slower, that is, if K is larger. This is logical since it corresponds to more attractive interactions. On the other hand, if K decreases, superconductivity decays faster, but the charge fluctuations (2.68) decay more slowly.

From the various correlations $R(r)$ we can define the susceptibilities

$$\chi(k,\omega_n) = \int_0^\beta d\tau \int dx\, R(x,\tau) e^{-ikx + i\omega_n \tau} \tag{2.79}$$

The analytical continuation of χ, $\chi(k, i\omega_n \to \omega + i\delta)$ gives the dynamical susceptibilities of the system (see Appendix A). We will see how to compute them later but let us first look at a simple scaling analysis. If R decays as a power law $R(r) \sim e^{i2k_F x}(1/r)^\nu$ then by simple scaling analysis, for $\beta = \infty$

$$\chi(k,\omega_n) \sim \max[\delta k, \omega_n]^{\nu-2} \tag{2.80}$$

where $k = 2k_F + \delta k$ for density correlations and $k = \delta k$ for superconducting ones. In a similar way at finite temperature the integral is cut at β. One has thus in a crude approximation

$$\chi(k,\omega,\beta) \sim \max[\delta k, \omega, T]^{\nu-2} \tag{2.81}$$

This is a crude approximation but essentially correct as a more detailed calculation will prove. Moreover, since the analytical continuation of a power law is

again a power law with the same exponent (except if the exponent is an integer), one can essentially replace ω_n by ω to get the retarded functions. This is a great advantage of one dimension. Because most of the things are power laws most results can be obtained by simple scaling analysis. Depending on the exponent ν the susceptibilities can thus be divergent. Such a divergent susceptibility indicates that any coupling to the corresponding operator, however weak, would induce a finite response. Such a weak coupling could, for example, be provided by the presence of other one-dimensional chains forming a three-dimensional network. We will see such examples in Section 6.4. A divergent susceptibility indicates the state that the system would like to order into, if it were not prevented by its one-dimensional nature. One can thus use the susceptibilities to build a sort of 'phase diagram' for the system. Here phase diagram means that we determine the most divergent fluctuation of the one-dimensional system, that is, the one most likely to be stabilized by a very weak three-dimensional coupling. Equation (2.81) shows that the susceptibility diverges for $\nu < 2$. For the density–density correlation (2.68) shows that this occurs for $K < 1$, that is, for repulsive interactions. The corresponding ordered state would be a periodic modulation of the charge of wavevector $2k_F$. If ϕ would take a classical value the expression of the density would be

$$\rho(x) = \frac{1}{(\pi\alpha)} \cos(2k_F x - 2\phi) \tag{2.82}$$

ϕ would just be the phase of the charge modulation. This periodic modulation of charge is called a charge density wave. We thus see that the one-dimensional electron gas has a tendency towards this kind of order, with a divergent susceptibility for repulsive interactions $K < 1$. We can thus view the one-dimensional electron gas as a charge density wave whose perfect order (ϕ is a constant) is destroyed by the quantum fluctuation. I will come back to these analogies in Section 3.3. Alternatively, when the interactions are attractive ($K > 1$), the system has a divergent susceptibility towards pair ordering. The superconducting phase θ would like to acquire a constant value. The fact that, when the superconducting phase likes to order, density fluctuations increase is a consequence of the standard duality between superconducting phase and charge. This is embedded in the commutations relations between the fields ϕ and θ. This allows to draw the phase diagram of Fig. 2.3 for a generic spinless interacting system.

Finally, one function of great interest is of course the single-particle Green's function. Its calculation is performed in Appendix C. For right movers it is given by

$$\begin{aligned} G_R(r) &= -\langle \psi_R(r)\psi_R^\dagger(0)\rangle \\ &= -\frac{e^{ik_F x}}{2\pi\alpha}\langle e^{i(\phi(r)-\theta(r))}e^{-i(\phi(0)-\theta(0))}\rangle \\ &= -\frac{e^{ik_F x}}{2\pi\alpha}e^{-[\frac{K+K^{-1}}{2}F_1(r)+F_2(r)]} \end{aligned} \tag{2.83}$$

which is again a power law. For $K = 1$, (2.83) gives

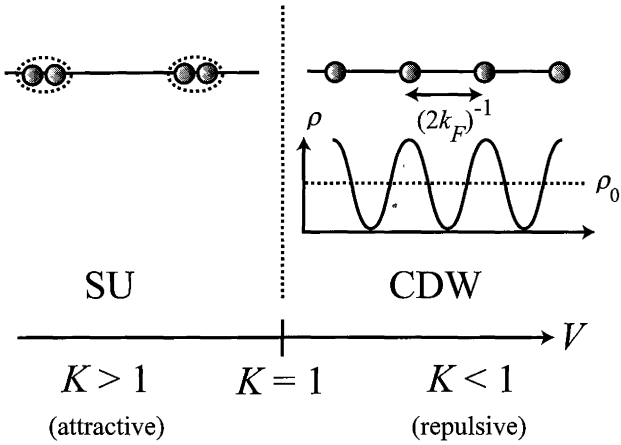

FIG. 2.3. Generic phase diagram for an interacting one-dimensional spinless system. V is the interaction. The system has either CDW diverging fluctuations ($K < 1$) or diverging superconducting fluctuations ($K > 1$).

$$\begin{aligned} G_R(r) &= -\frac{e^{ik_F x}}{2\pi\alpha} e^{-\log[(y_\alpha - ix)/\alpha]} \\ &= \frac{-ie^{ik_F x}}{2\pi} \frac{1}{x + i(v_F\tau + \alpha\,\mathrm{Sign}(\tau))} \end{aligned} \tag{2.84}$$

As expected this expression is *identical* to the one calculated directly in the fermion language. Note that if one comes back to the real time by performing the Wick rotation (Negele and Orland, 1988) $\tau = it + \epsilon\ \mathrm{Sign}(t)$ to go back to real time, the denominator has a zero for $x - v_F t = 0$, which is to be expected for particles moving with the velocity v_F. Note also that contrary to the density and superconducting correlations, the single-particle one depends on the angle between the space and time direction. Equation (2.83) shows that for an interacting system $G_R(r)$ is not a *universal* power law any more but decays with an exponent depending on the interaction. Note that this exponent is always greater than one regardless of the sign of the interaction. The decay of the single-particle Green's function is always *faster* than for a free fermion system. This shows that single-particle excitations are not welcome in the one-dimensional world but are converted into something else, again in agreement with our qualitative arguments.

The occupation factor $n(k)$ is simply the Fourier transform of the equal time Green's function (see Appendix A)

$$\begin{aligned} n(k) &= \int dx\, e^{-ikx} G_R(x, \tau = 0^-) \\ &= \int dx\, e^{i(k_F - k)x} \frac{-1}{2\pi\alpha} e^{-[\frac{K+K^{-1}}{2} F_1(x,\tau=0^-) + F_2(x,\tau=0^-)]} \end{aligned} \tag{2.85}$$

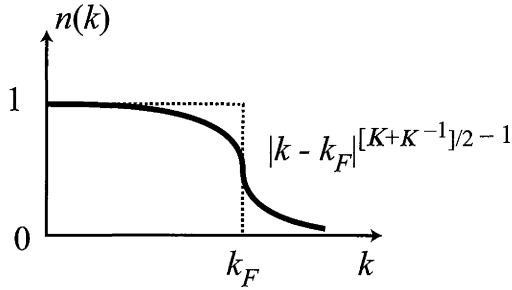

FIG. 2.4. The occupation factor $n(k)$. Instead of the usual discontinuity at k_F for a Fermi liquid, it has a power law essential singularity. This is the signature that fermionic quasiparticles do not exist in one dimension. Note that the position of the singularity is still at k_F. This is a consequence of Luttinger's theorem.

At $T = 0$ this gives

$$n(k) = \int dx\, e^{i(k_F - k)x} \frac{-1}{2\pi\alpha} \left(\frac{\alpha}{\sqrt{x^2 + \alpha^2}} \right)^{\frac{K+K^{-1}}{2}} e^{i\,\mathrm{Arg}(-\alpha + ix)} \tag{2.86}$$

Although a more precise calculation is possible along the lines explained in Appendix C as we will see in Chapter 7, the integral can again be easily determined by simple dimensional analysis. It is the Fourier transform of a power law and thus

$$n(k) \propto |k - k_F|^{\frac{K+K^{-1}}{2} - 1} \tag{2.87}$$

The occupation factor is shown in Fig. 2.4. Instead of the discontinuity at k_F that signals in a Fermi liquid that fermionic quasiparticles are sharp excitations (compare with Fig. 1.1), one finds in one dimension an essential power law singularity. Formally, this corresponds to $Z = 0$. This is the signature that individual fermionic excitations cannot survive in one dimension. As we already discussed, they are converted into collective ones. As a result, the decay of a single-particle Green's function is always *faster* than in a free electron gas. Note that the position of the singularity is still at k_F. This is a consequence of Luttinger's theorem. In a similar way one can define the single-particle 'density of states' (e.g. for right movers) as

$$n_R(\epsilon) = \frac{-1}{\pi} \int dt\, e^{i\epsilon t}\, \mathrm{Im}\, G_R^{\mathrm{ret}}(x = 0, t) = \frac{1}{\Omega} \sum_k A(k, \epsilon) \tag{2.88}$$

which coincides with the single-particle density of states for free fermions. We will make a more complete calculation in Chapter 7, but let us confine ourselves

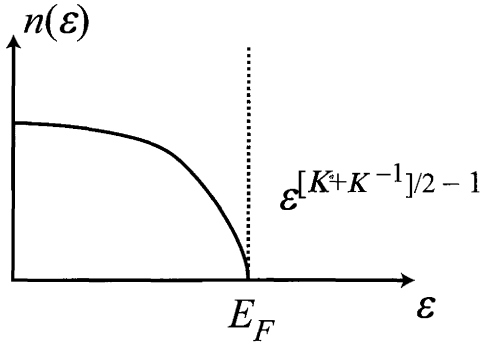

FIG. 2.5. Density of states in one dimension. It goes to zero as a power law, which shows that single-particle fermionic excitations do not survive in an interacting one-dimensional system but decompose in different (collective) objects.

again to simple scaling arguments. The Green function in imaginary time scales as

$$G(x=0,\omega_n) \sim (i\omega_n)^{\nu-1} \tag{2.89}$$

and the analytic continuation of a power law is a power law both for the real and imaginary parts since

$$z^\mu = e^{\mu \log(z)} \tag{2.90}$$

thus ($\mu = \nu - 1$)

$$G(\omega + i\delta) = e^{\mu[\log(\omega)+i\pi]} = e^{i\pi\mu}\omega^\mu \tag{2.91}$$

provided $\omega < 0$. Thus, unless μ is an integer both real and imaginary parts behave as ω^μ for negative frequencies. Thus, the density of states is

$$n(\epsilon) \propto \epsilon^{\frac{1}{2}[K+K^{-1}]-1} \tag{2.92}$$

The single-particle density of states thus *vanishes* at the Fermi level ($\epsilon = 0$) as shown in Fig. 2.5. As we will see in Chapter 7.2, the system remains perfectly metallic. This pseudogap in the density of state thus does not signal that no state is available close to the Fermi level. It signals that these states do not resemble single-particle excitations. We recover what we intuitively determined in Section 1.2, namely that single-particle excitations do not exist in an interacting one-dimensional system and are converted into collective excitations.

2.3 Model with spin; charge and spin excitations

Let us now turn to a system with spin. One can of course use the boson representation for each spin species separately and introduce the two sets of fields $(\phi_\uparrow, \theta_\uparrow)$ and $(\phi_\downarrow, \theta_\downarrow)$. In order to ensure the proper anticommutation relations

between the fermion fields Klein factors $U_\uparrow$ and $U_\downarrow$ should also be introduced for each spin species. The kinetic energy is obviously

$$H_{\text{kin}} = H^0_\uparrow + H^0_\downarrow \tag{2.93}$$

where H^0 is the quadratic Hamiltonian (2.29). The interaction is now given by all the processes of Fig. 1.9. g_4 processes are of the form

$$H_4 = \int dx \sum_{r=R,L} \sum_{\sigma=\uparrow,\downarrow} \left[\frac{g_{4\parallel}}{2}\rho_{r,\sigma}(x)\rho_{r,\sigma}(x) + \frac{g_{4\perp}}{2}\rho_{r,\sigma}(x)\rho_{r,-\sigma}(x)\right] \tag{2.94}$$

and g_2 terms are

$$H_2 = \int dx \sum_{\sigma=\uparrow,\downarrow} \left[g_{2\parallel}\rho_{R,\sigma}(x)\rho_{L,\sigma}(x) + g_{2\perp}\rho_{R,\sigma}(x)\rho_{L,-\sigma}(x)\right] \tag{2.95}$$

Obviously, these interactions introduce terms such as $\nabla\phi_\uparrow\nabla\phi_\uparrow$ and $\nabla\phi_\uparrow\nabla\phi_\downarrow$ and similar terms with θ. In the presence of the sole g_4 and g_2 processes the Hamiltonian thus remains quadratic in the fields ϕ and θ but is not diagonal any more in the spin index. This is normal since the interaction *a priori* couples the spin $\uparrow$ with the spin $\downarrow$. To diagonalize this quadratic Hamiltonian is it convenient to introduce the total charge and spin degrees of freedom defined as

$$\begin{aligned} \rho(x) &= \frac{1}{\sqrt{2}}[\rho_\uparrow(x) + \rho_\downarrow(x)] \\ \sigma(x) &= \frac{1}{\sqrt{2}}[\rho_\uparrow(x) - \rho_\downarrow(x)] \end{aligned} \tag{2.96}$$

This is a unitary transformation for the bosons and allows to introduce the new boson fields

$$\begin{aligned} \phi_\rho(x) &= \frac{1}{\sqrt{2}}[\phi_\uparrow(x) + \phi_\downarrow(x)] \\ \phi_\sigma(x) &= \frac{1}{\sqrt{2}}[\phi_\uparrow(x) - \phi_\downarrow(x)] \end{aligned} \tag{2.97}$$

and a similar relation for the θ fields. The ρ and σ fields commute whereas (ϕ_ρ, θ_ρ) and $(\phi_\sigma, \theta_\sigma)$ obey the standard commutation relations. The operators can easily be expressed in terms of these fields. For example, using (2.30) the single-particle fermion operator is

$$\psi_{r,\sigma}(x) = \frac{1}{\sqrt{2\pi\alpha}} U_{r,\sigma} e^{irk_F x} e^{-\frac{i}{\sqrt{2}}[r\phi_\rho(x) - \theta_\rho(x) + \sigma(r\phi_\sigma(x) - \theta_\sigma(x))]} \tag{2.98}$$

Other formulas are given in Appendix D. Substituting (2.97) in (2.93) gives for the kinetic energy

$$H_{\text{kin}} = H^0_\rho + H^0_\sigma \tag{2.99}$$

where H^0 is the quadratic Hamiltonian (2.29). The interaction Hamiltonian with g_4 processes is simply

$$H_4 = \frac{1}{4\pi^2}\int dx[g_{4\|} + g_{4\perp}][(\nabla\phi_\rho(x))^2 + (\nabla\theta_\rho(x))^2] + [g_{4\|} - g_{4\perp}][(\nabla\phi_\sigma(x))^2 + (\nabla\theta_\sigma(x))^2] \quad (2.100)$$

In a similar way, the g_2 process leads to

$$H_2 = \frac{1}{4\pi^2}\int dx[g_{2\|} + g_{2\perp}][(\nabla\phi_\rho(x))^2 - (\nabla\theta_\rho(x))^2] + [g_{2\|} - g_{2\perp}][(\nabla\phi_\sigma(x))^2 - (\nabla\theta_\sigma(x))^2] \quad (2.101)$$

The g_1 process needs a little bit more care. $g_{1\|}$ is identical to a $g_{2\|}$ by permuting two of the operators but the $g_{1\perp}$ will be different. In fermion language one has (using the standard anticommutation rules for fermions and the dictionary of Appendix D)

$$\begin{aligned} H_1 &= \int dx\, g_{1\|}\sum_\sigma[\psi^\dagger_{L,\sigma}\psi^\dagger_{R,\sigma}\psi_{L,\sigma}\psi_{R,\sigma}] + g_{1\perp}\sum_\sigma[\psi^\dagger_{L,\sigma}\psi^\dagger_{R,-\sigma}\psi_{L,-\sigma}\psi_{R,\sigma}] \\ &= \int dx(-g_{1\|})\sum_\sigma[\psi^\dagger_{L,\sigma}\psi_{L,\sigma}\psi^\dagger_{R,\sigma}\psi_{R,\sigma}] + g_{1\perp}\sum_\sigma[\psi^\dagger_{L,\sigma}\psi_{R,\sigma}\psi^\dagger_{R,-\sigma}\psi_{L,-\sigma}] \\ &= \int dx(-g_{1\|})\sum_\sigma[\rho_{L,\sigma}\rho_{R,\sigma}] + \frac{g_{1\perp}}{(2\pi\alpha)^2}\sum_{s=\uparrow,\downarrow}[e^{i(-2\phi_s(x))}e^{i(2\phi_{-s}(x))}] \end{aligned} \quad (2.102)$$

So we recover explicitly that $g_{1\|}$ is identical to a $g_{2\|}$ process but with a minus sign. One can thus simply replace in (2.101) $g_{2\|} \to g_{2\|} - g_{1\|}$. The $g_{1\perp}$ term can be bosonized using (2.97)

$$\begin{aligned} H_{1\perp} &= \int dx\frac{g_{1\perp}}{(2\pi\alpha)^2}\sum_{s=\uparrow,\downarrow}[e^{i(-2\phi_s(x))}e^{i(2\phi_{-s}(x))}] \\ &= \int dx\frac{2g_{1\perp}}{(2\pi\alpha)^2}\cos(2\sqrt{2}\phi_\sigma(x)) \end{aligned} \quad (2.103)$$

Putting all the interactions together one obtains a remarkable result. The interacting Hamiltonian of a generic interacting one-dimensional system *separates* into a charge Hamiltonian and a spin one

$$H = H_\rho + H_\sigma \quad (2.104)$$

The charge part is purely quadratic of the form (2.41) but with the coefficients u_ρ and K_ρ given by setting $\nu = \rho$ in the following formula:

$$
\begin{aligned}
u_\nu &= v_F \left[(1+y_{4\nu}/2)^2 - (y_\nu/2)^2\right]^{1/2} \\
K_\nu &= \left[\frac{1+y_{4\nu}/2+y_\nu/2}{1+y_{4\nu}/2-y_\nu/2}\right]^{1/2} \\
g_\nu &= g_{1\parallel} - g_{2\parallel} \mp g_{2\perp} \\
g_{4\nu} &= g_{4\parallel} \pm g_{4\perp} \\
y_\nu &= g_\nu/(\pi v_F)
\end{aligned}
\tag{2.105}
$$

(where the upper sign refers to ρ and the lower one to σ). The spin part is of the form

$$
H = H_\sigma^0 + \frac{2g_{1\perp}}{(2\pi\alpha)^2}\int dx\ \cos(2\sqrt{2}\phi_\sigma) \tag{2.106}
$$

where H_σ^0 is quadratic of the form (2.41) with the coefficients u_σ and K_σ given by (2.105). The result (2.104) shows that there is complete separation between the charge and the spin degrees of freedom. The full Hilbert space can be completely represented as a product of charge excitations and spin excitations. This is known as spin-charge separation and of course precludes any kind of single-particle excitations (which would carry both charge and spin) to exist. The physical interpretation of this spin-charge separation will be examined in more details in Section 3.1.

2.3.1 *Physical observables*

With (2.104) many properties of the system can easily be extracted. The compressibility of the system is the response to

$$
H = -\mu\int dx[\rho_\uparrow(x)+\rho_\downarrow(x)] = \frac{\mu\sqrt{2}}{\pi}\int dx\ \nabla\phi_\rho(x) \tag{2.107}
$$

In a similar way than (2.59) the compressibility is given by

$$
\kappa_\rho = \frac{2K_\rho}{\pi u_\rho} \tag{2.108}
$$

As can be expected it depends only on the charge sector. The uniform magnetic susceptibility is the response to

$$
H = -\mathbf{h}\int dx\frac{1}{2}[\rho_\uparrow(x)-\rho_\downarrow(x)] = \frac{\mathbf{h}}{\pi\sqrt{2}}\int dx\ \nabla\phi_\sigma(x) \tag{2.109}
$$

where $\mathbf{h} = g\mu_B h$, with h the magnetic field, μ_B the Bohr magneton and g the Lande factor. Calculating observables in the spin sector is more complicated because the spin Hamiltonian (2.106) is not simply quadratic, but of the sine-Gordon type. We will examine in Section 2.3.2 how to fully solve this Hamiltonian. For the moment let us assume that $g_{1\perp} = 0$. In that case the spin susceptibility is given by

$$\kappa_\sigma = \frac{K_\sigma}{2\pi u_\sigma} \tag{2.110}$$

Note that as for the spinless model, these results are 'Fermi liquid' like. One has a constant compressibility and susceptibility with coefficients renormalized by the interactions.

As for the spinless model, the effects of the interactions manifest themselves most remarkably in the $2k_F$ part of the various correlation functions. Various density like correlation functions can be defined: the charge density and the spin density correlations. Let us introduce the operators

$$\begin{aligned} O_\rho(x) &= \sum_{\sigma,\sigma'} \psi^\dagger_\sigma(x)\delta_{\sigma,\sigma'}\psi_{\sigma'}(x) \\ O^a_\sigma(x) &= \sum_{\sigma,\sigma'} \psi^\dagger_\sigma(x)\sigma^a_{\sigma,\sigma'}\psi_{\sigma'}(x) \end{aligned} \tag{2.111}$$

where σ^x, σ^y, σ^z are the Pauli matrices The operator O_ρ is simply the total density, whereas $O^a_\sigma(x)$ measures the spin density (along the direction $a = x, y, z$). To get the spin density a factor $1/2$ should be included in the spin operators since the spin is $1/2$ times the Pauli matrices, but it is convenient to define the operators that way since it makes explicit some symmetries that we will examine in detail in Chapter 7. As for the spinless model, the density contains a $q \sim 0$ component and a $q \sim 2k_F$ one. One has, for example, for O_ρ and $O^z_\sigma(x)$

$$\begin{aligned} O_\rho(x) &= \frac{-\sqrt{2}}{\pi}(\nabla\phi_\rho(x)) + (O_{\text{CDW}}(x) + \text{h.c.}) \\ O^z_\sigma(x) &= \frac{-\sqrt{2}}{\pi}(\nabla\phi_\sigma(x)) + (O^z_{\text{SDW}}(x) + \text{h.c.}) \end{aligned} \tag{2.112}$$

where the CDW and SDW are the operators measuring the $2k_F$ components of the charge and spin densities. They correspond, as for the spinless model to a charge or spin density wave order. If we forget for the moment the Klein factors U and use (2.98) these operators are given by

$$\begin{aligned} O_{\text{CDW}}(x) &= \psi^\dagger_{R\uparrow}\psi_{L\uparrow}(x) + \psi^\dagger_{R\downarrow}\psi_{L\downarrow}(x) = \frac{e^{-2ik_Fx}}{\pi\alpha}e^{i\sqrt{2}\phi_\rho}\cos(\sqrt{2}\phi_\sigma) \\ O^x_{\text{SDW}}(x) &= \psi^\dagger_{R\uparrow}\psi_{L\downarrow}(x) + \psi^\dagger_{R\downarrow}\psi_{L\uparrow}(x) = \frac{e^{-2ik_Fx}}{\pi\alpha}e^{i\sqrt{2}\phi_\rho}\cos(\sqrt{2}\theta_\sigma) \\ O^y_{\text{SDW}}(x) &= -i(\psi^\dagger_{R\uparrow}\psi_{L\downarrow}(x) - \psi^\dagger_{R\downarrow}\psi_{L\uparrow}(x)) = \frac{-e^{-2ik_Fx}}{\pi\alpha}e^{i\sqrt{2}\phi_\rho}\sin(\sqrt{2}\theta_\sigma) \\ O^z_{\text{SDW}}(x) &= \psi^\dagger_{R\uparrow}\psi_{L\uparrow}(x) - \psi^\dagger_{R\downarrow}\psi_{L\downarrow}(x) = \frac{e^{-2ik_Fx}}{\pi\alpha}e^{i\sqrt{2}\phi_\rho}i\sin(\sqrt{2}\phi_\sigma) \end{aligned} \tag{2.113}$$

The $q \sim 0$ part in (2.112) can easily be computed. It gives a $1/x^2$ decay in a way similar to (2.68). Given the spin-charge separation in H, the spin and charge

parts in the correlations of CDW and SDW *factorize*. If the spin part is simply quadratic the correlations are easily computed to give

$$\begin{aligned}
\langle O^\dagger_{\mathrm{CDW}}(r) O_{\mathrm{CDW}}(0)\rangle &= \frac{e^{2ik_F x}}{2(\pi\alpha)^2}\left(\frac{\alpha}{r}\right)^{K_\rho+K_\sigma} \\
\langle O^{x\dagger}{}_{\mathrm{SDW}}(r) O^x{}_{\mathrm{SDW}}(0)\rangle &= \frac{e^{2ik_F x}}{2(\pi\alpha)^2}\left(\frac{\alpha}{r}\right)^{K_\rho+1/K_\sigma} \\
\langle O^{y\dagger}{}_{\mathrm{SDW}}(r) O^y{}_{\mathrm{SDW}}(0)\rangle &= \frac{e^{2ik_F x}}{2(\pi\alpha)^2}\left(\frac{\alpha}{r}\right)^{K_\rho+1/K_\sigma} \\
\langle O^{z\dagger}{}_{\mathrm{SDW}}(r) O^z{}_{\mathrm{SDW}}(0)\rangle &= \frac{e^{2ik_F x}}{2(\pi\alpha)^2}\left(\frac{\alpha}{r}\right)^{K_\rho+K_\sigma}
\end{aligned} \tag{2.114}$$

As for the spinless model all these $2k_F$ correlations show non-universal power law decay with an exponent that depends on the interaction. Note that both the charge and spin exponent appear in these correlation functions. For the non-interacting case all correlation functions decay as $1/r^2$ as is fit for a free electron gas. In that case, the x, y, z components of SDW have the same decay as is imposed by spin rotation symmetry. We see that having $K_\sigma \neq 1$ breaks the rotation symmetry between the x, y plane and the z direction. For the moment we have set $g_{1\perp} = 0$, and we see from (2.105) that letting $g_{1\|} = 0$ indeed gives $K_\sigma = 1$, which ensures the same power law decay of the z and x, y components as is needed for interactions that obey spin rotation symmetry ($g_\| = g_\perp$).

In addition to the density operators, one can also look at pairing operators. As for the spinless model (2.75) they are defined by

$$\begin{aligned}
O_{\mathrm{SS}}(x) &= \sum_{\sigma,\sigma'} \sigma \psi^\dagger_{R,\sigma}(x)\delta_{\sigma,\sigma'}\psi^\dagger_{L,-\sigma'}(x) \\
O^a_{\mathrm{TS}}(x) &= \sum_{\sigma,\sigma'} \sigma \psi^\dagger_{R,\sigma}(x)\sigma^a_{\sigma,\sigma'}\psi^\dagger_{L,-\sigma'}(x)
\end{aligned} \tag{2.115}$$

where SS denotes singlet pairing whereas TS is triplet pairing. These operators describe paring with zero total momentum. Other pairings are of course possible but are usually less relevant. These operators become

$$\begin{aligned}
O_{\mathrm{SS}}(x) &= \psi^\dagger_{R\uparrow}\psi^\dagger_{L\downarrow}(x) + \psi^\dagger_{L\uparrow}\psi^\dagger_{R\downarrow}(x) = \frac{1}{\pi\alpha}e^{-i\sqrt{2}\theta_\rho}\cos(\sqrt{2}\phi_\sigma) \\
O^x_{\mathrm{TS}}(x) &= \psi^\dagger_{R\uparrow}\psi^\dagger_{L\uparrow}(x) + \psi^\dagger_{L\downarrow}\psi^\dagger_{R\downarrow}(x) = \frac{1}{\pi\alpha}e^{-i\sqrt{2}\theta_\rho}\cos(\sqrt{2}\theta_\sigma) \\
O^y_{\mathrm{TS}}(x) &= -i(\psi^\dagger_{R\uparrow}\psi^\dagger_{L\uparrow}(x) - \psi^\dagger_{L\downarrow}\psi^\dagger_{R\downarrow}(x)) = \frac{-1}{\pi\alpha}e^{-i\sqrt{2}\theta_\rho}\sin(\sqrt{2}\theta_\sigma) \\
O_{\mathrm{TS}}(x) &= \psi^\dagger_{R\uparrow}\psi^\dagger_{L\downarrow}(x) - \psi^\dagger_{L\uparrow}\psi^\dagger_{R\downarrow}(x) = \frac{e^{2ik_F x}}{\pi\alpha}e^{-i\sqrt{2}\theta_\rho}\sin(\sqrt{2}\phi_\sigma)
\end{aligned} \tag{2.116}$$

Note that there seems to be some arbitrariness in the above expressions in terms of the bosonic fields since by anticommuting two fermionic fields one can introduce a minus sine and thus change a sine into a cosine. We will see in Section 4.3.2 how to answer this question in an unambiguous way. The decay of these correlation functions is trivially obtained from (2.114) by letting $k_F = 0$ and $K_\rho \to 1/K_\rho$. Here again this is a power law decay. There is no true superconducting *order* (since $\langle O \rangle = 0$) due to the impossibility to break a continuous symmetry in one dimension. The best the system can do is to have slowly (power law) decaying correlations.

Having the correlation functions we could start building the phase diagram in the same way like that for spinless fermions. This would be valid for a system with $g_{1\perp} = 0$. However, the effects of the $g_{1\perp}$ terms are quite drastic so it will be good to understand them first. This is of course mandatory if we want to be able to deal with spin rotation invariant Hamiltonians. It is also a quite important calculation since sine-Gordon-type Hamiltonians are common in the one-dimensional world and we will have to learn how to deal with them in more complicated situations as well.

2.3.2 *Renormalization equations for sine-Gordon Hamiltonians*

To complete our analysis of the spin sector we have to treat the sine-Gordon Hamiltonian (2.106). There are many ways one can tackle such a problem. The fact that interactions (or other terms) can generate non-quadratic terms is a recurrent fact when dealing with one-dimensional systems. This is obvious from the exponential form of the single fermion operators. When putting together a certain number of these operators, quite generally exponentials of the boson fields will remain. Physically, the effect of the cosine is clear. Contrary to the quadratic term that lets the field ϕ fluctuate, the cosine term would like to lock the field ϕ in one of the minima of the cosine. There will thus be a competition between the quadratic part and the cosine. Since the quadratic part contains the conjugate momentum Π it does not like ϕ to be blocked and promotes fluctuations. In order to know who wins and to obtain the low-energy physical properties of (2.106) we use a renormalization procedure. The ideas of a renormalization procedure are explained in detail in Section 1.3.2 and I strongly encourage you to read this section to understand the philosophy of the procedure, before we start with the gory details of the calculation itself.

As discussed in Section 1.3.2 we change the cutoff of the system while keeping the low-energy properties of the system unchanged. This can be done by varying the coupling constants (and possibly generating new couplings). There are various ways to carry this renormalization procedure. I give in this section a derivation based directly on the correlation functions (José *et al.*, 1977). It has the advantage of being physically transparent and to extend easily to more complicated cases (see Section 4.4). An alternative derivation directly on the partition function is given in Appendix E.1.

Let us consider the correlation function

$$R(r_1 - r_2) = \langle e^{ia\sqrt{2}\phi(r_1)} e^{-ia\sqrt{2}\phi(r_2)} \rangle_H \tag{2.117}$$

If H was the quadratic Hamiltonian H^0 of (2.41), the correlation would be (for $r_1 - r_2 \gg \alpha$)

$$\langle e^{ia\sqrt{2}\phi(r_1)} e^{-ia\sqrt{2}\phi(r_2)} \rangle_{H^0} = e^{-a^2 K F_1(r_1 - r_2)} \simeq \left(\frac{\alpha}{r_1 - r_2} \right)^{a^2 K} \tag{2.118}$$

as shown in Appendix C. Since (2.106) contains a cosine, one cannot compute (2.117) exactly any more, but one can perform a perturbative expansion in the cosine term, assuming that the interaction $g_{1\perp}$ is small. In the following, to lighten the notations I will denote $g_{1\perp}$ simply by g. The first-order term is zero, and if we stop at second order the correlation function is given by

$$\begin{aligned} R(r_1 - r_2) = \langle e^{ia\sqrt{2}\phi(r_1)} e^{-ia\sqrt{2}\phi(r_2)} \rangle_{H_0} + \frac{1}{2} \left(\frac{g}{(2\pi\alpha)^2 u} \right)^2 \sum_{\epsilon_1 = \pm 1, \epsilon_2 = \pm 1} \\ \int \int d^2 r' \, d^2 r'' [\langle e^{ia\sqrt{2}\phi(r_1)} e^{-ia\sqrt{2}\phi(r_2)} e^{i\epsilon_1 \sqrt{8}\phi(r')} e^{-i\epsilon_2 \sqrt{8}\phi(r'')} \rangle_{H_0} \\ - \langle e^{ia\sqrt{2}\phi(r_1)} e^{-ia\sqrt{2}\phi(r_2)} \rangle_{H_0} \langle e^{i\epsilon_1 \sqrt{8}\phi(r')} e^{-i\epsilon_2 \sqrt{8}\phi(r'')} \rangle_{H_0}] \end{aligned} \tag{2.119}$$

where $r = (x, y = u\tau)$ and $d^2 r = dx \, dy$. The second term in the integral is the disconnected terms coming from the partition function in the denominator of the average. Since the averages are taken with the quadratic Hamiltonian (2.41) they can be readily performed (see Appendix C). One gets

$$\begin{aligned} R(r_1 - r_2) = e^{-a^2 K F_1(r_1 - r_2)} \Bigg[1 + \frac{g^2}{2(2\pi\alpha)^4 u^2} \sum_{\epsilon_1} \int \int d^2 r' d^2 r'' e^{-4K F_1(r' - r'')} \\ \left(e^{2a\epsilon_1 K [F_1(r_1 - r') - F_1(r_1 - r'') + F_1(r_2 - r'') - F_1(r_2 - r')]} - 1 \right) \Bigg] \end{aligned} \tag{2.120}$$

The terms with $\epsilon_2 \neq \epsilon_1$ vanish (see Appendix C). We can take a as we wish. It is clear that if one takes a small enough, due to the factor $e^{-4F(r' - r'')}$ (which is essentially a power law) the integral over $d^2 r' \, d^2 r''$ is dominated by configurations where r' and r'' are not too distant from each other. One can thus expand the exponential term linear in a in powers of $r' - r''$. In particular, if we introduce the center of mass and relative coordinates

$$\begin{aligned} R &= \frac{r' + r''}{2} \\ r &= r' - r'' \end{aligned} \tag{2.121}$$

we can rewrite the correlation function as

$$R(r_1 - r_2) = e^{-a^2 K F_1(r_1 - r_2)} \left[1 + \frac{g^2}{2(2\pi\alpha)^4 u^2} \sum_{\epsilon_1} \int \int d^2R \, d^2r \, e^{-4KF_1(r)} \right.$$
$$\left. \left(e^{2a\epsilon_1 K[r \cdot \nabla[F_1(r_1 - R) - F_1(r_2 - R)]} - 1 \right) \right] \quad (2.122)$$

Since r is small the exponential can be expanded. The first-order term is zero because of the sum over ϵ_1. Stopping at second order gives for the correlation function

$$R(r_1 - r_2) = e^{-a^2 K F_1(r_1 - r_2)} \left[1 + \frac{2g^2}{(2\pi\alpha)^4 u^2} \int \int d^2R d^2r \, e^{-4KF_1(r)} \right.$$
$$\left. (aK[r \cdot \nabla[F_1(r_1 - R) - F_1(r_2 - R)])^2 \right] \quad (2.123)$$

The expansion of the quadratic term leads to terms of the form

$$r_i r_j (\nabla_{R_i}[F_1(r_1 - R) - F_1(r_2 - R)])(\nabla_{R_j}[F_1(r_1 - R) - F_1(r_2 - R)]) \quad (2.124)$$

where i, j denote the two possible coordinates x and y. Let us make use of the rotation invariance in $(x, u\tau)$ of the quadratic Hamiltonian and choose a cutoff procedure that respects this invariance. The asymptotic properties are independent of the short distance cutoff so this choice is arbitrary. Such a cutoff procedure corresponds to restricting $r > \alpha$. In that case it is easy to see that because of the integral over d^2r in (2.123) only the terms with $i = j$ survive, the other terms being zero by symmetry $x \to -x$ or $y \to -y$. Since moreover $\int d^2r \, x^2 = \int d^2r \, y^2 = \int d^2r \, r^2/2$, one obtains by integration by part over R

$$R(r_1 - r_2) = e^{-a^2 K F_1(r_1 - r_2)} \left[1 - \frac{g^2}{(2\pi\alpha)^4 u^2} \int \int d^2R \, d^2r \, e^{-4KF_1(r)} a^2 K^2 r^2 \right.$$
$$\left. [F_1(r_1 - R) - F_1(r_2 - R)](\nabla_X^2 + \nabla_Y^2)[F_1(r_1 - R) - F_1(r_2 - R)] \right] \quad (2.125)$$

Since $F_1(r)$ is essentially a log ($F_1(r) = \log(r/\alpha)$ when $r \gg \alpha$) one can use

$$(\nabla_X^2 + \nabla_Y^2) \log(R) = 2\pi\delta(R) \quad (2.126)$$

This identity, well-known for two-dimensional Coulomb systems, can be directly proven by differentiating (C.25). More generally even with an isotropic cutoff

$$\int d^2q [1 - \cos(qr)] \frac{1}{q^2} e^{-\alpha q} = 2\pi \log \left[\frac{1}{2} (1 + \sqrt{1 + r^2/\alpha^2}) \right] \simeq 2\pi \log[r/\alpha] \quad (2.127)$$

Applying $(\nabla_X^2 + \nabla_Y^2)$ on (2.127) obviously gives back (2.126). I will come back to the analogy between this problem and two-dimensional Coulomb problems in Section 3.3. Using (2.126) in (2.125) one obtains

$$\int d^2R[F_1(r_1-R)-F_1(r_2-R)](\nabla_X^2+\nabla_Y^2)[F_1(r_1-R)-F_1(r_2-R)] = -4\pi F_1(r_1-r_2) \tag{2.128}$$

The terms $F_1(r_1-r_1)$ are finite (not logarithmically divergent) because the correlation function F_1 is regular at a short distance. With our original regularization scheme (2.64) this term would be zero. The term $F_1(r_1-r_2)$ is logarithmically divergent when the distance between r_1 and r_2 becomes large. The correlation function is thus

$$R(r_1-r_2) = e^{-a^2KF_1(r_1-r_2)}\left[1+\frac{g^2K^2a^2F_1(r_1-r_2)}{4\pi^3u^2\alpha^4}\int_{r>\alpha} d^2r\, r^2 e^{-4F_1(r)}\right] \tag{2.129}$$

where $d^2r = dx\, dy = 2\pi r\, dr$. One recognizes an expansion of an exponential form similar to (2.118) but with an effective exponent K_{eff}

$$K_{\text{eff}} = K - \frac{y^2K^2}{2}\int_\alpha^\infty \frac{dr}{\alpha}\left(\frac{r}{\alpha}\right)^{3-4K} \tag{2.130}$$

where I have used $y = g/(\pi u)$. The exponent of the correlation function is precisely what controls the asymptotic (low-energy) properties of the system. This exponent should remain unaffected by the cutoff. If we vary the cutoff from α to $\alpha' = \alpha + d\alpha$ in the limit of the integral one has

$$K_{\text{eff}} = K - \frac{y^2K^2}{2}\frac{d\alpha}{\alpha} - \frac{y^2K^2}{2}\int_{\alpha'}^\infty \frac{dr}{\alpha}\left(\frac{r}{\alpha}\right)^{3-4K} \tag{2.131}$$

To keep K_{eff} unchanged one should change the parameter K such that

$$K(\alpha') = K(\alpha) - \frac{y^2(\alpha)K^2(\alpha)}{2}\frac{d\alpha}{\alpha} \tag{2.132}$$

Similarly, to get back (2.130) but with α' one should rescale the integral and thus define

$$y^2(\alpha') = y^2(\alpha)\left(\frac{\alpha'}{\alpha}\right)^{4-4K(\alpha)} \tag{2.133}$$

The forms of (2.132) and (2.133) suggest to parametrize $\alpha = \alpha_0 e^l$ where α_0 is the original cutoff. Changing α is thus equivalent to change l into $l + dl$. Using this parametrization in (2.132) and (2.133) and making an infinitesimal change gives the renormalization equations

$$\begin{aligned}\frac{dK(l)}{dl} &= -\frac{y^2(l)K^2(l)}{2}\\ \frac{dy(l)}{dl} &= (2-2K(l))y(l)\end{aligned} \tag{2.134}$$

Note that these equations are only perturbative in y but are exact in K.

Before we analyze these equations let us understand them on a physical basis. The equation for y is simply the scaling dimension of the operator that appears in the action

$$y \int dx \int d\tau \ \cos(\sqrt{8}\phi_\sigma) \tag{2.135}$$

Since the correlation behaves as

$$\langle \cos(\sqrt{8}\phi_\sigma(r)) \ \cos(\sqrt{8}\phi_\sigma(0))\rangle = \left(\frac{\alpha}{r}\right)^{4K} \tag{2.136}$$

we can say that the operator behaves as

$$\cos(\sqrt{8}\phi_\sigma) \equiv L^{-2K} \tag{2.137}$$

Thus, the operator in the action behaves as

$$y \int dx \int d\tau \ \cos(\sqrt{8}\phi_\sigma) \equiv yL^{2-2K} \tag{2.138}$$

which gives back the equation for y. One can understand the equation for K by noting that K controls the fluctuations of ϕ_σ through the term

$$\frac{u}{K}(\nabla\phi_\sigma)^2 \tag{2.139}$$

in the Hamiltonian. Since the cosine term wants to order the field ϕ_σ its effect at a purely quadratic level would be to decrease K to make the fluctuations of ϕ_σ more difficult in (2.139). A similar physical picture is given by the Wilson renormalization of Appendix E.1.

The flow (2.134) is shown in Fig. 2.6. For an infinitesimal y, one sees from (2.134) that for $K < 1$ y is relevant (y grows upon a change of scale), whereas for $K > 1$ y is irrelevant (y decreases upon a change of scale). One thus expects a phase transition at $K = 1$. To further analyze the flow around this transition let us expand $K_\rho = 1 + y_\parallel/2$. Note that this corresponds to the original $y_{1\parallel}$ and $y_{1\perp}$ from (2.105). With these variables the flow becomes

$$\begin{aligned} \frac{dy_\parallel(l)}{dl} &= -y^2(l) \\ \frac{dy(l)}{dl} &= -y_\parallel(l)y(l) \end{aligned} \tag{2.140}$$

These equations that correspond to an expansion up to second order in the interactions are identical to the ones derived in the fermion language (1.58). They are also identical to the ones derived for the XY problem (Kosterlitz, 1974), as we will discuss more in Section 3.1. From (2.140) we see that $y\frac{dy}{dl} = y_\parallel \frac{dy_\parallel}{dl}$ and thus

$$A^2 = y_\parallel^2 - y^2 \tag{2.141}$$

is a constant of motion. The trajectories are thus hyperbolas. A real corresponds to the regions (a) and (c) in Fig. 2.6. A imaginary ($A^2 < 0$) is region (b). The

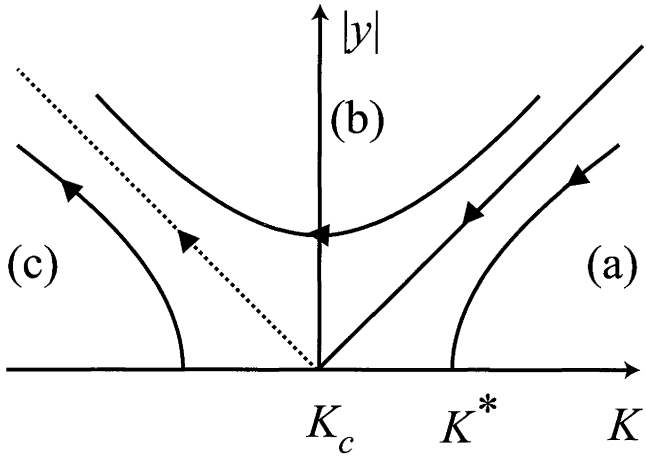

FIG. 2.6. Flow corresponding to the eqn (2.134). The trajectories are hyperbolas (see text). The first diagonal (thick line) is a separatrix between a regime where y is irrelevant and a regime where y flows to strong coupling.

equations depend only on $|y|$ and thus the flow is symmetric when changing $y \to -y$. It will be thus sufficient to analyze the case $y > 0$.

The line $y_{\|} = y$ is obviously a separatrix between two different regimes, as shown in Fig. 2.6. Using the constant of motion (2.141) in (2.140) the flow can be easily integrated. For example, for $y_{\|} > y$ one has

$$\begin{aligned} y_{\|}(l) &= A/(\tanh(Al + \operatorname{atanh}(A/y_{\|}^0))) \\ y(l) &= A/(\sinh(Al + \operatorname{atanh}(A/y_{\|}^0))) \end{aligned} \tag{2.142}$$

On the separatrix one has

$$y_{\|}(l) = y(l) = \frac{y^0}{1 + y^0 l} \tag{2.143}$$

When $A > 0$ and $y_{\|} > 0$, the operator $\cos(\sqrt{8}\phi_\sigma)$ is irrelevant. The fixed point corresponds to $y^* = 0$ and $y_{\|}^* = A$. Close to the fixed point the flow can be approximated by

$$\begin{aligned} \frac{dy_{\|}(l)}{dl} &= 0 \\ \frac{dy(l)}{dl} &= (2 - 2K^*)y(l) \end{aligned} \tag{2.144}$$

To obtain the correlation functions we should, strictly speaking, write the renormalization equations for the correlation functions themselves. This will be done

in Section 4.4. However, the trajectories are nearly vertical, thus $y \to 0$ while K converges to a fixed point value K^*. As a first approximation one can thus compute the correlation functions using the simple quadratic Hamiltonian (2.41) but with the renormalized parameters K^*. As a result the correlations have the asymptotic decay

$$\langle e^{ia\sqrt{2}\phi_\sigma(r)} e^{-ia\sqrt{2}\phi_\sigma(0)} \rangle \simeq \left(\frac{\alpha}{r}\right)^{a^2 K_{\text{eff}}} = \left(\frac{\alpha}{r}\right)^{a^2 K^*} \tag{2.145}$$

In this regime the RG flow thus allows to get the asymptotic behavior of the correlation functions. Because the cosine disappears from the asymptotic properties and the system is described by a pure quadratic Hamiltonian, this regime is called 'massless regime'.

When $y_\parallel = y$ the operator is marginally irrelevant, the flow is along the first diagonal. We thus see that if one starts from a spin rotation invariant problem $y = y_\parallel$ then the rotation invariance is preserved at each step of the renormalization as it should be. The fixed point corresponds to $y_\parallel^* = y^* = 0$ and thus $K^* = 1$. One can thus still use the expression (2.145), with $K^* = 1$. As we discussed in the previous section this is exactly the value that ensures spin rotation invariance of the correlation functions, which now is only natural. However, the fact that the corresponding operator is only marginal gives some additional contributions as shown in Section 4.4. For some correlation functions this gives rise to logarithmic corrections. For example,

$$\begin{aligned} \langle \cos(\sqrt{2}\phi_\sigma(r))\ \cos(\sqrt{2}\phi_\sigma(0)) \rangle &\simeq \frac{\alpha}{r} \log^{1/2}(r/\alpha) \\ \langle \sin(\sqrt{2}\phi_\sigma(r))\ \sin(\sqrt{2}\phi_\sigma(0)) \rangle &\simeq \frac{\alpha}{r} \log^{-3/2}(r/\alpha) \end{aligned} \tag{2.146}$$

See Section 4.4 for the general expressions.

When $y > y_\parallel$ the trajectories tend to $y_\parallel \to -\infty$ and $y \to \infty$. The flow goes to strong coupling. Of course, since the RG equations themselves have been established in a perturbation expansion in y they cease to be valid beyond a certain lengthscale for which $y(l) \sim 1$. Nevertheless, the equations can be used below this lengthscale. The flow can be integrated as

$$\arctan(y_\parallel^0/\overline{A}) - \arctan(y_\parallel/\overline{A}) = \overline{A} l \tag{2.147}$$

where

$$\overline{A} = \sqrt{y_0^2 - (y_\parallel^0)^2} \tag{2.148}$$

On the special line $y_\parallel = -y < 0$ (for which $\overline{A} = 0$) one has

$$y(l) = \frac{y^0}{1 - y^0 l} \tag{2.149}$$

note that this line corresponds also to the spin rotation invariant case since one can take $y = -y_{1\perp}$ when $y_{1\parallel} = y_{1\perp} < 0$. Since the flow goes to strong coupling we

need to guess the physics of this phase. This is one major advantage of the boson representation over the fermion one. We can try to analyze the Hamiltonian by looking at the limit $y \to \pm\infty$ (and $K_\sigma \to 0$). On the fermion representation having a coupling constant going to infinity does not help much, because fermions operators do not have a classical limit. On the boson Hamiltonian we can expect that when $y \to \pm\infty$ the term

$$\frac{yu}{2\pi\alpha^2}\int dx\ \cos(\sqrt{8}\phi_\sigma) \tag{2.150}$$

imposes that ϕ_σ is locked into one of the minima of the cosine. The field ϕ_σ thus orders and we go into a massive phase. If y is very large one can expand the cosine around the minimum. If $y \to -\infty$ the minimum is $\phi_\sigma = 0$ and the Hamiltonian would become

$$H = H^0 + \frac{2yu}{\pi\alpha^2}\int dx\ \phi_\sigma^2(x) \tag{2.151}$$

In Fourier space the action would thus become

$$S = \frac{1}{2\pi K}\frac{1}{\beta\Omega}\sum_{k,\omega_n}\left[\frac{1}{u}\omega_n^2 + uk^2 + \frac{4Kyu}{\alpha^2}\right]\phi^*(k,\omega_n)\phi(k,\omega_n) \tag{2.152}$$

Even at $k = 0$ excitations now cost a finite energy. The spectrum thus has a gap of order

$$M_P = \sqrt{\frac{4Kyu^2}{\alpha^2}} \tag{2.153}$$

These excitations are the 'phonons' (that is, the small oscillations) of the field ϕ which are now massive. They correspond to a variation of ϕ within one of the minima of the cosine. There are other excitations, the solitons, that take ϕ from one minimum of the cosine to the other. I will come back to such solutions later (see also Appendix E.3). Of course, such an expansion is valid only if y is very large. One can make a more sophisticated approximation using a variational approach as shown in Appendix E.2. A more accurate method is to combine the RG with a strong coupling analysis. The boson Hamiltonian is quite useful in that respect since, contrary to the fermion Hamiltonian, it is easy to analyze the limit where the coefficient of the cosine becomes large. Let us use the RG up to a point where the coupling y is of order one. The gap in the spectrum has the dimension of an energy and thus it renormalizes as

$$\Delta_\sigma(l) = e^l\Delta_\sigma(l=0) \tag{2.154}$$

When $y(l^*) \sim 1$ we can use the expansion (2.152), which would lead to a gap $\Delta_\sigma(l^*) \sim uy^{1/2}(l^*)/\alpha \sim u/\alpha$. The true gap of the system is thus simply given by

$$\Delta_\sigma(l=0) \simeq e^{-l^*}\Delta_0 \tag{2.155}$$

where l^* is the scale at which the coupling is of order one and $\Delta_0 = u/\alpha$ is a quantity of the order of the original bandwidth of the system. The complete

solution can easily be obtained from the flow (2.147). Let us examine it in three physically different limits.

$y \ll |y_{\|}|$. In that case one is deep in the massive phase. From Fig. 2.6 and the flow (2.147), one sees that the flow is nearly vertical. One can thus approximate it by

$$\begin{aligned} \frac{dK(l)}{dl} &= 0 \\ \frac{dy(l)}{dl} &= (2-2K)y(l) \end{aligned} \tag{2.156}$$

which gives $y(l) = y^0 e^{(2-2K)l}$. Thus, the lengthscale l^* is

$$e^{l^*} = \left(\frac{1}{y^0}\right)^{1/(2-2K)} \tag{2.157}$$

and the gap is

$$\Delta_\sigma(l=0)/\Delta_0 \simeq (y^0)^{1/(2-2K)} \tag{2.158}$$

The gap is thus a power law of the bare coupling constant, with an exponent controlled by K. This result can also be obtained by a variational approach (see Appendix E.2). If one gets closer to the transition $K \to 1$ the gap gets smaller as it should (remember that $y^0 \ll 1$).

$y_{\|} = -y$. This corresponds to a system which is invariant by spin rotation. In that case, (2.149) gives (for $y \ll 1$)

$$l^* = \frac{1}{y^0} - 1 \sim \frac{1}{y^0} \tag{2.159}$$

The gap is thus

$$\Delta_\sigma(l=0) \simeq \Delta_0 e^{-1/y^0} \tag{2.160}$$

and the gap is *exponentially* small in the coupling constant. This is clearly a highly non-perturbative result. I will come back to this result when discussing the Hubbard model in Section 7.1.1.

Close to the Transition. Finally let us get close to the separatrix. In that case using (2.147) gives

$$\overline{A} l^* \to \pi \tag{2.161}$$

since $\overline{A} \to 0$ close to the transition and thus $y_{\|}^0/\overline{A} \to \infty$ and $y_{\|}(l^*)/\overline{A} \to -\infty$. Thus, the gap becomes

$$\Delta_\sigma(l=0) \simeq \Delta_0 e^{-\pi/\overline{A}} \tag{2.162}$$

If we consider that one approaches the transition such as $y_0 \to y_{\|}$ then

$$\overline{A} \sim \sqrt{2y_0(y_0 - y_{\|}^0)} \tag{2.163}$$

and thus the gap is exponentially small in the square root of the distance to the transition.

We thus see that using the RG one can determine, up to a multiplicative constant, the behavior of the gap in the whole phase diagram. This behavior depends crucially of the original coupling constant. This will be specially relevant when we will focus at a given microscopic model as in Chapter 7.

2.3.3 *Phase diagram*

We can now use these results to get the generic phase diagram of a one-dimensional chain. There are two sectors depending on whether the spin Hamiltonian is massless or massive. Remember that for fermions with spins the g and the K are related by (2.105).

If we are in the massless sector for the spin part both the charge sector and the spin sector lead to power law decay for the correlation functions. For a spin rotation invariant problem this corresponds to $g_1 > 0$, that is, repulsive interactions. For the spin sector one has to use the renormalized parameter K_σ^*. The various instabilities have susceptibilities

$$\begin{aligned}
\chi_{\mathrm{CDW}} &\sim \omega^{K_\rho + K_\sigma^* - 2} \\
\chi_{\mathrm{SDW}_z} &\sim \omega^{K_\rho + K_\sigma^* - 2} \\
\chi_{\mathrm{SDW}_{x,y}} &\sim \omega^{K_\rho + 1/K_\sigma^* - 2} \\
\chi_{\mathrm{SS}} &\sim \omega^{K_\rho^{-1} + K_\sigma^* - 2} \\
\chi_{\mathrm{TS}_z} &\sim \omega^{K_\rho^{-1} + K_\sigma^* - 2} \\
\chi_{\mathrm{TS}_{x,y}} &\sim \omega^{K_\rho^{-1} + 1/K_\sigma^* - 2}
\end{aligned} \tag{2.164}$$

For a system with spin rotation symmetry $K_\sigma^* = 1$. The dominant instabilities are a spin or a charge density wave when $K_\rho < 1$ and triplet or singlet superconductivity when $K_\rho > 1$. Note that when $K_\rho < 1$ as far as the power law decay is concerned there is *as much* tendency towards spin density wave along z than a charge density wave. This is a rather counterintuitive result since, as shown in Fig. 2.7, one would expect the system to have antiferromagnetic tendency (SDW) but no charge density wave tendency. In fact this image is true at short distances. At large distance the spin up and spin down density waves are soft enough so that the *asymptotic* decay of both the spin and charge density waves have the same *exponent*. Of course, the amplitudes are not the same and for the spin isotropic case there are even log corrections that favor the SDW states. I will come back to this point in detail in Section 4.4.

When the spin sector is massive, the field ϕ_σ orders. A Luttinger liquid in which the spin modes have become massive is sometimes referred to as a Luther–Emery liquid. For a spin rotation invariant problem, this occurs when $g_1 < 0$, that is, for attractive interactions. For a general case that is not spin rotation invariant, we can have a massive phase because $K_\sigma < 1$ (that is $g_{1\parallel} < 0$) while at the same time one can have either $g_{1\perp} > 0$ or $g_{1\perp} < 0$. The value at which ϕ_σ orders minimizes

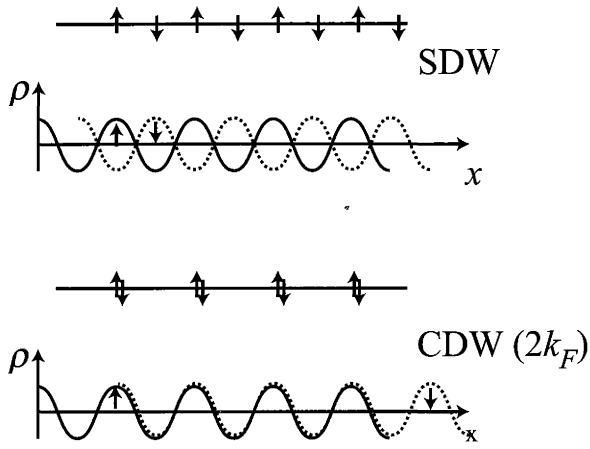

FIG. 2.7. Spin and charge density wave tendencies. In a spin density wave (antiferromagnetism) one has two waves of density for spin up and down with wavelength $2k_F$. The two waves are shifted relative to each other. The field ϕ_σ controls this dephasing (see text). The density is uniform and the spin modulation maximum. In a charge density wave, the two waves are in phase giving a density modulation and a zero spin modulation. Intuitively, one expects that repulsion between electrons favor the SDW order compared to the CDW one.

$$g_{1\perp} \int dx \, \cos(\sqrt{8}\phi_\sigma) \tag{2.165}$$

The ordered value $\langle \phi_\sigma \rangle$ is thus different depending on the sign of $g_{1\perp}$

$$\begin{aligned} \phi_\sigma &= \frac{\pi}{\sqrt{8}} + \frac{2\pi n}{\sqrt{8}}, \quad g_{1\perp} > 0 \\ \phi_\sigma &= 0 + \frac{2\pi n}{\sqrt{8}}, \quad g_{1\perp} < 0 \end{aligned} \tag{2.166}$$

It is important to note that the field is trapped in *one* of the minima of the cosine. Going from the massless phase to the massive one is thus a true phase transition. Since it occurs at $T = 0$ it is an example of a quantum phase transition (Sachdev, 1998). The parameter driving the transition is K that controls the amount of (quantum) fluctuations coming from the quadratic part. When one has a periodic structure such as a cosine and a quantum problem one can be worried that tunneling events from one minima to the other can restore the symmetry. For a single-particle in a cosine potential, the slightest amount of tunneling between two cosine minima leads to conduction bands, for example, and restores the translational symmetry. However, our sine-Gordon problem is a two-dimensional (one space one time) problem. In that case it is well-known that instantons with a finite action (instanton) that would connect two cosine

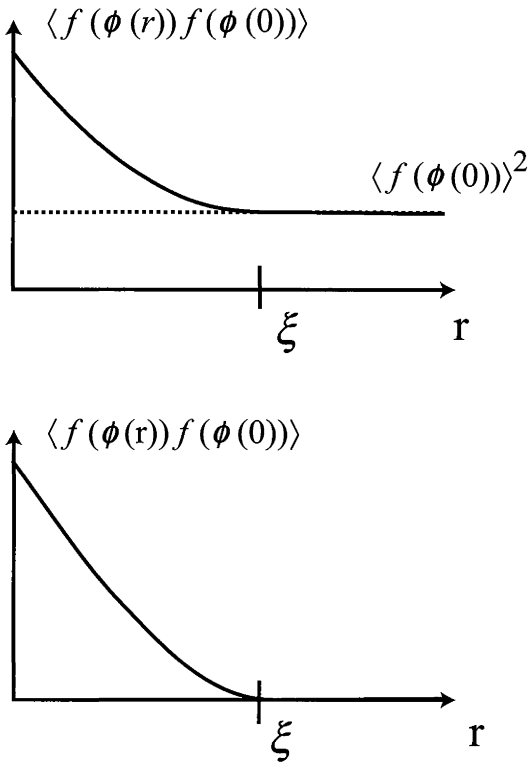

FIG. 2.8. When a field orders the correlation function decay exponentially, with a characteristic length that is the inverse of the gap $\xi = u/\Delta$. Depending on whether the average value of the operator $\langle f(\phi_\sigma)\rangle$ is zero or not the correlation is either asymptotically suppressed or tends rapidly to a constant.

minima cannot exist (Rajaraman, 1982). There is thus no restoring of symmetry and the field is truly locked in *one* of the minima. This is of course related to the Mermin–Wagner theorem stating that in two (classical) dimensions it is impossible to break a continuous symmetry but one can break a discrete one.

Since the field ϕ_σ orders, correlation functions containing this field now decay exponentially, thus

$$\langle f(\phi_\sigma(r'))f(\phi_\sigma(r))\rangle \to \langle f(\phi_\sigma(r'))\rangle\langle f(\phi_\sigma(r))\rangle = \langle f(\phi_\sigma(r))\rangle^2 \tag{2.167}$$

as shown in Fig. 2.8. Because the field ϕ_σ orders, the dual field θ_σ is totally disordered.

$$\langle\cos(a\theta_\sigma(r))\rangle = \langle\sin(a\theta_\sigma(r))\rangle = 0 \tag{2.168}$$

and all correlation functions decay exponentially to zero. Thus, all correlation functions containing the field θ_σ are exponentially suppressed and the corresponding susceptibilities are not divergent any more. This is the case for the x, y

components of the triplet superconductivity and of the SDW phase. For the z component or the SS and CDW phase, this depends on the value of the field ϕ_σ. Using (2.166) one gets

$$\begin{aligned} \langle \cos(\sqrt{2}\phi_\sigma(r))\rangle &= 0, \quad g_{1\perp} > 0 \\ \langle \sin(\sqrt{2}\phi_\sigma(r))\rangle &= 0, \quad g_{1\perp} < 0 \end{aligned} \tag{2.169}$$

whereas the other average is non-zero. Note that the physical quantities do not depend on which value of the minimum (value of n) we chose in (2.166). If the field was really stuck to the value given in (2.166), then the average value would be 1 and the corresponding correlation function would be constant. In fact, quantum fluctuations induced by the quadratic part of the Hamiltonian reduce the average value. We can use the variational approximation to get an estimate of this value. This calculation is performed in Appendix E.2.

Using (2.169) we see that for $g_{1\perp} < 0$ the correlation function of the SDW_z and TS_z order parameter are exponentially suppressed. This is intuitively reasonable. For attractive interactions between opposite spins $g_{1\perp} < 0$ one expects the electrons to pair into singlets, and thus that any spin correlation is exponentially suppressed. This is what we find here since all components x, y, z of the SDW and TS fluctuations are exponentially suppressed. In the CDW and SS correlations the spin part can be replaced by a constant and the asymptotic decay of the correlations is given by

$$\begin{aligned} \langle O^\dagger_{\mathrm{CDW}}(r) O_{\mathrm{CDW}}(0)\rangle &\propto C^2 \left(\frac{\alpha}{r}\right)^{K_\rho} \\ \langle O^\dagger_{\mathrm{SS}}(r) O_{\mathrm{SS}}(0)\rangle &\propto C^2 \left(\frac{\alpha}{r}\right)^{1/K_\rho} \end{aligned} \tag{2.170}$$

where $C = \langle \cos(\sqrt{2}\phi_\sigma)\rangle$. Compared to the case where the spin sector is massless the correlation functions decay more slowly since only the fluctuations of the charge part contributes to the decay. As a result *both* susceptibilities can be divergent simultaneously if $K_\rho \in [1/2, 2]$ since

$$\begin{aligned} \chi_{\mathrm{CDW}} &\sim \omega^{K_\rho - 2} \\ \chi_{\mathrm{SS}} &\sim \omega^{K_\rho^{-1} - 2} \end{aligned} \tag{2.171}$$

If the interactions are extremely repulsive $K_\rho < 1/2$ (resp. attractive $K_\rho > 2$) then only the CDW (resp. SS) is divergent, which is again reasonable physically. This leads to the phase diagram shown in Fig. 2.9.

If one has $g_{1\perp} > 0$ then the CDW and SS are exponentially suppressed while the SDW_z and TS_z have susceptibilities similar to the ones in (2.171). Note that having $K_\sigma < 1$ to be in the massive sector and $g_{1\perp} > 0$ corresponds to very spin anisotropic interactions since $K_\sigma \simeq 1 + g_{1\parallel}/(2\pi v_F)$ and thus one would have $g_{1\parallel} < 0$ and $g_{1\perp} > 0$. It is not thus surprising to have exponentially suppressed x, y SDW and TS fluctuations while having order in SDW_z.

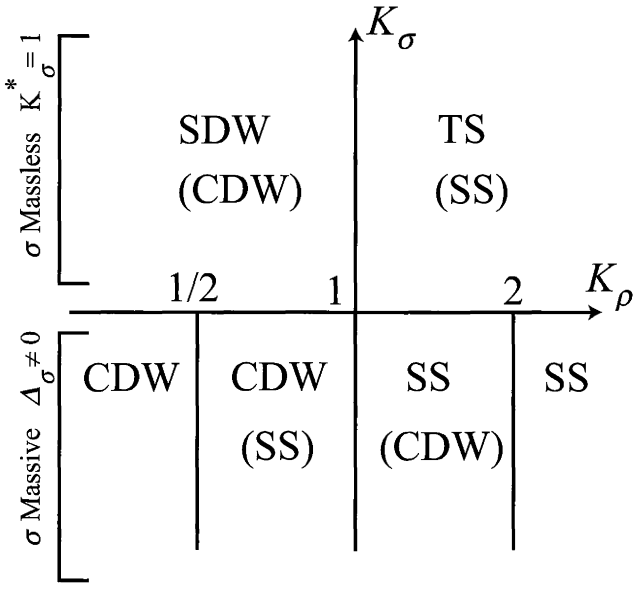

FIG. 2.9. Phase diagram of the system with spin for spin isotropic couplings. There are four sectors depending on the value of the parameters K_ρ and the sign of the backscattering term $g_{1\perp}$ (or alternatively the value of the bare parameter K_σ). The phases correspond to the most divergent susceptibility. I have indicated in parenthesis subdominant divergences. In the upper part ($K_\sigma > 1$) the spin sector is massless. In the lower part ($K_\sigma < 1$) the spin excitations are massive with a gap Δ_σ.

Thanks to the bosonization method we have now determined the *generic* properties of an interacting fermionic system with short-range interactions. It is worth emphasizing that *any* microscopic model with simple interactions falls in the phase diagram of Fig. 2.9. More complicated interactions and/or coupled chains can of course lead to more complex physics and we will see some examples in the next chapters. Although we started from a very specific model (the Tomonaga–Luttinger model) with the strictly linear dispersion relations we will see in the next chapter that most of the properties that we have obtained hold quite generally.

3

LUTTINGER LIQUIDS

> You can know the name of a bird in all the languages of the world, but when you're finished, you'll know absolutely nothing whatever about the bird. You'll only know about humans in different places and what they call the bird. So let's look at the bird and see what it's doing — that's what counts.
>
> Richard Feynman, quoting his father

In the previous chapter, we have seen, for fermions, a careful derivation of the bosonization formulas. The bosonization technique allows to solve the interacting problem and to extract a certain number of properties such as power law behavior of the correlation functions. However, this derivation is, strictly speaking, based on a linearization of the spectrum close to the Fermi energy. One can thus wonder what will remain of the results of the previous chapter when it is impossible to stay confined close to the Fermi level, for example, when the interactions become strong. In order to answer this question let us rederive the bosonization formulas, in a more phenomenological but more general way (Haldane, 1981*b*). I also give in this chapter a more physical interpretation for most of the results that were obtained in a rigorous way in the previous chapter. This allows to show that a similar concept as Fermi liquids exists in one dimension. This concept called Luttinger liquid encompasses most of the physics of simple one-dimensional systems and will be the starting point to study more complex situations.

This chapter is very simple technically and emphasizes the physical interpretations of the various formulas. Mathematical rigor has been set aside. If there is only one chapter you should read this is the one. You can then go back to the previous chapters to have the dots on the i and the crosses on the t of the bosonization.

3.1 Phenomenological bosonization

Let us start with any one-dimensional system (fermions or bosons). The density operator of such a system is

$$\rho(x) = \sum_i \delta(x - x_i) \tag{3.1}$$

where x_i is the position operator of the ith particle. Let us label the position of the ith particle by an 'equilibrium' position R_i^0 that the particle would occupy

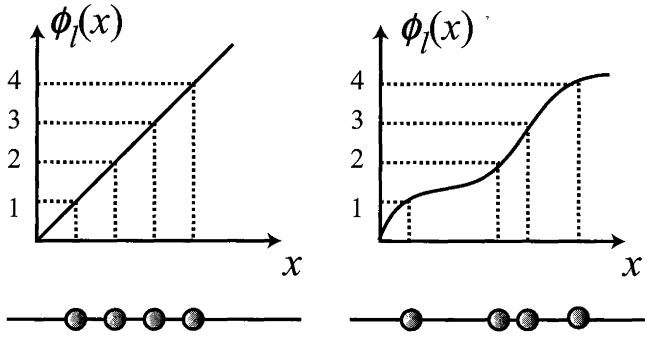

FIG. 3.1. Some examples of the labelling field $\phi_l(x)$. If the particles form a perfect lattice of lattice spacing d, then $\phi_l^0(x) = 2\pi x/d$, and is just a straight line. Different functions $\phi_l(x)$ allow to put the particles at any position in space.

if the particles were forming a perfect crystalline lattice, and the displacement u_i relative to this equilibrium position. Thus,

$$x_i = R_i^0 + u_i \tag{3.2}$$

If ρ_0 is the average density of particles, $d = \rho_0^{-1}$ is the distance between the particles. Then, the equilibrium position of the ith particle is

$$R_i^0 = di \tag{3.3}$$

The density operator written as (3.1) is not very convenient. To rewrite it in a more pleasant form we introduce a labelling field $\phi_l(x)$ (Haldane, 1981*b*). This field, which is a continuous function of the position, takes the value $\phi_l(x_i) = 2\pi i$ at the position of the ith particle. It can thus be viewed as a way to number the particles. Since in one dimension, contrary to higher dimensions, one can always number the particles in an unique way (e.g. starting at $x = -\infty$ and processing from left to right), this field is always well-defined. Some examples are shown in Fig. 3.1. Using this labelling field and the rules for transforming δ functions

$$\delta(f(x)) = \sum_{\text{zeros of } f} \frac{1}{|f'(x_i)|}\delta(x - x_i) \tag{3.4}$$

one can rewrite the density as

$$\begin{aligned} \rho(x) &= \sum_i \delta(x - x_i) \\ &= \sum_n |\nabla\phi_l(x)|\delta(\phi_l(x) - 2\pi n) \end{aligned} \tag{3.5}$$

It is easy to see from Fig. 3.1 that $\phi_l(x)$ can always be taken as an increasing function of x, which allows to drop the absolute value in (3.5). Using the Poisson summation formula this can be rewritten

$$\rho(x) = \frac{\nabla\phi_l(x)}{2\pi}\sum_p e^{ip\phi_l(x)} \tag{3.6}$$

where p is an integer. It is convenient to define a field ϕ relative to the perfect crystalline solution and to introduce

$$\phi_l(x) = 2\pi\rho_0 x - 2\phi(x) \tag{3.7}$$

The density becomes

$$\rho(x) = \left[\rho_0 - \frac{1}{\pi}\nabla\phi(x)\right]\sum_p e^{i2p(\pi\rho_0 x - \phi(x))} \tag{3.8}$$

Since the density operators at two different sites commute it is normal to expect that the field $\phi(x)$ commutes with itself. Note that if one averages the density over distances large compared to the interparticle distance d all oscillating terms in (3.8) vanish. Thus, only $p = 0$ remains and the smeared density is

$$\rho_{q\sim 0}(x) \simeq \rho_0 - \frac{1}{\pi}\nabla\phi(x) \tag{3.9}$$

We can go further by looking at the single-particle creation operator $\psi^\dagger(x)$. Such an operator can always be written as

$$\psi^\dagger(x) = [\rho(x)]^{1/2}e^{-i\theta(x)} \tag{3.10}$$

where $\theta(x)$ is some operator. The (anti-) commutation relations between the ψ impose some commutation relations between the density operators and the $\theta(x)$. For bosons, the condition is

$$[\psi_B(x), \psi_B^\dagger(x')] = \delta(x - x') \tag{3.11}$$

Using (3.10) the commutator gives

$$e^{+i\theta(x)}[\rho(x)]^{1/2}[\rho(x')]^{1/2}e^{-i\theta(x')} - [\rho(x')]^{1/2}e^{-i\theta(x')}e^{+i\theta(x)}[\rho(x)]^{1/2} \tag{3.12}$$

If we assume quite reasonably that the field θ commutes with itself ($[\theta(x), \theta(x')] = 0$), the commutator (3.12) is obviously zero for $x \neq x'$ if (for $x \neq x'$)

$$[[\rho(x)]^{1/2}, e^{-i\theta(x')}] = 0 \tag{3.13}$$

A sufficient condition to satisfy (3.11) would thus be

$$[\rho(x), e^{-i\theta(x')}] = \delta(x - x')e^{-i\theta(x')} \tag{3.14}$$

How to satisfy the above relation? One can guess the answer by replacing the exact density in (3.14) by the smeared density (3.9). Physically, one expects that

most of the commutator should come from this term since the fields $\phi(x)$ and $\theta(x)$ are expected to vary slowly at the scale of the interparticle distance ρ_0^{-1}. If the density is only the smeared density then (3.14) is obviously satisfied if

$$[\frac{1}{\pi}\nabla\phi(x), \theta(x')] = -i\delta(x - x') \tag{3.15}$$

as can be directly checked by using (A.9). The commutation relation (3.15) implies directly that the commutator between ϕ and θ is of the form (2.24) (see also the discussion in Section 3.2). The higher harmonics in the density give commutators of the form

$$\begin{aligned}[e^{-i2p\phi(x)}, e^{-i\theta(x')}] &= e^{-i2p\phi(x)}e^{-i\theta(x')}(1 - e^{2p[\phi(x),\theta(x')]}) \\ &= e^{-i2p\phi(x)}e^{-i\theta(x')}(1 - e^{ip\pi\mathrm{Sign}(x'-x)})\end{aligned} \tag{3.16}$$

Thus, for $x = x'$ all higher harmonics vanish (remember that the function $\mathrm{Sign}(x)$ in (2.24) is regularized to give zero at $x = 0$). Equation (3.14) works perfectly. This is not the case when $x \neq x'$ where odd harmonics remain. However, since these terms are multiplied by the oscillating factor $e^{i2p\pi\rho_0 x}$ we can expect them to play no role in the continuum limit. Note in particular that

$$[\rho(x), e^{-i2\theta(x')}] = 2\delta(x - x')e^{-i2\theta(x')} \tag{3.17}$$

is *perfectly* satisfied. So let us proceed for the moment by assuming that (3.15) is indeed the condition that ϕ and θ need to satisfy. Equation (3.15) proves that θ and $\frac{1}{\pi}\nabla\phi$ are canonically conjugate. Note that for the moment this results from totally general considerations and does not rest on a given microscopic model. Integrating by part (3.15) shows that

$$\pi\Pi(x) = \nabla\theta(x) \tag{3.18}$$

where $\Pi(x)$ is the canonically conjugate momentum to $\phi(x)$.

To obtain the single-particle operator one can substitute (3.8) into (3.10). Since the square root of a delta function is also a delta function up to a normalization factor the square root of ρ is identical to ρ up to a normalization factor that depends on the ultraviolet structure of the theory. Thus,

$$\psi_B^\dagger(x) = [\rho_0 - \frac{1}{\pi}\nabla\phi(x)]^{1/2}\sum_p e^{i2p(\pi\rho_0 x - \phi(x))}e^{-i\theta(x)} \tag{3.19}$$

where the index B emphasizes that this is the representation of a *bosonic* creation operator. How to modify the above formulas if we have fermions instead of bosons? The density can obviously be expressed in the same way in terms of the field ϕ. For the single-particle operator one has to satisfy an anticommutation relation instead of (3.11). We thus have to introduce in representation (3.10) something that introduces the proper minus sign when the two fermions operators are commuted. This is known as a Jordan–Wigner transformation and I will

come back to it when looking at spin chains in Chapter 6. Here, the operator to add is easy to guess. Since the field ϕ_l has been constructed to be a multiple of 2π at each particle, $e^{i\frac{1}{2}\phi_l(x)}$ oscillates between ± 1 at the location of consecutive particles. The Fermi field can thus be easily constructed from the boson field (3.10) by

$$\psi_F^\dagger(x) = \psi_B^\dagger(x) e^{i\frac{1}{2}\phi_l(x)} \tag{3.20}$$

This can be rewritten in a form similar to (3.10) as

$$\psi_F^\dagger(x) = [\rho_0 - \frac{1}{\pi}\nabla\phi(x)]^{1/2} \sum_p e^{i(2p+1)(\pi\rho_0 x - \phi(x))} e^{-i\theta(x)} \tag{3.21}$$

The above formulas are a way to represent the excitations of the system directly in terms of variables defined in the continuum limit. It is thus well suited to describe the asymptotic properties of the system.

In addition to the small oscillations, the fields ϕ and θ can have topological excitations. For periodic boundary conditions $\psi(x+L) = \psi(x)$, this implies that, for bosons, $\theta(x+L) = \theta(x) + \pi J$ where J is an even integer. In a similar way the periodicity condition on the density operator imposes $\phi(x+L) = \phi(x) + \pi N$ where N is an integer (Haldane, 1981*b*; Mironov and Zabrodin, 1991). Because of the extra operator for fermions, the boundary condition is now $N+J$ even. Compare (3.21) with the bosonization formula (2.30) of the previous chapter, derived for the Luttinger model. For spinless fermions $k_F/\pi = \rho_0$, thus (3.21) and (3.8) are a generalization of (2.30) and (2.62). They contain the $q \sim 0$ and $q \sim 2k_F$ components (for the density) and $q = \pm k_F$ (for the single-particle) components that are present in the Luttinger model. But in addition they contain all the higher harmonics. The absence of higher harmonics in the Luttinger model is an artefact of the strictly linear dispersion relation. I will come back to this point later.

The field ϕ and θ that we have derived in this chapter have a simple canonical commutation relation (ϕ and $\Pi = \nabla\theta/\pi$ are canonically conjugate). Irrespective of any Hamiltonian ϕ and Π thus have a simple expression in terms of bosonic operators b_p and $b_p^\dagger$ (one boson per momentum mode p since $\phi(x)$ depends on space). Since ϕ is real it should contain both b and $b^\dagger$. It is exactly equivalent to a standard harmonic oscillator representation (Mahan, 1981). Thus, the fields can be expressed in terms of the bosons b_p and $b_p^\dagger$ as shown in (2.23) in the previous chapter. As before the bosons represent the small oscillations of the density. The topological numbers N and J of this chapter are analogous to $N_+ + N_-$ (total number of particles) and $N_+ - N_-$ (total current) of the previous chapter. Here, the parameter α of (2.23) is a cutoff to regularize the theory at large momentum. It is of the order of the distance above which the continuum description applies, namely here the interparticle distance $d = \rho_0^{-1}$.

What is the Hamiltonian of the system? It should be written only in terms of the variables $\phi(x)$ and $\theta(x)$. It is easy to see that $(\nabla\phi(x))^2$ terms should be present. These terms would come, for example, from the interaction $\int dx\, \rho(x)^2$.

Similarly $(\nabla\theta(x))^2$ terms should also be there. For example, for bosons, they directly come from the kinetic energy

$$H_K = \int dx \frac{1}{2m}(\nabla\psi^\dagger(x))(\nabla\psi(x)) \tag{3.22}$$

Using

$$\psi^\dagger(x) = \rho_0^{1/2} e^{-i\theta(x)} \tag{3.23}$$

which is the part of the single-particle operator (3.10) containing less powers of $\nabla\phi$ and thus the most relevant, one gets

$$H_K = \int dx \frac{\rho_0}{2m}(\nabla\theta(x))^2 \tag{3.24}$$

The coefficient cannot be obtained reliably since both terms coming from the interactions and renormalization from irrelevant operators can change it. But the important result is that the most relevant terms in the Hamiltonian, that is, the ones that will control the low-energy properties are $(\nabla\theta(x))^2$ and $(\nabla\phi(x))^2$. It is easy to check that cross terms cannot appear. Indeed, if the system has an inversion symmetry, the energy is invariant by $x \to -x$. Changing $\rho(x) \to \tilde{\rho}(-x)$ and $\psi(x) \to \tilde{\psi}(-x)$ imposes that $\phi(x) = -\tilde{\phi}(-x)$ and $\theta(x) = \tilde{\theta}(-x)$. And thus one has $\nabla\phi(x) = \nabla\tilde{\phi}(-x)$ and $\nabla\theta(x) = -\nabla\tilde{\theta}(-x)$. This is nothing but the conservation of density and as we will soon see the inversion of the current. In such an inversion a cross term $\nabla\phi\nabla\theta$ would change sign and thus cannot appear in the energy. Thus, the most general Hamiltonian describing the low-energy properties of a *massless* one-dimensional system is

$$H = \frac{\hbar}{2\pi}\int dx[\frac{uK}{\hbar^2}(\pi\Pi(x))^2 + \frac{u}{K}(\nabla\phi(x))^2] \tag{3.25}$$

where I have put back the $\hbar$ for completeness. This leads to the action (see Appendix C)

$$S/\hbar = \frac{1}{2\pi K}\int dx\, d\tau[\frac{1}{u}(\partial_\tau\phi)^2 + u(\partial_x\phi(x))^2] \tag{3.26}$$

Parameters u and K are used to parameterize the two unknown coefficients in front of the two operators. These two coefficients *totally* characterize the low-energy properties of *any* massless one-dimensional system. In the absence of a good perturbation theory (e.g. in the interaction), it is difficult to compute these coefficients. Nevertheless, once they are fixed, all properties of the system are determined.

This is a very important step. It shows that *all* the bosonization formulas that we have established in the previous chapter are in fact non-perturbative. They are totally generic (provided all the harmonics are included). That was the only artefact of the Tomonaga–Luttinger model. Otherwise, all the properties, representation in terms of bosons of the various operators, calculation of the

correlation functions, phase diagram, etc., are generic and apply to *any* one-dimensional model. The bosonic representation and Hamiltonian (3.25) play in fact the same role for one-dimensional systems than the Fermi liquid theory plays for higher-dimensional systems. It is an effective low-energy theory that is the fixed point of all massless theories.[16] This theory, which is known as Luttinger liquid theory, depends only on the two parameters u and K. Provided that the correct value of these parameters are used, *all* asymptotic properties of the correlation functions of the system can be obtained *exactly* using (3.8) and (3.10) for bosons (or (3.21) for fermions).

Let me be more specific and show explicitly how to compute the correlation functions, using the standard operator technique. A calculation using the functional integral is given in Appendix C. Let us compute

$$G_{\phi\phi}(x,\tau) = \langle [\phi(x,\tau) - \phi(0,0)]^2 \rangle \tag{3.27}$$

Let us absorb the factor K in the Hamiltonian by rescaling the fields (this preserves the commutation relation)

$$\begin{aligned} \phi &= \sqrt{K}\tilde{\phi} \\ \theta &= \frac{1}{\sqrt{K}}\tilde{\theta} \end{aligned} \tag{3.28}$$

The fields $\tilde{\phi}$ and $\tilde{\theta}$ are expressed in terms of bosons operator as (2.23). It is easy to check (see the previous chapter) that Hamiltonian (3.25) with $K = 1$ is simply

$$\tilde{H} = \sum_{p\neq 0} u|p| b_p^\dagger b_p \tag{3.29}$$

This can be checked by a direct substitution of (2.23) in (3.25). In the limit $L \to \infty$ topological excitations are not important and can be ignored, so only the bosonic part remains. If $K \neq 1$ had still been there in the Hamiltonian the boson expression would have contained the unpleasant terms bb and $b^\dagger b^\dagger$. These terms should then have been diagonalized by a Bogoliubov transformation (Mahan, 1981) on the bosons. The rescaling of the fields is thus the equivalent of this Bogoliubov transformation and much simpler. The time dependence of the field can now be easily computed from (3.29), (2.23), and (A.25). This gives

$$\phi(x,\tau) = -\frac{i\pi}{L}\sum_{p\neq 0}\left(\frac{L|p|}{2\pi}\right)^{1/2}\frac{1}{p}e^{-\alpha|p|/2-ipx}(b_p^\dagger e^{u|p|\tau} + b_{-p}e^{-u|p|\tau}) \tag{3.30}$$

Beware that for operators the average $\langle\ \rangle$ means time-ordered product (see Appendix A) so just for the next few lines I put back explicitly the time-ordered

[16] There are of course some exceptions, otherwise life would be too simple.

product and denote $\langle\ \rangle_0$ the averages without the time-ordered product, that is, simply $\mathrm{Tr}[e^{-\beta(H-\mu N)}\ldots]/Z$

$$\begin{aligned} G_{\phi\phi}(x,\tau) &= K\langle T_\tau[\tilde{\phi}(x,\tau)-\tilde{\phi}(0,0)]^2\rangle_0 \\ &= 2K[\langle\tilde{\phi}(0,0)\tilde{\phi}(0,0)\rangle_0 - Y(\tau)\langle\tilde{\phi}(x,\tau)\tilde{\phi}(0,0)\rangle_0 \\ &\quad - Y(-\tau)\langle\tilde{\phi}(0,0)\tilde{\phi}(x,\tau)\rangle_0] \end{aligned} \tag{3.31}$$

where Y is the step function (see Appendix A). One then plugs (3.30) in (3.31). The calculation is thus reduced to the averages of factors such as

$$\langle b_p^\dagger b_{p'}\rangle_0 = \delta_{p,p'} f_B(\epsilon_p = u|p|) \tag{3.32}$$

and factors such as $bb^\dagger = 1 - b^\dagger b$ that can be easily reduced to the above form. f_B is the standard Bose factor. At $T=0$ since $\epsilon_p > 0$ (remember that $p \neq 0$ for the bosons modes) $f_B(\epsilon_q) = 0$. Thus, (3.31) becomes (taking the standard limit $L \to \infty$)

$$\begin{aligned} G_{\phi\phi}(x,\tau) &= K\int_0^\infty \frac{dp}{p} e^{-\alpha p}[1 - e^{-u|\tau|p}\cos(px)] \\ &= \frac{K}{2}\log\left[\frac{x^2+(u|\tau|+\alpha)^2}{\alpha^2}\right] \end{aligned} \tag{3.33}$$

Thus, up to the small cutoff α, this is essentially $\log(r)$ where r is the distance in space–time. This invariance by rotation in space–time reflects the Lorentz invariance of the action. One can introduce

$$\begin{aligned} r &= \sqrt{x^2+y_\alpha^2} \\ y_\alpha &= u\tau + \alpha\mathrm{Sign}(\tau) \end{aligned} \tag{3.34}$$

The same calculation with θ instead of ϕ gives exactly the same result with $1/K$ instead of K. One can either do it directly or notice that the Hamiltonian is invariant by $\phi \to \theta$ and $K \to 1/K$. Calculation of the $\phi\theta$ correlation function can be done exactly in the same way to give

$$\begin{aligned} G_{\phi\theta}(x,\tau) &= \langle T_\tau\phi(x,\tau)\theta(0,0)\rangle_0 \\ &= -\frac{i}{2}\mathrm{Sign}(\tau)\int_0^\infty \frac{dp}{p} e^{-\alpha p} e^{-u|\tau|p}\sin(px) \\ &= -\frac{i}{2}\mathrm{Sign}(\tau)\ \arctan\left[\frac{x}{u|\tau|+\alpha}\right] \end{aligned} \tag{3.35}$$

Since the time ordering product has a minus sign for fermions and a plus sign for bosons when permuting two operators one should in fact add an extra phase (see Appendix C) when computing correlation functions of objects such as (3.21). As explained in Appendix C this changes (3.35) into

$$G_{\phi\theta}(x,\tau) = -i\ \mathrm{Arg}(y_\alpha - ix) \tag{3.36}$$

where Arg is the argument of the complex number with a cut on the negative axis (i.e. for $a < 0$ $\mathrm{Arg}(a \pm i\epsilon) = \pm\pi$). This coincides with (3.35) for $x > 0$

and $\tau > 0$ but is different for $x < 0$ and $\tau < 0$. Since this extra phase is $\pm\pi$ it disappears in all other correlation functions of a *physical* quantity since the ϕ and θ fields appear with integer coefficients. One can thus always take (i.e. for $a < 0$ $\mathrm{Arg}(a \pm i\epsilon) = \pm\pi$) (3.36) for the $\phi - \theta$ correlations. More details and the expressions at finite temperature are given in Appendix C.

To compute exponentials of the fields one simply uses that for an operator A that is *linear* in terms of boson fields and a quadratic Hamiltonian one has (see Appendix C)

$$\langle e^A \rangle = e^{\frac{1}{2}\langle A^2 \rangle} \tag{3.37}$$

Thus, for example

$$\begin{aligned} \langle e^{i2\phi(x,\tau)} e^{-i2\phi(0,0)} \rangle &= e^{-2\langle [\phi(x,\tau)-\phi(0,0)]^2 \rangle} \\ &= e^{-2G_{\phi\phi}(x,\tau)} \end{aligned} \tag{3.38}$$

If from (3.8) we compute

$$\langle \rho(x,\tau)\rho(0) \rangle \tag{3.39}$$

we obtain, using (3.8) and the formulas of Appendix C (compare with (2.68))

$$\begin{aligned} \langle \rho(x,\tau)\rho(0) \rangle = \rho_0^2 + \frac{K}{2\pi^2} \frac{y_\alpha^2 - x^2}{(x^2 + y_\alpha^2)^2} + \rho_0^2 A_2 \cos(2\pi\rho_0 x) \left(\frac{\alpha}{r}\right)^{2K} \\ + \rho_0^2 A_4 \cos(4\pi\rho_0 x) \left(\frac{\alpha}{r}\right)^{8K} + \cdots \end{aligned} \tag{3.40}$$

Here, the lowest distance in the theory is $\alpha \sim \rho_0^{-1}$. The amplitudes A_i are non-universal objects. They depend on the precise microscopic model, and even on the parameters of the model. For example, for the Luttinger model introduced in Section 2.1, all amplitudes except A_2 are strictly zero, since only $q = 0$ and $q = 2k_F$ terms exist (keep in mind that for spinless fermions $\rho_0 = k_F/\pi$). Other examples will be examined in Chapter 7. Contrary to the amplitudes A_n, which depend on the precise microscopic model, the power-law decay of the various terms are *universal*. They *all* depend on the unique Luttinger coefficient K. Similarly, one can compute the single-particle Green's function. For the Luttinger model it had only a power law decay for Fourier components around $\pm k_F$ (see (2.83)). In fact, (3.21) shows that power law decay also occurs at $\pm 3k_F$, $5k_F$, etc., albeit with a higher exponent also controlled by K (Ogata and Shiba, 1990; Penc and Sólyom, 1991; Penc *et al.*, 1996).

The fact that *all* asymptotic properties are controlled by the *unique* parameter K is a remarkable result, as important as the theory of Fermi liquids for higher-dimensional systems. This result can be used in two ways that we will illustrate in the remaining of this book. Either one likes to work with a specific microscopic model. In that case, to get the low-energy properties of this model, it is *enough* to compute by one way or the other the two coefficients u and K. Since they control all correlation functions, and in particular the thermodynamics (see (2.46)), it is relatively easy and accurate to do this. This can

be done either analytically, using perturbation if the interactions are small, or by exact solutions as we will see in Chapter 5. Alternatively, if no exact solution is available these coefficients can be determined numerically as we will discuss in more details in Section 5.2. Since these coefficients can be extracted from thermodynamic quantities they are much less sensitive to finite size effects than the correlation functions themselves. The Luttinger liquid theory thus provides, coupled with the numerics, an incredibly accurate way to compute correlations and physical properties of a system.

But, of course, a much more important use of Luttinger liquid theory is to justify the use of the boson Hamiltonian and fermion–boson relations as starting points for any microscopic model. The Luttinger parameters then become some effective parameters. They can be taken as input, based on general rules (e.g. for fermions $K > 1$ means attractive interactions and $K < 1$ repulsive interactions), without any reference to a particular microscopic model. This removes part of the caricatural aspects of any modelization of a true experimental system. This use of the Luttinger liquid is reminiscent of the one made of Fermi liquid theory. Very often calculations are performed in solids starting from 'free' electrons and adding important perturbations (such as the BCS attractive interaction to obtain superconductivity). The justification of such a procedure is rooted in the Fermi liquid theory, where one does not deal with 'real' electrons but with the quasiparticles, which are intrinsically fermionic in nature. The mass m and the Fermi velocity v_F are then some parameters. The calculations in $d = 1$ proceed in the same spirit with the Luttinger liquid replacing the Fermi liquid. The Luttinger liquid theory is thus an invaluable tool to tackle the effect of perturbations on an interacting one-dimensional electron gas (such as the effect of lattice, impurities, coupling between chains, etc.). I will illustrate such use in the following chapters.

Now might be a good point to read the previous chapter if you skipped it, to get all the details on the bosonization procedure. A summary of the dictionary between bosons and fermions and the Luttinger liquid relations is given in Appendix D.

For systems with spins (or any flavor index) one can of course use the same procedure. Each species can be bosonized separately as we saw in Chapter 2.3 and I refer the reader to this section for details. For two species it is usually useful to introduce the charge and spin combinations $\phi_{\rho,\sigma} = (\phi_\uparrow \pm \phi_\downarrow)/\sqrt{2}$. There is however an important point to note when one computes the correlation functions. Let us look, for example, at the density–density correlation. Using (3.8) one would write for the total density $\rho_0 = \rho_{0,\uparrow} + \rho_{0,\downarrow}$

$$\rho(x) = \rho_0 - \frac{\sqrt{2}}{\pi}\nabla\phi_\rho(x) + 2\rho_0[e^{i(2k_F x - \sqrt{2}\phi_\rho(x))}\cos(\sqrt{2}\phi_\sigma(x)) + \text{h.c.}] \\ + 2\rho_0[e^{i(4k_F x - 2\sqrt{2}\phi_\rho(x))}\cos(2\sqrt{2}\phi_\sigma(x)) + \text{h.c.}] + \cdots \quad (3.41)$$

So in the higher harmonics both ϕ_ρ and ϕ_σ appear with the same coefficient. One

would thus naively think that in the correlation functions the $4k_F$ component would decay with a power law

$$\left(\frac{\alpha}{r}\right)^{4K_\rho+4K_\sigma} \tag{3.42}$$

in the same way that the $2k_F$ component was decaying with the exponent $K_\rho + K_\sigma$. This would be true if the spin part of the Hamiltonian was strictly quadratic, that is, if $g_{1\perp}$ was zero. However, for a generic interaction, due to the presence of $g_{1\perp}$ there is a $\cos(\sqrt{8}\phi_\sigma)$ term in the Hamiltonian (see Chapter 2). If we compute the density–density correlation function this term generates in perturbation in power of $g_{1\perp}$ terms of the form

$$\rho(x,\tau)\int dx_1\, d\tau_1\, \cos(\sqrt{8}\phi_\sigma(x_1,\tau_1)) \tag{3.43}$$

which contains, from the $4k_F$ components of the density, terms of the form

$$\cos(\sqrt{8}\phi_\sigma(x,\tau))\int dx_1\, d\tau_1\, \cos(\sqrt{8}\phi_\sigma(x_1,\tau_1)) \tag{3.44}$$

If the points (x,τ) and (x_1,τ_1) are separated this term leads after averaging to an additional power law decay and is thus in general less relevant than the terms containing only the $\cos(\sqrt{8}\phi_\sigma)$ term coming from the density. However, if (x_1,τ_1) is very close (within a cutoff distance α) of (x,τ) then one can approximate (3.44) as

$$\frac{\alpha^2}{u}\cos(\sqrt{8}\phi_\sigma(x,\tau))^2 \simeq \frac{\alpha^2}{2u}[1+\cos(2\sqrt{8}\phi_\sigma(x,\tau))] \tag{3.45}$$

$\cos(2\sqrt{8}\phi_\sigma)$ is an operator that leads to correlations decaying rapidly (with an exponent $16K_\sigma$) and is thus quite irrelevant. But we see from (3.45) that the seemingly irrelevant operator (3.44) is in fact *asymptotically* constant. It means that to compute the asymptotic decay of the $4k_F$ part of the correlation function one should compute, in presence of the $g_{1\perp}\ \cos(\sqrt{8}\phi_\sigma)$ term in the Hamiltonian, the decay of

$$\langle e^{i(4k_Fx-2\sqrt{2}\phi_\rho(x))}e^{i(2\sqrt{2}\phi_\rho(0))}\rangle \sim \left(\frac{\alpha}{r}\right)^{4K_\rho} \tag{3.46}$$

This leads to a much smaller power law decay than naively anticipated. Thus, a more faithful expression for the density operator would be

$$\rho(x) = \rho_0 - \frac{\sqrt{2}}{\pi}\nabla\phi_\rho(x) + \rho_0[e^{i(2k_Fx-\sqrt{2}\phi_\rho(x))}\cos(\sqrt{2}\phi_\sigma(x)) + \text{h.c.}] + \rho_0[e^{i(4k_Fx-2\sqrt{2}\phi_\rho(x))} + \text{h.c.}] \tag{3.47}$$

Remember that in the above sum, the precise coefficients in front of the cosines are meaningless since they are non-universal and depend on the ultraviolet cutoff of the theory.

The total density correlation function in a Luttinger liquid with spins is thus given by

$$\langle\rho(x,\tau)\rho(0)\rangle = \rho_0^2 + \frac{K}{\pi^2}\frac{y_\alpha^2 - x^2}{(x^2+y_\alpha^2)^2} + \rho_0^2 A_2 \cos(2\pi\rho_0 x)\left(\frac{\alpha}{r}\right)^{K_\rho+K_\sigma} + \rho_0^2 A_4 \cos(4\pi\rho_0 x)\left(\frac{\alpha}{r}\right)^{4K_\rho} + \cdots \quad (3.48)$$

The difference is important. In the naive answer one is always dominated by the $2k_F$ component of the density since the $4k_F$ one would be always less relevant. In fact, since the $4k_F$ component does not depend on the spin part, we see that (given that $K_\sigma = 1$ for spin isotropic repulsive interactions) for $K_\rho < 1/3$ the system is dominated by the $4k_F$ component of the density. This has important consequences to which I will come back in Chapters 4 and 7.

This example shows that one should be extremely careful when taking an operator to estimate its dimension. Contractions with other operators as in (3.44) can lead to a part that decays *more slowly* than each of the original operators. This is the well-known operator product expansion (Cardy, 1996). It is particularly crucial in one dimension since most of the operators are cosine like, and it is very easy to obtain squares of cosines as in (3.45). We will thus have many occasions to see this phenomenon again.

3.2 Semiclassical and physical interpretations

Many of the formulas that have been derived have simple physical interpretations. Let us examine some of them in this chapter and other interpretations will be apparent as we proceed with new examples.

First, the field ϕ is obviously related to the density of particles. Since the long wavelength part of the density is simply $\rho(x) = -\nabla\phi(x)/\pi$ we see immediately two facts, illustrated in Fig. 3.2. Let us add a single-particle. A particle at point x_0 would manifest itself as a kink in ϕ since $\rho(x) = \delta(x - x_0)$. Since

$$\int_{-\infty}^{x>x_0} dx'\, \rho(x') = 1 = \frac{-1}{\pi}[\phi(x) - \phi(-\infty)] \quad (3.49)$$

one sees that the step in ϕ is quantized and is a measure of the total charge added in the system. The converse is of course true. If we solve some model and find some kink-like excitations for ϕ then we can interpret these excitations as some charge carrying excitations whose charge (not necessarily integer) is given by (3.49). This gives a very simple interpretation for the single-particle operator. Since it is an operator creating a charge at point x is should create a π kink in ϕ for $x' \in]-\infty, x]$. In quantum mechanics the operator that translates some variable is the exponential of the conjugate variable. If $[X, P] = i\hbar$

$$Xe^{-iaP} = e^{-iaP}(X + a\hbar) \quad (3.50)$$

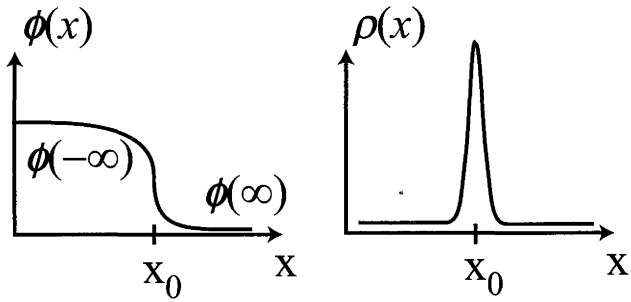

FIG. 3.2. A kink in ϕ at point x_0 corresponds to the creation of a particle at this point. The amplitude of the kink gives the charge of the particle. Thus, soliton excitations in ϕ define the quantum number of the 'particles' in the system.

Thus, the operator creating a charge 1, that is, a kink of amplitude π in ϕ is ($\hbar = 1$)

$$e^{-i\int_{-\infty}^{x} dy \pi \Pi(y)} = e^{-i[\theta(x)-\theta(x=-\infty)]} \tag{3.51}$$

For bosons this is all we need and we see that we recover our formula (3.10). The term $\theta(x = -\infty)$ is a simple choice of phase. It can safely be dropped in *physical* operators such as $\psi_B^\dagger$ since this phase always appears multiplied by an integer number. It would not be true if operators such as $e^{i\nu\theta}$ with ν non-integer would be considered. Although the theory in terms of the fields ϕ and θ can be pathological due to the non-local nature of θ these pathologies disappear when one computes physical objects. For fermions one sees that such an operator cannot be a fermionic creation operator since two such operators at different points would commute and not anticommute. One has thus to multiply it by a phase factor that gives a minus sign when commuting two operators. Using the relation (A.8) and the fact that the commutator between ϕ and θ is the sign function (see (2.24)), it is easy to check that

$$\psi^\dagger(x) \propto e^{i(\pm\phi(x)-\theta(x))} \tag{3.52}$$

does the job. Of course, one has to introduce an operator that changes the *global* charge by one (this is the Klein factor of (2.30)). Since this operator spreads the charge in the whole space it cannot give any contribution in the thermodynamic limit (beyond a global sign). Then the bosonic operator (3.52) ensures that this charge is concentrated at a given point in space. It is thus the only important part when computing correlation functions.

The fields ϕ and θ are very convenient variables since they give rise to semi-classical interpretations. ϕ allows for a semiclassical interpretation of the density operator. If we take a constant ϕ, then the long wavelength part of the density ($\nabla\phi$) vanishes and only the modulated part remains. The density is

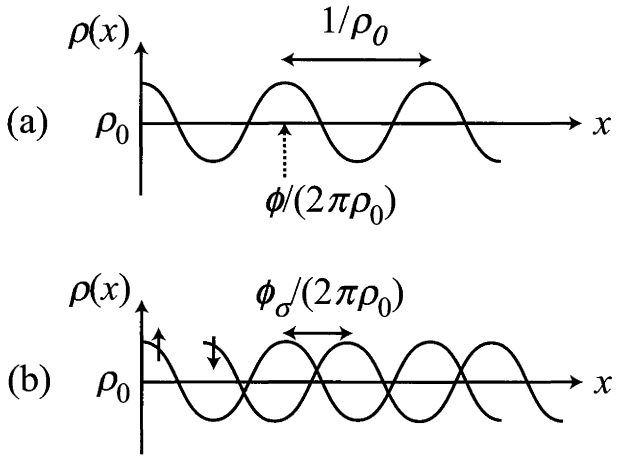

FIG. 3.3. A classical representation of the density. The field ϕ gives the position of the maxima of a wave of density. For systems with spins ϕ_ρ gives the maxima of charge, whereas ϕ_σ is the offset between the spin $\uparrow$ and $\downarrow$ density waves.

$$\rho(x) \propto \rho_0 \cos(2k_F x - 2\phi) \tag{3.53}$$

One can thus see the density as a density wave of period $2k_F$ or $2\pi\rho_0$ in general (see (3.8)). The value of ϕ gives the position of the maxima of the density, as shown in Fig. 3.3. For a system with spin the fields ϕ_ρ and ϕ_σ have a similar interpretation. One has for the density of each spin species in the approximation where ϕ is a constant:

$$\begin{aligned} \rho_\uparrow(x) &\propto \cos(2k_F x - \sqrt{2}\phi_\rho - \sqrt{2}\phi_\sigma) \\ \rho_\uparrow(x) &\propto \cos(2k_F x - \sqrt{2}\phi_\rho + \sqrt{2}\phi_\sigma) \end{aligned} \tag{3.54}$$

Thus, ϕ_ρ gives the phase of the charge density whereas ϕ_σ is the dephasing between the $\uparrow$ and $\downarrow$ density waves. As shown in Fig. 3.3, if $\phi_\sigma = 0$ the two waves are in phase. The spin density then is zero and the charge is modulated. On the contrary, if $\phi_\sigma = \pi/2\sqrt{2}$, the two densities are in opposite phase and thus the total charge is constant whereas the spin is modulated. One thus recovers the expressions for the various CDW and SDW_z operators (2.113).

Of course, this perfect wave exists only if the field ϕ orders. We will see such cases in the subsequent chapters. For Hamiltonian (3.25) the field ϕ fluctuates, which means that the precise phase of the wave changes with space and time and thus the correlation between different points of the wave are lost. This is what gives rise to the power law decay of the various density correlations. This interpretation in terms of wave also allows to derive the current. One can use the continuity equation

$$\frac{\partial \rho}{\partial t} + \nabla j = 0 \tag{3.55}$$

which together with the expression for the long wavelength part of the density (3.9) gives $j = \partial_t \phi/\pi$. One can interpret this result by saying that for a wave

$$\rho(x) = \rho_0 + \rho_0 \cos(2\pi\rho_0 x - 2\phi) \tag{3.56}$$

which has the proper average density, a change of phase of ϕ by π corresponds to the motion of a charge ρ_0 by a distance $1/\rho_0$. Using that the current is $j = \rho_0 v$ and taking for v the phase velocity gives back the expression for the current. The field θ has similar interpretations in terms of the phase of the particles (3.10). It is analogous to the standard superconducting phase in a BCS wavefunction. Such an interpretation allows to also recover the current from the standard expression (see, e.g. in a superconductor, Tinkham 1975). The possibility to have classical representations in mind is one of the great advantages of the boson representation, and specially of the ϕ, θ field representation. Indeed, if these fields are ordered, they are identical to the familiar mean field expressions for either a superconductor (θ) or a density mean field theory (ϕ). The fact that these fields are conjugate shows that their fluctuations compete and Hamiltonian (3.25) reflects this competition. The possibility for these bosonic fields to order also drastically simplifies the analysis of some strong coupling limit of the Hamiltonian.

Let us complete our tour of the semiclassical interpretations by looking at the excitations of a system with spins. As we saw the Hamiltonian separates into two parts, a charge part and a spin part. As a result, single-particle fermionic excitations do not exist. The excitations are the ones described by the fields ϕ_ρ and ϕ_σ. Let us represent again our ground state by a state in which ϕ_ρ and ϕ_σ are constant. For repulsive interactions this leads to a SDW. If now we remove a fermion it means that at a single site we create a kink *both* in ϕ_ρ and ϕ_σ. These two excitations are free to propagate completely independently. In the fermion language let us see what happens if we let the hole propagate as shown in Fig. 3.4(a). In that case one reaches the state of Fig. 3.4(b). At one point there is a site where a charge is lacking but the spin environment is purely antiferromagnetic. This corresponds to an excitation that is a kink in ϕ_ρ but no disturbance in ϕ_σ. This excitation is known as a holon. In another part of the system there is a place where no charge is missing but we have two neighboring spin up. This is a spin excitation with a spin 1/2 compared to the ground state. This excitation is known as a spinon, and corresponds to a kink in ϕ_σ. In one dimension, we see that the spinon and holon are free to separate, and thus any single-particle excitation dissociates into these elementary excitations. In higher dimension if we reproduce our cartoon, we see that because of the presence of other chains the spinon and the holon would be separated by a string of frustrated bonds. Indeed, all the spins between the spinon and the holon are parallel to the ones of the neighboring chains. This costs the antiferromagnetic exchange, and thus the spinon and holon are held together by a string whose energy grows linearly with the distance. They are thus confined and their bound state is the single-particle fermionic excitation.

Finally, let me define for (3.25) the two fields (see (C.46))

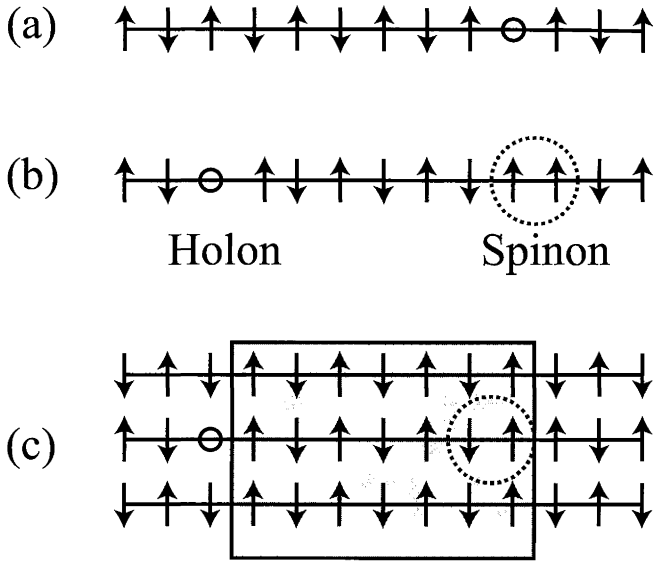

FIG. 3.4. In a one-dimensional system a single-particle excitation (a) is converted into an excitation that contains only charge degrees of freedom (holon) and spin degrees of freedom (spinon). This is represented schematically in (b). In (c) one sees that in a higher-dimensional system the spinon and holon would be held together by a string whose energy cost grows with distance. They thus form a bound that is the single-particle fermionic excitation.

$$\begin{aligned} \phi_R &= K\theta - \phi \\ \phi_L &= K\theta + \phi \end{aligned} \tag{3.57}$$

and the corresponding 'densities'

$$\tilde{\rho}_{R,L} = \pm\frac{1}{2\pi}\partial_x\phi_{R,L} \tag{3.58}$$

It is easy to check from (2.28) that for the non-interacting case $K = 1$ the $\tilde{\rho}_{R,L}$ do coincide for fermions with the densities of right and left movers. This is of course not the case for the interacting case, but the fields $\phi_{R,L}$ have interesting properties. First, they commute between each other and satisfy (using (2.24))

$$[\phi_R(x), \phi_R(x')] = -[\phi_L(x), \phi_L(x')] = i\pi K \operatorname{Sign}(x - x') \tag{3.59}$$

The total density $\tilde{\rho}_R + \tilde{\rho}_L$ is the true total density in the system (using (3.9)). These fields diagonalize Hamiltonian (3.25), which can be rewritten as

$$\frac{1}{4\pi K}\int dx[(\partial_x\phi_R)^2 + (\partial_x\phi_L)^2] \tag{3.60}$$

These fields thus satisfy the equation of motion

$$\frac{\partial \tilde{\rho}_{R,L}}{\partial t} = i[H, \tilde{\rho}_{R,L}] = \mp \partial_x \tilde{\rho}_{R,L} \tag{3.61}$$

Thus, the densities $\tilde{\rho}_{R,L}$ (and the fields $\phi_{R,L}$) are only functions of $x - ut$ and $x + ut$. These fields describe excitations that propagate only in the right (resp. left) direction. For this reason they are called chiral fields. They are the generalization to the interacting case of the right and left free fermions. In presence of interactions right and left fermions interact. But one can still find an excitation (that contains both right and left fermions) that propagates solely to the right or to the left. I will come back to these fields in Chapter 10.

3.3 Links with 2D statistical mechanics

There are many links between the one-dimensional Luttinger liquid problem and classical systems in $1 + 1$ dimension. This mapping between a quantum system in d dimensions and a classical system in $d + 1$, where the (imaginary) time direction plays the role of an extra spatial dimension, is of course very familiar. Path integral representation (see Appendix C) is a very convenient way to show such connections. It is of course a great advantage to be able to make such connections between different physical models since one can borrow the knowledge of one to solve the other. Let me examine here more precisely some of those links.

3.3.1 *Elastic systems*

Let us consider a classical crystal where we denote by R_i^0 the equilibrium position of the particles, and by u_i the displacements relative to their equilibrium positions. The interaction between the particles of the crystal can be approximated by an elastic Hamiltonian. Although it is possible in principle to stick to the lattice, it is much more convenient to go to the continuum. The Hamiltonian becomes

$$H = \frac{c}{2} \int d^d r (\nabla u(r))^2 \tag{3.62}$$

where c is the elastic constant. Of course, a true elastic Hamiltonian has more complicated (bulk, tilt, and shear) coefficients, but this isotropic elasticity will be enough for our purposes. The elastic approximation assumes that $|u_{i+1} - u_i| \ll a$. Let us take a scalar displacement and a two-dimensional system x, z. This represents a crystal of lines along the z direction as shown in Fig. 3.5. The Hamiltonian of our classical crystal is

$$H = \frac{c}{2} \int dx\, dz [(\nabla_z u(x,z))^2 + (\nabla_x u(x,z))^2] \tag{3.63}$$

It is exactly identical to the action (3.26) of the one-dimensional quantum problem (where the velocity has been absorbed in the change of variables $z = u\tau$).

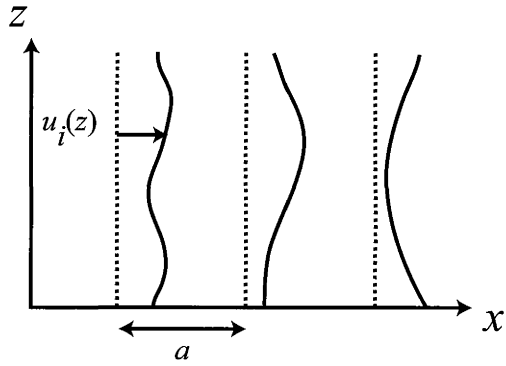

FIG. 3.5. A crystal of lines is defined by a scalar displacement $u_i(z)$ which in the continuum limit along x becomes the function $u(x, z)$. This classical system in its elastic limit is equivalent to a Luttinger liquid. The lines can be viewed as the space–time trajectories of the particles.

System	Quantum	Classical
Dimension	d	d+1
β	Temperature	$u\beta\hbar$ = Size of system in direction z
$\hbar$	quantum fluctuations	Temperature

Table 3.1 *Equivalence between a quantum system of dimension d and a classical system in dimension* $d+1$

The lines of our elastic system can be viewed as the space–time trajectories of the quantum particles (Pollock and Ceperley, 1987). As usual $u\beta\hbar$ for the quantum problem is the size along z of the classical problem, which is defined on a torus to ensure the periodicity. The elastic constant c is equivalent to $1/(\pi K)$ for the quantum problem, whereas T the temperature of the classical problem plays the role of $\hbar$ for the quantum problem. For a quantum system at zero temperature $\beta = \infty$ the role played by quantum fluctuations (whose amplitude is controlled by $\hbar$) is equivalent to the role played by the thermal fluctuations (controlled by T) in the two-dimensional classical system. Since we see that the combination $1/\hbar K$ (for quantum) or c/T (for classical) appears, changing K (or c for classical) is a way to control the amount of fluctuations in the system. The equivalence is recalled in Table 3.1. Since by changing the interactions in the system one changes the amount of quantum fluctuations, one-dimensional systems are a paradise for quantum phase transitions (Sachdev, 1998).

To go further let us express the density of the crystal in the continuum limit. The density is

$$\rho(x) = \sum_i \delta(x - R_i^0 - u_i) \tag{3.64}$$

To go to a continuum limit as we did for the elastic Hamiltonian is a little tricky. Indeed, one has to keep the discrete nature of u_i in (3.64) even if we performed the continuous limit in H. This is due to the fact that we want to have the density at scales comparable or smaller than the lattice spacing itself. This is relevant for systems such as vortices in type II superconductors (Tinkham, 1975) for which the lattice spacing is in fact quite large and thus many things (e.g. disorder) can vary at a lengthscale much shorter than the lattice spacing. It is thus crucial to remember the discrete nature of the lattice to compute the density at a given point r. On the other hand, we know (this is the elastic limit) that u itself varies very slowly at the scale of the lattice spacing a so we can use this fact to simplify (3.64). To derive the density for the classical crystal (Giamarchi and Le Doussal, 1995) we proceed exactly along the same lines and in the same spirit than the one we used to derive the phenomenological bosonization in the previous section. In order to take the continuum limit, one can introduce a smooth displacement field $u(r, z)$ by

$$u(r) = \int_{BZ} \frac{d^d q}{(2\pi)^d} e^{iqr} \sum_j e^{-iqR_j^0} u_j \tag{3.65}$$

such that $u(R_i) = u_i$ and which has no Fourier components outside of the Brillouin zone (BZ). In terms of the smooth field (3.65) one can introduce the relabelling field

$$\phi(r) = r - u(\phi(r)) \tag{3.66}$$

In the absence of dislocations there is a unique solution of (3.66) giving $u(r)$ as a function of $\phi(r)$. ϕ is the equivalent of ϕ_l of the quantum problem. At the location of the particles ϕ takes the integer value

$$\phi(R_i^0 + u_i) = R_i^0 \tag{3.67}$$

Substituting (3.66) in (3.64) one gets

$$\rho(r) = \sum_i \delta(R_i^0 - \phi(r)) \det[\partial_\alpha \phi_\beta(r)] \tag{3.68}$$

Using the integral representation of the δ function, (3.68) becomes

$$\rho(r) = \det[\partial_\alpha \phi_\beta] \int \frac{d^d q}{(2\pi)^d} \rho_0(q) e^{iq\phi(r)} \tag{3.69}$$

where

$$\rho_0(q) = \sum_i e^{iqR_i^0} \tag{3.70}$$

is the density of the associated perfect system. For the case of a perfect lattice $\rho_0(q)$ is

$$\rho_0(q) = \rho_0 (2\pi)^d \sum_K \delta(q - K) \tag{3.71}$$

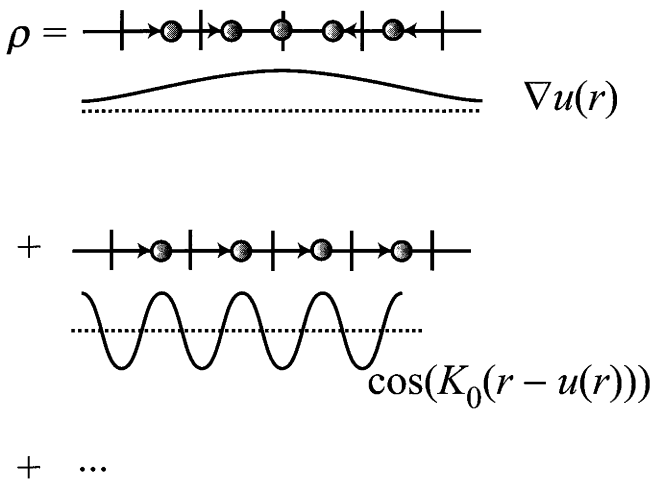

FIG. 3.6. Equation (3.73) realizes a Fourier decomposition of the density relative to the wavevectors corresponding to the lattice spacing. It is easy to see physically that the $q \sim 0$ component is $-\rho_0 \nabla u$. A variation of the density at the scale of the lattice spacing can be decomposed in $\cos(K_n(r-u))$ where a constant (at the scale of the lattice spacing) u would just shift the peaks of the cosine. K_n are the vectors of the reciprocal lattice. Putting all harmonics together gives back (3.73).

where K are the vectors of the reciprocal lattice. Using (3.71) in (3.69) one gets

$$\rho(r) = \rho_0 \det[\partial_\alpha \phi_\beta] \sum_K e^{iK\cdot\phi(r)} \tag{3.72}$$

Assuming that we are in the elastic limit $\partial_\alpha u_\beta \ll 1$ one can expand (3.72) to get

$$\rho(r) \simeq \rho_0[1 - \partial_\alpha u_\alpha(\phi(r)) + \sum_{K\neq 0} e^{iK(r-u(\phi(r)))}] \tag{3.73}$$

In (3.73), one can replace $u(\phi(r))$ by $u(r)$ up to terms of order $\partial_\alpha u_\beta \ll 1$. Note that in doing so u has negligible Fourier components outside the Brillouin zone, and thus there is a complete decoupling between the gradient term and higher K terms. We have realized a sort of Fourier decomposition of the density, separating terms varying at lengthscales much larger than the lattice spacing, from Fourier components varying with harmonics of the periodicity of the lattice. This can be schematically seen in Fig. 3.6. This representation of the density for a classical crystal holds provided we can define the labelling field. Physically this means that one can number in a unique way the atoms of the crystal. This is obviously possible if there are no defects such as dislocations in the crystal. For our two-dimensional crystal of lines this is always possible since one can always number

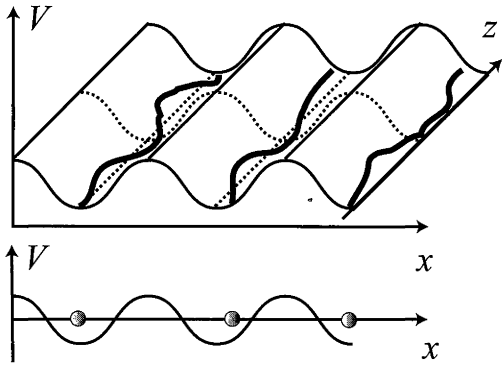

FIG. 3.7. A classical crystal in a potential periodic in the direction x (tin roof potential). This is analogous to a quantum problem on a lattice with a commensurate filling, and gives rise to the Mott transition.

the lines starting from (say) the left in a unique way. The formula for the density (3.73) is exactly identical to the one of our Luttinger liquid with $\phi/\pi = \rho_0 u$. One can thus carry the identity between the quantum problem and the crystal made of lines completely. For example, if one adds to the crystal a periodic potential $V(x,z) = V_0 \cos(K_0 x)$, which is shown in Fig. 3.7, this corresponds to a term in the classical Hamiltonian

$$H = \int dx\, dz\, V(x,z)\rho(x,z) \simeq V_0 \int dx\, dz\, \cos(K_0 u(x,z)) \tag{3.74}$$

using (3.73) and keeping only the terms that do not oscillate since the other terms vanish in the continuum limit. We recognize a sine-Gordon term. This problem is in fact analogous to the Mott transition that we will examine in detail in Section 4.2: the lines are pinned by the tin roof potential and would of course like to sit in the minima, but thermal fluctuations are shaking them. Which wins corresponds for the quantum problem to the Mott transition.

This equivalence is quite interesting. First, it provides a simple physical picture to help understanding the perhaps less intuitive quantum problem. It shows also clearly the spirit behind our representation procedure. We can define fields that vary slowly at the scale of the lattice, and the energy is a smooth function of these fields (displacements for the classical problem, field ϕ for the quantum one). We can thus retain *only* the long wavelength components of these fields (and thus take the continuum limit for them). However, the various operators can vary at a lengthscale comparable to the lattice (e.g. the density) and one cannot directly take the continuum limit for them. However, it is possible to express them as some involved functions of the slowly varying fields. We have thus gained a direct continuum representation, and thus a faithful low-energy description of the system in terms of simple fields. The price to pay is that the

operators themselves are complicated and hide in their form the complexity of the original (microscopic) problem.

Second and more important, the problem of a classical crystal submitted to various perturbations is of course a crucial problem of statistical mechanics. Fermion representation thus represent an interesting route to tackle such problems (and vice versa). For more details on various works on classical crystals I refer the reader to Blatter *et al.* (1994), Nattermann and Scheidl (2000) and Giamarchi and Bhattacharya (2002).

3.3.2 *Coulomb gas and XY model*

The equivalence between the Luttinger liquid and the crystal of lines was very direct. I examine now a more involved mapping based on the fact that the density of the system contains terms of the form $e^{i\phi}$. Let us consider a two-dimensional classical XY model, where on each site a classical spin is

$$\vec{S} = (\cos(\phi), \sin(\phi)) \tag{3.75}$$

The Hamiltonian of the system is

$$H = -\frac{J}{2}\sum_{i,a}\cos(\phi(i+a) - \phi(i)) \tag{3.76}$$

where a is a set of nearest neighbors vectors. The density–density correlations for the Luttinger liquid thus correspond to the spin–spin correlation of the XY model, if once again we assimilate one of the directions (say y) of space for the classical model to the imaginary time direction for the quantum problem and the field ϕ for the phase of the spin. What about the Hamiltonian? If ϕ was a smooth field one could expand

$$\phi(i+a) - \phi(i) = \vec{a}\cdot\vec{\nabla}\phi \tag{3.77}$$

and the XY Hamiltonian would become in the continuum limit (for a square lattice)

$$H_{XY} = \frac{J}{2}\int dx\, dy[(\nabla_x\phi)^2 + (\nabla_y\phi)^2] \tag{3.78}$$

that is, identical to our favorite elastic Hamiltonian in two dimensions. We know for the XY model that this expansion is valid provided that the temperature is low enough (Berezinskii, 1971; Kosterlitz and Thouless, 1973; Kosterlitz, 1974). At higher temperatures the XY model undergoes a transition (Berezinskii–Kosterlitz–Thouless or BKT) towards a disordered phase. For the low-temperature phase of the XY model we thus have equivalence with our LL Hamiltonian H_0. We know that at higher temperatures, vortex configurations, where the angle ϕ is singular, start to be important. Such a configuration is shown in Fig. 3.8. We can easily see that such a configuration should exist. Indeed, if one considers $\int dr\nabla\phi$ over a closed loop it should give $2\pi n$ since ϕ is defined modulo 2π. If

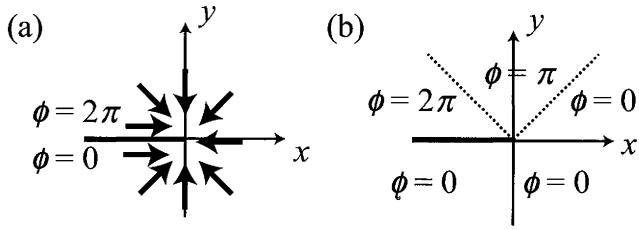

FIG. 3.8. (a) A vortex configuration for the classical XY model. (b) For the Luttinger liquid the operator $\cos(2\theta)$ creates such a vortex configuration.

only spin waves (smooth configurations of ϕ) are allowed, this integral is zero. Vortices should thus be added to H_0.

Let us now see how one could for the quantum problem create such a vortex. We start from a configuration where on each point (space, time) the field ϕ takes the value zero. This would correspond in the XY equivalence to a system where all spins point in the x direction. We saw in Section 3.2 that the operator $e^{i2\theta(x)}$ creates a kink of amplitude 2π on ϕ. Thus, if we apply $e^{i2\theta(x_0,\tau_0)}$ to our uniform configuration, it means that just after the time τ_0, ϕ has been shifted by 2π on the left of the point x_0. This leads to the configuration shown on Fig. 3.8(b). This configuration can be smoothly deformed to the more standard representation of a vortex (shown on Fig. 3.8(a)). The operator $e^{i2\theta(x)}$ (with the time ordering) is thus the vortex creation operator for the field ϕ. Since the Hamiltonian and commutation relations are symmetric the reverse is true and the operator $e^{i2\phi(x)}$ will create vortices in the field θ.

One can thus expect the analogy between the XY model and the Luttinger liquid to hold provided that these operators are included. To formalize this let us consider a Hamiltonian

$$H = H_0 + g_\phi \int dx\ \cos(\sqrt{8}\phi) + g_\theta \int dx\ \cos(\sqrt{8}\theta) \tag{3.79}$$

and compute the partition function. It is given by

$$Z = \sum_{n=0}^{\infty} \frac{1}{n!} \int d^2r_1\, d^2r_2 \cdots d^2r_n \langle (\frac{g_\phi}{u} \cos(\sqrt{8}\phi(r_1)) + \frac{g_\theta}{u} \cos(\sqrt{8}\theta(r_2))) \cdots$$
$$(\frac{g_\phi}{u} \cos(\sqrt{8}\phi(r_n)) + \frac{g_\theta}{u} \cos(\sqrt{8}\theta(r_n)))\rangle \tag{3.80}$$

a correlation function containing an arbitrary product of exponential factors of ϕ and θ is easily evaluated (see (C.38)). Let us take $g_\theta = 0$ to illustrate the result simply. Only even powers are non-zero, and if one expresses the cosine as $\sum_{\epsilon=\pm} e^{i\epsilon\sqrt{8}\phi}$ only 'neutral' configurations $\sum_i \epsilon_i = 0$ give a non-zero contribution. In that case one can arbitrarily take $\epsilon_1, \ldots, \epsilon_p = +1$ and $\epsilon_{p+1}, \ldots, \epsilon_{2p} = -1$. In that case the partition function is simply given by

$$Z = \sum_{p=0}^{\infty} \frac{1}{(p!)^2} \int d^2r_1\, d^2r_2 \cdots d^2r_{2p}\, g_\phi^{2p} e^{\sum_{i<j}[\epsilon_i\epsilon_j 4K]F_1(r_i - r_j)} \tag{3.81}$$

This is exactly the partition function of a gas of classical particles of fugacity g_ϕ (Chui and Lee, 1975). The exponential term can be identified with $e^{-E_{\text{class}}/T_{\text{class}}}$ where T_{class} and E_{class} are the temperature and the energy of the classical system. One can thus describe the classical system as a gas of classical charges that carry a charge ± 1, are at the 'temperature' $1/T_{\text{class}} = 2K$, and interact with each other with a potential $V(r_i - r_j) = -2F_1(r_i - r_j) \sim -2\log(r_i - r_j)$. Because of the form of the correlation functions in the LL only neutral configurations are allowed. This problem is exactly the well-known Coulomb gas problem in two dimensions. Indeed, a logarithmic potential satisfies the Poisson equation (see (2.126))

$$\Delta V(r) + 4\pi\delta(r) \tag{3.82}$$

The sine-Gordon model thus maps exactly to the Coulomb gas problem, which is known to be equivalent to the two-dimensional classical XY model (Kosterlitz, 1974). Our more complicated Hamiltonian (3.79) has also a simple Coulomb gas interpretation. We can still view the partition function as the partition function of a mixture of classical particles of two types with respective fugacities g_ϕ/u and g_θ/u. The first type are charged particles with charges $\pm\sqrt{K}$ interacting with the Coulomb potential $-2F_1$. The second type are magnetic monopoles with magnetic charges $\pm 1/\sqrt{K}$ interacting through the magnetic potential $-2F_1$. Indeed, taking Maxwell's equation it is easy to check that if a density of magnetic monopoles exists it will generate a magnetic potential obeying the same Poisson's equation than normal charges since

$$\nabla \cdot B(x) = \rho_m(x) \tag{3.83}$$

The $\phi\theta$ correlation F_2 describes the interaction between the charges and the magnetic monopoles. If a charge makes a circle around the origin then its phase must only change by a multiple of 2π due to the flux that its trajectory has enclosed. Computing this flux (Ahronov–Bohm flux) gives back F_2. Our complete Hamiltonian (3.79) can thus be viewed as a mixture of charges and magnetic monopoles, each species needing to have only neutral configurations.

Given the amount of physics known for the XY model and Coulomb gases, such mappings are extremely useful. For example, we can directly borrow the results for the BKT phase transition in the XY model to infer the existence of a quantum phase transition for the sine-Gordon problem and extract the properties of the various phases. This is what we did in Chapter 2, directly on the sine-Gordon Hamiltonian. We will see other applications in Chapter 4.4. The trick works of course both ways and one can use the fermionic approach to tackle interesting questions for the classical problems (Lecheminant *et al.*, 2002).

3.4 Basics of conformal theory

We have seen that the correlation of a Luttinger liquid in the massless phase corresponds to the correlation functions of a classical two-dimensional system that sits exactly at criticality. For such systems it is known for a long time that the correlation functions are invariant by a large class of transformations. These include, for example, the continuous rotation (between x and τ direction), and scale transformations. In addition, the systems at criticality are invariant by a much broader class of transformations: the conformal transformations. These are the transformations that preserve the angles between a triplet of points. Such transformations obviously include the rotations, symmetries such as reflection etc., and the dilatations. In three dimensions, there are not many more operations in the conformal group than these simple transformations. The situation is however quite different in two dimensions. In that case the conformal group is very large, and the fact that the correlation functions are invariant by such transformations provides severe constraints and allows to extract a lot of relevant information without effort. Since the scope of the conformal theory exceeds largely the level of this book, I refer the reader to Cardy (1996) and Di Francesco *et al.* (1997) for more details. Here we will just illustrate the power of the method on a few examples.

The idea of the conformal method is to generalize the scale invariance of a theory that is at criticality. If one takes, for example, a classical system that is at a critical point, the correlation functions decay as power laws. As a result a critical theory is invariant under rescaling. If ψ_i denotes fields of the theory one has

$$\langle \psi_1(r_1)\psi_2(r_2)\cdots\psi_n(r_n)\rangle = b^{-\nu_1}b^{-\nu_2}\cdots b^{-\nu_n}\langle \psi_1(r_1')\psi_2(r_2')\cdots\psi_n(r_n')\rangle \quad (3.84)$$

where $r_i' = b^{-1}r_i$. The quantities ν_i are the scaling dimensions of the operators ψ_i in the theory. For example, for a simple two-point correlation function

$$\langle \psi(r_1)\psi(r_2)\rangle \sim \left(\frac{1}{r_1 - r_2}\right)^{2\nu} \quad (3.85)$$

The rescaling is obviously satisfied with $\nu_1 = \nu_2 = \nu$. There are other transformations that can leave the correlation functions unchanged or trivially changed. This is, for example, the case of rotations or translations. In a critical theory one has thus simple transformations of the original coordinates for which we know exactly how to transform the correlation functions. The idea of the conformal theory is to generalize these transformations to a change of coordinates that are *locally* simple rescalings, rotations, or translations. If the Hamiltonian has only local interactions then one can expect that such a *local* transformation only affects the properties of the whole system locally and thus that one can still use the transformation formulas for the correlation functions if the points at which the correlations are computed are very far from each other. In other words, one can generalize formula (3.84) to obtain the asymptotic properties. The transformations that are locally identical to dilatations, rotations, translations are known

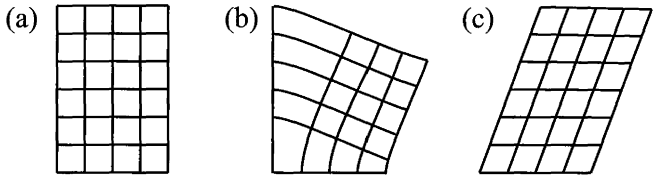

FIG. 3.9. (b) An example of a conformal transformation. It preserves locally the angles of the original lattice (a). (c) A forbidden transformation that causes shear in the coordinates.

as conformal transformations (they have to locally preserve angles). An example of such transformations is shown on Fig. 3.9. Such conformal transformations preserve locally the metric (length of an infinitesimal segment) of the system. Thus, if $r = (x_1, x_2, \ldots, x_n)$

$$\sum_i dx_i' \, dx_i' = b(r)^{-2} \sum_i dx_i \, dx_i \tag{3.86}$$

The 'number' of such conformal transformations depends very much on whether one is in three or two dimensions. In three dimensions, the group of conformal transformations has a finite number of parameters, and thus is not much more useful than the simple original transformations. In two dimensions, however, the situation is quite different. It is very useful in two dimensions to parametrize a point $r = (x, y)$ using the complex number $z = x + iy$. Using this parametrization the metric becomes

$$(dx)^2 + (dy)^2 = dz \, d\overline{z} \tag{3.87}$$

Upon a general transformation one has

$$dz' \, d\overline{z}' = \left(\frac{\partial z'}{\partial z} dz + \frac{\partial z'}{\partial \overline{z}} d\overline{z} \right) \left(\frac{\partial \overline{z}'}{\partial z} dz + \frac{\partial \overline{z}'}{\partial \overline{z}} d\overline{z} \right) \tag{3.88}$$

This transformation satisfies (3.86) if and only if

$$\frac{\partial z'}{\partial \overline{z}} = \frac{\partial \overline{z}'}{\partial z} = 0 \tag{3.89}$$

Thus, in the transformation z' depends only on z and $\overline{z}'$ only on $\overline{z}$. It means that *any* analytic function f of a complex variable z can generate a conformal transformation $z' = f(z)$. If one uses such a transformation the rescaling factor is, from (3.88) and (3.86)

$$dz' \, d\overline{z}' = |f'(z)|^2 dz \, d\overline{z} \tag{3.90}$$

and thus

$$b(r) = |f'(z)|^{-1} \tag{3.91}$$

The subgroup corresponding to rotations, dilatations, translations, and inversion is the so-called Möbius transformations

$$z' = \frac{Az + B}{Cz + D} \tag{3.92}$$

with $AD - BC \neq 0$. Of course, the fact that any analytic function can generate a conformal transformation gives an incredible number of possibilities. To write the transformation for the correlation functions we generalize (3.84) to a local transformation with (3.91)

$$\begin{aligned}\langle \psi_1(z_1, \overline{z}_1) \cdots \psi_n(z_n, \overline{z}_n) \rangle &= |f'(z_1)|^{\nu_1} \cdots |f'(z_n)|^{\nu_n} \\ &\times \langle \psi_1(z_1' = f(z_1), \overline{z}_1' = f(\overline{z}_1)) \cdots \psi_n(z_n' = f(z_n), \overline{z}_n' = f(\overline{z}_n)) \rangle \end{aligned} \tag{3.93}$$

Let us take a correlation function that can be written in terms of the complex variable z as

$$G(z_1, z_2) = \left(\frac{1}{z_1 - z_2}\right)^h \left(\frac{1}{\overline{z}_1 - \overline{z}_2}\right)^{\overline{h}} \tag{3.94}$$

Note[17] that $\overline{h}$ is not the complex conjugate of h but an independent real quantity. For example, for the correlation function (3.85) $h = \overline{h} = \nu$. If we now make a change of variables $z \to z'$, the correlation function transforms as

$$G(z_1', z_2') = \left[\frac{dz_1}{dz_1'}\right]^{h/2} \left[\frac{dz_2}{dz_2'}\right]^{h/2} \left[\frac{d\overline{z}_1}{d\overline{z}_1'}\right]^{\overline{h}/2} \left[\frac{d\overline{z}_2}{d\overline{z}_2'}\right]^{\overline{h}/2} G(z_1, z_2) \tag{3.95}$$

Formula (3.95) does not look much but is incredibly powerful. It allows us to obtain the correlation function in *any* restricted geometry that can be obtained by a conformal transformation of the plane. Here, let us just see how the use of conformal theory allows to get back the correlation functions at finite temperature. They can of course also be directly computed by standard methods (see Appendix C) but the conformal derivation is very general and can work for other geometries as well. At zero temperature the correlation function is simply

$$G(x, y = u\tau) = \left(\frac{1}{x^2 + y^2}\right)^{\nu} = \left(\frac{1}{z\overline{z}}\right)^{\nu} \tag{3.96}$$

G is thus a function of both z and $\overline{z}$. At $\beta = \infty$ the point (x, y) covers the whole complex plane. At finite temperatures the imaginary time is only between $\tau = 0$ and $\tau = \beta$ with periodic boundary conditions. We thus have to compute the correlation function on a torus, as shown in Fig. 3.10. We can make a conformal

[17] Notations are weird, but since they are the ones you find in the literature ... *vox populi, vox dei.*

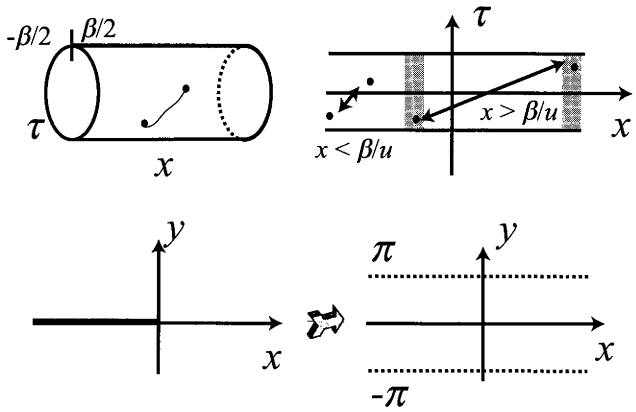

FIG. 3.10. Torus for finite-temperature correlation functions. When the distance between points is larger than β the system realizes that it is at finite temperature and becomes equivalent to a one-dimensional classical system. The bottom part shows that the complex plane with a cut on the negative real axis can be mapped on a torus by a conformal transformation. Thus, if we know the correlation functions at $\beta = \infty$ we also know them at any finite temperature.

transformation mapping the infinite plane into a torus. Such a transformation is obviously

$$z' = \frac{\beta}{2\pi} \log(z) \tag{3.97}$$

This imposes to put a cut in the complex plane. A possible choice is shown in Fig. 3.10. With this choice the imaginary part of the log is between $-\pi$ and $+\pi$. Transformation (3.97) thus maps the plane into a torus of size β along the imaginary axis. Let us call the correlation function on the torus

$$G(z_1', z_2', \overline{z}_1', \overline{z}_2') \tag{3.98}$$

Because of the translational invariance in space and time one can always take $z_2' = \overline{z}_2' = 0$. We can now use (3.95). We relate a point z' on the torus to a point z in the infinite plane by

$$z = e^{2\pi z'/\beta} \tag{3.99}$$

which is the inverse of (3.97). Equation (3.95) thus gives the correlation function on the torus in terms of the correlation function in the infinite plane whose expression (3.96) we know. Using

$$\frac{dz_1}{dz_1'} = \frac{2\pi}{\beta} e^{2\pi z_1'/\beta} \tag{3.100}$$

one obtains

$$G_{\text{torus}}(z_1', z_2' = 0, \overline{z}_1', \overline{z}_2' = 0) = \left[\frac{2\pi}{\beta} e^{2\pi z_1'/\beta}\right]^{\nu/2} \left[\frac{2\pi}{\beta} e^{2\pi \overline{z}_1'/\beta}\right]^{\nu/2} \left[\frac{2\pi}{\beta}\right]^{\nu} \times G_{\text{plane}}(z_1(z_1'), z_2 = 1, \overline{z}_1(\overline{z}_1'), \overline{z}_2 = 1) \quad (3.101)$$

We have used that $z(z' = 0) = 1$ from (3.99). Using expression (3.96) for the correlation function in the plane one gets

$$G_{\text{torus}}(z_1', z_2' = 0, \overline{z}_1', \overline{z}_2' = 0) = \frac{(\pi/\beta)^{2\nu}}{(\sinh(\pi z_1'/\beta)\ \sinh(\pi \overline{z}_1'/\beta))^{\nu}} \quad (3.102)$$

Expression (3.102) is exactly the expression that we got in Appendix C doing the boson averages at finite temperatures.

Let us comment on this result. At zero temperature the correlation function decays with an exponent

$$G(r) \sim \left(\frac{1}{r}\right)^{2\nu} \quad (3.103)$$

where $r = \sqrt{x^2 + (u\tau)^2}$. At finite temperatures, as long as both x and the time τ are much smaller than β the system has no way to know that it is on a torus, and thus that it is not a truly *two* dimensional (classical) system. The correlation function thus still reflects the criticality of the infinite two-dimensional system. When x becomes much larger than β, the correlation function can 'feel' the finite size of the torus, as illustrated in Fig. 3.10. In that case the system is in fact like a classical one-dimensional system and its correlation function has to decay exponentially with a certain characteristic lengthscale ξ. It is obvious that the crossover occurs when $x \sim \beta$ and that $\xi \sim \beta$. The full behavior of the correlation function is illustrated in Fig. 3.11. Using (3.102) and expanding for large x, we find that

$$G(x \to \infty, \tau) \sim e^{-2|x|\nu/\beta} \quad (3.104)$$

leading to

$$\xi = \beta \frac{2\nu}{\pi} \quad (3.105)$$

We thus see that indeed the correlation length ξ is proportional to β as could be expected but the proportionality coefficient is *precisely* fixed by the exponent of the critical theory. Thus, computing exponential decay of the correlation function at finite β is also a way to obtain the exponent for the infinite system. Of course a similar analysis can be done to study finite size effects in space (see, e.g. Cazalilla, 2002).

The conformal method is extremely powerful since it allows trivially to take into account all possible geometries, and thus many possible boundary conditions. This is specially useful when coupled with an RG calculations. Indeed, when some coupling goes to strong coupling one can often view its effect as

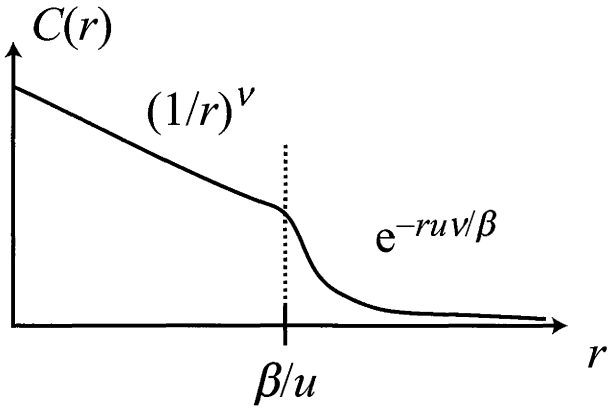

FIG. 3.11. Full behavior of the correlation functions at finite temperatures. Beyond the thermal length $\xi = \beta u$ the decay of the correlations become exponential instead of a power law. A good approximation is thus to consider that all correlations are lost beyond this lengthscale and that the system is like at zero temperature below.

a simple constraint on the field ϕ. This constraint correspond to a change in boundary conditions that can be taken into account using the conformal theory. We will see some examples in Section 10.1 and Section 11.2.

Besides the simple correlation functions the conformal invariance allows to predict many properties. Of special importance is the size dependence of the energy of the ground state. For the boson model (3.25) this is again something that can be computed directly from the boson representation. But the result is much more general than for the quadratic Hamiltonian (3.25). I will not give here the demonstration of the formula for the energy since it is rather involved and refer the reader to Belavin *et al.* (1984), Cardy (1996) and Di Francesco *et al.* (1997) for more details. For a conformally invariant theory, the size dependence of the energy of the ground state is

$$\epsilon_0 - \frac{E(L)}{L} = \frac{c\pi u}{6L^2} \tag{3.106}$$

where ϵ_0 is the ground state energy per unit length in the thermodynamic limit, u is the velocity of the massless mode. c is a number that is only dependent on the type of conformal theory, that is, on the very nature of the model and is known as the central charge. It roughly gives the number of independent bosons in the theory. For the quadratic Hamiltonian of the Luttinger liquids the conformal charge is $c = 1$, as can be checked by a direct calculation of (3.106) from the boson Hamiltonian. Such a relation can be very useful to compute the Luttinger liquid parameter u. I will come back to the calculation of the Luttinger liquid parameters in Chapter 5.

4

REFINEMENTS

Now that we have all this useful information, it would be nice to do something with it. (Actually, it can be emotionally fulfilling just to get the information. This is usually only true, however, if you have the social life of a kumquat.)

Unix Programmer's Manual

In this chapter, I present some additional complications that arise in addition to the simple Luttinger liquid theory of the previous two chapters. This chapter can thus be skipped for a first reading. After you have become familiar with your favorite microscopic model and want to treat a specific example you can come back to this chapter since there is a great chance that some way or the other you will need the material presented here.

4.1 Long-range interactions

Let us start with the simplest modification of the Luttinger liquid. We have now a fairly complete description of a system with finite range interactions. At the level of the LL description the change of range of the interaction does not change much. It just removes some bounds on the minimal value of K_ρ as we will see in Chapter 7. The physics of a system with truly long-range interactions for which the $q \sim 0$ Fourier component of the interaction is not finite is quite different. Such a term can be provided by the Coulomb interaction in a situation where it cannot be screened. Let me consider an interaction $V(x)$ with an arbitrary spatial dependence. This corresponds to a term

$$H = \frac{1}{2}\int dx\, dx'\, V(x-x')\rho(x)\rho(x') = \frac{1}{2\Omega}\sum_q V(q)\rho(q)\rho(-q) \tag{4.1}$$

Since we are mostly interested in the long-range part of the interaction one can keep in the density only the $q \sim 0$ part. Other Fourier components give contributions that fall in the general framework of the LL. The $q \sim 0$ part of the density is simply given by (3.9). Since the potential only involves the total density the $q \sim 0$ component does not affect the spin part of the Hamiltonian (beware, this would not be true for the $2k_F$ part). The interaction thus becomes

$$\frac{1}{\Omega\pi^2}\sum_q V(q)q^2\phi_\rho(q)^*\phi_\rho(q) \tag{4.2}$$

The full Hamiltonian (3.25) can thus be written

$$\tilde{H} = \sum_q \frac{u_\rho(q)}{2\pi\Omega} \left[K_\rho(q)\pi^2 \Pi(q)^* \Pi(q) + \frac{1}{K_\rho(q)} q^2 \phi(q)^2 \phi(q) \right] \tag{4.3}$$

where $u_\rho(q)$ and $K_\rho(q)$ are defined exactly as in (2.42) but with q dependent interactions

$$\begin{aligned} u_\rho(q) K_\rho(q) &= v_F \\ \frac{u_\rho(q)}{K_\rho(q)} &= v_F(1 + \frac{2V(q)}{\pi v_F}) \end{aligned} \tag{4.4}$$

Since Hamiltonian (4.3) is still quadratic one can compute the correlation functions exactly with the same technique used in Appendix C, simply keeping the q dependence of the coefficients $u_\rho(q)$ and $K_\rho(q)$ in the integrals over q. Two cases are possible.

If $V(x)$ has a finite Fourier transform for $q \to 0$ then the Luttinger parameters tend to a constant at very small q. The asymptotic (large distance or time) form of the correlation functions is thus exactly identical to the ones one would get by putting $u_\rho(q = 0)$ and $K_\rho(q = 0)$ in the LL expressions (see (2.71)). The asymptotic behavior of the system is thus identical to the one with a delta function interaction whose strength is simply $V(q = 0)$. Of course, there is a complicated crossover regime, but one can in principle compute it if one knows $V(q)$. We thus see that a system with any short-range interaction (that is, one for which $\int dx\ V(x)$ is finite), falls into the category of LL, that is, presents power law correlation functions.

On the other hand, if $V(x)$ is sufficiently long-range such that the Fourier transform at $q \to 0$ diverges, then the q dependence of the interactions is *crucial* to obtain the asymptotic properties and should be kept explicitly. A physical example is the case of the Coulomb potential between particles. In a macroscopic three-dimensional system made of one stacked one-dimensional chain the bare Coulomb potential between the electrons is screened by the presence of other electrons (Schulz, 1983). On the other hand, one can also realize single channels of one-dimensional electrons (quantum wire) that we will examine in more details in Section 9.3. Such systems are like a finite size confining potential of width d in which the electrons can propagate, as indicated in Fig. 4.1. In such systems the Coulomb potential can only be screened by external electrons (such as the ones in a gate). If such electrons are not present the electrons in the wire feel the bare Coulomb potential. The charges are spread over a width d, thus we can replace the system by a purely one-dimensional system at distances larger than d (which plays here the role of our lower distance cutoff α or lattice spacing). At distance larger than d, the particles feel the potential

$$V(r) = \frac{e^2}{4\pi\epsilon|r|} \tag{4.5}$$

where e is the charge of one electron, and ϵ the dielectric constant of the system. For distances smaller than d the $1/r$ behavior of the potential for point

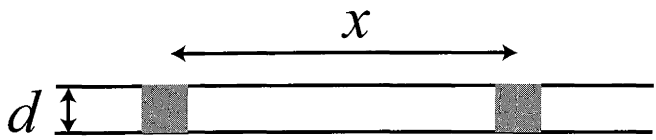

FIG. 4.1. A caricature of a quantum wire. The electrons are spread over a width d. As a result, charges at a distances larger than d see the bare Coulomb potential. The $1/r$ behavior gets cut at short distances due to the finite size of the wire.

charges is cut by the finite size d of the transverse wavefunction of the electrons inside the wire. The precise form of the potential depends on the precise shape of the wavefunction and thus on the shape of the well, but one can take the phenomenological form (Gold and Ghazali, 1990):

$$V(r) = \frac{e^2}{\kappa\sqrt{r^2 + d^2}} \tag{4.6}$$

where we have called $\kappa = 4\pi\epsilon$.[18] This form has the advantage to have a simple Fourier transform

$$V(q) = 2\frac{e^2}{\kappa} K_0(|q|d) \tag{4.7}$$

where K_0 is the Bessel function. The $q \to \infty$ behavior is dependent on the precise cutoff but the $q \to 0$ part is universal since it only reflect the divergence of the Fourier transform of the $1/r$ potential

$$V(q \to 0) \sim \int dx \frac{1}{x} \sim \log(1/q) \tag{4.8}$$

A more correct expression for $V(q)$ could thus be

$$V(q) = 2\frac{e^2}{\kappa} K_0(|q|d) + C(d) \tag{4.9}$$

where $C(d)$ is a constant that has a logarithmic dependence in d. In fact, (4.9) separates the short-range part $|x - x'| < d$ of the Coulomb interaction from the long-range part $|x - x'| > d$ for which the q dependence is crucial. Using (4.9) we can now extract from (4.3) the physical properties of the electron gas in presence of long-range interactions.

The first modification due to the long-range interaction shows up in the spectrum. For the charge mode the spectrum is given by

$$\omega(q) = u_\rho(q)|q| = \left(\frac{4v_F e^2}{\pi\kappa}\right)^{1/2} |q| \log^{1/2}\left(\frac{1}{qd}\right) \tag{4.10}$$

[18] for the nostalgics of the c.g.s. unit system.

whereas the spin sector which is not affected by the long-range interaction still has a linear dispersion relation $\omega(q) \sim u_\sigma |q|$. In the absence of long-range interactions the charge mode would also have a linear dispersion relation corresponding to the sound waves of the density oscillations. The long-range interactions replace the sound velocity by the standard plasmon dispersion relation, which in one dimension is indeed $\omega \sim q \log^{1/2}(1/q)$. By the way, the plasmon dispersion relation can be derived easily in any dimension by writing the elastic-like Hamiltonian (4.3) for the oscillations of the density. In dimension greater than one it is only useful for the collective modes, whereas in one dimension it gives all the excitations.[19] The Fourier transform of $1/r$ is by simple dimensional analysis

$$\begin{aligned} V(q) &\sim \log(1/q), \quad d=1 \\ V(q) &\sim 1/q, \quad d=2 \\ V(q) &\sim 1/q^2, \quad d=2 \end{aligned} \tag{4.11}$$

which immediately leads to

$$\begin{aligned} \omega(q) &\sim q \log^{1/2}(1/q), \quad d=1 \\ \omega(q) &\sim q^{1/2}, \quad d=2 \\ \omega(q) &\sim \text{cste}, \quad d=3 \end{aligned} \tag{4.12}$$

The difference between the charge and spin dispersion relation has been observed in one-dimensional quantum wires as shown in Fig. 4.2.

One could naively think that except for the small logarithmic correction in the spectrum the effect of long-range interactions are negligible. In fact they manifest quite strongly in the correlation functions (Glazman *et al.*, 1992; Schulz, 1993). One can guess it physically by looking at relation (4.4). Formally, since $V(q) \to \infty$ when $q \to 0$ it is like if one had a 'Luttinger liquid' with $K_\rho = 0$. Thus, instead of decaying as a power law, the correlation function containing the field ϕ_ρ will decay *more slowly* than any power law. The charge part of the Hamiltonian is thus nearly completely ordered, and in any case much more ordered than in a Luttinger liquid. A calculation of the correlation, performing the integrals as explained in Appendix C, gives

$$\begin{aligned} \langle[\phi_\rho(x,\tau) - \phi_\rho(0,0)]^2\rangle_0 &= C \log^{1/2} \frac{\sqrt{x^2 + (\tilde{u}|\tau| \log^{1/2}|\tau| + \alpha)^2}}{\alpha} \\ \langle[\theta_\rho(x,\tau) - \theta_\rho(0,0)]^2\rangle_0 &= \frac{1}{C} \log^{3/2} \frac{\sqrt{x^2 + (\tilde{u}|\tau| \log^{1/2}|\tau| + \alpha)^2}}{\alpha} \end{aligned} \tag{4.13}$$

where $C = (\pi u \kappa / e^2)^{1/2} = 2K_\rho/\sqrt{\alpha_c}$, $\tilde{u} = u\sqrt{\alpha_c}$. This is to be compared with the logarithmic growth in a LL. The ϕ_ρ correlation grows more slowly in agreement

[19] Of course, there are only collective modes.

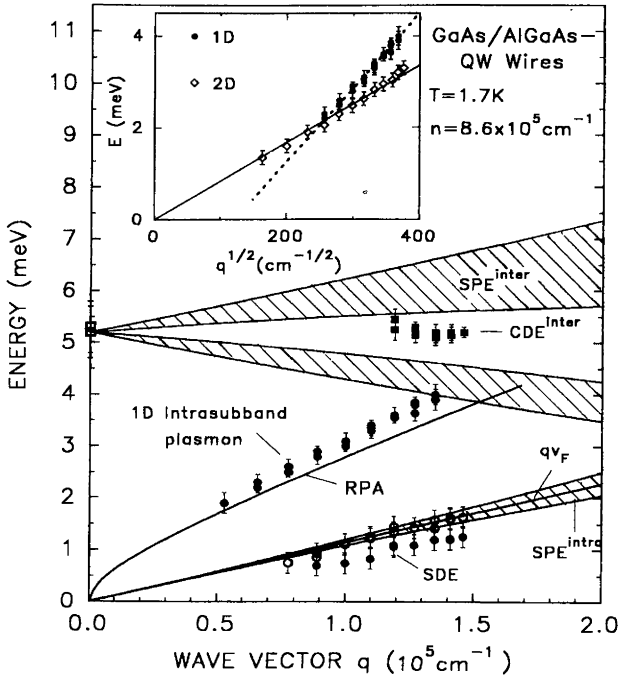

FIG. 4.2. Raman scattering on a one-dimensional quantum wire. Excitations that change the spin quantum number (bottom curve–SDE) show a linear behavior extrapolating to zero compatible with $\omega = u_\sigma|q|$. On the contrary excitations that only affect charges (intrasubband plasmon) show a 'linear' behavior but not extrapolating to zero, which is reasonably compatible with a $\omega \sim |q| \log^{1/2}(1/q)$ behavior. (From Goñi *et al.*, 1991 (Copyright (1991) by the American Physical Society).)

with our physical argument (the prefactor of the log should be $K_\rho = 0$) whereas the θ_ρ grows faster (the prefactor of the log would be $1/K_\rho = \infty$). The $2k_F$ and $4k_F$ parts of the density–density correlation function thus become (compare with (3.48))

$$\langle \rho(x)\rho(0)\rangle = \cdots + A_1' \frac{\cos(2k_F x)e^{-C\sqrt{\log x}}}{x} + A_2' \cos(4k_F x)e^{-4C\sqrt{\log x}} + \cdots \quad (4.14)$$

where A_1', A_2' are the non universal amplitudes. Since the spin part is still decaying as a power law the slowest decaying correlation is now the $4k_F$ charge density wave. This is in agreement with our argument of the previous chapter that for $K_\rho < 1/3$, $4k_F$ charge density wave correlation dominates. More importantly, the $4k_F$ correlation decays more slowly than any power law. The charge is thus as ordered as a one-dimensional system would permit given the fact that true order cannot exist, even at $T = 0$ without breaking a discrete symmetry (which

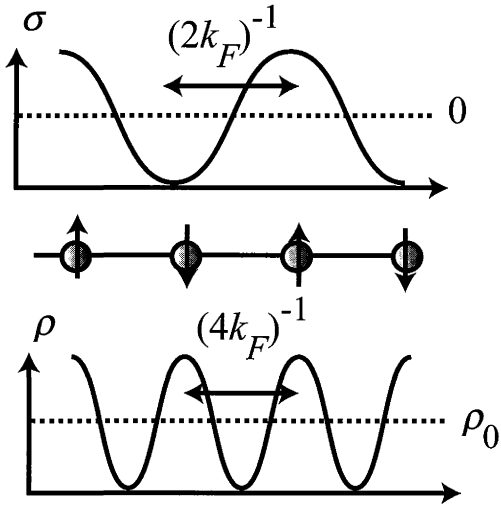

FIG. 4.3. A $4k_F$ charge density wave corresponds exactly to a modulation of the charge with the periodicity of the electronic lattice. Near order in this charge sector thus signals a tendency towards Wigner crystal formation. $2k_F$ corresponds to a periodicity of two sites and is usually the modulation corresponding to antiferromagnetic tendencies.

is not the case since there is no lattice). As shown in Fig. 4.3, a $4k_F$ charge density wave corresponds exactly to a modulation of the charge with a periodicity corresponding to the distance between the electrons. Near order means that the electrons have a strong tendency to crystallize because of the Coulomb repulsion between them. The resulting phase is thus nothing but the one-dimensional equivalent of a Wigner crystal (Wigner, 1934; Mahan, 1981). In higher dimensions, Wigner crystallization only occurs if the density is small enough so that the repulsion between particles can dominate over the kinetic energy to force the particles to crystallize. Of course, in higher dimensions a true crystal is possible where the density is perfectly ordered. In one dimension, Wigner crystallization occurs regardless of the density due to the too long-range nature of the Coulomb potential, but, on the other hand, quantum fluctuations still prevent the crystal to have perfect order. It does its best, having an order in the density–density correlation functions that decays more slowly than any power law (and thus leading to divergent Bragg peaks in a diffraction experiment). This order is to be compared to the faster decay of the density order in the Luttinger liquid phase where because of the short-range nature of the interaction the perfect crystalline order is now destroyed as a power law by the quantum fluctuations. Using the equivalence with a classical system of lines discussed in the previous chapter, the phases for the quantum problem have analogues for a two-dimensional classical crystal of lines.

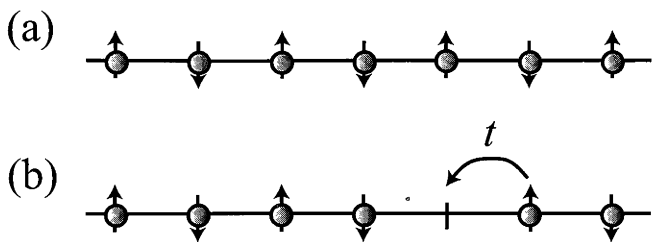

FIG. 4.4. (a) If there is one particle per lattice site and the repulsion among particles is strong, then it is more favorable to localize the particles on each site rather than to have them in plane wave states where their density is uniform. Such a state is a Mott insulator since hopping would cost an energy of the order of the interaction U among particles. All these effects concern the charge. For the spin degrees of freedom (if present) virtual hopping leads to superexchange and favors antiferromagnetic order. (b) If the system is doped the extra electrons or holes can propagate without any energy cost from the interactions and gain some kinetic energy $\sim 2t$. The system is then metallic.

4.2 Mott transition

So far we have essentially worked directly in the continuum and forgotten completely the presence of an underlying lattice on which the electrons move. We will examine specific lattice models in Chapter 7, but we can already start to explore without much effort one of the most important consequences of the existence of a lattice, namely the possibility for the electrons to give an insulator driven by the interactions known as the Mott insulator.

4.2.1 *Basic ingredients*

The physics of a Mott insulator is well-known and illustrated in Fig. 4.4. If the repulsion U among the particles is much larger than the kinetic energy t, then the plane wave state is not very favorable since it leads to a uniform density where particles experience the maximum repulsion. It is more favorable to localize the particles on the lattice sites to minimize the repulsion. If there is one particle per site it is easy to see that at large repulsion the system is an insulator. Such an insulating state driven by the interplay between lattice and interactions is known as a Mott insulator (Mott, 1949; Mott, 1990). If the system is weakly doped compared to a state with one particle per site it is clear that the holes can propagate without experiencing repulsion, the system is thus a metal again but with a number of carriers proportional to the doping. In high dimensions the Mott phenomenon is something that is widely studied as well. The above argument shows that one usually needs a finite (and in general of the order of the bandwidth) repulsion to reach that state. For further details on the Mott transition in higher dimension see Georges *et al.* (1996) and Imada *et al.* (1998).

Our boson representation should be able to capture this phenomenon as well. For that we just need to remember that a lattice exists. The existence of a lattice

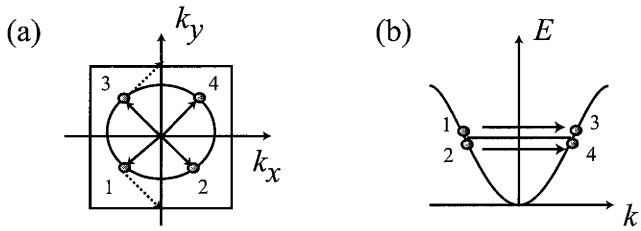

FIG. 4.5. (a) In high dimensions one can play with angles and easily get umklapp processes, practically regardless of the filling (provided $|k_F|$ is large enough). (b) In one dimension, since there is no angle to play with, one gets an umklapp process where two particles are scattered from one side of the Fermi surface to the other only if $4k_F = 2\pi$, that is, for half-filling.

means that the wavevector is in fact defined modulo a vector of the reciprocal lattice (that is, in one dimension a multiple of $2\pi/a$ with a the lattice spacing). It means that in an interaction process the momentum should now only be conserved modulo a vector of the reciprocal lattice. Thus, in addition to the processes that truly conserve momentum $k_1 + k_2 = k_3 + k_4$ one can now have processes such that $k_1 + k_2 - k_3 - k_4 = Q$ where Q is a vector of the reciprocal lattice. The electronic system can transfer momentum to the lattice and get it back. These processes are well-known and called umklapp processes.[20] Since umklapps do not conserve momentum they are the only ones that can lead to a finite resistivity, and are responsible for the T^2 law in a Fermi liquid. For these processes to contribute at low-energy one should of course look whether they occur for electrons on the Fermi surface. As shown in Fig. 4.5, in high dimension it is relatively easy to get such processes. The situation is quite different in $d = 1$. Since the Fermi surface is reduced to two points, conserving both momentum and interactions is not easy. If one wants the particles at the Fermi surface, imposing $k_1 + k_2 - k_3 - k_4 = 2\pi$ can only be realized for $4k_F = 2\pi$, that is, at half-filling. Away from such a commensurate filling the umklapp process cannot exist. This process is shown in Fig. 4.5(b). What are these terms? Let us take, for example, our favorite interaction of the form

$$H = \int dx\, U \rho_\uparrow(x) \rho_\downarrow(x) \tag{4.15}$$

when substituting the expressions for ρ in the continuum limit (2.35) one throws away the terms that are oscillating since they will be suppressed by the integration over x. This is the case for terms that contain $e^{i2k_F x}$ factors and usually terms that contain $e^{i4k_F x}$. These terms are of the form

[20] No capital since it is not the famous physicist Prof. Dr Umklapp.

$$H = \int dx\, U \frac{1}{(2\pi\alpha)^2} [e^{-i4k_F x} e^{i2(\phi_\uparrow(x)+\phi_\downarrow(x))} + \text{h.c.}]$$
$$= \int dx\, U \frac{1}{(2\pi\alpha)^2} [e^{-i4k_F x} e^{i2\sqrt{2}\phi_\rho(x)} + \text{h.c.}] \tag{4.16}$$

However, if one has a lattice and there is exactly one particle per site $4k_F = 2\pi/a$. Since $x = na$, the $e^{i4k_F x}$ is in fact equal to one and is not oscillating. The terms (4.16) are thus present in the continuum limit and should be kept. They are the one-dimensional umklapp processes. Physically these terms do correspond to the scattering of two fermions that are left movers (momentum $-k_F$) on the other side of the Fermi surface with a momentum transfer of $4k_F$ from the lattice. We thus recover that on a lattice the momentum needs only to be conserved modulo a vector of the reciprocal lattice. For spinless fermions one can make a similar calculation which will be done in Chapter 6.

Equation (4.16) shows that on a lattice for one fermion per site the charge part of the Hamiltonian becomes, because of the umklapp process,

$$H = H_0 + \frac{2g_3}{(2\pi\alpha)^2} \int dx\, \cos(\sqrt{8}\phi_\rho(x)) \tag{4.17}$$

while the spin part is unchanged. The coefficient g_3 is the strength of the umklapp process (U in our example) and of course depends on the microscopic model used. But the form of the Hamiltonian is universal. Our old friend the sine-Gordon Hamiltonian is back again. As we know from Chapter 2 this Hamiltonian has a quantum phase transition depending on the value of the parameter K_ρ. In fact, the form of the charge Hamiltonian at half-filling is exactly identical to the one of the spin Hamiltonian. This is not an accident but the consequence of a symmetry that allows to go from the charge sector to the spin sector. This symmetry, which is a particle–hole transformation on one of the spin species, will be examined in more details in the context of the specific microscopic model of Section 7.1.1.

Before we embark on the study of (4.17), let us see what happens if one wants to move away from half-filling. There are two ways to do it. The first one is to add to (4.17) a chemical potential term. This gives in boson representation (2.107). The second method is to work with a fixed number of particles. Let us call the doping d ($d = 0$ for half-filling and $d = 1$ for a filled band). Then, $4k_F = 2\pi/a + \delta$ with $d = \delta/(2\pi)$. The umklapp term has now an oscillatory factor

$$e^{i4k_F x} = e^{i\delta x} \tag{4.18}$$

If the doping is small this term oscillates with such a long wavelength that it is worth keeping it in the continuum limit. The cosine term thus becomes

$$H_u = \frac{2g_3}{(2\pi\alpha)^2} \int dx\, \cos(\sqrt{8}\phi_\rho(x) - \delta x) \tag{4.19}$$

Note that one could obtain (4.19) from (2.107) and (4.17) by absorbing the linear term in the quadratic part H_0 and introducing

$$\tilde{\phi}(x) = \phi(x) + \frac{\sqrt{2}K_\rho \mu}{u_\rho} x \tag{4.20}$$

which would give back the form (4.19). There is however an important difference. In the case of (4.19) we want to work with a fixed number of particles so δ is the true deviation from half-filling. As a result in this case

$$\langle \nabla \phi \rangle = 0 \tag{4.21}$$

whereas in the case of a chemical potential the number of particles is not fixed so $\langle \nabla \phi \rangle$ is not constrained. The field $\phi(x)$ can thus develop a linear dependence in x that would cancel the one coming from the μ term in (4.20). Physically this is the difference between a given chemical potential and a given doping. I will come back to that point later.

In fact, umklapps are not restricted to one particle per site (Giamarchi and Millis, 1992; Schulz, 1994). If we use the LL formula (3.47) with all the harmonics for the density we see that we directly recover the form of the umklapp term (4.16) by taking the $4k_F$ term of the density (the other densities in the interaction term being thus ρ_0). Keep in mind that in this formula the amplitudes are non-universal quantities. This provides us with another way to reintroduce the lattice. We could start directly from the continuum and then put back the lattice as a periodic potential acting on the electrons. To get one electron per site we need this potential to have the wavelength $4k_F$ (see Section 4.1). The interaction term is thus

$$H = \int dx\, V(x)\rho(x) = V_0 \int \cos(4k_F x)\rho(x) \tag{4.22}$$

which, keeping only the non-oscillating terms, gives back the umklapp term. I will come back in more details to this method for the case of bosons in Section 11.1. In addition to recovering the umklapp for one particle per site, the full formula for the density (3.8) shows us that we can get an umklapp term for any *commensurate* density. Indeed, if $2pk_F = 2\pi q/a$ (where p and q are integers) then the corresponding term stays in the Hamiltonian. For even commensurabilities ($p = 2n$) this gives a term

$$H_{\frac{1}{2n}} = g_{\frac{1}{2n}} \int dx\ \cos(n\sqrt{8}\phi_\rho(x))\ \cos(n\sqrt{8}\phi_\sigma(x)) \tag{4.23}$$

The spin part can be eliminated with the $\cos(\sqrt{8}\phi_\sigma(x))$ term in the Hamiltonian (see (3.44)), giving for the umklapp term

$$H_{\frac{1}{2n}} = g_{\frac{1}{2n}} \int dx\ \cos(n\sqrt{8}\phi_\rho(x)) \tag{4.24}$$

In the presence of doping one can thus write quite generally the umklapp as

$$H_{\frac{1}{2n}} = g_{\frac{1}{2n}} \int dx\ \cos(n\sqrt{8}\phi_\rho(x) - \delta x) \tag{4.25}$$

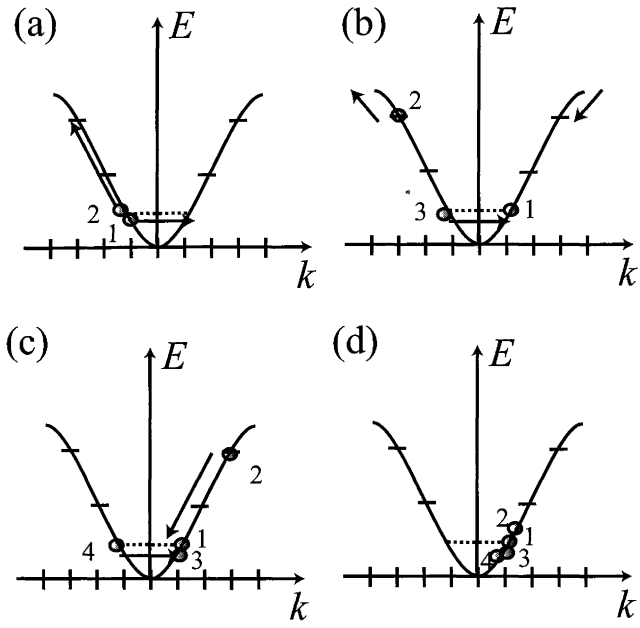

FIG. 4.6. A quarter-filled umklapp can be constructed from a third-order perturbation theory in the interaction U. Since one goes through two intermediate states of high-energy W of the order of the bandwidth, the amplitude for such a process is of order $U(U/W)^2$.

where n is the order of the commensurability ($n = 1$ for half-filling — one particle per site; $n = 2$ for quarter-filling — one particle every two sites and so on). The coupling constant $g_{1/2n}$ is the umklapp process corresponding to the commensurability n and δ the deviation (doping) from the commensurate filling. Odd commensurabilities can be treated in the same way. In that case the spin part cannot be eliminated (Schulz, 1994). I concentrate here on even commensurabilities for simplicity.

The derivation using the LL expression for the density cannot give access to the amplitudes and thus to the coefficients $g_{\frac{1}{2n}}$. For the half-filled case, using the more controlled expressions of Chapter 2 for the Luttinger model we see that in general $g_{\frac{1}{2}}$ is of the order of the interaction U. This depends of course on the specific microscopic model and we will discuss it in more details in Chapter 7. The higher commensurabilities can also be understood physically. Let us consider a quarter-filled band such that $8k_F = 2\pi$ (this corresponds to $n = 2$ in the above notations). To produce an umklapp we thus need to transfer *four* particles from one side of the Fermi surface to the other to get the proper $8k_F$ momentum transfer. This can be done in higher-order perturbation terms by doing three scatterings as shown in Fig. 4.6. For weak interactions the amplitude of such a

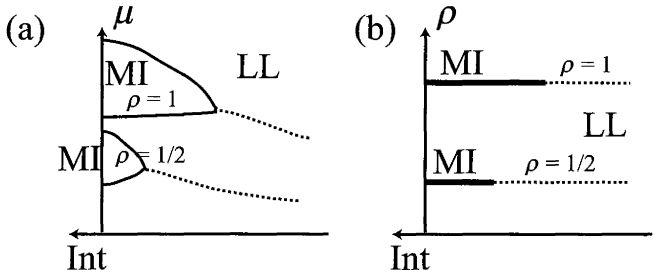

FIG. 4.7. Phase diagram of a generic system. Any commensurate filling can potentially lead to a Mott insulating (MI) phase depending on the interactions. The horizontal axis represents repulsive interactions increasing from right to left. Higher commensurabilities are the most relevant. (a) The chemical potential μ needs to exceed the Mott gap to change the density of particles. The dotted line is a line of constant density in the metallic (Luttinger liquid (LL)) phase. (b) As a function of density Mott phases only exist for commensurate densities.

process would thus be of order $U(U/W)^2$, where W is the bandwidth. Note that the two additional interaction processes correspond in the LL derivation to the two terms $g_1 \cos(\sqrt{8}\phi_\sigma(x))$ that one would have needed to introduce to cancel the spin factors in (4.23). Similar expressions can be derived for the case of bosons as we will see in Section 11.1. It is therefore remarkable that in one dimension $H_0 + H_{\frac{1}{2n}}$ provides the solution to *all* Mott transitions, for *all* systems, and *all* (for particles with spin: even) commensurabilities.

Thus, to change the physical properties of a commensurate system one has two control parameters. One can vary the strength of the interactions while staying at commensurate filling, or vary the chemical potential (or filling) while keeping the interactions constant. One can thus expect two different classes of transition to occur. The first one, when the interactions are varied will be called Mott-U. The second one Mott-δ. This leads to the phase diagram of Fig. 4.7.

4.2.2 *Commensurate case: Luther–Emery solution*

Let us deal first with the Mott-U transition. We have already encountered such a sine-Gordon Hamiltonian in Section 2.3.2 and solved it. There is a BKT (Berezinskii–Kosterlitz–Thouless) transition occurring at the critical value $K_c^* = 1/n^2$ where n is the order of the commensurability. For larger values of K the cosine is irrelevant and the system is massless. For $K < K_c^*$ the cosine is relevant and the system is massive. This opening of a gap corresponds to the Mott transition and one can guess that the system becomes an insulator. We will confirm it in Section 7.2. The larger the commensurability the smaller K needs to be for the system to become insulating. For a commensurability $n = 1$, that is, half-filling the critical value is $K = 1$. This means that any repulsive interactions turn the

system into an insulator. For a quarter-filled band ($n = 2$) the critical value is $K = 1/4$. To get the insulator one needs both pretty strong interactions *and* interactions of a finite range. This is physically obvious: in order to stabilize a structure in which there is a particle every two sites one cannot do it with purely local interactions. We thus see that the range of the interactions in addition of their strength controls the range of values of K that one is able to explore. I will come back to that point in Chapter 7.

The critical properties of the transitions are thus the ones of a BKT transition and were studied by RG in Section 2.3.2. K jumps discontinuously from the universal value K_c^* at the transition in the metallic (non-gapped) regime to zero in the Mott phase (since there is a gap). Since the velocity is not renormalized it means using (2.108) the charge compressibility goes to a constant at the transition and then drops discontinuously to zero inside the Mott phase. Note that the Mott transition involves *only* the charge degrees of freedom in one dimension and thus *all* spin properties (susceptibility, etc.) are totally unaffected by the transition. For quantum-phase transitions, in addition to the standard critical exponents it is useful to define an additional exponent (dynamical exponent) z, which tells how a characteristic length in the time direction is related to a length in the spatial direction $\xi_\tau \sim \xi_x^z$ (Sachdev, 1998). Indeed, for quantum problems, time plays a special role and this special 'direction' has no reason to have the same exponents than the spatial ones. In the Luttinger liquid phase the Hamiltonian remains quadratic up to the transition. As a result the action is of the form

$$[\omega_n^2/u + uk^2]\phi(k,\omega_n)^*\phi(k,\omega_n) \tag{4.26}$$

which means that space and time are equivalent, $\omega \sim k$. Thus, at the Mott-U transition the dynamical exponent is $z = 1$. The critical properties of the Mott transition are given in Fig. 4.8.

To study the massive phase one can of course use the approximate variational approach described in Section 2.3.2 and Appendix E. In addition, a remarkable solution was found (Luther and Emery, 1974). The procedure used is one of the most useful tricks of the bosonization method, and we will see many other applications. The Hamiltonian one wants to solve is

$$H = H_\rho^0 + g_{\frac{1}{2n}} \int dx \ \cos(n\sqrt{8}\phi_\rho(x)) \tag{4.27}$$

where H_ρ^0 is the standard quadratic Hamiltonian. One notices that for spinless fermions

$$\psi_R^\dagger(x)\psi_L(x) = \frac{1}{2\pi\alpha}e^{i2\phi(x)} \tag{4.28}$$

which is very similar to the cosine term in (4.27) but with the wrong coefficient inside the cosine. One can thus rescale the field ϕ_ρ. If we set $\tilde{\phi} = n\sqrt{2}\phi_\rho$, Hamiltonian (4.27) becomes

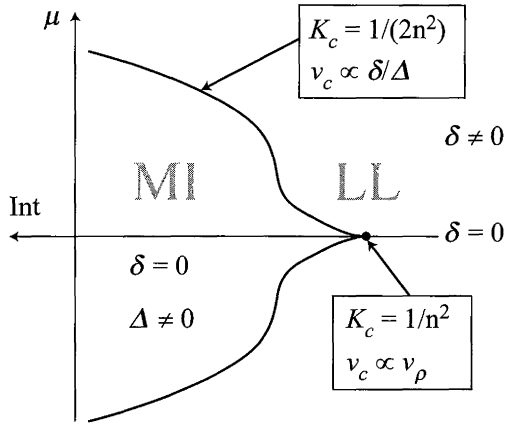

FIG. 4.8. Phase diagram close to a commensurability of order n ($n = 1$ for half-filling and $n = 2$ for quarter-filling). Int denotes a general (that is, not necessarily local) interaction (repulsion). μ is the chemical potential, δ the doping and Δ the Mott gap. MI means Mott insulator and LL the Luttinger liquid (metallic) phase. The critical exponent K_c and velocity v_c at the transition depend on whether it is a Mott-U or Mott-δ transition. (After Giamarchi, 1997.)

$$H = \frac{1}{2\pi}\int dx[u\tilde{K}(\pi\tilde{\Pi}(x))^2 + \frac{u}{\tilde{K}}(\nabla\tilde{\phi}(x))^2] + g_{\frac{1}{2n}}\int dx\ \cos(2\tilde{\phi}(x)) \tag{4.29}$$

where

$$\tilde{K} = K2n^2 \tag{4.30}$$

We can thus use the bosonization formulas backward and look at (4.29) as the bosonized form of a *spinless fermion* Hamiltonian. The quadratic part is simply the kinetic interaction plus the interaction between these fermions. The cosine term is a simple backscattering:

$$\int dx[\psi_R^\dagger(x)\psi_L(x) + \text{h.c.}] \tag{4.31}$$

Such a full fermion Hamiltonian (kinetic + interaction + backscattering) is known as the massive Thiring model. The important point is that if we start from an initial model with $K = 1/(2n^2)$, that is, in general a strongly interacting model, the resulting spinless fermion model corresponds in the boson language to $K = 1$, which means that it is *non-interacting*. For this special value of K the spinless fermions whose bosonized from is (4.29) are just free particles with a backscattering. This special value of K is known as the Luther–Emery line.

This is now a trivial problem to solve. One can get the spectrum for any value of $g_{\frac{1}{2n}}$. We have for the Hamiltonian

$$H_0 = \sum_k uk(c^\dagger_{R,k}c_{R,k} - c^\dagger_{L,k}c_{L,k}) + (\pi\alpha g_{\frac{1}{2n}})\sum_k c^\dagger_{R,k}c_{L,k} + \text{h.c.} \tag{4.32}$$

and H_0 can be diagonalized by a Bogoliubov transformation (Mahan, 1981), leading to the new eigenstates

$$\begin{aligned} c^\dagger_{\overline{u},k} &= \alpha_k c^\dagger_{R,k} + \beta_k c^\dagger_{L,k} \\ c^\dagger_{\overline{l},k} &= -\beta_k c^\dagger_{R,k} + \alpha_k c^\dagger_{L,k} \end{aligned} \tag{4.33}$$

where α_k and β_k are the usual transformation coefficients

$$\begin{aligned} \alpha_k &= [(1 + uk/\sqrt{(uk)^2 + \Delta^2})/2]^{1/2} \\ \beta_k &= [(1 - uk/\sqrt{(uk)^2 + \Delta^2})/2]^{1/2} \end{aligned} \tag{4.34}$$

These states have the energies (the upper sign is for $\overline{u}$)

$$E_{\overline{u},\overline{l}} = \pm\sqrt{(uk)^2 + \Delta^2} \tag{4.35}$$

which shows the opening of a gap Δ. From (4.32) one has $\Delta = \pi\alpha g_{\frac{1}{2n}}$. If one is away from the Luther–Emery line the interaction term gives a renormalization of the gap but the energies keep the form (4.35). The true gap Δ can either be obtained from the RG arguments as we discussed in Section 2.3.2 or from exact microscopic solutions (see Chapter 5). At commensurate filling the chemical potential is in the gap so that all $\overline{l}$ states are occupied and all $\overline{u}$ states are empty. At zero temperature the system is obviously an insulator, very reminiscent of a simple band insulator. However, the 'free' particles are not the original fermions but the eigenstates of the Luther–Emery Hamiltonian (4.32). What are these excitations? They are the spinless fermions corresponding to kinks (solitons) in the field ϕ_ρ through (4.28) and thus the holons of the original system. We thus see that these excitations behave as free fermions for the magic value of the original interaction $K = 1/(2n^2)$ of the original particles. In a more conventional Mott insulator the '$\overline{l}$' states would be the lower Hubbard band and the '$\overline{u}$' states the upper Hubbard band. The holons would thus simply be in an extreme limit the holes and the doubly occupied sites. This is depicted in Fig. 4.9.

The interest of the Luther–Emery solution is to provides a solution for the massive phase on the whole line $K = 1/(2n^2)$, $g_{\frac{1}{2n}}$ arbitrary. Since the umklapp operator is relevant for $K < K_c = 1/n^2$ this is deep in the massive phase and can be used in conjunction with the RG, to determine the properties of the *whole* massive phase. Since it provides a simple way to tackle the massive phase it also allows to study various perturbations on them. This is a very useful method that we will use repeatedly. As a first example of its use let us now investigate the Mott-δ transition.

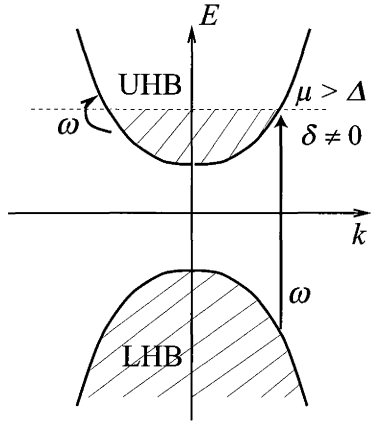

FIG. 4.9. Lower Hubbard band (LHB) and Upper Hubbard band (UHB). This concept can be made rigorous in one dimension by mapping the full interacting system to a massive Thiring model. Optical transitions can be made either within or between the two 'bands'. (After Giamarchi, 1997.)

4.2.3 *Doping; C–IC transition*

The first way to tackle the doped system is to extend the RG approach used for the commensurate case to treat a term like

$$H_{\frac{1}{2n}} = g_{\frac{1}{2n}} \int dx \ \cos(n\sqrt{8}\phi_\rho(x) - \delta x) \tag{4.36}$$

In fact, this problem has a well-known classical analogue. It represents lines in a periodic potential with a slight mismatch between the periodicity of the crystal of lines and the one of the underlying periodic potential (see Fig. 3.7). This is known as the commensurate-incommensurate transition (Japaridze and Nersesyan, 1978; Pokrovsky and Talapov, 1979; Schulz, 1980; Haldane *et al.*, 1983)

To illustrate the method I confine myself to the case of one particle per site ($n = 1$). I drop all the indices ρ on velocities and K to lighten the notations and take $g_{\frac{1}{2n}} = \frac{2g}{(2\pi\alpha)^2}$ to make contact with the standard notations in fermion language. It is easy to work out the same RG procedure than in Section 2.3.2 (Giamarchi and Schulz, 1988*a*; Giamarchi, 1991). The steps are identical except that now (2.123) should be replaced by

$$R(r_1 - r_2) = e^{-a^2 K F(r_1 - r_2)} \left[1 + \frac{2g^2}{(2\pi\alpha)^4 u^2} \int\int dR \, dr \, e^{-4KF(r)} \cos(\delta x) \right.$$
$$\left. (aK[r \cdot \nabla[F(r_1 - R) - F(r_2 - R)]])^2 \right] \tag{4.37}$$

Because of the $\cos(\delta x)$ term the x^2 and y^2 terms are not equivalent. Space and time thus have to be renormalized differently. Let us set

$$F(r-r') = \frac{1}{2}\log\left[\frac{(x-x')^2+(u(\tau-\tau'))^2}{\alpha^2}\right] + \frac{t}{K}\cos(2\theta_{r-r'}) \tag{4.38}$$

where θ_r is the angle between the vector $(x, u\tau)$ and the x-axis, and t parameterizes the anisotropy between the space and time directions. In the original Hamiltonian t is zero but will be generated during the renormalization due to the chemical potential. As this anisotropy parameter is of first-order in the interaction constants, we need to keep it only in the zeroth order term in the development. After a straightforward calculation one finds (I take $a = 1$):

$$R(r_1-r_2) = e^{-KF(r_1-r_2)}\left[1+\frac{y^2}{8\pi^2}K^2[J_+I_+(r_1-r_2)+J_-I_-(r_1-r_2)]\right] \tag{4.39}$$

with $y = g/\pi u$ and

$$\begin{aligned} I_\pm(r_1-r_2) &= \int d^2R\ \log\mid r_1-R\mid[\partial_X^2 \pm \partial_Y^2]\log\mid R-r_2\mid \\ J_\pm(r_1-r_2) &= \int \frac{d_2r}{\alpha^2}(x^2\pm y^2)\cos(\delta x)e^{-4KF(r)} \end{aligned} \tag{4.40}$$

Using eqn (4.38), we have

$$\begin{aligned} J_+ &= 2\pi\int_\alpha^{+\infty}\frac{dr}{\alpha}\left(\frac{r}{\alpha}\right)^{3-4K} J_0(\delta r) \\ J_- &= -2\pi\int_\alpha^{+\infty}\frac{dr}{\alpha}\left(\frac{r}{\alpha}\right)^{3-4K} J_2(\delta r) \\ I_+ &= 2\pi\log[\frac{r_1-r_2}{\alpha}] \\ I_- &= \pi\cos(2\theta_{r-r'}) \end{aligned} \tag{4.41}$$

Substituting back into eqn (4.39) and reexponentiating we find that the correlation function A has the same form as the free one but with the effective quantities

$$\begin{aligned} K^{\text{eff}} &= K - \frac{g^2}{2}K^2\int_\alpha^{+\infty}\frac{dr}{\alpha}\left(\frac{r}{\alpha}\right)^{3-4K} J_0(\delta r) \\ t^{\text{eff}} &= t + \frac{g^2}{4}K^2\int_\alpha^{+\infty}\frac{dr}{\alpha}\left(\frac{r}{\alpha}\right)^{3-4K} J_2(\delta r) \end{aligned} \tag{4.42}$$

Given the form (4.38) a renormalization of t is equivalent to a renormalization of the velocity u by

$$\frac{-2}{K}\frac{dt}{dl} = \frac{1}{u}\frac{du}{dl} \tag{4.43}$$

This leads to the renormalization equations

$$\begin{aligned}\frac{dK}{dl} &= -\frac{1}{2}y^2K^2J_0(\delta(l)\alpha)\\ \frac{dy}{dl} &= (2-2K)y\\ \frac{du}{dl} &= -\frac{y^2}{2}uKJ_2(\delta(l)\alpha)\end{aligned} \tag{4.44}$$

If we work at constant doping $\delta(l) = \delta e^l$ where δ is the doping, since δ has the dimensions of the inverse of a length (term δx in the Hamiltonian). There are several interesting points to note in these equations. First, there is a renormalization of the velocity. This is normal since now space and time are inequivalent. We see that the velocity is decreased by the commensurate potential. Since at this order the velocity does not feed back in the other equations, this renormalization of the velocity is not drastically important. The second important point is the presence of the Bessel function $J_0(\delta(l)\alpha)$ in the equation. The oscillatory nature of this function is not important and is related to the use of a sharp cutoff in real space, whereas a smooth cutoff would have led to non-oscillatory functions (Horowitz *et al.*, 1983). What matters is that the function is essentially one as long as $\delta(l)\alpha < 1$ and essentially zero when $\delta(l)\alpha > 1$. The renormalization coming from the cosine terms is thus suppressed at lengthscales x such that δx is of order one. Below this lengthscale the equations are essentially the commensurate ones, above this lengthscale we can throw away the cosine completely and we have a quadratic LL Hamiltonian with the renormalized parameters u^* and K^*. This is a very physical result if we look at the original cosine $\cos(\sqrt{8}\phi - \delta x)$ we see that for $\delta x \ll 1$ we can essentially forget the δx term. If on the other hand δx is large the cosine oscillates so much that we can throw it away. In other words δ^{-1} is roughly the distance at which the system realizes that it is not commensurate. As we will see this corresponds roughly to the distance between solitons in ϕ (see Fig. 4.10).

If we work at constant chemical potential (Horowitz *et al.*, 1983) we should also look at its renormalization. This can be done by ensuring that the number of particles is kept constant. Let me call $\delta_Q = 4K\mu/u$. This is the value that δ (that is, a quantity proportional to the number of particles $\delta = 2\pi d$) would take for a purely quadratic Hamiltonian. To compute δ for the general case one performs the change of variables (4.20), and then uses the thermodynamic relation

$$\delta = \frac{-2\pi}{L}\frac{\partial F}{\partial \mu} \tag{4.45}$$

Using $F = -\log(Z)/\beta$ and the expression of the partition function (see Appendix C) one gets

$$\delta = \delta_Q - \frac{4Kg}{u\pi\alpha^2}\frac{1}{\beta L}\int dx \int^{\beta} d\tau\, x\langle \sin(\sqrt{8}\tilde{\phi} - \delta_Q x)\rangle \tag{4.46}$$

As before we make a development in powers of g and find:

$$\delta = \delta_Q - \frac{1}{\beta L}\frac{g^2 K}{u^3\pi^3\alpha^4}\int d_2 r \int d_2 R\,(X + \frac{x}{2})\sin(\delta_Q x)e^{-4KF(r)} \tag{4.47}$$

where $r = (x, u\tau)$. The integration over X gives zero because of the parity and we are left with ($L = \int dX$):

$$\delta = \delta_Q - y^2 K \int_\alpha^{+\infty} \frac{dr}{\alpha}\left(\frac{r}{\alpha}\right)^{2-4K}\frac{1}{\alpha}J_1(\delta r) \tag{4.48}$$

If we change the cutoff δ is simply scaled as $\delta(l) = e^l\delta$ since it has the dimension of the inverse of a length. This gives the extra equation

$$\frac{d\delta_Q}{dl} = \delta_Q(l) - \frac{y^2}{\alpha}J_1(\delta_Q(l)\alpha) \tag{4.49}$$

In this equation the competition between the gradient term and the commensurate potential is apparent. The chemical potential would like to impose a slope that is given by the bare δ_Q (hence a simple scaling $\delta_Q(l) = \delta_Q e^l$ when the cutoff is changed). On the other hand, the cosine term would like this slope to be zero to keep ϕ in the minima of the cosine. It thus reduces the effective δ_Q. The finite slope, on the other hand, cuts the renormalization of the cosine. Which wins depends on the initial parameters and this competition is given by (4.49). This equation thus shows clearly that two phases exists depending on the value of the chemical potential. Note that for the case of constant doping (since $\delta(l) = \delta e^l$ instead of (4.49)), the δ term always cuts the flow at some lengthscale and one recovers that as soon as $\delta \neq 0$ the system is metallic and the cosine term irrelevant. Unfortunately, the RG approach does not allow to extract the critical properties of the transition. Indeed, close to the transition ($\delta \to 0$) the flow goes to strong coupling before the renormalization of the cosine term is stopped. One is thus always in the strong coupling regime in which the perturbative RG equations become unreliable, and one has to find another method.

A possible way to tackle this problem is provided by the Luther–Emery solution (Japaridze and Nersesyan, 1978; Schulz, 1980). Other methods can also be used with success (Papa and Tsvelik, 2001; Aristov and Luther, 2002). To describe the doped system we now have to add the chemical potential term (2.107) to (4.27). Quite generally (4.27) can be rewritten in terms of the spinless fermions (using the formulas of Appendix D)

$$H = H_0 + \frac{\pi u \sinh(2\vartheta)}{L}\sum_p [2\rho_R(p)\rho_L(-p) - f_1(\rho_R(p)\rho_R(-p) + \rho_L(p)\rho_L(-p))] \tag{4.50}$$

where the ρ operators are the density operators of the new spinless fermions. H_0 is the Hamiltonian (4.32) with, because of the interactions, a velocity v (instead of u in (4.32)) given by

$$\begin{aligned} v &= u(\cosh(2\vartheta) + f_1\ \sinh(2\vartheta)) \\ e^{2\vartheta} &= 1/(2n^2 K_\rho) \end{aligned} \tag{4.51}$$

Since the last term in (4.50) is just the kinetic energy written with boson operators, f_1 is at that stage totally arbitrary. Its interest will be apparent later. Note that we do not assume here that we are at the magic Luther–Emery value, hence the interaction term. If $K_\rho = 1/(2n^2)$ the interaction term of course vanishes ($\vartheta = 0$).

To be able to dope one needs to put a chemical potential higher than the gap Δ. It means that away from half-filling the chemical potential is in the upper band and in addition to the $\bar{l}$ states the $\overline{u}$ states are occupied up to a value $k_c = \pi d$, d being the doping. Then, assuming that we are interested only in very low frequency behavior the spectrum can again be linearized around k_c. We thus have to deal with a *new* Luttinger liquid made only of the residual particles (the holons) in the upper Hubbard band (the $\overline{u}$ states). This of course will only describe the correlation functions above a lengthscale roughly of the order of the distance between these particles. To characterize the asymptotic behavior of this new Luttinger liquid only the interaction processes scattering electrons at the (new) Fermi level need to be kept from (4.50). One thus first use (4.33) to reexpress (4.50) in terms of the new basis of $\bar{l}$ and $\overline{u}$ states. One then only keep the part containing the $\overline{u}$ operators. This is a new interacting Hamiltonian for which we need only to keep the processes close to the new Fermi level k_c, and define right and left goers from the $c_{\overline{u}}$ operators, using the same techniques than in Chapter 2. This leads to a standard Luttinger Hamiltonian (4.52) where α and β denote the right and left going particles corresponding to the $\overline{u}$ states around the new Fermi level. The trick (Schulz, 1980) is to use the freedom of choice of f_1 to cancel all the $\rho_r(p)\rho_r(-p)$ (where $r = R$ or $r = L$, that is a g_4 process) that would appear in this Luttinger Hamiltonian. Choosing such a value for f_1 ensures that after linearization one has

$$H = \sum_k v_c k(\alpha_k^\dagger \alpha_k - \beta_k^\dagger \beta_k) + 2\pi u \sinh(2\vartheta) f(k_c) \sum_p \rho_R(p)\rho_L(-p) \tag{4.52}$$

with $\rho_R(p) = \sum_k \alpha_{k-p}^\dagger \alpha_k$ and $\rho_L(p) = \sum_k \beta_{k-p}^\dagger \beta_k$ and

$$\begin{aligned} v_c &= \frac{\partial E_1(k)}{\partial k} = \frac{v^2 k_c}{\sqrt{(vk_c)^2 + \Delta^2}} \\ f_1 &= \frac{1}{1 + 2(vk_c)^2/\Delta} \\ f(k_c) &= v_c^2/v^2 \end{aligned} \tag{4.53}$$

The important point is that now the residual interaction term is proportional to k_c^2. Thus, sufficiently close to the commensurate filling the interaction term becomes negligible compared to the Fermi energy. Not only this justifies our linearization of the spectrum but it also means that our holons behave as *free* particles when the doping is very small. Note that this time we did not make any assumption on the original interaction so this result is valid *regardless* of

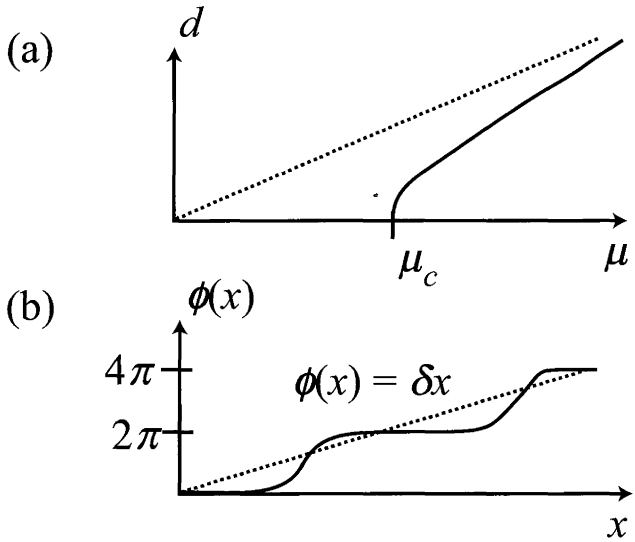

FIG. 4.10. (a) The doping is proportional to the square root of $\mu - \mu_c$. It corresponds to the filling of a band of free spinless fermions. (b) These fermions are the solitons in ϕ which are the best compromise between the gradient term (chemical potential) that wants a finite slope and the commensurate term that wants ϕ to be locked in the minima of the cosine. The average slope gives the doping.

the strength of the original coupling. Physically this is very reasonable. At very small doping the holons are so diluted that whatever is the original interaction they do not see each other. This allows immediately to determine the doping as a function of the chemical potential. As long as the chemical potential remains smaller than the gap Δ the doping remains zero. When $\mu > \mu_c = \Delta$ the doping is given by the filling of a band of free fermions and is thus simply given by $d = k_c/\pi$, which using expression (4.35) for the energy leads for small doping to

$$d \propto \sqrt{\mu - \mu_c} \tag{4.54}$$

which is shown in Fig. 4.10.

To determine the exponents of the correlation function one can use correlation functions that are easily computed both in the original language and in the spinless fermion language. For example

$$A(x) = \langle (\psi_R^\dagger \psi_L)_x (\psi_L^\dagger \psi_R)_0 \rangle = \langle e^{i2\tilde{\phi}(x)} e^{-i2\tilde{\phi}(0)} \rangle \tag{4.55}$$

If we assume that the original system is described by a Luttinger fixed point with renormalized parameters K^* and u^* then ($\tilde{\phi} = n\sqrt{2}\phi$)

$$A(x) \propto \left(\frac{\alpha}{x}\right)^{4n^2 K^*} \tag{4.56}$$

on the other hand the correlation function can also be computed from the spinless fermion Hamiltonian. If we assume that the spinless fermions are truly free then $A(x) \sim 1/x^2$, which allows to extract the universal value of the exponent right at the transition at zero doping $K^* = 1/(2n^2)$. Note that this value taken for the Mott-δ transition is exactly one-half of the universal value at the Mott-U transition. We can do a slightly better job by putting back the interaction using the perturbative formula for our Luttinger liquid of spinless fermions. This leads to

$$K = \frac{1}{2n^2}\left[1 - \frac{2uk_c}{\Delta}\sinh(2\vartheta)\right] \tag{4.57}$$

These universal values form a quite general result valid for *any* system. The approach to the universal value is proportional to the doping k_c, which again should be a universal behavior although the prefactor clearly depends on the detail of the model. We will compare these findings with exact results in Chapter 7. The velocity of the excitations is given by v_c and from (4.53) behaves as

$$v_c \sim k_c/\Delta \tag{4.58}$$

This has two important consequences. The compressibility (2.108) *diverges* at the Mott-δ transition, before dropping to zero in the Mott phase. In addition, since right at the transition the excitations are free spinless fermions at the bottom of a band the relation between energy and momentum is $\omega \sim k^2$. It means that for the Mott-δ transition the dynamical exponent is $z = 2$. A summary of the critical properties is given in Fig. 4.8. More can be found in Giamarchi (1991) and Mori *et al.* (1994).

4.3 Effects of magnetic field and magnetic anisotropy

Let us now see what happens when one breaks the spin rotation invariance in a Luttinger liquid with spin. There are two important ways of doing this, one is to add a magnetic field to the system, and the other to start with spin anisotropic interaction constants. Although we already examined partly the latter case by taking $g_{\parallel} \neq g_{\perp}$, a full treatment of this question allows to present some problems that occur with the operators U and that I swept under the rug in the previous chapters.

4.3.1 *Magnetic field*

Within the bosonization language the effects of a magnetic field are very similar to the ones of a chemical potential. Indeed, a magnetic field along the z direction gives

$$H = -\frac{\mathbf{h}}{2}\int dx[\rho_\uparrow - \rho_\downarrow] = \frac{\mathbf{h}}{\sqrt{2}}\int dx \frac{1}{\pi}\nabla\phi_\sigma(x) \tag{4.59}$$

where $\mathbf{h} = g\mu_B h$, with h the magnetic field, μ_B the Bohr magneton and g the gyromagnetic factor. The total Hamiltonian is thus

$$H = H_\sigma^0 + \frac{2g_{1\perp}}{(2\pi\alpha)^2}\int dx\ \cos(\sqrt{8}\phi_\sigma) + \frac{\mathbf{h}}{\sqrt{2}\pi}\int dx\ \nabla\phi_\sigma(x) \tag{4.60}$$

Let us first look at the case where the cosine term is marginal. This corresponds to spin isotropic repulsive interactions. In the charge sector we will see that similar effects can also occur. One can use the RG equations (4.44) to determine the effects of the magnetic field, since this is exactly the problem we studied in the previous section. Here, the cosine is marginal so the RG equations are valid at an arbitrary lengthscale. As we saw h cuts the flow of $g_{1\perp}$ when $h\alpha(l) \sim 1$. Let us start from the RG equation on the separatrix (2.143)

$$y(l) = \frac{y_0}{1 + y_0 l} \tag{4.61}$$

The flow stops at the scale

$$\frac{\mathbf{h}K_\sigma\alpha(l)}{\sqrt{2}u} \sim 1 \tag{4.62}$$

This corresponds to the scaling parameter $\alpha(l) = \alpha_0 e^l$

$$l = \log(\frac{\sqrt{2}u}{\mathbf{h}K\alpha_0}) \tag{4.63}$$

Thus, at the scale where the flow is cut, the interaction parameter becomes, for a weak enough magnetic field,

$$y(l^*) = 1/\log(\frac{\sqrt{2}u}{\mathbf{h}K\alpha_0}) \tag{4.64}$$

for weak enough magnetic field this value is independent of the initial coupling and depends in a quite singular way on the magnetic field. Since the parameter $y(l^*)$ is small one can use the perturbative expression (2.105) for the parameters u_σ and K_σ. For spin isotropic interactions one gets

$$\frac{K_\sigma(l^*)}{u_\sigma(l^*)} = \frac{1}{v_F}\frac{1}{1 - y(l^*)/2} \simeq \frac{1}{v_F}[1 + y(l^*)/2] \tag{4.65}$$

At this order in h the renormalization of the velocity is negligible (at least h^2 from (4.44)). Since at the scale l^* the cosine is irrelevant, we can use the formula for the spin susceptibility for a purely quadratic Hamiltonian but with the renormalized parameters. Using (2.110) we get

$$\kappa_\sigma = \kappa_\sigma^0 + \frac{1}{4\pi u_\sigma \log(\frac{\sqrt{2}u}{\mathbf{h}K\alpha_0})} \tag{4.66}$$

There is thus a very singular increase of the spin susceptibility ($d\kappa_\sigma/dh$ is infinite at the origin) with the magnetic field. This non-trivial logarithmic singularity of

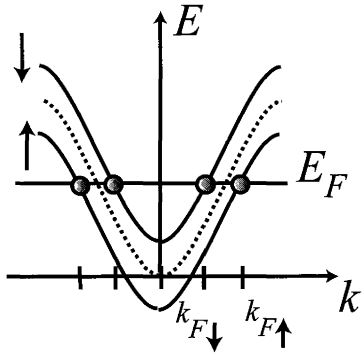

FIG. 4.11. The dispersion relation of a system with a magnetic field. There are now four points at the Fermi level.

the magnetic susceptibility is confirmed by exact solutions on microscopic models (Dzyaloshinskii and Larkin, 1972; Bourbonnais, 1993; Eggert *et al.*, 1994). Since K depends now on h the exponents of the various correlation functions thus depend on the magnetic field. The RG method allows for a reliable calculation of the magnetic field dependence of the exponents only if the field is very weak, otherwise other methods should be used. I will examine them in Chapter 5. At this level of approximation most of the features of the standard Luttinger liquid are preserved. There is still spin and charge separation. The only difference is that now the spin rotation symmetry is lost, which is quite natural, and the exponents for the spin part depend (in a quite singular way) on the magnetic field.

In the above study, I have assumed that one can still linearize the spectrum and the magnetic field acts only on the spin part of the Hamiltonian. For most systems this is a very reasonable approximation since a magnetic field of 1 Tesla corresponds in energy to 1 K, to be compared with the characteristic energies of a typical electron gas, of the order of 1 $eV \sim 12\,000K$. However, one could encounter situations where the Fermi energy is low enough so that such an approximation is not valid. In that case, a better starting point is to consider that the up and down electrons have different chemical potentials. As a consequence the up and down electrons have different Fermi velocities. The dispersion relations of the free system is the one shown in Fig. 4.11. The free electron Hamiltonian thus becomes

$$H = H_\uparrow + H_\downarrow \tag{4.67}$$

where

$$H_{\uparrow,\downarrow} = \frac{1}{2\pi}\int dx\, v_{\uparrow,\downarrow}[(\pi\Pi_{\uparrow,\downarrow})^2 + (\nabla\phi_{\uparrow,\downarrow})^2] \tag{4.68}$$

whereas the interaction term contains terms of the form (e.g. for a g_2 term)

$$U \int dx\ \rho_\uparrow(x)\rho_\downarrow(x) = \frac{U}{\pi^2} \int dx (\nabla\phi_\uparrow)(\nabla\phi_\downarrow) \tag{4.69}$$

Normally, we would diagonalize the Hamiltonian by going to the basis $\phi_\uparrow \pm \phi_\downarrow$. Because of the different velocities this is not a satisfactory basis any more. However, we see that we can still diagonalize the quadratic Hamiltonian by choosing a different linear combination of $\phi_\uparrow$ and $\phi_\downarrow$. As a price to pay we lose the charge and spin separation. Indeed, the $g_{1\perp}$ terms were of the form

$$\cos(\phi_\uparrow - \phi_\downarrow) \tag{4.70}$$

and now couple the new 'charge' and 'spin' modes that diagonalize the quadratic part of the Hamiltonian. I will not explore in much detail the full solution of this problem (Penc and Sólyom, 1993; Kimura *et al.*, 1996*a*; Pham *et al.*, 2000). We will have occasion to come back to it in a much more reasonable physical situation, namely the case where there is more than a single chain of electrons. This is the case of ladders that I will present in Chapter 8. Similar effects occur in the presence of strong spin–orbit coupling (Moroz *et al.*, 2000).

4.3.2 *Magnetic anisotropies*

Another source of magnetic anisotropy can come from the interactions themselves. This happens if the interactions depend on processes that couple the spin and the lattice. Such processes in the solids are due either to spin–orbit coupling or to dipole–dipole interactions. Since the precise computation of the microscopic constants would need a specific model, I will take here the interaction constants as given parameters and refer the reader to Giamarchi and Schulz 1988*a* for an example of such microscopic determination of the coupling constants.

The question is thus to obtain the most general coupling constants that describe spin–anisotropic interactions. We have already seen that one can take different coupling constants depending on whether the interaction was taking place between particles of the same spin ($g_\parallel$) or of opposite spins ($g_\perp$). In order to do so let us use the four operators for charge and spin density waves (see (2.111))

$$O_i = \sum_{\sigma,\sigma'} \psi^\dagger_{k_F,\sigma}(z)\sigma^{(i)}_{\sigma,\sigma'}\psi_{-k_F,\sigma'}(z) \tag{4.71}$$

Obviously O_0 is a scalar whereas $O_{1,2,3}$ is a vector operator under spin rotations. We can thus use the tensors $O_i^\dagger O_j$ ($\{i,j\} \in [0,3]$) as a basis to represent the most general interaction term H_{int}. The most general form is

$$H = \sum_{\alpha\beta} \int dx\ g_{\alpha\beta} O^\dagger_\alpha O_\beta \tag{4.72}$$

which is represented in Fig. 1.13. Note that now the spin indices are not conserved along one leg. The interaction is written as a g_1 type process. A g_2 type process

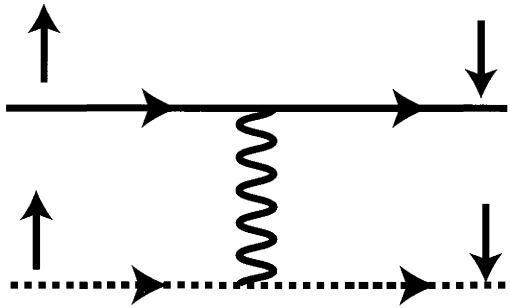

FIG. 4.12. g_f process. When written in the form of a g_2 term this term flips the two spins. It describes in fact the anisotropy in the XY plane.

can be obtained simply by permuting two external legs. Due to the time reversal symmetry there are no $O_0^\dagger O_i$ ($i \in [1,3]$) terms. As usual, the $O_i^\dagger O_j$ ($i,j \in [1,3]$) can be decomposed in one invariant, a vector operator, and an irreducible tensor operator. If we choose the axis system where the tensor part is diagonal and if we assume that the system has an inversion center we get for the most general interaction Hamiltonian (Giamarchi and Schulz, 1988*a*):

$$H_{\text{int}} = -\int dx \Big\{ (g_{2\parallel} - g_{1\parallel} - g_{1\perp}) O_0^\dagger O_0 + (g_{2\perp} + g_f) O_1^\dagger O_1 + (g_{2\perp} - g_f) O_2^\dagger O_2 + (g_{2\parallel} - g_{1\parallel} + g_{1\perp}) O_3^\dagger O_3 \Big\} \tag{4.73}$$

Since there are only four terms, only four independent coefficients are needed for the interactions. We can identify the contributions of the known terms $g_{1,2;\parallel,\perp}$ and have done so in the upper formula. Since $g_{2\parallel}$ and $g_{1\parallel}$ are in fact the same process, it means that to describe the most general spin non-conserving process one needs an additional constant that I name g_f. The g_f process is shown in Fig. 4.12. Equation (4.73) shows that for a system that is invariant under time reversal and inversion symmetry all the interaction effects are contained in the constants $g_{2\parallel} - g_{1\parallel}$, $g_{2\perp}$, $g_{1\perp}$, g_f in properly chosen axes. For the fermion system (4.73) the effect of each term is quite clear. The g_f constant represents the anisotropy in the x-y plane. $g_{2\parallel} - g_{1\parallel} - g_{2\perp} + g_{1\perp}$ parameterize the uniaxial anisotropy along the z-direction (of course, all coordinates refer here to the direction of the *spin* quantization axes).

Let us now bosonize our Hamiltonian. The g_f term is simply

$$-g_f \int dx (\psi_{R,\uparrow}^\dagger \psi_{L,\downarrow})(\psi_{L,\uparrow}^\dagger \psi_{R,\downarrow}) + \text{h.c.} \tag{4.74}$$

This becomes in terms of the bosons

$$-\frac{2g_f}{(2\pi\alpha)^2} \int dx \ \cos(2\sqrt{2}\theta_\sigma) \tag{4.75}$$

One would thus naively get for the full Hamiltonian

$$H = H_\rho^0 + H_\sigma^0 + \frac{2g_{1\perp}}{(2\pi\alpha)^2}\int dz\ \cos\sqrt{8}\phi_\sigma - \frac{2g_f}{(2\pi\alpha)^2}\int dz\ \cos\sqrt{8}\theta_\sigma \tag{4.76}$$

Equation (3.79) with both charges and magnetic monopoles is back. The flow equations for this system are interesting, since both cosines can be relevant but want to drive the system to opposite fixed points. Let us derive them rapidly since by now we are old pros in getting the RG equations. We use the same technique than in Section 2.3.2. The first-order terms are still zero and at second order the species of cosine do not mix since the total number of ϕ and θ charges (charges and magnetic monopoles in the classical analogy) should be zero. We have thus the familiar $g_{1\perp}^2$ term, already treated in Section 2.3.2, plus another correlation of the form

$$\begin{aligned}&\langle e^{ia\sqrt{2}\phi(r_1)}e^{-ia\sqrt{2}\phi(r_2)}e^{i\epsilon_1\sqrt{8}\theta(r')}e^{-i\epsilon_2\sqrt{8}\theta(r')}\rangle_{H_0}\\ &= e^{-a^2KF_1(r_1-r_2)}e^{-4K^{-1}F_1(r'-r')}e^{2a\epsilon_1[F_2(r_1-r')-F_2(r_1-r')+F_2(r_2-r')-F_2(r_2-r')]}\end{aligned} \tag{4.77}$$

Except for trivial factors of K replaced by K^{-1} the main difference is that some F_1 terms in (2.120) are replaced by F_2. However, we can proceed as before and make the gradient expansion. As before terms like $\nabla_X^2 F_2$ and $\nabla_Y^2 F_2$ appear. Since F_1 and F_2 are the real and imaginary parts of the complex function $\log(y_\alpha - ix)$, they obey the standard Cauchy relations

$$\begin{aligned}\nabla_X F_1 &= i\nabla_Y F_2\\ \nabla_Y F_1 &= -i\nabla_X F_2\end{aligned} \tag{4.78}$$

We can thus proceed exactly as before. The end result is a simple change of sign. The equations are thus

$$\begin{aligned}\frac{dK_\sigma}{dl} &= y_f^2 - K_\sigma^2 y_\perp^2\\ \frac{dy_\perp}{dl} &= (2-2K_\sigma)y_\perp\\ \frac{dy_f}{dl} &= (2-2/K_\sigma)y_f\end{aligned} \tag{4.79}$$

which at the lowest order in interaction gives (as usual $y = g/(\pi u)$ and $K_\sigma = 1 + y_\sigma/2$)

$$\begin{aligned}\frac{dy_\sigma}{dl} &= y_f^2 - y_\perp^2\\ \frac{dy_\perp}{dl} &= -y_\perp y_\sigma\\ \frac{dy_f}{dl} &= y_f y_\sigma\end{aligned} \tag{4.80}$$

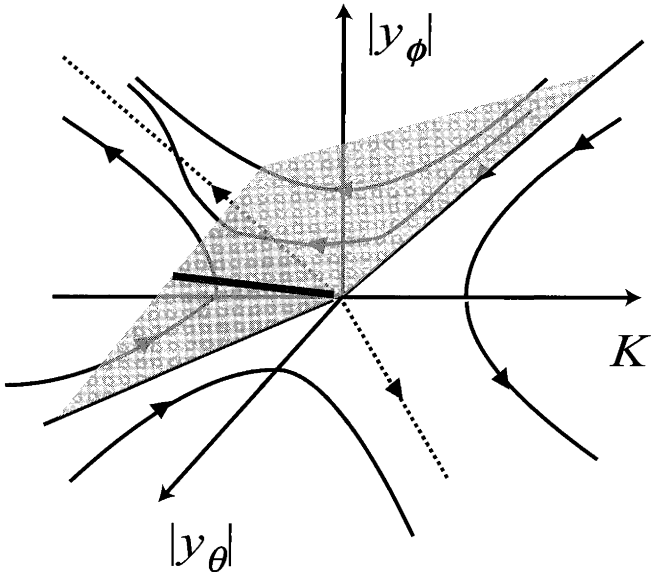

FIG. 4.13. Flow for a system with spin dependent interactions. Either the $\cos(\phi)$ or the $\cos(\theta)$ term becomes relevant. The dark grey plane separates these two regimes. The black line is a line of fixed points to which converges any starting point on the dark grey plane. (After Giamarchi and Schulz, 1988*a*.)

The $\cos(\sqrt{8}\theta)$ term wants to order θ and thus disorder ϕ whereas $\cos(\sqrt{8}\phi)$ wants exactly the opposite. The flow is indicated in Fig. 4.13. Depending on the initial values, a gap can open in the excitations of ϕ or θ. I will come back to such a competition in Section 6.4.1. For the moment let me just point out that $K = 1$ and $y_f = y_\phi$ is a fixed line in the flow. How can one understand it. Looking back at (4.73) we see that if we perform a rotation of the quantization axis we can directly read the new coupling constants from (4.73). For example, performing a rotation around the x axis to exchange y and z leads to the new coupling constants G (the charge part is invariant)

$$\begin{aligned} G_\sigma &= g_{1\perp} + g_f \\ G_{1\perp} &= \frac{1}{2}(g_\sigma + g_{1\perp} - g_f) \\ G_f &= \frac{1}{2}(g_\sigma - g_{1\perp} + g_f) \end{aligned} \tag{4.81}$$

The mysterious fixed line where the two cosine exactly equilibrated corresponds thus simply in the new axes to $G_f = G_{1\perp} = 0$ and $G_\sigma \neq 0$. This is a purely quadratic Hamiltonian with a given value K_σ. This example illustrates the fact that our bosonization formulas do not obviously exhibit the symmetries of the original problem. The same operator that is obviously rotation invariant in the

fermionic language can give terms that look as $(\nabla\phi)^2$, that is, quadratic terms that one knows how to treat, and cosine terms, that is, terms that in general we do not know how to deal with. Of course, if we can solve the problem fully the symmetry is perfectly respected, but sometimes not in an obvious way. This was, for example, the case of the spin rotation problem where the quadratic $g_{1\parallel}$ term and the cosine $g_{1\perp}$ terms conspire to keep the system right on the separatrix where the cosine renormalizes to zero and K_σ takes the magical value $K_\sigma^* = 1$. This is also the case in the present example where two operators that taken individually would open a gap in the spectrum conspire to keep the system critical. Such a situation requires care. A too crude approximate treatment of the system could break this non-obvious symmetry and make one think that the system becomes massive. If we known that the fermionic system obeys a symmetry we have to make sure that our boson solution *does* respect this symmetry, as it should. Any other result means that we have made a mistake.[21]

This situation occurs because in our bosonization method we have chosen explicitly a quantization axis (here the z-axis to quantize the spins) so the method breaks the rotational symmetry in implementing the operators. The method we have discussed, known as abelian bosonization since the fields are scalar, is thus adapted for systems that do not have a large symmetry group. This is the case for most of the examples that we will examine in this book. There is a generalization of the bosonization method that respects symmetries from the start. It is known as non-abelian bosonization. Its advantages is the respect of the symmetries. However, it is much more cumbersome to use than the abelian one, since many of the fermion operators cannot be written explicitly in terms of the boson ones. Which method to use depends thus on the problem at hand. For more details on non-abelian bosonization see Gogolin *et al.* (1999).

Our problem of magnetic anisotropies allows to illustrate another important point of the bosonization method. Let us reexpress our g_f process (4.74) in the more familiar g_2 form. This is simply done by permuting two fermion lines giving

$$g_f \int dx(\psi^\dagger_{R,\uparrow}\psi^\dagger_{L,\uparrow}\psi_{L,\downarrow}\psi_{R,\downarrow}) + \text{h.c.} \tag{4.82}$$

If we bosonize this expression, we get

$$\frac{2g_f}{(2\pi\alpha)^2}\int dx\ \cos(\sqrt{8}\theta) \tag{4.83}$$

which is exactly the same expression than before but with a minus sign! So obviously something is wrong. Note that the flow does not depend on the sign of g_f so one might think that the sign is arbitrary, but this is obviously not the case. Let us assume that one is in a regime where the g_f term is relevant and orders $\cos(\sqrt{8}\theta)$. According to our discussion of Chapter 2, $g_f > 0$ would mean that $\theta = \pi/\sqrt{8}$. If we use the boson representations (2.113) for the various correlations

[21] Usually simply being careful does the job!

we see that because θ orders, both the CDW and the SDW$_z$ correlation functions should now decay exponentially and because $\theta = \pi/\sqrt{8}$, $\cos(\sqrt{2}\theta)$ is essentially zero (hence the exponential decay of the corresponding correlation function) while $\sin(\sqrt{2}\theta)$ is a constant. Expression (4.83) would thus predict an SDW order along the y direction, whereas (4.75) would predict an SDW order along the x direction. Looking back at the fermionic operator in (4.73) it is easy to see (e.g. doing mean field) that the SDW$_x$ order is the correct one for $g_f > 0$ so (4.75) is correct and (4.83) is plain wrong.

Where is the mistake? Obviously, it comes from the fact that when one reorders fermion operators one can get a minus sign, whereas the order is essentially unimportant for the product of the boson operators of different species. To get the correct answer *for the ordered phases* we thus have to worry about the Klein factors (U operators) that are the only ones that can remember the original order of the fermions for different species, since their boson operators commute. As discussed before these factors do not have any spatial dependence so they do not contribute to the space–time decay of the correlation functions. This is totally controlled by the bosonic part. So we just have to find how to replace them by the proper *sign* in front of the boson operators. To do so we have first to write correctly the Hamiltonian taking the operators U into account. This gives

$$H = H_0 + \frac{g_{1\perp}}{(2\pi\alpha)^2}\int dx[U^\dagger_{R\uparrow}U^\dagger_{L\downarrow}U_{R\downarrow}U_{L\uparrow}e^{i\sqrt{8}\phi_\sigma(x)} + \text{h.c.}] - \frac{g_f}{(2\pi\alpha)^2}\int dx[U^\dagger_{R\uparrow}U^\dagger_{L\uparrow}U_{R\downarrow}U_{L\downarrow}e^{-i\sqrt{8}\theta_\sigma(x)} + \text{h.c.}] \quad (4.84)$$

In the same way one has to write the SDW and CDW operators with the operators U. Let me just write the two of them that are relevant here

$$\begin{aligned} O_{\text{SDW}_x} &\propto e^{-i(2k_F x - \sqrt{2}\phi_\rho(x))}\left[U^\dagger_{R\uparrow}U_{L\downarrow}e^{-i\sqrt{2}\theta_\sigma(x)} + U^\dagger_{R\downarrow}U_{L\uparrow}e^{i\sqrt{2}\theta_\sigma(x)}\right] \\ O_{\text{SDW}_z} &\propto e^{-i(2k_F x - \sqrt{2}\phi_\rho(x))}\left[U^\dagger_{R\uparrow}U_{L\uparrow}e^{i\sqrt{2}\phi_\sigma(x)} - U^\dagger_{R\downarrow}U_{L\downarrow}e^{-i\sqrt{2}\phi_\sigma(x)}\right] \end{aligned} \quad (4.85)$$

Let me recall that the U operators of different species anticommute while for a given species $UU^\dagger = U^\dagger U = 1$. In the thermodynamic limit one can forget about the fact that the U (resp. $U^\dagger$) lower (resp. raise) the total number of particles, and only focus on the *sign* due to these operators. A convenient mapping in that case is simply to replace U_r and $U^\dagger_r$ by a real (or so-called Majorana) fermion η_r. The correct (anti-) commutation relations are obeyed by imposing $[\eta_r, \eta_s] = 2\delta_{r,s}$. Although it is simpler to directly use the Majorana form to obtain the signs, I will stick in the following expressions to the U and $U^\dagger$ since this allows clearly to identify the various terms.

What we want to do is to compare (4.84) and (4.85) with similar expressions where the U operators have been suppressed, such as

$$H = H_0 + \frac{g_{1\perp}}{(2\pi\alpha)^2}\int dx[e^{i\sqrt{8}\phi_\sigma(x)} + \text{h.c.}] - \frac{g_f}{(2\pi\alpha)^2}\int dx[e^{i\sqrt{8}\theta_\sigma(x)} + \text{h.c.}] \quad (4.86)$$

and

$$\begin{aligned} O_{\mathrm{SDW}_x} &\propto e^{-i(2k_F x-\sqrt{2}\phi_\rho(x))}\left[e^{-i\sqrt{2}\theta_\sigma(x)}+e^{i\sqrt{2}\theta_\sigma(x)}\right] \\ O_{\mathrm{SDW}_z} &\propto e^{-i(2k_F x-\sqrt{2}\phi_\rho(x))}\left[e^{i\sqrt{2}\phi_\sigma(x)}-e^{-i\sqrt{2}\phi_\sigma(x)}\right] \end{aligned} \tag{4.87}$$

To get the correct properties we have thus to ensure that any order in the perturbation theory from (4.86) and (4.87) is identical to the ones of (4.84) and (4.85). This is not as formidable as it sounds. First, we do not have to worry at all about the spatial dependence since we know that the boson operators are faithfully taking care of it. We thus only have to worry about the signs in front of $g_{1\perp}$ and g_f. This means that we only have to look at the first-order perturbation theory to fix the signs. It is clear that the signs of $g_{1\perp}$ can be fixed independently of the sign of g_f (a change of sign is just a shift of either ϕ or θ by $\pi/\sqrt{8}$ which does not affect the other field). Let us first look at $g_{1\perp}$ and assume that we take for the O_{SDW_z} the sign convention of (4.87). In that case expanding the Hamiltonian to first-order in $g_{1\perp}$ and combining $\cos(\sqrt{8}\phi_\sigma)$ with the second term of O_{SDW_z} would give a term identical to the first one with a coefficient $g_{1\perp}$ (there is a minus sign coming from the expansion of $e^{-\beta H}$). Let us do the same operation with the operators U. One would find a term that is (from 4.84) and (4.85))

$$g_{1\perp}U^\dagger_{R\downarrow}U_{L\downarrow}U^\dagger_{R\uparrow}U^\dagger_{L\downarrow}U_{R\downarrow}U_{L\uparrow} \tag{4.88}$$

where I have just put the U operators since the boson factors are obviously correct. Using the anticommutation relations of the U operators of different species and $UU^\dagger = U^\dagger U = 1$ for the same species, this reduces to

$$g_{1\perp}U^\dagger_{R\uparrow}U_{L\uparrow} \tag{4.89}$$

which is exactly the first term (with the correct U operators) with a coefficient $g_{1\perp}$. So if we use for O_{SDW_z}, the bosonic expression $\sin(\sqrt{2}\phi_\sigma)$, then this forces us to use $g_{1\perp}\cos(\sqrt{8}\phi_\sigma)$ for the interaction term in the Hamiltonian, in order to correctly reproduce the fermion correlation functions. We could have arbitrarily decided to use $\cos(\sqrt{2}\phi_\sigma)$ for O_{SDW_z} but in that case to match (4.89) with the purely bosonic calculation we should have started from $-g_{1\perp}\cos(\sqrt{8}\phi_\sigma)$ in the Hamiltonian. It is easy to see that this change of convention corresponds to a shift $\phi \to \phi + \pi/\sqrt{8}$, which of course leaves the physics invariant. Let us now do the same analysis with g_f. At first-order in perturbation the combination of the second term of O_{SDW_x} gives

$$g_f U^\dagger_{R\downarrow}U_{L\uparrow}U^\dagger_{R\uparrow}U^\dagger_{L\uparrow}U_{R\downarrow}U_{L\downarrow} = g_f U^\dagger_{R\uparrow}U_{L\downarrow} \tag{4.90}$$

This is exactly identical to what one would have with the pure bosonic forms 4.86) and (4.87). It shows that choosing $\cos(\sqrt{2}\theta_\sigma)$ for O_{SDW_x} imposes to have $-g_f\cos(\sqrt{8}\theta_\sigma)$ in the Hamiltonian. Note that if one had written the g_f interaction in the g_2 form, which is the natural choice, and then bosonized stupidly

one would have got the wrong sign. When there are many species present it is necessary to pay attention to this point otherwise one simply swaps phases in the phase diagram. I will come back to that point in Section 6.4.1. The method explained here can of course be generalized to any number of fields. For more on this point, see Schulz 1996*b*.

4.4 Logarithmic corrections of correlation functions

Let us now look at the final little complication to the naive RG treatment performed in Chapter 2 to compute the correlation functions. So far we have determined the asymptotic behavior of the correlation functions just by plugging the renormalized LL parameters in the calculation performed with a purely quadratic Hamiltonian. In principle, one should write the renormalization equations for the correlation functions themselves. This is what I present in this section. In practice it justifies our naive treatment. However, when there are marginal operators logarithmic corrections to the correlation functions appear (Kosterlitz, 1974; Giamarchi and Schulz, 1988*a*; Voit, 1988; Affleck *et al.*, 1989; Giamarchi and Schulz, 1989; Eggert *et al.*, 1994), that this method is able to capture.

To illustrate the method we start from the Hamiltonian

$$H = H_0 + \frac{2g_\phi}{(2\pi\alpha)^2}\int dx\ \cos\sqrt{8}\phi - \frac{2g_\theta}{(2\pi\alpha)^2}\int dx\ \cos\sqrt{8}\theta \tag{4.91}$$

which can be for instance the Hamiltonian with spin anisotropies studied in the previous section. I introduce the notation

$$K = 1 + g_\sigma/2\pi u \tag{4.92}$$

The RG equations for (4.91) have already been computed (4.80). I consider the correlation functions

$$\begin{aligned} R_0 &= 2\langle T_\tau \cos(\sqrt{2}\phi(r_1))\cos(\sqrt{2}\phi(r_2))\rangle \\ R_1 &= 2\langle T_\tau \cos(\sqrt{2}\theta(r_1))\cos(\sqrt{2}\theta(r_2))\rangle \\ R_2 &= 2\langle T_\tau \sin(\sqrt{2}\theta(r_1))\sin(\sqrt{2}\theta(r_2))\rangle \\ R_3 &= 2\langle T_\tau \sin(\sqrt{2}\phi(r_1))\sin(\sqrt{2}\phi(r_2))\rangle \end{aligned} \tag{4.93}$$

which are the standard $2k_F$ parts of the CDW and SDW correlation functions (2.113). In the absence of g_ϕ and g_θ terms the functions R_i are easily computed (see Appendix C)

$$R_i(r_1 - r_2) = \exp[-K_i F_1(r_1 - r_2)] \tag{4.94}$$

where $K_0 = K_3 = K$ and $K_1 = K_2 = 1/K$. If $r \gg \alpha$ then

$$F_1(r) \sim \log(r/\alpha) \tag{4.95}$$

and I use this approximate form in the following. If now one includes the interactions $g_{1\perp}$ and g_θ and compute the R perturbatively, the development is divergent

for large $r_1 - r_2$. On the contrary, if we were working at fixed distance and for very small coupling constant the perturbation would be regular. The idea is thus to change the cutoff in the correlation function and find a function $I(\alpha', \alpha)$ such that

$$R(r_1 - r_2, \alpha') = I(\alpha', \alpha) R(r_1 - r_2, \alpha) \tag{4.96}$$

One then iterates the transformation up to a point where $r_1 - r_2 \sim \alpha$. In that case the correlation functions with such a cutoff can be evaluated perturbatively. Using the transformation (4.96) one has access to the original correlation function. In fact, R is not well adapted for such a transformation since even in the absence of interactions it has an intrinsic r dependence (and thus a dependence in α). It is much better to consider the functions $\overline{R}_i(r_1 - r_2) = R_i(r_1 - r_2) \exp[K_i F_1(r_1 - r_2)]$. In the absence of g_ϕ and g_θ, $\overline{R}_i$ reduces to the constant 1. In that case $I(\alpha', \alpha)$ would just be the constant 1, which also means that one can compute a perturbative expansion of $I(\alpha', \alpha)$ in powers of the interaction constants. Just a word for those who had the courage to read the end of Chapter 1. Since at the zeroth order in the interactions $K = 1$, we would compute in perturbation theory in *all* interactions the scaling equations for the functions $\overline{R} \sim rR(r)$ to eliminate the trivial scale dependence of $R(r)$. This is exactly the same procedure than taking the logarithmic derivative with respect of $\log(\omega)$ in (1.62) (a multiplication in real space is a derivative in Fourier space), to eliminate the trivial $\log(\omega)$ dependence of the correlation function at lowest order. As usual in one dimension, things are much more obvious in real space than in Fourier space.

We compute the functions $\overline{R}_i$ in a development in powers of g_ϕ and g_θ. If we define I such that

$$\overline{R}_i(r, \alpha e^l, g(l)) = I_i(dl, g(l)) \overline{R}_i(r, \alpha e^{l+dl}, g(l + dl)) \tag{4.97}$$

where the different $g(l)$ are the solutions of (4.80), for an infinitesimal transformation $\alpha(l + dl) = \alpha(l) e^{dl}$. Here and in the following α always denotes the initial short-distance cutoff, whereas the rescaled cutoff is written as $\alpha(l) = \alpha e^l$. If we use

$$\overline{R}_i(r, r, g(\log(r/\alpha))) = O(1) \tag{4.98}$$

provided that the couplings g are still small, and repeat (4.97) until the cutoff $\alpha(l)$ reaches r, we obtain:

$$\overline{R}_i(r, \alpha, g(\alpha)) = \prod_{l=0}^{l_r} I_i(dl, g(l)) = \exp[\int_0^{l_r} \log(I(dl, g(l)))] \tag{4.99}$$

where

$$l_r = \log(r/\alpha) \tag{4.100}$$

Computing the correlations in perturbation we find, for example, for R_0

$$
\begin{aligned}
R_0(r_1-r_2) &= e^{-KF_1(r_1-r_2)} \\
&- \frac{2g_\phi}{(2\pi\alpha)^2}\int dx_3\, d\tau_3 \langle T_\tau e^{i\sqrt{2}\phi(r_1)} e^{i\sqrt{2}\phi(r_2)} e^{-i\sqrt{8}\phi(r_3)}\rangle \\
&+ \frac{1}{2}\left(\frac{g_\phi}{4\pi^2}\right)^2 \sum_{\epsilon_i=\pm 1}\int \frac{dx_3\, d\tau_3}{\alpha^2}\,\frac{dx_4\, d\tau_4}{\alpha^2} \\
&\langle T_\tau e^{i\sqrt{2}\phi(r_1)} e^{-i\sqrt{2}\phi(r_2)} e^{i\sqrt{8}\epsilon_3\phi(r_3)} e^{-i\sqrt{8}\epsilon_4\phi(r_4)}\rangle_{\text{con.}} \\
&+ \frac{1}{2}\left(\frac{g_\theta}{4\pi^2}\right)^2 \sum_{\epsilon_i=\pm 1}\int \frac{dx_3\, d\tau_3}{\alpha^2}\,\frac{dx_4\, d\tau_4}{\alpha^2} \\
&\langle T_\tau e^{i\sqrt{2}\phi(r_1)} e^{-i\sqrt{2}\phi(r_2)} e^{i\sqrt{8}\epsilon_3\theta_\sigma(r_3)} e^{-i\sqrt{8}\epsilon_4\theta_\sigma(r_4)}\rangle_{\text{con.}}
\end{aligned}
\tag{4.101}
$$

where con. means the connected correlation (see Section 2.3.2). Computing the average values gives

$$
\begin{aligned}
\overline{R}_0(r_1-r_2) &= 1 - e^{2KF_1(r_1-r_2)}\frac{y_\phi}{2\pi}\int_\alpha \frac{d^2r_3}{\alpha^2} e^{-2KF_1(r_1-r_3)} e^{-2KF_1(r_2-r_3)} \\
&+ \frac{y_\phi^2}{2}K^2F_1(r_1-r_2)\int_\alpha^{+\infty}\frac{dr}{\alpha}\left(\frac{r}{\alpha}\right)^{3-4K} - \frac{y_\theta^2}{2}F_1(r_1-r_2)\int_\alpha^{+\infty}\frac{dr}{\alpha}\left(\frac{r}{\alpha}\right)^{3-4/K}
\end{aligned}
\tag{4.102}
$$

$\int_\alpha$ means that the domain of integration over r_3 excludes two circles of radius α around r_1 and r_2. The two last terms in (4.102) were already obtained in the previous section. They give rise to the renormalization of the coupling constants. The new term is the first-order term. This term only appears in the renormalization of the correlation functions of operators $\exp(ia\sqrt{2}\phi)$ with $a=1$ and does not contribute to the renormalization of the coupling constants. Physically it means that a term $\cos(\sqrt{8}\phi)$ in the Hamiltonian couples to

$$
\cos(\sqrt{2}\phi(r_1))\cos(\sqrt{2}\phi(r_2)) \tag{4.103}
$$

Indeed, as we already discussed (see (3.44)) when the two points are close these terms behave like a $\cos(\sqrt{8}\phi)$ term. Depending on the sign of the coupling constant this either favors or tries to reduce this order. If one changes α to $\alpha' = \alpha e^{dl}$, one finds

$$
\begin{aligned}
\overline{R}_0(r_1-r_2) &= 1 - y_\phi\, dl + \frac{1}{2}(K^2y_\phi^2 - y_\theta^2)F_1(r_1-r_2)\, dl \\
&+ y'_\phi\int_{\alpha'}\frac{dx_3\, d\tau_3}{\alpha'^2} e^{2KF_1'(r_1-r_2)} e^{-2KF_1'(r_1-r_3)} e^{-2KF_1'(r_2-r_3)} \\
&+ \frac{y_\phi'^2}{2}K^2F_1'(r_1-r_2)\int_{\alpha'}^{+\infty}\frac{dr}{\alpha'}\left(\frac{r}{\alpha'}\right)^{3-4K} - \frac{y_\theta'^2}{2}F_1'(r_1-r_2)\int_{\alpha'}^{+\infty}\frac{dr}{\alpha'}\left(\frac{r}{\alpha'}\right)^{3-4/K}
\end{aligned}
\tag{4.104}
$$

where

$$y'_\phi = y_\phi \left(\frac{\alpha'}{\alpha}\right)^{4-4K}, \quad y'_\theta = y_\theta \left(\frac{\alpha'}{\alpha}\right)^{4-4/K} \tag{4.105}$$

and F'_1 is the function F_1 with the new value of α. Equations (4.105) are nothing but the renormalization equations (4.80) for the coupling constants y_ϕ and y_θ. From (4.97) and (4.104) we deduce

$$I(\alpha'/\alpha, y_\phi, y_\theta) = e^{[-y_\phi + \frac{y_\phi^2}{2}\log(r/\alpha) - \frac{y_\theta^2}{2}\log(r/\alpha)]\, dl} \tag{4.106}$$

Therefore, we get

$$R_0(r) = \exp \int_0^{l_r} [-y_\phi(l) + \frac{1}{2}y_\phi^2(l) - \frac{1}{2}y_\theta^2(l)]\, dl \tag{4.107}$$

A similar derivation can be done for other correlation functions and we obtain

$$\begin{aligned}
R_0(r) &= e^{[-K\log(\frac{r}{\alpha}) + \int_0^{l_r} dl\, (-y_\phi(l) + \frac{1}{2}[y_\phi^2(l) - y_\theta^2(l)]\log(\frac{r}{\alpha(l)}))]} \\
R_1(r) &= e^{[-K^{-1}\log(\frac{r}{\alpha}) + \int_0^{l_r} dl\, (+y_\theta(l) - \frac{1}{2}[y_\phi^2(l) - y_\theta^2(l)]\log(\frac{r}{\alpha(l)}))]} \\
R_2(r) &= e^{[-K^{-1}\log(\frac{r}{\alpha}) + \int_0^{l_r} dl\, (-y_\theta(l) - \frac{1}{2}[y_\phi^2(l) - y_\theta^2(l)]\log(\frac{r}{\alpha(l)}))]} \\
R_3(r) &= e^{[-K\log(\frac{r}{\alpha}) + \int_0^{l_r} dl\, (+y_\phi(l) + \frac{1}{2}[y_\phi^2(l) - y_\theta^2(l)]\log(\frac{r}{\alpha(l)}))]}
\end{aligned} \tag{4.108}$$

From (4.80) we obtain

$$\frac{1}{2}\int_0^{l_r} dl[y_\theta^2 - y_\phi^2]\log(\frac{r}{\alpha(l)}) = -\frac{1}{2}y_\sigma \log(r/\alpha) + \frac{1}{2}\int_0^{l_r} y_\sigma(l)\, dl \tag{4.109}$$

As $K = 1 + y_\sigma/2$ this leads to

$$\begin{aligned}
R_0 &= \frac{\alpha}{r} L_1^{-1} L_2 L_3^{-1} \\
R_1 &= \frac{\alpha}{r} L_1 L_2 L_3 \\
R_2 &= \frac{\alpha}{r} L_1 L_2^{-1} L_3^{-1} \\
R_3 &= \frac{\alpha}{r} L_1^{-1} L_2^{-1} L_3
\end{aligned} \tag{4.110}$$

with

$$\begin{aligned}
L_1(r) &= \exp\left[\frac{1}{2}\int_0^{l_r} dl\; y_\sigma(l)\right] \\
L_2(r) &= \exp\left[\frac{1}{2}\int_0^{l_r} dl\; (y_\theta(l) - y_\phi(l))\right] \\
L_3(r) &= \exp\left[\frac{1}{2}\int_0^{l_r} dl\; (y_\theta(l) + y_\phi(l))\right]
\end{aligned} \tag{4.111}$$

(4.110) and (4.111) give the correlation functions to lowest non-trivial order in the coupling constants (Giamarchi and Schulz, 1989).

Let us just illustrate the solution on the simple case $g_\theta = 0$. We thus have from (4.111) $L_3 = 1/L_2$. If we sit on the separatrix $y_\sigma = y_\phi$, one can use $y_\sigma(l) = y_\sigma/(1 + y_\sigma l)$ and

$$L_1 = L_3 = \left(\frac{y_\sigma}{y_\sigma(l_r)}\right)^{1/2} \tag{4.112}$$

If $r \to \infty$ then $y_\sigma(l_r) \sim 1/l_r$ and

$$\begin{aligned} R_0(r) &= \frac{\alpha}{r}\log^{-3/2}(r/\alpha) \\ R_1(r) = R_2(r) = R_3(r) &= \frac{\alpha}{r}\log^{1/2}(r/\alpha) \end{aligned} \tag{4.113}$$

All the correlation functions decay with the same exponent, but logarithmic corrections enhance $R_{1,2,3}$ over R_0. Physically it means that for spin isotropic repulsive interactions the system 'remembers' that it prefers antiferromagnetic order to a charge density wave. This is enforced by the presence of the linear term. Indeed, if the $\cos(\sqrt{8}\phi)$ term had been able to order in the Hamiltonian instead of renormalizing to zero one would have had

$$\phi = \pi/\sqrt{8} \tag{4.114}$$

since the coefficient of the cosine is positive. This would have implied that $\cos(\sqrt{2}\phi)$ would have averaged to zero while $\sin(\sqrt{2}\phi)$ would have had a non-zero average value. In that case the CDW correlation would have decayed exponentially whereas the SDW_z ones would have been constant. Since the operator is marginal and renormalizes to zero the result is not as violent. But because the operator is marginal there is still a memory that a $\cos(\sqrt{2}\phi)$ is not the same as a $\sin(\sqrt{2}\phi)$ (this distinction would be completely lost if the Hamiltonian had been completely quadratic). This results into logarithmic corrections to the correlation functions. If the system is not on the separatrix, one can use solution (2.142). We thus have

$$\begin{aligned} L_1(r) &= [\cosh(Al) + \frac{y_\sigma}{A}\sinh(Al)]^{1/2} \\ L_3^2(r) &= C_3 \tanh[(Al + \operatorname{atanh}(A/y_\sigma))/2] \end{aligned} \tag{4.115}$$

with $C_3 = 1/\tanh[\operatorname{atanh}(A/y_\sigma)/2]$. Then, from (4.110)

$$\begin{aligned} R_0 &= \frac{\alpha}{r}L_1^{-1}L_3^{-2} \\ R_3 &= \frac{\alpha}{r}L_1^{-1}L_3^{2} \\ R_1 = R_2 &= \frac{\alpha}{r}L_1 \end{aligned} \tag{4.116}$$

As now we have $y_\phi \neq y_\sigma$, R_3 and $R_{1,2}$ are no longer degenerate. There are two different qualitative behaviors depending on the values of $l = \log(r/\alpha)$. If $Al \ll 1$

one can expand the hyperbolic functions and it is easy to check that to lowest order in A the results (4.113) are recovered. Thus, for short enough length the system behaves as if the couplings where isotropic ($A = 0$). In particular, all the correlation functions decrease with the *same* exponent, up to logarithmic corrections. At an 'anisotropy' length given by $\log(r/\alpha) = 1/A$ there is a crossover from a regime of isotropic correlation functions to a regime dominated by the anisotropies. By using $Al \gg 1$ one can expand L_1 and L_2 and find

$$\begin{aligned}
R_0(r) &= C_3^{-1}[(1+y_\sigma/A)/2]^{-1/2}(\frac{\alpha}{r})^{1+A/2}[1+2(\frac{y_\sigma - A}{y_\sigma + A})^{1/2}(\frac{\alpha}{r})^A + O((\alpha/r)^{2A})] \\
R_3(r) &= C_3[(1+y_\sigma/A)/2]^{-1/2}(\frac{\alpha}{r})^{1+A/2}[1-2(\frac{y_\sigma - A}{y_\sigma + A})^{1/2}(\frac{\alpha}{r})^A + O((\alpha/r)^{2A})] \\
R_1(r) &= R_2(r) = [(1+y_\sigma/A)/2]^{1/2}(\frac{\alpha}{r})^{1-A/2}[1+O((\alpha/r)^{2A})]
\end{aligned} \tag{4.117}$$

Thus, the correlation functions decay with different exponents: $1 + A/2$ for R_0 and R_3, $1 - A/2$ for R_1 and R_2. One recognizes the value that one would get by just using the renormalized K since from (2.141)

$$K^* = 1 + \frac{A}{2} \tag{4.118}$$

The result on the exponent validates our simple treatment of the previous chapters, simply replacing the exponents by their renormalized value. Physically it means that an irrelevant operator is not able to act on the asymptotic decay of the correlation functions. There are no logarithmic corrections but rather power law corrections to the main divergence that become negligible when $r \to \infty$. The fact that logarithmic corrections have existed up to the 'anisotropy' length manifest itself in the prefactor of the different correlation functions. If we go closer and closer to the isotropic limit the prefactor enhances $R_{1,2,3}$ over R_0. The presence of logarithmic corrections can be tested numerically (Hallberg *et al.*, 1995).

5

MICROSCOPIC METHODS

This is quite a three-pipe problem.
Sherlock Holmes, by Sir Arthur Conan Doyle (*The red headed league*)

So far I have discussed the universal features of one-dimensional models, and focussed on their low-energy properties. For this goal the bosonization method is an invaluable tool. A complementary approach is to start from a well-defined microscopic model and to extract *all* the physics from such a model. Some features will be specific to the model under consideration. This certainly includes the high-energy properties. The low-energy is supposed to be universal and well described by the LL theory. If one has a method to tackle the microscopic models it can thus be used to check the concept of LL and to determine the LL parameters in a regime where straightforward perturbation expansion fails.

Fortunately, such methods exist in one dimension,[22] and I present some of them in this chapter. On the analytic side the king of all methods in that respect is the Bethe-ansatz. It is a world in itself, thus this chapter contains only the very basics. In addition to this wonderful analytical method various numerical methods that have become incredibly accurate in $d = 1$ are also used. Without entering in the technical details, a short sketch of the various methods with their pros and cons will be given. I also show how to combine these methods with the bosonization method to get the best of both worlds.

5.1 Bethe-ansatz

Bethe-ansatz provides a nice analytical solution of various one-dimensional systems. It is very elegant but quite complicated method, so only a very basic description can be done in the context of this book. In particular, I will only discuss the exact solution of the Heisenberg model, to present the essential features of the method. The generalization to fermions with spins, although similar in spirit becomes very involved and I think difficult to explain here. The persons who want to become experts in Bethe-ansatz are referred to the excellent reviews on the subject to learn more about it (Baxter, 1982; Thacker, 1982; Gaudin, 1983; Korepin *et al.*, 1993; Andrei, 1994; Takahashi, 1999). I have also chosen to restrict myself to one form of Bethe-ansatz (the so-called coordinate Bethe-ansatz), which is quite simple to explain. Other approaches (such as S matrices) have been developed and proven quite useful in recent applications such as thermodynamic Bethe-ansatz or form factors. This would carry us too far so I refer the reader to the literature for more information on these techniques.

[22] Another miracle of the one-dimensional world.

It is important to note that Bethe-ansatz can be used for a large variety of models, both on a lattice and in the continuum. We will see various examples of models on a lattice in Chapters 6 and 7. Other applications[23] have been the massive Thiring model (Thacker, 1982), the Kondo model (Andrei *et al.*, 1983; Tsvelick and Wiegmann, 1983), many continuum models (sine-Gordon, $O(N)$, etc.) (Gaudin, 1967; Yang, 1967; Andrei and Lowenstein, 1979; Belavin, 1979), Haldane–Shastry models (spin chain with an $1/r^2$ interaction) (Haldane, 1988; Shastry, 1988), Schulz–Shastry models (Schulz and Shastry, 1998).

Note that the Bethe-ansatz gives the exact energies of the ground state and all the excited states in terms of the solution of a system of coupled nonlinear equations. On the other hand, the corresponding wavefunctions have a form so complicated that the explicit calculation of matrix elements, correlation functions, and other physical quantities has remained elusive so far. For models with gaps it is a very powerful method to compute the spectrum. For massless systems, the low-energy part corresponds very often to a Luttinger liquid. In the subsequent sections I shall describe how the knowledge of the energy spectrum obtained from exact solutions can be combined with the results of the preceding two chapters to obtain a rather detailed picture of the low-energy properties, in particular of correlation functions.

5.1.1 *Spin chain*

To illustrate the method I focus on the simplest microscopic model possible, namely one-dimensional spin chain

$$\begin{aligned} H &= J_{xy}\sum_j [S^x_{j+1}S^x_j + S^y_{j+1}S^y_j] + J_z\sum_j S^z_{j+1}S^z_j \\ &= \frac{J_{xy}}{2}\sum_j [S^+_{j+1}S^-_j + S^-_{j+1}S^+_j] + J_z\sum_j S^z_{j+1}S^z_j \end{aligned} \tag{5.1}$$

where $S^\pm = S^x \pm iS^y$ and the S are the standard spin matrices

$$\begin{aligned} S^+ &= (S^-)^\dagger = \begin{pmatrix} 0 & 1 \\ 0 & 0 \end{pmatrix} \\ S^z &= \frac{1}{2}\begin{pmatrix} 1 & 0 \\ 0 & -1 \end{pmatrix} \end{aligned} \tag{5.2}$$

Very often one chooses the parametrization $J_{xy} = J$, $J_z = J\Delta$. $\Delta = 1$ is the spin isotropic point that is ferromagnetic for $J < 0$ and antiferromagnetic for $J > 0$ (see next chapter). This model is known as the XXZ model. As we will see in the next chapter there is a nice representation of the spins in terms of either bosonic or fermionic particles. A spin down can be viewed as an empty site, whereas a spin up corresponds to the presence of a spinless fermion or a hard core boson

[23] The list is far from being exhaustive.

on the site. Solving the spin chain is thus equivalent to solving, for example, a chain of interacting spinless fermions with an energy of the form

$$H = -t\sum_i c_{i+1}^\dagger c_i + V\sum_i (n_{i+1} - 1/2)(n_i - 1/2) - \mu\sum_i n_i \tag{5.3}$$

This model describes fermions hopping on a lattice with a matrix element t. Only fermions on nearest neighbor sites feel an interaction V. In this chapter, I will stick with the spin description that is very visual. It is useful to remember however that a spin up or down can be thought of as the presence or the absence of a fermion. The J_{xy} term is essentially the kinetic energy since it moves a spin down to the neighboring sites while the J_z term is an interaction.

It is easy to check that the total S_z commutes with Hamiltonian (5.1). In the fermion language this is simply the conservation of the total number of particles. We can thus diagonalize the Hamiltonian in each sector of S_z independently.

5.1.2 *One, two, three*

To solve the problem we will try to guess the form of the wavefunction. This educated[24] guess rests on a simple hypothesis. Let us consider the fully polarized state $|\uparrow,\ldots,\uparrow\rangle$ with L up spins. The total z component of the spin is $S_z = L/2$ and the energy of this state is (with periodic boundary conditions) $E = LJ_z/4$. If now we look for a state with N spins down, the wavefunction is totally defined by the position of the N coordinates $x_1, x_2, \ldots, x_N$ of the down spins. So, for example, a wave function

$$\psi(x) = \delta(x - x_0) \tag{5.4}$$

means there is a single down spin at the site x_0 and that all other sites have spin up. In one dimension it is always possible to order unambiguously so we will always assume that $x_1 < x_2 < \cdots < x_N$.

The case of only one spin down is easy. The J_z term is trivial. If one has a bond $\uparrow\downarrow$ instead of $\uparrow\uparrow$ the energy of this bond changes from $J_z/4$ to $-J_z/4$. Thus, the change due to the J_z term is (there are two such bonds for a single spin down) $\delta E = -J_z$. The Schrödinger equation is thus

$$\begin{aligned} H\psi(x) &= E\psi(x) \\ &= J[-\Delta\psi(x) + \frac{1}{2}[\psi(x-1) + \psi(x+1)]] + E_0\psi(x) \end{aligned} \tag{5.5}$$

where E_0 is the energy of the totally polarized (all spin up) state. The J_{xy} term being just a kinetic-like term the eigenstates are clearly plane waves with a momentum k

$$\psi(x) = \frac{1}{\sqrt{L}} e^{ikx} \tag{5.6}$$

Here the lattice spacing is taken as $a = 1$ so both k and x are dimensionless. The total energy of this state is thus

[24] Inspired would be more close to the truth.

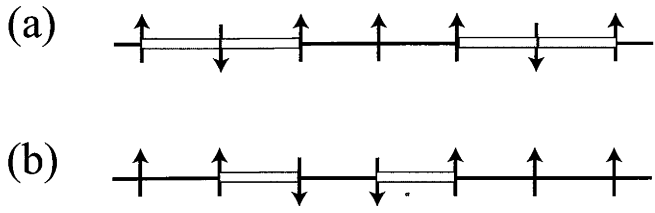

FIG. 5.1. Two down spins far away do not see each other (a). The equation is thus the same as for a single spin down. (b) If the two spins are close to each other both the interaction and the spin-flip term are different since a spin down can only move to the place where there is a spin up. The grey bonds represent an exchange of $-J_z/4$ and a black bond an energy of $J_z/4$.

$$E(k) = J[\cos(k) - \Delta + \frac{\Delta L}{4}] \tag{5.7}$$

The allowed momenta scan the first Brillouin zone $k \in [-\pi/2, \pi/2]$ and if one takes periodic boundary conditions the k are quantized as $k = 2\pi n/L$. For a ferromagnetic coupling this excitation is nothing but the standard magnon. For ferromagnetic systems the minimum of energy is at $k = 0$, which is a signature of the spin rotation symmetry of the system. The solution for one particle is thus (I is an integer).

$$\begin{aligned} E &= J[\cos(k) - \Delta] + \frac{J\Delta L}{4} \\ k &= \frac{2\pi I}{L} \\ \psi(x) &= \frac{1}{\sqrt{L}} e^{ikx} \end{aligned} \tag{5.8}$$

Two spins down is slightly more complicated. If the two down spins are far away, they do not see each other. On the other hand, if the two down spins are on adjacent sites the interaction between them is different from two far away down spins as shown in Fig. 5.1. One is thus facing the situation of two particles that can scatter when they get close to each other. One can thus imagine a scattering where the two particles would start with momentum k_1 and k_2 and far away would have momenta k_3 and k_4. Far away of the scattering the energy should be conserved. For two particles the conservation of momentum $k_1 + k_2 = k_3 + k_4$ and of the energy of the particles $E(k_1) + E(k_2) = E(k_3) + E(k_4)$ imposes that the momenta should either be conserved $k_3 = k_1$, $k_4 = k_2$ or exchanged $k_4 = k_1$, $k_3 = k_2$. Thus, the wavefunction with a given energy and momentum for two particles has to have the asymptotic form (for large separations of the particles)

$$\psi(x_1, x_2) = \alpha e^{i(k_1 x_1 + k_2 x_2)} + \beta e^{i(k_1 x_2 + k_2 x_1)} \tag{5.9}$$

The wavefunction is thus totally (asymptotically) determined by the ratio α/β, since the normalization fixes one of the parameters. The basic idea of Bethe's

ansatz is to extend this form of the wavefunction to *all* distances. Let us note immediately that $\psi(x,x)$ has of course no physical meaning since one cannot put two down spins one the same site, but is mathematically perfectly well-defined from (5.9). Such a form for the wavefunction is acceptable if the solution of the Schrödinger equation imposes only one additional condition (which fixes the parameter α/β). The allowed values of k are simply fixed by the boundary condition. For periodic boundary conditions (the origin can be put anywhere)

$$\psi(x_1,x_2) = \psi(x_2, x_1 + L) \tag{5.10}$$

This condition imposes from (5.9)

$$\alpha = \beta e^{-ik_2 L} = \beta e^{ik_1 L} \tag{5.11}$$

This imposes

$$k_1 + k_2 = \frac{2\pi n}{L} \tag{5.12}$$

This is the quantification of the total momentum $P = k_1 + k_2$. There is the second condition

$$\alpha/\beta = e^{ik_1 L} \tag{5.13}$$

The phase of the parameter α/β thus shifts the quantification of k_1, or equivalently of the difference $k_1 - k_2$, compared to what one would have for two totally independent particles. This is an effect of the interactions between the two down spins. One already sees at the level of two down spins that although each particle is still represented by a plane wave as a free particle, the allowed values of the momentum k for a given particle depend on the presence of the others.

Let us now go back to the Schrödinger equation. If the two down spins are not adjacent on the lattice, then the effect of H is totally independent on each down spin. The wavefunction (5.9) is thus a solution of the Schrödinger equation regardless of the value α/β. If the two particles are adjacent as shown in Fig. 5.1 then the situation is different. There are only two $\uparrow\downarrow$ bonds instead of four and the particle 1 can only jump to the left while particle 2 can only jump to the right. This gives (all energies are given relative to the fully polarized state)

$$H\psi(x,x+1) = J[-\Delta\psi(x,x+1) + \frac{1}{2}[\psi(x-1,x+1) + \psi(x,x+2)]] \tag{5.14}$$

Thus, if one wanted the Schrödinger equation to be exactly (5.5) for all positions of x_1 and x_2, it would work for all positions but for x_1 and x_2 adjacent and for this position there would be a missing term from the difference between (5.5) and (5.14).

$$J\Delta\psi(x,x+1) - \frac{J}{2}[\psi(x,x) + \psi(x+1,x+1)] \tag{5.15}$$

Thus, wavefunction (5.9) satisfies the Schrödinger equation *everywhere* if we choose α/β such that the missing term (5.15) is exactly zero. This imposes

$$2\Delta[\alpha e^{ik_2} + \beta e^{ik_1}] = (\alpha + \beta)[1 + e^{i(k_1+k_2)}] \tag{5.16}$$

that can be reexpressed as

$$\frac{\alpha}{\beta} = -\frac{\Delta e^{i\frac{k_1-k_2}{2}} - \cos(\frac{k_1+k_2}{2})}{\Delta e^{i\frac{k_2-k_1}{2}} - \cos(\frac{k_1+k_2}{2})} \tag{5.17}$$

We have thus reached our goal. We have the full wavefunction of the two-particle problem. The asymptotic wavefunction is in fact *exact* with the proper choice of α/β. Note that this remarkable result is a direct consequence of the fact that the interaction is only between nearest neighbors. If the two particles are further away than the nearest neighbor they are independent and the wavefunction is automatically exact. Thus, the Hamiltonian imposes a *unique* condition to fix the *only* parameter that we have at our disposal. We thus see that models with longer-range interactions will not in general (one can always find some magical fine-tuning between the interactions) be solvable by such a method since there will be more conditions than available free parameters.

Let us now have a look at the solution since it is instructive in the light of what will happen for more particles. For real k_1 and k_2 the ratio α/β is a pure phase

$$\frac{\alpha}{\beta} = -e^{i\Theta(k_1,k_2)} \tag{5.18}$$

with

$$\Theta(k_1, k_2) = 2\arctan\left(\frac{\Delta\sin(\frac{k_1-k_2}{2})}{\Delta\cos(\frac{k_1-k_2}{2}) - \cos(\frac{k_1+k_2}{2})}\right) \tag{5.19}$$

Note that $\Theta(k_1, k_2) = -\Theta(k_2, k_1)$. If we report α/β in the quantization condition (5.11) one finds

$$\begin{aligned} Lk_1 &= 2\pi I_1 + \Theta(k_1, k_2) \\ Lk_2 &= 2\pi I_2 + \Theta(k_2, k_1) \end{aligned} \tag{5.20}$$

where I_1 and I_2 are *half*-integers. Thus, the allowed values of k are shifted compared to the ones of a single down spin as shown in Fig. 5.2. Note that the shift on one k depends on the choice of the other k through $\Theta(k_1, k_2)$. This is the sign that the particles are *not* free excitations even if the wavefunction looks like a simple product of plane waves.

Two additional conditions can be worked out for $\Theta(k_1, k_2)$ The wavefunction can be written as

$$\psi(x_1, x_2) = e^{i(\frac{\Theta(k_1,k_2)}{2} + k_1x_1 + k_2x_2)} - e^{i(-\frac{\Theta(k_1,k_2)}{2} + k_1x_2 + k_2x_1)} \tag{5.21}$$

If one takes $k_1 = k_2$ the wavefunction is identically zero, and thus not allowed. It is thus necessary to have $k_1 \neq k_2$ to get an acceptable solution. Note also that if $\Delta = 0$ one has $\Theta(k_1, k_2) = 0$ and the solution is a simple plane wave where

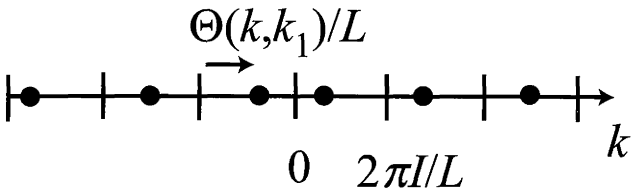

FIG. 5.2. Two particles are still described by a plane wave wavefunction. The effect of the interaction shows up in the shift of the quantization of the momentum k compared to the one of a free particle. The shift is due to the phase $\Theta(k,k_1)$ and depends on both momenta.

the ks are independent. As we will show in the next chapter this point is indeed equivalent to a free fermion problem.

Since this formulation was successful for two particles the idea is to try to continue with more. There are several reasons for why this should not work. First, for three particles in a scattering the conservation of energy and momentum is not enough to impose the conservation of the momenta. There is thus no reason to expect a wavefunction of the form (5.9) to work for more than two particles. The only case where it would work is if the scattering matrix was factorizable so that one of the particles is essentially unaffected in the collision. In general, this is a miracle that is not expected to happen. Well, miracles do happen for some models and in one dimension more often than would be reasonable to expect. It can be directly checked on three particles that a wavefunction of the form (5.9) is still a solution of the Schrödinger equation. This strongly suggests to tackle the N particle problem this way, which is what we do now.

5.1.3 *Many; Bethe-ansatz*

Let us now look at a system with N down spins at positions $x_1 < x_2 < \cdots < x_N$. Let us denote $\{x_i\} = x_1, x_2, \ldots, x_N$. As for two particles, if none of the x_i are adjacent, one has (I set $J = 1$ to lighten the notations since J only fixes the global energy scale)

$$\varepsilon\psi(\{x_i\}) = \frac{1}{2}\sum_{i=1}^{N} \delta_i \psi(\{x_i\}) \tag{5.22}$$

where $\varepsilon = E + \Delta(N - L/4)$, E is the eigenvalue for the energy, and the finite-difference operator δ_i is defined by

$$\delta_i\psi(\ldots, x_i, \ldots) = \psi(\ldots, x_i - 1, \ldots) + \psi(\ldots, x_i + 1, \ldots) \tag{5.23}$$

If two down spins are adjacent, for example, $x_{k+1} = x_k + 1$, as we saw there are two differences: displacement of the spin is partly suppressed and the J_z term is different. Thus, generalizing what we did for two down spins one finds instead of (5.22)

$$\varepsilon\psi(\ldots,x_k,x_k+1,\ldots)=\frac{1}{2}\sum_{i\neq k,k+1}^{N}\delta_i\psi(\ldots,x_k,x_k+1,\ldots)$$
$$+\frac{1}{2}[\psi(\ldots,x_k-1,x_k+1,\ldots)+\psi(\ldots,x_k,x_k+2,\ldots)]+\Delta\psi(\ldots,x_k,x_k+1,\ldots) \tag{5.24}$$

It is clear how this generalizes to the case of more than two x_i's adjacent: whenever a down spin has a down neighbor, the term representing displacement to that site disappears, and one finds an 'interaction term' (Δ) instead. To generalize our wavefunction (5.9) of two spins we now look for a wavefunction of the form

$$\psi(x_1,\ldots,x_N)=\sum_P A_P\exp\left[i\sum_{j=1}^{N}k_{Pj}x_j\right] \tag{5.25}$$

P are all possible permutations of the N index for the down spins. So the different momenta are permuted amongst all the particles (down spins). As for two spins, this wavefunction is a solution of the 'free' (5.22) for arbitrary coefficients A_P. As for two spins, we want now to determine the coefficients A_P so that (5.22) and (5.24) become identical, that is, one requires (compare with (5.15))

$$2\Delta\psi(\ldots,x_k,x_k+1,\ldots)=\psi(\ldots,x_k+1,x_k+1,\ldots)+\psi(\ldots,x_k,x_k,\ldots) \tag{5.26}$$

Inserting this into (5.24) one sees that one recovers (5.22), which is automatically solved by the plane wave form (5.25). To solve (5.26) for general N it is convenient to associate with each permutation P another permutation P' that differs from P only by the exchange of two adjacent elements: $P'(k)=P(k+1), P'(k+1)=P(k)$. One then has

$$\psi(\ldots,x_l+m,x_l+n,\ldots)=\sum_P{}' e^{\left[i\sum_{j\neq l,l+1}k_{Pj}x_j\right]}e^{i(k_{Pl}+k_{P'l})x_l}$$
$$\times\left(A_Pe^{i(mk_{Pl}+nk_{P'l})}+A_{P'}e^{i(mk_{P'l}+nk_{Pl})}\right) \tag{5.27}$$

where in (5.26) the cases $m,n=0,1$ are relevant, and the summation over P is restricted over half of the permutations (e.g. those with $P(k)<P(k+1)=P'(k)$), the other permutations being included explicitly by the term proportional to $A_{P'}$. Given that (5.26) is supposed to be valid for any set $\{x_i\}$, the coefficients of the plane wave factors in the left- and right- hand sides have to be equal, for example,

$$2\Delta(A_Pe^{ik_{P'k}}+A_{P'}e^{ik_{Pk}})=(A_P+A_{P'})(1+e^{i(k_{Pk}+k_{P'k})}) \tag{5.28}$$

This is an obvious generalization of (5.16) and leads to

$$\frac{A_P}{A_{P'}}=-\frac{1+e^{i(k_{Pk}+k_{P'k})}-2\Delta e^{ik_{Pk}}}{1+e^{i(k_{Pk}+k_{P'k})}-2\Delta e^{ik_{P'k}}}=-\exp(-i\Theta(k_{Pk},k_{P'k})) \tag{5.29}$$

The phase $\Theta(k_i, k_j)$ has thus exactly the form (5.19). Note that although an arctangent is only defined up to an additive multiple of π this indetermination has no effect on the phase Θ itself. This now fixes all the coefficients in (5.25) unambiguously, up to an overall normalization. Indeed, any permutation can be built as a sequence of elementary permutations of two adjacent elements (transpositions). One can thus fix $A_{1,2,3,\ldots,N}$ and determine the coefficient A_P by decomposing the permutation P in a sequence of transpositions and using (5.29). A_P is thus the product of such factors

$$\frac{A_P}{A_{1,2,3,\ldots,N}} = (-1)^{\eta_P} e^{\sum \Theta(k_i,k_j)} \tag{5.30}$$

where η_P is the number of transpositions required to build P and the sum in the exponential is on all these transpositions. Because of the antisymmetry of the phases $\Theta(k_i, k_j) = -\Theta(k_j, k_i)$ this product is independent of the sequence of individual permutations, for example,

$$(123) \to (213) \to (231) \to (321) \text{ and } (123) \to (132) \to (312) \to (321) \tag{5.31}$$

lead to the same factor. One should also notice that (5.29) was derived without any assumption on the other x_is, and consequently situations with three or more adjacent down spins are equally covered and the generalizations of (5.24) to these cases are therefore also fulfilled. It remains to determine the allowed k-values. This follows from the periodic boundary condition

$$\psi(1, x_2, \ldots, x_N) = \psi(x_2, \ldots, x_N, L+1) \tag{5.32}$$

Inserting into (5.25) and noting that (5.32) has to be satisfied for all $(x_2, \ldots, x_N)$, one obtains the condition

$$(A_P/A_{P'})e^{ik_{P'1}L} = 1 \tag{5.33}$$

which must be satisfied for every permutation P. Here, P' is a permutation obtained from P by a 'right shift' of all elements:

$$(P'1, P'2, \ldots, P'N) = (PN, P1, P2, \ldots, PN-1) \tag{5.34}$$

The ratio of coefficients in (5.33) now can be calculated by repeatedly permuting PN in (5.34) to the right and using (5.29). The resulting equation is

$$(-1)^{N-1} \exp\left(i \sum_{j=1}^{N} \Theta(k_j, k_l) \right) e^{ik_l L} = 1 \tag{5.35}$$

with Θ defined in (5.29) (or (5.19)). This leads to

$$Lk_i = 2\pi I_i + \sum_j \Theta(k_i, k_j) \tag{5.36}$$

where I_i are integers if N is odd and half-integer if N is even. This is of course in agreement with our results for one and two spin down. Note that from (5.27)

one sees that if two k are equal the wavefunction is identically zero. Thus, only solutions where all k are different are allowed.

We thus have computed the full equations determining the wavefunction, energy, and momentum of a system of L sites and N spins down. I summarize here the full equations for convenience

$$\begin{aligned}
\psi(x_1,\ldots,x_N) &= \sum_P A_P \exp\left[i\sum_{j=1}^N k_{Pj}x_j\right] \\
\frac{A_P}{A_{1,2,3,\ldots,N}} &= (-1)^{\eta_P} e^{\sum_{\eta_P}\Theta(k_i,k_j)} \\
\frac{A_P}{A_{P'}} &= -\frac{1+e^{i(k_{Pl}+k_{P'l})}-2\Delta e^{ik_{Pl}}}{1+e^{i(k_{Pl}+k_{P'l})}-2\Delta e^{ik_{P'l}}} = -\exp(-i\Theta(k_{Pl},k_{P'l})) \\
Lk_i &= 2\pi I_i + \sum_j \Theta(k_i,k_j)
\end{aligned} \tag{5.37}$$

where η_P and $\sum_{\eta_P}$ are, respectively, the number and the summations over the transpositions needed to build the permutation P from $1,2,3,\ldots,N$. P and P' differ by a transposition $P'(l) = P(l+1)$ and $P'(l+1) = P(l)$. I_i are integers for N odd and half-integer for N even. k_i should all be different. The energy and momentum are given by

$$\begin{aligned}
P &= \sum_i k_i \\
E/J &= \Delta\frac{L}{4} + \sum_j [\cos(k_j) - \Delta]
\end{aligned} \tag{5.38}$$

For all k_j reals (these are not *a priori* the only solutions) the phase $\Theta(k_i,k_j)$ takes the simple form

$$\Theta(k_1,k_2) = 2\ \arctan\left(\frac{\Delta\sin(\frac{k_1-k_2}{2})}{\Delta\cos(\frac{k_1-k_2}{2}) - \cos(\frac{k_1+k_2}{2})}\right) \tag{5.39}$$

5.1.4 *Bethe-ansatz and Luttinger liquids*

The remarkable equations (5.37) are the full solution to the spin chain problem. One has of course to realize what one means by full solution. There are two levels of complexity in going from (5.37) to the physics of the system. First, one has to solve the equations. This is a rather complicated task to do analytically, especially since one wants the thermodynamic limit $L \to \infty$ and N/L fixed. The equations have a nasty form and we will see how to partly deal with such a solution in the next section. More importantly, even if one has the solution the main question is what one can compute from the solution. Although one has the full form of the wavefunction, it is incredibly complicated and computing correlation functions

with the wavefunction (5.37) is a close to impossible task. As a result the only quantities that are relatively simple to extract from the solution are the total energy and the momentum. Since one gets these quantities as a function of the quantum numbers it is relatively easy to extract the thermodynamic quantities out of the solution.

This of course limits the use one can have for the Bethe-ansatz solution since one would mostly like to have the correlation functions of the system. There is however a trick that solves this problem and consists in coupling the Bethe-ansatz solution with the Luttinger liquid concept. Indeed, as we saw in Chapter 3, the full low-energy properties in a Luttinger liquid *only* depends on the two parameters u and K. Thus, one can use the Bethe-ansatz solution to compute two thermodynamic quantities. This fixes the two parameters u and K. One can then use the Luttinger liquid formulas to get the *exact* asymptotic decay for the given microscopic model. This method is extremely powerful since one does not even need to solve the equations analytically. Indeed, even if the Bethe-ansatz equations can be complicated to solve analytically (especially in the thermodynamic limit) they are quite easy to solve numerically for a finite L. Indeed, it is enough to start with an initial value for the k_i, for example, the solution where all Θ are zero. One then simply iterates (5.37) to get a new set of k_i as a function of the initial values. Iterating successively the equations rapidly converge to a solution. I do not know whether there is a proof that the Bethe-ansatz equations have the convexity property of converging to the solution but it does work. One can solve the equations for quite large number L and N. It is thus easy to compute the energy of the system, and then to use the energy to compute some thermodynamic quantities. Because it is a calculation of thermodynamic quantities the finite size effects are very small and one gets a very good accuracy on the results. This is a method that we will use repeatedly when looking at microscopic models in Chapters 6 and 7.

One only needs two relations to fix the two Luttinger parameters u and K. If there is more than one species (e.g. spin) then one needs two relations per species. Which quantity to compute is a matter of choice. A favorite candidate is the compressibility. Indeed, the compressibility is simply given by (see (2.50))

$$\begin{aligned} \kappa_{\text{true}}^{-1} &= \frac{N^2}{L}\frac{d^2E}{dN^2} \\ \kappa^{-1} &= L\frac{d^2E}{dN^2} \end{aligned} \tag{5.40}$$

The second derivative can be computed from a discrete number of particles by simply computing

$$\kappa^{-1} = L\left(\frac{E_0(N+2)+E_0(N-2)-2E_0(N)}{4}\right) \tag{5.41}$$

(one usually adds two particles to avoid even odd effects). The total energy can of course be easily computed from the Bethe-ansatz equations. One then uses

(2.59) to get the ratio u/K. One needs a second relation. The velocity can be extracted from the Bethe-ansatz solution directly in some cases. One can also use the size dependence of the ground-state energy (3.106), but because one needs to extract the size dependence it is not usually the most easy way. A very simple choice is to twist the boundary conditions $\psi(L) = e^{i\Phi}\psi(0)$ instead of taking the standard periodic ones. As we will see in Section 7.2 this is equivalent to threading a flux into the system. This simply changes the last relation in (5.37) into

$$Lk_i = 2\pi I_i + \Phi + \sum_j \Theta(k_i, k_j) \tag{5.42}$$

Now the energy of the system is a function of the flux. As we will see in Section 7.2 (see (7.80))

$$L\frac{\partial^2[E(\Phi)]}{\partial^2\Phi^2} = \frac{uK}{\pi} \tag{5.43}$$

Once again the derivative can be computed numerically. An example of the program using these relations to compute the Luttinger liquid parameters for the spin chain is given in Appendix F.

5.1.5 *Partial solution of the equations*

Let us now look how to tackle directly and analytically the equations. This is in itself a whole industry, so it is out of question to even scratch the surface of this problem. I will thus only discuss some simple consequences, and restrict the study to the case of the isotropic antiferromagnet ($\Delta = 1$, or the so-called Heisenberg model). I parametrize the equations by introducing the rapidities as

$$\begin{aligned} k &= \overline{k} + \pi \\ \lambda &= -\frac{1}{2}\tan(\overline{k}/2) \end{aligned} \tag{5.44}$$

The equations become

$$\begin{aligned} 2\pi\overline{I}_i &= 2L\arctan(2\lambda_i) - \sum_j 2\arctan(\lambda_i - \lambda_j) \\ E &= \frac{L|J|}{4} - |J|\sum_i [1 + \cos(\overline{k})] \\ P &= \sum_i \overline{k}_i + N\pi \end{aligned} \tag{5.45}$$

where $\overline{I}$ is integer if L and N have opposite parities and is half-integer if L and N have the same parity. The parametrization (5.45) works both for the isotropic antiferromagnet $J > 0$ and ferromagnet $J < 0$. From now on I drop the overline

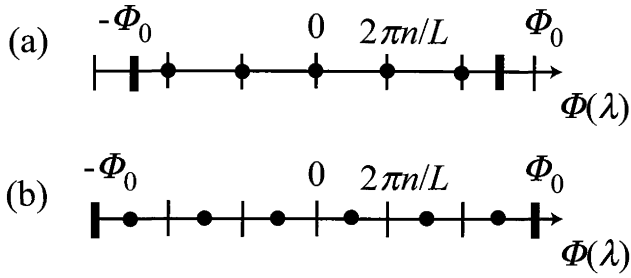

FIG. 5.3. Roots of the Bethe-ansatz solutions. (a) L and N have opposite parities. Since $\Phi(\lambda)$ is an increasing function going between $\pm\pi[L-N]$ the equation $\Phi(\lambda) = 2\pi I$ with I integer has exactly $L-N$ solutions. (b) L and N have the same parity. Since I is now a half-integer the number of solutions is still $L-N$.

in these equations to lighten the notations. To solve (5.45) one can give oneself a set of I_i and solve for the λ_i. In practice, one can define a function

$$\Phi(\lambda) = 2L\arctan(2\lambda) - \sum_j 2\arctan(\lambda - \lambda_j) \tag{5.46}$$

In principle, λ_j can be complex. I will come back to this point later. For the moment let me focus on real λ_i. Then the function Φ is obviously an increasing function of λ. Regardless of the precise values of λ_j it varies between $-\Phi_0$ and Φ_0 where

$$\Phi_0 = \pi[L-N] \tag{5.47}$$

One can thus start with a set of $\{\lambda_j\}$, which parametrize the function $\Phi(\lambda)$ and then solve the equation $\Phi(\lambda) = 2\pi I$. This defines a set of roots $\{\lambda_\alpha\}$. One should thus choose the original $\{\lambda_j\}$ such that it is a subpart of the final set of roots $\{\lambda_\alpha\}$. Needless to say finding this is a complicated thing. Since there are only N spin down (thus N original λ_j) there are in principle extra roots. Given the condition on I_i, it is easy to check that there are always $L-N$ solutions to the equation $\Phi(\lambda) = 2\pi I$. This is shown in Fig. 5.3. Among the $L-N$ solutions only N are occupied and intervene in the function Φ and the energy and momentum. The others are called holes in the possible rapidities. If they are present the holes are chosen in such a way that the total energy of the system is minimal. If one considers a chain in the absence of a magnetic field and thus with zero magnetization $L/2 = N_\uparrow = N_\downarrow$ (thus L is even), there are no holes and there is only one single set of $\{\lambda_j\}$ possible. Since the roots are given by the solution of $\Phi(\lambda) = 2\pi I$ and regularly spaced, one can define a density of states in the thermodynamic limit

$$\rho(\lambda) = \frac{1}{2\pi}\frac{d\Phi}{d\lambda} \tag{5.48}$$

With this density of states the function Φ becomes

$$\Phi(\lambda) = 2L\arctan(2\lambda) - 2\int_{-\infty}^{+\infty} d\lambda'\rho(\lambda')\arctan(\lambda-\lambda') \tag{5.49}$$

which using (5.48) gives the equation for $\rho(\lambda)$

$$2\pi\rho(\lambda) = \frac{4L}{1+4\lambda^2} - 2\int_{-\infty}^{+\infty} \rho(\lambda')\frac{d\lambda'}{1+(\lambda-\lambda')^2} \tag{5.50}$$

Since the integral is a convolution, it is trivial to solve this equation by Fourier transform. The solution is

$$\rho(\lambda) = \frac{L}{2\cosh(\pi\lambda)} \tag{5.51}$$

Now that we have the density of states of the roots we can easily compute the total energy and momentum. The energy of the ground state is given by

$$\begin{aligned} E_0 &= \frac{L|J|}{4} - |J|\sum_j [1+\cos(k_j)] \\ &= \frac{L|J|}{4} - |J|\sum_j \frac{2}{1+4\lambda_j} \\ &= \frac{L|J|}{4} - |J|\int d\lambda\, \rho(\lambda)\frac{2}{1+4\lambda} \\ &= L|J|[\frac{1}{4} - \log(2)] \end{aligned} \tag{5.52}$$

The total energy is thus $E_0 \simeq -0.44L|J|$. This is to be compared with the Neel state which would simply give $E = -\frac{1}{4}L|J|$. The true solution that takes into account the quantum fluctuations of the spins has a lower energy. The ground state is a spin singlet. The total momentum is $P_0 = \pi N$ since $\sum_j k_j$ is zero by symmetry.

Let us now look at what happens if we consider excited states compared to the ground state where one creates a few holes. I call the total density of states $\rho(\lambda)$ (it corresponds to the roots $\{\lambda_\alpha\}$). If we call $\rho_h(\lambda)$ the density of holes, the summation over the set $\{\lambda_j\}$ has to be performed with the density $\rho - \rho_h$. The equation for ρ and ρ_h becomes

$$\begin{aligned} 2\pi\rho(\lambda) + 2\int_{-\infty}^{+\infty} \rho(\lambda')\frac{d\lambda'}{1+(\lambda-\lambda')^2} \\ = \frac{4L}{1+4\lambda^2} + 2\int_{-\infty}^{+\infty} \rho_h(\lambda')\frac{d\lambda'}{1+(\lambda-\lambda')^2} \end{aligned} \tag{5.53}$$

This equation can be solved again by Fourier transform. If $\rho(\xi)$ is the Fourier transform of $\rho(\lambda)$ one has

$$\rho(\xi) = \rho_0(\xi) + \frac{\rho_h(\xi)}{1+e^{|\xi|}} \tag{5.54}$$

where $\rho_0(\xi)$ is the Fourier transform of the density of states in the absence of holes that we have already computed. The solution is thus of the form

$$\begin{aligned}\rho(\lambda) &= \rho_0(\lambda) + \int_{-\infty}^{+\infty} d\lambda'\ \rho_h(\lambda')\phi(\lambda-\lambda') \\ \phi(\lambda) &= \frac{1}{2\pi}\int_{-\infty}^{+\infty} d\xi \frac{e^{-i\xi\lambda}}{1+e^{|\xi|}}\end{aligned} \tag{5.55}$$

The holes have thus an action on the *whole* density of states. The energy of the system compared to the ground-state energy E_0 is

$$\begin{aligned}E - E_0 &= -|J| \int_{-\infty}^{+\infty} [\rho - \rho_0 - \rho_h] \frac{2d\lambda}{1+4\lambda^2} \\ &= \int_{-\infty}^{+\infty} \rho_h(\lambda)\epsilon(\lambda)\end{aligned} \tag{5.56}$$

The last line defines the energy $\epsilon(\lambda)$. Using the expression for ρ one obtains

$$\begin{aligned}\epsilon(\lambda) &= \int_{-\infty}^{+\infty} d\lambda'[\delta(\lambda-\lambda') - \phi(\lambda-\lambda')]\frac{2|J|}{1+4(\lambda')^2} \\ &= \frac{\pi|J|}{2\ \cosh(\pi\lambda)}\end{aligned} \tag{5.57}$$

The momentum can be computed in a similar way, defining $q(\lambda)$

$$\begin{aligned}P - N\pi &= \int_{-\infty}^{+\infty} d\lambda'\ \rho_h(\lambda')q(\lambda') \\ q(\lambda) &= \int_{-\infty}^{+\infty} d\lambda'[\delta(\lambda-\lambda') - \phi(\lambda-\lambda')]2\arctan(2\lambda')\end{aligned} \tag{5.58}$$

It is easy to check from (5.56) and (5.58) that

$$\frac{dq}{d\lambda} = \frac{2\epsilon}{|J|} \tag{5.59}$$

and using (5.57)

$$q(\lambda) = \arctan(\sinh(\pi\lambda)) + \text{Cste} \tag{5.60}$$

The constant can be fixed by looking at a single hole at $\lambda = 0$. In that case $P = 0$ by symmetry and thus the constant is zero. The energy and momentum of a distribution of holes with a density $\rho_h(\lambda)$ is given by

$$\begin{aligned}q(\lambda) &= \arctan(\sinh(\pi\lambda)) \\ \epsilon(\lambda) &= \frac{\pi|J|}{2\cosh(\pi\lambda)}\end{aligned} \tag{5.61}$$

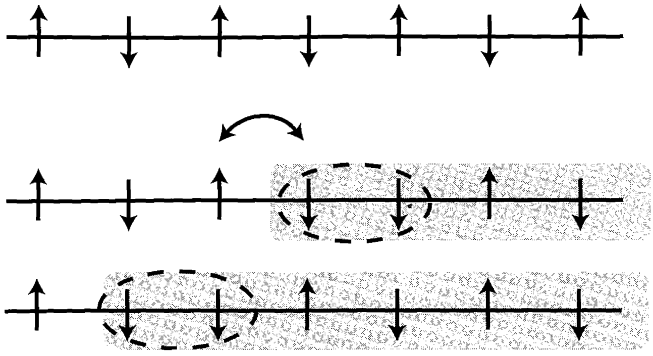

FIG. 5.4. Schematic representation of a spinon excitation corresponding to a single hole in the Bethe-ansatz equations. It consists in creating a domain wall by reversing all the spins beyond a certain point. The spinon carries a spin 1/2. When this spinon propagates because of the spin flip terms in the Hamiltonian it moves by two lattice spacings as shown in the bottom figure.

and thus the holes verifies

$$\epsilon = \frac{\pi|J|}{2}\cos(q) \tag{5.62}$$

This is a remarkable solution since it looks like the dispersion relation of a free particle. It is however important to note that the holes are not free particles since their presence affects the whole distribution ρ. The density of state is a very complex object to obtain, since contrary to true free particles λ are not regularly spaced any more. However, all these effects are hidden in the density of states and the dispersion relation is particularly simple.

Let us first look at a single hole. From (5.61) we see that the momentum is in the interval $[-\pi/2, \pi/2]$, that is, on only *half* of the Brillouin zone. This strange property can be understood by looking at the physical interpretation of a single hole. This excitation, shown in Fig. 5.4, is called a spinon. It consists in turning half of the chain upside down thus putting two neighboring spin up. It is a Bloch domain wall in the one-dimensional spin chain. The $x - y$ part of the spin Hamiltonian moves this excitation in the chain. A single flip moves the spinon by *two* lattice spacings. This explains why its momentum only spans half the Brillouin zone. Note that if a spinon makes a full circle on the chain the system does not go back to the same state but all spins have been reversed. The spinon should thus make two turns to leave the system in the same state. The quantification of q is thus twice as dense than for an excitation that leaves the system unchanged after only one turn. One thus recovers the proper number of states even if the 'Brillouin' zone for the spinon is only half of the normal one. We will see in the next chapter how to recover the spinons from the bosonization solution.

Let us now look at an excited state where one has made an excitation of spin 1. This can be done by flipping a spin down as indicated in Fig. 5.5. It is the

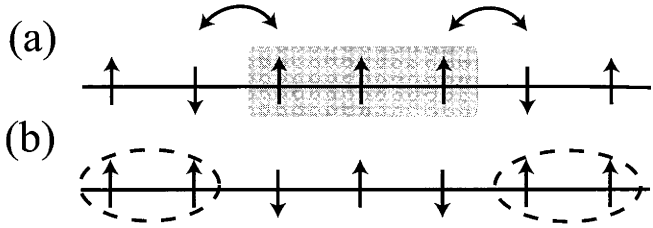

FIG. 5.5. A magnon excitation consists in flipping a single spin. (a) The central spin has been flipped up compared to the normal antiferromagnetic chain. The magnon carries a spin one. (b) This magnon decomposes under the effect of the spin flip terms in the Hamiltonian into two spinons.

standard magnon of a spin system. This excitation corresponds to $N = L/2 - 1$. Since the number of solutions of the equation is $L - N = L/2 + 1$, there are thus *two* holes in the spectrum to make a single magnon. Physically this means that the magnon decomposes into two spinons as shown in Fig. 5.5. The magnon excitation is made of two entities, and thus leads to a continuous spectrum, with a momentum q and energy ϵ given by

$$\begin{aligned} q &= q_1 + q_2 \\ \epsilon(q) &= \frac{\pi|J|}{2}[\cos(q_1) + \cos(q_2)] \end{aligned} \tag{5.63}$$

The corresponding dispersion relation $\epsilon(q)$ is shown in Fig. 5.6. We just saw how two spinons get combined symmetrically to give a spin 1 solution (the magnon). They can also combine antisymmetrically to give a spin 0 bound state. This involves solutions with complex λs. These solutions are referred as 'string solutions' in the literature. Their study falls outside of this brief presentation and I refer the reader to the above-mentioned reviews for more material on this point.

This is a small tour of the information that one can directly extract form the Bethe-ansatz equations. Most of the thermodynamic properties can also be extracted analytically, using the so-called 'thermodynamic Bethe-ansatz' (Takahashi, 1999). Recently, progress was also made for the calculation of correlation functions in massive phases with the so-called form factors (Gogolin *et al.*, 1999). I refer the reader to the literature for more details on these points.

5.2 A zest of numerics

Let me now present very briefly some of the numerical methods that have proved very useful in one dimension. Indeed, the numerical methods have gained a considerable importance. In one dimension the finite size effects are quite small in themselves compared to higher dimensions, since the volume/surface ratio is optimal. In addition, in the same way that we used Bethe-ansatz to determine the Luttinger parameters one can of course use a numerical solution of the problem for this purpose. Combining the numerics with the Luttinger liquid concept has thus proved to be a very powerful tool.

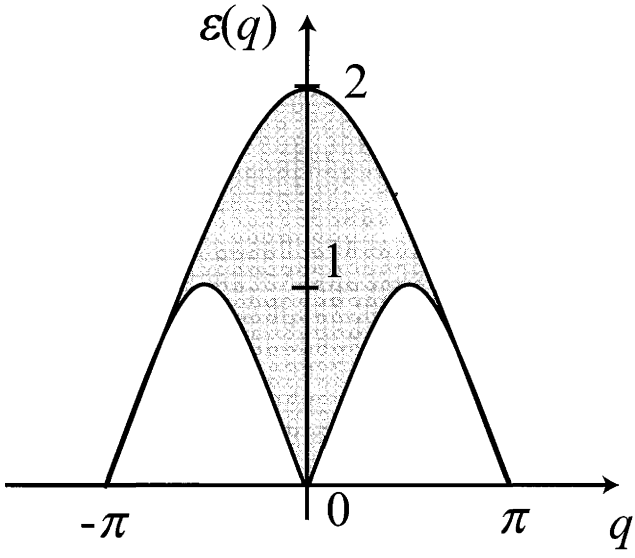

FIG. 5.6. Relation dispersion of a single magnon. Because the magnon decomposes into two entities, there is a continuum of excitations for a given vector q.

5.2.1 *Exact diagonalizations*

This is the simplest numerical method in principle. One simply diagonalizes the full interacting Hamiltonian and determines the eigenvalues and the eigenvectors. Although the principle is simplicity itself, it is clear that the implementation of the method cannot be. To diagonalize an interacting Hamiltonian is indeed a formidable problem. The dimension of the Hilbert space is humongous. Let us consider, for example, the case of a spin Hamiltonian where on each site there is a spin 1/2. In that case the number of states per site is 2, which means that the size of the Hilbert space is 2^N. One has thus in principle to diagonalize a matrix $2^N \times 2^N$. Even for 15 sites this would represent if the matrix was full about 10^9 elements, something hard to store and manipulate on most computers. Fortunately the situation is slightly better. Since usually only neighbors are coupled by the interaction the Hamiltonian is a very sparse matrix. Keeping only the non-zero elements decreases a lot its size. One can also make a maximal use of the symmetries of the original system to further reduce the size of the matrix. Even with all these tricks the memory size to store and manipulate the elements of the Hamiltonian is the most severe limitation. Given the state of the art of the present computers it is very hard to exceed 36 sites for a spin system. For a system where there are more than two states per site the situation is of course much worse. The industry of exact diagonalization is thus a very strong encouragement to find Hamiltonians where the unnecessary states have been

eradicated. This is, for example, the case of the t–J model that we will examine in much more details in Chapter 7. Even with all these tricks, diagonalizing such large Hamiltonians requires some special techniques, the method usually used being the Lanczos technique. I refer the reader to the literature for more details on the method itself (Lanczos, 1950; Bonner and Fisher, 1964; Oitmaa and Betts, 1978; Davidson, 1993).

The advantage of exact diagonalization is of course the exact and systematic character of it. Given a microscopic Hamiltonian one gets the lowest eigenstates and eigenvalues, without any approximation or intrinsic numerical limitation. The results are thus free of bias. Since both the eigenvalues and eigenvectors are known the correlation functions can be computed directly in real time or frequency without fudging. One can work directly at zero temperature (which can be also a drawback). Exact diagonalizations have been extremely useful to compute Luttinger parameters. One can directly compute numerically the compressibility and response to a twist in boundary conditions. Since the quantum numbers are known one can also extract the velocities directly from the spectrum. We will see examples of results based on exact diagonalization in Chapter 7.

The drawback is of course mainly the size limitation. Since the Hilbert space doubles every time one site is added, this is not a problem that will be solved in the future. This means that extracting the long-distance, low-energy behavior is a very tricky business. For the frequency dependence of the correlation functions, this limitation is very obvious. For a system with L sites one can expect that the lowest reachable frequency is of the order of W/L where W is the bandwidth of the system. Since $1K$ corresponds to 30 GHz, one is quite far from the low-frequency behavior in an experimental sense.

5.2.2 *Monte-Carlo*

Monte-Carlo is opposite in spirit to exact diagonalizations. It is a well-known technique at the classical level. One has a partition function

$$Z = \sum_{\text{config}} e^{-\beta H} \tag{5.64}$$

The sum over all configurations is an N-dimensional integral, with N very large. The best way to evaluate such multiple integrals is a statistical method. A lucid exposition of the technique is given in Binder (1984) and Landau and Binder (2000). For classical systems the 'only' drawback of the Monte-Carlo method is the fact that the error in evaluating the integral decreases only as $1/\sqrt{t}$ where t is the computing time. It means that given enough time (and thus money) any problem can be in principle solved.

Unfortunately,[25] the situation is highly more complicated in the case of quantum problems. First, the equivalent of the partition function for a classical system is provided by the functional integral, which is a way to evaluate the partition

[25] Fortunately for us analytical guys ....

function for a quantum problem. It means that the method can only compute the various quantities in *imaginary* time. Going back to the physically interesting (that is, the retarded) correlation function is a complicated business. There are various ways of doing the Monte-Carlo for fermions, too specialized and numerous to be examined here (see, e.g. Kalos, 1982; Ceperley, 1995; Grotendorst *et al.*, 2002). The simplest is to compute directly the functional integral (C.3). This of course works only for bosons. For fermions the functional integral is not over numbers but over weird objects known as Grassmann variables. It is thus necessary to integrate over fermions. There are various ways to do this. Let me just mention the simplest method known as the Hirsh–Fye algorithm (Hirsch and Fye, 1986). Let us assume that one starts with the Hubbard model (see Chapter 7)

$$H = H_0 + U \sum_i (n_{i\uparrow} - \frac{1}{2})(n_{i\downarrow} - \frac{1}{2}) \tag{5.65}$$

The partition function in a discrete path integral representation is

$$\begin{aligned} Z &= \mathrm{Tr}[\prod_{j=1}^{N_\tau} e^{-\Delta\tau H}] \\ &= \mathrm{Tr}[\prod_{j=1}^{N_\tau} e^{-\Delta\tau H_0} e^{-\Delta\tau H_U}] \end{aligned} \tag{5.66}$$

where $\Delta\tau N_\tau = \beta$ and terms of order $\Delta\tau^2$ have been discarded. The interaction term on each site can be decoupled by introducing an Ising variable $\sigma = \pm 1$ on each site (and at each time slice)

$$e^{-\Delta\tau U(n_{i\uparrow}-1/2)(n_{i\downarrow}-1/2)} = \frac{e^{-(\Delta\tau U)/4}}{2} \mathrm{Tr}_\sigma[e^{\lambda\sigma(n_{i\uparrow}-n_{i\downarrow})}] \tag{5.67}$$

where $\cosh(\lambda) = e^{\Delta\tau U/2}$. After the interaction has been decoupled using (5.67), the trace over the fermionic degrees of freedom can be done explicitly in (5.66). The evaluation of the partition function (and the various correlation functions) is thus reduced to the evaluation of the classical sum over the Ising variables σ. The weight of a given configuration of σ is given by the complicated determinant resulting from the integration over the fermionic degrees of freedom in (5.66). This integral over the σ can thus be done by a similar Monte-Carlo method than for a classical system.

The advantage of Monte-Carlo is its possibility to treat relatively large size systems. It is in principle also an unbiased method. The correlation functions are computed at finite temperatures that can either be viewed as an advantage or as a drawback.

Unfortunately, there are several drawbacks. The first problem is known as the sign problem. Since the weight of a given configuration is resulting (in our method) from the integrations over the fermionic degrees of freedom there is no

guarantee that it is a positive number. In general, this is not the case, contrary to the classical case where the weights $e^{-\beta H}$ are intrinsically positive. It thus means that to compute the correlation function, one has now to add positive and negative numbers. Each individual term can thus be much larger than the final sum. It means that the statistical error that one can get in evaluating such a sum can (and in general will!) grow extremely fast. This contains some physics: we have reduced a fermionic problem for which only antisymmetric wave functions are allowed to a classical problem where one sums freely over the configurations. There should thus be something in the sum that cancels the unwanted configurations of the σ to keep only the good ones. The consequence of this problem is that, contrary to the classical case, the error can grow very fast in the calculation making any evaluation of the correlation function unfeasible. Spending more money on the calculation does not guarantee any more an increased accuracy in the results. This problem is yet unsolved. Various cures have been proposed, but they always require some knowledge of what should be the structure of the true fermionic wave function, which biases the method. In some fortunate cases, however, one can show that the weights are indeed positive. This is, for example, the case for spin systems on unfrustrated lattices, or for the Hubbard model at half-filling. In that case the sign problem does not occur and Monte-Carlo is an extremely efficient method.

The second problem comes from the fact that the method evaluates the correlation functions in imaginary time. To make an 'analytical' continuation on a numerical result (with noise!) is black magic. Thus, it is not always easy to go from Monte-Carlo results to the physical correlation functions. Some 'voodoo' methods have been devised for that, known as Maximum Entropy methods. Monte-Carlo can also be used to determine Luttinger exponents. With this method the two easiest quantities are the compressibility and the response to a twist in boundary conditions. The parameter K can also in principle be extracted directly from the correlation functions since the systems that one can access are reasonably large.

5.2.3 *DMRG*

In one dimension there is a recent method that has allowed to make gigantic progress in our ability to obtain numerical solutions (White, 1993). It is at the moment the closest to an ultimate weapon as one can dream of. The idea is simple and directly inspired from the numerical renormalization group method used by Wilson for the Kondo problem. The idea is to diagonalize a problem but keeping only the low-energy states and then implement numerically a renormalization procedure. With such a method the drawbacks of the exact diagonalization due to the need to keep too many states are eliminated while in principle keeping an excellent accuracy for the low-energy physics.

However, the procedure is not so easy to do in practice. Let me illustrate the problem with free electrons. Let us assume that one has diagonalized a free electron system of size L. How can one obtain the low-energy physics for a segment of size $2L$ from the knowledge we have for the system of size L. If

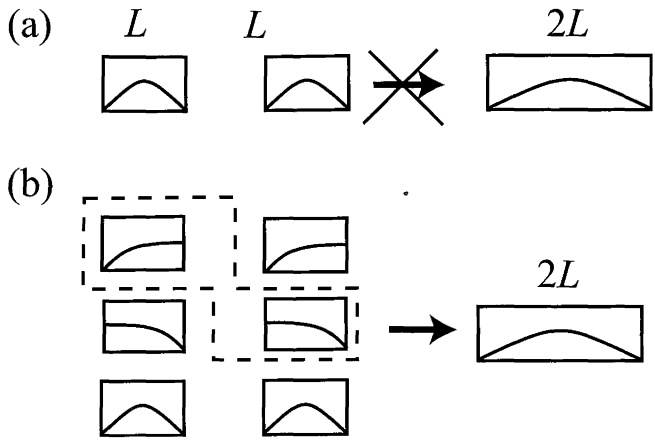

FIG. 5.7. To build a numerical renormalization group it is necessary to take into account various possible boundary conditions. (a) If one keeps only the low-energy of a system of size L with hard boundary condition then it is impossible to reproduce the low energy sector of a system of size $2L$ by coupling two such segments. (b) If all possible boundary conditions are allowed then it is possible to get a close approximate of a low-energy state in a segment of size $2L$ based on the low-energy properties of segments of size L. It is thus possible to build a numerical renormalization group.

one keeps all the states this is obviously easy, but let us assume that we have kept only the low-energy states of the segment of size L. In a renormalization group spirit we would only need the bottom of the spectrum to get the low-energy properties of the system and thus can throw away the states too far from the ground state since they will contribute little to the physical properties of the system. If there is a way to compute the low-energy of the segment of size $2L$, by reiterating the procedure one could in principle couple again two such segments and obtain ultimately the low-energy properties of a very long segment of material. In fact as noted by White, this method does not work very well if one does not pay special attention to the boundary conditions. Let us illustrate it by taking hard boundary conditions. In that case the ground state of the $2L$ segment has the form indicated in Fig. 5.7, with a maximum of density in the middle. On the other hand, the ground state of the L segments have a *minimum* of density at that point. It is thus practically impossible to reproduce the ground state of the $2L$ segment by combining low-energy states from L segments. The situation is quite different if one allows arbitrary boundary conditions as shown in Fig. 5.7. In that case it is very easy to reproduce the ground state of the $2L$ segment out of low-energy states of the L segment and the numerical RG can thus be constructed. The success of this procedure thus relies in the possibility to have the low-lying states for arbitrary boundary conditions without double

counting. For the interacting system, the clever solution found by White was to compute the density matrix of the system. Part of the system is used to compute the density matrix, whereas part of the system acts as a bath to provide the various boundary conditions. The renormalization procedure can then be used. The method is too complex to be exposed in detail here and I refer the reader to Peschel *et al.* (1998) for more information.

Since this is in essence a method that retains only the low-energy properties of the system, and thus focus on the relevant quantities it can look at incredibly long systems. This allows to get rid of most of the size-effect and to look directly at the correlation functions. This is one of the main advantages of this DMRG technique. It allows a nearly direct calculation of all *static* quantities.

There are still some drawbacks. It is more difficult to extract from the method dynamical quantities, although the situation is rapidly improving. It is also not so easy to play with the boundary conditions. This can make it difficult to compute quantities that require such a change. This makes, for example, the calculation of the Luttinger parameters more complicated by this method since one cannot use the response to a twist easily, so quite often the parameter K is extracted from the static correlation functions. The method is also better suited to compute zero temperature quantities than finite temperature ones. But except for these few drawbacks it is clearly the method of choice to tackle one-dimensional problems. We will see various examples of phase diagrams that are computed using this method in the subsequent chapters.

6

SPIN 1/2 CHAINS

Man is born free and everywhere he is in chains.

Jean-Jacques Rousseau (*The Social Contract*)

In this chapter, I examine the question of spin systems. Such systems are the simplest realization of Luttinger liquids. The peculiarities of one dimension make the solution of this problem quite surprising and different from what our intuition expects based on a classical vision of the spins. Of course, it is impossible to cover in this chapter all the richness of this subject, and the present chapter can only be an introduction. Fortunately, excellent reviews specifically devoted to this problem exist in the literature (Affleck, 1988), and I refer the reader to them for more information on this subject. From an experimental point of view, the progress in material research have allowed to synthesize many new materials with quite novel properties in the recent years. It is thus a very lively subject, the richness of which is far from being exhausted.

6.1 Physical properties of the spin 1/2 chain

6.1.1 *Hamiltonian*

To start using our one-dimensional technology let us take the simplest possible system: a chain of spin 1/2. On each site there is a spin $S_i = \sigma_i/2$ where σ_i are the Pauli matrices. The three components of the spin S^x, S^y, S^z thus obey the commutation relations

$$[S^\alpha, S^\beta] = i\epsilon_{\alpha\beta\gamma} S^\gamma \tag{6.1}$$

where $\epsilon_{\alpha\beta\gamma}$ is the totally antisymmetric tensor (that is, equal to zero if two indices are equal and $\epsilon_{xyz} = 1$). The spin operators on different sites commute. Let us assume that the spins interact via a nearest neighbor exchange

$$H = \sum_i J_{xy}(S^x_{i+1}S^x_i + S^y_{i+1}S^y_i) + J_z S^z_{i+1} S^z_i \tag{6.2}$$

I have kept rotation symmetry in the xy plane but chosen different exchanges in the xy plane and the z direction. This model is known as the XXZ Hamiltonian. If $J_z = J_{xy}$ the interaction between spins is totally invariant by rotation and this is the famous Heisenberg Hamiltonian. One can of course consider more complicated Hamiltonians, and this will be the object of Section 6.2. For the moment I illustrate the method with this simple one. If the J are positive, the energy is minimal if the spins on two neighbors tend to point in opposite directions, thus

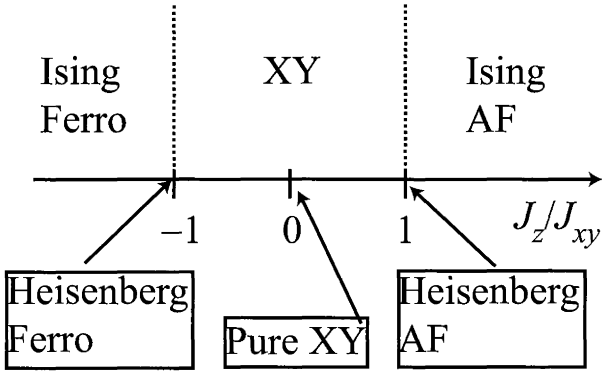

FIG. 6.1. Various regimes for a spin 1/2 chain as a function of J_z/J_{xy}.

$J > 0$ favors antiferromagnetic order. On the contrary $J < 0$ obviously favors the spins to be oriented ferromagnetically.

If there are only nearest neighbor interactions as in (6.2), some simplifications are possible. Indeed, on a bipartite lattice it is possible to change the spins to change the sign of the exchange. For a classical spin one would simply change $S \to -S$ on every other site to change $J \to -J$. For classical spins there is thus no difference between ferromagnetic and antiferromagnetic couplings on bipartite lattices. For quantum spins however this transformation is not possible since it violates the commutation relations (6.1). It is however possible to change the sign of two of the components. If we perform the transformation

$$\begin{aligned} S_i^x &\to (-1)^i S_i^x \\ S_i^y &\to (-1)^i S_i^y \\ S_i^z &\to S_i^z \end{aligned} \tag{6.3}$$

it respects the commutation relations. It changes $J_{xy} \to -J_{xy}$ and $J_z \to J_z$. Thus, regardless of the signs of the couplings it is enough to consider $J_{xy} > 0$. It is easy to see that $J_z = J_{xy}$ is the antiferromagnetic isotropic point. $J_z = -J_{xy}$ is the ferromagnetic isotropic point (using the transformation (6.3)). $J_z = 0$ is the pure XY point. This allows to represent the various domains as a function of J_z as shown in Fig. 6.1.

Working with spin operators is unpleasant since they have funny commutation relations. There are two useful mappings for the spins. The first one is to realize that on each site the raising and lowering operators can be replaced by bosonic operators $S^+ \to b^\dagger$ and $S^- \to b$. To get the proper commutation relations the S_z operator should be the density of bosons

$$S^z = b^\dagger b - \frac{1}{2} \tag{6.4}$$

Spin operators on different sites thus also naturally commute as it should be. Unfortunately, the Fock space for bosons on one site is too large since an arbitrary

large number of bosons can exist. To restrict the space to the only two states allowed for a spin 1/2, one has to introduce a hard core constraint stating that more than one boson on the same site is not allowed. A spin system can thus be mapped in any dimension to a hard core boson problem. Because of the constraint, solving the boson problem is quite complicated. I will come back to this question in Section 11.1. In order to get rid of the constraint it would be convenient to use the Pauli principle to enforce it, and thus to use spinless fermions instead of bosons. If we use

$$\begin{aligned} S^+ &\to c^\dagger \\ S^z &= c^\dagger c - 1/2 \end{aligned} \tag{6.5}$$

where the c are fermions, it is easy to check that the spin commutation relations are obeyed on each site. The space of allowed states has exactly the right size: the absence of a fermion means a spin state $|S_z = -\frac{1}{2}\rangle$, whereas a fermion means $|S_z = \frac{1}{2}\rangle$. Unfortunately, fermions on different sites anticommute whereas the spins should commute. Thus, one should modify the mapping (6.5) to transform a commutation into an anticommutation, without changing the local relations. In one dimension the solution was found by Jordan and Wigner. One attaches a string of operators to each fermion. This string produces the needed minus sign. This is in the same spirit than the method we used to construct the fermion operator in Section 3.2. The mapping becomes

$$\begin{aligned} S_i^+ &\to c_i^\dagger e^{i\pi \sum_{j=-\infty}^{i-1} c_j^\dagger c_j} \\ S^z &= c_i^\dagger c_i - 1/2 \end{aligned} \tag{6.6}$$

At first sight, the non-local character of the mapping makes it appear untractable. Fortunately many operators are usually quite simple in the fermion language. This is due to the fact that the string simplifies very often. Let us take for example the kinetic energy

$$S_{i+1}^+ S_i^- = c_{i+1}^\dagger e^{i\pi c_i^\dagger c_i} c_i = c_{i+1}^\dagger c_i \tag{6.7}$$

The XXZ Hamiltonian (6.2) thus becomes after the Jordan–Wigner transformation

$$H = \frac{J_{xy}}{2} \sum_i [c_{i+1}^\dagger c_i + \text{h.c.}] + J_z \sum_i (c_{i+1}^\dagger c_{i+1} - 1/2)(c_i^\dagger c_i - 1/2) \tag{6.8}$$

To get a more conventional fermionic Hamiltonian we make the canonical transformation, which consist in shifting the momentum of the fermions by π

$$c_i \to (-1)^i c_i \tag{6.9}$$

This is in the fermion language the equivalent of the transformation (6.3). It leads to the Hamiltonian

$$H = -t\sum_i [c_{i+1}^\dagger c_i + \text{h.c.}] + V\sum_i (c_{i+1}^\dagger c_{i+1} - \frac{1}{2})(c_i^\dagger c_i - \frac{1}{2}) \tag{6.10}$$

with $t = J_{xy}/2$ and $V = J_z$. The spin chain is thus equivalent to a chain of spinless fermions. Fermions can hop between neighboring sites with a hopping matrix element t. They experience a nearest neighbor interaction V. A local interaction is, of course, precluded for spinless fermions by the Pauli principle. Note that a magnetic field along z for the spin chain is simply a chemical potential for the fermions

$$-h\sum_i S_i^z = -h\sum_i (c_i^\dagger c_i - \frac{1}{2}) \tag{6.11}$$

In the absence of external magnetic field the average magnetization is zero. Since $\langle S_z \rangle = 0$ the fermion density is $\langle c_i^\dagger c_i \rangle = 1/2$. The fermionic band is half-filled ($k_F = \pi/2$). The totally polarized $\uparrow$ states corresponds to a filled band and the totally polarized $\downarrow$ states to an empty band. Hamiltonians (6.10) and (6.11) are written in such a way to obey the particle–hole symmetry. If we make the canonical transformation

$$c_i \to (-1)^i \tilde{c}_i^\dagger \tag{6.12}$$

then (6.10) written in terms of the $\tilde{c}$ is unchanged, whereas the chemical potential h in (6.11) is changed into $-h$. This particle–hole symmetry corresponds to the spin reversal symmetry.

The mapping (6.10) is remarkable. For $J_z = 0$ the solution is immediate since this is the free fermion Hamiltonian. The ground state is the filled Fermi sea, and the excitations have obvious fermionic character. This is surprising since one would have naively expected from the commuting nature of the spins the interactions to be bosonic in nature. Some correlations can be easily computed. For example, the $S_z\ S_z$ correlation is simply the density–density correlation for the fermions

$$\langle S^z(x,\tau) S^z(0,0) \rangle = \langle \rho(x,\tau)\rho(0,0) \rangle \tag{6.13}$$

which decays as $1/r^2$. Unfortunately, the $S^+\ S^-$ correlation functions have no simple fermionic representation because of the string. We will see soon how to compute such correlation functions.

The Jordan–Wigner transformation can be used in higher dimensions as well. One should just find a unique path going through all sites to define the string. Unfortunately, it means that some operators that were local in spins, such as the Hamiltonian itself, now become highly non-local because the string does not cancel anymore. This severely limits the use of the Jordan–Wigner transformation in dimensions larger than one.

6.1.2 *Bosonization solution*

Let us now use our new knowledge of one-dimensional interacting fermions to solve the spin chain problem. We take the continuum limit and define

$$\begin{aligned} S^+(x) &= S_i^+/\sqrt{a} \\ S^z(x) &= S_i^z/a \end{aligned} \tag{6.14}$$

where a is the lattice spacing. Alternatively, one can just set $a = 1$ and reintroduce the dimensions by simple dimensional analysis, the results being of course independent of our choice of a. Since the Hamiltonian is (6.10) we can use the bosonization representation of the various fermion operators. The kinetic energy is simple. The kinetic terms can be diagonalized by going to Fourier space

$$H_{xy} = \sum_k \epsilon_k c_k^\dagger c_k \tag{6.15}$$

where the energy is the standard tight binding one

$$\epsilon_k = -J_{xy}\ \cos(ka) \tag{6.16}$$

which gives close to the Fermi level a Fermi velocity

$$v_F = J_{xy} a\ \sin(k_F a) \tag{6.17}$$

The interaction part of the Hamiltonian becomes

$$\begin{aligned} H_{\text{int}} = a^2 J_z \sum_j &(\rho_R(r_{j+1}) + \rho_L(r_{j+1}) + e^{-i2k_F r_{j+1}} \tilde{\psi}_R^\dagger(r_{j+1}) \tilde{\psi}_L(r_{j+1}) + \text{h.c.}) \\ &(\rho_R(r_j) + \rho_L(r_j) + e^{-i2k_F r_j} \tilde{\psi}_R^\dagger(r_j) \tilde{\psi}_L(r_j) + \text{h.c.}) \end{aligned} \tag{6.18}$$

where $r_j = aj$. Since the fields $\tilde{\psi}$ vary slowly, one can take the continuous limit $r_{j+1} \sim r_j \to r$ *for the fields*. Such a continuum limit cannot of course be taken for the oscillating $e^{i2k_F r}$ factors. For these factors $r_{j+1} = r_j + a \to r + a$. Using the boson mapping of Appendix D, the Hamiltonian becomes

$$\begin{aligned} H_{\text{int}} = aJ_z \int dr &(-\frac{1}{\pi}\nabla\phi(r+a) + e^{-i2k_F(r+a)} \frac{1}{2\pi\alpha} e^{i2\phi(r+a)} + \text{h.c.}) \\ &(-\frac{1}{\pi}\nabla\phi(r) + e^{-i2k_F r} \frac{1}{2\pi\alpha} e^{i2\phi(r)} + \text{h.c.}) \end{aligned} \tag{6.19}$$

The terms that oscillate rapidly can be suppressed from the continuum limit. One is left with

$$\begin{aligned} H_{\text{int}} = aJ_z \int dr &\frac{1}{\pi^2}\nabla\phi(r+a)\nabla\phi(r) + (e^{-i2k_F a} \frac{1}{(2\pi\alpha)^2} e^{i2(\phi(r+a)-\phi(r))} + \text{h.c.}) \\ &+ (e^{-i4k_F r - 2k_F a} \frac{1}{(2\pi\alpha)^2} e^{i2(\phi(r+a)+\phi(r))} + \text{h.c.}) \end{aligned} \tag{6.20}$$

In this expression one can take α the cutoff as the lattice spacing. The second term can be expanded to give (for a cleaner calculation see (7.42))

$$\frac{1}{(2\pi\alpha)^2}e^{i2(\phi(r+\alpha)-\phi(r))} \simeq \frac{1}{(2\pi\alpha)^2}[1 + i2\alpha\nabla\phi(r) - 2\alpha^2(\nabla\phi(r))^2] \tag{6.21}$$

The first term is just the square of the average density. It is a simple (although infinite) constant in the Hamiltonian and can be discarded. The second term vanishes with the hermitian conjugate. The Hamiltonian becomes

$$H_{\text{int}} = aJ_z \int dr \frac{1}{\pi^2}[1 - \cos(2k_F a)](\nabla\phi(r))^2 + (e^{-i4k_F r - 2ik_F a}\frac{1}{(2\pi\alpha)^2}e^{i2(\phi(r+a)+\phi(r))} + \text{h.c.}) \tag{6.22}$$

Naively, one would like to drop the last term in (6.22) because of the oscillating $e^{i4k_F r}$. However, $r_j = ja$ and at half-filling $k_F = \pi/(2a)$ and $4k_F r_j = 2\pi j$. The exponential factor does not oscillate and should be retained. As we saw in Section 4.2, this is the standard situation for commensurate fillings. The $4k_F$ term is the umklapp process for our spinless fermions. In the continuum limit

$$\cos(2(\phi(r+a) + \phi(r)) \sim \cos(4\phi(r)) \tag{6.23}$$

Since at half-filling $2k_F = \pi$, $e^{i2k_F a} = -1$ and thus the interaction Hamiltonian is

$$H_{\text{int}} = aJ_z \int dr \frac{1}{\pi^2}[1 - \cos(2k_F a)](\nabla\phi(r))^2 - \frac{1}{(2\pi\alpha)^2}2\cos(4\phi(r)) \tag{6.24}$$

Note that the umklapp term $\cos(4\phi)$ for spinless fermions contains a larger coefficient inside the cosine than for fermions with spins. It is thus less relevant. This can be readily understood. In the fermion language this operator would be naively

$$\psi_R^\dagger \psi_R^\dagger \psi_L \psi_L \tag{6.25}$$

taking two spinless fermions from one side of the Fermi surface to the other. However, since there is now no spin index, if all operators are taken at the same point (continuum limit) the Pauli principle kills this term. What allows this term to survive is the fact that the two operators ψ_L are not exactly at the same point but on two neighboring sites. The term is, in fact,

$$\psi_L(x+a)\psi_L(x) \simeq [a\nabla\psi_L(x) + \psi_L(x)]\psi_L(x) = a\nabla\psi_L(x)\psi_L(x) \tag{6.26}$$

Contrary to fermions with spins, for spinless fermions the umklapp term has thus derivatives hidden in it and is thus less relevant. The bosonization formula (6.23) takes care of all that without any headache. Note that for a spin chain half-filling is the rule rather than the exception so taking proper care of the umklapp operator is specially important if one wants to get the proper physics. We will consider the effects of a finite magnetic field in Section 6.1.3, for the moment let us focus on the non-magnetized spin chains.

A word of caution in the bosonization derivation: writing the second term in the Hamiltonian in terms of the fermions would give

$$\psi_R^\dagger(r+a)\psi_L(r+a)\psi_L^\dagger(r)\psi_R(r) \tag{6.27}$$

One could be tempted to take the continuum limit $r+a \to r$ and reorder the operators to get

$$\psi_R^\dagger(r)\psi_R(r)\psi_L^\dagger(r)\psi_L(r) = \rho_R(r)\rho_L(r) = \frac{1}{\pi^2}((\nabla\phi)^2 - (\nabla\theta)^2) \tag{6.28}$$

At first sight there is nothing wrong with this result, except that it is different from our result (6.24) which contain only ϕ and its derivatives. In fact as we will see in Section 7.2, any Hamiltonian properly defined on a lattice cannot contain terms that change the coefficient of $(\nabla\theta)^2$. This is due to the fact that interactions only depend on the density and thus the commutator of the density and the Hamiltonian cannot be changed by interactions. Thus, the result (6.28) is wrong. The reason is the incorrect point splitting of the operators. $\rho_{R,L}(r) = \psi_{R,L}^\dagger(r)\psi_{R,L}(r)$ if the operators are *truly* at the same point. This is not the case in (6.18) since one of the field is at $r+a$ the other at r. One should thus be very careful when the Hamiltonian is defined on a lattice to properly identify the operators that are on the same site or on sites close by in order to correctly take the continuum limit. Another important, but much more obvious, point is to properly take into account the a terms in the oscillating factors such as $e^{i2k_F a}$. These terms are by no means small since k_F is itself of order $1/a$. Throwing these terms away would have given the wrong sign for the umklapp term in (6.24).

The spin chain Hamiltonian can thus be written as

$$H = H_0 - \frac{2g_3}{(2\pi\alpha)^2}\int dx\ \cos(4\phi(x)) \tag{6.29}$$

where $g_3 = aJ_z$ and H_0 is the quadratic Luttinger Hamiltonian (3.25) with the parameters

$$\begin{aligned} uK &= v_F = J_{xy}a\ \sin(k_F a) \\ \frac{u}{K} &= v_F(1 + \frac{2J_z a}{\pi v_F}[1-\cos(2k_F a)]) \end{aligned} \tag{6.30}$$

At half-filling $k_F = \pi/(2a)$. a is just there for dimensional reasons and one can set $a = 1$ (or absorb it in the coupling constants). These expressions are of course only valid in the perturbative limit, that is, not far from the XY limit where J_z is small. The phase diagram of (6.29) can be directly extracted from the results of Section 4.2. The umklapp term is irrelevant for $K > 1/2$. In this regime, the system flows to a fixed point which is Luttinger liquid like, with a quadratic Hamiltonian. Since $K = 1$ is the non-interacting point which corresponds to the XY limit, the whole Luttinger phase is thus an XY like phase. We will confirm

this by computing the correlation functions. For $K < 1/2$, the cosine term is relevant. The excitations of our spin chain thus develop a gap that one can compute along the lines of Section 2.3.2. Since this phase obviously corresponds to when the system is dominated by the J_z term, we see that it corresponds to an Ising phase along the z direction.

The expressions (6.30) are perturbative but since the spin chain model is exactly solvable by Bethe-ansatz one can go much further and get the exact values of the LL parameters in the whole massless phase (Luther and Peschel, 1975; Haldane, 1980). To do so one uses the tricks explained in Chapter 5. The simplest is to compute the compressibility (related to u/K) and the spin stiffness (related to uK). In the absence of magnetic field there is even an analytical solution

$$\begin{aligned} J_z/J_{xy} &= -\cos \pi\beta^2 \\ 1/K &= 2\beta^2 \\ u &= \frac{1}{1-\beta^2}\sin(\pi(1-\beta^2))\frac{J_{xy}}{2} \end{aligned} \tag{6.31}$$

We recover from (6.31) the perturbative expression (6.30) for small J_z/J_{xy}. Two interesting features, beyond the range of the perturbative expressions appear. First, the isotropic Heisenberg point corresponds to $K = 1/2$. This is exactly the value at which the umklapp operator is marginal, in agreement with our previous argument. The second important point is the fact that upon approaching the isotropic ferromagnetic point the velocity u vanishes and K diverges. The ferromagnetic side $J_z/J_{xy} < -1$ is thus not a Luttinger liquid. This is very reasonable, in a ferromagnet one expects spin wave dispersion relations $\omega \sim k^2$ instead of a linear dispersion relation. The phase diagram is given in Fig. 6.1.

To go further and determine the various physical properties, we first have to write the spin operators in the boson language. S_z is the most easy one since it is just the fermionic density

$$\begin{aligned} S_z(x) &= \rho - \frac{1}{2} = \rho_R + \rho_L + [e^{-i2k_F x}\tilde{\psi}_R^\dagger \tilde{\psi}_L + \text{h.c.}] \\ &= -\frac{1}{\pi}\nabla\phi(x) + \frac{1}{2\pi\alpha}2\ \cos(2\phi(x) - 2k_F x) \end{aligned} \tag{6.32}$$

keeping in mind that x is in fact defined on the lattice $x_j = aj$. So, for the specific case of $h = 0$ (1/2 filling for the fermions)

$$S_z(x) = -\frac{1}{\pi}\nabla\phi(x) + \frac{(-1)^x}{\pi\alpha}\cos(2\phi(x)) \tag{6.33}$$

The S^+ operator is more complicated because of the string. The string becomes (dropping the oscillating factors)

$$\begin{aligned} e^{i\pi\sum_{j<i} c_j^\dagger c_j} &= e^{i\frac{\pi}{2}x} e^{i\pi\int_{-\infty}^{x} dy[\rho_R(y)+\rho_L(y)]} \\ &= e^{ik_F x} e^{-i\int_{-\infty}^{x} dy[\nabla\phi(y)]} = e^{ik_F x} e^{-i(\phi(x)-\phi(-\infty))} \end{aligned} \tag{6.34}$$

where as usual one can throw away $\phi(-\infty)$ and I have used that the average density ρ_0 is related to k_F. The non-local string is thus wonderfully simple in terms of the boson fields. This makes the bosonization a method of choice to tackle spin chains. The raising operator becomes ($x = ai$)

$$\begin{aligned} S^+(x) &= (-1)^x c^\dagger(x) e^{i\pi \sum_{j<i}[c_j^\dagger c_j - \frac{1}{2}]} e^{ik_F x} \\ &= (-1)^x (\tilde{\psi}_R^\dagger(x) + \tilde{\psi}_L^\dagger(x) e^{i2k_F x}) e^{-i\phi(x)} \\ &= (-1)^x \frac{1}{\sqrt{2\pi\alpha}} (e^{-i\theta(x)} + e^{i(-2\phi(x)-\theta(x))+i2k_F x}) \end{aligned} \tag{6.35}$$

This expression contains $e^{-i\theta}$ operators and $e^{-i(\theta+2\phi)}$ operators. This asymmetry is unpleasant. Indeed, the Hamiltonian contains a $\cos(4\phi)$ operator. It will combine with $e^{-i(\theta+2\phi)}$ to give $e^{-i(\theta-2\phi)}$ operators. This is analogous to the production of the $4k_F$ density terms in Section 3.1. It would be much more pleasant to have both operators from the start, since this would allow to completely forget about the $\cos(4\phi)$ operator in the regimes where this operator is irrelevant. This can be obtained by taking a slightly different form for the string, which of course leads to the same mapping between fermions and spins, but is more symmetric

$$\frac{1}{2}(e^{i\pi \sum_{j<i}[c_j^\dagger c_j]} + \text{h.c.}) = \frac{1}{2}(e^{ik_F x - i\phi(x)} + \text{h.c.}) \tag{6.36}$$

Using this string leads to

$$S^+(x) = \frac{e^{-i\theta(x)}}{\sqrt{2\pi\alpha}}[(-1)^x + \cos(2\phi(x))] \tag{6.37}$$

The equations (6.33) and (6.37) are the mapping between the spins and the bosons. Note that when written in terms of the bosons the mapping is extremely simple since all the non-locality due to the string is hidden in the field θ. These expressions are recalled in Appendix D. This mapping leads to a very simple interpretation of the fields ϕ and θ for the spins. As shown in Fig. 6.2, they can be viewed as the polar and $x - y$ angle of the classical spin. Because the spin is a quantum object these two 'angles' cannot be defined simultaneously, hence the canonical commutation relations between ϕ and θ. We see that if the field θ orders, it favors ordering in the xy plane, whereas order in the ϕ fields means that correlations along z are favored.

In the LL region, one can easily compute the correlation functions. In that case the equal time correlation functions are

$$\begin{aligned} \langle S^z(x,0)S^z(0,0)\rangle &= C_1 \frac{1}{x^2} + C_2(-1)^x \left(\frac{1}{x}\right)^{2K} \\ \langle S^+(x,0)S^-(0,0)\rangle &= C_3 \left(\frac{1}{x}\right)^{2K+\frac{1}{2K}} + C_4(-1)^x \left(\frac{1}{x}\right)^{\frac{1}{2K}} \end{aligned} \tag{6.38}$$

where the C_i are non-universal amplitudes as usual. For the spin chain these amplitudes can be computed from the short distance expression of the operators

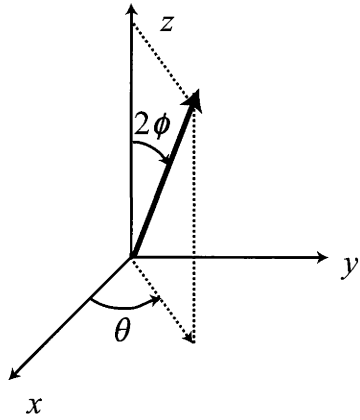

FIG. 6.2. Geometrical interpretation of the fields ϕ and θ. They can be roughly viewed at the two angles needed to define the spin as a classical vector. The quantum nature of the spin 1/2 is contained in the fact that the two 'angles' θ and ϕ do not commute. Imposing order in the xy plane thus scrambles the order along z and vice versa.

(Lukyanov, 1998; Lukyanov, 1999). We have for the spins the analogous of the slow decay of the $q \sim 0$ and $q \sim 2k_F$ components (with higher harmonics as well). For the spins, this represents the nearly ferromagnetic correlations and the nearly antiferromagnetic ones.

For the XY case $J_z = 0$ we recover with $K = 1$ the correlations of the free fermion case for S_z where both the $q \sim 0$ and $q \sim 2k_F$ part of the density decay as $1/x^2$. Note that for the S^+S^- correlation, the $q \sim 0$ part decays faster and the $q \sim 2k_F$ much slower. This is due to the contribution of the string. Physically, this traduces the fact that the XY phase has essentially antiferromagnetic order in the plane. The case $K > 1$ (attraction for the spinless fermions) corresponds to an enhancement of the ferromagnetic correlations as can be seen from the S_z correlation functions. On the other hand $K < 1$ (repulsion for the spinless fermions) enhances the antiferromagnetic part of the correlations. Indeed, at the isotropic antiferromagnetic point the S^z and S^+ correlations should be identical because of the spin rotation symmetry. This obviously imposes that $K = 1/2$, to get the same exponents. This is in agreement with the value we obtained from the Bethe-ansatz solution. Very often the simple use of a symmetry on the correlation functions can help getting the LL parameters at special points. In the whole antiferromagnetic regime where the cosine term is irrelevant $1/2 < K < 1$ we see from (6.38) that the slowest decaying correlation is the antiferromagnetic part of the XY correlation function. For the spin isotropic case $J_z = J_{xy}$ (that is $K = 1/2$) the decay of the antiferromagnetic part is $1/r$. However, since the cosine term is marginal there are logarithmic corrections as discussed in Section 4.4. The spin correlation function is thus

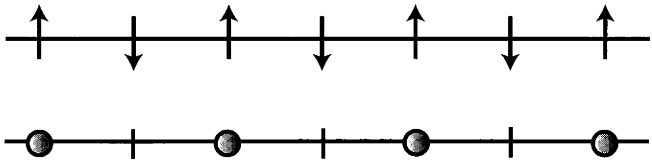

FIG. 6.3. Ising order along the z axis for the spins. This corresponds to a Mott insulator for the fermions. There are two possible degenerate ground states which depend on which value of ϕ is chosen to minimize the energy ($\phi = 0$ or $\phi = \pi/2$).

$$\langle S^\mu(x) S^\mu(0,0)\rangle = C_1 \frac{1}{x^2} + C_2(-1)^x \left(\frac{1}{x}\right) \log^{1/2}(x) \tag{6.39}$$

These logarithmic corrections have been checked in numerical DMRG calculations (Hallberg *et al.*, 1995). As we will see in Section 6.3 one can also probe the spin correlations by neutron diffraction. This provides an experimental check of the LL predictions.

For larger $J_z > J_{xy}$ the cosine term is relevant. The spinless fermions undergo a Mott transition whose properties were studied in Section 4.2. The field ϕ orders, and the system develops a gap. Because of the order in ϕ, all XY correlations decay exponentially since they contain the θ operator. The coefficient in from of the cosine being negative ϕ takes the value $\phi = 0 + \pi n/2$ to minimize the cosine term. We see from (6.33) that the $q \sim 0$ part of the correlation now decays exponentially, while the antiferromagnetic part orders. The spin along the z direction has thus an average value

$$\langle S_z(x)\rangle = (-1)^x \langle \cos(2\phi)\rangle \tag{6.40}$$

The average of the cosine which is non-zero can be computed by the methods of Appendix E.2. This order corresponds to an antiferromagnetic Ising order of the spins along the z directions. For the spinless fermions it means that there is a charge every two sites, which corresponds to the Mott insulating state. This is shown in Fig. 6.3. Depending on whether $\phi = 0$ or $\phi = \pi/2$ there are two different ground states where the spins are reversed. The Ising order thus breaks the discrete translational symmetry. Since this is the breaking of a discrete symmetry a true phase transition and order is allowed at $T = 0$ (the quantum system is the equivalent of a two-dimensional classical system).

6.1.3 *Finite magnetic field*

Let us now look at the effects of a finite magnetic field. To do so, we turn on a magnetic field H in the $\hat{z}$-direction. Note that the magnetic field breaks the $SU(2)$ symmetry. The interaction with the spins on the lattice is

$$H_m = -\mathbf{h} \sum_i g\mu_B H S_i^z \tag{6.41}$$

where $\mathbf{h} = g\mu_B h$ where g is the Lande factor, μ_B the Bohr magneton, and h the magnetic field. In the boson language this becomes

$$H_m = \frac{1}{\pi}\int dx \mathbf{h}\partial_x\phi \tag{6.42}$$

For the spinless fermions this is exactly a chemical potential term. The effect of a magnetic field is thus to dope the system compared to half-filling. The total Hamiltonian has thus exactly the same structure as the one we studied in Section 4.2 and we can directly use the results. In the region where the system is massless (the cosine is irrelevant), changing the chemical potential directly changes the magnetization. Using

$$m = \langle S_z\rangle = \frac{-1}{\pi}\langle\nabla\phi\rangle \tag{6.43}$$

one can simply absorb the finite magnetization in a shift of the field ϕ by

$$\phi = \tilde{\phi} - \pi m x \tag{6.44}$$

with $\langle\nabla\tilde{\phi}\rangle = 0$. In the massless regions, using the LL form of the Hamiltonian (3.25) one has $\tilde{\phi} = \phi + \frac{K\mathbf{h}x}{u}$, where u and K are the true LL liquid parameters of the system which gives

$$m = \frac{K\mathbf{h}}{u\pi} \tag{6.45}$$

in agreement with the general formula (2.59) for the compressibility of a LL.

Getting the LL parameters in presence of the magnetic field is not easy. Only special limits can easily be obtained. Since the system is invariant by changing $H \to -H$ (in the fermion language this corresponds to a particle–hole symmetry), we need only to consider $m > 0$ or $m < 0$. In the limit of a nearly empty fermionic band the particles are so separated they do not interact any more. One should thus have $K \to 1$. On the whole XY line the system is mapped to free fermions. In that case $K = 1$ regardless of the filling of the band. A map of the LL parameters is given in Fig. 6.4. For a general value of the field and the magnetization the LL parameters can be computed from the Bethe-ansatz equations (Luther and Peschel, 1975; Haldane, 1980). Since for finite magnetic field no simple analytical expression exists, the simplest is to solve the equations numerically. An example of solution is given in Appendix F, and an example of the value of the parameters is given in Fig. 6.5. When the cosine is relevant the zero magnetization case leads to a gap. From Section 2.3.2, this gap is of BKT type, in excellent agreement with the results of Bethe-ansatz. The magnetic field wants to break this gap, and one has a Mott-δ transition as explained in Section 4.2. As long as the field is smaller than the gap Δ, the magnetic field does not induce any magnetization. When the field exceeds the gap, the gap is

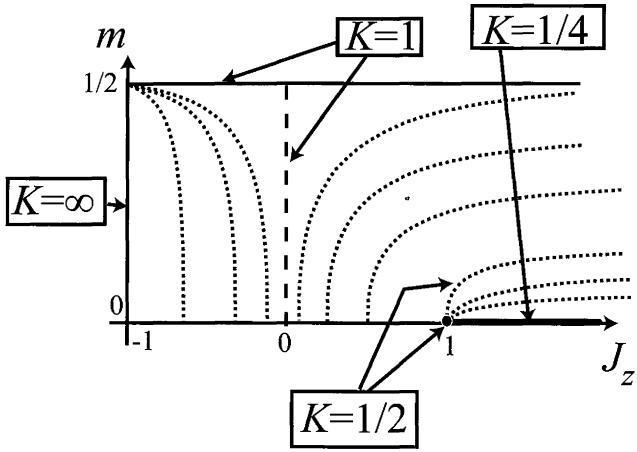

FIG. 6.4. A schematic map of the LL parameter K as a function of the magnetization m and J_z (in units of J_{xy}). Special limits can directly be extracted from the LL theory (see text). For an arbitrary field and magnetization the values are obtained by solving the Bethe-ansatz equations numerically. The thick line is the massive phase (Mott phase for the spinless fermions). The dotted lines are the lines of constant K value. Note the accumulation around the point $J_z = 1$ due to the difference in exponents for the Mott-U and Mott-δ transition.

destroyed and a finite magnetization appears. Using the results of Section 4.2, the magnetization is for $H \sim \Delta$

$$m \propto \sqrt{\mathbf{h} - \Delta} \tag{6.46}$$

We can use the general results of Section 4.2 to obtain that the LL parameter for small H tends to $K^* = 1/4$. These findings are in agreement with the exact Bethe-ansatz results and are indicated in Fig. 6.4. When the gap is destroyed and one is in the incommensurate phase, the system is again described by a LL quadratic Hamiltonian and the magnetic field can be absorbed in the shift (6.44).

In all cases a finite magnetization results in the shift (6.44). This has interesting consequences for the correlation functions. Injecting the new value (6.44) of the field ϕ in (6.33) and (6.37) we see that the correlations become

$$\begin{aligned}
\langle \mathcal{S}^z(r)\mathcal{S}^z(0,0)\rangle &= m^2 + \frac{K}{2\pi^2}\frac{y_\alpha^2 - x^2}{(x^2+y_\alpha^2)^2} + C_2\ \cos(\pi(1+2m)x)\left(\frac{1}{r}\right)^{2K} \\
\langle \mathcal{S}^+(r)\mathcal{S}^-(0,0)\rangle &= C_3\ \cos(2\pi m x)\left(\frac{1}{r}\right)^{2K+1/(2K)} + C_4\ \cos(\pi x)\left(\frac{1}{r}\right)^{1/(2K)}
\end{aligned} \tag{6.47}$$

The low-energy excitations of the system are thus not at $q \sim 0$ and $q \sim \pi$ anymore, as they were for the case of zero magnetic field. The S_zS_z correlation

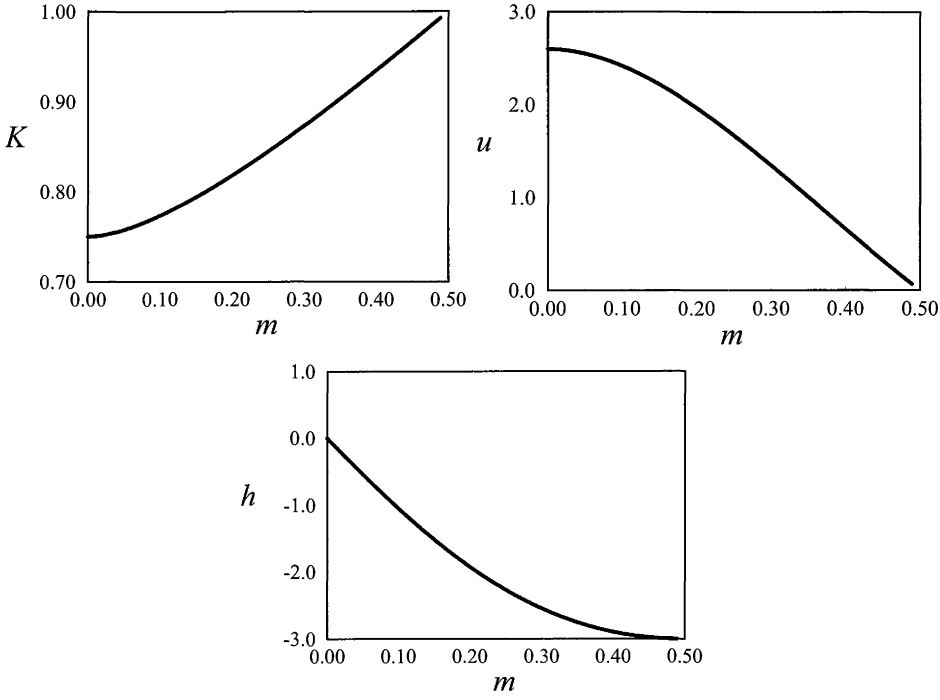

FIG. 6.5. LL parameters K and u and magnetic field h as a function of the magnetization m for a chain with an anisotropy parameter of $J_z/J_{xy} = 1/2$.

has low-energy modes at $q \sim 0$ and $\pi(1 \pm 2m)$. This is reasonable since the magnetic field creates kinks in the field ϕ and thus is equivalent in changing the effective $2k_F$ of the spinless fermion system. What is more surprising is the fact that the XY correlations also develop some incommensurability but this time around the mode $q \sim 0$ which is shifted to $q \sim \pm 2\pi m$. The $q \sim \pi$ mode remains commensurate. This is summarized in Fig. 6.6.

From the correlations (6.47), the retarded correlations can be computed using the methods of Appendix C. A knowledge of these quantities helps us extract various measurable quantities like neutron scattering intensities and nuclear magnetic resonance (NMR) rates. The susceptibilities are given by the following expression

$$\chi_{ij}(q,\omega,T) = -i \int dt\ dx\ e^{i(\omega t - qx)} Y(t) \langle [S^i(x,t), S^j(0,0)] \rangle \tag{6.48}$$

Here i, j refer to the components of the spin. Since rotations in the $x - y$ plane still leave the Hamiltonian invariant, there are no cross correlations, that is, $\langle S^i S^j \rangle = 0$ for i $\neq$ j. Using the expressions of the spin correlations in imaginary time (6.47) one can perform the analytic continuation and the Fourier transform as explained in Appendix C to get the retarded correlation functions (6.48) from

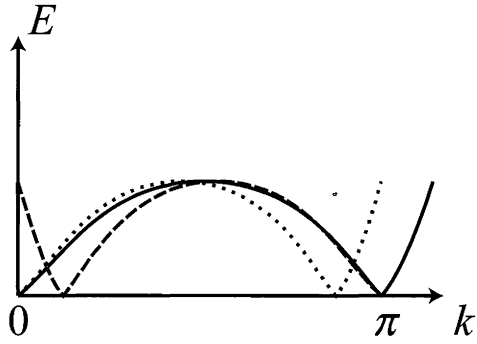

FIG. 6.6. Schematic picture of the field-dependent dispersion in presence of a magnetic field, compared to the commensurate (zero field) case (solid line). The correlations become incommensurate but in a different way for the spins parallel (S^zS^z (dotted line)) or perpendicular (S^+S^- (dashed line)) to the field. $k = 0$ and $k = \pi$ are the usual commensurate modes and $k = \pm 2\pi m$ and $k = \pi(1 \pm 2m)$ are the low-energy incommensurate modes.

(6.47) (Schulz, 1986). The dominant part of the susceptibility comes from q vectors close to one of the wavevectors for which the correlation has low-energy modes as shown in Fig. 6.6. I denote this mode by Q. The Fourier transform is done for q close to Q, that is, for $q = Q + \delta q$ with δq small. The susceptibility χ_{zz} in the direction parallel to the direction of the applied field is given for $q \sim Q = 0$ by

$$\chi_{zz}(q,\omega,T) = \frac{\delta q^2 K u}{\pi((u\delta q)^2 - (\omega + i\epsilon)^2)} \tag{6.49}$$

where $\epsilon = 0^+$. For $q \sim Q = \pi(1 - 2m)$ one has

$$\chi_{zz}(q,\omega,T) = C_2' T^{2K-2} B(\frac{K}{2} - \frac{i(\omega + u\delta q)}{4\pi T}, 1 - K) \times B(\frac{K}{2} - \frac{i(\omega - u\delta q)}{4\pi T}, 1 - K) \tag{6.50}$$

For the susceptibility perpendicular to the magnetic field one has $\chi_{xx} = \chi_{yy} = \frac{1}{2}\chi_{+-}$, because of rotation invariance perpendicular to the field. For $q \sim Q = 2\pi m$, one has

$$\begin{aligned}\chi_{xx}(q,\omega,T) = \\ - C_3' T^{2\gamma}[B(\frac{\gamma+2}{2} - \frac{i(\omega + u\delta q)}{4\pi T}, (-1-\gamma))B(\frac{\gamma}{2} - \frac{i(\omega - u\delta q)}{4\pi T}, (1-\gamma)) \\ + B(\frac{\gamma}{2} - \frac{i(\omega + u\delta q)}{4\pi T}, (1-\gamma))B(\frac{\gamma+2}{2} - \frac{i(\omega - u\delta q)}{4\pi T}, (-1-\gamma))]\end{aligned} \tag{6.51}$$

where $2\gamma = 2K + 1/(2K) - 2$. For $q \sim Q = \pi$, the susceptibility becomes

$$\chi_{xx}(q,\omega,T) = C_4 T^{2\gamma'-2} B(\frac{\gamma'}{2} - \frac{i(\omega + u(q-Q))}{4\pi T}, (1-\gamma'))$$
$$\times B(\frac{\gamma'}{2} - \frac{i(\omega - u(q-Q))}{4\pi T}, (1-\gamma'))] \quad (6.52)$$

where $\gamma' = \frac{1}{4K}$, $B(x,y)$ is the Beta function (see Appendix C) and u is the (magnetization dependent) spin velocity. Note that the prefactors C' are *a priori* magnetization dependent. The form of these susceptibilities can be directly compared with neutron data as I will discuss in Section 6.3. They also enter in other physical observable such as the NMR relaxation time (Sachdev, 1994; Chitra and Giamarchi, 1997).

To finish, let us look at the nature of the excitations. Based on the general discussion of Section 3.2, one can determine the spin of an elementary excitation by looking at the kinks of the umklapp term in (6.24). Indeed, as explained in Section 4.2, a magnetic field creates excitations that are the kinks of this operator. Since the system in the massless phase is the Luttinger liquid, these kinks give the quantum numbers of the excitations. One goes from a minimum of the cosine to the other by a shift $\phi \to \phi + \pi/2$. The spin of such an excitation is thus

$$\delta S_z = \frac{-1}{\pi} \int dx\, \nabla\phi(x) = -\frac{1}{2} \quad (6.53)$$

and is thus an excitation of spin 1/2. Furthermore, if we consider that ϕ is a constant, a shift of ϕ by $\pi/2$ corresponds using (6.32) to changing $S_z \to -S_z$. This kink thus corresponds exactly to the spinon excitation that we saw in Fig. 5.4, in agreement with the Bethe-ansatz results.

6.2 Extensions

The ideal spin 1/2 chain can be perturbed in many ways. Each of these perturbations can lead to quite rich physics. I examine here only the simplest of them. I focus, in this section, on perturbations that apply to strictly one-dimensional chains, and examine coupling between chains in Section 6.4.

6.2.1 *Frustrated chains*

The simplest perturbation consists in adding a second neighbor exchange J_2. For simplicity, I stick here to Heisenberg exchange. The second neighbor antiferromagnetic exchange frustrates the chain as shown in Fig. 6.7. Normally this should be a formidable problem. Thanks to the boson representation and a few tricks this is a relatively easier term to treat. The second neighbor exchange is

$$H = J_2 \sum_i S_{i+2} \cdot S_i \quad (6.54)$$

This term can thus be bosonized exactly like the nearest neighbor exchange. Let us just look at the easiest term which is the umklapp term. In the expression (6.22) one has just to replace $e^{i2k_F a}$ by $e^{2k_F(2a)}$. The rest of the derivation is

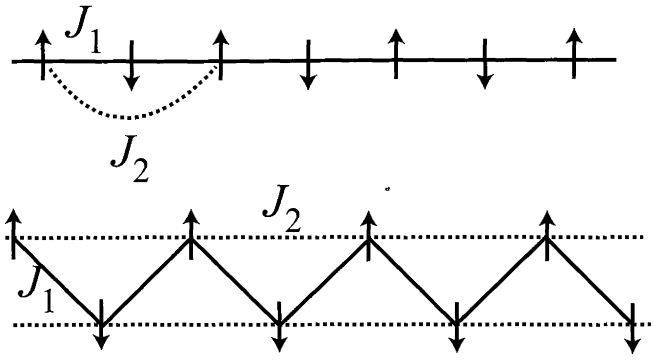

FIG. 6.7. A second neighbor antiferromagnetic exchange frustrates the chain, since the nearest neighbor exchange favors ferromagnetic alignment between second neighbors. Note that such a spin chain can also be viewed as a zig-zag ladder.

unchanged. It means that in the coefficient of the umklapp term we have now $J_1 - J_2$ instead of J_1. We could compute the quadratic part in the same way but this is not even necessary, and could be dangerous. Since we know that the system is spin rotation invariant, it means that it should stay *exactly* on the separatrix when renormalizing the cosine. The coefficient of the quadratic part should just match the changes of the coefficient of the umklapp term to respect this symmetry. Since the isotropic point is very far from the perturbative point $J_z \sim 0$ around which the coefficients can be obtained by perturbations, this condition would not have been satisfied by a perturbative expansion. This illustrates the rule that we were discussing before: symmetries should be implemented in order not to flow to a massive phase incorrectly. Of course, the coefficient of the umklapp term is also renormalized when J_z is strong but the tendency should be correct: the second neighbor exchange weakens the umklapp.

There are thus only two cases. Either $J_1 - J_2 > 0$, which means in fact that J_2 is smaller than some critical value J_{2c}. [26] In that case the cosine is marginal and flows to zero. The second neighbor exchange has essentially no effect on the system. On the contrary, if the coefficient of the cosine becomes negative, since one has to stay on the separatrix, the cosine is now relevant as shown in Fig. 6.8. Right at the transition point, the cosine disappears, and thus there are no logarithmic corrections to the correlation functions any more (Affleck *et al.*, 1989). Since the coefficient of the cosine is now positive the relevance of the cosine has a completely different physical consequence than for the simple spin chain. Indeed, now the ordered value of ϕ is $\phi = \pi/4 + n\pi/2$. The XY correlations that contain the θ operator still decay exponentially, but now the average value of the $\cos(2\phi)$ in the S_z correlation is *also* zero. This means that

[26] $J_{2c} \sim 0.245$ as determined numerically.

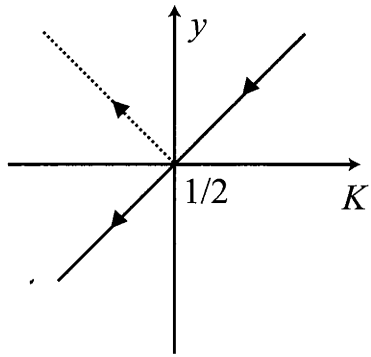

FIG. 6.8. When the coefficient of the umklapp term becomes negative, the cosine becomes relevant since the system is forced to sit on the separatrix due to spin rotation symmetry. In that case the frustration induces a gap, and the spins on the chain lock into singlets.

all spin correlation functions decay exponentially and that the spins in the chain have locked themselves into singlet states because of the frustration. Of course, putting a magnetic field on the chain is able to break the gap, and restore LL correlation functions, very much like in the case of the simple chain in the Ising limit. This is exactly the same Hamiltonian, and thus the same transition. Because it is exactly the same Hamiltonian, the excitations correspond to the same quantum numbers namely to $\delta S_z = \pm 1/2$, that is, to a spinon. I will not explore the frustrated chain further since we will have simpler systems on which to examine this singlet locking. I refer the reader to Haldane (1982*a*), Haldane (1982*b*), Chitra *et al.* (1995) and Chitra and Giamarchi (1997) for more details on the $J_1 - J_2$ chain and the quantum phase transition under magnetic field in this chain.

6.2.2 *Spin-Peierls*

An important effect, known as the spin-Peierls transition occurs when the exchange couplings are modulated. This can occur because the length of bonds between spins changes. For the equivalent spinless fermion model this corresponds to a modulation of the hopping parameters (or identically of the bond lengths). In the case of fermions, the phenomenon is known as the Peierls instability. For the spin chain we consider

$$H = \sum_i J(u_i, u_{i+1}) S_{i+1} \cdot S_i + H_{\text{phonon}}(u) \tag{6.55}$$

H_{phonon} is a Hamiltonian describing the energetic cost of making deformations u_i to the lattice. Note that although the spin system is one-dimensional the phonons can perfectly (and in general will) be three-dimensional. The detail of the model (optical versus acoustical phonons etc.) have of course their importance, but

there is a crucial feature discovered by Peierls about this system. To illustrate it in the simplest way, before tackling the full solution, let me take the XY limit for our spin chain. We can thus replace it by free spinless fermions. Let us assume that the change in J is linear in the phonons (for small displacements one can always expand J), that is, something of the kind (for acoustical phonons)

$$J = J_0 + \delta J(u_{i+1} - u_i) \tag{6.56}$$

or if we take optical phonons directly on the bonds $J = J_0 + \delta J u_i$. What would be the cost of making a *static* deformation of the lattice of amplitude u? The energetic cost is obviously proportional to u^2, since phonon Hamiltonians are quadratic in the displacements. To gain energy one can make a periodic deformation with a periodicity $2k_F$. This way one can open a gap at the Fermi level for our free fermions. The effect of the gap is to replace the energy ξ_k by $\sqrt{\xi_k^2 + (\delta J u)^2}$. This lowers the energy of the occupied states by roughly $\delta J u$. It also raises the energy of the states above the Fermi surface by the same amount but since they are empty it does not cost anything. The number of states affected by this change is roughly $\delta J u N(E_F)$, where $N(E_F)$ is the density of states. The total *gain* in energy on the spin chain is thus

$$\Delta E = -(\delta J u)^2 N(E_F) \tag{6.57}$$

So, normally for a small enough coupling δJ this does not compensate the cost in phonon energy and a static deformation is impossible. This is the normal situation in high dimensions. However, for one dimension I cheated in the above derivation. In one dimension, because of the gap, the density of state has a singularity and a better estimate of the gain in energy is

$$\int_0^\Lambda dk[\sqrt{(uk)^2 + \Delta^2} - uk] = \frac{\Delta^2 \log[4e\Lambda^2/\Delta^2]}{4} \tag{6.58}$$

where one integrates up to some large momentum cutoff Λ which mimics the bandwidth. Because of the logarithmic factor we see that the gain in energy due to the opening of the gap *always* overcome the cost of elastic energy to make the lattice distortion. In one dimension a chain of electrons or equivalently a spin chain is thus unstable towards a deformation of the lattice.

Let us now put the interactions and solve the problem. I will here simply examine two simple limits of this problem, since the full solution is a quite interesting but difficult and still an open question.

6.2.2.1 *Static potential* Let us first assume that there is a static deformation of the exchange constants. This amounts in neglecting all dynamics for the phonons. It is known as an adiabatic approximation for the phonons and is an accurate approximation if the timescale of evolution of the phonons (typically the inverse of the Debye frequency) is much larger than the typical timescale of evolution for the spins (typically the inverse of the exchange constant). In that case one

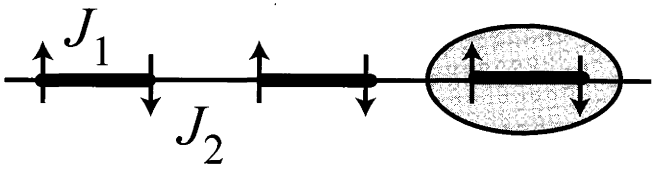

FIG. 6.9. A spin chain with an alternation of strong and weak bonds. The strong bonds lock the pair of spins into a singlet state.

can consider the phonons as static and assume that u is a constant. The precise value of u can then be determined by minimizing the total energy. For the spin chain we thus have to solve a problem where there is a static modulation of the exchange

$$J = J_0 + \delta J \ \cos(Qx) \tag{6.59}$$

Although one can of course consider any periodic deformation, as we discussed above the maximum effect of the deformation occurs when the deformation can open a gap at the Fermi level. We thus look at the case when $Q = 2k_F = \pi$. Let us consider here for simplicity the commensurate case, that is, the spin chain in the absence of an external magnetic field. In that case

$$J = J_0 + \delta J(-1)^x \tag{6.60}$$

In addition to the relevance to spin-Peierls systems, such a bond alternation is directly realized in some experimental compounds (Bonner *et al.*, 1983; Manaka and Yamada, 2001). To get an idea of the ground state of such a system let us go to strong coupling and assume $\delta J \sim J_0$. In that case the chain is an alternation of strong and weak links as shown in Fig. 6.9. If the weak bonds have exactly zero exchange the ground state is just a product of singlet states around the strong bonds. On these bonds there is a gap of order J_0 between the singlet (ground state) and one of the triplets (first excited state). Because of this energy gap any perturbation on this ground state is regular. This ground state is thus stable to a weak exchange on the weak bonds. The chain with the spin-Peierls distortion has, at least for strong coupling all the spins locked into singlet states. One can thus expect *all* spin correlation functions to decrease exponentially fast. In addition there is a gap between the (singlet) ground state and the first excited state. In this limit the gap is of order J_0.

To study the opposite limit of a small dimerization of the chain the simplest is to use bosonization. The bosonization in presence of the modulation is a little tricky so let us look at it in detail. We start with the S^+S^- terms. As we saw this term becomes in terms of the fermions

$$\begin{aligned} S^+_{i+1}S^-_i &\to -c^\dagger_{i+1}c_i \\ &= -(e^{-ik_F(x+a)}\tilde{\psi}^\dagger_R(x+a) + e^{ik_F(x+a)}\tilde{\psi}^\dagger_L(x+a)) \\ &\quad (e^{ik_Fx}\tilde{\psi}_R(x) + e^{-ik_Fx}\tilde{\psi}_L(x)) \end{aligned} \tag{6.61}$$

The uniform part gives the standard kinetic quadratic boson Hamiltonian (6.10). Let us look at the modulated term. It is given by

$$\begin{aligned}[S^+_{i+1}S^-_i]_{2k_F} &\to -e^{-ik_Fa}e^{-i2k_Fx}\tilde{\psi}^\dagger_R(x+a)\tilde{\psi}_L(x) + e^{ik_Fa}e^{i2k_Fx}\tilde{\psi}^\dagger_L(x+a)\tilde{\psi}_R(x) \\ &\simeq -e^{-ik_Fa}e^{-i2k_Fx}\tilde{\psi}^\dagger_R(x)\tilde{\psi}_L(x) + e^{ik_Fa}e^{i2k_Fx}\tilde{\psi}^\dagger_L(x)\tilde{\psi}_R(x) \\ &= -e^{ik_Fa}e^{-i2k_Fx}e^{i2\phi(x)} + e^{ik_Fa}e^{i2k_Fx}e^{-i2\phi(x)} \end{aligned} \tag{6.62}$$

Thus, one sees clearly that a modulation with a wavevector of $2k_F$ produces the maximum effect. Other modulations vanish in the continuum limit. For $2k_F = \pi$, one can write the Hamiltonian of the spin-Peierls term

$$\begin{aligned} H &= \frac{\delta J}{2}\sum_i (-1)^i [S^+_{i+1}S^-_i + \text{h.c.}] \\ &= \delta J \int dx\ \sin(2\phi) \end{aligned} \tag{6.63}$$

By spin rotation symmetry the J_z term should lead to the same physics. Performing the actual bosonization of the J_z term requires some care and I refer the reader to Orignac and Giamarchi (1998*a*) for a derivation. One recovers exactly the same term.

We thus end up again with a sine-Gordon Hamiltonian. The relevance of the periodic distortion depends on the LL parameter K. The spin-Peierls term is relevant if $4-2K \geq 0$, that is, for $K < 2$. This operator is thus violently relevant, unless very close to the ferromagnetic regime. It is in particular relevant at the XY point ($K = 1$) in agreement with our previous discussion, and of course at the Heisenberg point ($K = 1/2$). Far from the transition point $K = 2$ one can use the derivations of Section 2.3.2 to compute the gap for a small dimerization δJ

$$\Delta \propto (\delta J)^{1/(2-K)} \tag{6.64}$$

The gap is thus $\Delta \sim \delta J$ at the XY point in agreement with the free fermion results. At the Heisenberg point $K = 1/2$, the gap is (Cross and Fisher, 1979)

$$\Delta \propto (\delta J)^{2/3} \tag{6.65}$$

The gap (and hence the energy gain) is thus much enhanced at the Heisenberg point compared to the XY point. The dimerization has a very strong effect on the spin chain. Going to the Heisenberg limit strongly favors the spin-Peierls instability. Physically, this is readily understood in terms of the spinless fermions. The modulation creates a periodic potential. In the presence of repulsion the instability towards a CDW state is enhanced. Such a state easily pins on a periodic potential giving rise to the Mott state. In the gapped phase the field ϕ orders at the value

$$\begin{aligned} \phi &= \frac{\pi}{4} + \pi n, \quad \delta J < 0 \\ \phi &= \frac{-\pi}{4} + \pi n, \quad \delta J > 0 \end{aligned} \tag{6.66}$$

Because the field ϕ orders, all correlation functions of the θ field decay exponentially. Thus, all correlations of S^+S^- decay exponentially from (6.37). For S^z we see that $\langle \nabla\phi \rangle = 0$ and

$$\langle \cos(2\phi) \rangle = 0 \tag{6.67}$$

Thus, all correlations of S_z also decay exponentially. Note that the fact that $\sin(2\phi)$ and not another function of ϕ is the spin-Peierls term is absolutely crucial in this respect. Any other function would have given a finite average in (6.67). Since the shift of ϕ by π corresponds to a shift of the spin modulation by one lattice spacing (see (6.33)), we see that depending on the sign of δJ the ground state shifts by one lattice spacing the location of the spins. We thus recovers the interpretation of the ground state in terms of a locking of the spins in singlets on the strongest bonds. The weak and strong coupling thus give the same physics for the spin-Peierls state and are smoothly connected.

Adding a magnetic field can be done by exactly the same methods than in the previous sections. If the magnetic field is larger than the gap it destroys the commensurate state and give rise to an incommensurate state (the Mott-δ transition). Since one has again a sine-Gordon Hamiltonian, all critical properties of the transition are identical to the ones seen before. There are two important differences. The universal K^* very close to the transition is now $K^* = 1$ (instead of $K^* = 1/4$ for the Ising or the frustrated system). The second important difference is the quantum numbers of the excitations. Since the kink between minima is now $\delta\phi = \pi$ the excitations carry a spin $\delta S_z = 1$, instead of $\delta S_z = 1/2$ as we had before for the Ising and frustrated massive phases. This is a sign that the excitations here are triplets instead of spinons. This is compatible with the physical image of the magnetic field breaking one of the singlet bonds and giving two spin up instead (Affleck, 1966; Tsvelik, 1992; Uhrig and Schulz, 1996).

The case of strong dimerization with a magnetic field can also be studied by bosonization, but using a trick. In that case one has strong $J_1 \sim 2J_0$ and weak $J_2 \sim 0$ bonds. If we ignore J_2 then as discussed before, the ground state is made out of pairs of spins. A magnetic field on this state breaks a singlet and turns the pair of spins into a triplet as indicated in Fig. 6.10. Of course, in the presence of a residual coupling between the pairs, the triplet can jump from site to site and give rise to a band of width $\sim J_2$. When the field is close to the critical field $h_c \sim J_1$ it is thus *enough* to keep the singlet and the lowest triplet state. All other states are excited states of very high energy. On can thus map each bond to an effective spin 1/2 chain using

$$\begin{aligned} |\tilde{\downarrow}\rangle &= \frac{1}{\sqrt{2}}[|\uparrow\downarrow\rangle - |\downarrow\uparrow\rangle] \\ |\tilde{\uparrow}\rangle &= |\uparrow\uparrow\rangle \end{aligned} \tag{6.68}$$

where the tilde denotes the effective spin. An effective 'spin' down means a singlet on the bond, while a 'spin' up means a triplet. Using (6.68) it is easy to map the original spin operators $S_{1,2}$ of the bond in terms of the effective spin

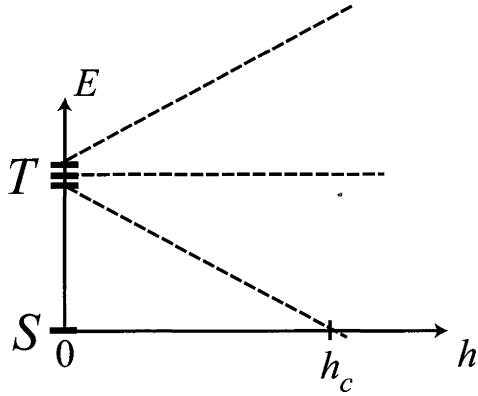

FIG. 6.10. In the absence of a magnetic field, a pair of spins is in a singlet ground state. The three states of the triplet are excited states. A magnetic field brings one of the component of the triplet to lower energy. Close to the critical field h_c where the singlet becomes unfavorable one can consider only the two low-energy states and thus replace the bond by an effective spin 1/2 degree of freedom.

$$\begin{aligned} S^+_{1,2} &= \mp\frac{1}{\sqrt{2}}\tilde{S}^+ \\ S^z_{1,2} &= \frac{[I + 2\tilde{S}^z]}{4} \end{aligned} \tag{6.69}$$

This mapping has several advantages. The spin 1/2 chain is exactly solvable and one can obtain the LL parameters *exactly* as a function of the magnetic field. Close to the critical field the band is nearly empty (nearly everybody is in a singlet state in the original system), and thus based on the discussion of the previous section $K^* \to 1$. One recovers the value obtained in the weak coupling regime, showing again that for this problem weak and strong coupling are smoothly connected (Chaboussant *et al.*, 1998; Mila, 1998; Giamarchi and Tsvelik, 1999; Furusaki and Zhang, 1999).

6.2.2.2 *Integration over the phonons* The adiabatic limit discussed in the previous section is not always applicable. Another approach to the spin-Peierls transition is thus to directly integrate over the phonons. I will briefly discuss this limit which is more complicated, and illustrate the main ideas. Let us do it only in the absence of a magnetic field. The action due to the dimerization is

$$S = \delta J \int dx\, d\tau\, u(x,\tau) \sin(2\phi(x,\tau)) \tag{6.70}$$

where I have made explicit the fact that the coupling constant is proportional to the displacement field u. The integration over the phonons can be easily performed leading to an action

$$S = -\frac{1}{2}\int dx\, dx'\, d\tau\, d\tau' G(x-x',\tau-\tau')\sin(2\phi(x,\tau))\sin(2\phi(x',\tau')) \quad (6.71)$$

where G is the Green function of the phonons. The phonons give rise to a non-local and retarded interaction between the electrons. Let us rewrite this term as

$$S = -\frac{1}{4}\int_{x,x',\tau,\tau'} G(x-x',\tau-\tau')[\cos(2(\phi(x,\tau)-\phi(x',\tau')))$$
$$-\cos(2(\phi(x,\tau)+\phi(x',\tau')))] \quad (6.72)$$

At large distances and times, the Green function of the phonons is local in space and time. For example, for optical phonons where each bond vibrates independently the Green function is (Mahan, 1981)

$$G(x,\tau) = \delta(x)e^{-\omega_0|\tau|} \quad (6.73)$$

where ω_0 is of the order of the Debye frequency of the phonons. Thus, for times shorter that ω_0^{-1} the interaction is essentially constant in time, and zero otherwise. The theory (6.72) is very difficult to solve. Let us have an idea of its physics by renormalizing the cutoff up to a point where the cutoff is of the order of ω_0^{-1}. Since one has to keep spin rotation symmetry the interaction keeps the form (6.72) albeit with a renormalized coupling constant. With that cutoff the Green function can be considered as local in space and time. The interaction (6.72) thus contains two parts. The first term can be expanded in powers of the gradient $(\nabla_x\phi)^2$ and $(\nabla_\tau\phi)^2$, and is a renormalization of the quadratic part of the Hamiltonian. The second term is simply the umklapp term $\cos(4\phi(x,\tau))$. The phonon coupling thus acts exactly as the frustration in the previous section and tends to reduce the coefficient of the umklapp term. The renormalization of the quadratic part ensures that one stays on the separatrix as it should be for a system with spin rotation symmetry. There are thus two cases. If the renormalized coupling to the phonons is not strong enough to make the umklapp coupling negative, the cosine is irrelevant. In that case the spin-Peierls instability does not take place. It is washed out by the quantum fluctuations of the phonons (Augier *et al.*, 1999). These quantum fluctuations were not taken into account in the adiabatic limit, where the phonon field was treated at a mean field level as a constant distortion. In that case the Peierls instability *always* occurs. If the phonon coupling is strong enough then the umklapp term becomes negative and the system develops a gap which corresponds in that case to having the Peierls distortion. Because here I took purely local phonons, the phonons themselves have a one-dimensional character and thus there cannot be any breaking of the translational symmetry into two sublattices as was the case in the mean field theory. To get closer to the mean field results some degree of three-dimensional coupling should be put either in the phonons or in the spins (see Section 6.4).

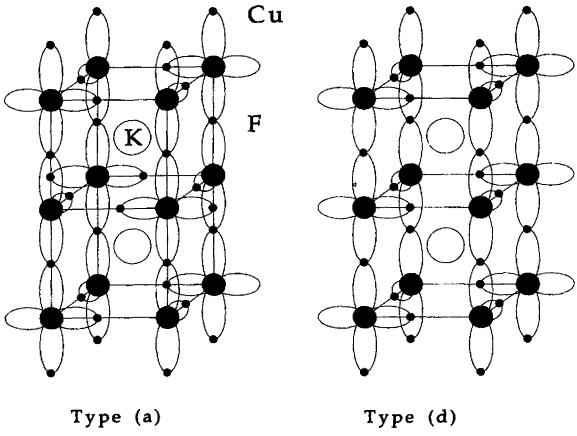

FIG. 6.11. Structure of $KCuF_3$. Because of a Jahn–Teller distortion the fluorines are displaced away from the midpoint of the Cu–Cu bond. This results in the two polytype structures (a) and (d). The unpaired electron on the Cu is in a $d_{x^2-y^2}$ orbital which has significant overlap with the F^- ions on the c-axis. (From Tennant *et al.*, 1995 (Copyright (1995) by the American Physical Society).)

6.3 Experimental realization of spin chains

Quite remarkably, there are several realization of spin chains. I examine some of them in this section and others together with the more specific theoretical analysis of the next sections. Of course, having a single chain of spins is not easily feasible so it much more common to have a three-dimensional material made up of stacks of chains, but where the magnetic exchange constants are such that exchange among different chains is much weaker than the intrachain exchange. This ensures that the chains are, from a magnetic point of view, nearly decoupled and behave as one-dimensional objects. We will see the effects of the weak residual coupling in Section 6.4.

One example of such material is $KCuF_3$. Its structure is shown in Fig. 6.11. Because of the structure, the unpaired spin on Cu is in a $d_{x^2-y^2}$ orbital which is oriented such that it has maximum overlap with the F^- ions in the c-axis direction. Thus, strong antiferromagnetic exchange occurs in the c direction with much weaker antiferromagnetic exchange along the a and b directions. Thus, at high enough temperatures (larger than the interchain exchanges) the system behaves as isolated spin chains. A method of choice to probe the spin systems is given by neutron scattering. The neutron scattering cross-section gives directly (up to trivial factors) (Mahan, 1981) the imaginary part of the Fourier transform of the spin–spin correlation function (6.48) (see Appendix A). Let us analyze the data in two steps.

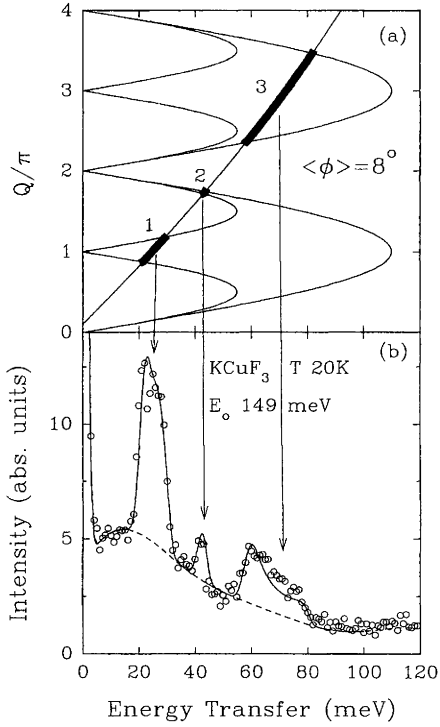

FIG. 6.12. (a) Spectrum of a one-dimensional spin chain. Three different zones (see text) designated by $1, 2, 3$ can be distinguished in the spectrum. (b) Scattering intensity for neutrons scattered by an angle of 8° compared to their incident direction. This gives the wavevector Q represented by a line on the top part. There is a peak of absorption each time $E(Q)$ is in the spectrum. (From Tennant *et al.*, 1995 (Copyright (1995) by the American Physical Society).)

On a crude level, if a system has excitations energies $E(q)$ then the absorption of neutrons is maximum when the frequency $\omega = E(q)$. One can thus expect peaks in the scattering cross-section (that is, in Im $\chi^{\mu\nu}(q,\omega)$) at these frequencies. The neutron scattering experiment is thus a way to probe the energy spectrum of the spin chain. This spectrum was determined from Bethe-ansatz in Fig. 5.6 and is recalled in Fig. 6.12. The neutron scattering for a given wavevector Q should thus give a peak when $E(Q)$ is in the spectrum. The calculated spectrum is in excellent agreement with the observed absorption as shown in Fig. 6.12. One can distinguish various sectors

- Zone 2 is the $q \sim 0$ part of the spectrum. Using the $\langle S_z S_z \rangle$ correlation function since one has spin isotropy, one obtains from (6.49)

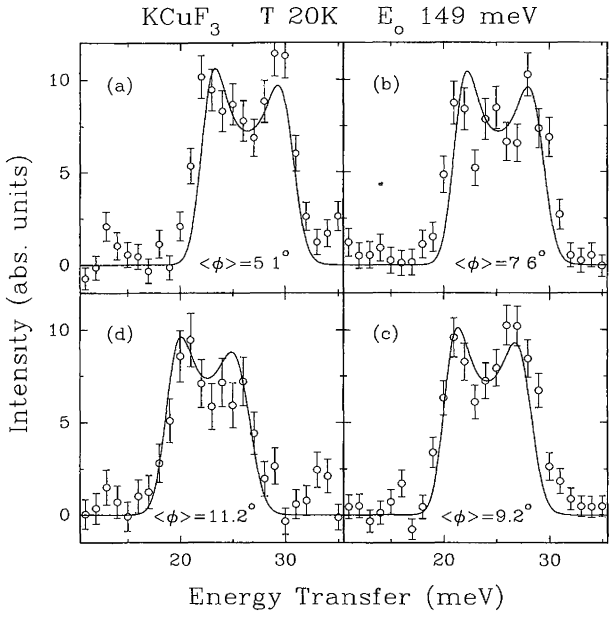

FIG. 6.13. Magnetic scattering where the incident neutrons are along c^* axis, for different scattering angles (that is, different vectors q). The solid line is a fit with the one-dimensional prediction for the correlation function. (From Tennant *et al.*, 1995 (Copyright (1995) by the American Physical Society).)

$$\text{Im}\,\chi^{zz}(q,\omega) \propto \delta(\omega - uk) + \delta(\omega + uk) \tag{6.74}$$

- Zone 1 is the $q \sim \pi$ part of the spectrum and correspond to the antiferromagnetic part of the correlations. This part is also well described by the bosonization as we already saw. I will come back to the detailed shape of this peak in a moment.
- Zone 3 is a continuum of spinons at high energies. This part of the spectrum is beyond the reach of bosonization. The spectrum itself can be obtained from Bethe-ansatz. To get the correlation function one can use a semi phenomenological description (see Tennant *et al.*, 1995).

In order to make a more stringent comparison between the experimental data and the one-dimensional theoretical prediction one can make a detailed comparison of the shape of the peak of Zone 1. Indeed, this part corresponds exactly to the correlation (6.52). The exponent γ' is here $\gamma' = 1/2$ since one is at the spin isotropic point $K = 1/2$. This is a highly non-trivial form, quite different in shape from spin wave predictions, which would give a Lorentzian like broadening of a δ function peak for the lineshape. A comparison of the experimental data with this formula is indicated in Fig. 6.13. There is excellent agreement between theory

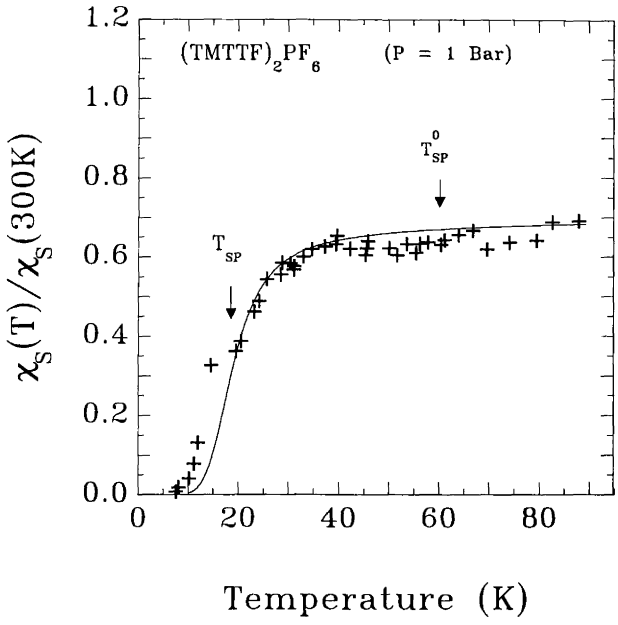

FIG. 6.14. Magnetic susceptibility of $(TMTTF)_2PF_6$. The system has a spin gap at $T = 0$ which is the signature of a spin-Peierls transition. The solid line is a theoretical calculation for a spin-Peierls instability. (From Bourbonnais and Dumoulin, 1996 (Copyright (1996) by EDP Sciences).)

and experiment confirming the special properties of one-dimensional spin chains. Many other probes and compounds can be used to test for one-dimensional spin chains, and it would be impossible to make a review here since this is an ever-expanding field. More information can be found in Oshikawa and Affleck (2002).

Another interesting one-dimensional system is provided by the organic conductor $(TMTTF)_2PF_6$. We will examine the whole family in Section 8.4 so I will not dwell on the structure here. These compounds are good realizations of spin chains. The susceptibility is shown in Fig. 6.14. The spin gap is a signature of the spin-Peierls instability with a dimerization of the structure. Different compounds correspond to different limits for the spin-Peierls transition (adiabatic or antiadiabatic). For example (Pouget, 2001) $(BCPTTF)_2PF_6$ has an exchange $J = 330K$, a Debye frequency $\Omega_0 = 50K$ and a spin-Peierls critical transition at $T_{SP} = 36K$. Its gap between singlet and triplet states is $\Delta = 44K$. This compound is thus likely to be well described by an adiabatic approximation. On the contrary, the inorganic compound $CuGeO_3$ corresponds to $J = 160K$, $\Omega_0 = 310K$ and $T_{SP} = 14.3K$, so it is in the antiadiabatic limit.

The spin-Peierls transition is an extremely rich and fascinating subject that we have only touched upon here. Many interesting questions are still to be solved

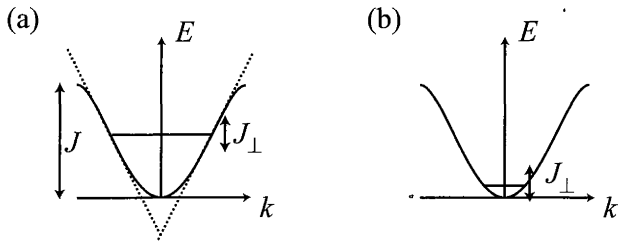

FIG. 6.15. (a) If the interchain coupling is much weaker than the intrachain one then one can use a bosonization description of each spin chain. (b) If the chain is nearly polarized, a one dimensional description is not possible since the coupling is larger than the 'Fermi energy' of a single chain.

such as the magnetic field effects, the effect of disorder, the precise treatment of the three-dimensional couplings, etc. There are also other systems in which the gap is created under a magnetic field, due to a staggered g factor. This allows to have *both* incommensurability and a gap (Dender *et al.*, 1997; Oshikawa and Affleck, 1999; Essler and Tsvelik, 1999).

6.4 Coupled chains

Let me now turn to the three-dimensional coupling of our beloved one-dimensional chains. This is, of course, of prime importance in order to compare with realistic compounds. This is a very complicated problem and I will only explore the basics in this section. In addition to the chain Hamiltonian I add now an antiferromagnetic coupling between the chains

$$H_{\text{inter}} = J_\perp \sum_{\langle\alpha,\beta\rangle} S_{i,\alpha} \cdot S_{i,\beta} \tag{6.75}$$

where i is the site index and α, β the chain index. $\langle\alpha, \beta\rangle$ denotes nearest neighbors in the two- or three-dimensional lattice of chains (depending on the system).

In the presence of the interchain coupling, one expects an ordered state for the spin system. The critical temperature at which the system orders has to be a function of the transverse couplings and has to go to zero when this coupling vanishes. If the interchain coupling is weak compared to the intrachain coupling, then it is legitimate to use the bosonization description for each spin chain. Indeed, in that case the perturbation caused by the three-dimensional coupling is negligible compared to the 'bandwidth' of the one-dimensional system, as shown in Fig. 6.15. Since the antiferromagnetic order is the slowest decaying correlation function in one dimension, one expects the three-dimensional coupling to stabilize this order. This is of course true for a generic coupling. Some special couplings might favor other types of order.

There are two questions one can ask for such a problem. The first one is what happens for an infinite number of coupled chains. This is the relevant question

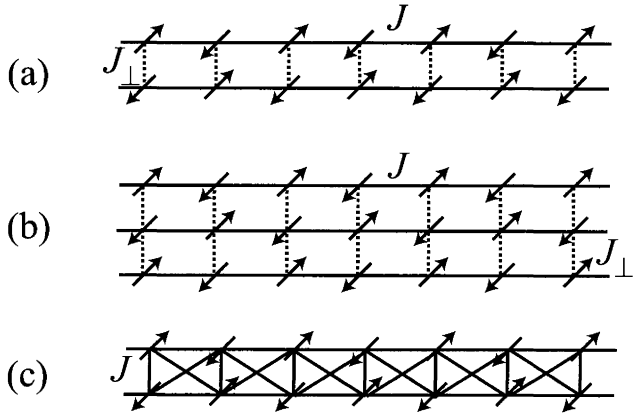

FIG. 6.16. (a) Two and (b) three-leg ladders. $J_\perp$ is the interchain coupling. (c) A spin one chain can be represented as a special ladder (see text).

to tackle most of the materials that are stacks of chains. Another question is how to go from the one-dimensional world to the two- or three-dimensional one and thus to consider a small number of coupled chains (two, three, four, etc.) and to see how the physical properties evolve with the number of chains. This second problem is known as the ladder problem.

6.4.1 *Spin ladders*

Let us therefore first start with the question of the physics of ladders. Ladders of various types (two, three, or more legs) are shown in Fig. 6.16. For simplicity, I confine myself to the system with isotropic couplings.

The physics of ladders can easily be understood in some special limits. The case where the transverse coupling $J_\perp$ is very large and ferromagnetic is the simplest. In that case all the spins in a rung are locked in a maximally polarized state. A rung is thus equivalent to a single spin $S = n/2$ where n is the number of legs in the ladder. The antiferromagnetic intrachain coupling couples these spins S. For large and negative $J_\perp$ the n-leg ladder is thus equivalent to a spin $S = n/2$ antiferromagnetic spin chain. The physics of such chains has been solved[27] by Haldane, who found that there is a drastic difference for the chains with integer and half integer spins (Haldane, 1983). I will come back to this solution later, but it already indicates that one can expect drastically different physics between ladders with odd and even number of legs, at least in this limit. The spin S chain admits another mapping onto a ladder. If we represent a spin $S = n/2$ by the sum of n spin 1/2 (Luther and Timonen, 1985; Schulz, 1986)

$$S = S_1 + S_2 + \cdots + S_n \tag{6.76}$$

[27]Curiously called Haldane's 'conjecture' (probably by people who did not believe in it).

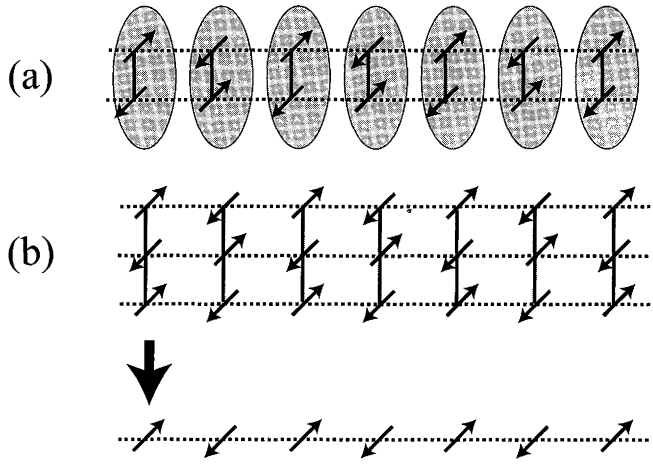

FIG. 6.17. (a) In an even leg antiferromagnetic ladder, the spins on a rung are locked into a singlet state. The ground state is essentially a collection of singlets. (b) For an odd leg antiferromagnetic ladder, one of the spins on the rung remains free. The system is thus essentially equivalent to a spin 1/2 system.

then it is clear that we get extra states. For example, for a spin one, instead of simply getting the three triplet states we get in addition a singlet state. But if one considers the spin S antiferromagnetic Hamiltonian

$$H = J \sum_j S_{j+1} \cdot S_j \tag{6.77}$$

when the spin S would be zero (singlet state) the chain is cut which costs an energy of order J. The extra states of this representation are thus very high-energy states, so to get the low-energy properties of the spin chain the representation (6.76) is a valid one. Substituting (6.76) into (6.77) shows that the spin S chain can be mapped on the n-leg ladder with the special couplings shown in Fig. 6.16.

For antiferromagnetic transverse coupling the large $J_\perp$ limit is also clear. Let us consider a two-leg ladder. In that case, for a very large $J_\perp$, the two spins of the rung lock into a singlet state. The singlets on the rungs have a gap towards triplet excitations of order $J_\perp$, and thus the $J_\parallel$ coupling cannot change this ground state. The ground state of the two-leg ladder is thus a series of singlets on each rung and totally gapped. On the other hand, for a three-leg ladder it is impossible to make a singlet state with the three spins on a rung and a spin 1/2 degree of freedom remains free. Each rung can thus be replaced by a spin 1/2 and the ladder is equivalent to a spin 1/2 chain, and thus gapless. One thus recovers an even/odd alternation, reminiscent of what happens for spin S chains. This is shown in Fig. 6.17.

6.4.1.1 *Bosonization solution* Let us now examine the opposite limit of weak interchain coupling and see how much of the above physics remains. We restrict our study to the two-leg ladder

$$H = \sum_{\alpha=1,2} H_\alpha^0 + J_\perp \sum_j S_{j,1} \cdot S_{j,2} \tag{6.78}$$

where H_α^0 is the single chain Heisenberg Hamiltonian. Each single chain Hamiltonian can be expressed in terms of fermion operators using the Jordan–Wigner transformation like in Section 6.1. One has to take care that the 'fermion' operators should have anticommutation relations inside one chain but *commutation* relations between the chains to respect the spin commutation relations. This causes no modification of the bosonized expressions (6.33) and (6.37) for the spin operators. Indeed, it is easy to check that these expressions preserve all the correct spin commutation relations. H^0 has been obtained in Section 6.1 and only the bosonized expression of H_{inter} is needed. Using the bosonized expressions and keeping only the most relevant operators[28] one obtains (Luther and Timonen, 1985; Schulz, 1986; Strong and Millis, 1992)

$$\begin{aligned} H_{\text{inter}} = \int \Bigg[& \frac{2g_1}{(2\pi a)^2} \cos(\theta_1 - \theta_2) + \frac{2g_2}{(2\pi a)^2} \cos 2(\phi_1 - \phi_2) \\ & + \frac{2g_3}{(2\pi a)^2} \cos 2(\phi_1 + \phi_2) \Bigg] dx + J_\perp^z a \int dx \frac{\partial_x \phi_1 \partial_x \phi_2}{\pi^2} \end{aligned} \tag{6.79}$$

Where:

$$\begin{aligned} g_1 &= \pi J_\perp^{xy} a \\ g_2 &= J_\perp^z a \\ g_3 &= J_\perp^z a \end{aligned} \tag{6.80}$$

If we had bosonized the ladder representing the spin S chain one would have gotten exactly the same Hamiltonian but with all coefficients being J since this is the only coupling constant in the problem (Schulz, 1986). We thus see that in the continuum limit there is no essential difference between the two problems.

The total Hamiltonian is rewritten in terms of the fields $\phi_a = \frac{\phi_1 - \phi_2}{\sqrt{2}}$ and $\phi_s = \frac{\phi_1 + \phi_2}{\sqrt{2}}$ giving

[28] Another operator appears $\cos(\theta_1 - \theta_2)\cos(2\phi_1)\cos(2\phi_2)$. Since it is marginal, it can be neglected together with the term $\partial_x \phi_1 \partial_x \phi_2$.

$$
\begin{aligned}
H &= H_s + H_a \\
H_s &= \int \frac{dx}{2\pi}\left[u_s K_s(\pi\Pi_s)^2 + \frac{u_s}{K_s}(\partial_x\phi_s)^2\right] + \frac{2g_2}{(2\pi\alpha)^2}\int dx\ \cos(\sqrt{8}\phi_s) \\
H_a &= \int \frac{dx}{2\pi}\left[u_a K_a(\pi\Pi_a)^2 + \frac{u_a}{K_a}(\partial_x\phi_a)^2\right] + \frac{2g_3}{(2\pi\alpha)^2}\int dx\ \cos(\sqrt{8}\phi_a) \\
&\quad + \frac{2g_1}{(2\pi\alpha)^2}\int dx \cos(\sqrt{2}\theta_a)
\end{aligned}
\tag{6.81}
$$

where

$$
\begin{aligned}
u_s &= u\left(1 + \frac{KJ_\perp^z a}{2\pi u}\right), \quad K_s = K\left(1 - \frac{KJ_\perp^z a}{2\pi u}\right) \\
u_a &= u\left(1 - \frac{KJ_\perp^z a}{2\pi u}\right), \quad K_a = K\left(1 + \frac{KJ_\perp^z a}{2\pi u}\right)
\end{aligned}
\tag{6.82}
$$

u, K are the LL parameters of a single chain as defined in (6.30). If the correct values of u and K are used, (6.81) only assumes $J_\perp a \ll u/K$. Because of our choice of an hermitian string operator, the $\cos(4\phi_1)$ and $\cos(4\phi_2)$ terms in $H^0_{1,2}$ can be dropped, since they always give terms that are less relevant than the terms that come from H_{inter}.

The particular case of isotropic interchain coupling (Strong and Millis, 1994) ($J_\perp^{x,y} = J_\perp^z$) corresponds to taking $g_2 = g_3 = g_1/\pi$ in (6.81). One can use another method (Shelton *et al.*, 1996) of derivation for isotropically coupled spin chains. Instead of using a Jordan–Wigner transformation one represents a spin chain as a system of fermions with one particle per site. As we saw in that case the charge sector has a gap. Only the spin degrees of freedom remain. Such a representation is particularly well adapted to describe an isotropic coupling since the superexchange leading to the spin Hamiltonian is automatically generated. Interestingly, one recovers the same bosonized Hamiltonian as (6.81) (with $K = 1/2$ due to isotropy), but with a different relation between the coefficients g. The coefficient satisfy $g_2 = g_3 = g_1 \propto J_\perp$. This difference comes from the fact that in the present derivation the calculation of the coefficients g is perturbative and the expression (6.80) is accurate for $J_z \ll J_{xy}$. In going to the isotropic point these coefficients get renormalized by irrelevant terms that do no affect the form of the low-energy Hamiltonian (6.81), but can change the explicit value of the coefficients compared to (6.80). Comparison of the two limits $J_z \ll J_{xy}$ and $J_z \sim J_{xy}$ shows that these renormalization effects are rather weak, and that (6.81) and (6.82) provide an extremely accurate description of the physics of the ladder system for all values of J_z, provided one does not need the *precise* values of the coefficients g.

Let us analyze the physics of (6.81) for the isotropic case. It is easy to see that one can also take into account anisotropy since this only affects the possible values of K_s and K_a. For the isotropic (Heisenberg) case $K = 1/2$. The symmetric part of the Hamiltonian is just a sine-Gordon one. Since $K_s = 1/2$

the cosine term is relevant (relevant for $K_s < 1$) and this sector is massive. The antisymmetric Hamiltonian is more complicated. It is very similar to the one studied in Section 4.3.2. The $\cos(\sqrt{8}\phi)$ and $\cos(\sqrt{2}\theta)$ compete. Contrary to the case studied in Section 4.3.2, here the $\cos(\sqrt{8}\phi)$ is relevant for $K_a < 1$ whereas $\cos(\sqrt{2}\theta)$ is relevant for $K_a > 1/4$. Both terms are thus relevant at the isotropic point $K = 1/2$. The most relevant operator is the first to attain the strong coupling regime under renormalization. In the strong coupling regime, this operator takes a mean value that minimizes the ground state energy. θ_a and ϕ_a being conjugated, when one of them develops a mean value the exponentials of the other one have zero expectation values and exponentially decaying correlations. Therefore, ϕ_a acquires a mean value while θ_a is disordered for $K_a < 1/2$ and the situation is reversed for $K_a > 1/2$. The antisymmetric sector is thus always massive. Since both the symmetric and antisymmetric sectors are massive all spin correlations decay exponentially, and one recovers that all the spins are locked into a singlet state, for any small $J_\perp$. One thus recovers the continuity with the strong coupling solution. A similar study can be made for a larger number of legs (Schulz, 1986; Cabra *et al.*, 1998; Kim and Solyom, 1999). Even-leg spin ladders are thus gapped, whereas odd-leg spin ladders are gapless. This physics is exactly identical to Haldane's result for the spin S system (see Affleck 1988 for more on the spin S problem). Thus, the passage from one chain to the two-dimensional system is not smooth. Using the bosonized form, many more physical properties can be computed in addition to the few that I showed here. There are many more studies that can be done on spin ladders, much of them too complicated for this book. I refer the reader to Schulz (1986), Kishine and Fukuyama (1997), Orignac and Giamarchi (1998*a*), Nersesyan *et al.* (1998), Gogolin *et al.* (1999) and Citro and Orignac (2002) for more.

Two final words before closing this chapter. The antisymmetric Hamiltonian has a remarkable solution (Shelton *et al.*, 1996; Gogolin *et al.*, 1999). Let us rescale the fields by $\tilde{\phi} = \sqrt{2}\phi$, $\tilde{\theta} = \theta/\sqrt{2}$. The antisymmetric Hamiltonian becomes (remember that for the isotropic case $K_a = 1/2$)

$$H_a = \int \frac{dx}{2\pi} u_a \left[(\pi\tilde{\Pi}_a)^2 + (\partial_x\tilde{\phi}_a)^2\right] + \frac{2g_3}{(2\pi\alpha)^2}\int dx\ \cos(2\tilde{\phi}_a) + \frac{2g_1}{(2\pi\alpha)^2}\int dx\ \cos(2\tilde{\theta}_a) \quad (6.83)$$

The first term is the kinetic energy of free spinless fermions. In the same spirit that the Luther–Emery solution one can refermionize the interaction which becomes

$$\propto g_3 \int dx[\psi_R^\dagger(x)\psi_L(x) + \text{h.c.}] + g_1 \int dx[\psi_R^\dagger(x)\psi_L^\dagger(x) + \text{h.c.}] \quad (6.84)$$

Quite remarkably the Hamiltonian H_a is thus a *quadratic* Hamiltonian of free spinless fermions and can thus be diagonalized by a Bogoliubov transformation.

The $\cos(2\phi)$ term is a backscattering of these fermions that favors order of the density wave type, whereas the $\cos(2\theta)$ is a Josephson term that favors superconducting pairing. One sees explicitly the competition between the two types of order. The solution of (6.84) can be made simpler by using Majorana fermions. This is a very elegant and powerful solution that allows to compute simply most of the physical properties of the two-leg ladder at the isotropic point.

Secondly, if one adds a magnetic field, the field couples to the total of the spins. It thus corresponds to a term

$$H = \mathbf{h}\frac{\sqrt{2}}{\pi}\int dx \nabla\phi_s(x) \tag{6.85}$$

with $\mathbf{h} = g\mu_B h$. It thus gives rise to the same type of Mott-δ transition than before, but only in the symmetric mode. The antisymmetric mode remains gapped. This means that some of the correlation functions in the ladder still decay exponentially even in the presence of magnetic field. See Chitra and Giamarchi (1997), Giamarchi and Tsvelik (1999) and Konik and Fendley (2002) for more details.

6.4.1.2 *Experimental realization of ladders* A good example of ladders is provided by the series $Sr_{n-1}Cu_{n+1}O_{2n}$ (Takano *et al.*, 1991). The compound $n = 3$, $Sr_2Cu_4O_6$ (in short $SrCu_2O_3$) can be seen as a stack of Cu_2O_3 planes separated by Sr planes. The magnetic coupling between Cu^{2+} ions is a superexchange through the O^{2-} ions. It is maximal and antiferromagnetic when the angle is about π. When the angle is close to $\pi/2$ the wavefunction overlap between Cu and O is small and the coupling is much weaker. From a magnetic point of view $SrCu_2O_3$ can thus be viewed as nearly uncoupled spin ladders, as shown in Fig. 6.18. As shown in Fig. 6.19, the ladder $SrCu_2O_3$ has a spin gap of the order of 36,2 meV. (Takano *et al.*, 1991). This gap can be observed by direct susceptibility measurement or by the NMR relaxation time $1/T_1$ on ^{63}Cu. This behavior is in good agreement with the theoretical expectations for an even-leg ladder. Identical measurements made on the three-leg ladder compound $Sr_4Cu_6O_{10}$ (or $Sr_2Cu_3O_5$) do not show any spin gap as indicated in Fig. 6.19. In addition muon spin relaxation (Kojima *et al.*, 1995) has shown that the three-leg ladder $Sr_2Cu_3O_5$ has antiferromagnetic order at $T = T_N = 52$ K, in agrement with what would be expected for a system that has a free spin 1/2.

The organic material $Cu_2(C_5H_{12}N_2)_2Cl_4$ (Chiari *et al.*, 1990) is another interesting system. This compound exhibits a spin gap (Chaboussant *et al.*, 1997; Hammar *et al.*, 1998). Structurally, the material is made of a stack of organic molecules. Initial studies suggested for the spins a ladder-like structure where the strongest bond would be $J_\perp$ (Chaboussant *et al.*, 1997; Hammar *et al.*, 1998). More recent neutron data seems, however, to favor a more three-dimensional structure with frustration (Stone *et al.*, 2002). What is the correct description for this compound is thus controversial at the moment. What makes this compound specially interesting, regardless of its dimensionality (quasi-one- or three-

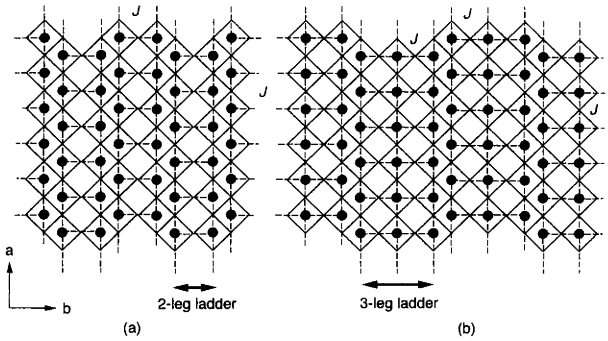

FIG. 6.18. Magnetic structure of $Sr_{n-1}Cu_{n+1}O_{2n}$ for $n = 2$ ($SrCU_2O_3$) and $n = 3$ ($Sr_2CU_3O_5$). The material is made of n-leg ladders. Due to the weak magnetic coupling and the frustration at the level of the double chains, the ladders are nearly magnetically decoupled. (From Azuma *et al.*, 1994 (Copyright (1994) by the American Physical Society).)

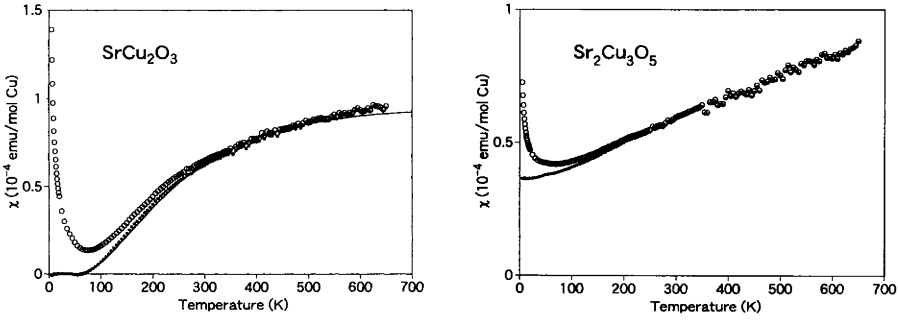

FIG. 6.19. (Left) Magnetic susceptibility of $SrCu_2O_3$. After subtracting a Curie tail due to the impurities, the susceptibility shows clearly the existence of a spin gap. This is in agreement with the expected behavior of even-leg ladders. (Right) Same measurement on the three-leg ladder compound $Sr_2Cu_3O_5$. After the subtraction of the Curie tails, the susceptibility becomes a constant, an indication that this compound has no spin gap. (from Azuma *et al.*, 1994 (Copyright (1994) by the American Physical Society).)

dimensional) is the fact that the couplings are such that the gap is humanly accessible, of the order of ~ 1 meV (to be compared with the 40 meV of $SrCu_2O_3$). This gap can thus be killed by an experimentally accessible magnetic field. This system is thus a prime candidate to study the type of quantum phase transitions discussed in the previous section where singlet states are destroyed by a magnetic field and lead to a massless phase. The existence of such a quantum critical point can be seen in relaxation time NMR measurements as shown in Fig. 6.20.

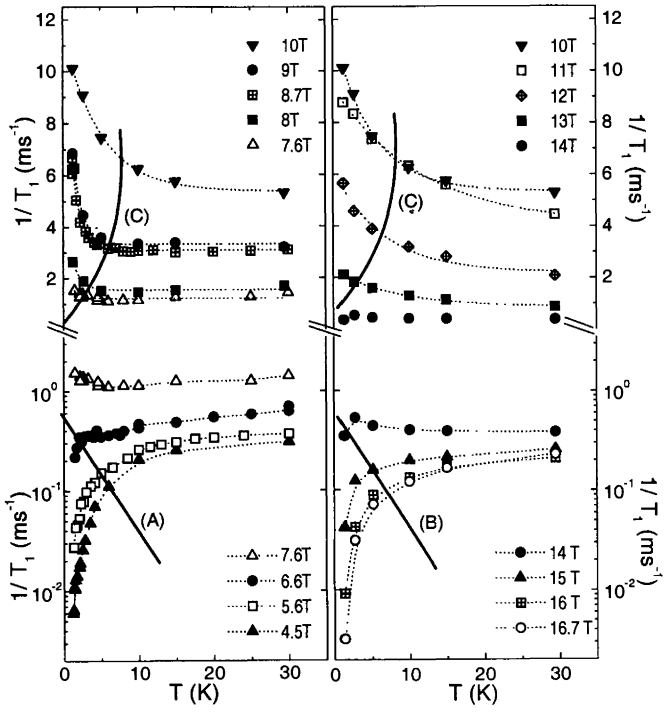

FIG. 6.20. Quantum critical point as seen by the NMR relaxation time. (Bottom left) The system is in a singlet state and the relaxation time drops for temperatures smaller than the spin gap (plotted as (A)). (Top left and right) The magnetic field exceeds the critical value h_c and the spin gap is destroyed. The low-temperature behavior of the relaxation rate is now quite different reflecting the nature of the excitations at low-energy. (Bottom right) If the magnetic field is large enough to completely polarize the system, then there is again a gap towards excitations (plotted as (B)). (From Chaboussant *et al.*, 1998 (Copyright (1998) by EDP Sciences).)

Many properties of this system are yet to be understood.

6.4.2 *Infinite number of chains*

Let us now move to an infinite number of coupled spin chains. This is of course a formidable problem and some approximations are needed. Again for simplicity let us confine the discussion here to the case without a magnetic field and with isotropic spin couplings. The interchain coupling has the same form than for the ladder

$$H_\perp = J_\perp \sum_{\langle \mu\nu \rangle} \int dx\, S_\mu(x) \cdot S_\nu(x) \tag{6.86}$$

where $\langle\mu\nu\rangle$ are neighboring chains in a three-dimensional lattice. At low temperatures, one expects the system to have an ordered state. Since the single chain has dominant antiferromagnetic correlations we expect, unless the perpendicular coupling is of a special kind, that this dominant fluctuation will be stabilized. One can thus try to treat the interchain coupling in a mean field approximation. We thus assume that the spin takes an average value $\langle S\rangle$ and that the fluctuations are small. Thus, $S = \langle S\rangle + \delta S$ and we can retain only terms linear in δS. In the ordered state, we can break the spin rotation symmetry by assuming that the order takes place say along the z direction. The interchain coupling thus becomes

$$\begin{aligned} H_\perp =& J_\perp \sum_{\langle\mu\nu\rangle} \int dx\, [\langle S_\mu(x)\rangle \cdot \langle S_\nu(x)\rangle + \delta S_\mu(x) \cdot \langle S_\nu(x)\rangle + \langle S_\mu(x)\rangle \cdot \delta S_\nu(x)] \\ =& J_\perp \sum_{\langle\mu\nu\rangle} \int dx\, [S_\mu(x) \cdot \langle S_\nu(x)\rangle + \langle S_\mu(x)\rangle \cdot S_\nu(x) - \langle S_\mu(x)\rangle \cdot \langle S_\nu(x)\rangle] \end{aligned} \tag{6.87}$$

The Hamiltonian of each chain is thus in the mean field approximation

$$\begin{aligned} H &= H_\mu^0 + J_\perp \sum_\nu S_\mu(x) \cdot \langle S_\nu(x)\rangle \\ &= H_\mu^0 + J_\perp \sum_\nu S_\mu^z(x) \langle S_\nu^z(x)\rangle \end{aligned} \tag{6.88}$$

assuming order in the z direction. The average value $\langle S_\nu^z(x)\rangle$ acts as a staggered magnetic field. We thus have to solve the problem of a spin chain in a staggered field

$$H = H_\mu^0 + h \int dx (-1)^x S^z(x) \tag{6.89}$$

where the field h is given by the self-consistency condition

$$h = Z J_\perp \langle S_\nu^z(x)\rangle = -Z J_\perp \langle S_\mu^z(x)\rangle \tag{6.90}$$

and Z is the coordination number of the lattice. This is a relatively easy problem to solve since we can use all our one-dimensional technology. If the interchain coupling is small compared to the intrachain we can use bosonization. In that case the Hamiltonian is

$$H = H_\mu^0 + \frac{h}{\pi\alpha} \int dx\ \cos(2\phi(x)) \tag{6.91}$$

which is our favorite sine-Gordon Hamiltonian. The self-consistency condition becomes

$$h = \frac{-Z J_\perp}{\pi\alpha} \langle \cos(2\phi(x))\rangle \tag{6.92}$$

There are of course several ways to tackle this self-consistency condition depending on the degree of accuracy needed. For an isotropic system $K = 1/2$ and thus

the cosine is relevant at $T = 0$ and opens a gap. The average of the cosine is non-zero and thus there is a solution to (6.92) showing that there is indeed an ordered state at $T = 0$. To solve (6.92) one can either use approximate solutions to compute the averages in the massive phase such as the variational method explained in Appendix E.2 or use exact solutions for the sine-Gordon model. To determine the temperature at which the system orders let us see when (6.92) has a non-zero solution. Since the field h is very small at the transition one can expand (6.92) to get

$$h = \frac{ZhJ_\perp}{(\pi\alpha)^2} \int dx \int_0^\beta d\tau \langle \cos(2\phi(x_0, \tau_0)) \cos(2\phi(x, \tau)) \rangle \tag{6.93}$$

which has in addition to the trivial solution $h = 0$ a non-zero solution at the temperature β_c where

$$\frac{1}{ZJ_\perp} = \frac{1}{(\pi\alpha)^2} \int dx \int_0^{\beta_c} d\tau \langle \cos(2\phi(x_0, \tau_0)) \cos(2\phi(x, \tau)) \rangle \tag{6.94}$$

The transition thus occurs when the *one-dimensional* susceptibility is equal to the inverse transverse coupling. If the one-dimensional susceptibility diverges there is always a temperature at which the system orders tridimensionally. This was our argument to draw a one-dimensional 'phase diagram' based on the divergence of one-dimensional susceptibilities in Chapter 2. On the other hand, if the susceptibility does not diverge at $\beta = \infty$ the system might not order if the transverse coupling is too weak. In our case, the self-consistent equation becomes

$$T_c \propto (J_\perp)^{\frac{1}{2-2K}} \tag{6.95}$$

where at the isotropic point $2-2K = 1$. The critical temperature is thus strongly renormalized by the *one-dimensional* fluctuations. For very weak $J_\perp$ it would be very incorrect to make a three-dimensional mean field theory. Such a theory forgets that in one dimensions quantum fluctuations can strongly disorder the system and thus reduce the tendency to order. It would grossly overestimate the critical temperature of the system (see e.g. what happens when $K \to 1$).

One can use the mean field approximation to extract other quantities. In particular for the correlation functions one can use an RPA approximation (Mahan, 1981) for the susceptibility

$$\chi(\omega, q, q_\perp) = \frac{\chi^{1D}(\omega, q)}{1 + 2J_\perp(\sum_\mu \cos(q_\perp^\mu))\chi^{1D}(\omega, q)} \tag{6.96}$$

The singularity in $\chi(\omega, q, q_\perp)$ gives the critical temperature. This is equivalent to our self-consistent condition. Using the expression for the one-dimensional correlation function one can compute the full susceptibility and compare with neutrons scattering experiments. I will stop here since this would carry us too far.

More can be found in Schulz (1998), Giamarchi and Tsvelik (1999) and Bocquet *et al.* (2001).

Note that treating the interchain coupling for spins is relatively simple since the spin has a well-defined average value. This allows us to use a mean field approximation, which is usually a very good approximation. We will see in Chapter 8 other coupled chain systems for which this is not the case, which complicates the treatment drastically.

7

INTERACTING FERMIONS ON A LATTICE

Models are to be used, not believed.

H. Theil (*Principles of Econometrics*)

Let us now turn towards the canonical microscopic models used to study interacting fermions. Most of these models are of course quite general and are not special to one dimension. They try to implement the essential ingredients to study a strongly interacting electronic system: the kinetic energy, the interaction and the lattice in order to be able to study effects such as the Mott transition.

7.1 Microscopic models

7.1.1 *Hubbard model*

Let us start with what is probably the 'Ising model' of strongly correlated fermions: the Hubbard model

$$H = -t \sum_{j,\sigma} c^\dagger_{j,\sigma} c_{j,\sigma} + U \sum_j n_{j\uparrow} n_{j\downarrow} \tag{7.1}$$

where $n_{i\sigma} = c^\dagger_{i\sigma} c_{i\sigma}$ is the number of particles of a given spin on site i. In addition one can include a chemical potential. The model can be rewritten in a convenient form as

$$H = -t \sum_{j,\sigma} c^\dagger_{j,\sigma} c_{j,\sigma} + U \sum_j (n_{j\uparrow} - 1/2)(n_{j\downarrow} - 1/2) - \mu \sum_j (n_{j\uparrow} + n_{j\downarrow} - 1) \tag{7.2}$$

In this model, electrons hop from site to site with a matrix element t. This is the standard tight binding kinetic energy. Electrons interact only if they are on the same site. Since the Pauli principle prevents two electrons of the same spin to be on the same site, it is enough to consider the local coupling between electrons of opposite spins (other terms would vanish because of the Pauli principle or simply become chemical potential terms). This model is the simplest generalization to fermions with spins of the spinless model we studied in Section 6.1.

Even without solving the Hubbard model one can have an idea of its basic physical properties. Let us first look at the symmetries. For that let us also consider a magnetic field along z (a factor of $g\mu_B/2$ has been included in h)

$$H_h = -h \sum_j (n_{j\uparrow} - n_{j\downarrow}) \tag{7.3}$$

The simplest symmetry is the particle–hole symmetry. If one changes

$$c_{j,\sigma} \to (-1)^j c^\dagger_{j,\sigma} \tag{7.4}$$

this leaves the kinetic energy and U invariant and changes $\mu \to -\mu$ and $h \to -h$. Thus, it is enough to study the system with either particle or hole doping. In the absence of magnetic field the system is spin rotation invariant (symmetry SU(2)). For a generic filling the only charge symmetry is the U(1) symmetry which is the multiplication of the operators by an arbitrary phase. A more interesting symmetry is the particle–hole symmetry on one of the spin species.

$$c_{j,\downarrow} \to (-1)^j c^\dagger_{j,\downarrow} \tag{7.5}$$

This leaves the kinetic energy invariant but changes $U \to -U$ and since

$$n_{j\uparrow} + n_{j\downarrow} \to n_{j\uparrow} - n_{j\downarrow} + 1, \quad n_{j\uparrow} - n_{j\downarrow} \to n_{j\uparrow} + n_{j\downarrow} - 1 \tag{7.6}$$

this changes $\mu \to h$ and $h \to \mu$. This transformation thus maps the charge sector of the Hubbard model on the spin sector and vice versa, while changing the repulsive system to the attractive one. At half-filling $\mu = 0$ and in the absence of magnetic field the only effect is to change $U \to -U$ and thus to go from attraction to repulsion. Since the spin sector becomes the charge sector, we see that at half-filling the Hubbard model has a hidden *charge* SU(2) symmetry which can be obtained by combining a spin rotation with the transformation (7.5). The total symmetry group is in that case $SU(2) \times SU(2) = SO(4)$. These symmetries will have very clear expressions in the boson representation. For repulsive interactions, one expects the system to be dominated by antiferromagnetic exchange, because of the superexchange between spins. At half-filling (one particle per site) and for large U the system is equivalent to a Heisenberg chain with an exchange constant $J \sim 4t^2/U$. For attractive and large interactions, on the other hand, one expects pairs of opposite spins to form a singlet on a site. This bound state behaves as a hard core boson since it is made of two fermions. In high dimensions the naive expectation would be that these bosons condense and the system becomes superconducting.

Let us now see how much of this intuitive picture actually survives in one dimension. Using the boson mapping of Appendix D the interaction in the Hubbard model (7.2) becomes (taking the lattice spacing $a = 1$)

$$\begin{aligned}\sum_j (n_{j\uparrow}-1/2)(n_{j\downarrow}-1/2) = \int dx \left[-\frac{1}{\pi}\nabla\phi_\uparrow(x) + \frac{1}{2\pi\alpha}(e^{i(-2k_F x + 2\phi_\uparrow(x))} + \text{h.c.})\right] \\ \times \left[-\frac{1}{\pi}\nabla\phi_\downarrow(x) + \frac{1}{2\pi\alpha}(e^{i(2k_F x - 2\phi_\downarrow(x)} + \text{h.c.})\right]\end{aligned} \tag{7.7}$$

We will examine later the case of commensurate fillings for which umklapp terms can appear. For the moment let us consider a generic filling. The only non oscillating terms for a generic filling are

$$\begin{aligned}
&\sum_j (n_{j\uparrow} - 1/2)(n_{j\downarrow} - 1/2) \\
&= \int dx \left[\frac{1}{\pi^2} \nabla\phi_\uparrow(x) \nabla\phi_\downarrow(x) + \frac{2}{(2\pi\alpha)^2} \cos(2\phi_\uparrow(x) - 2\phi_\downarrow(x)) \right] \\
&= \int dx \left[\frac{1}{2\pi^2} (\nabla\phi_\rho(x))^2 - (\nabla\phi_\sigma(x))^2 \right] + \frac{2}{(2\pi\alpha)^2} \cos(\sqrt{8}\phi_\sigma(x))
\end{aligned} \tag{7.8}$$

The full Hamiltonian is thus of the form studied in Section 2.3. The parameters are all functions of the single variable U with

$$\begin{aligned}
u_\rho K_\rho &= u_\sigma K_\sigma = v_F \\
u_\rho / K_\rho &= v_F (1 + \frac{U}{\pi v_F}) \\
u_\sigma / K_\sigma &= v_F (1 - \frac{U}{\pi v_F}) \\
g_{1\perp} &= U
\end{aligned} \tag{7.9}$$

If one is at half-filling then $4k_F = 2\pi$ and one should keep the corresponding umklapp term in (7.7), as explained in Section 4.2. The corresponding term is

$$H_u = \frac{2U}{(2\pi\alpha)^2} \int dx \ \cos(\sqrt{8}\phi_\rho(x)) \tag{7.10}$$

The strength of the umklapp is thus just U for the Hubbard model. The operators measuring the various correlations are given by (2.113). For the half-filled case, to write the boson form of these operators it is important to worry about the Klein factors (operators U) as explained in Section 4.3.2. Choosing the convention that the umklapp term is

$$H_u = \frac{-2U}{(2\pi\alpha)^2} \int dx \ \cos(\sqrt{8}\phi_\rho(x)) \tag{7.11}$$

The operators become

$$\begin{aligned}
O_{\text{CDW}}(x) &= \frac{e^{-2ik_F x}}{\pi\alpha} \sin(\sqrt{2}\phi_\rho) \cos(\sqrt{2}\phi_\sigma) \\
O^x_{\text{SDW}}(x) &= \frac{e^{-2ik_F x}}{\pi\alpha} \cos(\sqrt{2}\phi_\rho) \cos(\sqrt{2}\theta_\sigma) \\
O^y_{\text{SDW}}(x) &= \frac{e^{-2ik_F x}}{\pi\alpha} \cos(\sqrt{2}\phi_\rho) \sin(\sqrt{2}\theta_\sigma) \\
O^z_{\text{SDW}}(x) &= \frac{e^{-2ik_F x}}{\pi\alpha} \cos(\sqrt{2}\phi_\rho) \sin(\sqrt{2}\phi_\sigma)
\end{aligned} \tag{7.12}$$

Choosing the positive sign for the umklapp is equivalent in shifting ϕ_ρ by $\pi/\sqrt{8}$ and making the same change in (7.12). The chemical potential and magnetic

field are given by $\nabla\phi_\rho$ and $\nabla\phi_\sigma$ terms, respectively, as explained in Section 2.3. Another operator can exist

$$O_{\mathrm{BOW}}(x) = \frac{e^{-2ik_F x}}{\pi\alpha}\cos(\sqrt{2}\phi_\rho)\cos(\sqrt{2}\phi_\sigma) \tag{7.13}$$

It corresponds to a charge density wave where the density is located on the bonds (bond order charge density wave) rather than on the sites as a in the conventional CDW. For half-filling its expression is

$$\begin{aligned} O_{\mathrm{BOW}}(n) &= \frac{(-1)^n}{2}\sum_\sigma (c^\dagger_{n+1,\sigma}c_{n,\sigma} + \text{h.c.}) \\ &= \frac{1}{2}\sum_{r,\sigma}\psi^\dagger_{r,\sigma}(x+a)\psi_{-r,\sigma}(x) + \psi^\dagger_{r,\sigma}(x)\psi_{-r,\sigma}(x+a) \end{aligned} \tag{7.14}$$

The symmetries of the Hubbard model are explicit on the bosonized form. As we already discussed in Chapter 4 the SU(2) spin rotation is not obvious because of the abelian nature of the bosonization. But it is there and we know how to implement the rotation if needed (see Section 4.3.2). The particle–hole symmetry is present for all filling. This is an artefact of the linearization of the spectrum and would be broken by the irrelevant operators such as band curvature. The mapping of charge to the spin sector is simply the exchange $\phi_\rho \to \phi_\sigma$. This indeed changes $U \to -U$ and maps the charge correlation functions to the z component of the spin ones as can be seen from (7.12)

Based on the results of Section 2.3, one can thus distinguish two different regimes. If $U > 0$, the spin sector is massless. The operator $\cos(\sqrt{8}\phi_\sigma)$ is just marginal. The spin parameters flow to the fixed point $K^*_\sigma = 1$. Since $K_\rho < 1$ we see from Section 2.3 that charge/spin fluctuations dominates (that is, decay more slowly) than superconducting ones. The charge and the spin correlation functions have the *same* exponent. Since the operator $\cos(\sqrt{8}\phi_\sigma)$ is just marginal, logarithmic corrections appear as discussed in Section 4.4. The correlation functions are thus ($\delta\rho = \rho - \rho_0$)

$$\begin{aligned} \langle\delta\rho(x)\delta\rho(0)\rangle =& \frac{K}{\pi^2}\frac{y_\alpha^2 - x^2}{(x^2+y_\alpha^2)^2} + \rho_0^2 A_2\cos(2\pi\rho_0 x)\left(\frac{\alpha}{r}\right)^{K_\rho+1}\log^{-3/2}(\alpha/r) \\ &+ \rho_0^2 A_4\cos(4\pi\rho_0 x)\left(\frac{\alpha}{r}\right)^{4K_\rho} + \cdots \\ \langle S_\mu(x,\tau)S_\mu(0)\rangle =& \frac{K}{4\pi^2}\frac{y_\alpha^2 - x^2}{(x^2+y_\alpha^2)^2} \\ &+ A_2'\cos(2\pi\rho_0 x)\left(\frac{\alpha}{r}\right)^{K_\rho+1}\log^{1/2}(\alpha/r) + \cdots \end{aligned} \tag{7.15}$$

where $2\pi\rho_0 = 2k_F$ and other notations are in Appendix A. The dominant correlation is thus a $2k_F$ spin density wave. This is physically very satisfying since

this is the physics that one would expect from the repulsive Hubbard model in higher dimensions. Note that the modulation of the spin density wave is $2k_F$, which is an incommensurate modulation. This is the wavevector that one would get by simply assuming a commensurate modulation between holes. The whole analysis of the repulsive side of the Hubbard model can thus be directly borrowed from Section 2.3. The retarded correlation functions and their Fourier transform can be obtained directly from the formulas of Appendix C. The uniform charge and spin susceptibilities are 'Fermi liquid' like, that is, they tend to a constant at zero temperature. The small magnetic field response can directly be obtained from Section 4.3.1.

The spin correlations have a power law divergence at $Q = 2k_F$ that is given by

$$\chi(Q = 2k_F, \omega = 0, T) \sim T^{K_\rho - 1} \log^{1/2}(E/T) \tag{7.16}$$

where E is the band cutoff. Note that the charge susceptibility at $2k_F$ has in fact the same power law divergence and is only suppressed by logarithmic factors compared to the spin susceptibility. This divergence in the spin correlations can be probed for example in an NMR experiment. Indeed, the relaxation time in an NMR experiment is sensitive to the local spin correlation function

$$1/T_1 = A^2 T \sum_q \frac{\operatorname{Im} \chi(q, \omega)}{\omega} \tag{7.17}$$

where the A are the hyperfine coupling constants. The sum over q is just to reproduce the local spin correlation function. One can compute (7.17) rigorously from Appendix C, but let us be crude[29] and do it again by simple scaling analysis. The local spin–spin correlation function has two contributions (one from the $q \sim 0$ modes the other from the $q \sim 2k_F$ ones)

$$\langle S(x = 0, \tau) S(x = 0, 0) \rangle \sim \frac{1}{\tau^2} + \left(\frac{1}{\tau}\right)^{1+K_\rho} \tag{7.18}$$

The Fourier transform over time thus gives

$$\chi \simeq T + T^{K_\rho} \tag{7.19}$$

This would be essentially the function in Matsubara time. To go to real time or frequencies does not change the power laws. In the imaginary part of the susceptibility one power of ω has to appear (the imaginary part is odd), thus one power of T should be replaced by ω (ω and T scale the same way). One can

[29]This is very often sufficient and should in any case always be done before a more sophisticated calculation.

also obtain the same result using the retarded correlation function as computed with the techniques of Appendix C. The end result is

$$1/T_1 \propto T + T^{K_\rho} \tag{7.20}$$

The first term is nothing but the Korringa law that holds in Fermi liquids. This is reasonable since it comes from the fact that the susceptibility becomes a constant at low temperatures. This is indeed the case even in $d = 1$ for the $q \sim 0$ modes. In a Fermi liquid this is all there is. In a Luttinger liquid, the $2k_F$ contribution dominates ($K_\rho < 1$) at low temperatures and one expects strong deviations compared to the Korringa law.

To obtain the retarded single-particle Green's function two routes are possible. The simplest is to use the expression in imaginary time (2.83), which in presence of charge and spin modes now trivially becomes (see (2.83))

$$\begin{aligned} G_{R,s}(r) &= -\langle \psi_R(r)\psi_R^\dagger(0)\rangle \\ &= -\frac{e^{ik_F x}}{2\pi\alpha} e^{-[\frac{K_\rho+K_\rho^{-1}}{4}F_1(x,u_\rho\tau)+\frac{1}{2}F_2(x,u_\rho\tau)]} \\ &\quad e^{-[\frac{K_\sigma+K_\sigma^{-1}}{4}F_1(x,u_\sigma\tau)+\frac{1}{2}F_2(x,u_\sigma\tau)]} \end{aligned} \tag{7.21}$$

where the effective spin LL parameter is $K_\sigma = 1$ because of spin rotation symmetry. The expression of the *retarded* Green's function in real time can be obtained by the Wick rotation $\tau = it + \delta\ \mathrm{Sign}(t)$ where $\delta = 0^+$ (see Appendix C). For example the charge factor becomes (for $t > 0$)

$$\begin{aligned} e^{-[\frac{K_\rho+K_\rho^{-1}}{4}F_1(x,u_\rho\tau)+\frac{1}{2}F_2(x,u_\rho\tau)]} &\to \left(\frac{\alpha^2}{x^2+(it+\alpha)^2}\right)^{\frac{K_\rho+K_\rho^{-1}}{8}-\frac{1}{4}} e^{-\frac{1}{2}\log[(y_\alpha - ix)/\alpha]} \\ &= \left(\frac{\alpha^2}{x^2+(it+\alpha)^2}\right)^{\frac{K_\rho+K_\rho^{-1}}{8}-\frac{1}{4}} \frac{\sqrt{\alpha}}{\sqrt{i(u_\rho t - x)+\alpha}} \end{aligned} \tag{7.22}$$

Using the relation between the time-ordered Green's function and the retarded one (see Appendix C) one gets

$$\begin{aligned} G_{r,s}^{\mathrm{ret}}(x,t) &= -iY(t)\langle[\psi_{rs}(x,t),\psi_{rs}^\dagger(0,0)]_+\rangle \\ &= -i\frac{Y(t)}{2\pi}e^{irk_F x}\lim_{\epsilon\to 0}\left\{\frac{\alpha+i(v_F t - rx)}{\epsilon+i(v_F t - rx)}\right. \\ &\quad \times \prod_{\nu=\rho,\sigma}\frac{1}{\sqrt{\alpha+i(u_\nu t - rx)}}\left(\frac{\alpha^2}{(\alpha+iu_\nu t)^2+x^2}\right)^{\gamma_\nu} + \left.\begin{pmatrix} x\to -x \\ t\to -t\end{pmatrix}\right\} \end{aligned} \tag{7.23}$$

The first term originates from the momentum dependence of the velocities u_ν and describes the crossover from free fermion behavior at very short length (time)

scales to Luttinger liquid behavior in the asymptotic long distance (time) regime (Meden and Schönhammer, 1992; Voit, 1993). The exponent is

$$\gamma_\nu = (K_\nu + K_\nu^{-1} - 2)/8 > 0 \tag{7.24}$$

For a spin rotation invariant system such as the Hubbard model $K_\sigma^* = 1$ and $\gamma_\sigma = 0$. The other method is to directly compute the retarded correlation function by doing the averages in real time, using the real time evolution of the boson operators along the lines explained in Chapter 3.

The imaginary part of the retarded correlation function is the spectral function. This spectral function can be measured in a photoemission experiment. One shines a photon which kicks an electron out of the system. One can measure the energy and momentum of the particle. The interpretation of such an experiment can be quite complicated, but in a first approximation one can consider that this experiment directly measures the spectral function. It creates one electron with a given ω and k and this electron is measured. We discussed the spectral function of a Fermi liquid in Section 1.1, which is essentially a lorentzian. The spectral function of a Luttinger liquid (e.g. for right movers) is given by

$$A_{R,s}(q,\omega) = -\frac{1}{\pi}\mathrm{Im}G^{\mathrm{ret}}_{R,s}(k_F + q, \omega) \tag{7.25}$$

The Fourier transform can be done with techniques similar to the ones used in Appendix C, and gives the structure

$$A_{R,s}(q,\omega) \sim (\omega - u_\sigma q)^{\zeta - 1/2}|\omega - u_\rho q|^{(\zeta-1)/2}(\omega + v_\rho q)^{\zeta/2} \ . \tag{7.26}$$

where $\zeta = \sum_\nu \gamma_\nu$. Complete expressions can be found in Meden and Schönhammer (1992) and Voit (1993). The spectral function is shown in Fig. 7.1. There are two important things to note in this figure. First, there is not a single peak but two, at frequencies $\omega = u_\rho k$ and $\omega = u_\sigma k$. There are only peaks for the holon and the spinon. This clearly shows that no individual excitation exists in the LL but that the individual fermion decomposes in these elementary objects as discussed in Chapter 3. More importantly, since by accident the two velocities u_ρ and u_σ could be equal, the shape of the peak is *not* Lorentzian. It corresponds to the usual[30] power law divergence with an exponent controlled by the LL parameter K_ρ. As we already discussed in Chapter 2 the integrated (over k) intensity can also be computed. This can be directly measured, and for a Fermi liquid coincides with the density of states at the Fermi level. For a Luttinger liquid one finds (making the Fourier transform of the single-particle Green's function for $x = 0$ (see (2.92))

$$n(\epsilon) \propto |\epsilon|^{\frac{1}{4}[K_\rho + K_\rho^{-1}] - \frac{1}{2}} \tag{7.27}$$

The integrated intensity goes to zero at the Fermi level, which signals that no single-particle excitations do survive in the LL. I will come back to the experimental consequences when discussing the organic compounds in Section 8.4.

[30] By now it should be usual for you, it is always a power law.

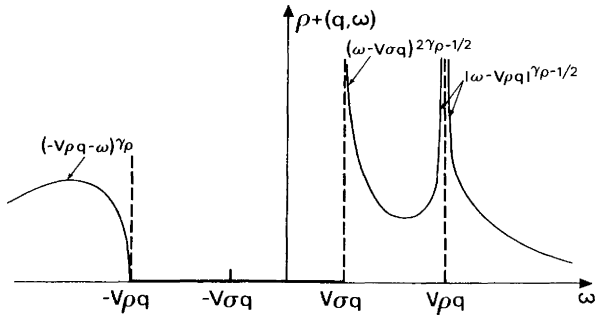

FIG. 7.1. Spectral function $\rho_+(q,\omega)$ of right movers in a LL. In this figure, V_ρ (resp. V_σ) denotes the charge (resp. spin) velocity (denoted u_ρ and u_σ in this book). Instead of a Lorentzian peak, one has power law divergences with an exponent that depends on the Luttinger liquid parameter. There are two peaks one corresponding to the holons ($\omega \sim u_\rho q$) and one to the spinons ($\omega \sim u_\sigma q$). Each peak has a power law structure. This clearly shows that no single-particle like excitations exist in a LL. (From Voit, 1993 (Copyright (1993) by the American Physical Society).)

Before we move to the attractive side, let us extract some additional information from the very form of the correlation functions. First, because the concept of Luttinger liquid should hold even when U is large we can extract the limit of K_ρ when $U \to \infty$ using a similar trick than for the spin chains. If U is very large, two fermions with opposite spins cannot sit on the same site. The system is thus equivalent as far as its charge properties are concerned to a free spinless fermion system. Since each state can be occupied only once the 'new' k'_F of this system is $2k_F$ of the original fermionic system. Thus, in the correlations (7.15), one should have $A_{2k_F}(U=\infty) = 0$ whereas to reproduce the $1/r^2$ decay of the $2k'_F$ component of free spinless fermions imposes $K_\rho(U=\infty) = 1/2$. This simple argument predicts that $K_\rho \to 1/2$ when $U \to \infty$. We thus see that very large interactions are not enough to reach arbitrarily low Luttinger parameters. The range is important as well as we already discussed in Section 4.2 for the Mott transition. For the velocities one can also obtain some simple limits in addition to the perturbative expressions (7.9). At very large U, since the charge properties are the ones of spinless fermions with a momentum $2k_F$ one expects the charge velocity to go to

$$u_\rho(U=\infty) = 2t\ \sin(2k_F) \tag{7.28}$$

On the other hand for very large U the spin exchange constant $J = 4t^2/U$ tends to zero. This means that the spin velocity approaches zero $u_\sigma(U=\infty) \to 0$.

The attractive side $U < 0$ can be treated in a similar way. The field ϕ_σ develops a gap. Given the spin SU(2) symmetry the system is on the separatrix and the gap is given by (see Section 2.3.2)

$$\Delta_\sigma \propto e^{-v_F/U} \tag{7.29}$$

for small U. Higher-order terms in the RG give a $U^{1/2}$ prefactor in agreement with the Bethe-ansatz value for the gap (Larkin and Sak, 1977). As we saw in Section 2.3.2 all the spin correlations decay exponentially. Physically, this corresponds to the fact that the fermions tend to pair in singlets. The only remaining correlations are the charge and the singlet superconducting fluctuations. These are given by (2.171). Since $U < 0$, the Luttinger parameter $K_\rho > 1$ and the superconducting correlations have the slowest decay, as is physically intuitive. For very large $|U|$, the physics is again quite transparent. Fermions form a bound state in site with an energy $|U|$. The pair can be viewed as a hard core boson. In order for the pair to jump to a neighboring site, it should break and thus the effective hopping is

$$t_{\text{eff}} \propto \frac{t^2}{U} \tag{7.30}$$

If two such pairs are on neighboring sites they interact. The large U Hubbard model is thus equivalent to a model of hard core bosons with a residual nearest neighbor interaction. We will examine this system in great detail in Section 11.1. Since the spin sector has a gap it means that when one computes the single-particle Green's function it is also gapped since it is the product of the spin part by the charge part even if the charge sector remains massless. In the presence of a gap either in the charge or the spin sector, spectral functions can also be estimated (Voit, 1998; Essler and Tsvelik, 2002).

Finally, let us discuss the commensurate case $n = 1/2$ of one particle per site. Because of the umklapp term, the system is a Mott insulator for $K_\rho < 1$, that is, for all repulsive interactions. It is metallic even at half-filling for $K_\rho > 1$, that is, on the attractive side. Because $K_\rho > 1/2$ regardless of the strength of the interaction, one particle per site is the only commensurate filling for which a Mott transition can take place (1/4 filling requires $K_\rho < 1/4$ to get the Mott state). All other fillings than one particle per site are thus metallic in agreement with our intuition (see Section 4.2). I will not dwell too much here on the nature of the two Mott transitions, both as a function of the strength of the interaction and as a function of the doping since they fall in the general framework studied in Section 4.2. Very close to half-filling, the LL parameter K_ρ takes the universal value $K_\rho = 1/2$. Because of the charge spin symmetry, the properties of the Mott phase for $U > 0$ can be deduced from the properties of the spin gapped phase for $U < 0$. In particular the Mott gap is exponentially small in U for small U as in (7.29). At exactly half-filling, the charge sector is massive, and $\langle\phi_\rho\rangle \to 0$. The spin sector remains massless. Thus, from (7.12) we see that the density correlation decays exponentially and that the average of the variation of the density is zero. This means that the density orders to give exactly one particle per site. The three components of the SDW are simply given by the spin part since $\langle\cos(\sqrt{2}\phi_\rho)\rangle$ is non-zero. One sees that by making the change $\phi_\sigma \to \sqrt{2}\phi_\sigma$ one recovers exactly the same correlations and Hamiltonian

than the bosonized version of the Heisenberg chain with $K \to K_\sigma/2 = 1/2$ which was indeed the value of the LL parameter at the spin isotropic point. One thus recovers directly on the bosonized Hamiltonian that the Hubbard model is identical to an Heisenberg chain where only the spin degrees of freedom are active at low-energy. This equivalence is exact even for very small U. Here the gap to make charge excitations is Δ_ρ the charge gap, which becomes U in the large U limit.[31] The spin exchange energy is given by the spin velocity u_σ which for small U is essentially the Fermi velocity. Note also that by using the symmetries of the Hubbard model one can extract the bounds for K_ρ on the attractive side. A naive derivation is to say that the LL quadratic Hamiltonian is symmetric by changing $K \to 1/K$ and $\phi \to \theta$, thus if K_ρ is limited by $1/2 < K_\rho$ on the repulsive side it should be limited by $K_\rho < 2$ on the attractive one. One can be more rigorous though. The attractive Hubbard model with a chemical potential can be mapped onto the repulsive one at half-filling ($h = 0 \to \mu = 0$) but in the presence of a magnetic field (corresponding to the original chemical potential). If $U \to -\infty$, the repulsive equivalent is exactly the Heisenberg chain. We thus have to determine the LL parameter of the Heisenberg chain as a function of the field, which we know goes from $\tilde{K} = 1/2$ for no field to $\tilde{K} \to 1$ close to the filled band. Thus, when translated in terms of the LL parameters of our original model this implies $K_\rho = 1$ at half-filling and $K_\rho < 2$ regardless of the chemical potential.

To get all the values of the parameters u_ρ, u_σ, K_ρ, one uses the tricks explained in Chapters 5 and 6. We use the Bethe-ansatz equations to determine the thermodynamic quantities. Doing the Bethe-ansatz for the Hubbard model would take us far above the level of this book. Although the procedure is totally similar in spirit to the one exposed in Chapter 5, the presence of the spin sector makes the algebra much more dense and tedious. As a result, other Bethe-ansatz methods have been developed to tackle these more complicated models in a relatively simpler way than the old Bethe approach.[32] I refer the reader who wants to know more on the procedure to the general references on Bethe-ansatz given in Chapter 5. I will just quote the results here.

For the repulsive side of the Hubbard model, the original study made by Schulz (1990) extracted the velocities directly from the Bethe-ansatz, and obtained K_ρ from the compressibility. Other choices are possible since the charge stiffness can also be extracted from the Bethe-ansatz (Shastry and Sutherland, 1990). The values of the Luttinger liquid parameters are shown in Fig. 7.2. The various limits are in agreement with the analysis performed directly on the LL Hamiltonian in the previous sections. K_ρ goes from 1 for $U = 0$ to $K_\rho = 1/2$ for $U \to \infty$. As a result the Hubbard model can only have a Mott phase at half-filling. At half-filling, the system is an insulator for any repulsive interac-

[31] U large compared to the kinetic energy t, a good measure of which is given by the bandwidth W.

[32] All is relative!

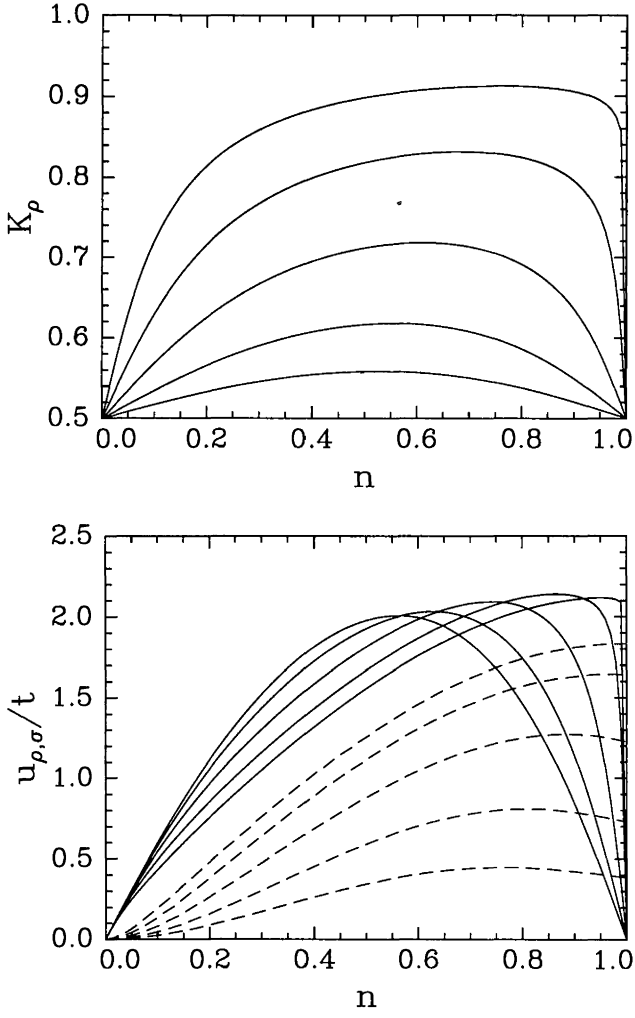

FIG. 7.2. Luttinger liquid parameters u_ρ (full lines), u_σ (dashed line) and K_ρ as a function of U and the density n. Curves are for $U = 1, 2, 4, 8, 16$. For K_ρ and u_σ this is from top to bottom and for u_ρ from bottom to top in the left part of the figure. (From Schulz, 1995 (Copyright (1995), with permission by Elsevier).)

tions. At very small doping $K_\rho \to 1/2$ in agreement with the universal value for the Mott-δ transition. The charge velocity goes linearly to zero as discussed in Section 4.2. The spin velocity goes to a constant which is simply given (for large U) by the superexchange $J = 4t^2/U$. For a very small number of particles (that is, either a nearly empty or full band) $K_\rho \to 1/2$. This result is also easy

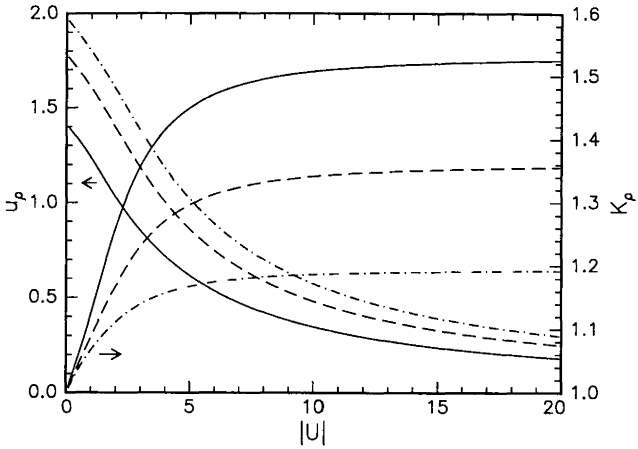

FIG. 7.3. Luttinger parameters u_ρ and K_ρ for the attractive Hubbard model as a function of the interaction $|U|$. These values are obtained by a numerical integration of the Bethe-ansatz equations on a system of $L = 200$ sites. Curves are for densities $n = 0.9$ (dash-dotted), $n = 0.7$ (dashed), $n = 0.5$ (full). (From Giamarchi and Shastry, 1995 (Copyright (1995) by the American Physical Society).)

to understand. The velocity is going to zero since one is at the bottom (or top) of the band. The effective local interaction $U/(\pi v_F)$ is thus going to infinity regardless of the strength of the initial interaction. Note that close the bottom or top of the band the LL behavior becomes valid only at large enough distances. Roughly speaking one needs to probe excitations that do not feel the bottom of the band. For the negative side the Luttinger parameter can again be determined exactly from the Bethe-ansatz equations (Kawakami and Yang, 1991; Giamarchi and Shastry, 1995). The result is shown in Fig. 7.3. The LL parameters in the limit of very large negative U can be easily determined by noting that, thanks to the mapping (7.5) the system becomes equivalent to an isotropic Heisenberg chain with a magnetic field (Hubbard model with a very large positive U and a magnetic field) whose exponents were determined in the previous chapter. The corresponding phase diagram is shown in Fig 7.4.

Let us finish by pointing out that directly from the Hamiltonian we can have an idea of the quantum numbers of the excitations, as we did for the spin chain. There are of course independent charge and spins excitations since the Hamiltonian decomposes into a charge and a spin part. The charge excitations are the solitons of $\cos(\sqrt{8}\phi_\rho)$, which correspond to $\delta\phi_\rho = \pi/\sqrt{2}$. They carry a charge

$$\delta Q = \frac{\sqrt{2}}{\pi}\nabla\phi_\rho = 1 \tag{7.31}$$

These are the holons depicted in Fig. 3.4, and correspond in the Hubbard picture

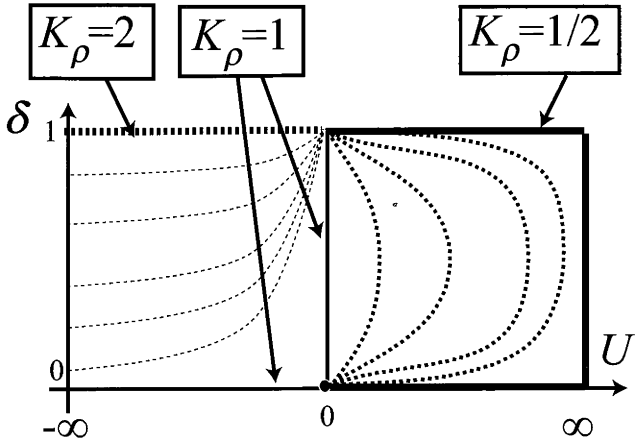

FIG. 7.4. Schematic plot of the Luttinger parameters for the Hubbard model as a function of the doping δ and interaction U. Only positive doping is shown the other part being identical by particle–hole symmetry. For positive U, the line $\delta = 0$ is a Mott insulator with a charge gap. Dotted lines are lines of constant K_ρ. $K_\sigma = 1$ for $U > 0$ by spin rotation symmetry and there is a spin gap for $U < 0$.

to the holes and doubly occupied sites. In the spin sector the excitations are the solitons of $\cos(\sqrt{8}\phi_\sigma)$ which gives for their spin

$$\delta S = \frac{1}{2}(n_\uparrow - n_\downarrow) = \frac{1}{\sqrt{2}\pi}\nabla\phi_\sigma = \frac{1}{2} \tag{7.32}$$

The spin excitations are spin 1/2 objects, and correspond to the spinons of Fig. 3.4, that is, to two neighboring spin up or down.

The Hubbard model is thus a remarkable model. It is simple enough to be integrable but has most of the generic features of a one-dimensional system. It however suffers from several peculiarities associated with the purely local nature of the interaction. Let us now investigate briefly some generalizations of the Hubbard model. These are popular microscopic Hamiltonians studied in the context of one-dimensional systems. Of course, the list is not exhaustive and increasingly complex models can be studied. I will consider the two most popular ones, here.

7.1.2 *t–J model*

The Hubbard model can be solved analytically in one dimension. In higher dimensions, however, it is a formidable model, which resists so far analytical treatments. Thus, the desire to tackle it numerically. From a numerical point of view the Hubbard model has several disadvantages. Although it can be nicely treated by Monte-Carlo methods (see Section 5.2), it is quite complicated for exact diagonalization. Indeed, the Hubbard model has four states per site, hence a Hilbert

space growing as 4^N where N is the number of particles. For very large U, doubly occupied states should not be too favorable and it is tempting to reduce the Hilbert space by throwing away these states. This is the procedure used at half-filling to reduce the Hubbard model to a pure spin system with superexchange. If one extends this procedure to the system with holes one obtains the so-called t–J model. This model has rapidly become a favorite microscopic model among numericians. Initially it was viewed as a large U limit of the Hubbard model, but acquired soon a life of its own.

The idea is simple. The t–J model is obtained by removing from the Hubbard model all states where there is double occupancy of a site (because of the particle symmetry we can confine ourselves to hole doping) (Hirsch, 1985). This is of course a good approximation when U is large since these states are energetically unfavorable. The simplest way to derive the t–J model is to make a canonical transformation

$$H_{t-J} = e^{iS} H_{\text{Hubbard}} e^{-iS} \tag{7.33}$$

to remove the doubly occupied states. Here, I will just give the physical results. If there was exactly one particle per site the charge would be frozen and as discussed in the previous section we would end up with a Heisenberg Hamiltonian

$$H = J \sum_i S_{i+1} \cdot S_i \tag{7.34}$$

If now some particles are removed, these holes can jump with the matrix element t on the neighboring sites. The full Hamiltonian is thus

$$H_{t-J} = P[-t \sum_{i,\sigma} c^\dagger_{i+1,\sigma} c_{i,\sigma} + J \sum_i (S_{i+1} \cdot S_i - \frac{n_{i+1} n_i}{4})]P \tag{7.35}$$

where the spin on site i is

$$S^\alpha_i = \frac{1}{2} \sum_{\sigma,\sigma'} c^\dagger_{i,\sigma} \sigma^\alpha_{\sigma,\sigma'} c_{i,\sigma'} \tag{7.36}$$

P is the projector on states with at most one electron per site. At half-filling, the t–J model reduces exactly to the Heisenberg model. If the t–J model is derived as the large U limit of the Hubbard model $J = 4t^2/U$ is the standard superexchange. However, within the t–J model one can consider t and J to be independent parameters. For large J, the t–J model cannot be linked any more to an 'honest' fermion Hamiltonian with a density–density interaction.

Because of the presence of the projector, any analytic treatment of the t–J model is extremely complicated. The constraint of at most one fermion per site is difficult to take into account. The number of approximations used to try to tackle this constraint are countless and I refer the reader to Douçot and Zinn-Justin 1995 for some of them.[33] Quite remarkably, there is still a Bethe-ansatz

[33] Most of them fail anyway!

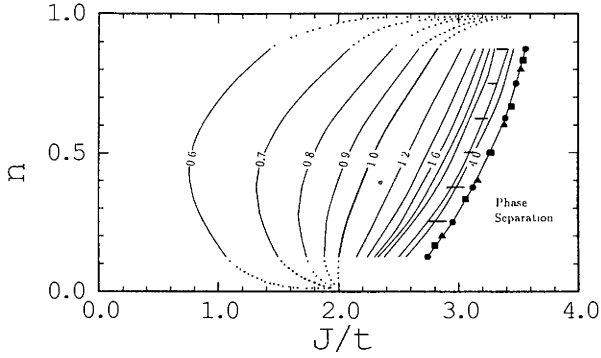

FIG. 7.5. Phase diagram of the t–J model as a function of J and the filling ($n = 1$ is half-filling). The LL parameter K_ρ whose values are given have been determined from an exact diagonalization. (From Ogata *et al.*, 1991 (Copyright (1991) by the American Physical Society).)

solution for this model but on the special line of parameters $J = 2t$ (Sutherland, 1975; Schlottmann, 1987; Bares *et al.*, 1991). The use of Bethe-ansatz for this model is thus somewhat restricted. On the contrary, because this model has at most three states per site, it is a dream for someone doing exact diagonalization, for example. The Luttinger liquid thus provides an extremely powerful way to tackle the t–J model in one dimension. Indeed, the Luttinger parameters can be determined with excellent accuracy from the numerics. Then they can be used to obtain *analytically* the correlation functions and thus the physical properties of the system. This is of course a much more powerful way than to try to extract directly the correlation functions from the numerics. Given the size limitations of exact diagonalization (about 25 sites), this would be a hopeless procedure. The result of the numerical determination of the LL parameters is shown in Fig 7.5. We see that when the parameter J is small the t–J model has essentially the same physics than the Hubbard model, as expected. The system is a Mott insulator for half-filling. Close to half-filling, the LL parameter K_ρ approaches the universal value $K_\rho \to 1/2$ as it should since this value is totally independent of the microscopic model and only depends on the filling at which the Mott transition occurs. I will not dwell much more on the correlation functions of the t–J model since they are the same as the ones we analyzed before.

On the contrary, when J becomes large many new features appear. There is a line of LL parameter $K_\rho = 1$ which occurs at finite J. Quite remarkably, the value corresponds to the value for which the model is exactly soluble by Bethe-ansatz. Since $K_\rho = 1$ corresponds in some sense to free fermions, this is not too surprising. When J is increased beyond this value, K_ρ becomes greater than one, which signals an attraction in the charge sector and superconducting instabilities. The t–J model has thus a whole attractive regime. When J becomes too large the attraction is so strong that it induces an instability. This can be seen on the

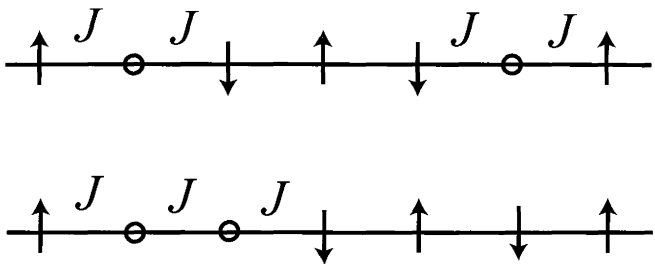

FIG. 7.6. Phase separation for the t–J model. At large J, putting two holes on separate sites costs $4J$ instead of $3J$ if the holes are on neighboring sites. For large enough J, all hole thus condense in a region of space.

LL parameters that become singular. This behavior is similar in some sense to what happened for the attractive spinless fermion model when $V = -2t$, and which signalled in the spin language the instability towards the ferromagnetic state. Here this instability can be interpreted as a phase separation where all holes condense in a finite region of space leaving the rest of the spins untouched. One can indeed check on Fig. 7.6 that this solution is energetically favorable for large J. Indeed, putting holes far apart costs $2J$ per hole whereas a string of holes costs only $(n+1)J$ for the whole string, plus the loss of kinetic energy (of order t per hole). Note that the Hubbard model has no such instability, so in some sense putting a large J is like having an effective attraction in the system.

7.1.3 *U–V model and beyond*

The purely local character of the Hubbard model is responsible for some of the peculiarities of the model. The most important peculiarities are: (i) the impossibility to explore the full phase diagram (2.9); (ii) the impossibility to have Mott transitions at other commensurate fillings than 1/2 filling; (iii) the limitations on K_ρ

A way to cure this is of course to put back longer-range terms in the interaction. The simplest term that one can add that respects spin rotation invariance is a nearest neighbor interaction

$$H_V = V \sum_i n_{i+1} n_i \tag{7.37}$$

This model is known as the U–V model. It can easily be generalized to a longer range interaction

$$\begin{aligned} H_V &= \sum_{i,r} V_r n_{i+r} n_i \\ &= V \sum_{i,r} V_r [n_{i+r,\uparrow} n_{i,\uparrow} + n_{i+r,\downarrow} n_{i,\downarrow}] + [n_{i+r,\uparrow} n_{i,\downarrow} + n_{i+r,\downarrow} n_{i,\uparrow}] \end{aligned} \tag{7.38}$$

For a small V_r the effects of such potential can be computed using the perturbative bosonization expressions. The first two terms should be treated with care. Using (2.35) in (7.38) one gets

$$V_{i-j}\{\frac{1}{\pi^2}(\nabla\phi_i)(\nabla\phi_j)+\frac{1}{(2\pi\alpha)^2}2\cos(2k_F(x_i-x_j)-(2\phi_i-2\phi_j))\} \quad (7.39)$$

where ϕ denotes either $\phi_\uparrow$ or $\phi_\downarrow$ for the corresponding term $n_{i,\sigma}n_{j,\sigma}$. Terms that depend on $i+j$ have been discarded since they oscillate and are eliminated by $\int dr_i \int dr_j$. By considering that the fields ϕ are slowly varying at the scale of the lattice, one can expand (7.39) (Capponi *et al.*, 2002). To expand *safely* the fields should be normal ordered. Since in a normal product all destruction operators are on the right, one has obviously from a simple series expansion in ϕ

$$\langle : \cos(\phi) : \rangle = 1 \quad (7.40)$$

Thus,

$$\cos(\phi) = \langle\cos(\phi)\rangle : \cos(\phi) : \quad (7.41)$$

This formula can be proven by a direct expansion in powers of ϕ and using the fact that ϕ is a linear combination of creation and destruction operators. One thus has

$$e^{i2(\phi(r_1)-\phi(r_2))} =: e^{i2(\phi(r_1)-\phi(r_2))} : e^{-\frac{1}{2}\langle[2(\phi(r_1)-\phi(r_2))]^2\rangle} \quad (7.42)$$

At the lowest order in V, (7.42) becomes

$$e^{i2(\phi(r_1)-\phi(r_2))} =: e^{i2(\phi(r_1)-\phi(r_2)} : \frac{\alpha^2}{(r_1-r_2)^2} \quad (7.43)$$

In the normal product one can expand $\phi(r_1)-\phi(r_2) \simeq (r_1-r_2)\nabla\phi(R)$, where $R=(r_1+r_2)/2$. The term thus becomes

$$\frac{1}{\pi^2}\int dx(\nabla\phi(x))^2\sum_r V_r[1+2\ \cos(2k_F r)] \quad (7.44)$$

Replacing $\phi_{\uparrow,\downarrow}$ as a function of $\phi_{\rho,\sigma}$ gives for the charge part a quadratic LL Hamiltonian with

$$\begin{aligned} u_\rho K_\rho &= v_F \\ u_\rho/K_\rho &= v_F\left(1+\frac{U+\sum_r 2V_r[1-2\ \cos(2k_F r)]}{\pi v_F}\right) \end{aligned} \quad (7.45)$$

where $r=1,2,3,...$ is the distance on the lattice. To compute the coefficients of the spin part it is simpler to get the coefficient of the $\cos(\sqrt{8}\phi_\sigma)$ directly and then use the spin rotation symmetry since computing the quadratic part is a mess (but can be done). To get such a term we can consider that the field ϕ_σ in the two densities in the second term in brackets in (7.38) are at the same

points since the expansion in gradients leads to less relevant operators. Beware one cannot of course do the same approximation for the term $e^{i2k_F r}$ since this term rapidly oscillates at the lengthscale of the lattice. One has thus a term

$$\sum_r 2V(r)\cos(2k_F r)\cos(\sqrt{8}\phi_\sigma(x)) \tag{7.46}$$

Thus, the backscattering term is given by

$$g_{1\perp} = U + 2V(r)\cos(2k_F r) \tag{7.47}$$

One can of course at half-filling, compute the umklapp term in the same way.

The above expressions are valid at the lowest order in V. For finite V the various coefficients in them will get renormalized by irrelevant operators. For a long-range potential the sum in (7.45) is dominated by the large r part and one recovers the expression for the long-range interactions given in Section 4.1. Due to the $2k_F$ oscillations in density the $2k_F$ component of the potential also occurs. This is similar to Friedel oscillations. Let us consider the case of nearest neighbor interaction only (the U–V model). In that case, the effective interaction in the charge and spin sectors are, respectively,

$$\begin{aligned} U_\rho &= U + 2V[1 - 2\cos(2k_F a)] \\ U_\sigma &= U + 2V\cos(2k_F a) \end{aligned} \tag{7.48}$$

Contrary to the case of the Hubbard model, depending on the values of U and V one can now tune attraction and repulsion in the charge and spin sectors separately. Close to half-filling, for example, $U_\rho \sim U + 6V$ while $U_\sigma = U - 2V$. Thus, both for repulsive U and V but $V > U/2$ the system becomes attractive in the spin sector *while* staying repulsive in the charge sector. The physics is easy to understand: if V is large enough, electrons will prefer to pair on the same site rather than pay the price of V. However, these pairs repel, and thus 'crystallize' to form a charge density wave. A cartoon of this scenario is shown in Fig. 7.7.

For commensurate fillings the model is of course a Mott insulator. This occurs at half-filling as for the Hubbard model. In the extended Hubbard model an intermediate BOW phase can appear between the SDW and the CDW phases (Nakamura, 1999; Tsuchiizu and Furusaki, 2002). In addition, since the interaction is now able to reach the nearest neighbor (and further) one can expect to be able to order a structure where electrons are spaced by one (or more) site. This is illustrated in Fig. 7.8. It is indeed easy to see that for $U = \infty$ and $V = \infty$ a quarter-filled system is an ordered Mott insulator. This proves that for the U–V model the Luttinger parameter K_ρ is able to go below $K_\rho = 1/4$, which is the critical value to get the quarter-filled Mott insulator, as explained in Section 4.2. The limit $U = \infty$ is also easy to analyze for the charge degrees of freedom in the quarter-filled system. In that case the charge behaves like spinless fermions since one cannot put two particles on the same site because of U. The system thus becomes equivalent to spinless fermions with one particle every two sites

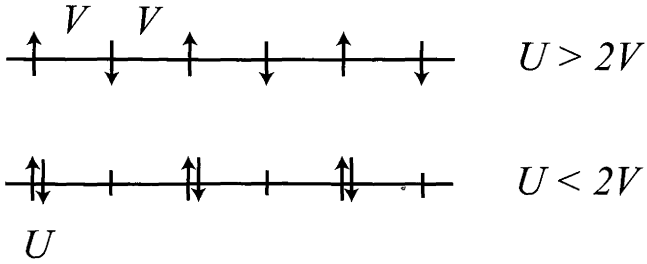

FIG. 7.7. In the presence of $V > U/2$ one can go from a SDW ground state to a CDW one to avoid to pay the repulsion V. A cartoon of this effect is shown in the case of one particle per site.

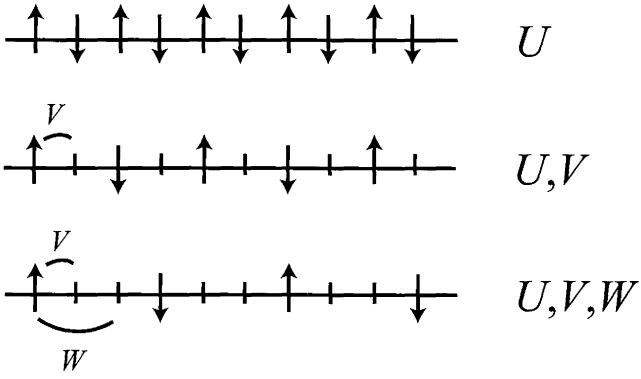

FIG. 7.8. In the U–V model one can have a Mott phase for 1/4 filling contrary to the case of the Hubbard model. For longer range interactions, one can stabilize a Mott insulating phase at even lower commensurability. For example, a 1/6 filling needs at least a U–V–W model.

plus a nearest neighbor interaction V. This is exactly the case we studied in the previous chapter and we know there from the Bethe-ansatz solution or the mapping to the spin chain, that there is a Mott transition for $V > 2t$. Clearly with interactions of increasing range one can stabilize insulating phases of lower and lower commensurabilities. For the Hubbard model only half-filling can become insulator (see Fig. 7.8). For the U–V model the 1/4 filling (one particle every two sites) can also have a Mott transition, but larger distance between the particles always remains metallic regardless of the strength of U and V. The longer the range (provided the interactions are strong enough) the lower the bound on K_ρ. For the case of truly long-range ($1/r$) interactions the properties can indeed be viewed as 'if' $K_\rho = 0$ as explained in Section 4.1.

The above analytic arguments can be completed by a microscopic calculation of the Luttinger liquid parameters. Since the U–V (and more) model is not inte-

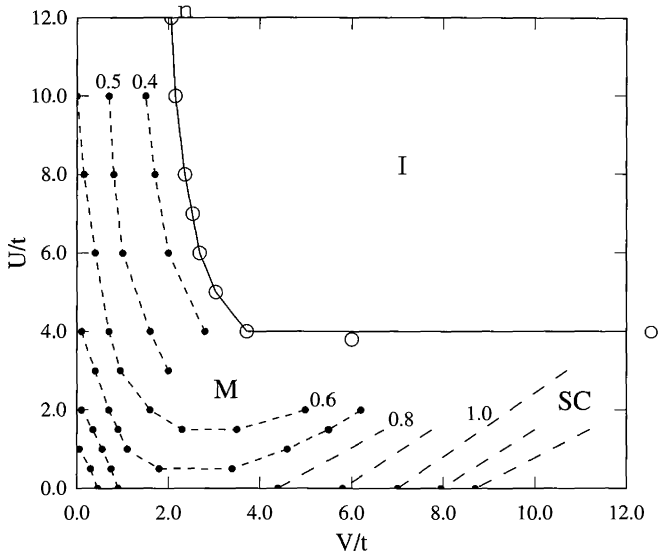

FIG. 7.9. The phase diagram and the LL parameter K_ρ for the U–V model at quarter filling as determined by an exact diagonalization. M and SC are massless LL phases. In SC the system has dominant superconducting fluctuations since $K_\rho > 1$. The phase I is the quarter-filled Mott insulator. (From Mila and Zotos, 1993 (Copyright (1993) by EDP Sciences).)

grable one should use numerics. A precise determination can be done for example using exact diagonalization and the standard tricks explained in Chapter 3. The results are shown in Fig. 7.9

7.2 Transport

So far we have focused mostly on equilibrium properties and phase diagrams. However, one of the most easy measurements on realistic one-dimensional systems are the transport ones. The one-dimensional world has very specific properties in this respect. This is the question we address in this section.

7.2.1 *Conductance, conductivity*

In this section, we examine the basic formulas to compute the transport properties. Most of the material is standard (Mahan, 1981) and based on the Kubo formula. However, there are some specificities in the implementation using bosonization that we now examine.

Let me first compute the linear response to an external electric field. The ratio between the current density and the local electric field defines the conductivity of the system

$$j(q,\omega) = \sigma(q,\omega) E_{\rm loc}(q,\omega) \tag{7.49}$$

For infinite systems the conductivity is the proper quantity to use. For a finite system it is sometimes more convenient to define the conductance (or resistance) of the system. Loosely speaking, the conductance is the ratio between the voltage difference at the edge of the system and the current through the system

$$I = GV \tag{7.50}$$

More generally, the standard law of associations of resistance tells that for a block in dimension d of size L, the current scales as $I = jL^{d-1}$ and the voltage is $V = EL$. The relation between conductivity and conductance is thus

$$\sigma L^{d-2} = G \tag{7.51}$$

Let us now recover the conductivity and conductance from the linear response. We can use the conservation law for the charge

$$\frac{\partial \rho_e(x,t)}{\partial t} + \vec{\nabla} \cdot \vec{j_e} = 0 \tag{7.52}$$

where $\rho_e = e\rho$ is the charge density. Since we are interested in the long wavelength properties $q \sim 0$, we can use the expression (2.55) for the density. In one dimension, (7.52) is a simple scalar equation and one obtains

$$j_e(x,t) = ej(x,t) = \frac{e}{\pi}\partial_t \phi(r,t) \tag{7.53}$$

for spinless fermions. Since transport only involves the charge sector it is very easy to go from spinless fermions to fermions with spins. One has to replace the density of spinless fermions by the total density $\rho_\uparrow + \rho_\downarrow$ and thus $\phi \to \sqrt{2}\phi_\rho$. In this subsection I give the formulas for spinless fermions. Formulas for fermions with spins are given in Appendix D. Using the Heisenberg equation of motion

$$\partial_t O(t) = \frac{i}{\hbar}[H, O(t)] \tag{7.54}$$

one obtains for the current operator.

$$j_e(x,t) = \frac{e}{\hbar}(uK)\Pi(x,t) \tag{7.55}$$

Superficially, the current operator seems to depend on u and K and thus on the interactions in the system. For a well-defined Hamiltonian on a lattice, it is impossible. Indeed, the interaction part *only* depends on the density, so $[H, \rho]$ is *only* dependent on the kinetic energy $[H, \rho] = [H_{\text{kin}}, \rho]$. The current operator is thus totally determined by the kinetic energy. This imposes that for a lattice Hamiltonian one has

$$uK = v_F \tag{7.56}$$

In other words, the interaction term cannot generate terms that directly change the coefficient of the $(\nabla\theta)^2$ operator. This is a theorem we had many occasions to

directly check by an explicit calculation in Chapter 6 and Section 7.1. Note that this is of course only true for the *bare* parameters. The interaction can perfectly generate terms (such as $\cos(\phi)$ terms) that have an impact on the *expectation value* of the current operator. Thus, the effective u and K to put in a low-energy theory can (and in general will) be different from $uK = v_F$.

We can now proceed with the usual Kubo formula (Mahan, 1981). Let us assume that the wire is submitted to a small electric field, uniform on the wire of length L: $E(t) = E_0 e^{-i(\omega+i\delta)t}$ (with $\delta = 0^+$) and that the field is zero outside the wire. This field corresponds to a vector potential such that $E = -\partial A/\partial t$. The current $\langle j(x,t)\rangle$ in the wire is given by (I put back the $\hbar$ for a while to show the proper conductance units)

$$\langle j_e(x,t)\rangle = \frac{E_0 e^{-i(\omega+i\delta)t}}{i(\omega+i\delta)}\left[-D - \int_{-L/2}^{L/2} dx'\, dt' \frac{e^{i(\omega+i\delta)(t-t')}\langle j_e(x,t); j_e(x',t')\rangle}{\hbar}\right] \tag{7.57}$$

where $\langle ; \rangle$ denotes the retarded correlation function (see Appendix A) and D designates here the diamagnetic term. To generate (7.55) by the standard minimal substitution in the Hamiltonian and

$$j_e(x,t) = -\frac{\partial H}{\partial A(x,t)} \tag{7.58}$$

where A is the potential vector, one has to make the substitution in (3.25)

$$\Pi(x,t) \to \Pi(x,t) - \frac{eA}{\pi} \tag{7.59}$$

Note the factor of π compared to the standard substitution $P \to P - qA$. It is simply due to the factor $1/\pi$ in the relation between the density and ϕ. The diamagnetic term is thus

$$D = -\frac{\partial^2 H}{\partial A \partial A} = \frac{e^2 uK}{\hbar\pi} \tag{7.60}$$

Before analyzing its properties further let us simplify the expression for the current–current correlation function. As usual, to compute the retarded correlation function one computes first the (imaginary) time-ordered function and then makes the analytical continuation (see Appendix A). The current–current correlation function in imaginary time is given by, using (7.55)

$$\begin{aligned}\chi(\tau-\tau') &= -\langle j_e(x,\tau) j_e(x',\tau')\rangle \\ &= -\left(\frac{euK}{\hbar}\right)^2 \langle \Pi(x,\tau)\Pi(x',\tau')\rangle\end{aligned} \tag{7.61}$$

Using the functional integral representation of Appendix C, the integral over Π can be performed to give

$$\langle \Pi(x,\tau)\Pi(x',\tau')\rangle = -\frac{\hbar^2}{(\pi u K)^2}\langle \partial_\tau \phi(x,\tau)\partial_{\tau'}\phi(x',\tau')\rangle + \frac{\hbar^2}{\pi u K}\delta(x-x')\delta(\tau-\tau') \tag{7.62}$$

If one goes to Fourier space, the above formula can be rewritten as

$$\langle \Pi(q,\omega_n)^*\Pi(q,\omega_n)\rangle = -\frac{\hbar^2}{(\pi u K)^2}\omega_n^2\langle \phi(q,\omega_n)^*\phi(q,\omega_n)\rangle + \frac{\hbar^2}{\pi u K} \tag{7.63}$$

This result is quite interesting. When put back in (7.57), the second term cancels exactly the diamagnetic term. This result can also be derived directly in operator language but requires to be careful with the time ordering (Shankar, 1990). The current–current correlation function in terms of the current operator $J \propto \partial_\tau \phi$ is

$$\chi(\tau-\tau') = -\langle T_\tau(\partial_\tau\phi)(\partial_\tau\phi)\rangle \tag{7.64}$$

To pull out an ω_n^2 term as in (7.63) the naive idea is to integrate twice by parts in the Fourier transform of χ. This gives the first term in (7.63). But the time ordering operator gives in fact also a step function

$$T_\tau j(\tau)j(\tau') = Y(\tau-\tau')j(\tau)j(\tau') + Y(\tau'-\tau)j(\tau')j(\tau) \tag{7.65}$$

which has to be differentiated with respect to τ in the integration by parts and give back exactly the term D in (7.63). The functional integral that directly replaces the operators by fields and gets rid of the time ordering operator, thus allows to get this result very simply. Formula (7.63) is very nice since it simplifies enormously the expression for the conductance/conductivity for a one-dimensional system.

Let me start with the conductivity. In that case one can take the limit $L \to \infty$. The current is thus independent of the point x. From the relation $j_e = \sigma E$ and using (7.63) in (7.57)

$$\sigma(\omega) = -\frac{e^2}{\pi^2\hbar} i(\omega + i\delta)\langle \phi(q=0,\omega_n)^*\phi(q=0,\omega_n)\rangle_{i\omega_n\to\omega+i\delta} \tag{7.66}$$

The diamagnetic term disappears and the conductance/conductivity is *directly* given by the retarded $\phi\phi$ correlation function. Note that one could also compute the response to a q dependent electric field by computing this correlator at q.

One can deal with the conductance in the same manner. In that case one keeps L finite and is interested in the static limit $\omega \to 0$. Note that the two limits $L \to \infty$ and $\omega \to 0$ do not commute. I will come back to that point. If one considers the static limit, the current is conserved in the wire and thus does not depend on the point where we compute it. Thus, one can compute the conductance from (7.57) by computing the current at $x = 0$. This gives using again (7.63)

$$
\begin{aligned}
G(\omega) &= \frac{e^2}{\pi^2\hbar} i(\omega + i\delta) \left[-\frac{1}{L} \int_{-L/2}^{L/2} dx' \int dt' e^{i(\omega+i\delta)(t-t')} \langle \phi(x=0,t); \phi(x',t') \rangle \right] \\
&= -\frac{e^2}{\pi^2\hbar} i(\omega + i\delta) \left[\frac{1}{L} \int_{-L/2}^{L/2} dx' \; \langle \phi(x=0,\omega_n)\phi(x',-\omega_n) \rangle |_{i\omega_n \to \omega + i\delta} \right] \\
&= -\frac{e^2}{\pi^2\hbar} i(\omega + i\delta) \frac{1}{L} \sum_q K(q,L) \; \langle \phi(q,\omega_n)\phi(-q,-\omega_n) \rangle |_{i\omega_n \to \omega + i\delta} \qquad (7.67)
\end{aligned}
$$

where

$$
K(q,L) = \frac{\sin(qL/2)}{qL/2} \qquad (7.68)
$$

Note that in the conductance (7.67) compared to the conductivity (7.66), one has to perform a sum over q instead of simply computing the propagator at $q = 0$. Note also the wonder of the thing. In higher dimensions, the current–current correlation function is a complicated object containing four fermion operators (bubble). Here the conductivity is related to the basic boson propagator of our Luttinger liquid. This is an object for which one can expect to have powerful ways to make either an analytical or numerical calculation.

7.2.2 *Clean case; persistent currents*

Let us start with the simplest case, namely a totally clean system, without any source of scattering. We even ignore here the presence of the lattice and forget about umklapp processes. In that case the momentum is conserved in any interaction process so we of course expect the conductivity of the system to be infinite. Indeed, if we take a purely quadratic LL Hamiltonian. The commutator of the current with the Hamiltonian is

$$
[j_e, H] \propto \int dx [\Pi(x), H] = i \int dx \frac{u}{2\pi K} \nabla_x^2 \phi(x) \qquad (7.69)
$$

which is zero using, for example, periodic conditions since $\nabla\phi$ is the density. The current is thus conserved by the quadratic LL Hamiltonian. Let us look first at an infinite system and compute the conductivity from (7.66)

$$
\begin{aligned}
\sigma(\omega) &= -\frac{e^2}{\pi^2\hbar} i(\omega + i\delta) \langle \phi(q=0,\omega_n)^* \phi(q=0,\omega_n) \rangle_{i\omega_n \to \omega + i\delta} \\
&= -\frac{e^2}{\pi^2\hbar} i(\omega + i\delta) \left. \frac{\pi u K}{\omega_n^2} \right|_{i\omega_n \to \omega + i\delta} \qquad (7.70)
\end{aligned}
$$

using (C.18) for the boson propagator. The conductivity is thus

$$
\sigma(\omega) = \frac{e^2}{\pi\hbar} \frac{iuK}{\omega + i\delta} = \frac{e^2}{\hbar} (uK) [\delta(\omega) + i\mathrm{P}\frac{1}{\pi\omega}] \qquad (7.71)
$$

where P denotes the principal part. The conductivity is thus a simple delta function peak (Drude peak). Using the favorite $e = 1, \hbar = 1$ of the theorist, the

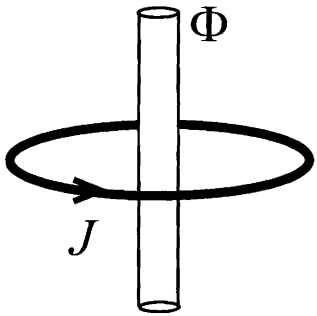

FIG. 7.10. A one-dimensional ring threaded by a flux. The flux induces a persistent current in the ring. The strength of the persistent current is proportional to the charge stiffness $\mathcal{D}$.

weight of the Drude peak is given by the product uK. The system is a perfect conductor with an infinite static conductivity. As imposed by the Kramers–Kronig relations the imaginary part of the conductivity is then simply $1/(\pi\omega)$ with the same weight.

The product uK thus measures the ability of the system to sustain a current without dissipation. It is Kohn's charge stiffness (Kohn, 1964). Another interpretation of uK can be found by looking at a ring threaded by a flux as shown in Fig. 7.10. Since there is no electric field or magnetic field exerted on the wire, the only effect of the flux is to give a static vector potential

$$A = \frac{f}{L} \tag{7.72}$$

where f is the flux threading the ring. Such a static vector potential can be absorbed by a gauge transformation on the fermions since $P \to P - eA$ in presence of a vector potential

$$\psi \to e^{i\frac{eAx}{\hbar}}\psi = e^{i2\pi\frac{fx}{f_0 L}}\psi \tag{7.73}$$

where $f_0 = h/e$ is the flux quantum. Since such a gauge transformation does not affect any local physical quantity such as the density, it leaves the interactions invariant. It can thus be absorbed at the expense of a twist in boundary conditions

$$\psi(L) = e^{i\Phi}\psi(0) \tag{7.74}$$

where Φ denotes the boundary angle $\Phi = 2\pi f/f_0$. For free electrons, such a gauge transformation is equivalent to changing $k \to k + \frac{\Phi}{L}$. As shown in Fig. 7.11, such a gauge term has two consequences: It increases the ground state energy of the system E_0 which is now a (periodic) function of the flux $E_0(\Phi)$ and induces

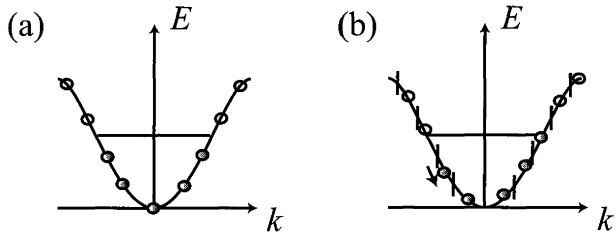

FIG. 7.11. A twist of boundary conditions changes the energy of the ground state (a) and induces a persistent current in the system since it shifts all values of the momentum as shown in (b). The shift is periodic in flux since for a flux equal to the flux quantum the shift replaces exactly one k by another.

a current in the system since this shifts all the values of k (Imry, 1997). This current is known as persistent current. Quite generally one has for the current density

$$J = \frac{1}{\hbar L}\sum_k \frac{d\epsilon_k}{dk} = \frac{1}{\hbar}\frac{d}{d\Phi}\sum_k \epsilon_k = \frac{1}{\hbar}\left.\frac{dE_0}{d\Phi}\right|_\Phi \tag{7.75}$$

At small flux the current is proportional to the flux, the proportionality constant is known as the charge stiffness

$$\mathcal{D} = \pi L \left.\frac{dJ}{df}\right|_{f=0} \tag{7.76}$$

Let us show using the boson representation that this charge stiffness is identical to the weight of the Drude peak. A vector potential couples to the current giving in the action an additional term

$$S_A = -\int dx\, d\tau\, A j_e(x,\tau) = -\frac{e}{\pi}\int dx\, d\tau\, A\partial_\tau\phi \tag{7.77}$$

This term can be absorbed in the quadratic part of the action in a way identical to the one used for the calculation of the compressibility in Section 2.1. This shows that the average current density is

$$J = \frac{1}{\pi}\langle\partial_\tau\phi\rangle = \frac{eKu}{\pi\hbar}A = \frac{uK}{\pi L}\Phi \tag{7.78}$$

and one recovers the expression for the charge stiffness extracted from the conductivity (7.71)

$$\mathcal{D} = uK \tag{7.79}$$

At $T = 0$, the charge stiffness can be generally related to the change of the ground state energy with respect to the flux (Kohn, 1964; Shastry and Sutherland, 1990; Scalapino *et al.*, 1992)

$$\mathcal{D} = \frac{\pi L}{\hbar} \frac{d^2 E_0}{d\Phi^2}\bigg|_{\Phi=0} \tag{7.80}$$

in agreement with our derivation in one dimension. A word of caution: one should not mix the charge stiffness with the superfluid stiffness (or Meissner fraction), which is

$$\rho_s = \frac{\pi L}{\hbar} \frac{d^2 F}{d\Phi^2}\bigg|_{\Phi=0} \tag{7.81}$$

where F is the *free* energy of the system. Although both of ρ_s and D are related to the current correlation function, they correspond to different limits. ρ_s, being a thermodynamic quantity corresponds to the limit $\omega \to 0$ first and then $q \to 0$, whereas $\mathcal{D}$ which is related to transport corresponds to the limits taken in the reverse order. For finite T, the two quantities are distinct (Giamarchi and Shastry, 1995). For a macroscopic system, ρ_s measures the superfluid density and will be zero for a non-superfluid system, whereas $\mathcal{D}$ can be non-zero if the system is perfectly conducting but not superconducting (e.g. free electrons in the absence of impurities). If one has a finite system, then ρ_s needs not be zero even if the system is not superconducting.

Since the charge stiffness is in fact a property of the ground state (that is, a *thermodynamic* quantity) even if it seems related to transport, it means that one can compute it from a low-energy effective Hamiltonian. If the system flows to a LL fixed point characterized by an effective u^* and K^* the stiffness is thus directly given by $\mathcal{D} = u^* K^*$. The charge stiffness can thus be used to extract the Luttinger liquid coefficients. This is a very convenient technique since twisting the boundary conditions is easy to implement both analytically and numerically. Note that if on a lattice the bare parameters satisfy $uK = v_F$ this is of course not the case of the effective low-energy ones $u^* K^*$ when one has reduced the full Hamiltonian to a purely quadratic form. Thus, depending on the interactions the charge stiffness can be much reduced as compared to the non-interacting case. In particular if the system is an insulator it is obvious that $\mathcal{D} = 0$, since there cannot be a Drude peak in the conductivity. I will come back to this point later.

Let us now turn to a finite size system of length L for which is it better to compute directly the conductance of the system. Note that the limits $\omega \to 0$ and $L \to \infty$ do not commute, since roughly speaking one can associate a lengthscale $L_\omega = u/\omega$ with the frequency. What we did before was to take first the limit of infinite size system $L \to \infty$ for a finite (eventually arbitrarily small) frequency. Thus, implicitly $L \gg L_\omega$ regardless of ω. For a finite system a static measurement of the conductance puts us in the opposite limit $L \ll L_\omega$, which is what led to (7.67). For the clean system one gets

$$G = \frac{e^2}{\hbar\pi} \lim_{\omega\to 0} \frac{i}{(\omega + i\delta)} \int_{-\pi/a}^{\pi/a} \frac{dq}{2\pi} K(q, L) \left[\frac{\omega_n^2 uK}{\omega_n^2 + u^2 q^2}\right]_{i\omega_n \to \omega + i\delta} \tag{7.82}$$

If one wants to take the static limit it means that we can consider ω, that is, ω_n, as tending to zero in (7.82). One can thus rescale q by using $\tilde{q} = q/\omega_n$. The conductance becomes in the limit where ω_n is very small

$$G = \frac{e^2}{\hbar\pi} \lim_{\omega\to 0} \int_{-\frac{\pi}{a\omega_n}}^{\frac{\pi}{a\omega_n}} \frac{d\tilde{q}}{2\pi} K(\tilde{q}\omega_n, L) \left[\frac{vK}{1+v^2\tilde{q}^2}\right] \tag{7.83}$$

If one takes the limit $\omega \to 0$ first, $K(\tilde{q}\omega_n, L) \to 1$. Note that in the opposite limit it becomes $\delta(q)$ instead which gives back the standard conductivity. Here the integral thus goes unrestricted from $[-\infty, \infty]$. For the clean finite size system it is as if we had taken the limit $L \to 0$. Performing the integral gives the conductance

$$G = \frac{e^2}{h} K \tag{7.84}$$

This is a quite remarkable result (Apel and Rice, 1982*a*; Kane and Fisher, 1992*a*). The conductance is finite. Note that this does not contradict the fact that the system is a perfect conductor since the conductivity of an infinite system is given by $\sigma = GL$ and thus will be perfectly infinite for a finite conductance. This is the generalization for interacting electrons of the famous Landauer result for the conductance (Landauer, 1970; Imry, 1997). Indeed, for non-interacting electrons the conductance of a wire can be related to the transmission coefficient $\mathcal{T}$ of the wire by

$$G = \frac{e^2}{h} \mathcal{T} \tag{7.85}$$

Thus, for a perfectly conducting system the transmission is one per channel of conduction and the conductance is quantized in units of e^2/h. This quantum of conductance corresponds to a resistance of ~ 25.83 kΩ. For non-interacting electrons $K = 1$ and one recovers exactly this result. For interacting electrons, the result (7.85) is curious since the conductance seems to depend on the interactions. For long-range Coulomb since, as we saw in Section 4.1, this corresponds formally to $K_\rho \to 0$ logarithmically one would even have a zero conductance for a pure system (Fabrizio *et al.*, 1994). Note that for the infinite system the charge stiffness was $\mathcal{D} = uK$, which was indeed independent of the interactions in the absence of any source of scattering since in that case $uK = v_F$. In fact the result (7.85) depends very much on the experimental situation. As we will see it is correct for some special cases as the case of the Hall effect (see Section 10.4). For the standard case of a wire in contact with two reservoirs, the result (7.85) is in fact incorrect. There are various elegant ways to show it (Safi and Schulz, 1995; Maslov and Stone, 1995). For a clean system the conductance depends at large times only of the properties of the leads. If the leads are Fermi liquid like, the interactions do not play a role and one recovers the quantization of the conductance in units of e^2/h. As we will see in Section 9.3, these properties can be checked in quantum wires.

7.2.3 *Mott insulator*

To obtain a finite conductivity one has thus to include a process that allows the momentum to relax. We will examine the case of disorder in Chapter 9 and focus here on the relaxation of the momentum due to scattering on the lattice. This can be due either to the presence of a periodic potential, or to the transfer of momentum to the lattice via umklapp processes. The two processes are of course very similar since, as we saw, umklapp processes can be interpreted as scattering on a $4k_F$ periodic potential.

Since the conductivity/conductance is simply given by the $\phi\phi$ correlation function, one could naively think that it is not much more complicated to compute than all the correlation functions that we have already obtained up to now. Some of them are indeed much more complicated but there is an important difference. To compute the correlations up to now, we have computed them using *only* the fixed point Hamiltonian, which was often the quadratic Luttinger liquid. We have thrown away all irrelevant operators. One can use such a procedure because the correlation with the fixed point action is meaningful. For the transport the situation is more complicated. As we saw, for a LL Hamiltonian the system is a perfect conductor, with only a $\delta(\omega)$ term in the conductivity. This is because a LL Hamiltonian commutes with the current. This is of course not the case in the real system with scattering. In order to get correctly the temperature or frequency dependence of the conductivity it is thus mandatory to retain at least the most important operator that violates current conservation, *even* if this operator is irrelevant. Doing so complicates of course the process. There is another complication. Usually, one cannot perform an exact calculation (which is the case here) and one only knows how to compute quantities in some perturbation expansion of the coupling. So we would like to be able to compute the conductivity in powers of the scattering operator. Unfortunately, this is not possible: in the absence of scattering the conductivity is infinite, whereas it is finite in the presence of scattering. The perturbation expansion in scattering is highly singular. This can be readily seen on the Drude formula $\sigma = ne^2\tau/m$ which shows that the conductivity is proportional to the scattering time, that is, *inversely* proportional to the scattering coupling constant. We will thus have to find a more sophisticated way to organize the perturbation theory. The fixed point Hamiltonian is not totally useless however, since it still gives the $\omega = 0$ limit, that is, the charge stiffness. By simply using the LL Hamiltonian we can get the contribution of the Drude peak, and decide whether the system is a metal or an insulator.

Let us examine what happens if we look at the intrinsic resistivity of the electron gas, that is, the resistivity due to interactions and umklapp processes. Such processes are necessary to get a finite resistivity since they are the only ones that relax momentum. In higher dimensions, these processes are responsible for the existence of a finite resistivity as well. However, there, because the Fermi surface is indeed a surface it is easy to play with the angle to find such processes for electrons very close to the Fermi surface (that is, for which the magnitude of the

momentum is close to k_F). This means that in higher dimensions as soon as you have 'normal' interactions you have umklapp regardless of the precise position of the Fermi surface. This umklapp gives the T^2 Fermi liquid resistivity. Note that this is true if the Fermi surface is large enough. If the filling is too low $4k_F$ is not able to reach the zone boundary. In that case, it is necessary to go to higher-order umklapps (Giamarchi and Millis, 1992). Even a Fermi liquid resistivity in that case will be T^n where n is the number of electrons involved in the momentum nonconserving process. In one dimension, there are no angles to play with, which makes the umklapp processes only efficient at commensurate densities as we saw in Section 4.2. It is easy to use the same Boltzman approach than in higher dimensions but taking into account the phase space restriction of one dimension. In that case one finds that the umklapp gives $\rho(T) \propto T$ instead of T^2. Of course, this approach is too primitive since it does not take into account the Luttinger nature of the one-dimensional electron gas (that is, the effect of the other interactions). To get the transport in the presence of umklapp one should just compute the $\phi\phi$ correlation with the sine-Gordon Hamiltonian. Unfortunately, even with such a relatively simple Hamiltonian getting the full correlation function is not feasible. So one has to devise some approximation scheme. The more systematic one is to compute the self-energy of the boson propagator $\phi\phi$ in powers of the scattering mechanism (Oshikawa and Affleck, 2002). However, getting the self-energy is slightly cumbersome. I therefore present another approximation scheme which is very well suited to one-dimensional systems, and physically quite transparent (Giamarchi, 1991). The two procedures are equivalent at the lowest order.

The idea is that since the conductivity is inversely dependent on the scattering mechanism it would be useful to try an expansion of the resistivity. A method trying to achieve this program is the so-called memory function formalism (Götze and Wölfle, 1972). The idea is to make a hydrodynamic approximation for the conductivity. A Drude-like expression gives, for the frequency dependent conductivity

$$\sigma(\omega) = \frac{ine^2/m}{\omega + i/\tau} \tag{7.86}$$

where τ is the scattering time. To reach a similar expression let us rewrite the Kubo expression in a convenient form. The Kubo formula can be written (see (7.57)), considering fermions with spins

$$\sigma(\omega) = \frac{i}{\omega}\left[\frac{2u_\rho K_\rho}{\pi} + \chi(\omega)\right] \tag{7.87}$$

where χ is the retarded current–current correlation function. If one assumes that the system is a normal conductor (σ finite) at zero frequency then from (7.87) one gets $\chi(0) = -2u_\rho K_\rho/\pi$, and one can express the conductivity in terms of the meromorphic memory function $M(\omega)$ by

$$\sigma(\omega) = \frac{i2u_\rho K_\rho}{\pi}\frac{1}{\omega + M(\omega)} \tag{7.88}$$

where

$$M(\omega) = \frac{\omega\chi(\omega)}{\chi(0) - \chi(\omega)} \tag{7.89}$$

So far this is an exact but useless expression. One can however make a hydrodynamic approximation assuming that $M(\omega)$ admits a regular expansion in the scattering term. Since $\chi(\omega \neq 0)$ is zero in the absence of scattering since the current commutes with the Hamiltonian, it means that

$$\chi(0) - \chi(\omega) \simeq \chi(0) \tag{7.90}$$

when the scattering is small and for a *fixed* frequency. To expand in a similar way the numerator, let us integrate by parts the Kubo formula

$$\begin{aligned}
\omega\chi(\omega) &= \int_0^\infty dt\omega e^{i\omega t}\langle[j(t), j(0)]\rangle \\
&= -i\int_0^\infty d\omega(\partial_t e^{i\omega t})\langle[j(t), j(0)]\rangle \\
&= i\int_0^\infty d\omega e^{i\omega t}\langle[\frac{\partial j(t)}{dt}, j(0)]\rangle \\
&= \int_0^\infty d\omega e^{i\omega t}\langle[[H, j(t)], j(0)]\rangle
\end{aligned} \tag{7.91}$$

This expression shows explicitly that if the current commutes with the Hamiltonian the numerator is zero. Let us call $F = [H, j]$. It is thus a very physically transparent approximation. F is obviously proportional to the scattering potential. In order to obtain a more symmetric expression, let us integrate by parts a second time to get

$$-\omega\chi(\omega) = [\langle F; F\rangle_\omega - \langle F; F\rangle_{\omega=0}]/\omega \tag{7.92}$$

Since F is proportional to the scattering one can approximate the above expression by its value computed with the Hamiltonian in the absence of scattering

$$-\omega\chi(\omega) \simeq [\langle F; F\rangle_\omega^0 - \langle F; F\rangle_{\omega=0}^0]/\omega \tag{7.93}$$

One has thus the full expression for the memory function

$$M(\omega) \simeq \frac{[\langle F; F\rangle_\omega^0 - \langle F; F\rangle_{\omega=0}^0]/\omega}{-\chi(0)} \tag{7.94}$$

The expression (7.94) is correct at high frequency for arbitrary temperatures. The hope is that it still captures the essential physics even at low frequencies when the temperature is finite. I will come back to this question later.

With the sine-Gordon Hamiltonian the memory function is very easy to compute. Indeed,

$$F = [j, H] = \frac{8g_3}{(2\pi\alpha)^2}(u_\rho K_\rho)\ i\ \sin(\sqrt{8}\phi_\rho(x,\tau) - \delta x) \tag{7.95}$$

where I have used the Hamiltonian for the Mott system (4.19). Since the correlation is computed with the quadratic Luttinger liquid Hamiltonian it is identical to the one we computed for spin chains (see (6.51)) using the methods of Appendix C. It gives

$$\langle F; F\rangle_\omega = \frac{2g_3^2(u_\rho K_\rho)^2}{\pi^4\alpha^2 u_\rho}\left[\sin(2\pi K_\rho)\left(\frac{2\pi\alpha T}{u_\rho}\right)^{4K_\rho-2} B[K_\rho - iS_+, 1-2K_\rho]\right.$$
$$\left. B[K_\rho - iS_-, 1-2K_\rho] - \frac{\pi}{1-2K_\rho}\right] \tag{7.96}$$

with $S_\pm = (\omega \pm u_\rho\delta)/(4\pi T)$ and B is the beta function. Using (7.94) one gets

$$M(\omega) = \frac{g_3^2 K_\rho}{\pi^3\alpha^2}\left(\frac{2\pi\alpha T}{u_\rho}\right)^{4K_\rho-2}\frac{1}{\omega}\left[B(K_\rho - iS_+, 1-2K_\rho)B(K_\rho - iS_-, 1-2K_\rho)\right.$$
$$\left. -B(K_\rho - iS_+^0, 1-2K_\rho)B(K_\rho - iS_-^0, 1-2K_\rho)\right] \tag{7.97}$$

where $S_\pm^0 = S_\pm(\omega = 0)$.

Equation (7.97) gives the full frequency and temperature dependence of the conductivity at every filling *provided* that a perturbative expansion in g_3 is possible. This is of course obvious when the umklapp operator is irrelevant (or marginal), but fails when the operator is relevant. A way to improve greatly on this procedure is to couple this method with the renormalization group. One uses the RG up to the point where the cutoff is of the order of the frequency or the temperature. In that case a perturbation expansion in $g_{1\perp}$ is well behaved and one can use the memory function with the renormalized parameters. Of course, if the umklapp operator is relevant and opens a gap this procedure can only be used for energy scales above the gap.

I will just discuss here the general features of the solution and refer the reader to the literature for more details (Giamarchi, 1991; Giamarchi, 1992; Controzzi *et al.*, 2001; Carmelo *et al.*, 2000; Jeckelmann *et al.*, 2000). For simplicity, I discuss only the case of half-filling, but all the results mentioned here are valid in a generic way provided one correctly replaces K_ρ by n^2K_ρ for higher commensurabilities (see Section 4.2). Let me first examine the optical conductivity at $T = 0$. For commensurate fillings one has a transition between a regime where the umklapp is irrelevant $K_\rho > K_c$ and a regime where the umklapp is relevant $K_\rho < K_c$ ($K_c = 1$ for half-filling). At commensurate fillings the memory function is given by

$$M(\omega) \simeq \frac{g_3^2 K_\rho}{\pi^3 \alpha^2} \sin(2\pi K_\rho)\Gamma^2(1-2K_\rho)e^{-i\pi(2K_\rho-1)}\frac{1}{\omega}\left(\frac{\alpha\omega}{2u_\rho}\right)^{4K_\rho-2} \tag{7.98}$$

For $K_\rho > K_c$ the cosine is irrelevant and the system is described by a LL fixed point with an effective parameter K_ρ^*. The system has thus a conductivity shown in Fig. 7.12 and given at low frequencies by

$$\text{Re}\ \sigma(\omega) = \mathcal{D}\delta(\omega) + \sigma_{\text{reg}}(\omega) \tag{7.99}$$

where

$$\sigma_{\text{reg}}(\omega) \propto g_3^2 \omega^{3K_\rho-4} \tag{7.100}$$

It is thus a perfect conductor. The weight of the Drude peak is *finite* up to the transition since the K jumps discontinuously to zero in the Mott phase (see Section 4.2). At the transition the weight takes the universal value $\mathcal{D}/u_\rho = 2K_c$. The 'regular' part of the conductivity is a power law with an exponent that is directly fixed by the LL parameter K_ρ^*. The optical conductivity is thus a very powerful tool to measure the LL exponent K_ρ. I will come back to that point in Section 8.4. Note that close to the transition the 'regular' part is itself divergent since $K_\rho \to K_c = 1$ when the cosine is marginal and the conductivity behaves as

$$\sigma_{\text{reg}}(\omega) = \frac{g_3^2}{\omega\ \log^2(\omega)} \tag{7.101}$$

the log correction is similar to the one of Section 4.3.1 and comes from the fact that right at the transition the umklapp operator is marginal $g_3(l) \sim 1/l \sim 1/\log(\omega)$. It is easy to see that such corrections are needed for low frequencies since the conductivity should obey the sum rule

$$\int_0^\infty d\omega\ \text{Re}\ \sigma(\omega) = D \tag{7.102}$$

where D is the diamagnetic term. The $1/\omega$ behavior is totally generic and does not depend on the value of K_c (that is, the order of commensurability).

If the umklapp is relevant it opens a gap 2Δ in the spectrum. The system is a Mott insulator and the weight of the Drude peak is zero. The memory function approximation even coupled with the RG cannot be used for frequencies below the gap. For frequencies above 2Δ, the behavior is still approximately given by

$$\sigma(\omega) \sim g_3^2 \omega^{3K_\rho-4} \tag{7.103}$$

as can be seen from (7.97). A more precise determination is to integrate the RG flow. The effect is a little bit similar than for the calculation of the gap in Section 2.3.2. There is not much difference if the trajectories are nearly vertical since in that case K is nearly scale independent. Otherwise the scale dependence of K as given by the flow should be taken into account (Giamarchi, 1991). In that

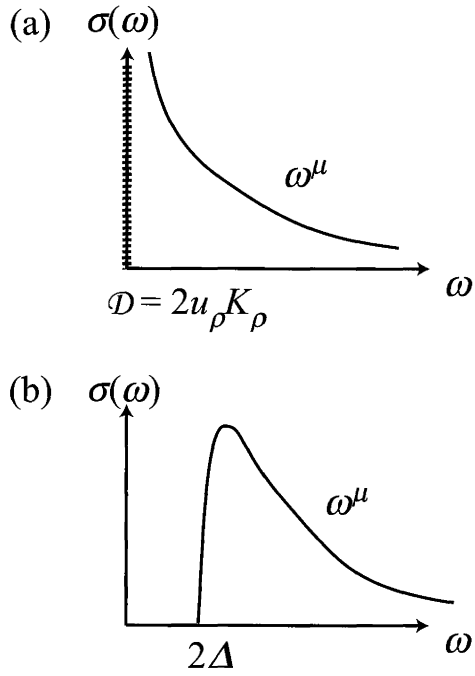

FIG. 7.12. Frequency dependence of the conductivity for the commensurate case. (a) When the umklapp is irrelevant the system is a perfect conductor with a Drude peak of finite weight up to the transition. The finite frequency part is a power-law like with an exponent depending on the interactions (see text). (b) When the umklapp is relevant it opens a gap. The system is an insulator and the conductivity is zero below the gap. The behavior for $\omega \gg 2\Delta$ is again power law like with a non-universal exponent controlled by the LL parameter (see text). Note that the optical gap is twice the thermodynamic one Δ (that is, the one entering in the temperature dependence of $\sigma(T)$).

case the exponent is renormalized leading to deviations compared to a simple power law. A sketch of the conductivity is shown in Fig. 7.12.

To get an idea of the behavior at the scale of the gap one can use the Luther–Emery method and map the sine-Gordon Hamiltonian on a system of spinless fermions (see Section 4.2). The current of the original Hamiltonian can be expressed in terms of the spinless fermions of (4.32) by

$$j = \frac{\sqrt{2}}{\pi}\partial_t\phi_\rho = \frac{1}{\pi}uK\partial_t\tilde{\phi} = \sum_k v(c^\dagger_{R,k}c_{R,k} - c^\dagger_{L,k}c_{L,k}) \tag{7.104}$$

and up to a numerical coefficient is the current of the spinless fermion problem. Thus, the conductivity is essentially the conductivity of the spinless fermions in a

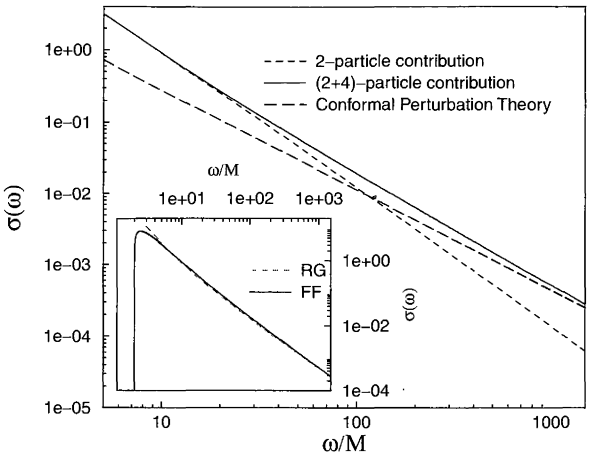

FIG. 7.13. Conductivity of the sine-Gordon model for parameters corresponding to a Hubbard model. M is here the optical gap. Dashed and full lines are form factor calculations with higher contributions included (full line). The long dashed line is the power law with a fixed exponent forgetting about the renormalization of the exponents. Although the result is good at very high frequencies it deteriorates rapidly since for a Hubbard model one is very close to the separatrix and the renormalization of the exponent is important. The insert is a comparison of form factors with the theory taking into account the renormalization of the exponents as explained in the text. The agreement is excellent up to very close to the gap. The two methods complement nicely each other to get the full behavior of the conductivity. (From Controzzi *et al.*, 2001 (Copyright (2001) by the American Physical Society).)

periodic potential. It is easy to see from Fig. 4.9 that one cannot have absorption for frequencies below the gap so the optical conductivity is zero for $\omega < 2\Delta$. A sketch of the full conductivity is given in Fig. 7.12. Right at the Luther–Emery line there is a divergence at the threshold $\chi \sim 2\Delta$ of the conductivity. This divergence is suppressed when one moves away from the Luther–Emery line. Another very powerful method is to use Bethe-ansatz. Quite recently, it has been possible to express, at $T = 0$ the correlation functions for integrable massive models (which is the case for sine-Gordon) in an expansion of ω/Δ. Such an expansion, known as form factors (Gogolin *et al.*, 1999), is thus valid close to the gap, but can be made better and better by including more terms. It is thus the perfect complement of the RG approach that works at higher energies than the gap and becomes bad at energy scales close to the gap. A plot of the conductivity for the sine-Gordon model using both methods is shown in Fig. 7.13. The agreement is excellent.

The temperature dependence can be obtained by the same method. In the

massless regime or for temperatures higher than the gap $T \gg \Delta$ one has for the memory function (since now $\omega \ll T$)

$$M(\omega) \simeq i\frac{g_3^2 K_\rho}{\pi^3\alpha^2} B^2(K_\rho, 1-2K_\rho)\cos^2(\pi K_\rho)\frac{1}{T}\left(\frac{2\pi\alpha T}{u_\rho}\right)^{4K_\rho-2} \tag{7.105}$$

This leads to

$$\sigma(T) \sim \frac{1}{g_3^2} T^{3-4K_\rho} \tag{7.106}$$

Note that for $K_\rho = 1$, this result is compatible with the naive Boltzman calculation. The interactions are again changing the exponent compared to the non-interacting case. Close to the transition $K_\rho \to K_c$ one has $\rho(T) \sim T$, which corresponds to the behavior $\sigma(\omega) \sim 1/\omega$ for finite frequencies.

Let us illustrate how this result can be obtained using the RG procedure. If one can neglect the scale dependence of K (vertical trajectories) one has (2.144)

$$g_3(l) = g_3 e^{(2-2K)l} \tag{7.107}$$

Let us stop the renormalization when $l = \log(u_\rho/T\alpha)$. We can then use (7.105) with the new cutoff $\alpha(l) = u_\rho/T$ to get (7.106). The prefactor is meaningless since it depends on the precise way of doing the renormalization and the precise value at which the renormalization is stopped. Of course, such an approximation is only valid if the initial value of g_3 is sufficiently small *and* the renormalization is stopped sufficiently early (high temperatures) that $g_{1\perp}$ remains small compared to K. If one takes, for example, the K and g_3 which would come from a one-dimensional Hubbard model (7.9) such an approximation would be seldom valid. If now g_3 is finite the renormalization of K has to be taken into account and the simple power law (7.106) is no longer valid. By numerically integrating (4.44) and using (7.105), one can obtain the full temperature dependance of the conductivity for various values of the interactions, at least in the regime where the equations are still valid, which corresponds roughly to $T > \Delta$. A summary of the temperature dependence of the conductivity is shown in Fig. 7.14. Below the gap one expects an exponential increase of the resistivity since the number of carriers is exponentially small ($\sim e^{-\Delta/T}$).

It is important to note that although the results for the frequency dependence of the conductivity are rock solid, the ones for the temperature dependence have some hidden assumption in them. I will just discuss its main features and refer the reader to the literature for more in depth discussions (Giamarchi, 1991; Zotos and Prelovsek, 1996; Sachdev, 1998; Zotos, 1999; Rosch and Andrei, 2000; Garst and Rosch, 2001). Indeed, one can really use the frequency as a cutoff in an RG procedure, but saying that the temperature produces a length $L_T = u/T$ above which the flow is cut *assumes* that the system looses coherence above this lengthscale. This is true if the system is in equilibrium with some phase breaking processes (phonons or such) that in addition to imposing the temperature can destroy the phase coherence. Although this is the physical situation

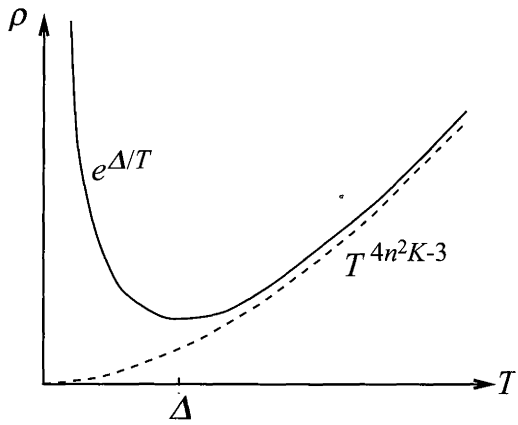

FIG. 7.14. Temperature dependence of the resistivity for the commensurate case. Above the gap one has a power law with a non-universal exponent depending on the LL parameter. Below the gap, number of carriers is exponentially small leading to an exponential resistivity (see, however, the text). (After Giamarchi, 1997.)

that is not the way the temperature is normally taken into account in the Kubo formula. The thermostat is put at time $-\infty$ and then removed (Mahan, 1981). As a result a one-dimensional system can perfectly have an infinite conductivity even at finite temperature. This is obvious, for example, if one takes the Luther–Emery solution. Our sine-Gordon Hamiltonian has been mapped to free spinless fermions with a gap. It is easy to see that at finite temperature although the number of thermally excited carriers at a given temperature is exponentially small $n \sim e^{-\Delta/T}$ these carriers do not scatter since the only source of scattering comes from the umklapp term already absorbed in the diagonalization of the Hamiltonian. So, strictly speaking, if the umklapp is the only source of scattering the conductivity would turn out to be infinite at every finite temperature. This occurs because although the umklapp term breaks the conservation of the current, there are other (hidden) conservation laws that are preserved by the umklapp. If these conservation laws are obeyed it is impossible to relax the current to zero and thus the conductivity would remain infinite even at finite temperature. In one dimension it is particularly easy to have many conservation laws, specially if the system is integrable. So in order to have a finite conductivity one should break all the conservation laws that would prevent the current to relax to zero. This is the assumption implicitly made when assuming that the temperature can be used as a cutoff in the flow. These phase breaking processes can also be taken into account in the memory function formalism.

Finally, let me briefly examine what happens in the doped system. One can of course use the memory function result (7.97) to compute the conductivity. At low temperature (7.97) gives an exponential increase of the conductivity as

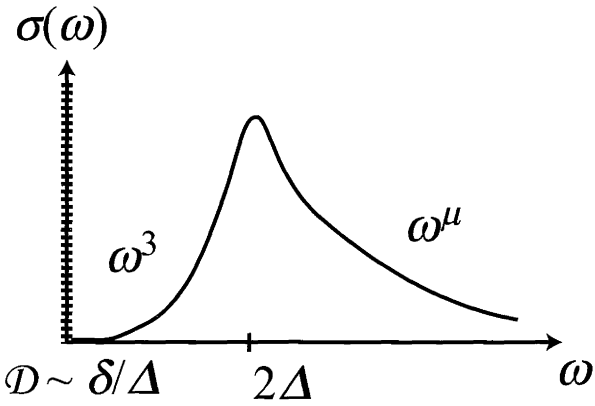

FIG. 7.15. Frequency dependence of the conductivity for the incommensurate case. There is a Drude peak whose weight is proportional to the doping δ and inversely proportional to the gap Δ at commensurate filling. At small frequency intraband transitions lead to an ω^3 dependence. For frequencies of the order of the gap, the system cannot make the difference between doped and undoped and the frequency behavior is the same as for commensurate filling.

$\sigma(T) \sim e^{(u\delta)/T}$ since the umklapps are frozen by the doping. For the frequency dependence one can have a clear picture by looking at the Luther–Emery model (see Fig. 4.9). At very high energy there are interband transitions and the system does not know whether it is doped or not, so the behavior is the same as at half-filling. For frequencies smaller than the gap interband transitions are again blocked so the conductivity should be zero. In fact, irrelevant operators such as band curvature terms give an ω^3 contribution (Giamarchi and Millis, 1992). At very small frequencies, the doped system can make intraband transitions and there is thus a Drude peak. The weight of the Drude peak is again given by $2u_\rho^* K_\rho^*$. As we saw for very small doping $K_\rho \to K_c/2$ while $u_\rho \sim \delta/\Delta$. The weight of the Drude peak is proportional to the doping, in agreement with the result from Bethe-ansatz (Shastry and Sutherland, 1990; Schulz, 1990). This is a very intuitive result, since one expects only the holes or doubly occupied states to be able to conduct. Note that the weight is also inversely proportional to the gap at half-filling Δ, which can thus be viewed here as an 'effective mass' for the holes. A sketch of the conductivity for the doped case is shown in Fig. 7.15.

8

COUPLED FERMIONIC CHAINS

To infinity and beyond!

Buzz Lightyear in Toy Story (Disney)

Now that we have a good understanding of the properties of a single electronic chain we can investigate how the one-dimensional physics is changed when one goes from a purely one-dimensional system to a two- or three-dimensional situation. We can reach such effect by considering a system of one-dimensional chains where the electrons can hop from one chain to the other with a term such as

$$H_\perp = -\int dx \sum_{\langle\mu,\nu\rangle} t_{\perp,\mu,\nu}[\psi_\mu^\dagger(x)\psi_\nu(x) + \text{h.c.}] \tag{8.1}$$

where $\langle\mu,\nu\rangle$ denotes a pair of chains. This is very similar to the effects we looked at in coupled spin chains in Section 6.4. There is, however, an important difference. For coupled spin chains, the spin has a well-defined classical limit so that the coupling term $S_\mu S_\nu$ can be viewed, in a mean field approximation, as an effective 'classical' field acting on a chain $S_\mu S_\nu \to \langle S_\mu\rangle S_\nu$. Thus, at least for an infinite number of chains for which one could expect a mean field approach to be qualitatively correct, the physics of such a term is transparent: it pushes the system to an ordered state. For the fermionic single-particle hopping (8.1) no such mean field description is possible since a single fermion operator has no classical limit. It is thus impossible to approximate $\psi_\mu^\dagger(x)\psi_\nu(x)$ as $\langle\psi_\mu^\dagger(x)\rangle\psi_\nu(x)$, which makes the solution of this problem much more complicated. This difference is apparent also on the bosonization representation. A spin can essentially be expressed in terms of a single bosonic field (either $e^{i\theta}$ for $S^\pm$ or $\cos(2\phi)$ for S_z). This is from where we got the mean field description in Section 6.4. On the contrary the single fermionic operator contains *both* ϕ and θ. Since these field are conjugate variables they cannot order simultaneously and no classical representation can exist.

In order to solve this problem we thus have to use other techniques. Of course, if $t_\perp \sim t_\parallel$ (where $t_\parallel$ is the intrachain hopping) the kinetic energy is essentially isotropic and one is in a high-dimensional situation to start with. Adding the electrons on such a system is very likely to lead to a Fermi liquid if the interactions are not too strong. In any case, a good starting point is to study an interacting high-dimensional problem. I consider here the other limit where $t_\perp$ is much smaller than the intrachain characteristic energy scales (e.g. the kinetic energy or the interactions). In that case the chains have a well-defined

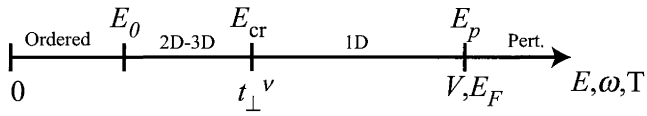

FIG. 8.1. Separation of energy scales if the interchain hopping $t_\perp$ is much smaller than the intrachain one $t_\parallel$. At energies larger than the intrachain hopping (or equivalently the Fermi energy E_F) and interactions (denoted generically V), simple perturbation theory is valid. Below this scale the system is a Luttinger liquid. The interchain hopping couples the chains at an energy $E_{\rm cr}$ and destroys the one-dimensional physics. For non-interacting particles $E_{\rm cr} \sim t_\perp$ but this scale is renormalized by interactions into $t_\perp^\nu$ (see text). In the coupled chains (two- or three-dimensional) regime the system can have a transition to an ordered state at an energy E_0.

Luttinger liquid regime before the processes due to interchain hopping can spoil the pure one-dimensional physics. This is summarized in Fig. 8.1

As for the spin chains, there are two interesting limiting cases for which one can study this problem. We can look at the coupling of a small number of chains. This corresponds to a fermion ladder. We can also look directly at an infinite number of coupled chains.

8.1 Fermionic ladders

Let us start with a small number of coupled chains. This is the equivalent of the spin ladder problem studied in Section 6.4. Here again one can expect interesting differences between an odd and an even number of chains. The question of ladders is a problem that has been the subject of intense analytical, numerical and experimental (see Section 8.2) studies and it is impossible to cover all the material here. A review can be found in Dagotto and Rice (1996) and Dagotto (1999). Here I confine myself to the simplest case of a ladder, namely a two-leg ladder.

8.1.1 *Spinless ladders*

To warm up let me start with two coupled chains of spinless fermions (Nersesyan *et al.*, 1993). The general Hamiltonian for such a system is

$$H = H_1 + H_{-1} - t_\perp \int dx[\psi_1^\dagger(x)\psi_{-1}(x) + \text{h.c.}] + U \int dx\, \rho_1(x)\rho_{-1}(x) \qquad (8.2)$$

where $\mu = 1$ and $\mu = -1$ are the chain indices and H_μ is the Hamiltonian describing a one-dimensional chain of interacting spinless fermions similar to the ones studied in Chapter 2. $t_\perp$ is the interchain hopping and U is some interchain interaction. For example, this Hamiltonian could come from the lattice Hamiltonian

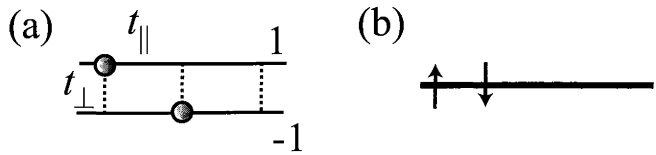

FIG. 8.2. A spinless ladder (a). $t_{\|}$ and $t_{\perp}$ are respectively the intra- and interchain hopping. This system can be viewed as a single chain of fermions with spins (b), where $S_z = \pm 1/2$ becomes the chain number. Since intra- and interchain interactions are a priori different the interactions of the effective chain with spin are spin anisotropic. The interchain hopping acts as a magnetic field along x in the effective chain with spins.

$$H = -t \sum_{i,p} [c_{i,p}^{\dagger} c_{i+1,p} + \text{h.c.}] + V \sum_{i} n_{i,p} n_{i+1,p} - t_{\perp} \sum_{i} [c_{i,1}^{\dagger} c_{i,-1} + \text{h.c.}] + U \sum_{i} n_{i,1} n_{i,-1} \quad (8.3)$$

The ladder is shown in Fig. 8.2.

To solve this problem, we can of course introduce one boson species per chain and then use the standard bosonization technique. However, this is a problem that we have in fact already solved in this book in Section 4.3.2. Indeed, since we have spinless fermions and two chains we can consider the chain index as the two $S_z = \pm 1/2$ components of a spin index. The ladder (8.3) or (8.2) is thus equivalent to a *single chain* of fermions with spin, as shown in Fig. 8.2. If $t_{\perp}$ and U are zero the 'up' spins are totally disconnected from the 'down' spins. This is equivalent to say that all $g_{\perp}$ processes are zero. The process U introduces some interaction between up and down spins. The interaction in this effective chain are thus very spin anisotropic, but except for that it is a regular fermionic chain. In the absence of $t_{\perp}$ this is exactly the problem we have considered in Chapter 2 by taking $g_{\|} \neq g_{\perp}$ (here $g_{\|} \sim V$ and $g_{\perp} \sim U$). For example, for repulsive interactions $g_{\|} > g_{\perp} > 0$ (physically one would expect interchain interactions to be weaker than intrachain ones), one gets a massless spin sector, and thus a Luttinger liquid where both 'charge' (that is $\rho_1 + \rho_{-1}$) and 'spin' (that is $\rho_1 - \rho_{-1}$) sectors are massless.

The $t_{\perp}$ term slightly complicates matters. In the spin language this term corresponds to

$$-t_{\perp} \int dx [\psi_1^{\dagger}(x) \psi_{-1}(x) + \text{h.c.}] = -t_{\perp} \int dx [\psi_{\uparrow}^{\dagger}(x) \psi_{\downarrow}(x) + \text{h.c.}] \quad (8.4)$$

This term thus corresponds exactly to a magnetic field applied along the x axis. If we used a boson representation in the chain (spin) index one would have

$$-t_\perp \int dx\ \psi_1^\dagger(x)\psi_{-1}(x) = -t_\perp \int dx[\psi_{R\uparrow}^\dagger(x)\psi_{R\downarrow}(x) + \psi_{L\uparrow}^\dagger(x)\psi_{L\downarrow}(x) + \text{h.c.}]$$
$$= \frac{-4t_\perp}{2\pi\alpha} \int dx\ \cos(\sqrt{2}\phi_\sigma(x)) \cos(\sqrt{2}\theta_\sigma(x)) \tag{8.5}$$

This is a very unpleasant operator since it contains both ϕ and θ. This is normal given our previous discussion on $t_\perp$, but it means that beyond writing RG equation for this operators we will have a hard time studying it. In fact in the bosonization representation it would be much more convenient to have the magnetic field along the z direction since in that case the magnetic field has the much more simple representation $\nabla\phi_\sigma$, that we know very well how to treat.

It is thus much more convenient to make a rotation of spin axis to put the magnetic field in the z direction. The price to pay is that the interactions transform in the non-trivial way given by (4.81), with in particular a spin flip term appearing. Our ladder problem is thus exactly identical to the study of the effect of a magnetic field along z on the Hamiltonian (4.86). The effect of a simple gradient term is something that we have analyzed in detail in Section 4.2 (see e.g. (4.44)). We see that by this simple spin rotation we have reduced the $t_\perp$ term to something which is now very manageable with the bosonization method.

What is the physical interpretation of this spin rotation. The transformation to go from the x axis to z axis is to use the basis $\psi_{\pm x} = (\psi_\uparrow \pm \psi_\downarrow)/\sqrt{2}$. In the original chain language, it simply means that we go to the bonding and antibonding bands that are the eigenstates of the rung kinetic energy

$$E(k, k_\perp) = E_{1\text{d}}(k) - 2t_\perp\ \cos(k_\perp a) \tag{8.6}$$

Since here we have only two chains $k_\perp = 0$ and $k_\perp = \pi/a$ are the only two allowed values. The eigenstates are

$$\begin{aligned} \psi_o &= \frac{\psi_1 + \psi_{-1}}{\sqrt{2}} \\ \psi_\pi &= \frac{\psi_1 - \psi{-1}}{\sqrt{2}} \end{aligned} \tag{8.7}$$

The transformation thus takes us from the chain basis to the bonding–antibonding representation as shown in Fig. 8.3. In the bonding–antibonding representation, it is no wonder that $t_\perp$ is simpler since we have diagonalized the kinetic energy. The price to pay is that now we have four Fermi points instead of two, which allows for more complicated interaction processes. This is the reason for the existence of the new interaction g_f in the spin language even if one started from perfectly usual interactions. In the spin language, this transformation is very natural since it is nothing but a simple rotation. Note that because of the nonlinear relation between the fermion and the boson operators the simple transformation on the fermions (8.7) leads to a very complicated relation between the boson operators of the new and old base (compare (8.5) with $\nabla\phi_\sigma$).

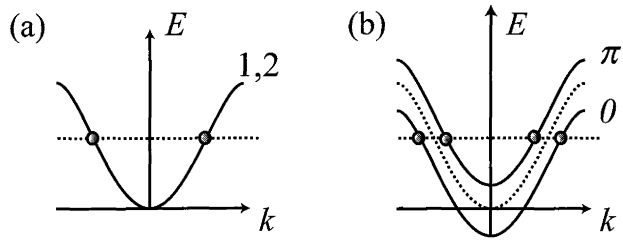

FIG. 8.3. Chain and bonding representation. In the chain representation (a) we have two species with the dispersion relation of a single chain. In the bonding–antibonding basis (b) the kinetic energy has been diagonalized. As a results the dispersion relation of the bonding and antibonding species are different. There are thus four different points at the Fermi level.

Let us now complete our solution of the full Hamiltonian. We use the bonding bands base, instead of the chain base. We further introduce the symmetric and antisymmetric combinations in this base

$$\rho_{\rho,\|} = \frac{\rho_o \pm \rho_\pi}{\sqrt{2}} \tag{8.8}$$

These are the equivalent of the charge and the spin sectors in the single chain mapping. In terms of these fields the Hamiltonian becomes (Nersesyan *et al.*, 1993)

$$\begin{aligned} H =& H_\rho + H_\| \\ H_\rho =& \int \frac{dx}{2\pi}\left[u_\rho K_\rho(\pi\Pi_\rho)^2 + \frac{u_\rho}{K_\rho}(\partial_x\phi_\rho)^2\right] \\ H_\| =& \int \frac{dx}{2\pi}\left[u_\| K_\|(\pi\Pi_\|)^2 + \frac{u_\|}{K_\|}(\partial_x\phi_\|)^2\right] + \int dx t_\perp \frac{\sqrt{2}}{\pi}\partial_x\phi_\| \\ &+ \int dx\left[\frac{2g_\perp}{(2\pi\alpha)^2}\cos(\sqrt{8}\phi_\|) + \frac{2g_f}{(2\pi\alpha)^2}\cos(\sqrt{8}\theta_\|)\right] \end{aligned} \tag{8.9}$$

The $\|$ part is identical to (4.76) with $t_\perp$ playing the role of a magnetic field along z. The K and g depend of course on the initial interactions. For example, for the microscopic Hamiltonian (8.3), one finds for small $t_\perp$ (for larger values of $t_\perp$ see Ledermann and Le Hur 2000)

$$\begin{aligned} g_f &= -Va(1-\cos(2k_F a)) \\ g_\perp &= Ua - Va(1-\cos(2k_F a)) \end{aligned} \tag{8.10}$$

and

$$
\begin{aligned}
K_{\parallel} &= 1 + \frac{Ua}{2\pi v_F} \\
u_{\parallel} &= v_F(1 - \frac{Ua}{2\pi v_F} + \frac{Va}{\pi v_F}(1 - \cos(2k_F a))) \\
K_{\rho} &= 1 - \frac{Ua}{2\pi v_F} - \frac{Va}{\pi v_F}(1 - \cos(2k_F a)) \\
u_{\rho} &= v_F(1 + \frac{Ua}{2\pi v_F} + \frac{Va}{\pi v_F}(1 - \cos(2k_F a)))
\end{aligned}
\tag{8.11}
$$

with $v_F = 2ta\ \sin(2k_F a)$. Therefore, for the pure t–V model, one has $K_\rho < 1$ (resp. $K_\rho > 1$) and $g_f < 0$ (resp. $g_f > 0$) for repulsive (resp. attractive) interactions and $K_\parallel = 1$ for all t, V. As in previous chapters, the boson Hamiltonian (8.9) is quite general provided that one goes beyond the perturbative expressions of the LL parameters. More complicated (that is, longer-range and interchain interactions) lead only to a change in the parameters K, u and g. By adding interchain interactions such as U in formulas (8.11) and (8.10) or longer range interactions one can in particular access the other regimes $K_\rho > 1$ and $g_f < 0$ or $K_\rho < 1$ and $g_f > 0$.

The physics of the system is readily seen in (8.9). The charge part is simple, so let us focus on the *parallel* (spin) part. In the absence of $t_\perp$ the system is totally described by the flow (4.80) shown in Fig. 4.13. Let us concentrate here on the simplest case $U = 0$. In that case the system starts on the fixed line $g_\perp = g_f$, $K_\parallel = 1$. This is natural since it corresponds to the massless phase of the two decoupled chains. The $t_\perp$ term kills the $\cos(\sqrt{8}\phi_\parallel)$, as explained in Section 4.2. The system now flows with the RG equations resulting from $\cos(\sqrt{8}\theta_\parallel)$ only. Given the initial condition $K_\parallel = 1$, this flows to strong coupling. In presence of interchain hopping the field $\theta_\parallel$ thus develops a gap. It means that the antisymmetric modes (bonding minus antibonding) become massive. The symmetric mode (bonding plus antibonding) always remain massless. This is a simple consequence of the galilean invariance of the ladder since we have not put any umklapp terms. The total charge density of the system should be able to slide at zero energy cost, thus the Hamiltonian should be invariant by $\phi_\rho \to \phi_\rho + \text{Cste}$. The total charge Hamiltonian can thus only be a quadratic LL one and cannot contain any $\cos(\phi_\rho)$ terms. This would of course not be true for commensurate fillings for which umklapp terms can appear and the total charge mode can become massive.

For the t–V model, θ becoming massive is the only possibility since one starts from $K_\parallel = 1$. A more general model allows to explore the whole phase diagram. Let us consider here only the case where θ is massive. As usual its value and thus the nature of the ordered fields depends on the sign of g_f. The various possibilities are summarized in Table 8.1. To compute the physical properties of the system, we have to compute the dominant correlation functions as for the single chain system. As for one chain, two main type of instabilities are possible: particle–hole (density, current etc.) instabilities or particle–particle (that is, superconducting)

Table 8.1 *The four sectors of the pure two-chain spinless fermion model, as a function of K_ρ and g_f. The average values of the massive field $\langle\theta_\parallel\rangle$ are indicated together with the phase with the most divergent susceptibility. (After Orignac and Giamarchi, 1997.)*

	I	II	III	IV
g_f	$+$	$+$	$-$	$-$
K_ρ	<1	>1	>1	<1
$\langle\theta_\parallel\rangle =$	$\pi/\sqrt{8}$	$\pi/\sqrt{8}$	0	0
Phase	OAF	SC^s	SC^d	CDW^π

ones. But because of the presence of the two chains, one can construct new operators. Since $\phi_\parallel$ is gapped, any operator that contains this field either decays exponentially or tends to a constant at large distance as explained in Fig. 2.8. The operators that have potentially a non exponential decay are thus

$$\begin{aligned}
O_{\mathrm{CDW}^\pi} &= \psi^\dagger_{R,1}(x)\psi_{L,1}(x) - \psi^\dagger_{R,-1}\psi_{L,-1}(x) \sim e^{i\sqrt{2}\phi_\rho}\cos(\sqrt{2}\theta_\parallel)\\
O_{\mathrm{SC}^s} &= \psi_{L,o}(x)\psi_{R,0} + \psi_{L,\pi}\psi_{R,\pi} \sim e^{i\sqrt{2}\theta_\rho}\sin(\sqrt{2}\theta_\parallel)\\
O_{\mathrm{OAF}} &= i(\psi^\dagger_{R,1}(x)\psi_{L,-1}(x) - \psi^\dagger_{R,-1}(x)\psi_{L,1}(x)) \sim e^{i\sqrt{2}\phi_\rho}\sin(\sqrt{2}\theta_\parallel)\\
O_{\mathrm{SC}^d} &= \psi_{L,0}\psi_{R,0} - \psi_{L,\pi}\psi_{R,\pi} \sim e^{i\sqrt{2}\theta_\rho}\cos(\sqrt{2}\theta_\parallel)
\end{aligned} \tag{8.12}$$

Note that to get correctly the operators, it is mandatory to pay attention to the Klein factors as explained in Section 4.3.2, otherwise one can exchange some of the phases.[34] In the language where the two chains are represented by a pseudo spin, the above operators are easily identified to the charge and spin density waves (for CDW^π and OAF) and to the superconducting operators (along x and y) for SC^s and SC^d (see (2.116)). Note the change of $\cos(\sqrt{2}\theta_\parallel)$ into $\sin(\sqrt{2}\theta_\parallel)$ compared to (2.116)), due to the change of sign of the factor g_f in the Hamiltonian (8.9) compared to (4.84).

The operator O_{CDW^π} describes an out-of-phase CDW. As shown in Fig. 8.4 it corresponds to two charge density waves which are locked together with a dephasing of π. This configuration is obviously optimal for intrachain repulsion and since one charge on a chain is in front of an empty site on the other chain the electrons can still gain some energy from $t_\perp$ by doing virtual jumps on the other chain. O_{SC^s} is the standard superconducting phase. In terms of the lattice operators this is

$$O_{\mathrm{SC}^s}(n) = c_{n+1,1}c_{n,1} + c_{n+1,-1}c_{n,-1} \tag{8.13}$$

Particles are paired on the chains, for example by a negative V and then these pairs have dominant superconducting fluctuations (they would Bose condense in

[34]The two superconducting phases in Nersesyan *et al.* (1993) should be exchanged for this reason.

higher dimensions). These two phases are a natural extension to two chains of the phases of a single spinless fermionic chain seen in Chapter 6.

There are two other possible phases that are more specific of the ladder. The operator O_{SC^d} creates the ladder equivalent of d-wave superconductivity in a two-dimensional system. The pairing occurs essentially between particles on the two chains. The equivalent of the operator is

$$O_{\mathrm{SC}^d}(x) = \psi_{L,1}(x)\psi_{R,-1}(x) + \psi_{L,-1}(x)\psi_{R,1}(x) \tag{8.14}$$

It corresponds to superconductivity across the rung. Note that the operator giving the naive pairing across the rung would be

$$O = c_{n,1}c_{n,-1} \tag{8.15}$$

and would correspond to

$$\begin{aligned} O &= \psi_{L,1}\psi_{R,-1} - \psi_{L,-1}\psi_{R,1} \\ &\propto e^{i\sqrt{2}\theta_\rho}\cos(\sqrt{2}\phi_{\|}) \end{aligned} \tag{8.16}$$

But because $\theta_{\|}$ orders, this operator decays exponentially. To get the pairing one should thus shift one of the particles to the neighboring site, as when the pairing occurs inside the chain. A more correct microscopic pairing operator is thus

$$O_{\mathrm{SC}^d}(n) = c_{n+1,1}c_{n,-1} \tag{8.17}$$

Because this operator is essentially

$$(\psi_1 + \psi_{-1})_{x+a}(\psi_1 - \psi_{-1})_x \tag{8.18}$$

(the extra parts are irrelevant), the sign of the wavefunction changes when one turns by $\pi/2$ reminiscent of a 'd-wave' like symmetry for the superconducting order parameters. Of course, there is no continuous rotation. In fact, the order parameter is also odd under parity, so a better description is to see this order as p-wave type (Ledermann and Le Hur, 2000). I will nevertheless stick to the denomination d-wave for simplicity, and to ensure a smooth connection with the fermions with spins. The O_{OAF} operator describes orbital currents circulating around a plaquette of length π/k_F. It is the one-dimensional analogue of the so-called flux phases in higher dimension (Kotliar, 1988; Affleck and Marston, 1988). The phase diagram is shown in Fig. 8.4.

The phase diagram of the spinless ladder thus presents interesting features compared to the one of the single chain. It shows, in particular, that the interchain hopping changes drastically the physical properties as compared to a single chain, because of the gap it opens in the transverse degrees of freedom. This study also suggests that the bonding–antibonding base is a very good starting point to take into account the effects of $t_\perp$ using bosonization. Of course, many other properties are interesting to compute such as the effect of different velocities (Ledermann and Le Hur, 2000) such as commensurability effects (Donohue *et al.*, 2001) and I refer the reader to the appropriate papers for more details.

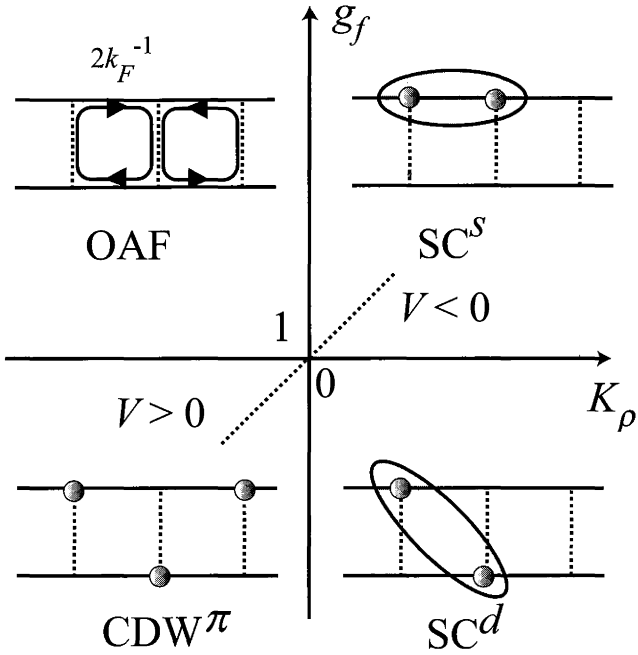

FIG. 8.4. Phase diagram of a spinless ladder as a function of the LL parameter K_ρ and the 'chain' flip interaction g_f. SC^s and SC^d are dominated by either s- or 'd'-wave (or p-wave) superconducting fluctuations. CDW$^\pi$ is a charge density wave with density alternating between the chains. OAF is an orbital antiferromagnet with orbital currents circulating on a plaquette. The dashed line indicates the phase reachable for a pure t–V model in the chains. (After Nersesyan *et al.*, 1993; Orignac and Giamarchi, 1997.)

8.1.2 *Ladders with spins*

Let us now examine the more complicated case of fermions with spins. This is a more complicated problem but its physics is much richer. Here again the literature is gigantic. This problem has been analyzed in great detail both analytically (Fabrizio, 1993; Finkelstein and Larkin, 1993; Kveschenko and Rice, 1994; Nagaosa, 1995; Balents and Fisher, 1996; Schulz, 1996*a*; Shelton and Tsvelik, 1996) and numerically (Dagotto *et al.*, 1992; Noack *et al.*, 1994; Poilblanc *et al.*, 1994; Tsunetsugu *et al.*, 1994; White *et al.*, 2002).

To understand what can happen, let us go back for a moment to our spin ladder. As we saw in Section 6.4.1 such a system has a spin gap. If the transverse exchange $J_\perp$ is large the spins on a rung are locked into a singlet state. We have seen that this physics was essentially correct even if $J_\perp$ was small. Let us now assume that we dope such a ladder. This system can be the realization of the so-called t–J ladder, where each chain is described by a t–J model (see Section 7.1.2)

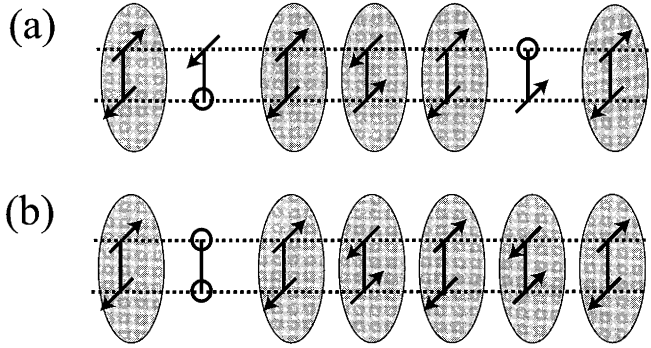

FIG. 8.5. Doping of a t–J ladder. (a) Putting two holes on two different rungs costs twice the spin gap. (b) For large exchange J, it is energetically favorable to confine the holes on the same rung. The spin gap forces the holes to pair.

and a $t_\perp$ and $J_\perp$ couple the two chains. Putting holes in the structure can be done in two ways as shown in Fig. 8.5. As was pointed out by T.M. Rice *et al.*, if one puts two holes on two different rungs one has to break two spin gaps, whereas putting the two holes on the same rung costs only one spin gap. The holes are thus paired on a t–J ladder (in the limit of large $t_\perp$ at least). Note that in such a ladder all spin properties are gapped contrary to what happens for a single chain. Of course, having pairs is not enough to decide of the phase, since these pairs can either crystallize and form a charge density wave, or 'Bose condense' and give rise to superconductivity. But it is strongly suggestive that superconductivity with repulsive interactions can occur in this system. In the last case superconductivity can be expected to be of the d-wave type, since as for the spinless ladder the pairing would occur through the rung.

Let us now investigate the ladder in the opposite limit of weak interactions. A possible microscopic model is for example

$$\begin{aligned} H = &-t \sum_{i,\sigma,p} [c^\dagger_{i+1,\sigma,p} c_{i,\sigma,p} + \text{h.c.}] - t_\perp \sum_{i,\sigma,p} c^\dagger_{i,\sigma,p} c_{i,\sigma,-p} \\ &+U \sum_{i,p} n_{i,\uparrow,p} n_{i,\downarrow,p} + V \sum_{i,p} n_{i,p} n_{i+1,p} \end{aligned} \tag{8.19}$$

where $p = \pm 1$ is the chain index and $\sigma = \uparrow, \downarrow$ labels the spin. In order to treat this Hamiltonian using bosonization, one can separate the bonding o and antibonding π bands as was done for spinless fermions. Then, within each band, one can apply the standard bosonization formulas for fermions with spins. As a consequence, the system is described by four fields $\phi^\pi_\rho, \phi^\pi_\sigma \phi^o_\rho, \phi^o_\sigma$ instead of two for the spinless case. As for the spinless case it is convenient to introduce the symmetric and antisymmetric combinations (both for the charge and spin sectors)

$$\phi_{\nu\pm} = \frac{1}{\sqrt{2}}(\phi_{\nu,o} \pm \phi_{\nu,\pi}) \tag{8.20}$$

Using the bosonization dictionary of Appendix D one can bosonize (8.19). As usual the bosonized Hamiltonian is quite general and would hold for more complex interactions than in (8.19). The Hamiltonian is

$$H = H_0 + H_{\text{int},2} + H_{\text{int},1} - \frac{2t_\perp}{\pi}\int dx\, \nabla\phi_{\rho-} \tag{8.21}$$

where H_0 is the usual quadratic part

$$H = \sum_{\substack{\nu=\rho,\sigma \\ r=\pm}} \int \frac{dx}{2\pi}\left[u_{\nu r}K_{\nu r}(\pi\Pi_{\nu r})^2 + \frac{u_{\nu r}}{K_{\nu r}}(\partial_x\phi_{\nu r})^2\right] \tag{8.22}$$

There are two sine-Gordon like parts coming from the interactions. Because of the presence of $t_\perp$ the cosines containing $\phi_{\rho-}$ are wiped out. One can thus forget these operators in the Hamiltonian (for the complete Hamiltonian see e.g. Tsuchiizu *et al.* 2001). Keeping only the remaining cosines, one can regroup the interactions in two terms. The first one is associated with the interband processes induced by intrachain forward scattering

$$H_{\text{int},2} = \frac{g_2}{2(\pi\alpha)^2}\int dx\ \cos 2\theta_{\rho-}\ (\cos 2\phi_{\sigma-} + \cos 2\theta_{\sigma-}) \tag{8.23}$$

The other one is associated with the intrachain backward scattering

$$H_{\text{int},1} = \frac{2g_1}{(2\pi\alpha)^2}\int dx\,[\cos 2\phi_{\sigma+}(\cos 2\theta_{\rho-} + \cos 2\phi_{\sigma-} + \cos 2\theta_{\sigma-}) - \cos 2\theta_{\rho-}\cos 2\theta_{\sigma-}] \tag{8.24}$$

The parameters u, K and g_1, g_2 depends on the microscopic model. For example, for (8.19) the symmetric charge mode has the LL parameter

$$K_{\rho+} = \left(\frac{2\pi v_F + (g_1 - 2g_2)}{2\pi v_F - (g_1 - 2g_2)}\right)^{1/2} \tag{8.25}$$

with

$$\begin{aligned} g_1 &= Ua + 2Va\cos(2k_F a) \\ g_1 - 2g_2 &= -(Ua + 2Va(2 - \cos(2k_F a)) \end{aligned} \tag{8.26}$$

as usual a is the lattice spacing. Of course, for a more general microscopic Hamiltonian the bosonized Hamiltonian remains valid but with different g_1 and g_2.

To determine the physics of the system one should, as for the spinless problem, write the RG equations, and follow the flow. The equations are relatively messy,

Table 8.2 *The four sectors of the pure two-chain Hubbard model, as a function of $K_{\rho+}$ and g_1. The average value of the field developing a gap are indicated together with the phase with the most divergent susceptibility (After Orignac and Giamarchi, 1997.)*

	I	II	III	IV
g_1	$+$	$+$	$-$	$-$
$K_{\rho+}$	<1	>1	>1	<1
$\langle\theta_{\rho-}\rangle$	0	0	0	0
$\langle\phi_{\sigma+}\rangle$	$\pi/2$	$\pi/2$	0	0
$\sigma-$	$\langle\phi_{\sigma-}\rangle=\pi/2$	$\langle\theta_{\sigma-}\rangle=0$	$\langle\phi_{\sigma-}\rangle=0$	$\langle\theta_{\sigma-}\rangle=\pi/2$
phase	SC^d	OAF	SC^s	CDW^π

so we will not do it here (Varma and Zawadowski, 1985; Balents and Fisher, 1996; Schulz, 1996*a*). I will just give a physical argument for the fixed point in the case of the Hubbard model ($g_1 = g_2 \propto U$). Given that the field $\theta_{\rho-}$ appears in the Hamiltonian in (marginally) relevant terms and that all $\cos 2\phi_{\rho-}$ are not present, one expects the field $\theta_{\rho-}$ to order. The presence of the term $\cos 2\phi_{\sigma+}\cos 2\theta_{\rho-}$ implies that the field $2\phi_{\sigma+}$ also orders. Determining the order for the field $\sigma-$ is more complex since both $\phi_{\sigma-}$ and $\theta_{\sigma-}$ appear in the Hamiltonian and they compete for different orders. One of these two fields orders depending on the value of the coupling constants. One has an Hamiltonian similar to (4.76) with coefficients for the $\cos(\sqrt{2}\phi_{\sigma-})$ term (resp. $\cos(\sqrt{2}\theta_{\sigma-})$), which are proportional to g_2 (resp. $g_2 - g_1$) (the other part are symmetric in the two dual fields). The bigger coefficient wins. This depends on the relative signs of g_1 and g_2. For example for $g_2 > 0$ and $g_1 < 0$ $\cos(\sqrt{2}\theta_{\sigma-})$ wins and $\langle\theta_{\sigma-}\rangle = \pi/2$ to minimize the energy. We thus see that three of the modes are gapped. The only one that remains massless is the total charge field, for the same reasons of Galilean invariance than for the spinless case. The mean values of the three other fields are determined by minimizing the energy of the ground state. Thus, depending on the interactions one can distinguish four sectors that are summarized in Table 8.2. All physical quantities thus depend only on the parameter $K_{\rho+}$ of the symmetric charge mode, analogous to the K_ρ of the spinless problem.

As for the spinless case, one has to consider the various operators with divergent susceptibilities. The possible candidates are

$$
\begin{aligned}
O_{\mathrm{CDW}^\pi}(n) &= \sum_{p,\sigma} p c^\dagger_{n,\sigma,p} c_{n,\sigma,p} \\
O_{\mathrm{OAF}}(n) &= \sum_{p,\sigma} p c^\dagger_{n,\sigma,p} c_{n,\sigma,-p} \\
O_{\mathrm{SC}^s}(n) &= \sum_{p} c_{n,\sigma,p} c_{n,-\sigma,p} \\
O_{\mathrm{SC}^d}(n) &= \sum_{p} c_{n,\sigma,p} c_{n,-\sigma,-p}
\end{aligned}
\tag{8.27}
$$

When taking the continuum limit these expressions become

$$
\begin{aligned}
O_{\mathrm{CDW}^\pi} &= \sum_{\sigma} (\psi^\dagger_{L1\sigma}\psi_{R1\sigma} - \psi^\dagger_{L-1\sigma}\psi_{R-1\sigma}) \\
O_{\mathrm{OAF}} &= \imath \sum_{\sigma} (\psi^\dagger_{L1\sigma}\psi_{R-1\sigma} - \psi^\dagger_{L-1\sigma}\psi_{R1\sigma}) \\
O_{\mathrm{SC}^s} &= \sum_{\sigma} (\psi_{L0\sigma}\psi_{R0,-\sigma} + \psi_{L\pi\sigma}\psi_{R\pi,-\sigma}) \\
O_{\mathrm{SC}^d} &= \sum_{\sigma} (\psi_{L0\sigma}\psi_{R0,-\sigma} - \psi_{L\pi\sigma}\psi_{R\pi,-\sigma})
\end{aligned}
\tag{8.28}
$$

As usual (see Section 2.2) for the SC operators, the $q \sim 0$ component gives the dominant contribution, while for the OAF and CDW$^\pi$ the $q \sim 2k_F$ component is the one with the slowest decay. These operators have the same physical meaning than for the spinless case. Note that in the ladder of fermions with spins the spin sector is totally gapped (both the symmetric and antisymmetric mode are gapped). The spin degrees of freedom thus play *no role*. Because there are two spin modes, there are in fact *two* spin gaps in the system. Putting a uniform magnetic field, for example, would only kill the cosines containing the symmetric spin mode since it couples to the total spin density only.

To get the correct bosonized expression one has to pay extra care to the anticommuting Klein factors (there are here eight different fields to take care of!). This can be done by the methods of Section 4.3.2. One obtains

$$
\begin{aligned}
O_{\mathrm{CDW}^\pi} &= \frac{2}{\pi\alpha} e^{\imath\phi_{\rho+}} \cos\phi_{\sigma+} \sin\theta_{\sigma-} \\
O_{\mathrm{OAF}} &= \frac{2\imath}{\pi\alpha} e^{\imath\phi_{\rho+}} \sin\phi_{\sigma+} \cos\theta_{\sigma-} \\
O_{\mathrm{SC}^s} &= \frac{2}{\pi\alpha} e^{-\imath\theta_{\rho-}} \cos\phi_{\sigma+} \cos\phi_{\sigma-} \\
O_{\mathrm{SC}^d} &= \frac{2}{\pi\alpha} e^{-\imath\theta_{\rho+}} \sin\phi_{\sigma+} \sin\phi_{\sigma-}
\end{aligned}
\tag{8.29}
$$

From the bosonized form of these operators (simplified by the fact that $\langle\theta_{\rho-}\rangle = 0$ everywhere) and the expressions given in Table 8.2 one can deduce that sector

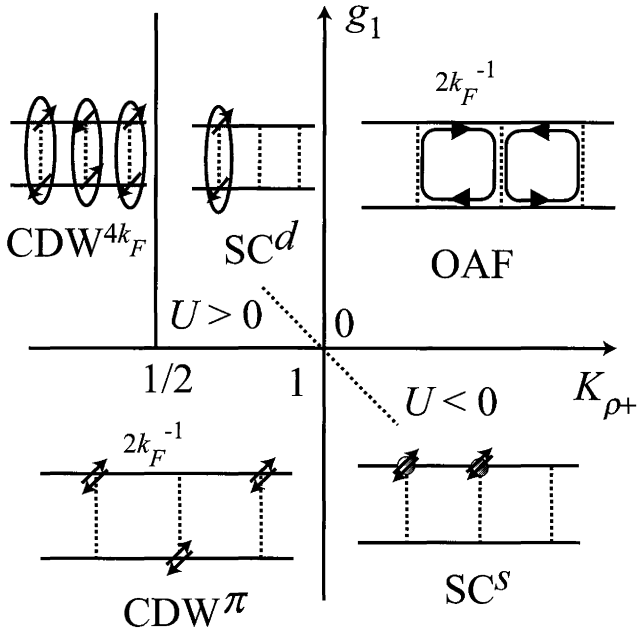

FIG. 8.6. Phase diagram of a ladder of fermions with spins as a function of the LL parameter of the symmetric charge mode $K_{\rho+}$ and the backscattering term g_1. All modes other than the totally symmetric charge mode are gapped. Possible phases are s- and d-wave superconducting phases (SC^s and SC^d), an orbital antiferromagnet with staggered orbital moments OAF and two charge density waves phases CDW$^{\pi}$ and CDW^{4k_F}. The dashed line indicates the phases reachable for a Hubbard model in the chains.

I is a SC^d phase, sector II an OAF phase, sector III a SC^s phase and sector IV a CDW$^{\pi}$ phase. In sector I there is another order parameter that competes with the SC^d one. It corresponds to a $4k_F$ charge density wave, as described in Chapter 4, where the *total* density is modulated with a period $4k_F$. Since this order parameter depends only on the total density it is simply given by

$$O_{\mathrm{CDW}^{4k_F}} \propto e^{i2\phi_{\rho+}} \tag{8.30}$$

Using (8.29) one sees that the SC^d order decays as $(1/r)^{1/(2K_{\rho+})}$ whereas the CDW^{4k_F} order decays as $(1/r)^{2K_{\rho+}}$. The CDW^{4k_F} thus dominates for $K_{\rho+} < 1/2$. The phase diagram is summarized in Fig. 8.6.

Note that for the pure Hubbard model, which corresponds to $V = 0$ in (8.26), one simply goes from the SC^d phase (for $U > 0$) to the SC^s phase (for $U < 0$). The other phases could be obtained for a more general model such as the extended Hubbard model. There are several observations on this phase diagram.

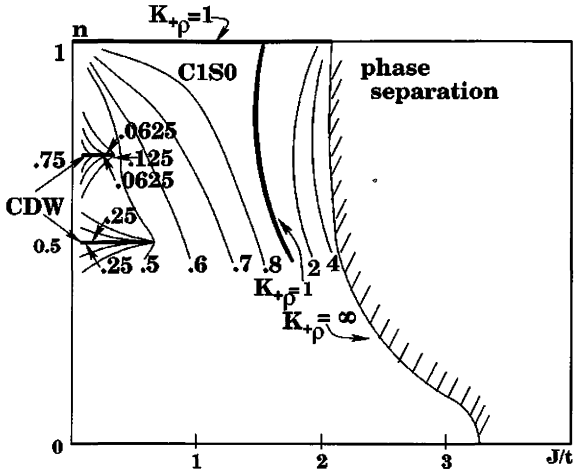

FIG. 8.7. Phase diagram of the t–J ladder obtained from DMRG, as a function of the electron density n and the ratio J/t. Values of the LL parameter $K_{\rho+}$ for the symmetric charge mode are indicated. There are Mott insulating phases for some range of the interactions for the commensurate densities $n = 1$, $n = 3/4$ and $n = 1/2$. (From White *et al.*, 2002 (Copyright (2002) by the American Physical Society).)

First, for repulsive interactions the physics we saw from the strong coupling t–J ladder is essentially correct and carries to arbitrarily weak interactions. The SDW instability of a single chain is suppressed because of the presence of the spin gap(s) and the dominant instability is a d-wave superconducting instability. Compare this phase diagram with the one of a single chain in Fig. 2.9. This is a very rare case where one can explicitly show that superconductivity is induced by purely repulsive interactions. This mechanism is the implementation in one dimension of the advocated RVB mechanism (Anderson, 1997). Another very interesting phase is the OAF phase. This phase has charge currents circulating on plaquettes of period π/k_F. Although this phase has no free spin because of the spin gaps, the orbital currents induce and orbital moment so this phase has still antiferromagnetic correlations of the orbital moment. It is the equivalent of the flux phases that have been studied in the case of the two-dimensional systems (Affleck and Marston, 1988). This phase has remarkable transport properties (Orignac and Giamarchi, 1997) and has been the subject of recent studies (Tsutsui *et al.*, 2001; Marston *et al.*, 2002).

The ladder phase diagram can also be studied numerically (Hayward and Poilblanc, 1996; White *et al.*, 2002), confirming the presence of dominant d-wave superconducting correlations. In Fig. 8.7, the phase diagram of a t–J ladder as obtained by a DMRG calculation is shown. The t–J and (extended) Hubbard

ladder described above, give of course the same physics when $J \ll t$ since this is the limit where one can map one model on the other for large repulsion. This is not the case for large J as we already noted in Chapter 7 for the Hubbard and t–J single chain. Although large J allows to reach values of $K_{\rho+}$ larger than one, it does not correspond to the attractive sector of the Hubbard or extended Hubbard model, and thus gives different phases.

The ladders thus offer an interesting bridge between the one- and the two-dimensional worlds. They possess many features that one would hope to find in the two-dimensional Hubbard model. Of course, many other physical properties are interesting to compute, for example what happens for a larger number of chains (Arrigoni, 1996; Kimura *et al.*, 1996*b*; Lin *et al.*, 1997).

When the filling becomes commensurate the ladders can become Mott insulators. This problem can be studied analytically (Lin *et al.*, 1998; Schulz, 1999; Le Hur, 2001; Tsuchiizu *et al.*, 2001) and numerically (White *et al.*, 2002). Because of the spin gap the critical values of $K_{\rho+}$ are different than for a single chain. However, they are again given by the same arguments based on the sine-Gordon mapping as described in Section 4.2. Some values are shown in Fig. 8.7.

8.2 Physical realizations of Ladders

Unfortunately, there are not that many realizations of fermionic ladder systems so far. In bulk systems a variation of the spin ladders that we have seen are made of fermionic ladders. Most experiments have been made on $Sr_{14}Cu_{24}O_{41}$ that has proved more easy to dope than $SrCu_2O_3$. The structure is shown in Fig. 8.8. In this system, there is transfer upon pressure of holes from the chains into the ladders. A superconducting phase under pressure (30 kbars) was obtained for the first time by Uchara *et al.* 1996 at low temperatures (10 K) in $Sr_{0,4}Ca_{13,6}Cu_{24}O_{41}$. The resistivity is shown in Fig. 8.9. It is thus tempting to attribute the superconductivity of this material to the superconductivity stemming from ladder physics as explained above. However, this interpretation poses several problems. First the superconductivity in ladders is inordinately sensitive to disorder, which suggests that if the ladders were well separated even a very weak disorder would make them insulating. It was thus suggested that the two-dimensional nature of this material was crucial in getting the superconductivity (much more than just stabilizing the one-dimensional phase), which seemed confirmed by later measurements of transverse conductivity, showing that transverse coherence strongly increases under pressure (Orignac and Giamarchi, 1997; Nagata *et al.*, 1998; Dagotto, 1999). The superconductivity in this material thus keeps its secrets for the moment.

One can also realize in principle ladders with more mesoscopic systems that we will see in the examples given in the next chapters, such as quantum wires, nanotubes, and Josephson junction arrays .

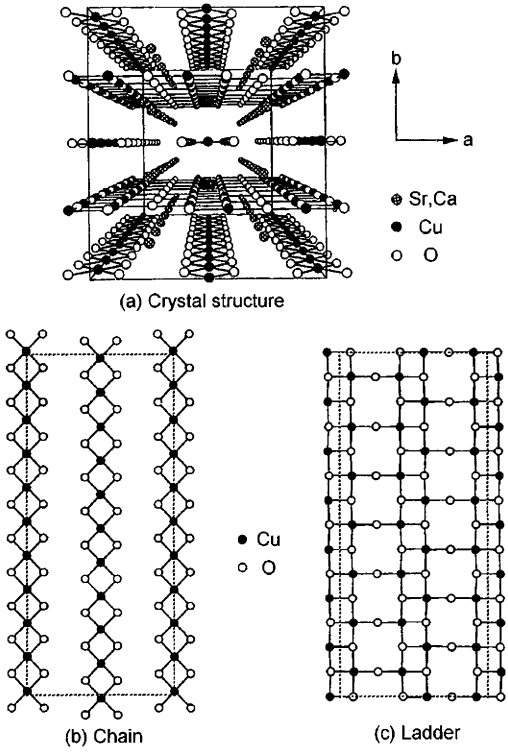

FIG. 8.8. The compound $Sr_{14}Cu_{24}O_{41}$ is made of a plane with CuO_2 chains, another plane with Cu_2O_3 chains and a plane with Sr. These planes are stacked along b. c is the direction parallel to chains and ladders and a the perpendicular direction. (From Magishi *et al.*, 1998 (Copyright (1998) by the American Physical Society).)

8.3 Infinite number of chains

Up to now we have kept a finite number of chains. In that case the physics remains very close to the one of a Luttinger liquid. The totally symmetric mode still gives the power law behavior with non-universal exponents. The other modes give different contributions, depending on whether they are gapped or not. However, as the number of chains increases the size of the gaps of many modes decreases. Thus, although the asymptotic physics at zero temperature is the one of a Luttinger liquid, if one works at finite temperature or looks at the physical properties at a given energy scale, many gaps will be smaller than this energy scale. The asymptotic physics is not important in that case, and it is a much better approximation to approach the problem from the opposite limit of the infinite number of chains. Let us thus see what happens in that case.

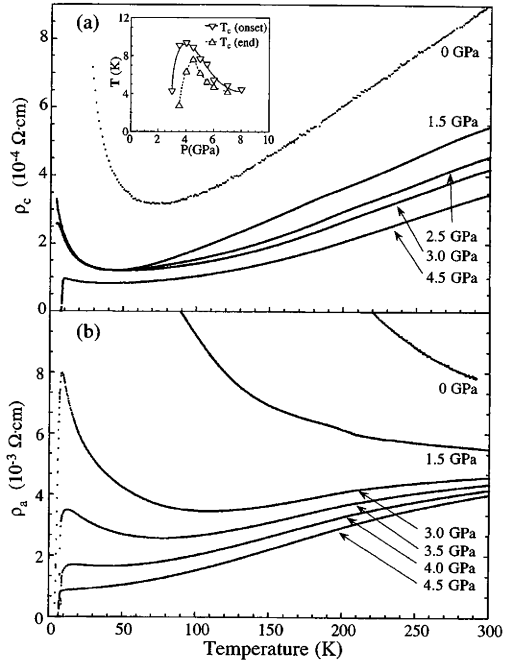

FIG. 8.9. (a) Resistivity of $Sr_{14-x}Ca_xCu_{24}O_{41}$ for various pressures. One clearly sees that the system under pressure becomes superconducting. (b) The transport transverse to the ladder direction strongly suggests that the system becomes two-dimensional again under pressure. (From Nagata *et al.*, 1998 (Copyright (1998) by the American Physical Society).)

8.3.1 *Hopping between chains*

Let us now consider the single electron hopping term between the chains (8.1) and restrict for the moment to hopping between nearest neighbors. In the absence of interaction it is easy to go to Fourier space. The hopping gives the energy (e.g. for one perpendicular direction)

$$\epsilon(k_\parallel, k_\perp) = -t_\parallel \cos(k_\parallel a) - t_\perp \cos(k_\perp b) \tag{8.31}$$

If the perpendicular hopping $t_\perp$ is much smaller than the parallel one $t_\parallel$, then (8.31) leads to the open Fermi surface of Fig. 8.10. We can see already on this simple example the effect of the interchain hopping. If one is at an energy scale (let us say, e.g. at a given temperature T) larger than the warping of the Fermi surface then the warping is washed out. In that case the system is indistinguishable from one with a flat Fermi surface. It can thus be considered as a one-dimensional system. There is no coherent hopping between the chains. On the other hand if the temperature is much smaller than the warping of the Fermi surface all correlation functions are sensitive to the presence of the warping, and

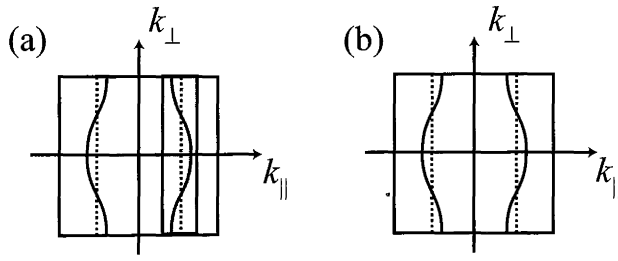

FIG. 8.10. (a) If the temperature (or any other external energy scale) is larger than the warping of the Fermi surface due to interchain hopping the system cannot feel the warping and is thus behaving as a one-dimensional system. (b) At lower temperature/energy the system feels the two (or three) dimensional nature of the dispersion. There is thus a dimensional crossover as the temperature/energy is lowered.

the system is two- or three-dimensional. We thus see that such a system has a *dimensional crossover* as a function of a parameter (temperature, frequency, energy, etc.). For free electrons, this crossover occurs at an energy scale of the order of the interchain hopping. This is summarized in Fig. 8.10.

An important question is of course how the interactions change this dimensional crossover. In order to determine this let us look at the renormalization of the interchain hopping (Brazovskii and Yakovenko, 1985; Bourbonnais and Caron, 1986; Wen, 1990*a*; Bourbonnais and Caron, 1991; Yakovenko, 1992; Boies *et al.*, 1995; Schulz, 1996*b*). If we look at second order in perturbation theory of let us say the partition function, the interchain hopping term contributes to

$$-t_\perp^2 \sum_{\langle i,j\rangle,\sigma} \int dr_1\, dr_2 \langle c_{i,\sigma}^\dagger(r_1) c_{i,\sigma}(r_2)\rangle \langle c_{j,\sigma}^\dagger(r_2) c_{j,\sigma}(r_1)\rangle \tag{8.32}$$

This term scales as $L^{4-2\zeta}$ where ζ is the single-particle Green's function exponent (see Chapter 3). Upon rescaling the renormalization equation for $t_\perp$ can thus easily be obtained

$$\frac{dt_\perp}{dl} = t_\perp(2-\zeta) \tag{8.33}$$

Note that this result is quite general. In the absence of interactions $\zeta = 1$ and we recover that $t_\perp$ is a relevant perturbation. We can determine the crossover scale by the energy at which the renormalized interchain hopping is of order one $t_\perp/W \sim 1$ where W is of the order of the intrachain hopping or the intrachain bandwidth. If we neglect the renormalization of ζ by the interchain hopping, then we have (Bourbonnais and Caron, 1986)

$$E^* \sim We^{-l^*} = W\left(\frac{t_\perp}{W}\right)^{\frac{1}{2-\zeta}} \tag{8.34}$$

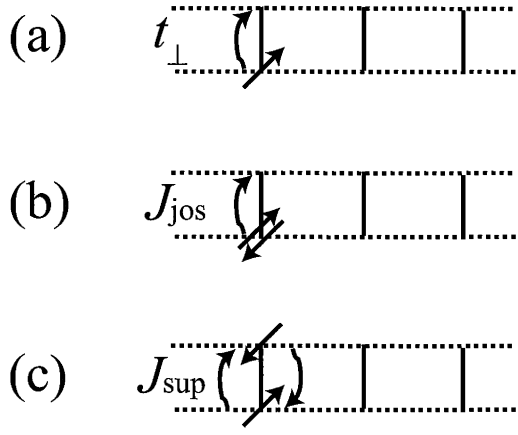

FIG. 8.11. (a) The single-particle hopping is renormalized by interactions since a particle that hops leaves behind particles (or holes) with which it interacts. The single-particle hopping generates at second order particle–particle (pair) hopping (Josephson coupling) shown in (b) and particle–hole (density–density interaction and superexchange) shown in (c). These couplings can become relevant even if the single-particle hopping itself is irrelevant.

We thus see that the interactions strongly renormalize the scale at which the dimensional crossover takes place. For the non-interacting case one recovers $E^* \sim t_\perp$. Since ζ for an interacting system is always larger than one, we see that the scale at which the dimensional crossover takes place is always *smaller* than for free fermions. Interactions thus tend to make the system more one-dimensional. If the LL parameter K is such that one can reach $\zeta > 2$ then (8.33) shows that $t_\perp$ is an irrelevant perturbation. Naively, one could think that this means that the system remains one-dimensional as the temperature is lowered. In fact the situation is slightly more complicated; I will come back to that. Why is the system more one-dimensional in the presence of interactions? This can easily be visualized if the interactions are attractive, in that case an electron that tries to hop leaves behind a particle to which it was attracted. This makes the hopping more difficult. With repulsive interactions it is the same mechanism, the attraction being between an electron and a hole rather than between two electrons. This is shown in Fig. 8.11.

This renormalization of the hopping between chains occurs due to the absence of single-particle excitations in a Luttinger liquid. Indeed, a naive tunneling formula would depend on the 'density of states', which indeed tends to zero in a Luttinger liquid (see Fig. 2.5). Worse situations induced by interactions can also happen. Indeed, if the system on each chain develops a gap, either, for example, by having a spin gap (e.g. for attractive interactions) or in the charge part (e.g. for commensurate filling by being a Mott insulator), it means that the

single-particle Green's function decays *exponentially.* The single-particle hopping is now an irrelevant variable. Physically this means that a single-particle cannot hop from one chain to the other without breaking a pair. The formation of a gap is thus in direct competition with the interchain hopping and leads to the so-called confinement of the particles in the chains. Of course, the single-particle hopping tends to break the gap so there is a competition between the two mechanisms.

8.3.2 *Two-body hopping*

One could naively conclude from the previous analysis that if α is large enough or if there is a gap, a weak enough $t_\perp$ is totally irrelevant. This is perfectly true as far as *single-particle* hopping is concerned, but it is not the end of the story. This is another example of an irrelevant operator hiding something that is in fact relevant (see Section 3.1). Let us look at the terms generated by the interchain hopping at second order. Among all the terms one can find terms of the form

$$\begin{aligned} J_1 &= t_\perp^2 \sum_{i,j,\sigma} \int dr_1\, dr_2\, c^\dagger_{i,\sigma}(r_1) c_{j,\sigma}(r_1) c^\dagger_{i,-\sigma}(r_2) c_{j,-\sigma}(r_2) \\ J_2 &= t_\perp^2 \sum_{i,j,\sigma} \int dr_1\, dr_2\, c^\dagger_{i,\sigma}(r_1) c_{j,\sigma}(r_1) c^\dagger_{j,-\sigma}(r_2) c_{i,-\sigma}(r_2) \end{aligned} \tag{8.35}$$

These terms are represented in Fig. 8.11. If r_1 and r_2 are different this represent the hopping of two uncorrelated particles. This mechanism is thus irrelevant if $t_\perp$ is irrelevant. However, one can consider the particular case where $r_1 = r_2$, that is, the case where the two objects (either two particles or a particle and a hole) jump at the same place and at the same time. In that case the process becomes

$$\begin{aligned} J_1 &\propto t_\perp^2 \sum_{\langle i,j\rangle,\sigma} \int dr_1\, c^\dagger_{i,\sigma}(r_1) c^\dagger_{i,-\sigma}(r_1) c_{j,\sigma}(r_1) c_{j,-\sigma}(r_1) \\ J_2 &\propto t_\perp^2 \sum_{\langle i,j\rangle,\sigma} \int dr_1\, c^\dagger_{i,\sigma}(r_1) c_{i,-\sigma}(r_1) c^\dagger_{j,-\sigma}(r_1) c_{j,\sigma}(r_1) \end{aligned} \tag{8.36}$$

The first process describes the hopping of a pair of electron from one chain to the other. One easily recognize the Josephson coupling. Written in bosonization language this process becomes (compare with the $O_{\rm SS}$ operator in (2.116))

$$J_1 \propto t_\perp^2 \sum_{i,j,\sigma} \int dr_1\, e^{i\sqrt{2}\theta_{\rho,i}(r_1)} e^{-i\sqrt{2}\theta_{\rho,j}(r_1)} \cos(\sqrt{2}\phi_{\sigma,i}(r_1)) \cos(\sqrt{2}\phi_{\sigma,j}(r_1)) \tag{8.37}$$

where I have used (see Appendix D)

$$c^\dagger_{i,\sigma}(r_1) c^\dagger_{i,-\sigma}(r_1) \propto e^{i\sqrt{2}\theta_{\rho,i}(r_1)} \cos(\sqrt{2}\phi_{\sigma,i}(r_1)) \tag{8.38}$$

If the interactions are such that the system opens a spin gap (see Fig. 2.9) then only the θ_ρ part remains, the $\cos(\sqrt{2}\phi_{\sigma,i}(r_1))$ giving then a constant as

explained in Section 2.3.2. If we interpret θ_ρ as the 'superconducting' phase, this is the standard expression of the Josephson coupling. The RG equation of this term can be easily written. It is simply

$$\frac{dJ_1}{dl} = J_1(2 - \frac{1}{K_\rho} - K_\sigma) \tag{8.39}$$

If the spin sector is gapped, one can formally replace K_σ by zero in the above equation. This equation is quite remarkable in connection with (8.33). Indeed, since (8.39) only contains $1/K_\rho$ it is clear that attractive interaction make J_1 more and more relevant. This goes well with the physics of a Josephson coupling that tends to order the superconducting phases of the whole system, and is thus favored by attractive interactions. On the other hand, the $t_\perp$ term itself has an exponent that contains both K_ρ and $1/K_\rho$ and is thus *irrelevant* if the interactions become *either* too attractive *or* too repulsive. We thus have here another example of the case of an operator that can be irrelevant itself but generate at a higher-order relevant operators if contracted in the proper way.

Physically, this means that for too attractive interactions the *single-particle* hopping is irrelevant. On the other hand, if the interactions become attractive enough it is perfectly possible and now much better for the particles to jump in pairs. Although this process is much smaller to start with since it is second order in $t_\perp$, it is relevant. This would remain perfectly true even if there is a gap in the proper sector, for example, a spin gap caused by attractive interactions since it will not prevent (in fact it helps) the Josephson term from becoming relevant. For repulsive interactions one has an identical mechanism with the term J_2. It corresponds to particle–hole hopping. It can easily be recognized as either a density–density coupling or a spin–spin exchange (superexchange) term of the form

$$\sum_{\langle\mu,\nu\rangle} \int dx [\vec{S}_\mu(x) \cdot \vec{S}_\nu(x) + \rho_\mu(x)\rho_\nu(x)] \tag{8.40}$$

If these processes where there alone they would lead to an ordered state. Indeed, both the Josephson coupling, the exchange and density–density couplings have well-defined classical limits. They can thus be treated by mean-field like approximations. This is exactly what we did for spin systems in Chapter 6. We could do the same thing here. Let me take, for example, the Josephson coupling. It can be rewritten as an effective 'pairing field'

$$-J \sum_{\langle\mu,\nu\rangle} \int dx\, e^{i\theta_{\rho,\mu}(x)} e^{-i\theta_{\rho,\nu}(x)} \simeq -\frac{J}{2} \sum_\mu \int dx\, Z \langle e^{-i\theta_{\rho,\nu}(x)}\rangle e^{i\theta_{\rho,\mu}(x)} \tag{8.41}$$

where Z is the connectivity of the lattice (compare with (6.88)). The averages have to be determined self-consistently. One can also extract the transition temperature from the RG equation. The transition occurs when the effective coupling becomes of order one. The transition temperature to the ordered state (here a

superconducting phase) is thus (neglecting again the renormalization of the LL parameter K_ρ by J and assuming one has attractive interactions so that the spin sector is gapped)

$$T_{x2} \simeq We^{-l^*} = W\left(\frac{J}{W}\right)^{\frac{1}{2-1/K_\rho}} \tag{8.42}$$

This is exactly identical to the result we would have obtained by treating the coupling in mean field (see (6.95)). Taking into account the renormalization of the Ks by J allows to get a more precise result.

We thus have two different phenomena taking place. On the one hand, the single-particle hopping induces a dimensional crossover at an energy scale determined by (8.34), which I call from now on T_{x1}. On the other hand, the interchain hopping generates couplings that want to induce an order state at a temperature that I call T_{x2}. We of course only know how to compute T_{x2} by the above method if the chains stay in the one-dimensional limit, that is, if $T_{x2} > T_{x1}$. Otherwise if the dimensional crossover happens first the transition to an ordered state should be computed from the proper two- or three-dimensional limit (e.g. starting from a Fermi liquid theory) and the above result for T_{x2} has no meaning any more. Usually, these two-particle processes being of order $t_\perp^2$ are much smaller than the single-particle hopping and thus one is dominated by the single-particle hopping. The system has a dimensional crossover way before these processes can play a role. But in one dimension the things are more subtle if the interactions are strong enough .

How can we take both processes into account? One can write the renormalization equations for all the couplings. Of course, the two-particle hoppings are zero initially but they will get generated. Indeed, we saw that putting two hoppings at the same point (in space–time) is equivalent to a two-particle hopping. Thus, one has

$$-t_\perp^2 \int\int_{|r_1-r_2|<\alpha} dr_1 \int dr_2 \to -t_\perp^2 \alpha^2 \int dr_1 \equiv J \int dr_1 \tag{8.43}$$

Thus, if in a renormalization procedure one changes $\alpha \to \alpha + d\alpha$ there is a contribution to J coming from the $t_\perp^2$ term. Let us take, for example, the case of single-particle hopping and spin exchange J_S.

$$\begin{aligned} \frac{dt_\perp}{dl} &= (2 - \frac{1}{4}(K_\rho + K_\rho^{-1}) - \frac{1}{4}(K_\sigma + K_\sigma^{-1})) \\ \frac{dJ_S}{dl} &= (2 - K_\rho - K_\sigma)J_S + t_\perp^2 \end{aligned} \tag{8.44}$$

There are equivalent equations for the density–density and Josephson coupling. For spin isotropic repulsive interactions $K_\sigma = 1$. The $t_\perp^2$ term in the second equations shows the generation of the spin exchange by the single-particle hopping. $t_\perp(l) \sim 1$ and $J_S(l) \sim 1$ define, respectively, the dimensional crossover T_{x1} and the transition to an ordered state T_{x2}. The result is shown in Fig. 8.12. If $t_\perp$ is

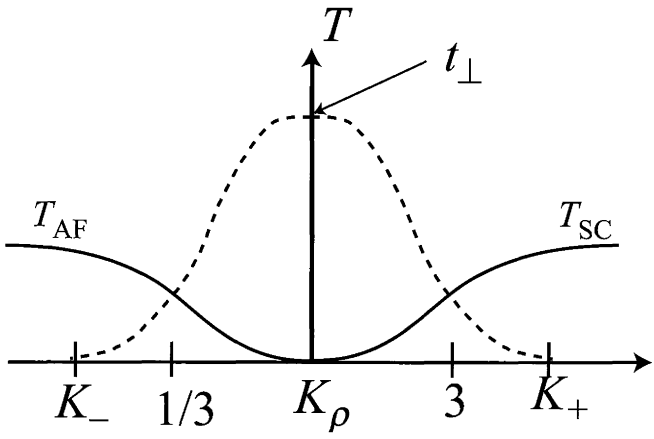

FIG. 8.12. Crossover temperatures. If $t_\perp$ is small and the interactions not too strong the crossover due to single-particle hopping (dashed line) occurs first. The system thus stops to be one-dimensional before being able to order. If the interactions are strong enough the single particle hopping is weakened and can even become irrelevant both for attractive ($K > K_+$) or repulsive enough ($K < K_-$) interactions. However, it always generates a two particle (or particle–hole) hopping that drives the system to an ordered state. For repulsive interactions, the system becomes antiferromagnetic at the temperature $T_{\rm af}$ and for attractive ones, superconducting at the temperature $T_{\rm sc}$. (After Schulz, 1996*b*.)

very small or the interactions not too large $T_{x1} > T_{x2}$. In this case of course T_{x2} should be recomputed properly. This is the difficult case since we now flow to a two- or three-dimensional system that is still in the 'normal state'. Since in such system the interactions can still be strong the resulting low-dimensional phase is a complicated problem. Even if it is a Fermi liquid, since this Fermi liquid stems from the high temperature non-Fermi liquid phase, its features are certainly quite special. Determining its characteristics is a major challenge. Note that the RG analysis is quite useless in this respect since the flow goes to strong coupling so one needs other techniques below T_{x1}. Studying these techniques would take us too far and I refer the reader to Biermann *et al.* 2002 for a review of some attempts that have been made to tackle this problem. Note that I mostly talked here about temperature, but any energy scale will do. In particular if one studies optical conductivity, the frequency also allows to scan through the dimensional crossover. If the interactions become too strong then $T_{x1} < T_{x2}$. This case is of course much more easy to analyze, since in that case one can use more simple mean field approaches as seen in Chapter 6.

To finish, let us see what happens when there is a charge or spin gap. The energy scales are still given by the flow (8.44) to which one should add (2.140)

to get the flow of K_ρ (for a charge gap). Of course, there are now also terms depending on $t_\perp$ in the flow but if $t_\perp$ is very small one can ignore them. If the flow for the term that creates the gap (e.g. the umklapp) reaches strong coupling first then the gap is formed and the single-particle hopping is suppressed. On the other hand, if $t_\perp$ reaches a value of order one before the gap is formed then the single-particle hopping induces the dimensional crossover and the gap does not form (at least not because of the one-dimensional physics). A rule of thumb to get the position of this deconfinement transition is thus to compare the two scales l_{x1} and l_Δ for which $t_\perp$ and the umklapp reaches order one. Thus, roughly if $T_{x1} > \Delta$ one is deconfined, whereas for $T_{x1} < \Delta$ the gap wins and the chains are confined, only allowing for two particles hopping. Of course, this is only a rule of thumb and one should, in principle, solve the full coupled problem. More on this question can be found in Bourbonnais and Caron (1991), Yakovenko (1992), Schulz (1996*b*), Giamarchi (1997), Tsuchiizu and Suzumura (1999) and Tsuchiizu *et al.* (2001).

8.4 Organic quasi-one-dimensional conductors

A wonderful system to study these questions is provided by the Bechgaard salts $TMTSF_2X$. These were the first organic compounds to exhibit superconductivity, and have thus been the focus of intense experimental and theoretical studies. In addition to the superconducting phase, these materials have an extremely rich phase diagram and exhibit a host of remarkable properties (e.g. non-FL metallic behavior, quantized Hall conductance, Fröhlich conductivity), many of which are still poorly understood. It is of course impossible to study all the fascinating properties of these materials here. For more extensive reviews of the physical properties of quasi one-dimensional organics, see for example, Jérome and Schulz (1982), Jérome (1994) and Bourbonnais and Jérome (1999).

All these compounds crystallize in stacks of TM (short for TMTSF or TMTTF) molecules separated by the counterions X (for example PF_6 or ClO_4) as shown in Fig. 8.13. These molecules have double bonds between the carbon atoms and the π orbitals of the selenium atoms. In the parent TMTTF compounds (Fabre salts), the selenium atoms are replaced by sulphur ones. The counterions are here to provide the charge neutrality, as in a standard salt. The transfer of charge between the ion and the TM stacks is total. Since there is one ion for two TM molecules, the chains are quarter-filled. In addition the chains are slightly dimerized. It is important to note that the commensurate filling is fixed by the chemistry of the compound, and so far it has not been possible to move away from such a commensurate filling. No doubt that if this could be done this would prove very interesting.

The overlap of the π orbitals of the selenium or sulphur atoms leads to a high mobility of electrons along the stacking direction; the hopping integrals in the perpendicular directions are indeed smaller by more than one order of magnitude. Estimated values of the hopping integrals along the stack direction (a-axis) and the two perpendicular axes pointing towards neighboring stacks (b-axis) and

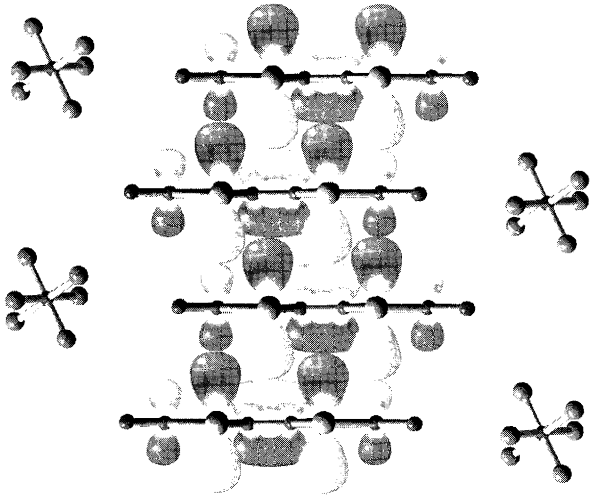

FIG. 8.13. Structure of the Bechgaard salts $(TMTSF)_2X$. Electronic transport takes place preferentially along the stacks of TMTSF molecules (vertical, a-axis). The horizontal axis (c-axis) for which the stacks are separated by the counterions is the least conducting one. (From Bourbonnais and Jérome, 1999 (Copyright (1999), with permission by Elsevier), figure courtesy of J.Ch. Ricquier.)

towards the anions (c-axis), respectively, are: $t_a : t_b : t_c = 1000K : 100K : 30K$. Therefore, one can think of these materials as one-dimensional chains coupled by small interchain hoppings. Given the hierarchy of transverse coupling the system is first expected to become two-dimensional and then three-dimensional at low temperatures. At very low temperatures the system has various ordered phases (spin-Peierls (SP), antiferromagnetic (AF), spin-density wave (SDW)) and superconducting (SC)). The nature of the molecule (TMTTF versus TMTSF) or of the ions slightly changes the interchain hopping and the dimerization. Such changes can also be induced by applying pressure to the system. This modifies the relative importance of the kinetic energy and Coulomb interaction and leads to a very rich phase diagram. The chemical and pressure changes have similar effects, which can be summarized by the unified phase diagram of Fig. 8.14.

Experimentally, at ambient pressure, the $(TMTTF)_2PF_6$ compound displays insulating behavior (MI). Upon increasing pressure, a transition to a metallic phase is found, and the properties of the TMTTF compounds evolve toward those of the compounds of the TMTSF family, which are good conductors. This evolution is clear from the a-axis resistivity measurements in Fig. 8.15. The minimum of the resistivity (followed by an activated law as temperature is lowered)

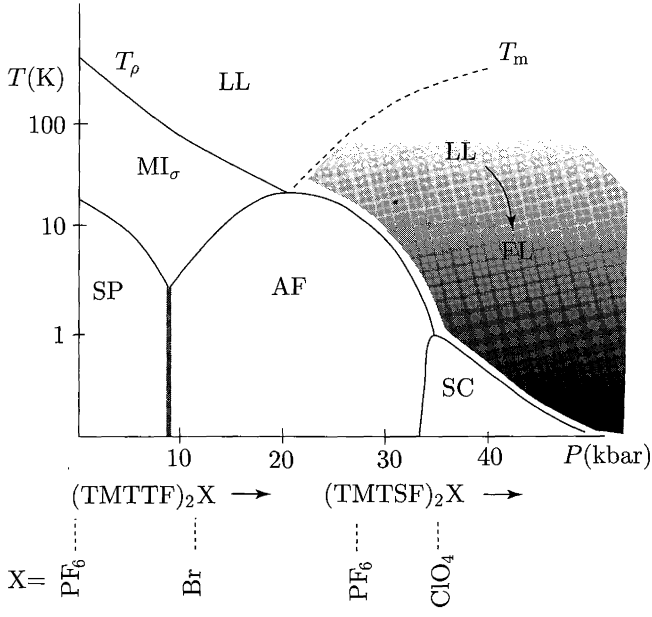

FIG. 8.14. Unified experimental phase diagram for the TM compounds. Either pressure or chemical changes (increasing pressure corresponds to going from the TMTTF to the TMTSF family and changing the anions) yields the same phases (MI: Mott insulator, LL: Luttinger liquid metal, FL: Fermi liquid metal, SP: spin-Peierls, AF: antiferromagnetic spin-density wave, SC: superconducting). The TMTTF family is insulating at ambient pressure whereas the TMTSF family shows good metallic behavior at room temperature. (From Bourbonnais and Jérome, 1999 (Copyright (1999), with permission by Elsevier).)

defines the onset of the MI regime on Fig. 8.14. Such an insulating behavior is well consistent with what one would expect for a one-dimensional Mott insulator (see Section 7). Since the chains are dimerized such a Mott insulating behavior could come either from the half-filled nature of the band (because of the dimerization), or if the interactions are large enough from the quarter-filled nature of the band (see Section 4.2). I will come back to this point later. It is thus clear that the interactions play a crucial role in the TMTTF family even at relatively high energies. For the TMTSF, the question is more subtle in view of the metallic behavior at ambient pressure and it was even suggested that such compounds could be described by a FL behavior with weak interactions (Gorkov, 1997). Another important question is of course the reason for such a difference between the very close families TMTTF and TMTSF, for which the various characteristics (bandwidth, dimerization, interactions) vary relatively little.

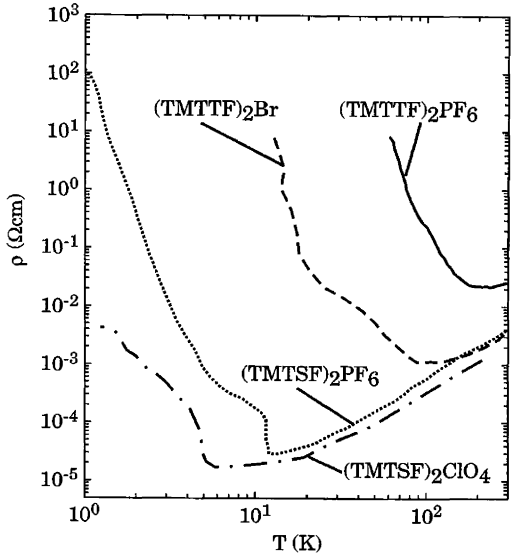

FIG. 8.15. Resistivity along a-axis for a series of compounds showing the gradual evolution to metallic behavior as pressure is increased. (From Vescoli *et al.*, 2000 (Copyright (2000) by EDP Sciences).)

A blatant proof of the importance of interactions for *both* the TF and SF compounds is provided by the optical conductivity (Dressel *et al.*, 1996; Schwartz *et al.*, 1998), as shown in Fig. 8.16. The optical conductivity clearly shows that the high-energy structure is the one of a Mott insulator, with a decreasing gap (of the order of 2000 cm^{-1} for the $TMTTF_2(PF_6)$ to 200 cm^{-1} for $TMTSF_2(PF_6)$. Nearly (99%) of the spectral weight is in this high-energy structure. In the metallic compounds there is in addition a very narrow Drude peak. The optical conductivity shows thus clearly that this compounds are very far from simple Fermi liquids. The data of optical conductivity can be compared with the expectations for a one-dimensional Mott insulator (see Fig. 7.12) as shown in Fig. 8.17. The data above the gap fits very well the power law LL behavior and thus shows quite convincingly that these compounds are indeed well described by a LL theory down to a scale of a few hundred Kelvin (temperature or frequency). This is the first direct proof of a Luttinger liquid behavior in an electronic system.

The a-axis optical measurements described above even allow for a quantitative determination (Schwartz *et al.*, 1998) of the LL parameter K_ρ, yielding $K_\rho \simeq 0.23$, indicating very strong electron–electron interactions. This estimate of the LL parameter agrees reasonably well with measurements of the longitudinal resistivity in the range 100–300K (Jérome, 1994). The optical data is consistent with an interpretation of the insulating state as a quarter-filled Mott insulator, suggesting that the dimerization plays little role at least in the TMTSF family. I refer the reader to Schwartz *et al.* 1998 for more discussion on this point. These

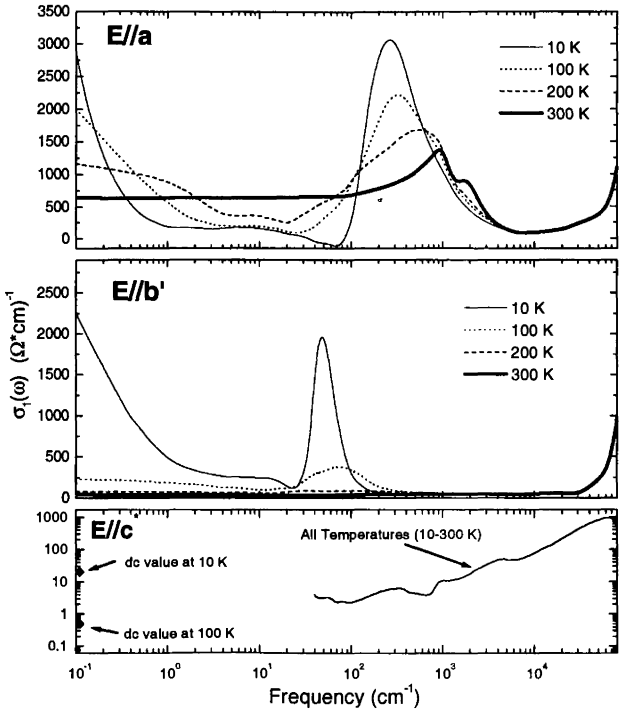

FIG. 8.16. Optical conductivity along the three axis for $TMTSF_2(ClO_4)$, at various temperatures. Although such compound seems to have a rather 'standard' dc conductivity, all the dc transport is in fact due to a very narrow Drude peak containing only 1% of the spectral weight, whereas 99% of the spectral weight is above an energy gap (of the order of 200 cm^{-1}), and is reminiscent of a Mott insulating structure. Depending on the temperature a different behavior is observed along the b direction which signals a dimensional crossover from essentially uncoupled chains to coherent planes. (From Henderson *et al.*, 1999 (Copyright (1999) by EDP Sciences).)

results are in good agreement with other measurements. The measured values of K_ρ are consistent with the photoemission data (Dardel *et al.*, 1993; Vescoli *et al.*, 2000). Photoemission in these system should be looked at with a grain of salt because of possible surface problems due to the ionic nature of the system (for other systems see, e.g. Denlinger *et al.*, 1999). The optical data along the c-axis (Henderson *et al.*, 1999) is consistent with the predictions of LL (Georges *et al.*, 2000). These measurements directly probe the density of excited states in the a-b plane. We note however that, although clearly revealing that electrons are confined in the chains above $\sim$ 100K, the measurements of dc transport along the c-axis (Moser *et al.*, 1998) (see Fig. 8.18) are not yet fully understood theoretically from a LL picture (see Georges *et al.*, 2000 for a discussion).

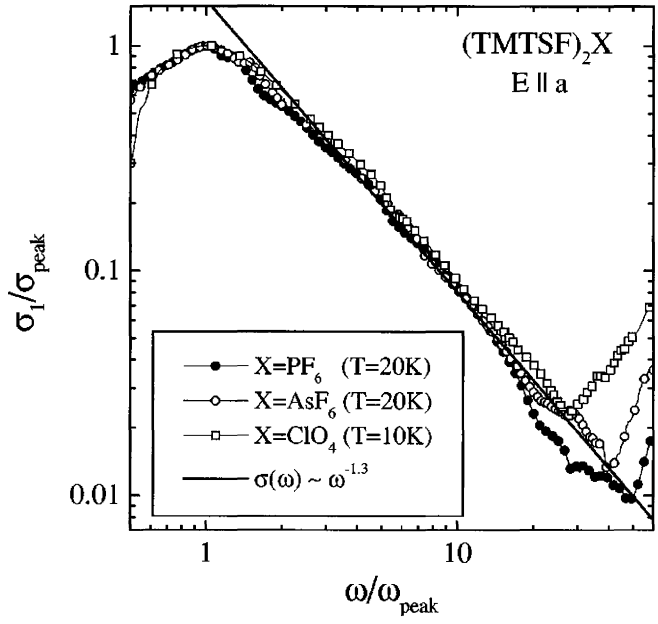

FIG. 8.17. Optical conductivity along the chain axis in the TMTSF family. The conductivity is rescaled by the gap in various samples. A fit of the ω dependence of the conductivity above the gap is well consistent with Luttinger liquid behavior. (From Schwartz *et al.*, 1998 (Copyright (1998) by the American Physical Society).)

These compounds are of course excellent systems to study the deconfinement transition discussed in the previous section. Since the isolated chains would be insulators the system will thus crossover from a regime where one has essentially uncoupled (insulating) chains to one of metallic planes. A dimensional crossover is observed in the optical conductivity along the b direction (intermediate axis perpendicular to the chains) as shown in Fig. 8.16. Transport along the c-axis shown in Fig. 8.18 would be also consistent with such an interpretation. From this experiment, we see that the dimensional crossover takes place around 100K in $(TMTSF)_2PF_6$. This is in agreement with the change of behavior from T (LL behavior) to T^2 observed in dc transport along the a axis (Jérome, 1994), and with the change of behavior in the transverse optical conductivity . The interpretation of the change of behavior between the insulating and metallic regimes as due to such deconfinement transition (Giamarchi, 1997) can be strengthened by the optical data (see Fig. 8.19). A measure of the gap extracted from the optical conductivity shows that the change of nature occurs when the observed gap is roughly of the order of magnitude of the interchain hopping (Vescoli *et al.*, 1998). There are, however, many mysteries in these compounds. In particular, the nature of the normal phase below 100K is very far from being understood. This

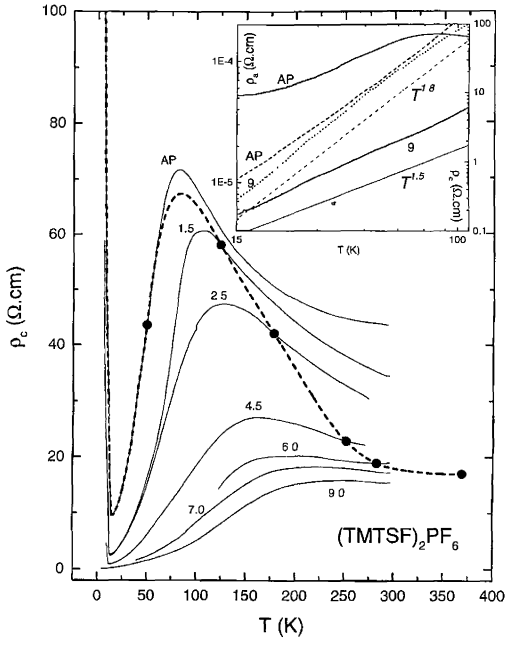

FIG. 8.18. Transport along the least conducting axis. This is in effect a tunneling experiment between the *ab* planes and thus a measure of the single-particle density of states in such planes. In the one-dimensional regime, there is no single-particle excitation and the resistivity increases with decreasing temperature, whereas when the chains couple coherently one recovers a more conventional (metallic) behavior. The one-dimensional Mott insulating behavior also leads to an insulating-like resistivity. The increase of resistivity with decreasing temperature is thus linked to the one-dimensional regime, whereas the metallic regime corresponds to a regime where the chains are coupled. The maximum in resistivity thus measures the scale for the dimensional crossover. (From Moser *et al.*, 1998 (Copyright (1998) by EDP Sciences).)

phase shows in particular very anomalous NMR behavior (Bourbonnais *et al.*, 1984). I refer the reader to Bourbonnais and Jérome (1999) and Biermann *et al.* (2002) for more details.

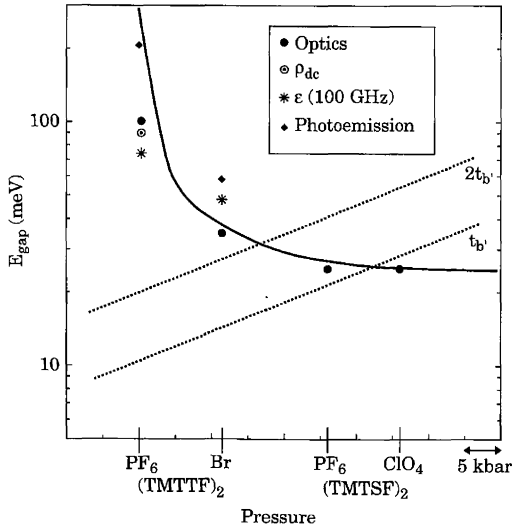

FIG. 8.19. A comparison of the measured gap in the optical conductivity with the interchain hopping. The change of behavior from insulator to metallic occurs when the two quantities are of the same order of magnitude showing that the difference between the various members of the TM families is indeed linked to a deconfinement transition. (From Vescoli *et al.*, 2000 (Copyright (2000) by EDP Sciences).)

9

DISORDERED SYSTEMS

One of the advantages of being disorderly is that one is constantly making exciting discoveries.

A. A. Milne

So far we have been interested in infinite and clean systems. Many of the experimental realizations of Luttinger liquids however present additional challenges. The first complication comes from the presence of the disorder. Disorder is ever present, or can be artificially introduced in a controlled way. As we will see it has particularly powerful and interesting effects in one dimension. Even if we have by now a good understanding of the effects of disorder in a Fermi liquid, we are far from having reached the same level of understanding in a Luttinger liquid.

Other challenging problems come from the size of the devices itself and the constraints that one is able to impose on them. Indeed, because many realizations of one-dimensional systems are made using nanotechnology, the size of the sample is usually relatively small. This is, for example, the case for quantum wires and nanotubes. In such systems it is also possible to impose special boundary conditions at a given point (boundary, single impurity, etc.). I examine these effects in the two coming chapters and discuss their consequences for some realizations of Luttinger liquids.

9.1 Effect of disorder; Anderson localization

The question of disorder in Luttinger liquids is an extremely challenging one. Indeed, even in higher dimensions the effects of disorder are mostly to be understood. For free electrons we know that disorder can give rise to very strong effects such as Anderson's localization. When interactions are included the question is largely open. Before we move on to Luttinger liquids let us examine some of the questions and techniques for disordered systems in more details.

9.1.1 *Generalities on disordered systems*

Quite remarkably disorder in fermionic systems exhibits marked differences with disorder in classical systems. Indeed, the very existence of a Fermi energy E_F 'reduces' the effects of disorder since the relative strength of the disorder compared to the Fermi energy D/E_F or the mean free path compared to the Fermi length $k_F l$ now becomes the relevant parameter. Of course, nature would not remain as simple as that and quantum effects lead in fact also to reinforcement of disorder effects and turn in low dimensions a free electron system into an insulator, as pointed out in Anderson (1958) and Mott and Twose (1961). We

have now gained a very good understanding of the properties of such disordered free electron systems. To tackle them an arsenal of methods ranging from diagrams (Lee and Ramakhrishnan, 1985) to scaling theory (Abrahams *et al.*, 1979), replicas (Wegner, 1979; Efetov *et al.*, 1980), supersymmetry (Efetov, 1983) have been developed. Because of quantum effects, disorder, if strong enough, can lead to a complete localization of the electrons. The wave function decays exponentially with a characteristic length known as localization length ξ_{loc}. The system is thus an insulator with a resistance increasing exponentially with the size of the system as $\rho \sim e^{L/\xi}$. In three dimensions, the disorder needs to be larger than a certain threshold to cause the localization. Weak disorder leaves the system metallic with a finite conductivity. Disorder can thus induce a metal insulator transition. In two dimensions, the scaling theory predicts that a free electron system is always localized. However, the localization length can be very large, of the form

$$\xi_{\text{loc}} \sim l \exp\left[\frac{\pi}{2} k_F l\right] \tag{9.1}$$

where l is the mean free path. In one dimension, the situation is much more drastic, and one finds from exact solutions (Berezinskii, 1974; Abrikosov and Rhyzkin, 1978) that the localization length is of the order of the mean free path itself. It means that after bumping a couple of times on the impurities the electrons are localized. This shows already that there are important differences for the disorder effects between the one-dimensional world, where localization occurs because electrons bump back and forth between impurities and the higher dimensional world where Anderson's localization is a rather subtle interference mechanism.

Life becomes much less simple when interactions among fermions are taken into account. The naive approach would be to say that for a Fermi liquid interactions are not so important and the free electron picture is a good starting point. This is certainly true, at least from a practical (that is, experimental) point of view if the disorder is very weak and the localization length is large. Note that if we had considered bosons instead of fermions then interactions would have to be included from the start. I will come back to this interesting case in Section 11.1. But both from a conceptual point of view and for practical purposes, when the disorder is moderately strong this intuitive feeling that interactions should not play a major role is totally incorrect. Even if in the pure system interactions can be 'removed' from the system by resorting to Fermi Liquid theory, this is not the case when disorder is present. Because disorder renders electrons slowly diffusive rather than ballistic, they feel the interactions much more strongly, with explosive results (Finkelstein, 1984; Altshuler and Aronov, 1985; Lee and Ramakhrishnan, 1985; Abrahams *et al.*, 2001). Effective interactions increase when looking at low-energy properties and Fermi liquid theory breaks down. In addition, when the dimension is small or the interactions strong to start with (like in systems undergoing Mott transitions) it is of course impossible to start from the non-interacting limit and one has to solve the full problem.

In that respect one dimension is a very interesting case. The separate effects of disorder and interactions are at their strongest. The disorder gives rise in the non-interacting system to a very strong localization. Since there is no diffusive regime the derivation used in higher dimensions for the increase of interactions cannot be applied, but one would naively expects similar effects to hold. If the electrons cannot move, then the interactions will be felt differently: either not at all if the electrons are pinned at different points in space, or extremely strongly if they are trapped at the same place. The interactions also give rise to extremely strong effects, as we saw in the rest of the book. In particular, the charge susceptibility in one dimension is divergent at $2k_F$. One can thus expect very strong response to any potential having such Fourier components, which is the case of the disorder (it is present at all wavevectors) and thus a strong reinforcement of the disorder due to the Luttinger liquid effects.

Before we move on to the study of the one-dimensional problem, let us see which tools of our theoretical toolbox one can use to tackle a disordered problem. If we put a random term in our Hamiltonian, then every observable depends on the specific realization of the random potential. What is needed is then to take an average of these observables with respect of the probability distribution of the disorder to get the average response of the system. This is of course a theoretical trick. A real experimental system has usually only one realization of the disorder, and the self-averaging comes from the fact that the system is large enough so that little pieces of the system more or less behave as independent sub-systems. Solving the problem for a given specific realization of the disorder and averaging afterwards is of course a totally impossible program. In addition of being impossible it is in general stupid, since a given realization of the disorder breaks many symmetries of the system. Since a given realization of the disorder is not invariant by translation, all correlation functions depend now on both coordinates x and x' at which they are computed and not simply on the difference $x - x'$ as in a translationally invariant system. On the other hand, the *averaged* correlation function is invariant by translation so it is much simpler. Of course, averages can be done order by order in a perturbation theory, but if one wants to go beyond perturbation one wants a method to average over disorder *from the start*. Unfortunately, many techniques that were useful for the non-interacting systems (such as supersymmetry) fail when interactions are included. I present here a quite general method that still works and is known as the replica method. We will barely use it in this book, but since it is a fairly important method I still feel it is worth having seen it at least once in one's life. The other useful method is the dynamical method (the so-called Keldysh technique) but it is of a more complex use. For a recent review on dynamical methods see Kamenev (2002).

Let us assume we want to compute the average value of some observable O for a system with a random potential V. The average value can be written as a functional integral over the configurations of the system as

$$\langle O\rangle_V = \frac{\int \mathcal{D}\phi O(\phi) e^{-S_V(\phi)}}{\int \mathcal{D}\phi e^{-S_V(\phi)}} \tag{9.2}$$

where $S_V(\phi)$ is the action of the system for a given realization of the random potential V. Of course, $\langle O\rangle_V$ depends on V itself, so we have to average over all realizations of V. If we assume that the disorder has a probability distribution $p(V)$ the average over disorder is

$$\overline{\langle O\rangle} = \frac{\int \mathcal{D}V p(V)\langle O\rangle_V}{\int \mathcal{D}V p(V)} \tag{9.3}$$

In general, $S_V(\phi)$ is linear in V, something like

$$S_V = S_0(\phi) + \int dx\, d\tau\, V(x) A(\phi(x,\tau)) \tag{9.4}$$

Note that for a quantum problem the disorder is time independent. For the disorder one takes in general a gaussian disorder. This is very often justified by the central limit theorem.[35] For example using a distribution

$$p(V) = e^{-\frac{1}{2D}\int dx\, V(x)^2} = e^{-\frac{1}{2D\Omega}\sum_q V_q^* V_q} \tag{9.5}$$

corresponds, using the techniques explained in Appendix C, to the average

$$\overline{V(x)V(x')} = D\delta(x-x') \tag{9.6}$$

I will come back to the physical significance of this type of disorder in the next section. With distribution (9.5) it would be very easy to perform the average (9.3) if it were not for the denominator in (9.2). Indeed, in the absence of such denominator one has

$$\frac{1}{\int \mathcal{D}V e^{-\frac{1}{2D}\int dx V(x)^2}} \int \mathcal{D}V e^{-\frac{1}{2D}\int dx V(x)^2} e^{-\int dx \int d\tau V(x) A(\phi(x,\tau))}$$
$$= e^{\frac{D}{2}\int dx \int d\tau \int d\tau'\, A(\phi(x,\tau))A(\phi(x,\tau'))} \tag{9.7}$$

One would end up with an effective action where the disorder has been eliminated and has given after average an interaction term so the action would be

$$S_{\text{eff}} = S_0(\phi) - \frac{D}{2}\int dx \int d\tau \int d\tau'\, A(\phi(x,\tau))A(\phi(x,\tau')) \tag{9.8}$$

we could then treat this problem using our favorite method since it would not be more complicated than the type of problems that we already encountered in this book. Compare in particular with the integration over phonons for the spin-Peierls transition in Section 6.2.

[35] And also because these are essentially the only integrals one knows how to do!

Unfortunately, the presence of the denominator in (9.2) prevents us from doing the average as in (9.7). The idea of the replica method (Edwards and Anderson, 1975) is thus to get rid of the denominator and to transform it into a numerator. As with any really great method the idea is very simple. One can rewrite

$$\frac{1}{\int \mathcal{D}\phi e^{-S_V(\phi)}} = \left[\int \mathcal{D}\phi e^{-S_V(\phi)}\right]^{n-1} \tag{9.9}$$

with $n = 0$. If we forget $n = 0$ for a moment and consider n as a positive integer $n = 2, 3, 4, \ldots$, then

$$\left[\int \mathcal{D}\phi e^{-S_V(\phi)}\right]^{n-1} = \left[\int \mathcal{D}\phi_2 e^{-S_V(\phi_2)}\right] \cdots \left[\int \mathcal{D}\phi_n e^{-S_V(\phi_n)}\right] \tag{9.10}$$

where we have introduced the fields ϕ_2, ϕ_3, etc. The denominator can thus be rewritten as the product of $n-1$ copies. The average (9.2) can thus be rewritten

$$\begin{aligned}\langle O\rangle_V &= \left[\int \mathcal{D}\phi_1 O(\phi_1) e^{-S_V(\phi_1)}\right]\left[\int \mathcal{D}\phi_2 e^{-S_V(\phi_2)}\right] \\ &\quad \left[\int \mathcal{D}\phi_3 e^{-S_V(\phi_3)}\right] \cdots \left[\int \mathcal{D}\phi_n e^{-S_V(\phi_n)}\right] \\ &= \int \mathcal{D}\phi_1 \mathcal{D}\phi_2 \ldots \mathcal{D}\phi_n O(\phi_1) e^{-\sum_{a=1}^{n} S_V(\phi_a)}\end{aligned} \tag{9.11}$$

There is no denominator anymore. The price to pay is the introduction of n copies of the system. Of course, one would only recover (9.2) if one can take the limit $n \to 0$ at the end. Before averaging over disorder in (9.11) all replicas (copies) are independent. Since there is no denominator in (9.11) one can do the average over disorder in the manner described above. One thus finds

$$\overline{\langle O\rangle} = \int \mathcal{D}\phi_1 \mathcal{D}\phi_2 \ldots \mathcal{D}\phi_n O(\phi_1) e^{-S_{\text{eff}}} \tag{9.12}$$

where the effective action is now

$$S_{\text{eff}} = \sum_{a=1}^{n} S_0(\phi_a) - \frac{D}{2} \sum_{a=1,b=1}^{n} \int dx \int d\tau \int d\tau' \; A(\phi_a(x,\tau)) A(\phi_b(x,\tau')) \tag{9.13}$$

This is nearly the same form except that now one has n fields and the interaction couples all fields together. We have thus traded a disordered system with only one field for a clean interacting problem of n coupled fields. Of course, the second one is more complicated due to the presence of the n fields, but as explained before we should be more equipped to tackle it. One important difficulty is of course that we should obtain a good enough solution for any n to be able to make the analytic continuation to $n \to 0$ at the end, since it is only in this limit that one

recovers the disordered solution. Taking this limit is far from being obvious and contains hidden difficulties that I will briefly allude to later in this chapter.

A few remarks to conclude. The interaction in (9.13) is totally non-local in time. This is a direct consequence of the fact that the disorder is time independent. In Fourier space this would mean that the frequency is conserved upon scattering on the impurities. This is very useful for the non-interacting problem since it allows to solve for a given energy, but for the interacting problem this does not help much. The fact that the effective interaction between replicas is non-local in time is a pain in the neck. A final remark for the professionals of diagrams: the role of replicas in a perturbative expansion is simply to remove the diagrams that are disconnected *before* the averaging over the disorder. Such diagrams correspond to connected diagrams when one uses the replicated action (9.13), and thus remain in the perturbative expansion. However, they are proportional to n and thus vanish in the $n \to 0$ limit, as they should since they correspond in fact to a disconnected process.

9.1.2 *Collective versus single individual pinning*

Let us now consider the disorder in more details. Electrons are scattered by impurities. The disorder term is simply

$$H_{\text{dis}} = \int dx\, V(x)\rho(x) = \frac{1}{\Omega}\sum_{k,q} V_q c^\dagger_{k+q} c_k \tag{9.14}$$

where $V(x)$ is the random potential produced by impurities. A good approximation for it would be

$$V(x) = \sum_i f(x - R_i) \tag{9.15}$$

where f is the potential of a single impurity, and R_i the random positions of the impurities. In standard systems the impurity potential is relatively short-range so that very often one takes $f(x) = V_0\delta(x)$. If the impurities are uniformly distributed this is a poissonian disorder. It is characterized by *two* independent variables, the strength of one impurity V_0 and the density of impurities n_i. Varying each one of these parameters leads to quite different physical effect. There are various interesting cases. The first one is when the impurities are dense enough and weak enough so that the effect of each impurity is negligible. They can only act collectively. In that case the scale of variation of the physical quantities is much larger than the distance between the impurities (n_i^{-1} in one dimension). In a volume where the physical parameters are thus practically constant, there are many impurities. In that case the central limit theorem tells us that the disorder is equivalent to a gaussian disorder. Physically it means that one can replace the original disorder by a coarse grained version

$$\frac{1}{|\Xi|}\int_\Xi dx\, V(x) = \tilde{V}(x) \tag{9.16}$$

where Ξ is some volume small compared to the scale of variation of the physical quantities, but large compared to the distance between impurities. $\tilde{V}(x)$ is the coarse grained potential. Since there are many impurities in the volume Ξ the central limit theorem imposes that $\tilde{V}$ has a gaussian distribution of the form

$$p(\tilde{V}) = e^{-\frac{1}{2}\int D^{-1}(x-x')\tilde{V}(x)\tilde{V}(x')} \tag{9.17}$$

ensuring that

$$\overline{\tilde{V}(x)\tilde{V}(x')} = D(x-x') \tag{9.18}$$

where $D(x-x')$ is a short-range function, which is zero beyond a few impurity distances n_i^{-1}. Since the scale of variation of physical constants is much larger one usually approximates $D(x) \sim D\delta(x)$. In that case the disorder is gaussian and uncorrelated from point to point. The strength of the gaussian disorder can easily be estimated from (9.15) to be

$$D = n_i V_0^2 \tag{9.19}$$

Notice that the gaussian disorder now depends on *only one* parameter. The distance between impurities has completely disappeared from the problem (or only stays as the correlation length of the disorder). Mathematically, the gaussian disorder corresponds to taking infinitely dense impurities $n_i \to \infty$ but each one infinitely weak $V_0 \to 0$ so that the effect can only be collective. A single impurity gives a very weak effect. The product $n_i V_0^2$ is kept constant and measures the strength of this 'collective' disorder. This is the case we will examine in Section 9.2. The totally opposite limit that we will examine in detail in Chapter 10 corresponds to the case where the density of impurities is weak, and the strength of a single impurity V_0 is getting very large. In this case each impurity is having a strong effect in its immediate vicinity, and one can essentially forget about collective effects and has to solve the problem of a single impurity.

9.2 Many impurities

9.2.1 *Basics*

Let us thus consider one-dimensional electrons subject to weak and dense impurities. In that case one can replace the disorder by its gaussian limit, so the disorder is (9.14) with the correlations for V (I drop the tilde from now on) given by (9.18). If the disorder strength D is much smaller than the Fermi energy, one can again consider that disorder produces effects only close to the two Fermi points. One can thus approximate

$$H_{\text{dis}} = \frac{1}{\Omega}\sum_{q\sim 0} V_q \sum_k c^\dagger_{k+q} c_k + \frac{1}{\Omega}\sum_{q\sim\pm 2k_F} V_q \sum_k c^\dagger_{k+q} c_k \tag{9.20}$$

There are of course also the $4k_F$, etc., harmonics. If one wants both k and $k+q$ to be close to a Fermi point, one obtains in the continuum limit

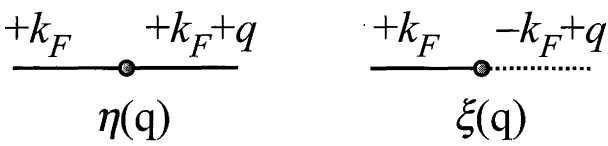

FIG. 9.1. (left) Forward scattering on impurities. In the continuum this conserves the chirality of a Fermion (that is, a right mover stays a right mover). (right) Backscattering that changes a right mover into a left mover.

$$H_{\text{dis}} = \int dx\, \eta(x)[\tilde{\psi}_R^\dagger(x)\tilde{\psi}_R(x) + \tilde{\psi}_L^\dagger(x)\tilde{\psi}_L(x)] + \int dx[\xi(x)\tilde{\psi}_L^\dagger(x)\tilde{\psi}_R(x) + \xi^*(x)\tilde{\psi}_R^\dagger(x)\tilde{\psi}_L(x)] \quad (9.21)$$

where $\eta(x)$ and $\xi(x)$ are the continuum limits corresponding to the $q \sim 0$ and $q \sim -2k_F$ components of the random potential. They are given by

$$\begin{aligned} \eta(x) &= \frac{1}{\Omega}\sum_{q\sim 0} V_q e^{iqx} \\ \xi(x) &= \frac{1}{\Omega}\sum_{q\sim 0} V_{q-2k_F} e^{iqx} \end{aligned} \quad (9.22)$$

It is easy to see that η is real since $V_q = V_{-q}$ ($V(x)$ is real). Naively, the field ξ is complex. In fact, this depends on the precise value of $2k_F$ and whether one is on a lattice or not. I will come back to this point. Physically the field η describes forward scattering ($q \sim 0$) on the impurities whereas the fields ξ and ξ^* are the backscattering where the momentum of an electron changes by $\mp 2k_F$. These processes are shown in Fig. 9.1. This is a very specific feature of one-dimensional systems. In higher dimensions, by playing with angles one can exchange an arbitrary momentum while staying close to the Fermi surface. In one dimension, since one has to stay close to one of the Fermi points, either the particle continues in the same direction (forward scattering) or it bumps back on the impurity (backward scattering)

There are important things to notice about (9.22). Because η and ξ only contain $q \sim 0$ terms in the Fourier sum, they vary slowly at the scale of k_F^{-1} and are thus well suited for a continuum limit. Since $\overline{V_q V_{q'}^*} = D\delta_{q,q'}$ from (9.18), the $q \sim 0$ and $q \sim \pm 2k_F$ fields are essentially independent random variables. So

$$\overline{\eta(x)\xi(x')} = 0 \quad (9.23)$$

From the correlations of $V(x)$ (I take $V(x-x') = D\delta(x-x')$) one has

$$\begin{aligned} \overline{\eta(x)\eta(x')} &= D_f\delta(x-x') = D\delta(x-x') \\ \overline{\xi(x)\xi(x')} &= 0 \\ \overline{\xi(x)\xi^*(x')} &= D_b\delta(x-x') = D\delta(x-x') \end{aligned} \quad (9.24)$$

The forward and backward scatterings can thus be treated independently. The fact that $\overline{\xi(x)\xi(x')}$ correlations are zero, traduces the fact that one cannot have two consecutive scatterings of $2k_F$ since it would take the particle away from the Fermi surface. This is of course true if one is in the continuum. On a lattice, if $2k_F = \pi$ (that is $4k_F = 2\pi$) a $4k_F$ scattering brings the particle back to the Fermi surface. One can indeed directly see from (9.22) that if one is on a lattice and $2k_F = \pi$, then because $e^{i2k_F x} = (-1)^x$, the field ξ is now *real*. For such commensurate cases the disorder becomes instead of (9.21)

$$H_{\text{dis}} = \int dx\, \eta(x)[\tilde{\psi}_R^\dagger(x)\tilde{\psi}_R(x) + \tilde{\psi}_L^\dagger(x)\tilde{\psi}_L(x)] + \int dx\, \xi(x)[\tilde{\psi}_L^\dagger(x)\tilde{\psi}_R(x) + \tilde{\psi}_R^\dagger(x)\tilde{\psi}_L(x)] \quad (9.25)$$

This has drastic physical consequences as I will briefly discuss later. I will also skip the interesting case where the potential is quasi-periodic, which is intermediate between commensurate systems and disordered ones (Kolomeisky, 1993; Vidal *et al.*, 1999; Hida, 2001).

For the moment let me focus on the incommensurate case. For the non-interacting system, powerful techniques exist that allow to solve rather completely this problem (Berezinskii, 1974; Abrikosov and Rhyzkin, 1978; Efetov, 1983). The first important point is that forward scattering does not affect the conductivity at all. This can be shown directly on the fermionic Hamiltonian but we will show it more generally later. Physically this can be understood easily. Since the forward scattering does not change the chirality it cannot affect the current. If one remembers the Boltzmann expression of the transport time (Mahan, 1981) it is weighted compared to the lifetime by

$$\tau_{\text{trans}}^{-1} = \int d\theta \tau_{\text{imp}}^{-1}\, (1 - \cos(\theta)) \quad (9.26)$$

where θ is the scattering angle. In one dimension, the only 'allowed' angles are $\theta = 0$ (forward scattering) and $\theta = \pi$ (backward scattering). So we see that forward scattering will not affect transport. The backward scattering is the one giving rise to localization. One finds exponential decay of the correlation functions with a characteristic length

$$\xi_{\text{loc}} = \frac{1}{D_{\text{b}}} \quad (9.27)$$

The conductivity is of the form shown in Fig. 9.2. The low frequency behavior of the conductivity can easily be understood in the fermion language in the strong pinning regime (Mott, 1990). Let us assume that each electron is pinned individually on an impurity as shown in Fig. 9.3. The power absorbed in an external field is $P = \sigma(\omega)E^2$. To absorb a photon the system should be able to make a transition from one occupied localized state of energy E_i to an empty one of energy $E_f = E_i + \hbar\omega$. If one assumes that the density of states $N(E)$ is

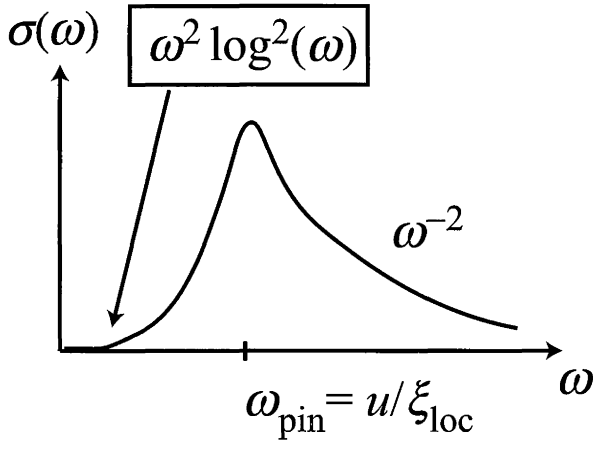

FIG. 9.2. Conductivity for the non-interacting one-dimensional electron system. The main characteristic is the existence of a pinning frequency of the order of $\omega_{\text{pin}} = v_F/\xi_{\text{loc}}$. The low-frequency behavior is $\sigma(\omega) = \omega^2 \log^2(1/\omega)$.

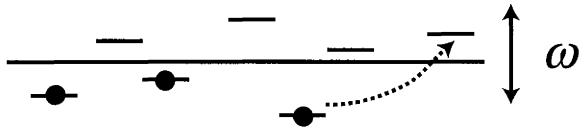

FIG. 9.3. Interpretation of the conductivity in the strongly localized regime. Transitions are absorption of the photons from one occupied localized state to an empty state. This can occur only within a layer $\hbar\omega$ around the Fermi level.

roughly unchanged by the disorder then the number of such states, which are within an energy range $\hbar\omega$ below the Fermi level, is $\sim N(E_F)\hbar\omega$. Each transition absorbs $\hbar\omega$, so the conductivity is $\sigma(\omega) \sim \omega^2$. This simple result can be refined to show that logarithmic corrections should be present. The result is confirmed by more rigorous calculations.

The non-interacting system is thus rather well understood. When interactions are included the question becomes much more complicated. However, since the bosonization form provides a natural framework to treat the interactions in one dimension, one can hope that the disorder problem in the presence of interactions will be tractable in the boson form. So, let me first rewrite the disorder Hamiltonian (9.21) in this much more convenient form. Using Appendix D one gets

$$H_{\text{dis}} = -\int dx\, \eta(x)[\frac{1}{\pi}\nabla\phi] + \int dx \frac{\xi^*(x)}{2\pi\alpha} e^{i2\phi(x)} + \text{h.c.} \tag{9.28}$$

for spinless fermions and

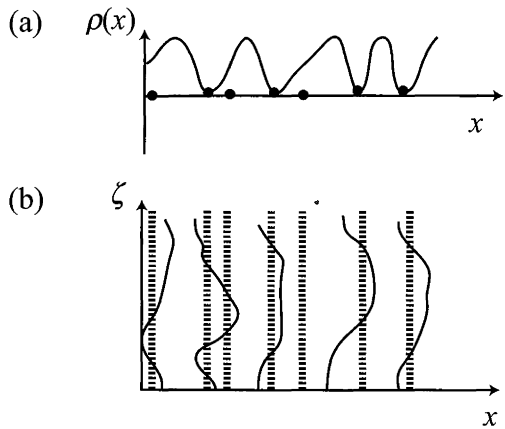

FIG. 9.4. (a) The disordered interacting electron system can be viewed as a charge density wave of periodicity $2k_F$ that tries to pin on impurities. It should distort to take advantage of the impurity potential. Quantum fluctuations of the charge density wave are measured by the LL parameter K and compete with pining. (b) It can also be viewed as a periodic array of lines that get pinned by columnar disorder, that is, by disorder that is independent of one of the coordinates z which is the imaginary time for the quantum problem. The lines are the space–time trajectories of the particles.

$$H_{\text{dis}} = -\int dx\, \eta(x)[\frac{\sqrt{2}\nabla\phi_\rho}{\pi}] + \int dx \frac{\xi^*(x)}{2\pi\alpha} e^{i\sqrt{2}\phi_\rho(x)} \cos(\sqrt{2}\phi_\sigma(x)) + \text{h.c.} \tag{9.29}$$

for fermions with spin. Of course, now all interactions are included in the 'free' Luttinger liquid Hamiltonian H^0, which is essentially quadratic. This is of course the main advantage of using the boson representation. Before we move to the solution let us use the physical images explained in Chapter 3 to make two interesting analogies. We first see that we can interpret the total Hamiltonian (3.25) and (9.28) or (9.29) as one describing a charge density wave where the density is of the form (3.53), which tries to pin on the impurities, as shown in Fig. 9.4. The phase has to distort to take advantage of the impurity potential. Quantum fluctuations that are taken into account by the Π^2 term in the Hamiltonian H^0 prevent the phase ϕ to have a too well-defined value at a point and thus fight pinning. These quantum fluctuations are controlled by the LL parameter K. If $K = 0$ the problem would be purely classical. When K increases the amount of quantum fluctuations increases. Another analogy is provided by our analogy with a classical system of lines as explained in Chapter 3. We see that in that language since the disorder is independent of time the disorder would be a so-called columnar disorder as shown in Fig. 9.4. The system is thus equivalent

to a 'crystal' of lines pinned by columnar disorder. This allows to make contact with the body of literature devoted to such problems (Nelson and Vinokur, 1993; Blatter *et al.*, 1994).

Let us now solve the problem. The forward scattering acts as a random chemical potential (compare with (2.57)). The backward scattering gives rise to a cosine-like potential not dissimilar to the one of the Mott transition. In fact if the disorder had *only* one Fourier component at $2k_F$ it would give rise exactly to a sine-Gordon term. This would be exactly similar to the Mott problem except for the fact that the most relevant periodicity is at $2k_F$ instead of $4k_F$ for the Mott problem. Since the forward scattering is like a random chemical potential it can be eliminated by the same techniques than in Chapter 2. One completes the square in H^0 by defining

$$\tilde{\phi}(x) = \phi - \frac{K}{u}\int^x dy\ \eta(y) \tag{9.30}$$

The Hamiltonian becomes (e.g. for spinless fermions)

$$H = H^0[\tilde{\phi}] + \int dx \frac{\xi^*(x)e^{i\frac{2K}{u}\int^x dy\ \eta(y)}}{2\pi\alpha} e^{i2\tilde{\phi}(x)} + \text{h.c.} \tag{9.31}$$

The only effect of the forward scattering is thus to redefine the phase of the backward scattering. Since ξ is a complex random variable with a gaussian distribution $\tilde{\xi}^*(x) = \xi^*(x)e^{i\frac{2K}{u}\int dx\ \eta(x)}$ is a random variable with exactly the same distribution. Thus, the absorption of the forward scattering in (9.30) has absolutely no effect on the Hamiltonian. Another way to see this is to use the replica method. Since forward and backward scatterings are independent random variables with gaussian distributions one can perform the averages independently. If one performs the average over the backscattering only the action becomes (e.g. for spinless fermions in the incommensurate case)

$$\begin{aligned} S = &\sum_{a=1}^{n} S_a^0 - \int dx\ \eta(x) \sum_{a=1}^{n} [\frac{1}{\pi}\nabla\phi_a] \\ &- \frac{D_\text{b}}{(2\pi\alpha)^2} \sum_{a=1,b=1}^{n} \int dx\ d\tau\ d\tau'\ \cos(2\phi(x,\tau)_a - 2\phi(x,\tau')_b) \end{aligned} \tag{9.32}$$

where S^0 is the Luttinger action (3.26). One can absorb the forward scattering by using (9.30) for each replica. Since each field is shifted by the same amount and the replicated backward term is local in space, it is absolutely invariant. The forward scattering can thus be treated *exactly*, and completely eliminated from the Hamiltonian. It does not mean of course that the correlation functions are not affected by it since ϕ should be replaced by $\tilde{\phi}$. However, since (9.30) is a simple shift $\tilde{\theta} = \theta$, it means that *any* correlation function containing only θ is invariant. This is in particular the case of the current–current correlation

function and the superconducting correlation functions. Another way to see that is to say that $j \sim \partial_\tau \phi$ and the shift depends only on space. The conductivity is thus totally independent of the forward scattering even in the presence of interactions, in agreement with our physical arguments. The other correlation functions are easily computed. For example, the $2k_F$ density is

$$\langle e^{i2\phi(r)} e^{-i2\phi(0)} \rangle_{S[\phi]} = e^{i2\int_0^x dx \frac{K}{u}\eta(x)} \langle e^{i2\tilde{\phi}(r)} e^{-i2\tilde{\phi}(0)} \rangle_{S[\tilde{\phi}]} \tag{9.33}$$

The correlation function for $\tilde{\phi}$ is the one that contains only backscattering. In the absence of backscattering it would thus just be the standard LL power law. Averaging over the disorder gives for the first term

$$\overline{e^{i2\int_0^x dx \frac{K}{u}\eta(x)}} = e^{-\frac{2K^2}{u^2}\int_0^x dx \int_0^x dx' D_f \delta(x-x')} = e^{-\frac{2K^2 D_f}{u^2}|x-x'|} \tag{9.34}$$

The forward scattering thus causes an exponential decay of the density–density correlation functions. Let me again emphasize that this *does not* correspond to Anderson's localization since the current is unchanged.

The difficult, but physically interesting part is thus to solve the backward scattering Hamiltonian

$$S/\hbar = \int dx\, d\tau \left[\frac{1}{2\pi K} \left[\frac{1}{v}(\partial_\tau \phi)^2 + v(\partial_x \phi)^2 \right] + \frac{\xi^*(x)}{2\pi\alpha\hbar} e^{i2\phi(x)} + \text{h.c.} \right] \tag{9.35}$$

I have reintroduced in the above formula $\hbar$ and other pesky constants to show explicitly the various physical limits. Note that although we are mainly concerned here with fermions (9.35) describes in fact nearly every one-dimensional disordered problem since all this problems have essentially the same boson representation. I will examine dirty bosons in Section 11.1. To understand the physical effects of the backward scattering let us go back to the interpretation of (9.35) in terms of a charge density wave that gets pinned on impurities. The elastic term in (9.35) wants the phase of the density wave to be as constant as possible, and have a nice sinusoidally modulated density, since phase and density are related by (3.53). The disorder term on the contrary wants to pin this charge density on the impurities by distorting the phase, as shown in Fig. 9.4. The problem of localization of interacting fermions is thus very similar to the one of the pinning of classical charge density waves (Fukuyama and Lee, 1978). The charge density wave is here intrinsic to the one-dimensional interacting electron gas and not due to a coupling to phonons (Phononic formation of CDW is the Peierls transition analogous to the one seen in the spin chain context in Section 6.2.2). The main features are nevertheless similar, the main difference being the fact that the effective mass of the 'CDW' is much smaller in the absence of the electron–phonon coupling (the phononic CDW has to carry the lattice distortion with it which gives a very large mass) and hence the importance of the quantum fluctuations is much higher. In the absence of quantum fluctuations, ϕ would be a classical field and we would have a good idea of what happens. This is the way Fukuyama

and Lee (1978) looked at this problem. Such an approximation is of course very good for 'phononic' charge density waves (Grüner, 1988) since the quantum term is $\Pi^2/(2M)$ and thus very small. For fermions this corresponds to the 'classical' limit $\hbar \to 0$, $K \to 0$ keeping $\overline{K} = K/\hbar$ fixed, and thus to very repulsive interactions. In that case we can ignore all quantum fluctuations, and look for a *static* solution for ϕ. It is of course crucial for the existence of such solution that the disorder does not depend on time. This solution $\phi_0(x)$ describes the static distortion of the phase imposed by the random potential. In the absence of kinetic energy $(\nabla\phi)^2$, it would be easy to 'determine' ϕ_0. If we write the random field ξ^* as an amplitude $-|\xi(x)|$ and a random phase -2ζ, the disorder term is proportional to

$$-\int dx|\xi(x)|e^{i2(\phi(x)-\zeta(x))} + \text{h.c.} \tag{9.36}$$

The optimum is thus for $\phi_0(x)$ to follow the random phase on each point. For point-like impurities located on random positions R_i, $|\xi|$ would just be the strength of each impurity potential and $\zeta = k_F R_i$. Thus, $\phi_0(x) = \zeta(x)$ is the generalization to any type of disorder (and in particular to the gaussian disorder so dear to the theorist) of the physics expressed in Fig. 9.4: get the density minimum at each impurity. In presence of kinetic energy, following the random phase would cost too much kinetic energy. We do not know exactly how to determine the optimal $\phi_0(x)$ but we can use some scaling arguments. Let us assume that ϕ remains constant for a lengthscale ξ_{loc}. On this lengthscale ϕ takes the value that optimizes the disorder term, which now reads

$$E_{\text{dis}} = \left[\int_0^{\xi_{\text{loc}}} \xi^*(x)\right] e^{i2\phi} + \text{h.c.} \tag{9.37}$$

Because the average of a gaussian random variable on a box of size ξ_{loc} is proportional to the square root of the size of the box, the disorder contributes as

$$E_{\text{dis}} = -\sqrt{D_{\text{b}}\xi_{\text{loc}}}e^{i(2\phi_0-2\Xi)} \tag{9.38}$$

where Ξ is some phase. It clear that the optimum energy is reached if ϕ_0 adjusts to this (now unknown) phase. The global energy gain now scales as $\sqrt{\xi_{\text{loc}}}$. Between two segments of size ξ_{loc} the phase has to distort to reach the next optimal value. This is sketched in Fig. 9.5. The distortion being of the order of 2π the cost in kinetic energy reads

$$E_{\text{kin}} \propto \frac{1}{\xi_{\text{loc}}} \tag{9.39}$$

minimizing the total cost shows that the length over which ϕ_0 remains constant is given by

$$\xi_{\text{loc}} \propto \left(\frac{1}{D_{\text{b}}}\right)^{\frac{1}{3}} \tag{9.40}$$

This tells us that the system *does* pin on the impurities and that below ξ_{loc} the system looks very much like an undistorted system. Since at the scale ξ_{loc},

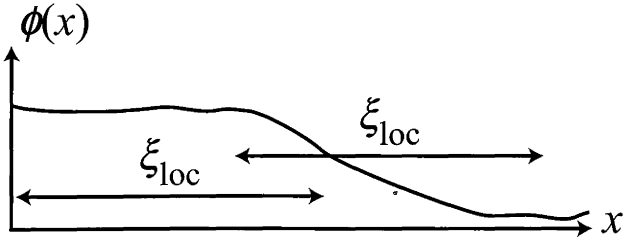

FIG. 9.5. The phase ϕ adjusts to the random phase over a length $\xi_{\rm loc}$. This length results from the best compromise between the 'elastic' energy and the pinning on disorder.

ϕ_0 varies randomly one naively expects the $2k_F$ density–density correlations to decay exponentially with a characteristic size $\xi_{\rm loc}$. It is thus very tempting to associate $\xi_{\rm loc}$ with the Anderson localization length. In the context of charge density waves this is known as the Fukuyama-Lee length (Fukuyama and Lee, 1978). The same arguments were introduced earlier in the context of classical systems, to show the existence of an analogous lengthscale for the pinning of vortices (the Larkin-Ovchinikov length, Larkin 1970; Larkin and Ovchinnikov 1979) or for random field Ising models (Imry-Ma length, Imry and Ma 1975).

Note that for the free fermion point $\xi_{\rm loc} \propto 1/D_{\rm b}$ instead of (9.40), so the above formula is clearly missing a piece of physics when K is not zero. Nevertheless, from this simple scaling argument we have obtained: (i) the fact that classical CDW or very repulsive fermions are pinned (localized) by disorder; (ii) the localization length; (iii) the fact that the ground state should contain a static distortion of the phase due to the disorder. Unfortunately, we have no other information on ϕ_0, which is certainly a drawback. Even with our limited knowledge of the statics we can nevertheless try to extract the dynamics. Let us assume that all deformations of the phase that are not contained in the static distortion are small and thus we can write

$$\phi(x,\tau) = \phi_0(x) + \delta\phi(x,\tau) \tag{9.41}$$

with $\delta\phi(x,\tau) \ll \phi_0(x)$ in a very vague sense since we deal with random variables. One can try to expand the random term in power of $\delta\phi$

$$\begin{aligned} S_{\rm dis} &= -\int d\tau\, dx\, |\xi(x)| \cos(2(\phi(x,\tau) - \zeta(x))) \\ &\simeq 2\int d\tau\, dx\, |\xi(x)| \cos(2(\phi_0(x) - \zeta(x)))(\delta\phi(x,\tau))^2 \end{aligned} \tag{9.42}$$

One can thus use in principle (9.42) to compute the various physical quantities. Note that the conductivity (see Section 7.2) will *not* depend *directly* on the static solution ϕ_0 since $\partial_t\phi_0 = 0$, so we can hope to compute it. Of course, the dependence of the fluctuations $\delta\phi$ in ϕ_0 is hidden in (9.42). If ϕ_0 was following the

random phase at every point, then the cosine in (9.42) would just be a constant. Disorder would just lead to a mass term for the fluctuations and the optical conductivity would show a gap as in Fig. 7.12. In fact, this is not true at every point so (9.42) leads to a distribution of masses for the fluctuations. Unfortunately, the knowledge of ϕ_0 is too crude to compute the conductivity accurately and depending on what exactly is $\xi_{\rm loc}$ one can find either a gap, a non-analytic behavior or a $\sigma(\omega) \sim \omega^2$ behavior at small frequencies (Fukuyama and Lee, 1978). Based on physical intuition Fukuyama and Lee opted for the later (Fukuyama and Lee, 1978), but the method shows its limitations here and does not allow a reliable calculation of the physical quantities. More precise calculations of ϕ_0 and the conductivity can be performed in the classical limit $K \to 0$ using a transfer matrix formalism (Feigelmann and Vinokur, 1981). A self-consistent harmonic approximation, similar to the variational method of Appendix E.2, can be used to approximately take into account quantum fluctuations in the localization length (Suzumura and Fukuyama, 1983). It gives

$$\xi_{\rm loc} \propto \left(\frac{1}{D_{\rm b}}\right)^{\frac{1}{3-2K}} \tag{9.43}$$

This expression for the localization length suggests that a delocalization transition is induced by the quantum fluctuations and occurs at $K = 3/2$. In the fermion language this corresponds to extremely attractive interactions.

9.2.2 *Physical properties*

The previous method starts directly from the localized phase. It provides some limited information about this phase, but suffers from serious limitations. An alternative approach is to start from the pure Luttinger liquid and investigate the effects of disorder perturbatively, and build a renormalization group analysis. The RG provides us with the best possible description of the delocalized phase and the critical properties of the transition. It also gives a very accurate description of the localized phase *up to* lengthscales of the order of the localization length $\xi_{\rm loc}$. To build an RG we use the same techniques that were described in Section 2.3.2. It is even simpler since the replicated disorder term already contains a double integral over time and we can thus expand to first-order only. Note that in fact this corresponds to an expansion to second order in the random potential V since $D_{\rm b} \sim VV$. Before we start with the RG itself one has to notice that it is necessary to introduce a cutoff in the double time integral. This cutoff is not there in the original disorder term, since the double integral over time should be unrestricted to give the elastic scattering on the impurities. We thus replace

$$D_{\rm b} \int\int d\tau\, d\tau' \to D_{\rm b} \int\int_{|\tau-\tau'|>\alpha} d\tau\, d\tau' \tag{9.44}$$

Introducing this cutoff has consequences that I will examine in detail in Section 9.2.3, but for the moment we will ignore this little difference.

Using the methods of Section 2.3.2 or Appendix E.1 one can easily get the renormalization equations for the spinless case. The renormalization of D_b is the easiest since it is only the dimension of the operator (9.32). At this order only terms diagonal in replica index survive upon average since the quadratic part of the action is diagonal in replicas:

$$\frac{\partial D_\mathrm{b}}{dl} = (3-2K)D_\mathrm{b} \tag{9.45}$$

The 3 comes from the two integrations in time and the integration over space, and the $-2K$ from the correlation $\langle e^{i2\phi}e^{-i2\phi}\rangle \sim (1/r)^{2K}$. In a similar way to that for the Mott transition (9.32) gives also a renormalization of the quadratic part of the action

$$\begin{aligned} -D_\mathrm{b}\int dx \int_{\alpha<|\tau-\tau'|<\alpha'} d\tau d\tau' \cos(2\phi_a(x,\tau)-2\phi_a(x,\tau)) \\ \propto \int dx\, d\tau\, (\partial_\tau\phi(x,\tau))^2 \end{aligned} \tag{9.46}$$

Such a term renormalizes the coefficient $1/(uK)$ in the action (3.26). Since the disorder generates only $(\partial_\tau\phi(x,\tau))^2$ terms and no $(\partial_x\phi(x,\tau))^2$, the coefficient u/K is not renormalized. Disorder thus gives both a renormalization of K and the velocity, since it breaks the space–time invariance. The RG equations are

$$\begin{aligned} \frac{dK}{dl} &= -\frac{K^2}{2}\tilde{D}_\mathrm{b} \\ \frac{d\tilde{D}_\mathrm{b}}{dl} &= (3-2K)\tilde{D}_\mathrm{b} \\ \frac{du}{dl} &= -\frac{uK}{2}\tilde{D}_\mathrm{b} \end{aligned} \tag{9.47}$$

where

$$\tilde{D}_\mathrm{b} = \frac{2D_\mathrm{b}\alpha}{\pi u^2} \tag{9.48}$$

We now briefly analyze these equations. The flow is shown in Fig. 9.6. In the variables $K, \sqrt{\tilde{D}_\mathrm{b}}$ the flow is identical to the one obtained in Section 2.3.2. The equation for the disorder indicates that two fixed points are possible. If $K > K_c$ the disorder flows to zero, whereas it increases under renormalization if $K < K_c$. Note that the critical value K_c depends on the disorder. However, at the transition the whole boundary renormalizes to the *universal* value $K^* = 3/2$, thus in particular $K_c(D_\mathrm{b} \to 0) = 3/2$. The phase where the disorder flows to zero is a Luttinger liquid, with renormalized parameters K^* and u^*. Note that since $K^* > 3/2$ this phase has strong superconducting fluctuations. From Section 7.2, it is a perfect conductor, with a finite charge stiffness $\mathcal{D} = u^*K^*$. The naive interpretation of this phase is thus that it is a delocalized phase in

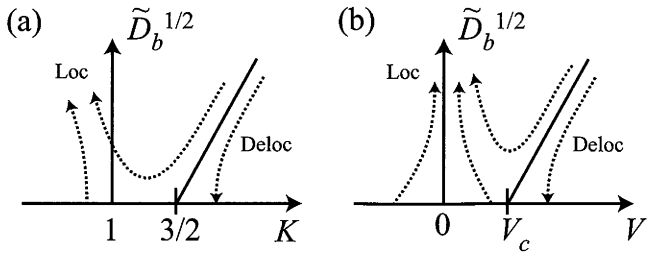

FIG. 9.6. Phase diagram and flow for spinless fermions in presence of disorder: (a) flow in $\tilde{D}_\mathrm{b}$ and K variables; (b) flow in $\tilde{D}_\mathrm{b}$ and interactions V. Disorder kills inelastic interactions.

which the disorder has been screened by the strongly attractive interactions. Below the transition line the disorder flows to strong coupling. Since the flow is going to strong coupling one cannot use the perturbative RG equations above the lengthscale for which $\tilde{D}_\mathrm{b} \sim 1$. To understand the physics of this phase we can proceed in two ways. The simplest is to notice that this phase contains the free electron line $K = 1$ for which we know that electron localization takes place. This phase is thus a localized phase. The other method is to use the fact that the disorder becomes large so one can try to tackle the strong coupling action. I will come back to this in Section 9.2.3.

Although one cannot use the RG equations above a certain lengthscale one can still use them to extract many physical quantities, in a way similar to what we did for the Mott transition. For example, one can extract the localization length. Let us renormalize up to a point where $\tilde{D}_\mathrm{b}(l^*) \sim 1$. The true localization length of the system is given by

$$\xi_\mathrm{loc} = e^{-l^*}\xi_\mathrm{loc}(l^*) \tag{9.49}$$

but if $\tilde{D}_\mathrm{b}(l^*) \sim 1$ the localization length of such a problem is of the order of the lattice spacing (this is the same trick than the one used to compute the gap for a Mott phase). Thus,

$$\xi_\mathrm{loc} \sim \alpha e^{-l^*} \tag{9.50}$$

One can then integrate the flow to get l^*. As for the Mott phase this depends on the position in the phase diagram. When one is deep in the localized phase (far from the transition) one can consider K as constant (see Section 2.3.2) and thus

$$\tilde{D}_\mathrm{b}(l) = \tilde{D}_\mathrm{b}(l=0)e^{(3-2K)l} \tag{9.51}$$

Thus,

$$\xi_\mathrm{loc} \sim \alpha \left(\frac{1}{\tilde{D}_\mathrm{b}}\right)^{\frac{1}{3-2K}} \tag{9.52}$$

One recovers the form (9.43). Thus, we see that the self-consistent harmonic calculation corresponds in fact to the limit of infinitesimal disorder, which is a

fact that we already noticed in Section 2.3.2 for such variational methods. For $K = 1$ one does recover that $\xi_{\text{loc}} \sim 1/\tilde{D}_{\text{b}}$, in agreement with the exact solution for free fermions, a sign that we have taken the right physics into account. Close to the transition the localization length diverges in a different way (setting $K = 3/2 + \eta$) (see Section 2.3.2)

$$\xi_{\text{loc}} \sim e^{2\pi/\sqrt{9\tilde{D}_{\text{b}}-\eta^2}} \tag{9.53}$$

As for the Mott transition, one can extract the frequency and temperature dependence of the conductivity. Let us here look at the temperature dependence by a very simple technique (Giamarchi and Schulz, 1988*b*). The idea is simply to renormalize until the cutoff is of the order of the thermal length $l_T \sim u/T$ corresponding to $e^{l^*} \sim l_T/\alpha$. At this lengthscale the disorder can be treated in the Born approximation. As the conductivity is a physical quantity it is not changed under renormalization and we have

$$\sigma(n(0), \tilde{D}_{\text{b}}(0), 0) = \sigma(n(l), D(l), l) = \sigma_0 \frac{n(l)\tilde{D}_{\text{b}}(0)}{n(0)\tilde{D}_{\text{b}}(l)} = \sigma_0 \frac{e^l \tilde{D}_{\text{b}}(0)}{\tilde{D}_{\text{b}}(l)} \tag{9.54}$$

where $\sigma(n(l), \tilde{D}_{\text{b}}(l), l) = \sigma(l)$ and $n(l)$ are, respectively, the conductivity and the electronic density at the scale l. $\sigma_0 = e^2 v_F^2/2\pi\hbar D_{\text{b}}$ is the conductivity in the Born approximation, expressed with the initial parameters. This is the simplified version of coupling RG with the memory function calculation as explained in Section 7.2. If one is deep in the localized phase, one can again retain only the RG equation for the disorder and consider K as constant and one has

$$\sigma(T) \sim \frac{1}{\tilde{D}_{\text{b}}} T^{2-2K} \tag{9.55}$$

This result is schematized in Fig. 9.7. It poses a paradox since (9.45) gives a localized–delocalized boundary at $K = 3/2$ whereas (9.55) gives perfect conductivity above $K = 1$ (that is, the non-interacting point). This shows that the RG equation for the disorder *cannot* be considered alone. Indeed, the RG equation for the disorder traduces in fact the dressing of the scattering on the disorder by the interactions. Such an effect has been derived long ago using either diagrams or RG (Gorkov and Dzyaloshinski, 1973; Mattis, 1974; Luther and Peschel, 1974; Apel, 1982; Apel and Rice, 1982*a*; Apel and Rice, 1982*b*; Giamarchi and Schulz, 1987; Giamarchi and Schulz, 1988*b*). In fact (9.45) would not allow in itself to really determine the metal–insulator transition point. One can immediately see that if one introduces a new variable such as

$$\overline{D_{\text{b}}} = e^{-al} D_{\text{b}} \tag{9.56}$$

the dimension of such a variable would be $(3-a-2K)$, leaving the location of the transition point as determined from (9.45) *alone* quite arbitrary. For example,

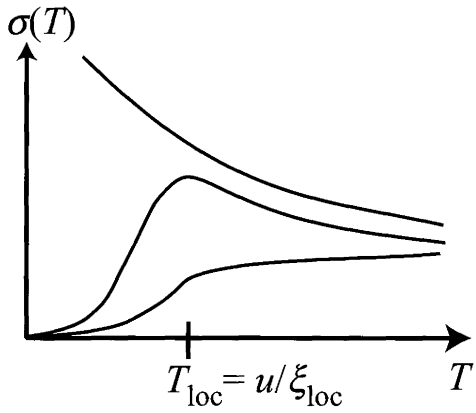

FIG. 9.7. Temperature dependence of the conductivity. For $K > 3/2$ (top) the system is delocalized and the conductivity increases with decreasing temperature. For $1 < K < 3/2$ (middle) the system is localized but the conductivity starts increasing with decreasing temperature. The renormalization of K due to disorder pushes the system to the localized side forcing the conductivity to decrease with decreasing temperature. For $K < 1$ (bottom) the conductivity decreases with temperature even at high temperatures. Below temperatures of the order of $u/\xi_{\rm loc}$, the system is strongly localized and the conductivity decreases exponentially.

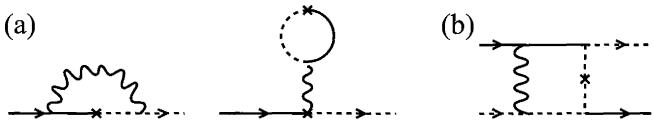

FIG. 9.8. Diagrams describing the renormalization of the disorder by the interactions (a) and the renormalization of the interactions by the disorder (b). Solid and dotted lines are fermions with $\pm k_F$, the wiggly line is the interaction and the cross is the impurity scattering.

remembering that $D_{\rm b} = n_i V_0^2$ one would get for the renormalization of the strength of one impurity (n_i scales as e^l)

$$\frac{dV_0}{dl} = (1-K)V_0 \tag{9.57}$$

One could naively conclude (incorrectly) from this result that the metal–insulator transition takes place at $K = 1$. The answer to this simple paradox is of course that (9.45) is complemented by the other RG equation that describes the renormalization of the interactions by the disorder. Both RG equations (9.45) and (9.47) have a diagrammatic representation shown in Fig. 9.8. In the presence of (9.47) one cannot rescale arbitrarily the variable $\tilde{D}_{\rm b}$ and the position of the

transition is now unambiguously fixed to $K = 3/2$. One easily checks that if one starts with $1 < K < 3/2$ the resistivity starts by *decreasing* with decreasing temperature but then the renormalization of K takes over and when $K(l) < 1$ starts shooting up again as shown in Fig. 9.7. Note that the advantage of the bosonization derivation is to allow to reach the non-perturbative point in interactions $K = 3/2$ where such a metal–insulator transition would take place. These predictions are directly relevant for spin chains, using the equivalence between spins and spinless fermions. The predictions for the phase diagram have been confirmed by numerical calculations (Schmitteckert *et al.*, 1998).

Let us stop here for spinless fermions and go to the case of fermions with spin, since this presents some twists compared to the much simpler spinless case. I will not give here the full derivation of the equations. The methodology to derive them is identical to the one presented in Chapter 2 and the derivation is well detailed in the literature (Giamarchi and Schulz, 1988*b*). I will rather focus on the salient points of this problem. To obtain the RG equations one starts with (9.29) and uses the methods of Chapter 2 and also sketched in this chapter for spinless fermions. One obtains

$$\begin{aligned}
\frac{dK_\rho}{dl} &= -\frac{u_\rho}{2u_\sigma} K_\rho^2 \tilde{D}_{\mathrm{b}}(l) \\
\frac{dK_\sigma}{dl} &= -\left[\frac{\tilde{D}_{\mathrm{b}}(l)}{2} + \frac{y^2(l)}{2}\right] K_\sigma^2 \\
\frac{dy}{dl} &= (2 - 2K_\sigma(l))y(l) \\
\frac{d\tilde{D}_{\mathrm{b}}}{dl} &= (3 - K_\rho(l) - K_\sigma(l))\tilde{D}_{\mathrm{b}}(l) \\
\frac{du_\rho}{dl} &= -\frac{u_\rho^2}{2u_\sigma} K_\rho \tilde{D}_{\mathrm{b}}(l) \\
\frac{du_\sigma}{dl} &= -\frac{u_\sigma K_\sigma}{2}\, \tilde{D}_{\mathrm{b}}(l)
\end{aligned} \tag{9.58}$$

where now

$$\tilde{D}_{\mathrm{b}} = \frac{2D_{\mathrm{b}}\alpha}{\pi u_\sigma^2}\left(\frac{u_\sigma}{u_\rho}\right)^{K_\rho} \tag{9.59}$$

and $y = g_{1\perp}/(\pi v_F)$. The equations look formidable but are in fact quite simple. The equation for $\tilde{D}_{\mathrm{b}}$ is as before the dimension of the disorder operator. There is now a renormalization of the charge and spin LL parameters K_ρ and K_σ due to the disorder. Of course, there is still the standard renormalization of K_σ due to the backscattering $g_{1\perp}$. Note that one recovers the spinless fermions case by setting $y = 0$ and $K_\rho = K_\sigma$ as one should (all couplings between different spin species are zero). Unfortunately, these equations are incomplete since it is easy to see that they do not obey spin rotation symmetry. The disorder $\tilde{D}_{\mathrm{b}}$ appears in the renormalization of K_σ but the equivalent term is not present in

the renormalization of y. So the flow will not stay on the separatrix $g_{1\parallel} = g_{1\perp}$ as it should. This is due to the fact that we have not collected all the contributions of order two. The precise details are given in Giamarchi and Schulz 1988*b* but let me present here the basic idea. This is again due to the fact that one can bring two operators at the same point as explained in Chapter 3. For example, if one combines one backscattering operator $g_{1\perp}$ with a disorder term (9.29) one gets

$$y\tilde{D}_{\mathrm{b}} \int dx\ \cos(\sqrt{8}\phi_\sigma(x)) \int dx'\ e^{i\sqrt{2}\phi_\rho(x')} \cos(\sqrt{2}\phi_\sigma(x')) \tag{9.60}$$

If the two points are within a cutoff distance of each other $|x - x'| < \alpha$ one can combine the two cosines to get (forgetting less relevant operators)

$$\sim y\tilde{D}_{\mathrm{b}} \int dx\ e^{i\sqrt{2}\phi_\rho(x)} \cos(\sqrt{2}\phi_\sigma(x)) \tag{9.61}$$

which is exactly a disorder term. In the same way combining two disorder terms at the same point cancels the ϕ_ρ contributions and gives

$$\tilde{D}_{\mathrm{b}}^2 \int dx\ \cos(\sqrt{2}\phi_\sigma(x))^2 \sim \frac{\tilde{D}_{\mathrm{b}}^2}{2} \int dx\ \cos(\sqrt{8}\phi_\sigma(x)) \tag{9.62}$$

which is a backscattering term. When varying the cutoff there is thus a renormalization of the disorder by terms of the order of $y\tilde{D}_{\mathrm{b}}$ and a renormalization of the backscattering by terms of order $\tilde{D}_{\mathrm{b}}^2$. The total equations are thus

$$\begin{aligned}
\frac{dK_\rho}{dl} &= -\frac{u_\rho}{2u_\sigma} K_\rho^2 \tilde{D}_{\mathrm{b}}(l) \\
\frac{dK_\sigma}{dl} &= -\left[\frac{\tilde{D}_{\mathrm{b}}(l)}{2} + \frac{y^2(l)}{2}\right] K_\sigma^2 \\
\frac{dy}{dl} &= (2 - 2K_\sigma)y - \tilde{D}_{\mathrm{b}} \\
\frac{d\tilde{D}_{\mathrm{b}}}{dl} &= (3 - K_\rho - K_\sigma - y)\tilde{D}_{\mathrm{b}}
\end{aligned} \tag{9.63}$$

where I have not written again the equations for the velocities. In particular, the renormalization of the disorder is changed, and the coefficient is not the simple dimension of the operator any more. This has serious consequences that I will examine in Section 9.2.3.

By now we are old hands at looking at fixed points so we can analyze the flow rapidly. For systems invariant by spin rotation ($g_{1\parallel} = g_{1\perp}$) one is forced to stay on the separatrix so there are only two possibilities: $K_\sigma \to 1$ and $y \to 0$ or $y \to -\infty$. If one is in the first case, then the disorder is irrelevant for $K_\rho > 2$. This regime is thus delocalized with a LL fixed point. By comparing with Fig. 2.9 we see that this region is dominated by triplet superconducting correlations. If

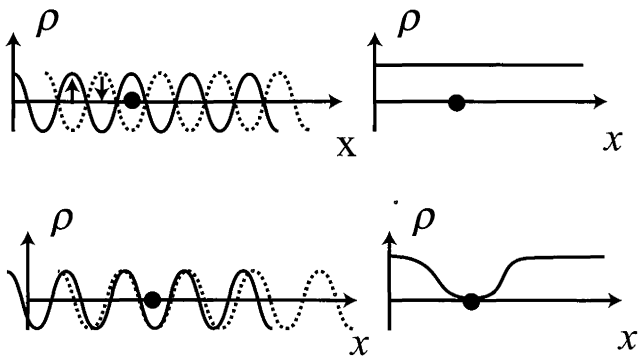

FIG. 9.9. Distortion of the charge order imposed by the impurity. In a totally rigid spin density wave state the density is uniform, so naively the disorder would not couple at lowest order. In fact, the disorder shifts locally the positions of the two density waves of spin up and down electrons to create locally a charge density wave modulation and pins it.

$K_\rho < 2$ then the disorder is relevant and the system localizes. Note that in our equations if $\tilde{D}_\mathrm{b} \to \infty$ it seems that it always forces $y \to -\infty$. This is obviously an artefact of the lowest-order RG equations. $y \to -\infty$ means a CDW ground state that is very efficiently pinned on impurities since the density varies spatially. On the other hand, $y \to 0$ gives a SDW type phase. In such a phase the density is uniform while the spin density is modulated. Thus, at lowest order the average of the coupling (9.29) vanishes. Of course, what happens in fact is that locally the disorder shifts the SDW order to make a distortion of density to which it can couple as shown in Fig. 9.9. This process occurs at next order, this is why in the lowest order RG when the disorder is relevant it always favors the CDW phase over the SDW. If the repulsion between opposite spins is very strong the electrons localize individually, as shown in Fig. 9.10, giving rise to a random SDW. Because the electrons are localized, only the spin degrees of freedom exist and since the distance between the electrons is random, one has a random exchange antiferromagnet as shown in Fig. 9.10.

The localization length can be computed by the method explained above. Far from the transition one can replace in (9.63) $K_\sigma^* = 1$ and $y = 0$ in the RG equation for the disorder and one gets

$$\xi_\mathrm{loc} \sim \left(\frac{1}{\tilde{D}_\mathrm{b}}\right)^{\frac{1}{2-K_\rho}} \tag{9.64}$$

Close to the transition extracting the localization length from the RG is more tricky because all equations have to be taken into account. One finds an exponential divergence of the localization length (Giamarchi and Schulz, 1988*b*).

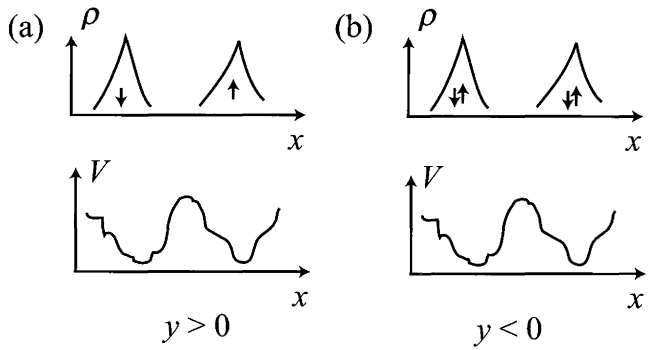

FIG. 9.10. For repulsive and strong enough interactions it is more favorable for the electrons to localize individually. The charge degrees of freedom are frozen but spin degrees of freedom remain and the resulting phase is thus a random antiferromagnet (a). If the interactions are not repulsive enough or attractive the electrons want to localize by pair and form singlet states. The spin degrees of freedom are gapped and the ground state is a pinned charge density wave (b).

If y is not large enough, then the disorder term pushes y to negative values. When y is negative it renormalizes to $-\infty$. As we saw in Section 2.3.2 this means that the system opens a spin gap. The electrons thus tend to pair. Because of the spin gap $\cos(\sqrt{2}\phi_\sigma)$ acquires a finite average value. Thus, at energies smaller than the spin gap the effective disorder is

$$H_{\text{eff}} = \int dx \frac{C\xi^*(x)}{(2\pi\alpha)} e^{i\sqrt{2}\phi_\rho(x)} \tag{9.65}$$

where

$$C = \langle \cos(\sqrt{2}\phi_\sigma) \rangle \tag{9.66}$$

Since the fluctuations due to the ϕ_σ field are suppressed the disorder is more efficient. I will come back to this paradoxical result in the next section. The system is now consisting (at low-energy) of pairs of electrons bound together. These 'molecules' act as a hard core bosons able to hop from site to site. If the spin gap was large the hopping element would be $t_{\text{eff}} = t^2/\Delta_\sigma$. This part of the phase diagram has thus strong connections with the boson problem that I will examine in Section 11.1. The RG equations can be derived (Giamarchi and Schulz, 1988*b*) for the effective disorder (9.65). Since only the charge part remains the derivation is very similar to the one we showed for spinless bosons. One obtains

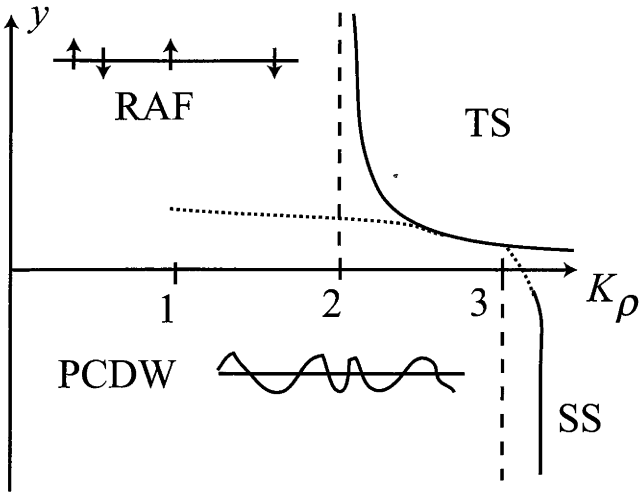

FIG. 9.11. Phase diagram for a one-dimensional disordered system. Solid lines denote the parts that can be extracted from the RG approach (see text). The dashed lines are the parts that cannot be extracted reliably from the weak coupling RG. TS and SS are, respectively, triplet and singlet superconductivity. RAF is a random antiferromagnet. PCDW is a pinned charge density wave. (After Giamarchi and Schulz, 1988*b*.)

$$\begin{aligned} \frac{dK_\rho}{dl} &= -\frac{K_\rho^2}{2}\tilde{D}_\mathrm{b} \\ \frac{d\tilde{D}_\mathrm{b}}{dl} &= (3-K_\rho)\tilde{D}_\mathrm{b} \\ \frac{du_\rho}{dl} &= -\frac{u_\rho K_\rho}{2}\tilde{D}_\mathrm{b} \end{aligned} \tag{9.67}$$

where $\tilde{D}_\mathrm{b} = 2CD_\mathrm{b}\alpha/(\pi u_\rho^2)$. Notice the change in dimension for the disorder from $(3-K_\rho-K_\sigma-y)$ to $(3-K_\rho)$, due to the fact that all spin fluctuations are now frozen. As a result the transition now occurs for $K_\rho^* = 3$, that is, for even more attractive interactions. The disorder pins much more effectively the system with a spin gap. The delocalized regime is a Luther–Emery liquid (Luttinger liquid with a spin gap). It corresponds to dominant singlet superconducting fluctuations. The charge stiffness is finite $\mathcal{D} = 2u_\rho^* K_\rho^*$. In the localized regime since the spins are paired the system has only charge fluctuations. The localized phase is thus a pinned charge density wave. The generic phase diagram is shown in Fig. 9.11. The localization length is now given (deep in the localized phase) by

$$\xi_\mathrm{loc} \propto \left(\frac{1}{\tilde{D}_\mathrm{b}}\right)^{\frac{1}{3-K_\rho}} \tag{9.68}$$

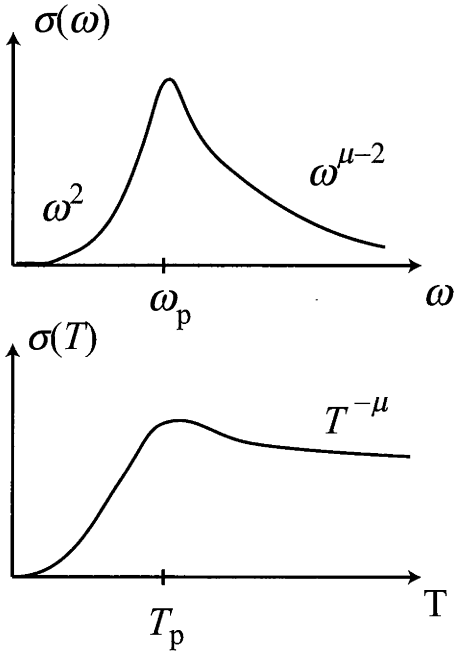

FIG. 9.12. Frequency and temperature dependence of the conductivity in a LL liquid. $T_p = \omega_p = u_\rho/\xi_{\rm loc}$ is the pinning frequency or temperature. $\mu = K_\rho - 1$ for a system with spin and spin isotropic interactions ($K_\sigma^* = 1$) provided that $K_\rho > 1/3$. For $K_\rho < 1/3$ the disorder pins the $4k_F$ density fluctuations and $\mu = 4K_\rho - 2$. For a spinless fermion system $\mu = 2K - 2$.

while it has a Berezinskii–Kosterlitz–Thouless form similar to (9.53), close to the transition.

For the system with spin the temperature dependence or frequency dependence of the conductivity can be extracted from the RG, down to energy scales where the disorder is of order one (see Section 7.2) and that correspond to $\omega \sim u_\rho/\xi_{\rm loc}$ or $T \sim u_\rho/\xi_{\rm loc}$. Deep in the localized phase one can neglect the renormalization of the LL parameter K in the initial steps of the RG, since the RG trajectories are nearly vertical (see Section 7.2). The temperature and frequency dependence of the conductivity is thus given by

$$\begin{aligned} \rho(T) &\sim D_{\rm b} T^{K_\rho - 1} \\ \sigma(\omega) &\sim \left(\frac{1}{\omega}\right)^{3-K_\rho} \end{aligned} \tag{9.69}$$

This is summarized in Fig. 9.12. Of course, more generally the LL parameters are renormalized by the disorder and all equations should be used (see Section 7.2), leading to a more complicated functional dependence than a simple power law.

Below the pinning frequency and temperatures, the RG cannot be used. For the frequency dependence one can use the method explained in the next section to show that the conductivity behaves as ω^2 (up to logarithmic terms) in good agreement with the solution for free fermions. For the temperature dependence calculations are more subtle (Lee and Larkin, 1978; Nattermann *et al.*, 2003). One finds a variable range hopping law of the form $\rho(T) \sim e^{(1/T)^{1/2}}$.

A final word. For systems with spin, the above values of the exponents apply when the interactions are not too repulsive. Indeed, we have retained the coupling of disorder to the $2k_F$ component of the density. This is correct as long as this component is the most relevant one. We have seen in Chapter 3 that for $K_\rho < 1/3$ the $4k_F$ component of the density is in fact the one that has the slowest decay. This component should thus be kept for the coupling to disorder, which becomes

$$H = \int dx\, \xi^*(x) e^{i\sqrt{8}\phi_\rho(x)} \tag{9.70}$$

The RG equation for the disorder becomes

$$\frac{d\tilde{D}_\mathrm{b}}{dl} = (3 - 4K_\rho)\tilde{D}_\mathrm{b} \tag{9.71}$$

Thus, $\sigma(T) \sim T^{2-4K_\rho}$ and $\sigma(\omega) \sim (1/\omega)^{4-4K_\rho}$. Note that for the case of Coulomb interactions $K_\rho \to 0$ and thus one recovers universal exponents (Maurey and Giamarchi, 1995) for the transport properties (up to log corrections).

9.2.3 *Extensions and pitfalls*

Let us examine some further consequences of the RG equations derived in the previous section and discuss some of the finer points. Since it is a relatively specialized section it can be safely skipped unless you are interested in the dirty detail of the disordered systems.

9.2.3.1 *Inelastic scattering* The first point to notice is that quite remarkably (9.47) seems wrong. Indeed, K naively depends on the (inelastic) interactions. Perturbatively, for the pure system $K = 1 - V/(2\pi v_F)$. If one starts for $K = 1$, that is, for the non-interacting system, it would thus seem from (9.47) that the *elastic* scattering on the impurities can generate *inelastic* fermion–fermion interactions. The solution of this paradox is hidden in the precise way the RG procedure is build. In order to have the elastic nature of the scattering on impurities, the time integrations in (9.28) should be done independently for τ and τ'. When we have performed the RG we have introduced a cutoff and imposed $|\tau - \tau'| > \alpha$. Thus, a part is left out of (9.44) which is

$$D_\mathrm{b} \int dx \int_{|\tau-\tau'|<\alpha} d\tau\, d\tau'\, \rho(x,\tau)\rho(x,\tau') \simeq 2D_\mathrm{b}\alpha \int dx \int d\tau\, \rho(x,\tau)\rho(x,\tau) \tag{9.72}$$

This is exactly an inelastic interaction term. Thus, K contains not only the original inelastic interactions V but also a small correction coming from the disorder itself. In order to determine the flow for V it is thus necessary to take this

small correction into account (Giamarchi and Schulz, 1988*b*), which gives the flow of Fig. 9.6(-b). One thus sees that the elastic case $V = 0$ indeed remains elastic and also that for spinless fermions, the perturbative flow indicates that the inelastic interactions are reduced by the disorder. This is compatible with the physical image that one would get at strong disorder: fermions localize individually and since the overlap of wavefunctions is exponentially small, so is the effect of interactions. One could thus naively expect that below $\xi_{\rm loc}$ the effect of interactions are strong but disappear above $\xi_{\rm loc}$. For fermions with spin the exchange interaction between the localized spins remains even in the localized phase.

9.2.3.2 *RG equations* The second important point is the consequences of getting the proper RG equation (9.63) for the disorder. This is in particular crucial if one tries to relate the variation of some physical quantity to microscopic parameters. Let us, for example, see how the localization length varies with the interaction U for a Hubbard model. Indeed, for a Hubbard interaction the relation between the LL parameters and U is given by (7.9) at small U. Substituting in the RG equation gives for the initial steps of the flow

$$\frac{d\tilde{D}_{\rm b}}{dl} = (1 - \frac{U}{\pi v_F})\tilde{D}_{\rm b} \tag{9.73}$$

whereas the substitution in the *incorrect* equation (9.58) or at the fixed point $K_\sigma = 1$, $y = 0$ would lead to $(1 + \frac{U}{\pi v_F})$, leading to quite different physics. Equation (9.73) implies that for Hubbard type interactions repulsive interactions make the system *less* localized (Giamarchi and Shastry, 1995) than for attractive interactions, that is, $\xi_{\rm loc}^{U>0} > \xi_{\rm loc}^{U<0}$. Similar effects exist for the charge stiffness and the persistent currents, that is, for a system with spin the persistent currents are in fact enhanced by repulsive interactions. Of course, for the Hubbard model both the repulsive and the attractive sides are always localized since $K_\rho < 2$ (see Chapter 7) and for the attractive side one needs $K_\rho > 3$ to delocalize. The counter-intuitive increase of the localization length by a positive U can be explained physically: interactions have two effects: (i) They tend to reinforce, when attractive, the superconducting fluctuations in the system. This screens disorder and makes it less effective. This is the only effect occurring for spinless fermions. (ii) When spin degrees of freedom exist, repulsive interactions also tend to make the density more uniform by spreading the charge (see Fig. 9.9). This makes it more difficult to couple to disorder. These two effects compete and for the Hubbard model (purely local interaction) the second effect wins, hence the decrease of localization length when the interactions become more attractive. Note that for the Hubbard model, since $K_\rho < 2$ both the repulsive and the attractive side are always localized. To reach delocalization one needs attractive interactions with a range of at least nearest neighbors. For more on this problem see Bouzerar *et al.* (1994), Giamarchi and Shastry (1995), Berkovits and Avishai (1995) and Gambetti-Cesare *et al.* (2002).

9.2.3.3 *Strong coupling* Can we analyze the strong coupling in the same way than what we did for the Mott phase. Indeed, if the coefficient of the cosine becomes large one would naively think that one can expand the cosine, leading to the disorder term

$$D_{\mathrm{b}} \int dx \int \int d\tau \, d\tau' \sum_{a,b} (\phi_a(x,\tau) - \phi_b(x,\tau'))^2 \tag{9.74}$$

Unfortunately, it is easy to see that this is essentially wrong. In particular, this only gives $\phi(\omega_n = 0)$ contributions to the action that does not modify the current. Thus, no trace of localization will be found in the conductivity, which is obviously incorrect. Even a better approximation for the cosine such as the variational approach of Appendix E.2 does not improve the result.

This peculiarity is due to the fact that we have ultimately to take the limit $n \to 0$ to get the physics of the disordered system. There are various ways to take this limit. One is the so-called replica symmetric way, which is the one the expansion of the cosine would give. The correlation $\langle \phi_a \phi_b \rangle$ has a value for equal replica indices and another one for different replica indices. This is the natural choice since it corresponds to the structure of the action. Unfortunately, this solution is unstable, as it often happens in disordered problems, and one has to break the replica symmetry. It would take us too far to explain the process here so I refer the reader to Giamarchi and Le Doussal (1996) and Giamarchi and Orignac (2003) for more details. Taking into account replica symmetry breaking it is possible to use a variational method along the lines of Appendix E.2 to analyze the strong coupling regime. It is a very nice approach since it can reach the energy regimes that the RG cannot reach.

9.2.3.4 *Commensurate disorder* How much of this physics is modified if one is at commensurate filling and the disorder Hamiltonian is (9.25) instead of (9.21)? We see immediately two important differences. First, ξ is real since there is no random phase any more to which the phase ϕ will try to adjust. The physics of the disordered phase is thus very different. The backward scattering term is

$$H = \int dx \, \xi(x) \cos(2\phi(x)) \tag{9.75}$$

Thus, the system has only two different minima $2\phi = 0$ or $2\phi = \pi$ depending on whether ξ is positive or negative. The physics of the commensurate systems is not about ϕ trying to adjust to a random phase, as for the incommensurate one, but about how to make kinks between these two minima at favorable places as indicated in Fig. 9.13. This leads to quite different properties. In particular, the commensurate system has a state at zero energy that is localized only as

$$\psi \sim e^{-\sqrt{|x|}} \tag{9.76}$$

so formally the localization length diverges at zero energy. There are other interesting properties and I refer the reader to Fisher (1994), Monthus *et al.* (1998) and Damle and Huse (2002) for more details.

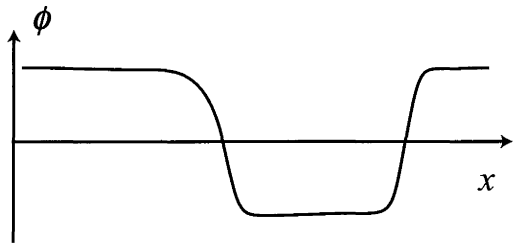

FIG. 9.13. Commensurate disorder. The phase now has only two values that lead to degenerate energy of the ground state. The physics of the system with such a disorder is thus controlled by the excitations that bring the phase from one value to the other. This is very different from the standard case where the phase has to adjust to a random value.

One last word about commensurate systems. Because of the form of disorder (9.75) one cannot eliminate the forward scattering any more by transformation (9.30). Since the elimination of the forward scattering was giving a random phase to ξ it thus replaces the commensurate backward scattering by a 'normal' one when present. For this reason the commensurate case is not very relevant for the case of fermions. For the case of spins, on the other hand, it is easy to find a form of the disorder that does not generate forward scattering such as random exchange. Indeed, random exchange does not change the spin density by spin rotation symmetry, it thus does not contain any component that would be for the fermions the equivalent of a chemical potential (that is, the forward scattering). Its effect has been worked out in (6.63) for the spin-Peierls distortion. The coupling to a staggered modulation of the exchange is $\sin(2\phi)$. A random exchange thus produces a term

$$\int dx\, \delta J(x) \sin(2\phi(x)) \tag{9.77}$$

Random spin chains are thus prime candidates to study the effects of commensurate disorder.

9.3 Quantum wires

An experimental realization of Luttinger liquids is provided by the so-called quantum wires. The idea is to confine the electron gas in a narrow enough channel, so that only one direction of motion matters. For example, let us assume that one starts with a two-dimensional electron gas. Such systems are routinely made for quantum hall devices and semiconducting industry. One can then either by lithography or by applying a potential repelling the electrons from a gate confine the electrons in a channel of width L_y as explained in Fig. 9.14. The

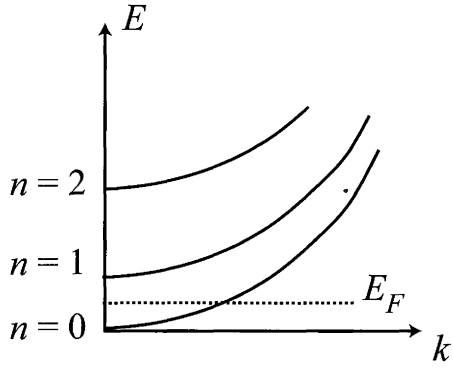

FIG. 9.14. Confinement of the electron gas in a one-dimensional wire. Only half of the dispersion relation $E(k)$ is shown for clarity. k is the momentum parallel to the wire direction. The degrees of freedom transverse to the wire direction lead to the formation of minibands, labelled by a quantum number n. If the channel in which the electrons are confined is narrow enough the distance between minibands can be made large compared to the temperature. One can be in a situation where only one miniband is occupied and the quantum wire is equivalent to a one-dimensional system. If two (or more) minibands are occupied the wire is equivalent to a ladder system.

wavefunction of the system is thus of the form

$$\psi(x, y) = e^{ikx}\phi(y) \tag{9.78}$$

where ϕ depends on the precise form of the confining potential (for an infinite well ϕ is also a combination of plane waves). The energy is of the form

$$E = \frac{k^2}{2m} + \frac{k_y^2}{2m} \tag{9.79}$$

where for simplicity I have taken ϕ to be a plane wave. The important point is the fact that due to the narrowness of the transverse channel l, the quantization of k_y is sizeable. Indeed, the change in energy by changing the transverse quantum number n_y is at least (e.g. $n_y = 0$ to $n_y = 1$)

$$\Delta E = \frac{(2\pi)^2}{2ml^2} \tag{9.80}$$

This leads to minibands as shown in Fig. 9.14. If the distance between the minibands is larger than the temperature one can by changing the chemical potential (with an external gate) be in a situation where only one miniband is occupied. The transverse degrees of freedom are thus frozen and only k matters. The system is a one-dimensional electron gas.

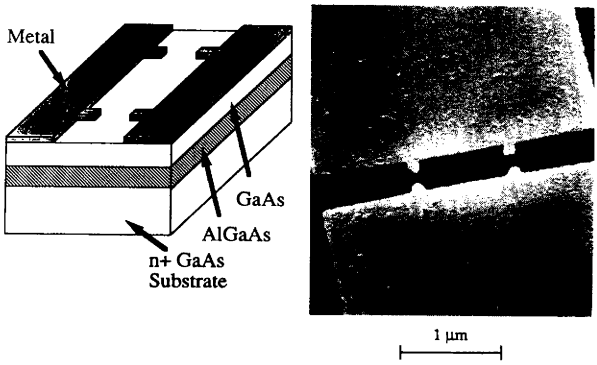

FIG. 9.15. A two-dimensional electron gas formed at the interface between GaAs and the insulating AlGaAs. The carrier density is controlled by the application of a voltage V_g to the substrate. To transform the 2DEG into a one-dimensional wire, metal electrodes on the surface confine the electron gas into a one-dimensional channel. The voltage v_b on the electrodes allows to control the width of the channel. (From Meirav *et al.*, 1990 (Copyright (1990) by the American Physical Society).)

An actual example is shown in Fig. 9.15 (Meirav *et al.*, 1990). Various variants can be found (Thornton *et al.*, 1986; Scott-Thomas *et al.*, 1989; Calleja *et al.*, 1991; Goñi *et al.*, 1991; Tarucha *et al.*, 1993; Hwang *et al.*, 1994). Typically, so far the possible length of a wire using these techniques is about 10 μm. The Fermi energy in these systems is quite small $\sim$100K, which imposes to work at very low temperatures. This has the advantage of allowing to forget most of the phonons, but has the drawback that the length of the wire is becoming a real limitation since the thermal length $L_T \sim u/T$ can become comparable to the size of the wire. Although in practice one could imagine getting a wire as thin as desired, it is much less easy to do so in practice, without cutting the wire due to some potential fluctuations.

We already saw some spectroscopy data in Fig. 4.2, which was in good agreement with the expectations for a one-dimensional electron gas. Let us examine here the transport properties in such wires. An example of conductance is shown in Fig. 9.16. One clearly sees the conductance quantization at the value e^2/h (per spin). This is in agreement with the theoretical expectation (see Section 7.2) and clearly shows that there is only one miniband at the Fermi level. From these data one sees that there are deviations to the perfect conductance quantization when the temperature is lowered. It is tempting to interpret these deviations as due to the disorder present in the wire following the analysis presented in this chapter. One indeed observes a decrease of conductance with temperature as shown in Fig. 9.16.

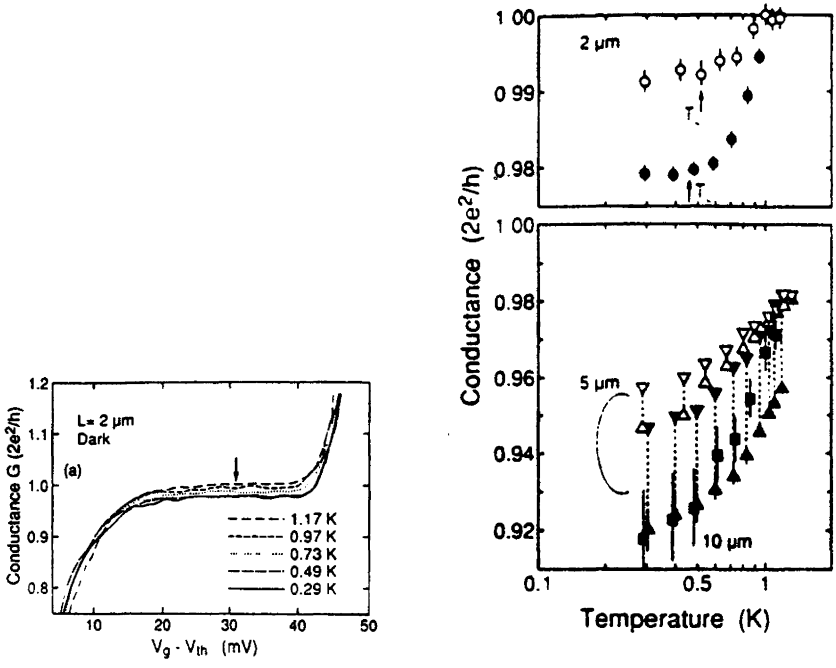

FIG. 9.16. Conductance of a quantum wire. One observes quantization of the conductance at a value of e^2/h per spin. This is an indication that there is only one channel of conduction at the Fermi level. The deviations from the perfect quantization can be interpreted as being due to the disorder in the wire. The data are consistent with the expected behavior for a LL but given the short-range of temperatures it is difficult to draw definite conclusions. (From Tarucha *et al.*, 1995 (Copyright (1995), with permission by Elsevier).)

Another very interesting technique (Yacoby *et al.*, 1996; de Picciotto *et al.*, 2000) consists in making the wire at the edge of a two-dimensional electron gas. This technique allows to have a very uniform width for the wire. The interpretation of the data in these systems is however more complex due to large contacts between the one-dimensional electron gas and the large 2D–1D scattering (de Picciotto *et al.*, 2001). These systems allow however for beautiful experiments both in transport and in tunneling between wires (Auslaender *et al.*, 2002; Carpentier *et al.*, 2002; Tserkovnyak *et al.*, 2002).

It would be impossible to review here all possible measurements that can be made in these systems. This is a field in constant expansion given the progress in the experimental realization of these systems. Quantum wires are clearly one of the ultimate weapons to study individual one-dimensional systems.

10

BOUNDARIES AND ISOLATED IMPURITIES

There is only one object on earth that frightens me: a physicist working on a new trick.

Nero Wolfe by Rex Stout (*A Family Affair*)

Let us look in this chapter at the effects of individual impurities and boundaries in a Luttinger liquid. Such effects are specially important in Luttinger liquids realized in mesoscopic (or nanoscopic) devices.

10.1 Effect of a boundary

We start with the effects of a boundary. Such a boundary can be produced either by the physical end of the device (such as in a nanotube) or by putting very strong impurities in the one-dimensional system. Such impurities will in effect cut the chain. For simplicity, I illustrate the calculations on spinless fermions. Similar results are obtained for fermions with spin. I consider a LL that terminates at $x = 0$ as indicated in Fig. 10.1. If we look at the correlation functions far from the boundary, it is clear that one should recover the correlation functions of the infinite LL. On the other hand if one sits very close to the boundary $x = 0^+$ and looks at the temporal decay of the correlation functions one can a priori expect some modifications compared to the same correlation functions deep in the LL. Let me illustrate this effect by looking at the single-particle Green's function. Far from the boundary one has (2.83)

$$\langle \psi(x,\tau)\psi^\dagger(x,0)\rangle \propto \left(\frac{\alpha}{u\tau}\right)^{(K+K^{-1})/2} \tag{10.1}$$

To compute this correlation function close to the boundary $x = x_b$, one has to take into account the constraint that at the boundary the wavefunction vanishes

$$\psi(x_b,\tau) = e^{ik_F x_b}\tilde{\psi}_R(x_b,\tau) + e^{-ik_F x_b}\tilde{\psi}_L(x_b,\tau) = 0 \tag{10.2}$$

The general condition at the boundary is thus

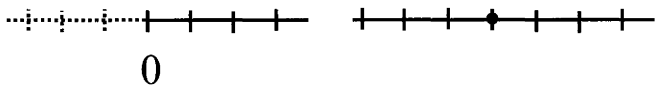

FIG. 10.1. A Luttinger liquid with a hard boundary. This can also be produced by putting a very strong impurity in an infinite chain.

$$\tilde{\psi}_R(x_b,\tau) = e^{i(\pi-2k_F x_b)}\tilde{\psi}_L(x_b,\tau) = e^{-i2\delta}\tilde{\psi}_L(x_b,\tau) \tag{10.3}$$

The precise phase shift δ depends on the position of the boundary. Let us take an example. If one takes a spinless fermion chain at half-filling ($k_F = \pi/(2a)$) starting at $x = 0$ one wants the wavefunction to be zero at $x_b = -a$ so that all the negative space is blocked. In that case the phase shift is zero and $\tilde{\psi}_R(-a,\tau) = \tilde{\psi}_L(-a,\tau)$. Note that since the fields $\tilde{\psi}$ vary slowly at the scale of the lattice the condition is approximately $\tilde{\psi}_R(0,\tau) = \tilde{\psi}_L(0,\tau)$. Re-expressing the fermion operators in terms of the boson fields gives for the bosons

$$\phi(x_b) = \delta + \pi n \tag{10.4}$$

In the following, I take $\delta = 0$ and $x_b = 0$ to illustrate the physics. Putting another phase shift is straightforward. Note that the constraint on the field ϕ comes from the fact that the boundary that we have chosen imposes that the density is fixed (zero in our case). Choosing other boundary conditions such as putting the LL in contact with a superconductor would impose a constraint on the field θ instead. The condition on ϕ has several consequences. First, since ϕ is constrained at $x = 0$ it means that very close to the boundary ϕ has to go to a constant. Indeed, ϕ is a continuous variable otherwise the term $(\partial_x\phi)^2$ in the Hamiltonian would be infinite. Thus, $\phi(x \to 0,\tau) \to 0$. One could thus naively think that it is enough to block ϕ and compute the correlations with the field θ free. This would give for the correlation

$$\begin{aligned}\langle\psi_R(x\simeq 0,\tau)\psi_R^\dagger(x\simeq 0,0)\rangle &\propto \langle e^{-i(\phi(x\simeq 0,\tau)-\theta(x\simeq 0,\tau)}e^{i(\phi(x\simeq 0,0)-\theta(x\simeq 0,0))}\rangle \\ &= \langle e^{i\theta(x\simeq 0,\tau)}e^{-i\theta(x\simeq 0,0)}\rangle \\ &= \left(\frac{\alpha}{u\tau}\right)^{(K^{-1})/2}\end{aligned} \tag{10.5}$$

Although this method is partly correct, and shows that the decay close to the boundary is drastically different than in the bulk, because some fluctuations are frozen, it contains an important mistake. Because of the boundary the fluctuations of the field θ are also changed and cannot be computed as if one was far away from the boundary. The exponent obtained from (10.5) is thus incorrect, and one needs a more careful calculation to obtain it (Eggert and Affleck, 1992).

Let us now correctly calculate the effects of the constraint. The constraint (10.4) can be expressed in terms of the chiral fields (3.57)

$$\phi_L(0,\tau) - \phi_R(0,\tau) = 2\delta \tag{10.6}$$

But since the chiral fields R, L are respectively functions of $x - ut$ and $x + ut$ *only*, this local constraint immediately extend to all space and time

$$\phi_L(x,\tau) - \phi_R(-x,\tau) = 2\delta \tag{10.7}$$

What we are considering is a Luttinger liquid living in half a space (the positive x) with right *and* left going particles. Because of the boundary one has to take

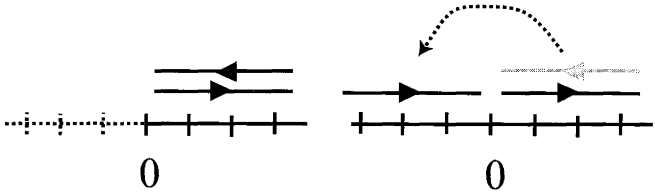

FIG. 10.2. A half Luttinger liquid with right and left movers can be viewed as a full Luttinger liquid. Only the right movers are important in that case. It is important to get rid of the interactions before doing this mapping to avoid very non-local interactions.

the constraint on ϕ into account for this problem. An alternative representation is to extend the problem to the whole space, the left goers for the positive x being identical to the right goers of the negative space using (10.7). This is schematically shown in Fig. 10.2. But before doing this, one has to get rid of the interactions. Indeed, if there is an interaction in the original problem, the new problem will have a crazy interaction. For example, if one has in the original Hamiltonian

$$\int_0^\infty \rho_R(x)\rho_L(x) \tag{10.8}$$

because of the mapping

$$\begin{aligned} \tilde{\psi}_R(x) &= \tilde{\psi}_R^e(x) \\ \tilde{\psi}_L(x) &= \tilde{\psi}_R^e(-x) \end{aligned} \tag{10.9}$$

the interaction becomes

$$\int_0^\infty \rho_R(x)\rho_L(x) = \int_0^\infty \rho_R^e(x)\rho_R^e(-x) \tag{10.10}$$

which is a non-local interaction and thus particularly unpleasant. However, one can always eliminate the interaction of the fermion problem simply by rescaling the fields, in the same way we did in Chapter 3 and Section 4.2. If one introduces the fields

$$\begin{aligned} \phi &= \sqrt{K}\tilde{\phi} \\ \theta &= \frac{1}{\sqrt{K}}\tilde{\theta} \end{aligned} \tag{10.11}$$

the problem defined in terms of $\tilde{\phi}$ and $\tilde{\theta}$ has $\tilde{K} = 1$ and thus corresponds to *free* fermions. For this system, one can thus use the trick of extending the system into the whole space without any cost. Since this becomes a little complicated, let me take the concrete example of computing the correlation

$$\langle \psi_R(x_{,1}\,\tau_1)\psi_R^\dagger(x_2,\tau_2)\rangle \tag{10.12}$$

Note that because of the boundary the correlation now depends explicitly on x_1 and x_2 and not on the difference. The operator we need is given by

$$\psi_R(x,_1 \tau_1) \propto e^{-i[\phi(x_1,\tau_1)-\theta(x_1,\tau_1)]} \tag{10.13}$$

In terms of the rescaled fields this becomes

$$\begin{aligned}\psi_R(x,_1 \tau_1) &\propto e^{-i[\sqrt{K}\tilde{\phi}(x_1,\tau_1)-\frac{1}{\sqrt{K}}\tilde{\theta}(x_1,\tau_1)]} \\ &= e^{-i[\sqrt{K}(\frac{\phi_L-\phi_R}{2})-\frac{1}{\sqrt{K}}(\frac{\phi_L+\phi_R}{2})](x_1,\tau_1)}\end{aligned} \tag{10.14}$$

where I have used the chiral field (3.57) corresponding to the fields $\tilde{\phi}$ and $\tilde{\theta}$ ($\tilde{K}=1$ for these fields). Now in presence of the boundary one uses the mapping (with $\delta = 0$) on the whole space (10.7)

$$\begin{aligned}\tilde{\phi}_R(x,\tau) &= \phi_R^e(x,\tau) \\ \tilde{\phi}_L(x,\tau) &= \phi_R^e(-x,\tau)\end{aligned} \tag{10.15}$$

Since the theory for $\tilde{\phi}$ is a free theory the Hamiltonian on the whole space is a *free* Hamiltonian. Note that the presence of the boundary leaves, in the appropriate variables, the theory free. This is a general feature that has been used to solve impurity problems. I will come back on that in Section 11.2. The single-particle operator becomes

$$\begin{aligned}\psi_R(x,_1 \tau_1) &\propto e^{\frac{-i}{2}[(\sqrt{K}-\frac{1}{\sqrt{K}})\phi_R^e(-x_1,\tau_1)-(\sqrt{K}+\frac{1}{\sqrt{K}})\phi_R^e(x_1,\tau_1)]} \\ &= e^{\frac{-i}{2}[(\sqrt{K}-\frac{1}{\sqrt{K}})[\theta^e-\phi^e](-x_1,\tau_1)-(\sqrt{K}+\frac{1}{\sqrt{K}})[\theta^e-\phi^e](x_1,\tau_1)]}\end{aligned} \tag{10.16}$$

Using (10.16) the correlation function can now be computed using the standard formulas of Appendix C (remember that the fields are free so that $K^e = 1$). Since (10.16) contains the fields at x and $-x$ the correlation will contain $x_1 + x_2$ and $x_1 - x_2$ and one recovers that in presence of a boundary the correlation depends separately in x_1 and x_2 and not only on the difference. Although there is no difficulty of principle in computing the full formula it is a little bit tedious so let me illustrate the calculation on the correlation function very close to the boundary ($x_1 = x_2 = 0$). In that case (10.16) becomes

$$\psi_R(0,\tau_1) \propto e^{-i[\frac{1}{\sqrt{K}}[\phi^e-\theta^e](0,\tau_1)]} \tag{10.17}$$

The correlation thus decays as

$$\langle\psi_R(0,\tau_1)\psi_R^\dagger(0,\tau_2)\rangle = \left(\frac{\alpha}{u|\tau_1-\tau_2|}\right)^{\frac{1}{K}} \tag{10.18}$$

The exponent close to the boundary is thus $1/K$ instead of $[K + 1/K]/2$ in the bulk. Note that the correct exponent is indeed different from the naive (incorrect)

one of (10.5). The decay close to the boundary is faster, since the fluctuations of θ are in fact enhanced compared to the bulk. This is very reasonable: since ϕ and θ are conjugate variables the fact that ϕ is frozen at the boundary should reinforce the fluctuations of θ. For the case of the correlation at the boundary one can recover this result in a simple way. The action written in terms of the field θ is

$$S = \frac{1}{2\pi}\int_0^\infty dx \int_0^\beta d\tau K[(\partial_\tau\theta)^2/u + u(\partial_x\theta)^2] \tag{10.19}$$

In Fourier transform, this would give

$$S = \frac{1}{2\pi}\frac{1}{2\beta L}\sum_{q,n} K[\omega_n^2/u + uq^2]\theta(q,\omega_n)^*\theta(q,\omega_n) \tag{10.20}$$

one has a coefficient $1/(2\beta L)$ instead of the usual $1/(\beta L)$ since the integral over x in (10.19) runs only on *half space*. It is as if one had replaced K by $K/2$ in the standard formulas. So if one computes the $\theta(x=0,\tau)\theta(x=0,\tau')$ correlation in (10.5) one should use $K/2$ instead of K giving back the correct exponent.

It means that if one can probe for example the single-particle density of states close to an edge in a LL one will see a different result than the bulk exponent (2.92). Note that the boundary exponent is still a function of the bulk parameter K, only the functional form is changed. For more on the effect of boundaries in other systems see, for example, Eggert and Affleck (1995), Fabrizio and Gogolin (1995) and Rommer and Eggert (2000).

10.2 Isolated impurities

Let us examine the case of a Luttinger liquid in which one has put a single impurity (Glazman *et al.*, 1992; Kane and Fisher, 1992*b*; Kane and Fisher, 1992*a*). Although such a description is not very realistic in a natural system, it can be obtained easily in an artificial one, where one puts a constriction in the Luttinger liquid. I will present later examples of such systems. For simplicity, let us start with spinless fermions. In that case the interaction between the impurity potential and the LL is (see (9.14))

$$H_{\text{sing}} = \int dx\, V(x)\rho(x) = V_0\rho(x=0) \tag{10.21}$$

if we replace the impurity potential by a delta function $V(x) = V_0\delta(x)$. We assume that V_0 is still weak compared to the Fermi energy so that one can use the bosonization representation. Using the decomposition of the density one gets

$$H_{\text{sing}} = V_0[-\frac{1}{\pi}\nabla\phi(x=0) + \frac{1}{\pi\alpha}\cos(2\phi(x=0))] \tag{10.22}$$

It is the very dilute limit of impurities for the disorder seen in Section 9.1. As we saw in the previous chapter, the forward scattering can be straightforwardly

eliminated from the problem by a redefinition of the field ϕ (see (9.30)). Since only the value of the field at $x = 0$ appears in the backward scattering term one can always choose the transformation as

$$\tilde{\phi} = \phi(x) - \frac{K}{u} \int_0^x dy\, \eta(y) \tag{10.23}$$

so that the field at $x = 0$ is not affected. I thus drop the forward scattering term in the following and look only at the effects of the backscattering terms.

10.2.1 *Weak coupling*

The backward potential can be treated by the very method we used in Section 9.1. Let us examine the renormalization due to the disorder term. The renormalization of the potential V_0 itself can be seen directly from the second-order term

$$\begin{aligned} S_2 &= V_0^2 \int\int d\tau\, d\tau' \langle \cos(2\phi(x=0,\tau)\cos(2\phi(x=0,\tau')\rangle \\ &= \frac{V_0^2}{2} \int\int d\tau\, d\tau' \left(\frac{\alpha}{u|\tau-\tau'|}\right)^{2K} \end{aligned} \tag{10.24}$$

Thus, this term has a dimension L^{2-2K}. The renormalization equation for V_0 is thus (see (9.45) and (9.57))

$$\frac{dV_0^2}{dl} = V_0^2(2-2K) \tag{10.25}$$

It is exactly identical to the one we obtained for the disorder (9.57). The renormalization of the disorder is thus identical for a single impurity to the one for many impurities (remember that for many impurities the disorder was $D = n_i V_0^2$). The main difference between the case of many impurities and the case of an isolated one is the renormalization of the parameter K. For many impurities the disorder was able to renormalize the interaction parameter K. Here, the second-order term (10.24) occurs only at a single point (compare with (9.28)). Thus, the term that was at the root of the renormalization of K does not appear, and K is not renormalized. This is physically very reasonable: since the impurity acts only at one point it cannot renormalize a bulk quantity such as the Luttinger parameter K. The full equations for the single impurity are thus

$$\begin{aligned} \frac{dK}{dl} &= 0 \\ \frac{dV_0}{dl} &= (1-K)V_0 \end{aligned} \tag{10.26}$$

This set of equations is similar to the ones for weak uniform disorder (9.47), so many physical properties will be very similar. There are, however, very important physical differences due to the absence of renormalization of K. I will come back,

later in this section, in more details to the comparison of isolated impurities and extended disorder. As for the extended disorder, (10.26) defines two regimes. If $K > 1$ the strength of the impurity potential goes down. The fixed point in this regime is thus a LL where the impurity is absent. One recovers a perfect conductor. On the contrary if $K < 1$ the strength of the impurity potential goes up. The system is thus more and more strongly pinned by the impurity. Note that because of the absence of feedback of the disorder in K the transition between the pinned and free regime is now for $K = 1$ (instead of $K = 3/2$ for uniform disorder), although the RG equation for the disorder are in fact *identical* in the two cases. This confirms, as already discussed in Chapter 9, that *both* the RG equations for the disorder and K determine the physical properties. In a similar way than in Section 9.2 (see (9.52)) the scale at which the impurity strength becomes of order one is

$$e^l = \left(\frac{\pi v_F}{V_0}\right)^{\frac{1}{1-K}} \tag{10.27}$$

Note that now we do not know what is the physics of the strong coupling with a single impurity, and we have to analyze it specifically. This will be done in the next section.

More importantly, one can compute the transport properties (Kane and Fisher, 1992*a*). Since the impurity exists only at one site, conductivity which is a bulk quantity would not be useful and one wants to compute the conductance of a segment of wire. We use formula (7.67). As we saw for a pure system, computing the static limit for the conductance was equivalent to taking $L \to 0$. Here, the impurity only exists at $x = 0$ so one can simply compute

$$G = \frac{e^2}{\hbar\pi^2} \lim_{\omega\to 0} i(\omega + i\delta)\left[\langle\phi(x=0);\phi(x=0)\rangle_\omega\right] \tag{10.28}$$

At finite temperature, the conductance can thus be computed in an expansion in powers of the scattering V_0. One can make a precise calculation of the perturbation expansion, but let us just obtain the scaling behavior here. We will do the precise calculation for the strong coupling regime. We renormalize the scattering up to a scale for which the cutoff is of the order of the temperature. This scale is given by

$$e^{l^*} = \left(\frac{L_T}{\alpha}\right) = \left(\frac{u}{\alpha T}\right) \tag{10.29}$$

At that lengthscale the correction to the conductance is of the form

$$G = \frac{e^2}{h}[K - V_0(l^*)^2 \int \langle\phi\phi\cos(\phi)\cos(\phi)\rangle] \tag{10.30}$$

where I have loosely noted $\int\langle\rangle$ the correlation function corresponding to the expansion up to second order in the scattering (the first-order vanishes). Because

the renormalized cutoff is of the order of the temperature this correlation function is of order one. The correction to the conductivity thus scales as

$$\delta G/G_0 \sim -V_0(l^*)^2 \sim -V_0^2 e^{(2-2K)l^*} \sim -V_0^2 \left(\frac{u}{\alpha T}\right)^{2-2K} \tag{10.31}$$

One thus recovers that when $K > 1$ the correction to the conductance vanishes at low-energy ($T \to 0$) and the system becomes a perfect conductor. When $K < 1$ on the contrary the correction to the conductance grows reducing the conductance compared to its perfectly conducting value. The disorder is relevant and this behavior is suggestive of the fact that the system might become an insulator at strong coupling. Note that the exponent for the correction of the conductance is exactly the opposite of the one we had obtained for the temperature dependence of the conductivity for extended disorder. I will come back to that point at the end of the section. The system with spin has exactly the same behavior except that the RG equation for the impurity potential should be replaced by

$$\frac{dD}{dl} = (2 - K_\rho - K_\sigma^*)D \tag{10.32}$$

where I have taken the equation at the fixed point for the spin part for simplicity (however, see (9.63) and the discussion in Section 9.2.3). Taking a spin rotation invariant system $K_\sigma^* = 1$ one finds that the exponent for the correction to the conductance is $(1/T)^{1-K_\rho}$. Note that here we have stopped the flow using the temperature as a cutoff. One could also use the voltage difference V across the system. Indeed, a voltage gives a in the Hamiltonian

$$H_V = -\int a(\tau)\partial_\tau \phi \tag{10.33}$$

(see Section 7.2), where $a \propto V$ is the vector potential and thus acts as a cutoff in a similar way than the magnetic field (which is $\sim \int \nabla\phi$) did in Section 4.2. One would have thus a voltage dependent correction to the conductance (at $T = 0$) of the form

$$G(V) = \frac{e^2}{h}[K - \text{Cste } V_0^2 V^{2K-2}] \tag{10.34}$$

which allows to get the leading nonlinear I–V characteristics using $I = G(V)V$.

10.2.2 *Strong coupling*

What happens when the potential has reached strong coupling. One can solve this problem in a physical way or use a more formal solution. Physically, we saw in the previous section that the impurity potential grows under renormalization. One would thus expect that the strong coupling corresponds to a situation where the impurity is so strong that the field ϕ is blocked to the minimum of the cosine. Note that this is true if the *backward* component of the potential is strong. This is not necessarily the same thing as to start from a strong potential for which the

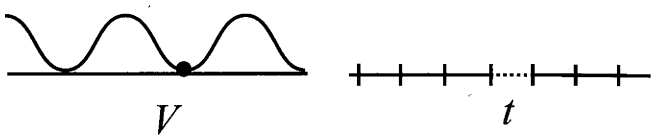

FIG. 10.3. Weak and strong coupling representations of a single impurity. If the potential V is weak it tries to pin the electron density. If the potential is strong one can view this problem as a system where the density wave wants to always put a minimum of density at the position of the impurity and the motion occurs by tunneling events (see text). An alternative representation of the strong coupling is to say that the impurity has cut the chain into two parts. The fact that the impurity potential is not infinite is taken into account by allowing a small tunneling t between the two segments of the chain.

forward component is also strong. If the field $\phi(x=0)$ was totally blocked at the site this would correspond to cutting the chain into two disconnected pieces as we saw in Section 10.1. Of course, this cannot be true at intermediate energy scales, so to analyze the strong coupling regime one has to take into account the fact that electrons can still jump across the impurity. Phenomenologically, this can be done by considering that the system is now described by two disconnected half chains and a hopping term (Kane and Fisher, 1992*b*; Kane and Fisher, 1992*a*). A very reasonable candidate for the strong coupling Hamiltonian is thus

$$H = H_1 + H_2 - t[\psi_1^\dagger(x=0)\psi_2(x=0) + \text{h.c.}] \tag{10.35}$$

where 1 and 2 are the two half chains. This is represented in Fig. 10.3.

Let us examine how the hopping changes the behavior of the system compared to the two unconnected chains. This can be done by looking at the RG equations for the hopping. As for the impurity potential in the weak coupling case, it is obvious that this is the only equation to examine. Since the hopping is only local it cannot renormalize the LL parameter of the chains. To determine the RG equation for the hopping let us go to second order in perturbation since the first-order term vanishes when averaged. It gives

$$\int d\tau_1 d\tau_2 \langle \psi_1^\dagger(\tau_1)\psi_2(\tau_1)\psi_2^\dagger(\tau_2)\psi_1(\tau_2)\rangle = \int d\tau_1 d\tau_2 \langle \psi_1^\dagger(\tau_1)\psi_1(\tau_2)\rangle_1 \langle \psi_2(\tau_1)\psi_2^\dagger(\tau_2)\rangle_2 \tag{10.36}$$

The correlations close to a boundary have been computed in the previous section and are

$$\langle \psi_j^\dagger(\tau_1)\psi_j(\tau_2)\rangle_j \sim \left(\frac{1}{\tau_1 - \tau_2}\right)^{\frac{1}{K}} \tag{10.37}$$

The scaling dimension of this term is thus $L^{2-2/K}$. This gives for the renormalization equation for the hopping

$$\frac{dt}{dl} = (1 - 1/K)t \tag{10.38}$$

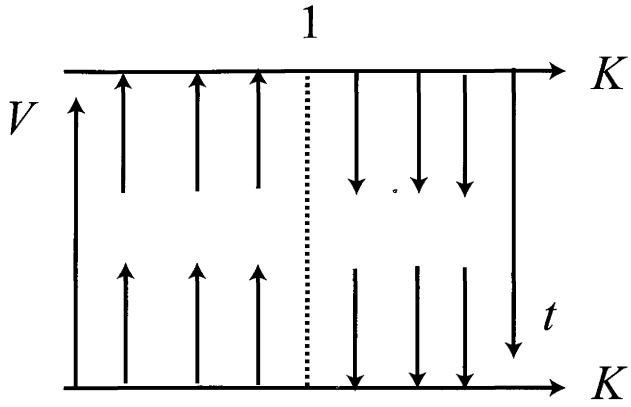

FIG. 10.4. RG flow for a single impurity. For weak coupling the impurity can be modelled by the potential V which is relevant for $K < 1$ and irrelevant for $K > 1$. The weak tunneling between two half chains, which is a way to model the strong impurity potential has the opposite behavior and is irrelevant for $K < 1$ and relevant for $K > 1$. These two limits allow to fully characterize the behavior of the impurity. (After Kane and Fisher, 1992*a*.)

One sees that for $K > 1$ the hopping between the two half parts increases connecting the chains more and more. For $K < 1$ the hopping decreases at low-energy leaving the chains less and less connected. This dual vision of the system offers thus a nice continuity with the weak coupling analysis and is shown in Fig. 10.4.

The dual representation (10.35) also provides a very nice way to study the physical properties in the strong coupling regime, since t becomes weaker and weaker when the chain is cut. For example, in the absence of t the conductance would be zero. The conductance is thus given by the lowest expansion in powers of t in the expression (10.28). The first-order vanishes and the dominant contribution is given by the second order term. We use the same scaling analysis than for the weak coupling. We stop the flow when the cutoff is of the order of the temperature. The conductance is thus given by (all correlations are of order one at that scale)

$$G \sim \frac{e^2}{h} t^2(l^*) \sim \frac{e^2}{h} t^2 \left(\frac{u}{\alpha T}\right)^{2-2/K} \tag{10.39}$$

The strong coupling analysis thus confirms that the decrease of the conductance that was seen in the weak coupling regime continues. The system is indeed a perfect insulator. But the decay of the conductance follows in the strong coupling regime a power law with a *different* exponent, than in weak coupling. A plot of the temperature dependence of the conductance is shown in Fig. 10.5. In a similar way the current–voltage characteristics is now given by

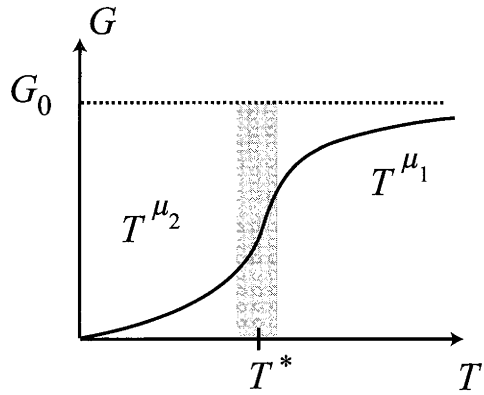

FIG. 10.5. The temperature dependence of the conductance for a single impurity for $K < 1$. The system becomes a perfect insulator at $T = 0$. At high temperature there are power law corrections to the perfect conductance $G_0 = e^2/h$, with an exponent $\mu_1 = 2K - 2$. There is a crossover scale T^* for which the renormalized impurity parameter is of order one. Below this lengthscale the transport proceed essentially by weak tunneling (instantons) through the impurity. The conductance has thus a different power law dependence than at high temperature $\mu_2 = 2/K - 2$.

$$I = G(V)V \sim V^{2/K-1} \tag{10.40}$$

The derivation of the strong coupling Hamiltonian is very reasonable physically but still phenomenological. To put this nice physical result on a firmer ground, let us take the runaway flow of the potential V seriously and consider

$$S_{V_0} = \frac{V_0}{\pi\alpha} \int d\tau \ \cos(2\phi(x = 0, \tau)) \tag{10.41}$$

with a very large V_0. For V_0 large but finite ϕ is not really blocked. It is constrained to stay in the minima of the cosine most of the time, so

$$2\phi = \pi + 2\pi n \tag{10.42}$$

If V_0 is very large then ϕ is forced to tunnel from one minimum of the cosine to the other. It stays very long in one of the minima and then makes a kink in time to go to the next minimum. This is shown in Fig. 10.6. We can thus analyze the whole physics of the system in terms of this tunneling event (Furusaki and Nagaosa, 1993*a*; Furusaki and Nagaosa, 1993*b*). To describe it let us consider the partition function

$$Z = \int \mathcal{D}\phi(\tau) e^{-S/\hbar} \tag{10.43}$$

where I have put back the $\hbar$ for a while. If $\hbar$ is very small, the functional integral would be dominated by the trajectories $\phi(\tau)$ that minimize the action. This is

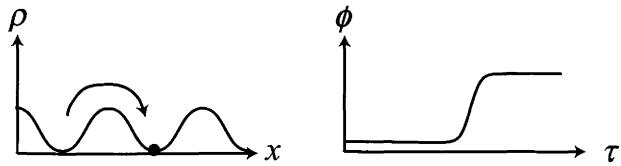

FIG. 10.6. The physics for a large V_0 can be described in terms of instantons. The phase stays locked very long in the minima of the cosine and then goes fast to the next minima to pay the minimum price in the action. Such a process is known as an instanton.

the standard saddle point approximation to compute tunneling events. One has to find the optimal trajectories that go from one of the minima of the potential to the other (Coleman, 1977; Schmid, 1983). Since we want these classical trajectories to contribute to the partition function they should obviously have a finite action. Such trajectories are known as instantons (Rajaraman, 1982). We will use the same trick for a large V_0 (and now $\hbar$ disappears again). To determine the trajectories for a large V_0 let us rewrite the quadratic part of the action. Since the action contains only the field $\phi(x = 0, \tau)$ one can integrate over all other modes. The action for this field is given by

$$S_0 = \frac{1}{2\beta} \sum_n G^{-1}(\omega_n)\phi(\omega_n)^* \phi(\omega_n) \tag{10.44}$$

with (see Appendix C)

$$\langle \phi(x = 0, \omega_n)^* \phi(x = 0, \omega_n) \rangle = \beta G(\omega_n) \tag{10.45}$$

G is thus easily computed

$$G(\omega_n) = \frac{1}{L} \sum_k \frac{\pi K u}{\omega_n^2 + u^2 k^2} = \frac{\pi K}{2|\omega_n|} \tag{10.46}$$

The action thus becomes

$$S_0 = \frac{1}{2\beta} \sum_n \frac{2|\omega_n|}{\pi K} \phi(\omega_n)^* \phi(\omega_n) \tag{10.47}$$

It is easy to rewrite this as

$$S_0 = \frac{1}{2\beta^2 K} \int_0^\beta d\tau \int_0^\beta d\tau' \frac{(\phi(\tau) - \phi(\tau'))^2}{(\sin(\pi(\tau - \tau')/\beta))^2} \tag{10.48}$$

Of course, the $|\omega_n|$ behavior is not valid for large frequencies, due to the cutoff on k in (10.46). At very short times, formula (10.48) should thus be regularized. It can be done naturally by adding to (10.48) a term of the form

$$S_0' = \frac{1}{2}\int_0^\beta d\tau\ M(\partial_\tau \phi(\tau))^2 \tag{10.49}$$

This term is the limiting value at short time of S_0. In the same way if β is very large we can approximate the sine in (10.48) by its argument. We have of course to remember that this is still in fact a periodic function and that the linearization is only an approximation. The total action of the system is thus

$$S = S_0 + S_0' + S_{V_0} \tag{10.50}$$

I denote in the following $\tilde{V}_0 = V_0/(\pi\alpha)$. If V_0 is large, in order to obtain a saddle point approximation, let us rescale the time by $\tau \to \tau/\sqrt{\tilde{V}_0}$. We see that S_0 is not affected by such a rescaling when β is very large. On the other hand, the two other terms of the action become proportional to $\sqrt{V_0}$. The action is thus

$$S = \sqrt{\tilde{V}_0}\left[\int d\tau \frac{M}{2}(\partial_\tau\phi(\tau))^2 - \int d\tau\ \cos(2\phi(\tau))\right] + S_0 \tag{10.51}$$

In the limit where V_0 is very large we can thus use a saddle point approximation for the action. The contribution of S_0 is *negligible* and the trajectories are obtained by minimizing the term in brackets in (10.51).

$$M\frac{d^2\phi(\tau)}{d\tau^2} = \frac{dV(\phi)}{d\phi} = 2\ \sin(2\phi(\tau)) \tag{10.52}$$

The solution starting from $2\phi = 0$ at $\tau = -\infty$ and ending at $2\phi = 2\pi$ at $\tau = \infty$ is easily found. One integrates once the equation (10.52) by multiplying by $\partial_\tau\phi$ to obtain

$$\frac{M}{2}\left(\frac{d\phi(\tau)}{d\tau}\right)^2 = V(\phi) - V(\phi = 0) \tag{10.53}$$

which is nothing but the conservation of energy. The solution of this equation is easily obtained as

$$\tilde{\phi}(\tau) = \frac{\pi}{2} + 2\arctan\left[\tanh[\sqrt{\tilde{V}_0/M}\ \tau]\right] \tag{10.54}$$

Using (10.53) in the action and the solution (10.54) one can easily show that the action is indeed finite for such an instanton and is

$$S_{\text{inst}} = 4\sqrt{M\tilde{V}_0} \tag{10.55}$$

This represents the cost to go through the barrier to tunnel between one minimum of the cosine to the other. This value is identical to the one that one would obtain in the WKB approximation (Coleman, 1977). Since the time to tunnel through the barrier is very small if the barrier is high, one can look for a general solution that is a sequence of such tunneling events. To tunnel from $\phi = 0$ to

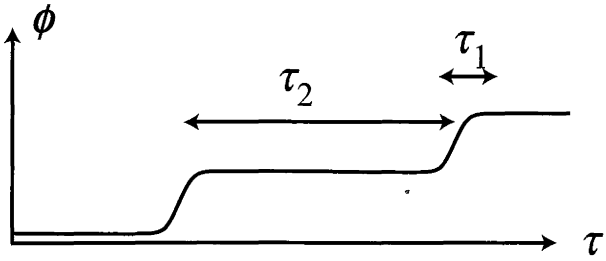

FIG. 10.7. Dilute instanton approximation. The width of an instanton τ_1 is quite small because the barrier is high. The time between instantons τ_2 is thus much larger than the width of an individual instanton. Physically, it means that the system is stuck for a long time between tunneling events.

$\phi = 4\pi$ it is much better to do it sequentially by two tunneling events rather than do it directly. Doing it directly would imply a much larger action cost and thus have a negligible weight for large V_0. This is known as the dilute instanton approximation (Rajaraman, 1982). The general solution we consider is thus

$$\phi(\tau) = \sum_i \epsilon_i \tilde{\phi}(\tau - \tau_i) \tag{10.56}$$

The $\epsilon_i = \pm 1$ indicates the direction in which the tunneling takes place. Such a solution is represented in Fig. 10.7. Regardless of the precise form of the instanton solution, the very fact that the tunneling though the barrier is extremely small allows to make the approximation

$$\frac{d\phi(\tau)}{d\tau} = \pi \sum_i \epsilon_i \delta(\tau - \tau_i) \tag{10.57}$$

This allows to compute the action of the solution (10.56). One injects the solution in (10.50) and integrates by parts the term S_0 to have $\partial_\tau \phi$ appear. Because they are short-range the terms S_0' and S_{V_0} do not couple the instantons. The contribution to the action is thus

$$S_0' + S_{V_0} = nS_{\text{inst}} \tag{10.58}$$

On the contrary the long-range nature of S_0 couples the instantons. Using (10.57) the partition function of the system is

$$Z = \sum_{p=0}^{\infty} \Delta_0^{2p} \sum_{\epsilon_1=\pm,\ldots,\epsilon_{2p}=\pm}' \int_0^\beta \frac{d\tau_{2p}}{\delta} \int_0^{\tau_{2p}-\delta} \frac{d\tau_{2p-1}}{\delta} \cdots \int_0^{\tau_2-\delta} \frac{d\tau_1}{\delta}$$
$$e^{\frac{2}{K}\sum_{i>j}\epsilon_i\epsilon_j \log\left(\frac{|\tau_i-\tau_j|}{\delta}\right)} \tag{10.59}$$

where

$$\Delta_0 = e^{-S_{\text{inst}}} \tag{10.60}$$

and δ is a short time cutoff of the order of the instanton width $\sqrt{M/\tilde{V}_0}$ since the approximation (10.57) can only be used for larger time separations. One has to sum over all possible ϵ_i since the tunneling can take place in both directions. However, since one computes a partition function (trace over all configurations), the value of ϕ at large time should be the same as the initial value, which imposes that $\sum_i \epsilon_i = 0$. We thus recognize the partition function of a Coulomb gas (see Section 3.3). The fugacity is given by the action needed to go trough the barrier. The logarithmic potential between the charges depends on the LL parameter K. If we compare to (3.81) we see that $1/K$ appears instead of K, and we thus recover that this is indeed the partition function of an action of the form of sine-Gordon but with a $\cos(2\theta(x=0,\tau))$ instead of $\cos(2\phi(x=0,\tau))$. Let us compare this result with the phenomenological strong coupling Hamiltonian (10.35). As we saw in the previous section, due to the presence of the boundary the action for one half space is (10.20). It means that if one integrates all the modes except the ones at $x=0$ one has (compare with (10.47))

$$S_j = \frac{1}{2\beta}\sum_n \frac{|\omega_n|K}{\pi}\theta_j(\omega_n)^*\theta_j(\omega_n) \tag{10.61}$$

for each half chain. Note that one has $K/2$ instead of K if one had had a full chain. The tunneling term is

$$-t[\psi_1^\dagger(x=0)\psi_2(x=0) + \text{h.c.}] \sim -t[e^{i(\theta_2(x=0)-\theta_1(x=0))} + \text{h.c.}] \tag{10.62}$$

It is thus useful to introduce the fields $\theta_\pm = (\theta_1 \pm \theta_2)/\sqrt{2}$. In terms of these fields the quadratic part of the action becomes

$$S_0 = S_1 + S_2 = S_+ + S_- \tag{10.63}$$

where $S_\pm$ have exactly the form (10.61). The hopping term becomes

$$-t[e^{-i\sqrt{2}\theta_-(\tau)} + \text{h.c.}] \tag{10.64}$$

It is easy to see, reproducing the calculation of Section 3.3, that (10.64) gives back the expansion for the partition function (10.59). The instanton method thus justifies the phenomenological strong coupling Hamiltonian and allows to compute a value of the hopping parameter t. The instantons correspond to the particles that tunnel in the effective Hamiltonian, using the general argument of quantification of charge (3.49).

In addition to the perturbative technique exposed here, this model is also solvable by Bethe-ansatz as well as reasonably accessible by numerical calculations. This would take us too far, so I refer the reader to Moon *et al.* (1993) and Fendley *et al.* (1995*a*) for more on that point.

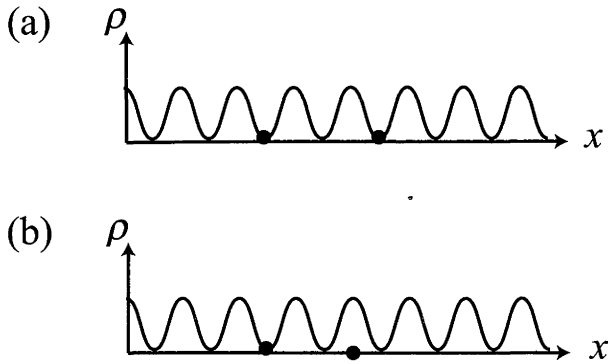

FIG. 10.8. The charge density couples to the two impurities. If the coupling is very weak the density is fixed by the unperturbed Hamiltonian. Two different cases are possible. (a) For a generic position of the impurities the density wave has a preferred position. This corresponds to pinning by the impurities, and is very similar to the case of a single impurity. (b) For a special position of the impurities there is no preferred position and the density wave can slide freely over the two impurities.

10.2.3 *More than one impurity*

The same type of calculations can be used to tackle the case of more than one impurity or of impurities with a structure. Let me focus on the case of two impurities that allows to illustrate some important concepts of mesoscopic systems.

If we put two impurities in positions $-a/2$ and $a/2$ the term in the Hamiltonian describing the interaction with these impurities is

$$V_{-a/2}\cos(2\phi(x=-a/2)+k_F a)+V_{a/2}\cos(2\phi(x=a/2)-k_F a) \tag{10.65}$$

If the potentials of the impurities are different the system has asymptotic properties that are essentially equivalent to the ones of a single impurity. There is a complicated crossover towards this behavior that I will not examine here. An interesting behavior appears if the potentials of the impurities are equal $V_{-a/2}=V_{a/2}=V_0$. Let us first examine physically what happens when the coupling to the impurities is very weak $V_0/v_F \ll 1$. In that case the phase can be viewed as roughly constant to minimize the Luttinger liquid Hamiltonian (3.25). One can thus see the density of the electron gas as a rigid charge density wave given by (3.53) as shown in Fig. 10.8. One can thus estimate the coupling with the impurity potential by assuming that the phase ϕ is roughly constant. In that case one can regroup the two cosines to get

$$V_0 2\ \cos(2\phi)\cos(k_F a) \tag{10.66}$$

Thus, for a generic position of the impurities, that is, when $2k_F a \neq \pi + 2\pi n$ the total potential produced by the two impurities looks very much like the potential produced by a single impurity. This case is shown in Fig. 10.8. The charge density wave has a preferred equilibrium position that minimizes the potential due to the two impurities. They thus act collectively as a localized pinning potential very much like the one of a single impurity. One can thus expect the same behavior than the one we studied in the above section. The situation is quite different when $\cos(2k_F a) = 0$. In that case the backscattering produced collectively by the two impurities vanishes. As shown in Fig. 10.8, this corresponds to a charge density wave that has no preferred position relative to the two impurities. When one part of the density is lower at one impurity, the density is maximum at the other. As a result, the density wave is now free to slide over the two impurities whereas it would be pinned by a single one. One can thus expect for that case a quite different behavior than the standard pinning on an impurity.

Of course, to derive this result we have assumed that the phase was constant, but this cannot be too wrong at low-energy if the coupling to the impurities is weak. Let us make a better job by looking at the action in an expansion to second order in V. One has

$$\delta S = \int d\tau_1\, d\tau_2 \left[V_{-a/2}^2 \langle e^{i2(\phi(-a/2,\tau_1)-\phi(-a/2,\tau_2))} \rangle + V_{a/2}^2 \langle e^{i2(\phi(a/2,\tau_1)-\phi(a/2,\tau_2))} \rangle \right.$$
$$\left. + 2V_{a/2}V_{-a/2}\cos(2k_F a) \langle e^{i2(\phi(-a/2,\tau_1)-\phi(a/2,\tau_2))} \rangle \right] \quad (10.67)$$

All three terms decay as a power law $(1/r)^{2K}$. In the first two terms $r = u|\tau_1 - \tau_2|$ while $r = \sqrt{a^2 + u^2(\tau_1 - \tau_2)^2}$ in the last term. At large time difference however this makes no difference in the asymptotic decay. This term is thus very similar to a single impurity but with the impurity potential

$$V_{\text{eff}}^2 = V_{a/2}^2 + V_{-a/2}^2 + 2V_{a/2}V_{-a/2}\cos(2k_F a) \quad (10.68)$$

If V_{eff} is non-zero then this term leads to the same RG flow than a single impurity (after some crossover). On the other hand, if $V_{a/2} = V_{-a/2}$ and $\cos(2k_F a) = -1$ the effective potential vanishes, leading to a much weaker singularity in the perturbation

$$\left(\frac{1}{\tau}\right)^{2K} - \left(\frac{1}{a^2+\tau^2}\right)^{2K} \sim K\left(\frac{1}{\tau}\right)^{2K+2} \quad (10.69)$$

which is always irrelevant. We thus recover from the RG the results of our simple physical reasoning.

Now let us examine what happens if the impurity potential is strong. In that case, as for one impurity, one should mandatorily have a minimum of density at the position of the impurity. As a result, one should in general stretch or extend the density wave as shown in Fig. 10.9. Let us consider two simple cases. The first one is the case where the two impurities would naturally sit in the minima of the density wave, that is, $\cos(2k_F a) = 1$. In that case the extra energy cost

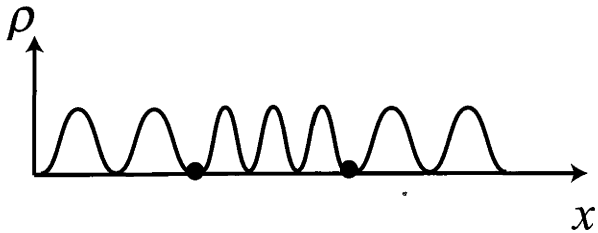

FIG. 10.9. Strong pinning. To accommodate for the two impurities the density wave should be stretched or compressed. This implies an extra cost of energy.

to accommodate the impurities is zero. In the island between the two impurities there are exactly $N = 3$ charges. As we saw for one impurity, the conduction can only occur by solitonic excitations where one full charge passes one impurity. This corresponds to the tunneling of one period of the charge density wave in Fig. 10.6. If a charge tunnels as shown in Fig. 10.9, this corresponds to a compression of the charge on the island. This can be viewed as making a change of the phase ϕ to accommodate the extra period over the length of the island. This change $\delta\phi$ is given by

$$\delta\phi = \pi\frac{x}{a} \tag{10.70}$$

(using (2.55)). The extra cost in energy compared to the case where $\phi = 0$ is thus

$$\begin{aligned} E_0 &= \frac{1}{2\pi}\int_0^a \frac{u}{K}(\nabla\phi)^2 \\ &= a\frac{u}{2\pi K}(\frac{\pi}{a})^2 = \frac{\pi u}{2aK} \end{aligned} \tag{10.71}$$

Note that this cost contains a contribution coming both from the kinetic energy of the electrons, which increases due to the compression in the island, and from the short-range interactions. Both these contributions are hidden in the parameters u and K. It thus means that to increase the charge of the island to $N+1$ the energy increases by the finite amount (10.71). If one wanted to remove one charge, it would be necessary to stretch the density wave in the island and this would cost exactly the same energy. The energy versus charge curve is shown in Fig. 10.10. The states with charge N and $N \pm 1$ have thus different energy. In fact one can consider the island as a capacitor and the energy E_0 to be of the form

$$E_0 = \frac{(Q - Q_{\min})^2}{2C} \tag{10.72}$$

where C is the capacitance of the island. It is easy to check from (10.71) that

$$C = \frac{Ka}{\pi u} \tag{10.73}$$

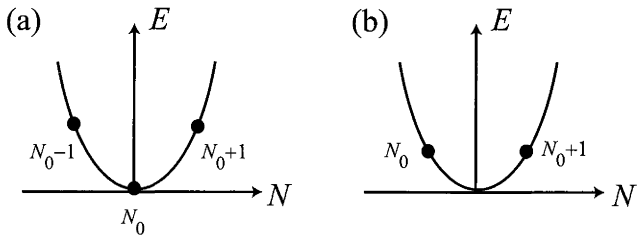

FIG. 10.10. Energy vs charge for the island. (a) the energy of states with N and $N+1$ (or $N-1$) states are different. Adding or removing a charge from the island costs a finite energy. It thus leads to the phenomenon known as Coulomb blockade where the charge cannot tunnel in and out of the island. (b) the energy of N and $N+1$ are degenerate. Thus, charge can tunnel in and out of the island at no energy cost.

Since the states with different charge on the island have different energy, it means that any tunneling in and out of the island requires a finite amount of energy to take place. Such processes have an energy gap and cannot take place at low-energy. This is the phenomenon known as Coulomb blockade that occurs quite generally in mesoscopic systems for which the charging energy of adding or removing an electron from an island can be sizeable (Imry, 1997). The one-dimensional system is a very nice illustration of this mechanism. Of course, here we go beyond the simple classical interpretation of the capacitance since the 'capacitance' contains contributions from the kinetic energy of the electrons as well as from the interactions. In this situation we can thus expect the charge on the island to be frozen and the tunneling processes to be suppressed at low-energy. Motion of charge should thus happen by cotunneling processes where a charge has to move in the island at the same moment that another charge goes out. Since this is a much more complicated process we expect the conductance through the island to vanish at low-energy. Note that the strong coupling analysis exactly agrees with the weak coupling criterion.

On the contrary if $\cos(2k_F a) = 0$ it means that the density wave should be stretched (or compressed) by half a period to put a minimum of density at the second impurity. In that case comparing with (10.70) the field ϕ is (we have stretched the density wave)

$$\delta\phi = -\frac{\pi}{2}\frac{x}{a} \tag{10.74}$$

which corresponds to a cost in energy of $E_0/4$ when comparing with (10.71), for N charges in the island. If now an additional charge tunnels in the island the extra phase of the field ϕ becomes

$$\delta\phi = +\frac{\pi}{2}\frac{x}{a} \tag{10.75}$$

which again corresponds to an energy $E_0/4$ but this time for $N+1$ charges in the island. In that case one has thus the quite different situation where the states

with charge N and charge $N+1$ are degenerate in energy. There is thus no problem to have charge tunnel in and out from the island and one thus expects to have easy conduction through the island. Once again this agrees well with the weak coupling analysis.

To make our analysis more quantitative let us follow the same route than for one impurity and integrate over all the modes but the ones at the impurity sites. We can introduce the symmetric and antisymmetric modes

$$\begin{aligned}\phi_+ &= \frac{1}{2}(\phi(\frac{a}{2}) + \phi(\frac{-a}{2}))\\ \phi_- &= (\phi(\frac{a}{2}) - \phi(\frac{-a}{2}))\end{aligned} \tag{10.76}$$

We rewrite the cosines as

$$2\tilde{V}_0 \ \cos(2\phi_+)\cos(\phi_- - k_F a) \tag{10.77}$$

To get the effective action the simplest is to introduce the two new fields as constraints

$$\int \mathcal{D}\phi(x,\tau)\mathcal{D}\phi_+(\tau)\mathcal{D}\phi_-(\tau)e^{-S}$$
$$\delta(\frac{\phi(-\frac{a}{2}) + \phi(+\frac{a}{2})}{2} - \phi_+(\tau))\delta((\phi(\frac{a}{2}) - \phi(-\frac{a}{2})) - \phi_-(\tau)) \tag{10.78}$$

The constraint can be expressed as

$$\delta(A(x,\tau)) = \int \mathcal{D}\lambda(x,\tau)e^{i\int dx\, d\tau\ \lambda(x,\tau)A(x,\tau)} \tag{10.79}$$

One can then integrate over ϕ and $\lambda_\pm$ using the methods of Appendix C. The effective action is thus

$$S = \frac{1}{2\beta K}\sum_{\omega_n}\left[\frac{4}{I_+(\omega_n)}\phi_+^*(\omega_n)\phi_+(\omega_n) + \frac{1}{I_-(\omega_n)}\phi_-^*(\omega_n)\phi_-(\omega_n)\right]$$
$$+\tilde{V}_0\int d\tau 2\cos(\phi_+)\cos(\phi_- + 2k_F a) \tag{10.80}$$

where

$$I_\pm(\omega_n) = \int_0^\Lambda dk\frac{2u(1\pm\cos(ka))}{\omega_n^2 + u^2k^2} \tag{10.81}$$

Let us examine the low-energy part of this action $\omega_n \to 0$. For small ω_n the integrals $I_\pm$ are dominated by what happens at small k. In the integral I_+ the term $1+\cos(ka)$ is equivalent to 2 at small k. This integral thus behaves as

$$I_+(\omega_n) \sim \int_0^\Lambda dk\frac{4u}{\omega_n^2 + u^2k^2} \sim \frac{2\pi}{|\omega_n|} \tag{10.82}$$

	Extended disorder	Single impurity
Disorder parameter D_b in RG	$n_i V^2$	V^2
dK/dl	$-D_b(l)$	0
dD_b/dl	$3-\mu(l)$	$2-\mu$
Transition	Strong attraction	Non-interacting
σ or δG	$\sigma \sim T^{2-\mu[T]}$	$\delta G \sim T^{\mu-2}$
Strong coupling phase	Anderson localization	Decoupled chain

Table 10.1 *Renormalization of the various parameters, physical properties and transport properties both in the case of uniform disorder and of a single impurity. For the relation between σ and δG see (10.87). For fermion with spin, the LL parameter is $K = K_\rho$. $\mu = 2K$ for spinless fermions and $K_\rho + K_\sigma$ for fermions with spins (see also Chapter 9). $\mu(l)$ or $\mu[T]$ reminds that via the renormalization of the LL parameter K the parameter μ depends on the scale of the problem and both the RG equations for disorder and for K should be taken into account. (After Giamarchi and Maurey, 1996.)*

This mode has thus an action similar to the modes in a single impurity problem. On the contrary in I_- the term $1-\cos(ka)$ is equivalent to k^2 and thus regularizes the integral. The integral is convergent at small ω_n. It can be estimated as

$$I_-(\omega_n = 0) = \int_0^\Lambda dk \frac{2u(1-\cos(ka))}{u^2k^2} = \frac{\pi a}{u} \tag{10.83}$$

Thus, the action of the ϕ_- mode is a mass term

$$S_- = \frac{1}{2C}\int d\tau(\phi_-(\tau)/\pi)^2 \tag{10.84}$$

where $C = aK/(u\pi)$. The relative phase on the two impurities is thus frozen at low-energy, and the field ϕ_- cannot fluctuate any more. Any change in ϕ_- costs an action (10.84). One recovers the charging energy that we have obtained phenomenologically. I will stop here with the double barrier problem, since when going further the calculations become much more involved. I refer the reader to the literature for more on this subject (Kane and Fisher, 1992*a*; Furusaki and Nagaosa, 1993*b*; Ogata and Fukuyama, 1994; Sassetti *et al.*, 1995; Maurey and Giamarchi, 1997).

Finally, let me comment briefly on the similarities and differences between uniform disorder and isolated impurities. A summary of the various equations and physical behaviors for a single and many impurities is given in Table 10.1. As is obvious from Table 10.1, the two systems offer striking similarities as well as some important physical differences. As can be expected on physical grounds since D_b has the meaning of $n_i V_0^2$ at weak coupling the behavior of a single impurity corresponds exactly to taking *first* the limit of infinitesimal disorder $D_b \to 0$ in the equations (9.47) (and therefore formally to the $n_i \to 0$ limit, that

is, a single impurity). This limit is non-trivial since in principle the gaussian approximation corresponds to infinitely dense (very weak) impurities $n_i \to \infty$. However, if one takes $D_\mathrm{b} \to 0$ first, since the equation (9.45) does not depend on the strength of D_b, the only effect is to neglect the renormalization of the exponents by the disorder. To match the conductivity and conductance one notices that in the limit $n_i \to 0$ the impurities are well separated, enough to be considered as independent scatterers, and their scattering add up. We have computed the scattering due to one impurity which gives the correction to the conductance

$$G = G_0 - \delta G \tag{10.85}$$

which leads, for the correction to the resistance

$$R = R_0 + \delta R = \frac{1}{G_0} + \frac{\delta G}{G_0^2} \tag{10.86}$$

Thus, for N_i impurities in a wire of length L the conductivity would be

$$\sigma(T) = LG = \frac{L}{R} = \frac{L}{R_0 + N_i \delta R} \tag{10.87}$$

assuming that the impurities act *independently* and that their resistances simply add up. For a long wire both L and N_i are large thus

$$\sigma(T) = \frac{1}{n_i \delta R} = \frac{G_0^2}{n_i \delta G} \tag{10.88}$$

One recovers that the conductivity is inversely proportional to the concentration of impurities. The temperature dependence of the conductivity in this limit is given by an exponent which is the opposite of the one of δG, as we found. The collective effects of impurities (that is, the fact that they cannot be considered as independent scatterers) manifest themselves in the renormalization of the exponents. This leads to a *faster* decay of the conductivity/conductance when the temperature decreases compared to that of independent impurities.

For gaussian disorder, collective effects manifest themselves at any lengthscale since again formally $n_i \to \infty$. On the other hand the scattering on a single impurity can never become strong. For realistic (Poissonian) disorder corresponding to many impurities with both an average distance a between the impurities and a strength of the potential of one impurity V, one can therefore expect a competition between two lengthscales: the temperature T_2 for which the thermal length u/T is equal to the distance between impurities and the crossover temperature $T_{1,\mathrm{cr}}$ for which *one* impurity goes to strong coupling. These two situations are reminiscent of the 'weak pinning' and 'strong pinning' cases of the classical charge density waves, and could in principle be observed in quantum wires. The various situations are summed up on Fig. 10.11.

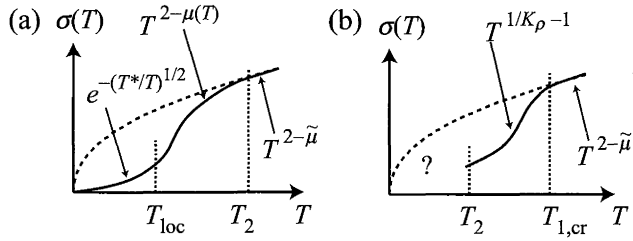

FIG. 10.11. Temperature dependence of the conductivity. The dashed line is the prolongation of the $T^{2-\tilde{\mu}}$ law where $\tilde{\mu} = 1 - K_\rho$ for fermions with spins. (a) 'Weak pinning': $T_{1,cr} < T_2$. Collective effects occur before each impurity can reach strong coupling. Below T_2, renormalization of the exponents gives a faster decay of the conductivity. For gaussian disorder T_2 is infinite. Below $T_{\rm loc}$ the system is collectively localized by pinning on the impurities, leading to a variable range hopping-like conductivity (Nattermann *et al.*, 2003). (b) 'Strong pinning': the opposite situation, $T_{1,cr} > T_2$. Each impurity goes to the tunneling limit before collective effects can take place. (After Giamarchi and Maurey, 1996.)

10.3 Nanotubes

A remarkable one-dimensional system is provided by the recently discovered carbon nanotubes. This is a subject currently quite active ranging from chemistry to applied physics. It is of course impossible to cover all the ground here, and I refer the reader to the literature for more (Dresselhaus *et al.*, 1995). I will confine myself here to the very basic ideas, and the direct connection with Luttinger liquids.

The nanotubes are carbon sheets that are wrapped up as shown in Fig. 10.12. Depending on the wrapping vectors the electronic properties are different. Indeed, the infinite carbon sheet has a semimetal dispersion relation. The wrapping vector can thus lead either to an insulating structure or to a metallic structure where two bands cross the Fermi level, as shown in Fig. 10.13. The nanotubes can thus be viewed as special one-dimensional systems where there would be four points at the Fermi level. There are thus two species of Fermions (each with two spin orientations), and thus four degrees of freedom instead of two in a normal Luttinger liquid. Such systems are thus like the ladder systems that we examined in Chapter 8 and their properties are somehow different from simple Luttinger liquids. This difference is due to the fact that the backscattering interaction between the two different species of fermions opens gaps in the spectrum. However, the nanotubes are rather special in this respect. Indeed, the extension of the transverse wavefunction is rather large (of the order of the diameter of the tube). There is thus a separation of the energy scales in the interactions. To understand this, let us use that the wavefunction of each electron species is of the form (x denotes the axis of the tube and y the transverse direction)

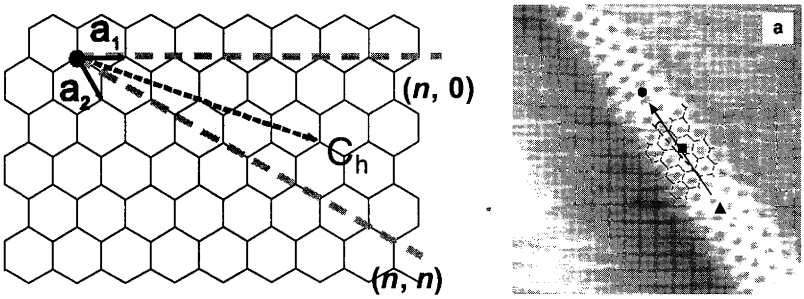

FIG. 10.12. A carbon nanotube is made of a wrapped up graphite sheet. Depending on the wrapping angle the electronic properties of the system are different. (left) A graphene sheet with the two unit vectors a_1 and a_2 and the roll up vector $c_h = na_1 + ma_2$. The so-called zigzag $(n, 0)$ and armchair (n, n) tubes are indicated with dashed lines. (right) Atomic structure and spectroscopy of metallic tubes. The tube axis is indicated by the solid arrow and the zigzag direction by a dashed line. (From Odom *et al.*, 1998 (Copyright (1998) by the Nature Publishing Group).)

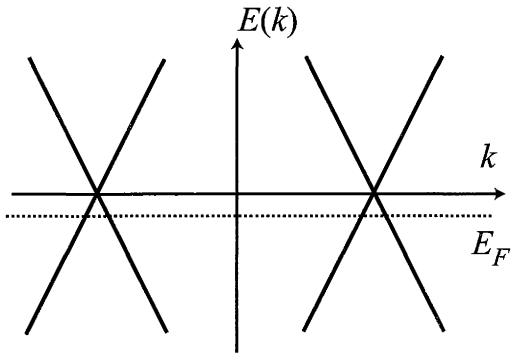

FIG. 10.13. Dispersion relation of metallic carbon nanotubes. Two bands cross the Fermi level. The dispersion relation is identical to the one in a two-leg ladder (see Chapter 8).

$$\psi_j(x, y) = \psi_{x,j}(x)\psi_{y,j}(y) \tag{10.89}$$

essentially the wavefunction along the tube is a plane wave. The interaction is of the form

$$\int dx_1 \int dx_2 \int dy_1 \int dy_2 \; V(r_1 - r_2)\rho(r_1)\rho(r_2) \tag{10.90}$$

The density is a complicated function of ψ, but one can distinguish terms that do not change the index number and terms that do change it. The first ones are of the form

$$\rho \sim \psi^\dagger_{x,j}(x)\psi_{x,j}(x)\psi^\dagger_{y,j}(y)\psi_{y,j}(y) \tag{10.91}$$

Because the transverse wave function is spread on the tube $\psi_y \sim 1/\sqrt{N}$ where N is the number of sites in the transverse direction. Thus, $\psi^\dagger_{y,j}(y)\psi_{y,j}(y) \sim 1/N$ and the integration over y removes the factor $1/N$. Physically, it means that for such terms, that are the forward scattering, only the total density counts. Even if the charge is spread over the width of the tube as long as the two charges are separated by more than the diameter of the tube the forward scattering feels the total charge. This is the same situation than the one we already discussed for the long-range interactions (see Section 4.1). On the contrary, if the index changes (backward scattering) then $\int dy\ \psi^\dagger_{y,j_1}(y)\psi_{y,j_2}(y)$ would be zero since the two wave functions are orthogonal. The only case where these terms do not cancel is when $y_1 = y_2$ in (10.90). In that case, one has

$$\int dy_1 |\psi_{y,j_1}(y)|^2 |\psi_{y,j_2}(y)|^2 \sim \frac{1}{N} \tag{10.92}$$

which is still down by a factor of $1/N$ compared to the forward scattering interaction. If the temperature is not too low and if the tube is not too narrow, one can, as a first approximation neglect all backward scattering and only a take into account the forward scattering (Kane *et al.*, 1997; Egger and Gogolin, 1997). In that case only the total charge mode feels the interaction. It is thus convenient to use the same collective modes than the ones we used for the ladder (8.20). Contrary to the ladder, since for the nanotube only the interaction between the total charge is taken into account terms like (8.23) and (8.24) do not exist and the four modes are totally decoupled. The Hamiltonian is essentially trivial since each mode is described by (3.25). Furthermore, since the interaction only couples the total charge it only affects the total charge mode, thus $K_{\rho-} = K_{\sigma+} = K_{\sigma-} = 1$ and only $K_{\rho+} \neq 1$ (smaller than one for repulsive interactions). The nanotube is thus essentially described by a simple Luttinger liquid with trivial modifications due to the presence of four modes instead of two. Of course, this is only true if the length of the tube is not too long. For longer tubes a crossover towards ladder behavior, where gaps appear in the other sectors, should occur.

Let us examine some of the physical consequences. The single-particle Green's function is given by the product over the four modes. In the absence of interactions each mode contributes as $(1/x)^{1/4}$ to give back the $1/x$ decay of the non-interacting system. In the presence of interactions only the total charge mode is modified. In a similar way than shown in Chapter 2 for the LL with two modes, its exponent becomes $(K_{\rho+} + K_{\rho+}^{-1})/8$ instead of $1/4$. The total exponent of the single-particle Green's function is thus $(K_{\rho+} + K_{\rho+}^{-1})/8 + (3/4)$. This gives a single particle density of state varying as

$$n_{\text{bulk}}(\epsilon) \sim \epsilon^{(K_{\rho+}+K_{\rho+}^{-1}-2)/8} \tag{10.93}$$

From the preceding chapter, one can also compute the single-particle density of states close to an edge. We saw that close to an edge for a single mode $(K + K^{-1})/2$ is replaced by $1/K$. With the four modes this occurs for each of

the modes, each one contributing to 1/4 of the final result. Since three of them are non-interacting $K = 1$ for three of the modes. The edge exponent of the correlation function is thus $(1/K + 3)/4$. The single-particle density of states close to the edge is thus

$$n_{\text{edge}}(\epsilon) \sim \epsilon^{(K_{\rho+}-1)/4} \tag{10.94}$$

This density of states can be measured in a tunneling experiments. Such an experiment can be realized by connecting the nanotube with 'bad' contacts and measuring the conductance of the system. If the contacts are bad the resistance is dominated by the tunneling process between the contacts and the nanotube. The data is shown in Fig. 10.14. The conductance is indeed a power law, which gives the very reasonable value $K_{\rho+} = 0.22$ when fitted to (10.93). One can check the consistence of the LL explanation by putting a strong impurity in the tube by bending it. In that case the conductance across the kink is dominated by the tunneling across the impurity as we discussed in this chapter. Such an experiment measures thus the square of the density of states (10.94) since each side of the impurity has this density of states at the edge. The same value of $K_{\rho+} = 0.22$ would then give an exponent of 1.8 indeed close to the one observed experimentally, leading good credence to the Luttinger liquid description of the nanotubes. A word of caution however, similar results are observed in ropes (Bockrath *et al.*, 1999) which are made of many nanotubes closely packed together. In such systems it is less obvious why naively one should expect a Luttinger liquid behavior, and more analysis of these results are clearly needed to make sure that one is indeed observing a Luttinger liquid. There are many open questions and challenges posed by the nanotubes. One of the puzzling questions at the moment is the behavior of nanotubes with good contacts and the possibility to have superconductivity in these systems (Kociak *et al.*, 2000).

10.4 Edge states in quantum Hall systems

So far we have dealt with Luttinger liquids whose microscopic origin was relatively natural. Let us now examine a more devious, but quite interesting realization. If we take a two-dimensional electron gas and put it in a strong magnetic field, it is now well-known that it leads to the famous quantum Hall effect (von Klitzing *et al.*, 1980; Tsui *et al.*, 1983). I will not review here the physics of the quantum hall effect and the reader can find very nice reviews and further references in Stormer (1999), Glattli (2002) and Shankar (2002). Although one starts from a two-dimensional electron gas, the transport is in fact ensured by one-dimensional electrons. There are two ways of visualizing this. The simplest is to think of the semiclassical trajectories of the electrons. Because of the magnetic field, they describe circles of radius the cyclotron length $l_c = eB/m$. The electrons trapped in such orbits cannot contribute to transport. On the other hand close to the edge of the sample the electrons can only describe half an orbit and can carry a current as shown in Fig. 10.15. This can also be seen by looking at the dispersion relation of the electrons in the system. In the bulk the

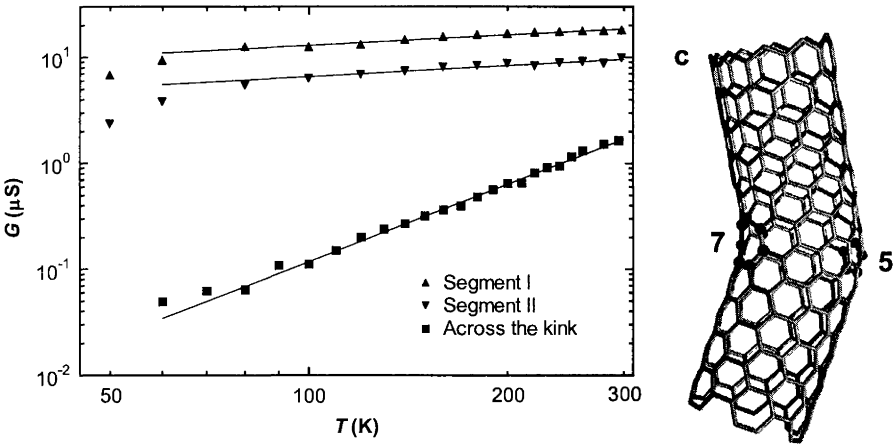

FIG. 10.14. Conductance of a nanotube as a function of temperature. The conductance inside the bulk (triangles) leads to a power law behavior with an exponent of $\alpha = 0.34$–0.35. When fitted to the Luttinger liquid formula (see text) this exponent leads to a reasonable value of the Luttinger parameter $K_{\rho+} = 0.22$. A kink can be created by bending the nanotube to measure the density of states close to an edge. The conductance through the kink (squares) gives a power law with an exponent 2.2 well consistent with what is expected for edge to edge tunneling (see text) with the value of $K_{\rho+}$ determined from the bulk. (From Yao *et al.*, 1999 (Copyright (1999) by the Nature Publishing Group).)

system is in Landau level states, that is, the energy is a constant. But due to the confining potential keeping the electrons inside the sample, the energy of the Landau levels has to raise close to the edges. Thus, even if the chemical potential is between two Landau levels inside the sample (this corresponds to a filled Landau level) it will cut the dispersion relation at the edges. One is thus back to the dispersion relation of a one-dimensional electron gas. This is a peculiar one-dimensional system however, since the right going electrons are physically separated from the left going electrons. Naively, one would thus say that there are no interactions and thus $K = 1$. However, this would lead us to trouble. Indeed, since the right and left goers are separated, let us see the effect of a different potential for right and left, that is, of a term in the Hamiltonian

$$H_V = -\frac{Ve}{2}\int dx[\rho_R(x) - \rho_L(x)] = -\frac{Ve}{2\pi}\int dx\, \partial_x\theta(x) \tag{10.95}$$

This term is identical to the chemical potential of Chapter 2, except it acts on θ instead of ϕ. It is very similar to the $\partial_\tau\phi$ term of Section 7.2 corresponding to threading a flux in the system since it couples to the current. It can be absorbed in the quadratic part of the LL Hamiltonian by shifting θ as

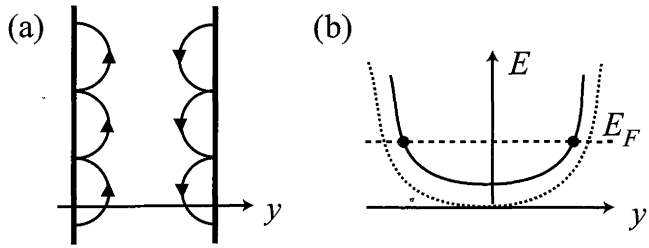

FIG. 10.15. (a) The current is carried by the edges of the sample while the electrons in the bulk do not carry current. (b) Because of the potential confining the electrons inside the sample the Fermi level crosses the dispersion relation at the edges leading to a one-dimensional dispersion.

$$\nabla\tilde{\theta} = \nabla\theta - \frac{Ve}{2(uK)} \tag{10.96}$$

Using the definition of the current (7.55) this would produce a current

$$J = \frac{euK}{\hbar}\langle\frac{\nabla\theta}{\pi}\rangle = \frac{e^2V}{2\pi\hbar} \tag{10.97}$$

This term is nothing but the conductance that we computed for our standard Luttinger liquid. However, here this terms measures the current in response to a difference of potential *between the edges*. It is thus the Hall conductance. Since the Hall value is quantized with a value that depends of the Hall plateau, we see that (10.97), and thus $K = 1$, cannot be correct. The only way to get the correct conductance is thus to assume that in the Hall system there is in fact some interaction between the right and left goers leading to a non-zero K. In addition, since our edges are well separated and contain only excitations that can move right or left, they cannot be simply the right and left fermions, since those would be mixed by an interaction leading to a non-zero K. Our edges must thus be the chiral excitations that were defined in Section 3.2, and which remain uncoupled even when there is a non-zero K. The density at the edge is $\tilde{\rho}_{R,L}$. A Hall voltage thus couples to

$$-\frac{Ve}{2}\int dx[\tilde{\rho}_R - \tilde{\rho}_L] = \frac{-VeK}{2\pi}\int dx\ \partial_x\theta \tag{10.98}$$

Note the factor of K that has appeared now, since we have considered the chiral modes to be the modes associated to each edge. Correcting (10.96) for the factor of K one obtains,[36] instead of (10.97), for the current

$$J = \frac{euK}{\hbar}\langle\frac{\nabla\theta}{\pi}\rangle = \frac{e^2VK}{2\pi\hbar} \tag{10.99}$$

[36]Alternatively, one can consider that the extra density of right chiral carriers leads to a current $J = eu\tilde{\rho}_R$.

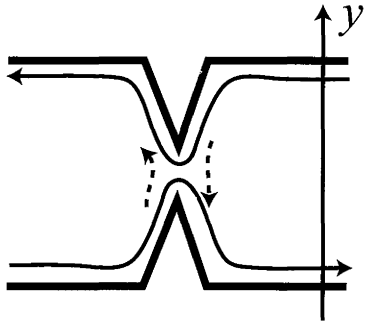

FIG. 10.16. A constriction in a Hall system acts as an isolated impurity, and can transform a left mover into a right mover. It is the equivalent of the single impurity in a Luttinger liquid that we have examined earlier in this chapter.

leading to the correct Hall conductance *provided* one takes $K = \nu$ (where $\nu = 1/m$ is the filling fraction corresponding to the Hall plateau). Viewing the edges as the chiral fields of a Luttinger liquid has other advantages. Using the commutation relation between the chiral fields (3.59) shows that the operator

$$e^{-i\phi_R(x)} \tag{10.100}$$

creates a kink of size K in the field ϕ_R itself. Thus, the electron creation operator which should create a charge one in the density at the edge should create a kink of unit size in ϕ_R. This can be written as (see (3.51))

$$\psi^e(x) \sim e^{-i\frac{\phi_R(x)}{K}} \tag{10.101}$$

which means, from the commutation relations (3.59), that two such operators when commuted get a factor

$$\psi^e(x)\psi^e(x') = e^{i\frac{\pi}{K}}\psi^e(x')\psi^e(x) \tag{10.102}$$

instead of the usual $e^{i\pi} = -1$. But since two fermions operators must anti-commute this imposes that $1/K = 1/\nu$ is an odd integer. This is one of the characteristic features needed to have a Laughlin state in the bulk (Laughlin, 1983). Other important characteristic features such as the fractional statistics are also reproduced. A proof of this mapping can be given by a Chern–Simons theory (Wen, 1990*b*; Wen, 1995). This mapping works well for simple fractions such as $1/(2m+1)$ or integer Hall effect but things are more complicated for other fractions (e.g. 2/3).

The Hall system is thus an excellent system to study backscattering in a Luttinger liquid since one can easily make isolated impurities as shown in Fig. 10.16. Some data (Milliken *et al.*, 1996) is shown in Fig. 10.17 for a $\nu = 1/3$ Hall plateau. One can compare it with the simple scaling estimates given in this chapter. With

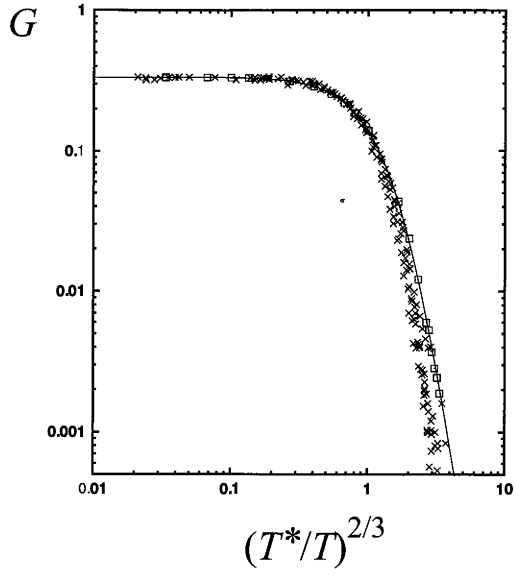

FIG. 10.17. Conductance in a Hall constriction in units of e^2/h. The experimental data from Milliken *et al.* (1996) is plotted as crosses. The full line is the Bethe-ansatz solution from Fendley *et al.* (1995*b*), and the squares are Monte-Carlo data from Moon *et al.* (1993). The simple scaling arguments of scattering on an impurity in a LL (see text) would give a $T^{2/3}$ and T^2 behaviors at high and low temperatures, which traduces on the figure into a constant an a line of slope -3. (After Fendley *et al.*, 1995*b*.)

a LL parameter of $K = 1/3$ the exponents for the temperature dependence of the conductance are $T^{K-1} = T^{-2/3}$ for the correction of the conductance in the high-temperature regime and $T^{1/K-1} = T^2$ in the low-temperature regime. In addition the conductance can be computed in a 'tour de force' calculation using Bethe-ansatz (Fendley *et al.*, 1995*b*) which allows a clean description of the full curve. The agreement between the three results is quite good. Many other physical quantities can be explored and in particular the question of noise. For more details on the question of Luttinger liquids and edge states in quantum hall systems see Fisher and Glazman (1997).

11

SIGNIFICANT OTHERS

I only know two pieces; one is 'Clair de Lune' and the other one isn't.

Victor Borge

To conclude our tour of Luttinger liquids, let us now look at less usual realizations than the ones coming from fermionic systems. The first realization we will examine is provided by interacting bosons. Indeed, in one dimension it is impossible to decouple completely the statistics from the interactions and one- and quasi-one-dimensional bosons are also described by Luttinger liquids. Then we will see how the techniques used to tackle one dimension can be used in higher dimensions as well. An important class of problems, that I will also examine, is the case of impurities coupled with a three-dimensional electron gas.

11.1 Interacting one-dimensional bosons

Bosons are particularly interesting systems to investigate. From the theoretical point of view bosons present quite interesting peculiarities and are in fact a priori much more difficult to treat than their fermionic counterpart. Indeed, for fermions, the free fermion approximation is usually a good starting point, at least in high enough dimension where Fermi liquid theory holds. Some perturbations such as disorder can be studied for the much simpler free fermion case, the Pauli principle ensuring that even in the absence of interactions the perturbation remains small compared to the characteristic scales of the free problem (here the Fermi energy). One can thus gain valuable physical intuition on the problem before adding the interactions. For bosons, on the contrary, interactions are needed from the start since there are radical differences between a non-interacting boson gas and an interacting one. Indeed, for the free boson gas, at $T = 0$, all particles can condense into the lowest energy state. For a free system this is the state with momentum $k = 0$, but in presence of disorder this would be the lowest eigenstate of the single boson Hamiltonian. There would be a *macroscopic* occupation of such a state. Any infinitesimal interaction would make such a state unstable since the interaction cost would grow roughly as N^2 where N is the total number of particles. It is thus mandatory for bosons to include the interactions (repulsion) from the start. In addition for one-dimensional bosons there cannot be a breaking of the continuous charge ($U(1)$) symmetry, so no condensate can form.

Interacting bosons thus constitute a remarkable theoretical challenge. Fortunately, this is not a purely abstract question since quite remarkably there are good realizations of interacting low dimensional bosons. I will examine these experimental realizations in Section 11.1.3.

In order to model the bosons, two slightly different starting points are possible. One can start directly in the continuum, where bosons are described by

$$H = \int dx \frac{(\nabla\psi)^\dagger(\nabla\psi)}{2M} + \frac{1}{2}\int dx\, dx'\, V(x-x')\rho(x)\rho(x') - \mu \int dx\, \rho(x) \quad (11.1)$$

The first term is the kinetic energy, the second term is the repulsion V between the bosons and the last term is the chemical potential. A famous model, exactly solvable by Bethe-ansatz (Lieb and Liniger, 1963) uses a local repulsion

$$V(x) = V_0\delta(x) \quad (11.2)$$

In such a model, there is no lattice so no commensurability effect is possible. It is however possible to reintroduce the lattice by adding to (11.1) a periodic potential $V_L(x)$ coupled to the density

$$H_L = \int dx\, V_L(x)\rho(x) \quad (11.3)$$

This term, which favors certain points in space for the position of the bosons, mimics the presence of a lattice of period a, the periodicity of the potential $V_L(x)$. Another starting point is to define the bosons directly on a lattice and to use a Bose–Hubbard Hamiltonian

$$H = -t\sum_i (b_{i+1}^\dagger b_i + \text{h.c.}) + U\sum_i n_i(n_i - 1) - \mu\sum_i n_i \quad (11.4)$$

The repulsion term acts if there are two or more bosons per site. Of course, it is possible to also add to (11.4) longer range interactions. One naively expects the two models (11.1) plus the lattice terms (11.3) and (11.4) to have the same asymptotic physics. There are several mappings that we can use. As we saw a spin chain is equivalent in the absence of magnetic field to a hard core boson system with one particle every two sites. It can thus be described by (11.4) in the limit $U \to \infty$ (and a proper nearest neighbor interaction to mimic J_z) to discourage double occupancy with the proper chemical potential. This immediately shows that there are in one dimension tight connections between bosons and spinless fermions since the same chain can also be represented by spinless fermions via a Jordan–Wigner transformation. If one has commensurate bosons, for example, one boson per site, and the repulsion is very large, one can naively expect a similar Mott transition than for fermions. I will come back to that point in Section 11.1.1. Let us first assume that the filling is incommensurate with the lattice or that we are directly in the continuum.

The boson representation of Section 3.1 is a very efficient way to represent a bosonic system, for the same reasons than for a fermionic system. Using the dictionary given in Appendix D, the kinetic energy becomes

$$H_K = \int dx \frac{\rho_0}{2M}(\nabla e^{i\theta})(\nabla e^{-i\theta}) = \int dx \frac{\rho_0}{2M}(\nabla\theta)^2 \quad (11.5)$$

If we assume for simplicity a local interaction (11.2), the interaction term becomes

$$H_{\text{int}} = \int dx V_0 \frac{1}{2\pi^2} (\nabla\phi)^2 \tag{11.6}$$

As discussed in Chapter 3, the higher harmonics can also give a contribution $(\nabla\phi)^2$ that renormalizes the coefficient in (11.6). The low-energy properties of interacting bosons are thus described by a Luttinger Hamiltonian of the form (3.25). As for fermions, the validity of this Hamiltonian exceeds the simple perturbative derivation that I have given and is really a low-energy effective Hamiltonian, whose parameters K and u control the asymptotic properties of the system. As can be seen from the perturbative derivation, the coefficient K goes to infinity when the interaction goes to zero. The fact that the system is a Luttinger liquid with a finite velocity u, implies that in one dimension an interacting boson system has a linear spectrum $\omega = uk$, contrary to a free boson system where $\omega \propto k^2$. Such a system is thus a *true* superfluid at $T = 0$ since superfluidity is the consequence of the linear spectrum (Mikeska and Schmidt, 1970). An even better criterion for superfluidity is provided by the correlation functions. The various correlations can be obtained from the Luttinger liquid expressions for the boson operators. They are derived in Chapter 3. The boson Green's function and the density (3.40) are given by

$$\begin{aligned} \langle\psi(r)\psi^\dagger(0)\rangle &= A_1 \left(\frac{\alpha}{r}\right)^{\frac{1}{2K}} + \cdots \\ \langle\rho(r)\rho(0)\rangle &= \rho_0^2 + \frac{K}{2\pi^2}\frac{y_\alpha^2 - x^2}{(y_\alpha^2 + x^2)^2} + A_3 \cos(2\pi\rho_0 x)\left(\frac{1}{r}\right)^{2K} + \cdots \end{aligned} \tag{11.7}$$

where the A_i are the non-universal amplitudes (other notations are defined in Appendix A). For the non-interacting system $K = \infty$ and we recover that the system possesses off-diagonal long-range order since the single-particle Green's function does not decay with distance. The system has condensed in the $k = 0$ state. As the repulsion increases (K decreases), the correlation function decays faster and the system has less and less tendency towards superconductivity. The Fourier transform of the single-particle Green's function is thus a power law as explained in Chapter 2. The example of the equal time correlation is shown in Fig. 11.1.

For a purely local interaction, one can obtain the parameter K when the repulsion is infinite. In that case the density of the system becomes equivalent to the one of a system of spinless fermions since two particles cannot be on the same site and the particles are totally free except for this constraint. The decay of the density (11.7) should be the one of free fermions. This can be realized if $K = 1$. In that case $2\pi\rho_0$ is equivalent to $2k_F$. Note that the Green function of the bosons *does not* become the correlation function of spinless fermions since they still represent different statistics. For a purely local repulsion, this is the minimal value that K can reach. Of course, similarly than for fermions, longer

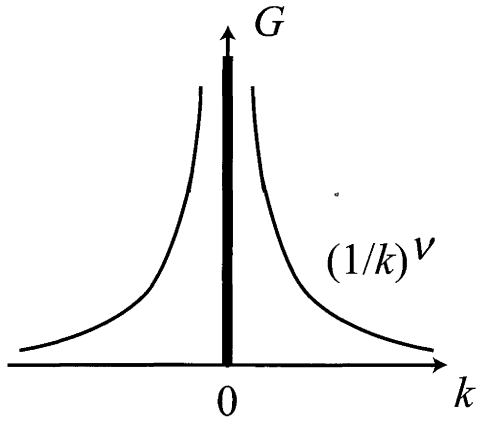

FIG. 11.1. Equal time Green's function correlation for the bosons as a function of the momentum k. For non-interacting bosons all bosons are in $k = 0$ state, thus $G(k) \propto \delta(k)$ (thick line). As soon as interactions are introduced the Green function decays as a power law with an exponent $1/(2K)$. This leads to a power law divergence of $G(k)$, with an exponent $\nu = 1 - 1/(2K)$ (solid line).

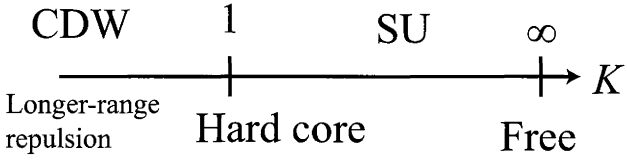

FIG. 11.2. Phase diagram for (incommensurate) one-dimensional bosons, as a function of the parameter K. Some characteristic values of K are indicated. For $K < 1$ the system is dominated by charge fluctuations (CDW) and for $K > 1$ by superfluid fluctuations (SU).

range repulsion between bosons can make the system reach smaller values of K. This is obvious when comparing, for example, (11.7) with the correlation functions of S^+S^- for a spin chain (see Chapter 6), which correspond to bosons with a hard core repulsion (that is $U = \infty$) and a nearest neighbor interaction J_z. K goes from $K = 1$ for $J_z = 0$ to $K = 1/2$ for $J_z = J_{xy}$. The smaller the K, the more slowly density correlations decay. Since the $2\pi\rho_0$ oscillations of the density decay with an exponent $2K$, $K = 1$ is the separatrix between dominant superfluid fluctuations and dominant charge fluctuations. This leads to the phase diagram of Fig. 11.2. As usual, one can either consider the parameters u and K as given parameters, or try to link them to a given microscopic model. In that case, as for fermions, it is very convenient to extract them directly from the compressibility

and the charge stiffness of the system as explained in Section 5.1. This can be done analytically for the model with a δ function repulsion in the continuum which is solvable by Bethe-ansatz, and numerically for other models.

11.1.1 *Commensurate bosons*

Let us now investigate the effects of a lattice on such a bosonic system (Haldane, 1981*b*; Fisher *et al.*, 1989; Scalettar *et al.*, 1991; Giamarchi, 1992; Giamarchi, 1997). This discussion is very similar to the study of the Mott transition for fermionic systems and I refer the reader to Section 4.2 for the calculations. Let us first take a lattice defined as a periodic potential by (11.3). I define $V_L(x)$ to be periodic of period a, which can be realized by taking

$$V_L(x) = \sum_n V_n^0 \cos(Qnx) \tag{11.8}$$

with $Q = 2\pi/a$. Using (11.3) and the expression (3.8) for the density, we see that a non oscillating term remains in the continuous limit if

$$nQ = 2\pi\rho_0 p \tag{11.9}$$

If we use $\rho_0 = 1/d$ where d is the distance between particles one has

$$nd = pa \tag{11.10}$$

The corresponding term in the Hamiltonian is

$$H_L \propto V_n^0 \int dx \ \cos(2p\phi(x)) \tag{11.11}$$

The analysis is thus very similar to the one for fermions. The most relevant commensurabilities are the ones with the smallest p. $p = 1$ corresponds to a commensurability of one (or 2, 3, ..., which would correspond to higher n) boson per site ($n = 1$). This is shown in Fig. 11.3. The periodicity leads to a Mott transition (see Section 4.2) for $K^* = 2$, with the generic characteristics of the Mott transition for a Luttinger liquid as explained in Section 4.2. The next commensurability corresponds to $p = 2$. It is one boson every two sites as shown in Fig. 11.3. Higher odd n would correspond to an integer number of bosons per site plus one boson every two sites. The corresponding term is relevant for $K = 1/2$. One recovers exactly the same umklapp term than the one that was obtained in the fermion representation for a spin chain.

The analysis of the Mott transition for bosons are thus totally similar to the ones I presented for fermionic systems in Section 4.2 and Section 7.2. In the Mott phase the single-particle Green's function decays exponentially since the field θ is dual to the field ϕ which is ordered. At the transition the single-particle Green's function decays with a *universal* exponent $1/(2K_c)$ (1/4 for one boson per site, 1 for one boson every two sites, etc.). This is summarized in Fig. 11.4 (compare

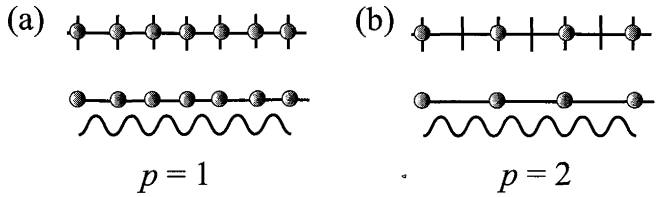

FIG. 11.3. Commensurabilities for the boson system. (Bottom) Bosons in the continuum. The lattice is reintroduced as a periodic potential. (Top) The bosons are defined directly on a lattice. The two descriptions lead of course to the same physics. (a) A commensurability of one boson per site. For the periodic potential it means that the density modulation has the same period than the external periodic potential. (b) A commensurability of one boson every two sites. In that case the period of the density modulation is twice the one of the external potential.

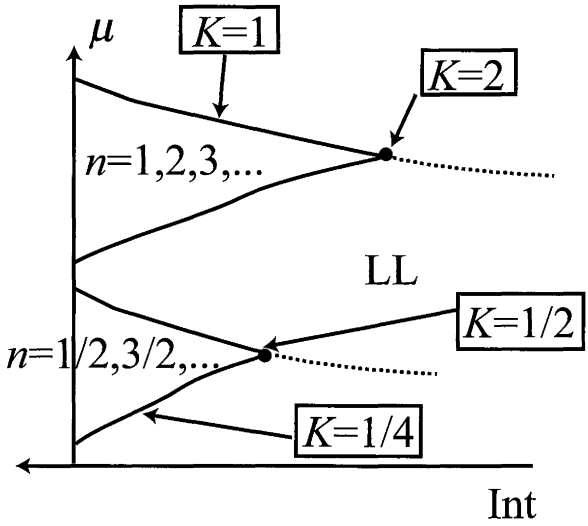

FIG. 11.4. Phase diagram for commensurate bosons as a function of the chemical potential μ and the interactions. Only the commensurabilities of one boson per site and one boson every two sites have been shown. The Mott phase for the bosons occurs for a commensurate filling and depends on the strength of the interactions. The Luttinger liquid parameters take a universal value both for the Mott-U and Mott-δ transitions. The value depends on the order of commensurability (see text).

with Figs 4.7 and 4.8). Similarly the transport properties can be directly deduced from Section 7.2, and I just briefly recall here the salient points. In the LL phase the system is a perfect conductor with a finite charge stiffness $D = u^* K^*$. This charge stiffness jumps discontinuously to zero at the Mott-U transition (constant density). The finite frequency part of the conductivity behaves at the transition as (see (7.101))

$$\sigma(\omega) \sim \frac{1}{\omega \ \log^2(\omega)} \tag{11.12}$$

In the Mott phase, the gap is given by the expressions computed in Section 2.3.2 and is thus exponentially small close to the Mott-U transition. The system is incompressible. The transition by varying the density occurs when the chemical potential equals the charge gap. The density in the incommensurate phase varies as $n \sim (\mu - \mu_c)^{1/2}$ (see Section 4.2). At the Mott-δ transition the universal value of the LL parameters is $K^* = 1$ for one (2, 3, ..) boson every site, $K^* = 1/4$ for one boson every two sites (plus 0,1,2, .. bosons per site), etc. The compressibility diverges at the transition. There is a Drude peak in the conductivity whose weight is given by $D \sim \delta/\Delta$ where δ is the doping and Δ the Mott gap.

This behavior is of course identical to the one that one would get starting directly from the tight binding description (11.4). In that case umklapp terms appear for exactly the same reasons than for a fermionic system (compare with (4.16)). $2k_F x$ in the expressions for the density of fermions is here replaced by $2\pi\rho_0 x$ (see Chapter 3 and Appendix D). The part of the interaction term corresponding to the umklapp is thus (on the lattice $x = ja$)

$$\rho\rho \rightarrow \rho_0^2 e^{ip(2\pi\rho_0 x - 2\phi)} \tag{11.13}$$

Thus, one recovers that if $2\pi\rho_0 pa = 2\pi n$ the corresponding term does not oscillate. $p = 1$ corresponds to $\rho_0 a = n$, that is, to an integer number of bosons per site. The corresponding umklapp term is

$$\propto \cos(2\phi) \tag{11.14}$$

which is identical to (11.11). These predictions of the LL theory can be tested on a given microscopic model. In order to reach the Mott transition with one boson every two sites it is necessary to have a Bose–Hubbard model with a nearest neighbor interaction. This is the boson equivalent of the U–V model of Section 7. The exponents can be computed using the DMRG method (see Chapter 5). Here, a determination from the compressibility and the correlations (for K) was used. The resulting phase diagram is given in Fig. 11.5.

11.1.2 *Disorder: Bose glass*

The bosonization representation is also particularly useful to deal with the effects of disorder on the one-dimensional boson gas. As we already discussed, contrary to the case of fermions, here the non-interacting limit is totally useless. Indeed, in the absence of interactions bosons can always find a large enough region of

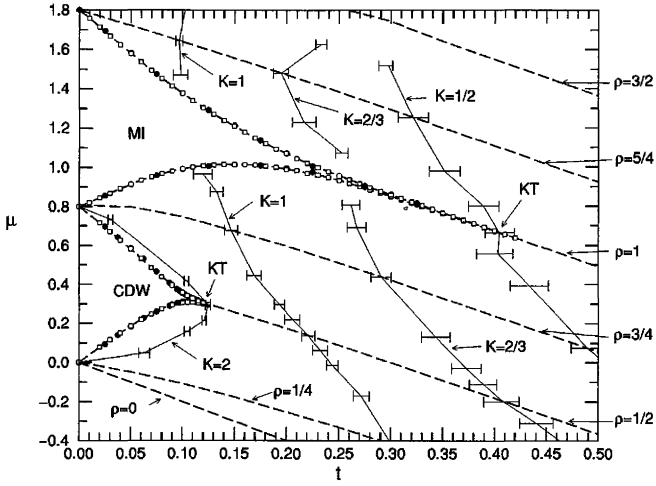

FIG. 11.5. Phase diagram for the Bose–Hubbard model with nearest neighbor interaction. μ is the chemical potential, t is the hopping term, the on-site interaction is taken as $U = 1$ and the nearest neighbor one as $V = 0.4$. One can reach the Mott insulating (MI) phase both for a commensurability of one boson per site and of one boson every two sites. The shape of the Mott lobe reflects the exponential nature of the gap close to the Mott-U transition. The Luttinger liquid parameters are indicated (K in this figure is $1/K$ of this book). They are in very good agreement with the analytic predictions. (From Kühner *et al.*, 2000 (Copyright (2000) by the American Physical Society).)

size L where the disorder is minimum (say $-V$ taking a bounded disorder). If the bosons are confined in such a region, the loss in kinetic energy is $E \propto (1/L)^2$ since the momentum cannot be strictly $k = 0$. On the other hand, the gain in potential energy is $-V$. For a large enough L it is thus favorable to condense all the bosons in such a region. Since such regions can be realized with a probability $p \sim e^{-L}$ (rare events), this scenario where *all* particles condense in a *finite* size region of size L is always possible. On the other hand since one has a *macroscopic* number of particles in a finite size region the density is infinite. Thus, any infinitesimal interaction makes this ground state unstable, and pushes the particles into other minima of the disorder (see Fig. 11.6).

Fortunately, the bosonization allows to treat the interacting disordered system quite simply (Giamarchi and Schulz, 1988*b*). As for fermions (see Section 9.1) the disorder can be introduced as a random potential coupled to the density. For simplicity I stick here to the incommensurate case. The disorder is

$$H_{\text{dis}} = \int dx\, V(x)\rho(x) \tag{11.15}$$

Using the representation (3.8) of the density one has (keeping only the lowest, that is, most relevant harmonics)

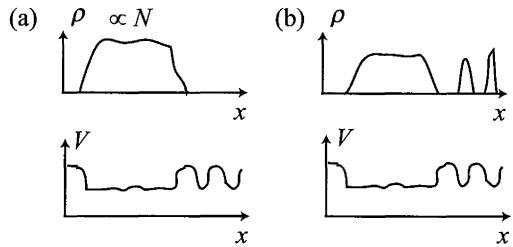

FIG. 11.6. A cartoon of free versus interacting bosons in the presence of disorder. (a) Free boson all condense in a large enough well of the random potential. Since the density is infinite, this situation is unstable when interactions are added. (b) the repulsion prevents the bosons to condense in the same site. Their behavior is thus much closer to fermions, where various minima of the random potential have to be used. Since one can still pile up many bosons in the same minima, the deep minima of the random potential are well smoothed by the bosons.

$$H_{\text{dis}} = \int dx\, V(x)[-\frac{1}{\pi}\nabla\phi(x) + \rho_0(e^{i(2\pi\rho_0 x - 2\phi(x))} + \text{h.c.})] \tag{11.16}$$

This expression is quite similar to the one for spinless fermions (9.28), where again $2\pi\rho_0$ plays the role of $2k_F$. There is thus for bosons the equivalent of forward and backward scattering on the disorder. The forward scattering is the pinning of the density fluctuations on Fourier components of the disorder that vary at a lengthscale much larger than the average boson–boson distance. The backward scattering corresponds to the pinning of the charge density on a periodic potential, which has a periodicity close to the boson periodicity. Using the analogy (see Fig. 3.5) with the classical systems explained in Chapter 3 one recognize a problem of a periodic array of lines which is pinned by columnar defects (that is, by a disorder independent of the τ direction). Compare with Fig. 3.7.

We can then proceed along the same lines than for Section 9.1. The forward scattering is absorbed in a redefinition of the field ϕ. Although this gives an exponential decay of the density–density correlation function this does not affect the current (hence the transport properties) and the θ correlation functions (hence, e.g. the single-particle Green's function). The backward scattering can be treated by the various techniques described in Section 9.1. In particular, the RG equations are

$$\begin{aligned} \frac{dK}{dl} &= -\frac{K^2}{2}\tilde{D}_{\text{b}} \\ \frac{d\tilde{D}_{\text{b}}}{dl} &= (3-2K)\tilde{D}_{\text{b}} \end{aligned} \tag{11.17}$$

where $\tilde{D}_b = D_b/(\pi^2 u^2 \rho_0)$ and D_b is the backward scattering (9.24). This leads to an irrelevant disorder for $K > 3/2$, that is, weakly repulsive bosons, and a localized phase for $K < 3/2$, that is, if the repulsion between the bosons are strong enough. On the separatrix the parameter K takes the universal value $K^* = 3/2$. Thus, the correlation functions decay with universal exponents. For example, the single-particle correlation function decays with an exponent 1/3. Most of the properties of the transition have been investigated in Section 9.1. This calculation thus point out the existence for the bosons of a localized phase. This phase, nicknamed Bose glass, whose existence can be established microscopically in one dimension has been generalizable to higher dimensions as well (Fisher *et al.*, 1989). In one dimension, one can compute the critical properties of the transition between the superfluid and the Bose glass. This parallels the analysis of Section 9.2.2. The localization length diverges exponentially as in (9.53) with the distance to localization. Formally, if one defines a critical exponent ν by $\xi_{\rm loc} \sim (\delta g)^{-\nu}$ where δg is the distance to the transition, one has thus $\nu = \infty$. Since the system is described by a LL the dynamical exponent is $z = 1$ ($\omega = uk$). The question of the nature of the transition between the superfluid and the Bose glass is an important question for which scaling hypothesis have been put forward to extend these properties to the higher dimensional case for which there is so far no microscopic solution. The charge stiffness $\mathcal{D}$ (see Section 7.2) jumps discontinuously to zero in the Bose glass phase and $\mathcal{D}/u = K$ takes the universal value 3/2 at the transition. At the transition the disorder is marginal. The regular part of the conductivity thus behaves as (Giamarchi, 1992) (see also (7.101))

$$\sigma(\omega) \sim \frac{1}{\omega \, \log^2(\omega)} \tag{11.18}$$

In the Bose glass phase, the localization is very similar to the one for spinless fermions. The bosonic nature of the particles is not so important any more. Since for zero interactions the localization is of a very different nature, the interesting question of the possibility of two different localized phases naturally arises for the bosonic system. I refer the reader to Giamarchi and Schulz (1988*b*) for more discussions on this, still open question.

There are many important properties of the bosonic system that can be studied using the bosonization methods. I refer the reader to the literature for some examples such as the bosonic ladder (Orignac and Giamarchi, 1998*b*; Orignac and Giamarchi, 2001; Donohue and Giamarchi, 2001) and the combination of disorder and commensurability (Fisher *et al.*, 1989; Scalettar *et al.*, 1991; Giamarchi *et al.*, 2001).

11.1.3 *Experimental realizations*

At the moment, the main realizations of one-dimensional bosonic systems is provided by Josephson junction arrays. However, Bose–Einstein condensate in optical traps could soon provide excellent systems to tackle these problems.

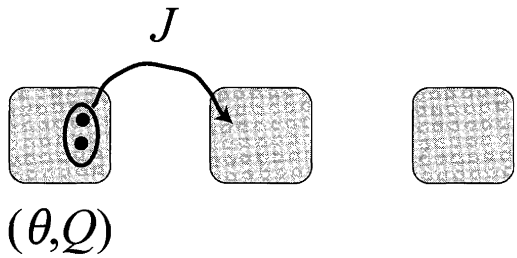

FIG. 11.7. A Josephson junction array. Each dot is a superconducting island characterized by a superconducting phase (supposed uniform on the dot) and a charge Q. These two parameters are conjugate variables as usual in a superconductor. The dots have a charing energy of the form $Q^2/2C$ where C is the capacitance of the dot. The phases between dots are coupled by the Josephson coupling J. This corresponds to the hopping of a Cooper pair from one dot to the other.

Josephson junction arrays are made of dots of weakly connected superconducting islands, as shown in Fig. 11.7 (for a review see, e.g. Schon and Zaikin, 1990; Fazio and van der Zant, 2001). Since each dot is a homogeneous system, it is characterized by a superconducting BCS wavefunction

$$\psi = Ae^{i\theta} \tag{11.19}$$

Since one is well below the superconducting temperature of each grain, the amplitude A is non-zero and well fixed. Having amplitude fluctuations cost a lot of energy so we can safely take the amplitude as a constant. The phase on the other hand is free to fluctuate. In addition to the phase, one can characterize the state of the grain by its charge Q. It is important to notice that neither θ nor Q is a classical object. Charge and phase obey the standard commutation relation (Tinkham, 1975)

$$[Q, \theta] = i\hbar \tag{11.20}$$

If we now consider a weak coupling between the grains, two main terms enter. The first one is the simple electrostatic coupling. Each grain has a certain capacitance and charging it costs energy. In the same spirit, there is a mutual capacitance between grains, so the charging energy can be written

$$E = \frac{1}{2}\sum_{ij}(C^{-1})_{ij}(Q_i - Q_0)(Q_j - Q_0) \tag{11.21}$$

where ij are the grain indices, and C_{ij} is the capacitance matrix. Q_0 is an average charge imposed for example by an external gate. This is nothing but the standard electrostatic energy. In addition to this electrostatic coupling there is also the possibility for the electrons to go from one dot to the other. Because of

the existence of the BCS gap the tunneling of a single electron from one dot to the other is exponentially suppressed. This is identical to what was discussed in Chapter 8 (see Fig. 8.11). It is much more energetically favorable for the electrons to hop by pairs. The Hamiltonian of such a system is thus

$$H = -J \sum_i \cos(\theta_{i+1} - \theta_i) + \frac{1}{2C} \sum_i (Q_i - Q_0)^2 \tag{11.22}$$

where J is the Josephson coupling between the grains. For simplicity I have taken the capacitance to be only local $C^{-1}_{i \neq j} = 0$. This amounts in taking only the charging energy of the grains and to neglect their mutual coupling.

In the continuum limit, this Hamiltonian is very similar to the Luttinger liquid Hamiltonian (3.25). One can make the approximation

$$-J \cos(\theta_{i+1} - \theta_i) \sim -J[1 - \frac{\alpha^2}{2}(\partial_x \theta(x))^2] \tag{11.23}$$

where α is the distance between grains. If in addition one defines the charge density as ($x = \alpha j$)

$$\rho(x) = Q_i/\alpha \tag{11.24}$$

one can then introduce the field ϕ related to the density as in (3.9). Given the commutation relation between θ and the charge Q the fields ϕ and θ verify similar commutation relations than the corresponding ϕ and θ of the Luttinger liquid, and have the same physical interpretation since ϕ is related to the density and θ to the superfluid phase of a 'site' (a grain). The Hamiltonian (11.23) can thus be mapped to the Luttinger liquid Hamiltonian (3.25). Note that the current in a superconductor is simply the gradient of the phase (if the amplitude is fixed), so we recover our favorite expression (7.55) for the current. In fact one should be more careful in the expansion of the cosine term $\cos(\theta_{i+1} - \theta_i)$ since doing so forgets about configurations where the phase has a vortex. However, we saw in Chapter 3 that it is possible to create vortices in the phase θ by adding to the Hamiltonian a term $\cos(2\phi)$. Josephson junction arrays thus give back our favorite sine-Gordon Hamiltonian (Bradley and Doniach, 1984; Glazman and Larkin, 1997).

Another mapping for the Josephson junction array is simply to consider each grain as a site, and to define a density n_i on this site. The Josephson term destroys a boson (a Cooper pair) on the site and creates it on the neighboring site. One can thus represent the array as

$$H = -J \sum_i b_i^\dagger b_i + \frac{1}{2C} \sum_i n_i^2 - \mu \sum_i n_i \tag{11.25}$$

which is identical to the Bose–Hubbard Hamiltonian (11.4). Of course, the precise mapping requires more care specially if one wants to worry about the effect of amplitude fluctuations or of dissipation. I refer the reader to Fazio and van der Zant (2001) for more material on this subject.

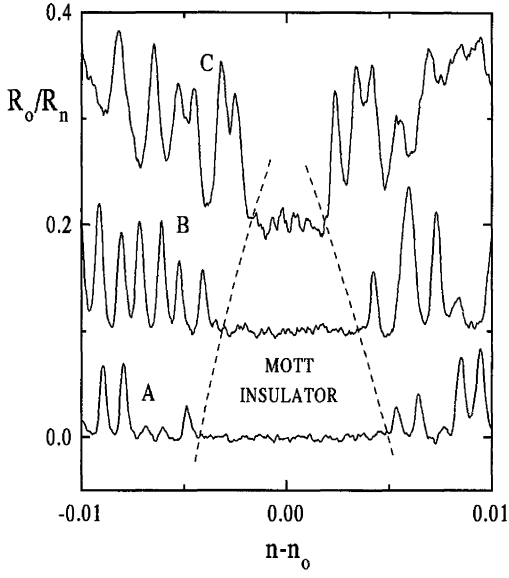

FIG. 11.8. Mott transition in Josephson junction arrays (see text). The resistance R_0 (normalized to the normal resistance R_n of the array) is shown for three samples A, B and C with different charging energies. When the chemical potential $n-n_0$ for the vortices is small enough the vortices are pinned by the periodic potential of the array and thus are in a Mott insulating phase (which means zero resistance for the superconductor). (From van Oudenaarden and Mooij, 1996 (Copyright (1996) by the American Physical Society).)

One can thus use Josephson junction arrays to probe the physics of one-dimensional bosons. I show here the example of the Mott transition. In this system a magnetic field is applied to create vortices in the superconducting phase. If vortices can move then the system has a high resistance. On the other hand if the vortices are pinned by the commensurate potential of the lattice then the system is still a good superconductor with low resistance. It is thus a Mott transition but where the periodic potential pins the phase θ instead of the field ϕ and where the 'chemical potential' couples to the current, that is, to $\nabla\theta$. By measuring the resistance one can thus check whether the phase θ is gapped or not. Transport is thus a way to map the phase diagram. The data is shown in Fig. 11.8 in very good agreement with the existence of a Mott transition. Note that Josephson junction arrays can also provide a good realization of bosonic ladders since the geometry is totally controlled.

Finally, let me now briefly examine the Bose condensate systems. Having bosons is relatively easy in condensed matter, but confining them into a one-dimensional geometry is very difficult, since one lacks the equivalent of the lithographic process for the fermions in quantum wires or the wonders of chemistry as

in nanotubes or organic materials. However, in recent years it has been possible to reach Bose–Einstein condensation in optical traps (see Anglin and Ketterle, 2002 for a review). Such systems are thus prime candidates to study the physics described here since one has a total control over the potential in which the Bosons are put. This is a field that is exploding at the moment and it is clear that many progress will occur in the coming years. At the time where these lines are written it is still too early to have a real one-dimensional Bose gas in which the LL properties can be tested. There are, however, very promising steps that have been taken (Görlitz *et al.*, 2001; Schreck *et al.*, 2001; Gerbier *et al.*, 2002). There is thus no doubt that one-dimensional geometry can be reached in these systems. A periodic potential can be imposed. For three-dimensional traps it has been possible to reach the Mott transition (Greiner *et al.*, 2002). One-dimensional realizations of Bose-Mott insulators should be possible soon. These systems offer several characteristics that are difficult to reach in conventional condensed matter systems, and are thus complementary of the conventional ones. For example, it is possible to apply electric fields much larger than in conventional systems (comparable to characteristics kinetic energy). It is also possible to switch on and off potentials, which allows to study the response to time dependent Mott potentials, an impossible thing to do in conventional systems.

11.2 Impurities in Fermi liquids

In this section, I present some extensions of the bosonization technique to higher dimensional cases. Various applications have been proposed that it is impossible to treat here both because of lack of space and because some of them are still quite speculative or go beyond the level of this book. This includes, and is not limited to bosonization in higher dimensions (Houghton *et al.*, 2000), direct application of Luttinger liquids in high Tc (Anderson, 1997), stripes[37] (Kivelson *et al.*, 1998). I refer the reader to the literature for more on these subjects. Instead I focus here on problems that can be reduced by some trick to a one-dimensional situation. This is in particular the case of the problem of a single impurity embedded in a fermion gas.

There is, for three-dimensional systems, a considerable interest in studying situations where a single impurity interacts in some way with the electron gas. Originally, such a problem is aimed at studying effects produced in realistic systems by very diluted impurities. Famous examples of such situations are the X-ray edge problem and the Kondo problems that we will examine in the next sections. Another famous example is the well-known Anderson model. Quite recently the progress of nanotechnology have made it possible to directly realize experimental devices in which these single impurity models describe directly the experimental situation. This is the case, for example, for quantum dots or quantum corals. The literature on the subject is quite impressive. Lack of space

[37]Since stripes are relatively conventional one-dimensional systems, much of the material of this book is directly useful.

prevents here to examine these experimental realizations in any reasonable detail, and I just[38] refer the reader to some reviews in the literature on these subjects (Kouwenhoven and Markus, 1998).

11.2.1 *X-ray edge problem*

Let us start with the famous X-ray edge problem, initially examined to describe the interaction of an electron band with a deep hole that can be created sending an X-ray on the system. Since we consider three-dimensional electrons in a metal where the Fermi liquid theory is expected to hold, one can describe these electrons as non-interacting. One also assumes that the hole is too heavy to move, and thus stays at the site where it is created. Its only effect is thus a local interaction with the conduction electrons on this site. This model was the prototype of a fermionic problem with a divergent perturbation theory, and has been instrumental in understanding more complicated problems such as the Kondo problem. I cannot recall here all the physics on this problem and refer the reader to Mahan (1981) and Nozieres and de Dominicis (1969) for more details. The Hamiltonian is

$$H = \sum_k \epsilon_k c_k^\dagger c_k + E d^\dagger d + \frac{1}{\Omega} \sum_{k,k'} V u_k u_{k'} c_k^\dagger c_{k'} d^\dagger d \tag{11.26}$$

where c are the conduction electrons and d is the deep hole. E is the energy of the hole. Since the hole stays localized the energy does not depend on k. The last term is the interaction (usually attractive $V < 0$) between the hole and the local density of electrons $\psi^\dagger(x=0)\psi(x=0)$ (one assumes that the hole cannot propagate and stays at $x = 0$). To simplify the problem, one assumes a constant density of states for the conduction electrons. It is thus necessary to impose a finite bandwidth. This is the role of the u_k in the above Hamiltonian. The u_k are one if the momentum is in the bandwidth $\epsilon_k \in [-E_0, E_0]$ and zero otherwise. Sending an X-ray kicks an electron from the deep band into the conduction band. It thus creates both a hole and a conduction electron at the origin. The coupling to the X-ray is

$$H_x = \frac{1}{\sqrt{\Omega}} \sum_k u_k c_k^\dagger d^\dagger \tag{11.27}$$

Since this is an impurity problem and the momentum is not conserved because of the local character of the impurity, all terms in the perturbation theory can be reexpressed as integrals over energy

$$\sum_k u_k \to \int_{-E_0}^{E_0} d\epsilon\, N(\epsilon) = N(0) \int_{-E_0}^{E_0} d\epsilon \tag{11.28}$$

[38] Much to my regret since the subject is really fascinating.

assuming a constant density of states $N(0)$. The problem is thus totally independent of the spatial dimension. One can thus replace the original three-dimensional problem by an effective one-dimensional one, with a linearized spectrum (that is, a constant density of states) and such that the Fermi velocity is $N(0)/\Omega = 1/(\pi v_F)$. This ensures that the effective one-dimensional problem has *the same* density of states than the original three-dimensional one. Both in the interaction term in (11.26) and in the coupling to the X-ray (11.27) the fermions only intervene through the combination (and its hermitian conjugate)

$$\sum_k c_k = \sum_k (c_{k,R} + c_{k,L}) \tag{11.29}$$

where I have used the expression of the single-particle operator for the effective one-dimensional problem (2.34) in terms of right and left movers. This suggests to perform the canonical transformation

$$\begin{aligned} A_{k,R} &= \frac{1}{\sqrt{2}}(c_{k,R} + c_{-k,L}) \\ A_{k,L} &= \frac{1}{\sqrt{2}}(-c_{k,R} + c_{-k,L}) \end{aligned} \tag{11.30}$$

It is easy to check that the transformation (11.30) preserves the anticommutation relations of the fermions, and thus that the A are true fermion operators. Note that such a transformation is non-local in space since it involves both k and $-k$. The Fourier transform of the A_k would contain a fermionic part both at point x and at point $-x$. It is thus only useful if the fermion Hamiltonian does not contain an interaction term. Otherwise, the interaction will become non-local in terms of the new operators. This is exactly the same procedure than the one used in Chapter 10 to treat the boundary. The Hamiltonian (11.26) and coupling (11.27) become

$$\begin{aligned} H &= \sum_k \epsilon_k [A^\dagger_{k,R} A_{k,R} - A^\dagger_{k,L} A_{k,L}] + E d^\dagger d + \frac{2V}{\Omega} \sum_{k,k'} u_k u_{k'} A^\dagger_{k,R} A_{k,R} d^\dagger d \\ H_x &= \sqrt{\frac{2}{\Omega}} \sum_k u_k A^\dagger_{k,R} d^\dagger \end{aligned} \tag{11.31}$$

Let us forget for a moment the limitation imposed by u_k, that is, assume that the bandwidth E is very large or that we are at very low-energy. Since the fermion operator at the origin is for right movers

$$\psi^\dagger_R(x=0) = \frac{1}{\sqrt{\Omega}} \sum_k A^\dagger_{k,R} \tag{11.32}$$

The Hamiltonian and coupling can be rewritten as

$$
\begin{aligned}
H &= \sum_k \epsilon_k [A^\dagger_{k,R} A_{k,R} - A^\dagger_{k,L} A_{k,L}] + E d^\dagger d + 2V \psi^\dagger_R(0) \psi_R(0) d^\dagger d \\
H_x &= \sqrt{2} \psi^\dagger_R(0) d^\dagger
\end{aligned}
\tag{11.33}
$$

Formula (11.33) shows two important properties. First, only the right going fermions are coupled to the impurity. This means that the impurity does not couple to the full one-dimensional fermions but only to half of the degrees of freedom. This property of our effective one-dimensional problem can easily be understood. Since the impurity is purely local one can always use for the original three-dimensional problem a distance $r > 0$ and angular momentum basis for the conduction electrons instead of the cartesian coordinates. Since the impurity is point-like the interaction conserves the angular momentum quantum number, and the impurity couples to the s channel. The properties thus depend only on the *distance* $r \geq 0$ to the impurity. This is why the problem is independent of dimension, and also why only *half* the degrees of freedom of the effective one-dimensional problem are needed. In fact, one can see that we can consider the system coupled to a full one-dimensional fermion gas (with left and right going fermions), but to only a half line $x > 0$. As in Chapter 10 we can use the fact that the space $x < 0$ is not physical to say that the left going fermions in $x > 0$ are identical to right going fermions on $x < 0$: $\psi_L(x > 0) = \psi_R(-x)$, and thus consider a full one-dimensional world but with only right going fermions coupling to the impurity. This is the equivalent of the transformation (11.30). The second important point in (11.33) is the fact that the impurity only couples to the fermionic operators at $x = 0$. If we think of the fermions living in a half space, in the absence of impurity we know their boundary condition. The effect of the impurity is to modify this boundary condition. I will come back to this very important point.

To be able to use our powerful one-dimensional arsenal is of course one of the interests of the mapping of the impurity problem to a one-dimensional system. Let us now use the bosonization method to solve the problem (Schotte and Schotte, 1969). Using the boson description of Appendix D one gets for (11.33)

$$
\begin{aligned}
H &= E d^\dagger d + \sum_{p \neq 0} \epsilon_p b^\dagger_p b_p + 2V d^\dagger d \sum_{p>0} \left(\frac{p}{2\pi L} \right)^{1/2} [b^\dagger_p + b_p] \\
H_x &= \sqrt{\frac{2}{2\pi\alpha}} U^\dagger_R e^{\sum_{p>0} \left(\frac{2\pi}{Lp}\right)^{1/2} [b^\dagger_p - b_p]} d^\dagger
\end{aligned}
\tag{11.34}
$$

where $\epsilon_p = v_F |p|$. I have used in (11.34) the standard boson operators instead of the fields ϕ and θ since the physics is more transparent using these variables, but this is of course strictly identical. We see that (11.34) is still a free Hamiltonian for the oscillators associated to the bosons operators b_p. The only effect of the coupling to the impurity is to shift these oscillators. It is easy to directly determine the new bosonic operators by completing the square in the Hamiltonian H. An alternative method to perform this shift is to remark that a canonical

transformation of the operators can be enforced by an unitary operator W. If H_0 is the free boson Hamiltonian (that is, (11.34) with $V = 0$), then let us compute

$$H_f = W^\dagger H_0 W \tag{11.35}$$

with W defined as

$$W = e^{iS} = e^{\sum_{p>0} \frac{2V}{\epsilon_p}\left(\frac{p_x}{2\pi L}\right)^{1/2}[b_p^\dagger - b_p]} \tag{11.36}$$

We can use the formula

$$H_f = H_0 - [iS, H_0] + \frac{1}{2}[iS, [iS, H_0]] + \cdots \tag{11.37}$$

The term $-[iS, H]$ is exactly the interaction term in (11.34). The second term is a simple constant

$$C = \frac{1}{2}[iS, [iS, H]] = \sum_{p>0} \frac{V}{\pi L v_F} \tag{11.38}$$

and thus all higher terms of the series in (11.37) are zero. H_f is thus, up to a constant term, exactly the interacting Hamiltonian H in (11.34) when a hole is present $d^\dagger d = 1$. The constant term is the zero point energy that corresponds to the shift of the oscillators. All the effects of the impurity can thus be removed by the canonical transformation (11.35) which is just a way to implement the change of variable corresponding to the shift of the oscillators in (11.34).

The correlation functions

$$\begin{aligned} G(\tau) &= -\langle 0_F; n_d = 0 | T_\tau d_\tau d_0^\dagger | 0_F; n_d = 0\rangle \\ F(\tau) &= -\langle 0_F; n_d = 0 | H_x^\dagger(\tau) H_x(0) | 0_F; n_d = 0\rangle \end{aligned} \tag{11.39}$$

can now be computed very simply. In the above formulas 0_F is the Fermi sea (I stick to zero temperature), and thus the ground state of the Fermions in the absence of holes. G is the Green function of the hole, while F is the linear response to an X-ray creating a hole and exciting an electron in the conduction band. These correlation functions can be computed exactly (Nozieres and de Dominicis, 1969). To compute them using the boson representation we use our canonical transformation. Let us take first $F(\tau)$. Since the hole has no dynamics between its creation and destruction, the correlation function is given by (for $\tau > 0$)

$$\begin{aligned} F(\tau) &= -2\langle 0_F; n_d = 0 | e^{H\tau} d\psi(x=0) e^{-H\tau} \psi^\dagger(x=0) d^\dagger | 0_F; n_d = 0\rangle \\ &= -2\langle 0_F | e^{H_0\tau} \psi(x=0) e^{-H_1\tau} \psi^\dagger(x=0) | 0_F\rangle \\ &= -2e^{C\tau}\langle 0_F | e^{H_0\tau} \psi(x=0) W^\dagger e^{-H_0\tau} W \psi^\dagger(x=0) d^\dagger | 0_F\rangle \\ &= -2e^{C\tau}\langle 0_F | e^{H_0\tau} \tilde{\psi}(x=0) e^{-H_0\tau} \tilde{\psi}^\dagger(x=0) | 0_F\rangle \end{aligned} \tag{11.40}$$

where H_1 is the Hamiltonian in presence of the hole ($d^\dagger d = 1$ in (11.34)) and H_0 the one in the absence of the hole ($d^\dagger d = 0$). The prefactor $e^{C\tau}$ where C is

(11.38) is unimportant since it is a simple shift of the energies, and I will ignore it from now on. One has thus to compute the correlation function for a free fermionic Hamiltonian but with a modified ψ which is now

$$\tilde{\psi}^\dagger = W\psi^\dagger = \frac{1}{\sqrt{2\pi\alpha}} e^{[1+\frac{V}{\pi v_F}]\sum_{p>0}\left(\frac{2\pi}{Lp}\right)^{1/2}[b_p^\dagger - b_p]} \tag{11.41}$$

Since everything is computed with free fermions, that is, the free boson Hamiltonian H_0, the correlation $F(\tau)$ is trivial to compute using Appendix C and gives

$$\begin{aligned} F(t) &= -\frac{1}{\pi\alpha} e^{\sum_{p>0}[1+\frac{V}{\pi v_F}]^2\left(\frac{2\pi}{pL}\right)(e^{-i\epsilon_p t}-1)e^{-\alpha p}} \\ &= \frac{1}{\pi\alpha}\left(1+\frac{iv_F t}{\alpha}\right)^{-(1+\gamma)^2} \end{aligned} \tag{11.42}$$

where

$$\gamma = N(0)V = \frac{V}{\pi v_F} \tag{11.43}$$

is the dimensionless interaction and I have used $\tau = it$ to go back to real time. The cutoff α is there, as usual, to mimic the finite bandwidth $\Lambda \sim 1/\alpha$. $G(\tau)$ can be computed in exactly the same way. The only difference is the fact that the operator ψ is absent from $G(\tau)$. Thus, in (11.41), $\tilde{\psi}^\dagger$ is now simply $\tilde{\psi}^\dagger = W$. One has thus to replace $1+\gamma$ by γ in (11.42), leading to

$$G(t) \propto t^{-\gamma^2} \tag{11.44}$$

Quite remarkably, the bosonization solution allows to reproduce in a few lines the main features of the X-ray problem, namely the power law dependence of the correlation functions (11.42) and (11.44). One even recovers the precise relation between the exponents. The bosonization formulation also allows to prove extremely easily some key results of the X-ray problem. In particular, it is easy to see that computing the correlations of

$$\psi \cdots \psi \tag{11.45}$$

leads to a bosonic operator

$$e^{[n+\gamma]\sum_{p>0}\left(\frac{2\pi}{Lp}\right)^{1/2}[b_p^\dagger - b_p]} \tag{11.46}$$

instead of (11.41) and thus to a time decay of

$$G_n(t) \sim \left(\frac{1}{t}\right)^{(n+\gamma)^2} \tag{11.47}$$

which is known as Hopfield rule, and not easy to prove in the Fermion representation. The only difference with the exact solution (Nozieres and de Dominicis,

1969) is the fact that instead of having $\gamma = \delta/\pi$ where $\tan(\delta) = \pi N(0)V$ is the standard phase shift associated with a local potential, one has now $\delta = \pi N(0)V$. Except for this unusual phase shift, all the relations between the exponents are *exact*. It is thus not a simple weak coupling expansion in the interaction. This can also be seen on the result (11.38). The shift of energy of an electronic system as a function of the phase shifts is given by Fumi's theorem (Mahan, 1981)

$$\Delta E = -\frac{1}{L\pi} \sum_p \delta(p) \tag{11.48}$$

This is exactly the result (11.38) if one admits that the phase shift is given by $\delta = \pi N(0)V$ and not the standard formula.

What is the explanation of this remarkable difference? Let us examine the Dirac equation that corresponds to the linearized Hamiltonian that we have used for the fermions. In the presence of an impurity the Hamiltonian

$$H = \int dx \left[\frac{v_F}{i} \psi_R^\dagger(x) \partial_x \psi_R(x) + V(x) \psi_R^\dagger(x) \psi_R(x) \right] \tag{11.49}$$

can easily be solved. The solutions obey

$$\frac{v_F}{i} \partial_x \psi(x) + V(x)\psi(x) = E\psi(x) \tag{11.50}$$

If one wants to get a plane wave at $x = -\infty$ the only solution is

$$\psi_R(x) = e^{ikx}\, e^{-\frac{i}{v_F}\int_{-\infty}^{x} dy\, V(y)} \tag{11.51}$$

Thus, the phase shift due to the impurity is defined by

$$\psi(x = +\infty) = e^{ikx}\, e^{-i\delta} \tag{11.52}$$

For a local potential $V(x) = V_0 \delta(x)$ it is given by

$$\delta = \frac{1}{v_F} \int_{-\infty}^{+\infty} dy\, V(y) = \frac{V_0}{v_F} = \pi N(0) V_0 \tag{11.53}$$

Thus, for the Dirac equation, that is, for a *strictly* linear spectrum the Born approximation for the phase shift is exact, which is of course not the case if one had taken the original dispersion relation (and the Schrödinger equation). This explains why in our bosonization solution we get exact exponents in terms of the parameter γ but with a different γ than the conventional phase shift of the three-dimensional theory. To track the source of the discrepancy between our original three-dimensional theory and the bosonized one, we have to go back to the Dzyaloshinskii–Larkin solution of Section 1.3. We have seen in this section that for a purely linear theory, all fermionic bubbles with more than two interaction lines attached cancel in the perturbation theory. This is also enforced

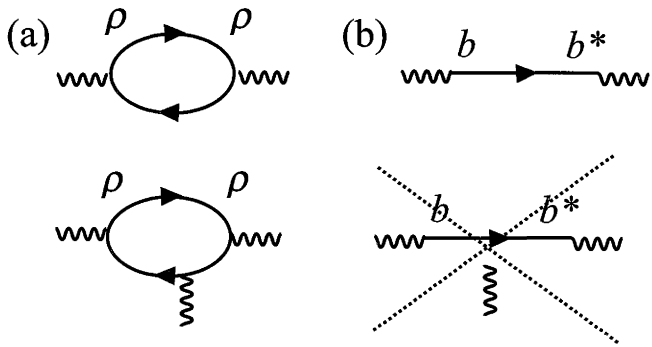

FIG. 11.9. Only bubbles with two interaction lines can survive with a strict linear spectrum. In the fermion language this is not obvious and is proven by the Dzyaloshinskii–Larkin theorem. In the bosonization representation the density bubble (a) becomes simply the boson propagator (b). It is then clear that a third interaction line cannot be attached any more to the graph.

by the bosonization theory since a bubble is a density–density correlation and is thus simply a *boson single line propagator* in the bosonization. Nothing can thus be attached to the bubble as shown in Fig. 11.9. However, such a result is not true for the original model for which fermionic bubbles with more than two interaction legs can perfectly exist. This difference is responsible for the difference between the phase shifts of the linearized theory and the phase shifts of the original one. We see that the bosonization theory can be again seen as an effective low-energy theory that captures *exactly* the low-energy properties of the system (that is, correlation functions, relations between exponents etc.). The relation between the fixed point parameters and the Luttinger liquid parameters can be renormalized by irrelevant operators and can be reliably determined in perturbation only or by some other exact method. If one wanted to make an exact calculation in this case, one should go back to the starting Hamiltonian (11.31). The linear spectrum *is exact* since in three dimensions one also assumes a constant density of states. But in the interaction one should keep the parameters u to enforce the *finite bandwidth* for the *three* dimensional system. Keeping them leads to the interaction

$$H_{\text{int}} = \int dx\, \tilde{u}(x)\psi_R^\dagger(x) \int dx'\, \tilde{u}(x')\psi_R(x') \tag{11.54}$$

where $\tilde{u}(x)$ is one if $x \in [-1/\Lambda, 1/\Lambda]$ and zero otherwise. The interaction is thus *non-local*, as shown in Fig. 11.10 and cannot be reduced simply to the form (11.33). Because of this non-locality the Dzyaloshinskii–Larkin result does not apply, and now more than two interaction lines are possible. This Hamiltonian would thus reproduce *exactly* the phase shift of the three-dimensional model, but is of course more complicated to solve. In other words, the limit $\alpha \to 0$ in the bosonization and the limit of $\tilde{u}(x) = \delta(x)$ do not commute. Letting $\Lambda \to \infty$

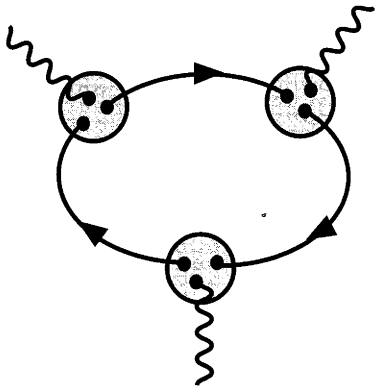

FIG. 11.10. Because of the cutoffs to impose the finite bandwidth, the interaction is in fact non-local in space if one wants to write it exactly as for the three-dimensional system. Here a full line is a fermion line, and a wiggly line is an interaction with the impurity. The non-local character of the interaction now allows for 'bubbles' (that are in fact not real bubbles any more) with more than two interaction lines to contribute.

but keeping a finite α in the bosonization formula is correct as far as the physics is concerned but does not give the exact phase shift. Note that the fermion operators can still be expressed in terms of the boson ones using the dictionary of Appendix D.

Once again rather than trying to obtain the phase shift from microscopic parameters that are approximate anyhow, it is much better to take the bosonization formulation as an effective low-energy formulation. In that case the parameter γ is the physical parameter and the bosonization formulas give the exact asymptotic behavior in terms of this parameter. As for the standard Luttinger liquid parameters (see Chapter 3) is it important to remember that γ is physically a phase shift in this problem. This means if γ comes from a three-dimensional problem it will be impossible to exceed $\gamma = 1$ even if naively one could have thought from (11.43) to be able to reach much higher values. Not taking into account this limitation can lead to incorrect physics. This limitation is reminiscent of the limitations on the Luttinger parameters for fermions (see, e.g. Chapter 7).

Finally, let us see how the bosonization result connects with the orthogonality catastrophe, which states that the ground states of two systems with and without a local impurity are orthogonal (Anderson, 1967). In the absence of the impurity the ground state of the system is the vacuum $|0_b\rangle$ with respect to the boson operators b. This is the state such that

$$b_k|0_b\rangle = 0, \quad \text{for all } k \tag{11.55}$$

In the presence of the impurity the ground state of the system changes and becomes the vacuum of the new operators $\tilde{b}_k$, which represent the shifted oscillators. It is simply the canonical transformation of the old vacuum

$$|\tilde{0}_b\rangle = W|0_b\rangle \tag{11.56}$$

with W given by (11.30). Keeping in mind that the boson operator $b_p^\dagger$ creates, in fermionic language, particle–hole excitations of total momentum p, we see that the new vacuum contains an infinite number of such excitations. We thus recover the orthogonality catastrophe. The overlap between the two vacua is

$$\langle 0_b|\tilde{0}_b\rangle = \langle 0_b|W|0_b\rangle \propto e^{-\frac{\pi\gamma^2}{L}\sum_{p>0}\frac{1}{p}} \tag{11.57}$$

For an infinite system the sum over p in (11.57) transforms into a divergent integral, and the overlap between the two vacua is zero. For a finite system the minimum value of p is $p_m = 2\pi/L$. Transforming the sum in (11.57) into an integral with a lower cutoff p_m the overlap is thus given by

$$\langle\phi|\tilde{\phi}\rangle \propto L^{-\frac{\gamma^2}{2}} \tag{11.58}$$

which shows again that the orthogonality is controlled by the phase shift due to the impurity. This overlap is in fact also given by the hole Green's function. Indeed, since the hole has no dynamics the correlation G measures the overlap at time τ of the two ground states with zero and one hole

$$\begin{aligned} G(\tau) &= -\langle 0_F; n_d = 0|e^{H\tau}de^{-H\tau}d^\dagger|0_F; n_d = 0\rangle \\ &= -\langle 0_F, n_d = 0|e^{H_0\tau}e^{-H_1\tau}|0_F, n_d = 1\rangle \\ &= -\langle 0_F, n_d = 0, \tau||0_F, n_d = 1, \tau\rangle \end{aligned} \tag{11.59}$$

The decay of the correlation with time is another way to prove that the two ground states with and without impurity are orthogonals.

Finally, let me comment on the solution. The presence of the impurity still leaves a problem of free bosons. Simply these bosons are not the original ones. The only effect of the impurity is thus to change the boundary condition. This is exactly similar to what happened for the boundary for the Luttinger liquid. Quite generally one can solve impurity problems by finding what is the proper boundary condition to take into account. This very powerful method has been used with great success. I refer the reader to Affleck and Ludwig (1994), Affleck (1995) and Di Francesco *et al.* (1997) since this is beyond the scope of this book.

11.2.2 *Kondo problem*

Let us now look at the case of a magnetic impurity. This is the famous Kondo problem, which has been one of the major headaches of the 1970s. The free fermion gas is coupled to an impurity with a spin degree of freedom. Here again I refer the reader to Mahan (1981), Tsvelick and Wiegmann (1983), Andrei *et al.* (1983) and Cox and Zawadowski (1998) for a discussion on the physics of the Kondo problem. Let us confine here to a spin 1/2. More general cases are of course possible. The coupling term is

$$H_{\text{int}} = \frac{V}{\Omega}\sum_{k,k'}\sum_{\sigma} c^{\dagger}_{k,\sigma}c_{k,\sigma} + \frac{J}{2\Omega}\sum_{k,k',\sigma,\sigma'} c^{\dagger}_{k,\sigma}\vec{\sigma}_{\sigma,\sigma'}c_{k,\sigma}\cdot\vec{S} \tag{11.60}$$

where the σ^i are the Pauli matrices and $\vec{S}$ is the spin of the impurity. Keep in mind that

$$\frac{1}{\sqrt{\Omega}}\sum_{k} c_{k,\sigma} = \psi_{\sigma}(x=0) \tag{11.61}$$

so the impurity couples to the fermions at the origin only. The first term in (11.60) is the potential coupling to the impurity. Since the charge of the impurity is totally inert, contrary to the case of the X-ray problem, we do not expect any non-trivial effect from this term. The second term describes the coupling of the electrons to the spin S of the impurity. The fermionic part in this term contains

$$\frac{J}{2\Omega}\sum_{k,k',\sigma,\sigma'} c^{\dagger}_{k,\sigma}\sigma^{\alpha}_{\sigma,\sigma'}c_{k,\sigma} = \frac{J}{2}\sum_{\sigma,\sigma'}\psi^{\dagger}(x=0)_{\sigma}\sigma^{\alpha}_{\sigma,\sigma'}\psi(x=0)_{\sigma'} \tag{11.62}$$

which is the component $\alpha = x, y, z$ of the fermionic spin at the origin. It is convenient for the following to study an anisotropic Kondo model where the coupling along x, y is different from the coupling along the z direction. In that case the spin interaction can be rewritten as

$$\frac{J_z}{2}(\psi^{\dagger}_{\uparrow}(0)\psi_{\uparrow}(0) - \psi^{\dagger}_{\downarrow}(0)\psi_{\downarrow}(0))S_z + \frac{J_{xy}}{2}(\psi^{\dagger}_{\uparrow}(0)\psi_{\downarrow}(0)S^{-} + \psi^{\dagger}_{\downarrow}(0)\psi_{\uparrow}(0)S^{+}) \tag{11.63}$$

where $S^{\pm} = S_x \pm iS_y$ are the spin raising and lowering operators for the impurity.

For small J, this problem can be studied by conventional RG techniques, similar to the ones of Chapter 1 (Anderson, 1970; Sólyom and Zawadowski, 1974). The perturbation theory has logarithmically divergent couplings that can be analyzed with an RG procedure. V totally decouples from the spin part and does not scale $\frac{dV}{dl} = 0$ showing that potential scattering has only trivial effects. The RG equations for the spin couplings are

$$\begin{aligned} \frac{d\tilde{J}_z}{dl} &= \tilde{J}^2_{xy} \\ \frac{d\tilde{J}_{yx}}{dl} &= \tilde{J}_z\tilde{J}_{xy} \end{aligned} \tag{11.64}$$

where $\tilde{J} = J/(\pi v_F)$ are the dimensionless couplings. The flow is thus exactly similar to the flow of Fig. 2.6 (with $K \equiv -\tilde{J}_z$ and $y = \tilde{J}_{xy}$). There are two regimes. In the ferromagnetic Kondo regime J_{xy} scales to zero. For isotropic couplings this corresponds to initial ferromagnetic couplings $J_z = J_{xy} < 0$, hence the name. Note that for the isotropic couplings both J_z and J_{xy} scale to zero so the impurity asymptotically decouples. In the antiferromagnetic Kondo

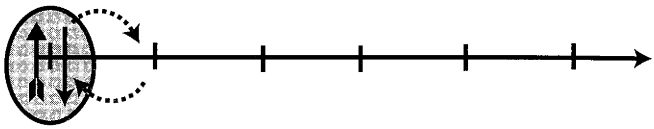

FIG. 11.11. The strong coupling image of the Kondo model. The impurity spin has bound a conduction electron in a singlet ground state. The site of the impurity is thus essentially excluded for the other electrons since if an electron hops in or out the impurity site it would break the singlet. The ground state is thus stable with respect of a weak hopping. Note that the strong coupling problem is again essentially a free electron problem but with one site excluded.

regime the couplings scale to large values. For the isotropic couplings $\frac{d\tilde{J}}{dl} = \tilde{J}^2$ and the coupling becomes of order one at a scale

$$1 \sim \tilde{J}(l^*) = \frac{\tilde{J}}{1 - \tilde{J}l^*} \tag{11.65}$$

which corresponds for small $\tilde{J}$ to the famous Kondo temperature

$$T_K = E_0 e^{-l^*} \sim E_0 e^{-\frac{1}{\tilde{J}}} \tag{11.66}$$

Since couplings flow to large values the perturbative RG is not applicable in this regime any more and the strong coupling needs to be understood. This is a very complicated problem. Physically if the coupling J becomes large one can expect that the local spin captures an electron to form a singlet as shown in Fig. 11.11. If the coupling J is very large this singlet has a gap to spin excitations of order J. Thus, electrons cannot hop in and out of the impurity site without paying this energy (if two conduction electrons are on the site they have to be in a singlet state because of the Pauli principle, and thus the impurity spin is free). For large J the system thus just behaves as if the impurity site is excluded for the other electrons, but except for this constraint the other electrons are free. The physics of the antiferromagnetic Kondo regime is thus the one of a Fermi liquid (Nozieres, 1974). Note that we have another example of the fact that the solution of an impurity problem is a change of boundary conditions (here the site zero is forbidden whereas it would be allowed if $J = 0$).

Of course, from the perturbative RG there is *no certainty* that the couplings indeed flow to infinity, since the equations are not valid beyond $J \sim 1$. For example going to next order in the RG equations gives $J^2 - J^3$ which would make believe that an intermediate fixed point $J \sim 1$ could exists. This intermediate fixed point is in fact an artefact and disappears when higher-orders are included. The fact that the strong coupling fixed point (J large) is stable towards a small kinetic energy (it has a gap of order J) is a good indication that no intermediate fixed point exists. But clearly one needs a better method to tackle the antiferromagnetic regime. This can be done by numerical RG (Wilson, 1975), which

is essentially exact for low energies or exact solutions (Tsvelick and Wiegmann, 1983; Andrei *et al.*, 1983). Both these methods are relatively heavy so let us see how bosonization can help us.

As for the X-ray, one finds the equivalent one-dimensional Hamiltonian with the same density of states and performs the canonical transformation (11.30) to couple only to right going fermions. The Hamiltonian (11.60) thus becomes

$$H = \sum_{k,\sigma} \epsilon_k [A^\dagger_{k,R,\sigma} A_{k,R,\sigma} - A^\dagger_{k,L,\sigma} A_{k,L,\sigma}] + 2V\rho(x=0) + 2J_z \mathbf{S}_z(x=0) S_z + J_{xy}[\psi^\dagger_{R,\uparrow}(0)\psi_{R,\downarrow}(0) S^- + \text{h.c.}] \quad (11.67)$$

where

$$\begin{aligned} \rho(x=0) &= \sum_\sigma (\psi^\dagger_{R,\sigma}(0)\psi_{R,\sigma}(0)) \\ \mathbf{S}_z(x=0) &= \sum_\sigma \frac{1}{2}(\sigma\psi^\dagger_{R,\sigma}(0)\psi_{R,\sigma}(0)) \end{aligned} \quad (11.68)$$

are respectively the charge density and spin density along z. As for standard fermionic problems (see Section 2.3) it is convenient to decouple charge and spin excitations using (2.97). In terms of the charge and spin excitations the various terms in (11.67) are

$$\begin{aligned} \rho(x=0) &= \frac{1}{\pi\sqrt{2}}[\nabla\theta_\rho(x=0) - \nabla\phi_\rho(x=0)] \\ \mathbf{S}_z(x=0) &= \frac{1}{2\pi\sqrt{2}}[\nabla\theta_\sigma(x=0) - \nabla\phi_\sigma(x=0)] \\ &= \frac{1}{\sqrt{2}}\sum_{p>0} e^{-\alpha|p|/2}\left(\frac{p}{2\pi L}\right)^{1/2}[b^\dagger_{\sigma,p} + b_{\sigma,p}] \\ \psi^\dagger_{R,\uparrow}(0)\psi_{R,\downarrow}(0) &= \frac{1}{2\pi\alpha} e^{i\sqrt{2}(\phi_\sigma(x=0) - \theta_\sigma(x=0))} \end{aligned} \quad (11.69)$$

where I have given the expressions both in terms of the ϕ and θ fields and in terms of the b operators. As usual the free fermion part separates in two decoupled sectors of charge and spin excitations (see Chapter 2). Thus, the total Kondo Hamiltonian is the sum of a charge and spin Hamiltonian $H = H_\rho + H_\sigma$. The charge part is

$$H_\rho = H^0_\rho + \frac{V\sqrt{2}}{\pi}[\nabla\theta_\rho(x=0) - \nabla\phi_\rho(x=0)] \quad (11.70)$$

It is the Hamiltonian of a system in presence of a static impurity. It can be diagonalized by the techniques of Section 11.2.1. Since the impurity is static none of the dynamical effects of the X-ray edge problem are present and thus the charge part is essentially trivial. Quite importantly the bosonization formulation shows

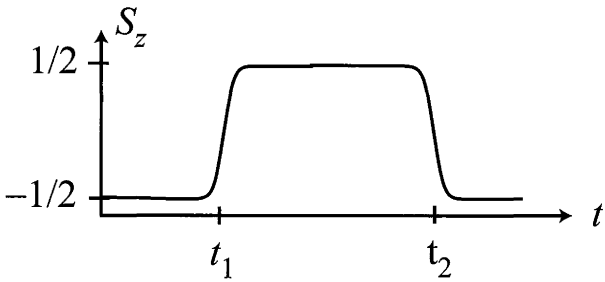

FIG. 11.12. Kondo problem as a succession of X-ray processes. The spin flip term J_{xy} makes the impurity flip between the two states $S_z = \pm 1/2$. Due to the J_z term the conduction electrons see two different local potentials depending on the spin S_z of the impurity. Thus, each time the spin flips there is an X-ray edge like problem where the ground state of the conduction electrons has to readjust to accommodate the new local potential.

immediately that the charge properties decouple completely from the spin properties. This is a result that was established perturbatively by the RG solution, and which is seen without effort in the bosonization. The spin part is non-trivial and given by

$$H = H_\sigma^0 + \frac{J_z S_z}{\pi\sqrt{2}}[\nabla\theta_\sigma(x=0) - \nabla\phi_\sigma(x=0)] + \frac{J_{xy}}{2\pi\alpha}[S^- e^{i\sqrt{2}(\phi_\sigma(x=0)-\theta_\sigma(x=0))} + \text{h.c.}] \quad (11.71)$$

The first line in (11.71) describes an X-ray edge problem. The potential changes as a function of time when the impurity spin S_z changes. In the absence of the J_{xy} term, the spin S_z is conserved and the problem is trivial. This J_{xy} interaction makes the impurity spin change as a function of time and thus starts an X-ray edge singularity. One can view the Kondo problem as a succession of X-ray edge singularities (Anderson *et al.*, 1970). Each time the impurity spin S_z flips, the ground state of the system has to rearrange and tries to become orthogonal to the previous ground state. This orthogonalization is interrupted by a new J_{xy} process. A summary is shown in Fig. 11.12.

The boson representation is again a very powerful way to tackle the Kondo problem. The X-ray part of (11.71) can be solved using the same canonical transformation than for the X-ray problem. Let us introduce

$$W = e^{i\gamma S_z(\phi_\sigma(x=0)-\theta_\sigma(x=0))} \quad (11.72)$$

with

$$\gamma = \frac{J_z}{\sqrt{2}\pi v_F} \quad (11.73)$$

As for the X-ray edge, the Hamiltonian H_z (which is (11.71) with $J_{xy} = 0$) is simply (up to a non-important constant shift of the energies)

$$H_z = W^\dagger H_0 W \tag{11.74}$$

In the absence of J_{xy}, one can easily compute the correlations of the S^+ operators

$$G^{+-}(\tau) = -\langle T_\tau S^+(\tau) S^-(0)\rangle \tag{11.75}$$

where

$$\begin{aligned} S^+(\tau) &= e^{H_z\tau} S^+ e^{-H_z\tau} \\ &= W^\dagger e^{H_0\tau} W S^+ W^\dagger e^{-H_0\tau} W \end{aligned} \tag{11.76}$$

Using (11.76), the correlation function becomes

$$G^{+-}(\tau) = -\langle T_\tau (W S^+ W^\dagger)_0(\tau)(W S^- W^\dagger)_0(0)\rangle \tag{11.77}$$

where the label $_0$ means that the time evolution is computed with the free Hamiltonian H_0. Using the expression for W it is easy to see that

$$W S^+ W^\dagger = e^{i\gamma(\phi(x=0)-\theta(x=0))} S^+ \tag{11.78}$$

The correlation function thus becomes

$$G^{+-}(\tau) = -\langle T_\tau S^+_\tau S^-_{\tau=0} e^{i\gamma(\phi(x=0,\tau)-\theta(x=0,\tau))} e^{-i\gamma(\phi(x=0,\tau=0)-\theta(x=0,\tau=0))}\rangle \tag{11.79}$$

where all time evolutions in (11.79) are computed with the free Hamiltonian H_0. Since in H_0, S_z is conserved, the spin and boson part decouple and the correlation can thus be very easily computed

$$G^{+-}(\tau) = \left(\frac{\alpha}{\tau}\right)^{\left(\frac{J_z}{\sqrt{2}\pi v_F}\right)^2} \tag{11.80}$$

Result (11.80) prompts for various remarks. First we see that this result, which is exact if we start from $J_{xy} = 0$ would also correspond to the fixed point Hamiltonian of the whole ferromagnetic sector of the Kondo problem (replacing J_z by the fixed point value J_z^*). The ferromagnetic Kondó sector thus leads to the non-Fermi liquid behavior (11.80) with non-universal power laws for the correlation functions. It is only for the *isotropic* ferromagnetic Kondo problem ($J_z = J_{xy} < 0$) that the fixed point corresponds to $J_z^* = 0$ and a universal behavior for (11.80) is recovered. In fact, as usual since the operator J is marginal there are logarithmic corrections to this correlation function. We see that the bosonization method, coupled to the renormalization equations allows to fully solve the ferromagnetic Kondo problem. The second remark is the fact that although J_z itself seems to appear in the exponent, one has to keep in mind that

the exponent is in fact the phase shift associated to the potential J_z. This is exactly similar to what we saw for the X-ray edge problem.

Using the solution of the Hamiltonian H_z and the expression (11.71), one can make a perturbation expansion in J_{xy} and treat this perturbation expansion using the same renormalization technique than in Section 2.3.2. It is easy to extract the RG equations directly from the bosonization method

$$\begin{aligned} \frac{\partial \gamma}{dl} &= (\sqrt{2}-\gamma)\frac{J_{xy}^2}{4(\pi v_F)^2} \\ \frac{\partial J_{xy}}{dl} &= [1-\frac{1}{2}(\sqrt{2}-\gamma)^2]J_{xy} \end{aligned} \tag{11.81}$$

It is worth comparing these equations to the ones one got directly in the fermion language (11.64). Contrary to (11.64) that are a *double* expansion in J_z and J_{xy} the equations (11.81) are *exact* in the phase shift γ (associated to J_z), and are perturbative (up to second order) *only* in J_{xy}. Of course, expanding up to first-order in J_z in (11.81) allows to recover exactly (11.64). Since (11.81) are still perturbative in J_{xy} they do not bring much more than (11.64) on the antiferromagnetic side of the Kondo problem. Indeed, both J_{xy} and J_z scale to strong coupling and the perturbative RG equations will stop to be valid at the Kondo energy scale (Kondo temperature). However, using the bosonization expression (11.71) for the Hamiltonian, it is possible to find an exact solution to the Hamiltonian for some specific value of the variables, in a spirit similar to the Luther–Emery solution of Section 4.2. One can thus again couple the RG analysis with the knowledge of an exact solution in the strong coupling regime. This is the method we now examine.

The idea of mapping the antiferromagnetic Kondo Hamiltonian to some exactly solvable problem has a long history (Toulouse, 1969; Wiegmann and Finkelshtein, 1978). The bosonization method provides a very easy way to perform this mapping (Schlottmann, 1978), and this is the derivation I follow here. In (11.71) the following operator appears

$$\psi_\uparrow^\dagger \psi_\downarrow = e^{i\sqrt{2}(\phi_\sigma(x=0)-\theta(x=0))} \tag{11.82}$$

whereas a single-particle creation operator of a spinless fermion would look like

$$\psi_R^\dagger(x=0) \propto U^\dagger e^{i(\phi_\sigma(x=0)-\theta(x=0))} \tag{11.83}$$

If one could change the coefficient in the exponential in (11.82) one could transform the quadratic $\psi^\dagger\psi$ into a single fermion operator. This is analogous to the Luther–Emery case where one transforms a four fermion operator into a two fermion operator (see Section 4.2). Such a modification of the exponent is performed by the canonical transformation (11.72). As can be seen from (11.78), using such a transformation on (11.71) gives

$$WHW^\dagger = H_0 + (2J_z - 2\sqrt{2}\pi\gamma v_F)S_z\mathbf{S}_z + \frac{J_{xy}}{\pi\alpha}[S^+ e^{-i(\sqrt{2}-\gamma)(\phi_\sigma-\theta_\sigma)} + \text{h.c.}] \tag{11.84}$$

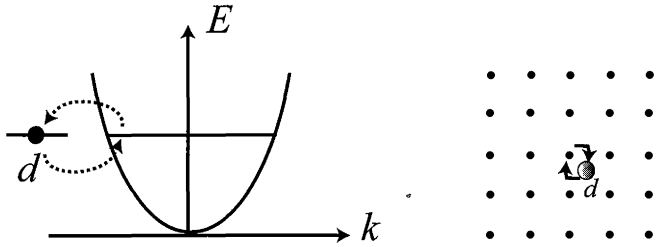

FIG. 11.13. Resonant level model. A conduction band of electrons (denoted c) can hybridize with a localized impurity denoted d. For a special value of the coupling J_z the spin part of the Kondo model can be mapped on this free electron problem.

If one chooses a $\gamma = \sqrt{2} - 1$ such that the exponential factor is simply the one of a single fermion operator, the J_{xy} part of the Hamiltonian now becomes trivial to solve in fermion language. The impurity spin can be mapped on a fermion operator

$$\begin{aligned} S_z &= d^\dagger d - \frac{1}{2} \\ S^+ U &= d^\dagger \end{aligned} \tag{11.85}$$

The Klein factor U ensures that $d^\dagger$ is a true fermionic operator (remember that S^+ has commutation relations). It is easy to check that the standard spin commutation relations are satisfied by (11.85). In terms of these variables the Hamiltonian becomes

$$\tilde{H} = H_0 + [\sqrt{2}J_z - 2\pi\gamma v_F]\rho_{sp,R}(x=0)(d^\dagger d - \frac{1}{2}) + \frac{J_{xy}}{\sqrt{2\pi\alpha}}[d^\dagger \psi_{sp,R}(x=0) + \text{h.c.}] \tag{11.86}$$

where sp designates some fictitious spinless fermionic field, denoted c in what follows, that is, the refermionization of the boson operators. I have also used that the boson field

$$\rho_{sp,R}(x=0) = \frac{1}{2\pi}(\nabla\theta - \nabla\phi) \tag{11.87}$$

is simply the density of right movers of the spinless fermionic field.

Hamiltonian (11.86) describes a resonant level model (see Fig. 11.13), where a localized level can hybridize with a conduction band. The localized level interacts with the conduction band through the density term. The hybridization is controlled by J_{xy}, whereas the interaction is controlled by J_z

$$\begin{aligned} t_{cd} &= \frac{J_{xy}}{2\sqrt{\pi\alpha}} \\ U_{cd} &= \frac{J_z}{\sqrt{2}} - v_F\pi(\sqrt{2}-1) \end{aligned} \tag{11.88}$$

In the absence of interaction between the localized state and the conduction band the fermionic Hamiltonian is trivial to solve since it is quadratic (Mahan, 1981). To get $U_{cd} = 0$ one needs to choose a special value for J_z

$$\frac{J_z^*}{\pi v_F} = \sqrt{2}(\sqrt{2} - 1) \tag{11.89}$$

which can be realized only for antiferromagnetic coupling. This special value of J_z is known as the Toulouse line. For this special value of J_z (in fact of the phase shift δ_z) the Kondo problem can thus be solved 'exactly'. As for the Luther–Emery solution of Chapter 2, coupling this exact solution for a special value of J_z with the RG equations allows to obtain the physical behavior in the whole antiferromagnetic regime. One starts from the bare couplings, renormalizes up to the point where $J_z(l) = J_z^*$ and at that point uses the exact solution. One thus recovers that the physics of the strong coupling Kondo problem corresponds to free fermionic excitations (the Hamiltonian of the fictitious spinless fermions is quadratic). This of course allows to compute simply most physical properties. For example the $\langle S^+ S^- \rangle$ spin–spin correlation is simply the single-particle Green's function of the d fermions.

$$G_{dd}(i\omega_n) = \frac{1}{i\omega_n - \Sigma(i\omega_n)} \tag{11.90}$$

where the self-energy is

$$\Sigma(i\omega_n) = \frac{t_{cd}^2}{L} \sum_k G_{cc}(i\omega_n, k) \tag{11.91}$$

The analytical continuation is easy to do and one gets

$$G_{dd}(\omega + i\delta) = \frac{1}{\omega + i\pi t_{cd}^2 N(0)} \tag{11.92}$$

This resonance indicates that the impurity correlation decays with time as $e^{-|t|/\tau_l}$ with $\tau_l^{-1} = \pi t_{cd}^2 N(0)$ as a consequence of the hybridization with the c electrons.

Let me make two remarks. The first one is that the trick works both ways and the knowledge of the Kondo problem can also be used to solve the interacting resonant level model, which is not trivial when $U_{cd} \neq 0$ (Giamarchi *et al.*, 1993). For example if one starts from such a model, an attractive interaction larger than $U_c = -v_F \pi(\sqrt{2} - 1)$ would correspond in the Kondo language to a negative J_z. In that case we know that the system renormalizes to the ferromagnetic fixed point (provided that the hybridization $t_{cd} \propto J_{xy}$ is small enough). Since

$$\langle S^+(\tau) S^- \rangle = \langle d^\dagger(\tau) d \rangle \tag{11.93}$$

the impurity correlation has a non Fermi liquid behavior (see (11.44))

$$\langle d^\dagger(\tau)d\rangle \propto \left(\frac{1}{\tau}\right)^\nu \tag{11.94}$$

There are of course many more physical quantities that can be extracted and I refer the reader to the literature to get more details. The second remark concerns the transformation itself. One might wonder why not simplify even more the Hamiltonian (11.71) by choosing a γ that would *completely* suppress the exponential. This is realized for

$$\gamma = \sqrt{2} \tag{11.95}$$

The Kondo model would then simply become

$$\tilde{H} = H_0 + [\sqrt{2}J_z - 2\pi\gamma v_F]\rho_{sp,R}(x=0)S_z + \frac{J_{xy}}{\sqrt{2\pi\alpha}}[S^+ + S^-] \tag{11.96}$$

This is the resonant tunneling model (Caldeira and Leggett, 1983). Since all dynamics has disappeared from the J_{xy} term it is clear that this model cannot be equivalent to the Kondo problem. There is thus a mistake in the mapping between the two models. The problem comes from the fact that in such transformations $\gamma = \delta/\pi$ where δ should in fact be a phase shift, since it ultimately appears in front of the density in the Hamiltonian. The value (11.95) would be unphysical since it would correspond to a phase shift larger than π. On the other hand the value $\gamma = \sqrt{2} - 1$ is within the allowed values for a phase shift, and the mapping to the resonant level model is valid. This limitation in playing with the transformations has to be kept in mind to obtain physical results.

11.2.3 *Multichannel Kondo problem*

Let us finally move to a more complicated, and physically different version of the Kondo problem, the so-called multichannel Kondo problem (Nozieres and Blandin, 1980). This model is particularly interesting theoretically since it exhibits a non-trivial non-Fermi liquid behavior. In view of the recent applications of impurity problems to quantum dots, it is also of practical importance experimentally. Let us assume that the impurity spin is now coupled to fermions that can carry a flavor index

$$H = \sum_i H_i^{\text{kin}} + J\sum_i \vec{\mathbf{S}}_i \cdot \vec{S} \tag{11.97}$$

where i is the flavor index and as before $\mathbf{S}_i$ is the spin at the origin due to the electrons of flavor i and S the spin of the impurity. For simplicity, I stick in what follows to the case of two fermion species (two-channel Kondo problem). A larger number of flavors would not change the salient points of the solution. I have not written the potential term, which as for the normal Kondo problem, does not play any role. The modification due to the presence of different species of fermions might seem minor but has a profound effect on the physics. The perturbative

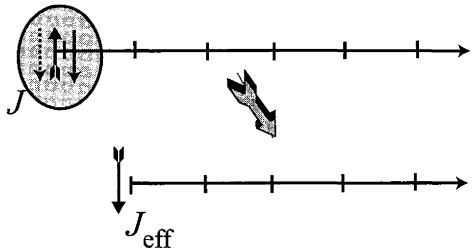

FIG. 11.14. In a two-channel Kondo problem the strong coupling is unstable. Indeed, for a large J the impurity (represented by an arrow) binds two electrons of different flavor (represented by solid and dashed lines) on the impurity site. The impurity site thus becomes equivalent to an effective spin 1/2. Due to the hopping of the conduction electrons in an out of the site, this effective spin has a weak residual antiferromagnetic coupling with the other sites. This weak coupling is a relevant perturbation. Since both the weak coupling and strong coupling fixed points are unstable the two-channel Kondo problem corresponds to some intermediate coupling fixed point, which makes it quite hard to solve and leads to a very rich physics.

RG equations are essentially identical to the ones of the single channel Kondo problem (sticking here to the spin isotropic case)

$$\frac{d\tilde{J}}{dl} = \tilde{J}^2 - \tilde{J}^3 + \cdots \tag{11.98}$$

So J grows on the antiferromagnetic side. The question is thus whether it goes to infinity as for the single channel Kondo problem or whether some intermediate coupling fixed point is now physical. The answer can be guessed by looking at the limit of J very large. In that case *two* electrons (one for each species) go on the impurity site and lock antiferromagnetically with the impurity spin. The resulting total spin on the impurity site is thus a spin 1/2 again instead of the spin $S = 0$ for the single channel Kondo problem. Second-order perturbation theory in the kinetic energy easily shows that the coupling between this effective spin and the neighboring sites is antiferromagnetic. One is thus back to the original situation of the two-channel Kondo but this time with a weak effective coupling $J_{\text{eff}} \sim E_{\text{kin}}^2/J$ between the effective spin and the rest of the conduction electrons. This is summarized in Fig. 11.14. Since one has an effective two-channel Kondo problem the coupling of this problem grows under RG following (11.98). The strong coupling fixed point is thus *unstable* and the most natural conclusion is that, contrary to the case of the single channel problem, an intermediate fixed point now exists. Of course, this complicates enormously the solution of the two-channel Kondo problem. Here again numerical RG and exact solutions are of help in understanding the physics of this fixed point.

I will again take the simple path of bosonization to tackle the problem. The method is similar to the one we use in the previous section for the standard Kondo problem. For each flavor one introduces the charge and spin bosons

$$\phi_{i,c,s} = \frac{1}{\sqrt{2}}[\phi_{i,\uparrow} \pm \phi_{i,\downarrow}] \tag{11.99}$$

where the upper sign is for the charge and the lower sign for the spin sector. In terms of these modes the Hamiltonian (11.97) becomes (I have removed the charge part that is again trivial and totally decouples as for the single channel Kondo problem)

$$\begin{aligned} H = H_{1,\sigma} + H_{2,\sigma} + \frac{J_z}{\sqrt{2}\pi}[(\nabla\theta - \nabla\phi)_1(x=0) + (\nabla\theta - \nabla\phi)_2(x=0)]S_z \\ + \frac{J_{xy}}{2\pi\alpha}[S^+ e^{-i\sqrt{2}[\phi-\theta]_1(x=0)} + S^+ e^{-i\sqrt{2}[\phi-\theta]_2(x=0)} + \text{h.c.}] \end{aligned} \tag{11.100}$$

Using again the standard renormalization techniques for the boson Hamiltonian one can recover the RG equations, but as for the Kondo problem this will bring very little since the fixed point is at intermediate coupling. Let us instead use the same trick than the one that worked so well for the Kondo problem (Emery and Kivelson, 1992). We introduce the symmetric and antisymmetric fields

$$\phi_{S,A} = \frac{1}{\sqrt{2}}[\phi_{1,\sigma} \pm \phi_{2,\sigma}] \tag{11.101}$$

and a similar relation for θ. The S and A fields commute. Let us use the chiral field $\phi_R = \theta - \phi$ (3.57). The two-channel Kondo Hamiltonian can be rewritten as

$$\begin{aligned} H = H_{0,S} + H_{0,A} + \frac{J_z}{\pi} S_z \nabla\phi_{R,S}(x=0) \\ + \frac{J_{xy}}{\pi\alpha}[S^+ e^{i\phi_{R,S}(x=0)} \cos(\phi_{R,A}(x=0)) + \text{h.c.}] \end{aligned} \tag{11.102}$$

where $H_{S,A}$ are the standard quadratic boson Hamiltonians (3.25) (with $K = 1$). The idea is now to eliminate the $\phi_{R,S}$ field in the exponentials to recover simple fermionic operators when refermionizing the $\phi_{R,A}$ part. We thus introduce the canonical transformation

$$W = e^{-i\phi_{R,S}(x=0)S_z} \tag{11.103}$$

The new Hamiltonian $\tilde{H} = WHW^\dagger$ is

$$\begin{aligned} \tilde{H} = H_{0,S} + H_{0,A} + (\frac{J_z}{\pi} - 4v_F)S_z \nabla\phi_{R,S}(x=0) \\ + \frac{J_{xy}}{\pi\alpha}[S^+ \cos(\phi_{R,A}(x=0)) + \text{h.c.}] \end{aligned} \tag{11.104}$$

As for Kondo, we introduce the fictitious spinless fermion

$$\psi_R(x) = \frac{U}{\sqrt{2\pi\alpha}} e^{-i(\phi_A - \theta_A)} \tag{11.105}$$

and the mapping of the impurity spin on the Abrikosov fermions $S^+ \to d^\dagger$ (incorporating again the Klein factor). As before we can get rid of the unpleasant density term in (11.104) by taking the special value of the parameter (Emery–Kivelson line)

$$J_z^* = 4\pi v_F \tag{11.106}$$

The Hamiltonian becomes

$$\tilde{H} = H_S + H_A + \frac{\sqrt{2}J_{xy}}{\sqrt{\pi\alpha}}[(d^\dagger - d)(\psi_R^\dagger(x=0) + \psi_R(x=0))] \tag{11.107}$$

Two remarkable things occur in (11.107). First, the symmetric bosonic degrees of freedom completely decouple. Secondly, the impurity only couples to the *real* part of the fermionic operator $\psi^\dagger + \psi$. It is as if the conduction electrons were hybridizing with only 'half' of the impurity (compare with (11.86)). Since the hybridization was what led to the Fermi liquid behavior for the standard Kondo problem we see that the behavior of the two-channel Kondo problem will be radically different.

To compute the correlation functions let us introduce the Majorana (real) fermions

$$\begin{aligned} a &= \frac{d + d^\dagger}{\sqrt{2}} \\ b &= \frac{d^\dagger - d}{i\sqrt{2}} \end{aligned} \tag{11.108}$$

The correlation function of the d electrons can thus be written as

$$\langle d(\tau)d^\dagger\rangle = \langle a(\tau)a\rangle + \langle b(\tau)b\rangle \tag{11.109}$$

Since the a fermions do not couple at all in the Hamiltonian (11.107) their spectral function is simply $\delta(\omega)$ (see (11.90), with $\Sigma = 0$ since there is no hybridization for the a fermions), whereas the b fermions have a spectral function similar to the one of the single-channel Kondo problem (11.90). The spectral function of the impurity spin is thus of the form

$$A(\omega) \propto \delta(\omega) + \frac{\Gamma}{\omega^2 + \Gamma^2} \tag{11.110}$$

which again shows that only 'half' of the impurity spin couples to the conduction electrons. This can be understood from Fig. 11.14 by seeing that every time the conduction electrons tries to screen the spin of the impurity, this leaves a spin

1/2 on the impurity site, which then starts a new Kondo effect and thus a new tentative of screening. It is as if 'half' of the impurity spin could survive this screening process. This has several consequences that can be directly computed from (11.107). First, there is a residual entropy $\log(2)/2$ in the ground state, consequence of this fact. This clearly shows that the two-channel Kondo problem is not a Fermi liquid. Secondly, the presence of the $\delta(\omega)$ part creates some singularities in the correlation functions. Let me illustrate this on the simple example of the transverse impurity spin susceptibility. Using

$$\tilde{S}^- = WS^-W^\dagger = \sqrt{2\pi\alpha}\psi_{R,S}(x=0)Ud \tag{11.111}$$

where U is again a Klein factor for the fermion. $\psi_{R,S}$ is a free fermion operator since the field $\phi_{R,S}$ does not appear any more in the coupling with the impurity. We thus have

$$\begin{aligned}\chi^{-+}(\tau) &= \langle S^-(\tau)S^+(0)\rangle_H \\ &= \langle \tilde{S}^-(\tau)\tilde{S}^+(0)\rangle_{\tilde{H}} \\ &= 2\pi\alpha\langle\psi_{R,S}(0,\tau)\psi^\dagger_{R,S}(0,0)\rangle\langle d(\tau)d^\dagger(0)\rangle\end{aligned} \tag{11.112}$$

the final line coming from the fact that the d fermion and the $\psi_{R,S}$ fermion are non-interacting on the Emery-Kivelson line. As seen from (11.110), the propagator of d fermions has a piece that is free ($\delta(\omega)$ in the spectral function). This free part dominates the large-τ behavior of $\chi^{-+}(\tau)$. We therefore have

$$\chi^{-+}(\tau) \simeq 2\pi\alpha\{\theta(\tau)\langle\psi_{R,S}(0,\tau)\psi^\dagger_{R,S}(0,0)\rangle + \theta(-\tau)\langle\psi^\dagger_{R,S}(0,0)\psi_{R,S}(0,\tau)\rangle\} \tag{11.113}$$

Note the crucial sign change, central to Kondo-type problems, of $\chi^{-+}(\tau)$ relative to $\langle T_\tau\psi_{R,S}(0,\tau)\psi^\dagger_{R,S}(0,0)\rangle$. This is due to the fact that the d are fermion operators even if they do not introduce here any time dependence in the correlation function. The transverse susceptibility becomes

$$\chi^{-+}(\omega,T) \sim -\alpha\int_{-1/\alpha}^{1/\alpha} dk\,\frac{\tanh\frac{uk}{2T}}{\omega - uk + i\delta} \tag{11.114}$$

where as usual $1/\alpha$ mimics a bandwidth cutoff. Thus, the static transverse impurity susceptibility is

$$\chi^{-+}(\omega=0,T) = \frac{2\alpha}{u}\log\frac{u}{\alpha T} \tag{11.115}$$

and has a logarithmic divergence. Another signature that the state is not a Fermi liquid state. This logarithmic divergence can be thought of simply in the following way: on the Emery-Kivelson line the canonical transformation removes all coupling to S_z *and* 'attaches' a fermion to the spin flip operators. As a result the $S_z = \frac{1}{2}$ and $S_z = -\frac{1}{2}$ ground states are *orthogonal* in the sense that they

are not connected by the spin flip operators. This removes the Curie divergence (which is the direct result of $S_z = \frac{1}{2}$ and $S_z = -\frac{1}{2}$ ground states being connected by a spin flip), replacing it by a weaker logarithmic one. There are many more interesting properties of the two (and higher) channel Kondo problem and I refer the reader to the literature (Glazman and Raikh, 1988; Affleck, 1995; Affleck and Ludwig, 1991; Eggert and Affleck, 1992; Clarke *et al.*, 1993; Sengupta and Georges, 1994; Eggert *et al.*, 2001).

APPENDIX A

BASICS OF MANY-BODY

In this appendix, I fix some of the notations and I recall the basics of many-body theory. This is merely to fix the notations for some formulas used in the rest of the book. These few pages do not pretend to be an introduction to many-body and diagrammatic theory and I refer the reader to Mahan (1981) for such a complete description.

A.1 Notations and formulas

I denote $Y(x)$ the Heaviside step function[39]

$$\begin{aligned} Y(x) &= 1, \quad x > 0 \\ Y(x) &= 0, \quad x < 0 \end{aligned} \tag{A.1}$$

Space is denoted x, real time t, imaginary time τ. The coordinates in space–time (imaginary) are denoted

$$r = (x, u\tau) \equiv (x, y_\alpha) \tag{A.2}$$

In presence of a small cutoff α the imaginary time can be regularized as

$$y_\alpha = u\tau + \alpha \,\mathrm{Sign}(\tau) \tag{A.3}$$

where u is a velocity. In the same way $\mathbf{q}$ denotes

$$\mathbf{q} = (k, \omega_n/u) \tag{A.4}$$

This will be used in Fourier transforms. I denote

$$\mathbf{q}r = kx - \omega_n\tau \tag{A.5}$$

For bosons $f_B(\xi)$ is the Bose factor

$$f_B(\xi) = \frac{1}{e^{\beta\xi} - 1} \tag{A.6}$$

where $\beta = 1/(k_B T)$ is the inverse of the temperature. $f_F(\xi)$ is the Fermi factor

$$f_F(\xi) = \frac{1}{e^{\beta\xi} + 1} \tag{A.7}$$

[39] Normally, I prefer to call the Heaviside function θ but this would be rather confusing, since θ is heavily used for another quantity.

We will use repeatedly the following useful formulas. For two matrices A and B that commute with their commutator $[A, B]$ one has

$$e^A e^B = e^{A+B} e^{\frac{1}{2}[A,B]} \tag{A.8}$$

and

$$[A, f(B)] = [A, B] f'(B) \tag{A.9}$$

where f is any function and f' the derivative of f. Other useful relations are

$$\begin{aligned} [AB, CD] &= A[B, CD] + [A, CD]B \\ [A, BC] &= [A, B]_+ C - B[A, C]_+ \end{aligned} \tag{A.10}$$

A.2 Digest of many-body

For a many-body system of fermions or bosons the antisymmetrisation or symmetrization of the many-body wave function can be automatically ensured by going to the Fock space. Given a complete basis of one-body states $|\alpha)$ (generally either the positions or the momentum), one introduces a vacuum $|\phi\rangle$. On this vacuum operate operators $c_\alpha^\dagger$ and c_α which create and destroy particles in the state α. For example, one has

$$c_\alpha^\dagger |\phi\rangle = |\alpha) \tag{A.11}$$

To ensure the proper symmetry of the total wavefunction the operators c should commute for bosons and anticommute for fermions. So for bosons:

$$\begin{aligned} [c_\alpha, c_\beta] &= [c_\alpha^\dagger, c_\beta^\dagger] = 0 \\ [c_\alpha, c_\beta^\dagger] &= \delta_{\alpha,\beta} \end{aligned} \tag{A.12}$$

with $[A, B] = AB - BA$. For fermions one has identical formulas with the commutator replaced by the anticommutator $[A, B]_+ = AB + BA$. The anticommutation of fermion operators ensures in particular that the Pauli principle is satisfied since $c_\alpha^\dagger c_\alpha^\dagger = 0$.

Useful formulas allow to write totally symmetric one- and two-body operators in the Fock space. If $A^{(1)}$ is a one-body operator and $A_i^{(1)}$ the corresponding operator acting on the ith particle, the operator $A = \sum_i A_i$ can be written in second quantization as

$$A = \sum_{\alpha,\beta} (\alpha|A^{(1)}|\beta) c_\alpha^\dagger c_\beta \tag{A.13}$$

where α, β span a complete basis of the one-body Hilbert space. For example, the total density $\rho(x)$ at point x can be expressed in terms of the one-body density $|x\rangle\langle x|$ as

$$\rho(x) = \sum_{\alpha,\beta} (\alpha|x)(x|\beta) c_\alpha^\dagger c_\beta$$

If one chooses for the complete basis the position basis $|\alpha) = |x)$ then

$$\rho(x) = c_x^\dagger c_x \tag{A.14}$$

where c_x destroys a particle at point x[40] One can also chose the basis of eigenstates of momentum $|\alpha) = |k)$, where

$$(x|k) = \frac{1}{\sqrt{\Omega}} e^{+ikx} \tag{A.15}$$

are the plane waves, suitably normalized for a volume Ω. In that case the density operator takes the form

$$\rho(x) = \sum_{k,k'} \frac{1}{\Omega} e^{i(k-k')x} c_{k'}^\dagger c_k = \sum_{k,q} \frac{1}{\Omega} e^{-iqx} c_{k+q}^\dagger c_k \tag{A.16}$$

and c_k destroys a particle of wavevector k.

Similarly, a symmetric sum over two-body interactions $V_{ij}^{(2)}$ coupling the particles i and j can be written in Fock space as

$$V = \frac{1}{2} \sum_{i,j} V_{ij}^{(2)} = \frac{1}{2} \sum_{\alpha\beta\gamma\delta} (\alpha\beta|V^{(2)}|\gamma\delta) c_\alpha^\dagger c_\beta^\dagger c_\delta c_\gamma \tag{A.17}$$

where in $(\alpha\beta|V^{(2)}|\gamma\delta)$ terms like $|\gamma, \delta)$ denote a wavefunction (non-antisymmetrized) where the first particle is in the state γ and the second one in the state δ. Similarly, for $(\alpha\beta|$ the first particle is in the state α and the second one in the state β. For example, an interaction such as the Coulomb interaction, which depends only on the positions of the particles $V_{ij}^{(2)} = V(R_i - R_j)$, becomes

$$V = \frac{1}{2} \int d^d x \, d^d x' \, V(x - x') \, c_x^\dagger c_{x'}^\dagger c_{x'} c_x \tag{A.18}$$

Note that the form (A.18) reduces to the standard form

$$V = \frac{1}{2} \int d^d x \, d^d x' \, V(x - x') \, \rho(x) \rho(x') \tag{A.19}$$

up to chemical potential terms coming from the (anti-) commutation of c_x and $c_{x'}^\dagger$. In momentum space the interaction becomes

$$V = \frac{1}{2\Omega} \sum_{k,k',q} V(q) c_{k+q}^\dagger c_{k'-q}^\dagger c_{k'} c_k \tag{A.20}$$

where $V(q)$ is the Fourier transform of the potential $V(x)$. Note that since $V(x)$ is real and symmetric (the particles are undiscernible) $V(x) = V(-x)$, one has $V(q) = V(-q)$. I take for the Fourier transform the convention

[40] very often noted in the literature $\psi(x)$ for some mysterious reason.

$$V(k) = \int d^d x \, e^{-ikx} V(x)$$
$$V(x) = \frac{1}{\Omega} \sum_k e^{ikx} V(k) \tag{A.21}$$

In the limit of infinite volume

$$\frac{1}{\Omega} \sum_k \to \int \frac{d^d k}{(2\pi)^d} \tag{A.22}$$

One can rewrite the interaction in the form (up to chemical potential terms)

$$V = \frac{1}{2\Omega} \sum_q V(q)\rho(q)\rho(-q) \tag{A.23}$$

Let us now turn to the time dependence of the various quantities. To compute physical quantities at different times I introduce the Heisenberg representation of the operator A

$$A(t) = e^{iHt} A e^{-iHt} \tag{A.24}$$

It is also convenient to define the evolution in imaginary time τ, where $\tau \in [0, \beta]$

$$A(\tau) = e^{\tau H} A e^{-\tau H} \tag{A.25}$$

At finite temperature the average value of a given operator is given by

$$\langle A \rangle = \frac{\mathrm{Tr}[e^{-\beta K} A]}{\mathrm{Tr}[e^{-\beta K}]} \tag{A.26}$$

where $K = H - \mu N$ and N is the number of particles. For a general Hamiltonian H, it is usually quite complicated to compute physical correlations at different times. To define correlation functions that can be easily computed in perturbation theory or that have a well-defined representation in terms of functional integrals (see Appendix C) one introduces the time ordering operator T_τ. It orders the operators such that they are written from right to left in order of increasing time. For fermions there is an overall plus or minus sign that corresponds to the signature of the permutation (that is, plus for an even number of inversions and minus for an odd number of inversions) between the initial order and the order as a function of the time. For example, for two operators

$$T_\tau(A(\tau_1)B(\tau_2)) = Y(\tau_1 - \tau_2)A(\tau_1)B(\tau_2) + \epsilon Y(\tau_2 - \tau_1)B(\tau_2)A(\tau_1) \tag{A.27}$$

where $Y(z)$ is the step function (A.1). $\epsilon = 1$ if A and B are boson-like operators (that is, either made of bosonic operators or of an even number of fermionic ones) and $\epsilon = -1$ if A and B are fermion-like operators (that is, made of an odd

number of fermions ones). One defines the so-called time-ordered correlation functions (in imaginary time) as

$$G_{AB}(\tau) = -\langle T_\tau A(\tau) B(0)\rangle \tag{A.28}$$

Of special interest is the single-particle Green's function, which can be written in k space for translationally invariant systems as

$$G(k,\tau) = -\langle T_\tau c_k(\tau) c_k^\dagger(0)\rangle \tag{A.29}$$

For bosons (resp. fermions) these Green's functions are periodic (reps. antiperiodic) functions of τ on the period β. They are thus conveniently represented in frequency by a Fourier series

$$\begin{aligned} G(i\omega_n) &= \int_0^\beta d\tau\, G(\tau) e^{i\omega_n \tau} \\ G(\tau) &= \frac{1}{\beta}\sum_n G(i\omega_n) e^{-i\omega_n \tau} \end{aligned} \tag{A.30}$$

the notation $i\omega_n$ is historic and is to remind that the correlation functions were computed with the evolution in imaginary time τ. Because of the periodicity or antiperiodicity the frequencies are discrete. These frequencies, known as Matsubara frequencies, take the values $\omega_n = 2\pi n/\beta$ for bosons and $\omega_n = (2n+1)\pi/\beta$ for fermions, where n is an integer.

For free fermions or bosons with an energy $H = \sum_k \epsilon(k) c_k^\dagger c_k$ the single-particle Green's function is

$$G(i\omega_n, k) = \frac{1}{i\omega_n - \xi(k)} \tag{A.31}$$

where $\xi(k) = \epsilon(k) - \mu$, μ being the chemical potential.

Time-ordered Greens function can be easily computed in perturbation theory (Feynmann diagrams), or have a nice expression in terms of a functional integral (see Appendix C). Unfortunately, they do not represent direct physical objects. The physical correlations are the ones that measure the response of the system to a perturbation added to the Hamiltonian. Let us assume that in presence of such a perturbation the Hamiltonian H becomes

$$H_p = H + \int d^d x\, h(x,t) B(x) \tag{A.32}$$

where $h(x,t)$ is some external field, (real) time and space dependent. The linear response of the system to such a perturbation is given by

$$\langle A(x,t)\rangle_{H_p} = \langle A(x,t)\rangle_H + \int d^d x'\, dt'\, \chi(x-x', t-t') h(x',t') \tag{A.33}$$

plus higher powers of h. The 'susceptibility' χ is given by the so-called retarded correlation function

$$\chi(x-x',t-t') = -iY(t-t')\langle[A(x,t),B(x',t')]_{\mp}\rangle_H \tag{A.34}$$

where the upper sign (commutator) is for bosons and the lower (anticommutator) is for fermion-like operators.

The correlation functions that directly measure the physical response are thus the retarded ones. The step function ensures that causality is obeyed. To shorten the notation I denote them as

$$\chi(x-x',t-t') \equiv \langle A(x,t);B(x',t')\rangle_{\text{ret}} \tag{A.35}$$

These retarded correlation functions have no simple perturbative expansion. Fortunately, their Fourier transform is simply related to the time-ordered correlations. I define

$$\chi_{\text{ret}}(\omega) = \int dt\, e^{i\omega t}\chi_{\text{ret}}(t) \tag{A.36}$$

note that because of the factor $Y(t)$ the integral in fact goes only from $t=0$ to $t=\infty$. Thus, it can be regularized by adding a small imaginary part to the frequency. ω is in fact $\omega+i\delta$ with $\delta=0^+$. This small imaginary part comes from the fact that the perturbation is applied adiabatically from $t=-\infty$, and thus a factor $e^{-\delta|t|}$ is in fact hidden in $h(t)$. The relation between the retarded and the time-ordered correlation function is a simple analytic continuation

$$\chi_{\text{ret}}(\omega) = \chi(i\omega_n \to \omega+i\delta) \tag{A.37}$$

Let us look at some examples. The retarded single-particle Green's function for free particles is simply (from (A.31))

$$G(k,\omega) = \frac{1}{\omega-\xi(k)+i\delta} \tag{A.38}$$

Quite generally the imaginary part of the single-particle Green's function is the spectral function

$$A(k,\omega) = \frac{-1}{\pi}\text{Im}\, G(k,\omega) \tag{A.39}$$

which gives the probability of finding an excitation with momentum k and energy ω. For free particles one thus recovers from (A.38)

$$A(k,\omega) = \delta(\omega-\xi(k)) \tag{A.40}$$

Another interesting quantity is the occupation factor $n(k)$. It is simply given by

$$n(k) = \int dx\, e^{-ikx}G(x,\tau=0^-) \tag{A.41}$$

as can be easily seen by using the definition of G in terms of the $c_k^\dagger$ and c_k.

APPENDIX B

NOT SO IMPORTANT FINE TECHNICAL POINTS

B.1 Explicit form of U operators

Let me give an explicit form for the operators U_r. I follow Haldane (1981*a*) and define the states with a given number of (right and left) fermions $|N_+, N_-\rangle$ by

$$c^\dagger_{r,k} c_{r,k} |N_+, N_-\rangle = \theta(k_F + 2\pi \mathcal{N}_r/L - rk)|N_+, N_-\rangle \tag{B.1}$$

in doing so periodic conditions on a segment of size L are assumed so that k is quantized as $k = 2\pi n/L$ and the Fermi level lies in the middle of two values of k so that k_F is of the form $k_F = \pi(2n_0 + 1)/L$. I denote by $\mathcal{N}_r$ the number of electrons (eigenvalues) to distinguish them from the operator N_r (see (2.8))

$$N_r|N_+, N_-\rangle = \mathcal{N}_r|N_+, N_-\rangle \tag{B.2}$$

$\mathcal{N}_r = 0$ corresponds to the Dirac sea filled up to the Fermi level. Changing $\mathcal{N}_r$ corresponds to creating electrons or holes on the branch r relative to this ground state. The operators U_r should obey

$$\begin{aligned} U^\dagger_+|N_+, N_-\rangle &= |N_+ + 1, N_-\rangle \\ U^\dagger_-|N_+, N_-\rangle &= |N_+, N_- + 1\rangle \end{aligned} \tag{B.3}$$

and they should commute with the boson operators to be useful. In order to create a charge uniformly and to obey the above relations we could use

$$U^\dagger_r = \frac{1}{\sqrt{L}} \int_0^L dx\ \psi^\dagger_r(x) e^{ir(k_F + \frac{\pi(2N_r+1)}{L})x} \tag{B.4}$$

which simply created a particle with the lowest available momentum. However, this expression does not commute with the boson operators so it is useless. However, an expression that does commute with the boson operators is

$$U^\dagger_r = \frac{1}{\sqrt{L}} \int_0^L dx\ e^{irk_F x} e^{-i\phi^\dagger_r(x)} \psi^\dagger_r(x) e^{-i\phi_r(x)} \tag{B.5}$$

with

$$\phi_r(x) = -\frac{\pi r x}{L} N_r + \lim_{\epsilon \to 0} i \sum_{p \neq 0} \left(\frac{2\pi}{L|p|} \right)^{1/2} e^{-L\epsilon|p|/(2\pi)} Y(rp) b_p e^{ipx} \tag{B.6}$$

$\phi_r(x)$ are the chiral fields whose commutation relations with the bosons are

$$[\rho_r^\dagger(p), e^{-i\phi_{r'}(x)}] = -\delta_{r,r'} Y(rp)(1-\delta_{p,0}) e^{ipx} e^{-i\phi_r(x)}$$
$$[\rho_r^\dagger(p), e^{-i\phi_{r'}^\dagger(x)}] = -\delta_{r,r'} Y(-rp)(1-\delta_{p,0}) e^{ipx} e^{-i\phi_r^\dagger(x)} \tag{B.7}$$

In addition, the only part of the field $\phi_r(x)$ that does not destroy the state $|N_+, N_-\rangle$ is the term with N_r. Simply expanding to all orders the term $e^{-i\phi_r^\dagger(x)}$ gives

$$\begin{aligned} U_r^\dagger |N_+, N_-\rangle &= \frac{1}{L} \sum_{k,n_p} \int_0^L dx\, e^{ir(k_F + \frac{\pi(2\mathcal{N}_r+1)}{L} - rk)x} \\ &\quad \prod_{rp>0} (-1)^{n_p} \frac{(b_p^\dagger)^{n_p}}{n_p!} e^{-ipn_p x} a_{rk}^\dagger |N_+, N_-\rangle \\ &= \sum_{k,n_p} \delta_{k,r[k_F + \frac{\pi(2\mathcal{N}_r+1)}{L} - \sum_{rp>0} |p| n_p]} \prod_{rp>0} (-1)^{n_p} \frac{(b_p^\dagger)^{n_p}}{n_p!} a_{rk}^\dagger |N_+, N_-\rangle \\ &= a^\dagger_{r,r[k_F + \frac{\pi(2\mathcal{N}_r+1)}{L}]} |N_+, N_-\rangle \end{aligned} \tag{B.8}$$

which indeed adds a fermion on the top of the Fermi (Dirac) sea. This completes the proof that (B.5) is indeed the correct operator.

The relation (B.5) giving the operator $U^\dagger$ in terms of the fermion creation operator can easily be inverted giving the fermion creation operator on the basis of the boson excitations and the operators U:

$$\begin{aligned} \psi_r^\dagger(x) &= \frac{1}{\sqrt{L}} e^{-irk_F x} e^{i\phi_r^\dagger(x)} U_r^\dagger e^{i\phi_r(x)} \\ &= \lim_{\epsilon \to 0} \frac{1}{\sqrt{2\epsilon L}} e^{-ir(k_F - \pi/L)x} e^{i\phi_r^\dagger(x) + i\phi_r(x)} U_r^\dagger \end{aligned} \tag{B.9}$$

In the same way, the Hamiltonian should take into account the presence of states with different fermion numbers in addition to the bosonic excitations described by (2.16) and (2.17). Let us look at right movers. Adding $\mathcal{N}_+$ fermions on the top of the Dirac sea adds an energy

$$\sum_{p=1}^{\mathcal{N}_+} v_F(2p-1) = v_F \frac{\pi}{L} \mathcal{N}_+^2 \tag{B.10}$$

using (2.1). Adding a similar contribution from the other branch and the boson contribution leads to the full Hamiltonian (2.22).

B.2 Completness of Hilbert space

If the bosonic Fock space is complete it means that each state of the original fermionic Fock space can be expressed in the new basis. A state in the boson basis is characterized by the total number of fermions of each species N_r (cannot be

changed by the boson operators) and by the bosonic numbers for each momentum n_p. Since the operators U commute with the boson operators, a state of the basis is thus of the form

$$|N_R, N_L, n_p\rangle = \prod_p \frac{(b_p^\dagger)^{n_p}}{(n_p!)^{1/2}} (U_R^\dagger)^{N_R} (U_L^\dagger)^{N_L} |0\rangle \tag{B.11}$$

where $|0\rangle$ is the vacuum. To check the completeness of the boson representation let us compute the partition function of the free electron gas in the original fermion system and also in the boson representation. In the fermion representation one has for the energy

$$\xi_{r,k} = v_F(rk - k_F) = v_F(r\frac{2\pi n}{L} - \frac{2\pi n_F}{L} - \frac{\pi}{L}) \tag{B.12}$$

using the quantification relation for k and putting the Fermi level exactly between two occupied states. A single state excited above the Dirac sea (particle or hole) contributes to the partition function as

$$Z_1 = 1 + e^{-\beta|\xi_{r,k}|} = 1 + w^{|2(rn-n_F)-1|} \tag{B.13}$$

with

$$w = e^{-\beta\pi v_F/L} \tag{B.14}$$

Keeping in mind that there are two branches of excitations (right and left going fermions) the total partition function is thus

$$Z = \left[\prod_{n=1}^{\infty} [(1 + w^{2n-1})^2\right]^2 \tag{B.15}$$

note that each term gives a strictly positive contribution to the correlation function. Let us now evaluate the partition function in terms of the bosons excitations and the total number of fermions N_r. The contribution of a single boson of energy $\epsilon_n = v_F 2\pi|n|/L$ is

$$Z_{1B} = \sum_{m=0}^{\infty} e^{-\beta m\epsilon} = \frac{1}{1 - w^{2n}} \tag{B.16}$$

The total boson partition function is thus

$$Z_b = \prod_{n\neq 0} \frac{1}{1 - w^{2n}} = [\prod_{n=1}^{\infty} \frac{1}{1 - w^{2n}}]^2 \tag{B.17}$$

Using (2.22) the partition function associated to the states $|N_+, N_-\rangle$ is thus

$$Z_N = \left[\sum_{m=-\infty}^{m=+\infty} w^{m^2}\right]^2 \tag{B.18}$$

Thus, the full partition function in the boson representation is

$$Z_{\text{bos}} = \left[\prod_{n=1}^{\infty} \frac{1}{1 - w^{2n}} \sum_{m=-\infty}^{m=+\infty} w^{m^2}] \right]^2 \tag{B.19}$$

At first sight (B.19) and (B.15) are quite different. However, there is an identity for the Jacoby function

$$\theta_3(0, q) = \sum_{m=-\infty}^{m=+\infty} q^{m^2} = \prod_{n=1}^{\infty} (1 + q^{2m-1})^2 (1 - q^{2m}) \tag{B.20}$$

which shows that (B.19) and (B.15) are in fact identical (Haldane, 1981*a*). The boson and U operators are thus a complete basis. There are other ways to show that the boson representation is complete, and I refer the reader to Schönhammer (2002) for this other derivation.

APPENDIX C

CORRELATION FUNCTIONS

C.1 Path integral

A very convenient representation to compute the time-ordered Green's functions (see Appendix A) is given by the functional integral. I just recall in this section the main formulas, specializing to the boson case. I refer the reader to Negele and Orland (1988) for more details.

Let us take a system characterized by two canonically conjugate variables ϕ and Π that can depend on a continuum variable such as the spatial position

$$[\phi(x), \Pi(x')] = i\hbar\delta(x - x') \tag{C.1}$$

and a Hamiltonian $H(\phi, \Pi)$. The partition function

$$Z = \mathrm{Tr}[e^{-\beta H}] \tag{C.2}$$

can be expressed via a functional integral

$$Z = \int \mathcal{D}\phi(x,\tau)\mathcal{D}\Pi(x,\tau) e^{\frac{1}{\hbar}\int_0^{\beta\hbar} d\tau \int dx [i\Pi(x,\tau)\partial_\tau\phi(x,\tau) - H(\phi(x,\tau),\Pi(x,\tau))]} \tag{C.3}$$

where $\int \mathcal{D}\phi(x,\tau)$ means the integration on all possible functions $\phi(x,\tau)$. Because of the trace and the bosonic character of the system only periodic functions in time are allowed $\phi(x,\tau+\beta) = \phi(x,\tau)$. Time-ordered correlation functions can be also obtained from the functional integration. If $\hat{O}$ and $\hat{A}$ are some operators, functions of the operators ϕ or Π, then the time-ordered correlation function is simply (let us take, e.g. operators that are functions of ϕ):

$$\langle T_\tau \hat{O}(\tau)\hat{A}(0)\rangle = \frac{1}{Z}\int \mathcal{D}\phi(x,\tau)\mathcal{D}\Pi(x,\tau) O(\phi(\tau)) A(\phi(0))$$
$$e^{\frac{1}{\hbar}\int_0^{\beta\hbar} d\tau \int dx [i\Pi(x,\tau)\partial_\tau\phi(x,\tau) - H(\phi(x,\tau),\Pi(x,\tau))]} \tag{C.4}$$

where $O(\phi(\tau))$ and $A(\phi(\tau))$ are the values of the operators. In order to lighten the notation and since the functional integral representation automatically ensures the time-ordered products, I simply denote by $\langle\cdots\rangle$ the time-ordered correlation functions. The cornerstone formula for using path integral is the formula for gaussian integrals over N complex variables u

$$\left(\prod_i \int \frac{du_i\, du_i^*}{2i\pi}\right) e^{-\sum_{ij} u_i^* A_{ij} u_j + \sum_i h_i^* u_i + h_i u_i^*} = \frac{e^{\sum_{ij} h_i^* (A^{-1})_{ij} h_j}}{\mathrm{Det} A} \tag{C.5}$$

A is an $N \times N$ matrix. Another useful formula, which one can deduce from (C.5), is

$$\langle u_i^* u_j \rangle = \frac{\left(\prod_i \int \frac{du_i\, du_i^*}{2i\pi}\right) u_i^* u_j e^{-\sum_{ij} u_i^* A_{ij} u_j}}{\left(\prod_i \int \frac{du_i\, du_i^*}{2i\pi}\right) e^{-\sum_{ij} u_i^* A_{ij} u_j}} = A_{ij}^{-1} \tag{C.6}$$

An important case is when matrix A is diagonal. Remember that for a real field $u(r)$ its Fourier transform satisfies $u(q)^* = u(-q)$:

$$\langle u^*(q_1) u(q_2) \rangle = \frac{\int \mathcal{D}u[q] u^*(q_1) u(q_2) e^{-\frac{1}{2}\sum_q A(q) u^*(q) u(q)}}{\int \mathcal{D}u[q] e^{-\frac{1}{2}\sum_q A(q) u^*(q) u(q)}} = \frac{1}{A(q_1)} \delta_{q_1, q_2} \tag{C.7}$$

C.2 Basic correlations

The path integral formulation is particularly convenient with quadratic Hamiltonians such as the Luttinger liquid one (2.29). Let us start simply by computing

$$\langle [\phi(r) - \phi(0)]^2 \rangle \tag{C.8}$$

It can be rewritten as

$$\begin{aligned} &\langle [\phi(r_1) - \phi(r_2)]^2 \rangle \\ &\quad = \frac{1}{(\beta\Omega)^2} \sum_{\mathbf{q}_1, \mathbf{q}_2} \langle \phi(\mathbf{q}_1) \phi(\mathbf{q}_2) \rangle (e^{i\mathbf{q}_1 r_1} - e^{i\mathbf{q}_1 r_2})(e^{i\mathbf{q}_2 r_1} - e^{i\mathbf{q}_2 r_2}) \end{aligned} \tag{C.9}$$

where $r = (x, u\tau)$, $\mathbf{q} = (k, \omega_n/u)$, and $e^{i\mathbf{q}r} = e^{i(kx - \omega_n \tau)}$ (see Appendix A). One has thus to compute averages such as

$$\langle \phi(\mathbf{q}_1) \phi(\mathbf{q}_2) \rangle \tag{C.10}$$

This correlation function can be represented as the functional integral

$$\frac{1}{Z} \int \mathcal{D}\phi(x,\tau) \mathcal{D}\theta(x,\tau)\ \phi(\mathbf{q}_1) \phi(\mathbf{q}_2)\ e^{-\frac{S}{\hbar}} \tag{C.11}$$

where S is the action in imaginary time associated with Hamiltonian (2.29) (from now on I revert to $\hbar = 1$)

$$-S = \int_0^\beta d\tau \int dx [i \frac{1}{\pi} \nabla\theta(x,\tau) \partial_\tau \phi(x,\tau) - \frac{1}{2\pi}(uK(\nabla\theta)^2 + \frac{u}{K}(\nabla\phi)^2)] \tag{C.12}$$

where I have used θ instead of Π and (2.26). To compute these averages let us rewrite the action in Fourier space

$$e^{-S} = e^{\frac{1}{\beta\Omega} \sum_{\mathbf{q}} [-\frac{ik\omega_n}{\pi} \phi(\mathbf{q}) \theta(-\mathbf{q}) - \frac{uK}{2\pi} k^2 \theta(\mathbf{q}) \theta(-\mathbf{q}) - \frac{u}{2\pi K} k^2 \phi(\mathbf{q}) \phi(-\mathbf{q})]} \tag{C.13}$$

Let us also rewrite the action in a form that will be useful for some correlation functions

$$S = \frac{1}{2}\frac{1}{\beta\Omega}\sum_{\mathbf{q}}(\theta^*_{\mathbf{q}}, \phi^*_{\mathbf{q}})M^{-1}\begin{pmatrix}\theta_{\mathbf{q}}\\ \phi_{\mathbf{q}}\end{pmatrix} = \frac{1}{2}\frac{1}{\beta\Omega}\sum_{\mathbf{q}}(\theta^*_{\mathbf{q}}, \phi^*_{\mathbf{q}})\begin{pmatrix}\frac{k^2uK}{\pi} & \frac{ik\omega_n}{\pi}\\ \frac{ik\omega_n}{\pi} & k^2\frac{u}{K\pi}\end{pmatrix}\begin{pmatrix}\theta_{\mathbf{q}}\\ \phi_{\mathbf{q}}\end{pmatrix} \tag{C.14}$$

which defines the matrix M^{-1}. Since the quantity to average does not depend on θ one can perform the sum over θ in (C.11). To do so one completes the square of the θ part to get rid of the linear term in θ. This leads to

$$e^{-S} = e^{\frac{1}{\beta\Omega}\sum_{\mathbf{q}}[-\frac{\omega_n^2}{2\pi uK}\phi(\mathbf{q})\phi(-\mathbf{q}) - \frac{uK}{2\pi}k^2[\theta(\mathbf{q})+\frac{i\omega_n\phi(\mathbf{q})}{uKk}][\theta(-\mathbf{q})+\frac{i\omega_n\phi(-\mathbf{q})}{uKk}] - \frac{u}{2\pi K}k^2\phi(\mathbf{q})\phi(-\mathbf{q})]} \tag{C.15}$$

Using the new variable $\tilde{\theta}(\mathbf{q}) = \theta(\mathbf{q}) + \frac{i\omega_n\phi(\mathbf{q})}{uKk}$ one has a gaussian integration on $\tilde{\theta}$. Since the quantity to average depends only on ϕ one can integrate over $\tilde{\theta}$. The gaussian average cancels with the similar one in Z in the denominator. One is thus left with an average over ϕ only of the form

$$\frac{1}{Z_\phi}\int \mathcal{D}\phi(x,\tau)e^{-S_\phi}\phi(\mathbf{q}_1)\phi(\mathbf{q}_2) \tag{C.16}$$

where $Z_\phi = \int \mathcal{D}\phi(x,\tau)e^{-S_\phi}$ is the partition function. The action written in terms of the field ϕ only is thus

$$\begin{aligned} S_\phi &= \frac{1}{\beta\Omega}\sum_{k,\omega_n}\frac{1}{2\pi K}[\frac{\omega_n^2}{u} + uk^2]\phi(k,\omega_n)^*\phi(k,\omega_n) \\ &= \frac{1}{2\pi K}\int dx\int_0^\beta d\tau[\frac{1}{u}(\partial_\tau\phi(x,\tau))^2 + u(\partial_x\phi(x,\tau))^2] \end{aligned} \tag{C.17}$$

On this form the Lorentz invariance of the theory is manifest. Integral (C.16) can easily be done by using Fourier coordinates and using (C.7) to give

$$\langle\phi^*(\mathbf{q}_1)\phi(\mathbf{q}_2)\rangle = \frac{\pi K\delta_{\mathbf{q}_1,-\mathbf{q}_2}\Omega\beta}{\frac{\omega_n^2}{u} + uk_1^2} \tag{C.18}$$

Note that one can also use directly (C.6) and expression (C.14). The inverse of matrix (C.14) is

$$M = \frac{\pi}{k^2(u^2k^2+\omega_n^2)}\begin{pmatrix}k^2\frac{u}{K} & -ik\omega_n\\ -ik\omega_n & k^2uK\end{pmatrix} \tag{C.19}$$

whose $\phi^*\phi$ component gives the same result like (C.18).

Using this expression in (C.9) one gets

$$\begin{aligned} \langle[\phi(r)-\phi(0)]^2\rangle &= \frac{1}{(\beta\Omega)}\sum_{\mathbf{q}_1}\frac{\pi K}{\omega_n^2/u + uk_1^2}(2 - 2\cos(\mathbf{q}_1(r_1-r_2))) \\ &= \frac{1}{\beta}\sum_{\omega_n}\int\frac{dk}{2\pi}\frac{2\pi K}{\omega_n^2/u + uk^2}(1-\cos(kx+\omega_n\tau)) \end{aligned} \tag{C.20}$$

$\theta-\theta$ correlation can be computed in the same way. One simply uses the fact that the Hamiltonian is invariant by $\phi \to \theta$ and $K \to 1/K$ to recover (C.20) with

K replaced by $1/K$. One can also see this directly from (C.19). Finally, $\phi - \theta$ correlations give (using (C.19))

$$\begin{aligned}\langle\phi(r_1)\theta(r_2)\rangle &= \frac{1}{(\beta\Omega)^2}\sum_{\mathbf{q}_1,\mathbf{q}_2}\langle\phi(\mathbf{q}_1)\theta(\mathbf{q}_2)\rangle e^{i\mathbf{q}_1 r_1 + i\mathbf{q}_2 r_2} \\ &= \frac{-1}{\beta\Omega}\sum_{\mathbf{q}}\frac{i\omega_n k\pi}{k^2(u^2k^2+\omega_n^2)}e^{i\mathbf{q}(r_1-r_2)}\end{aligned} \tag{C.21}$$

So for these correlations one has to compute

$$\begin{aligned}F_1(r) &= \frac{1}{\beta\Omega}\sum_{\mathbf{q}}[1-\cos(kx+\omega_n\tau)]\frac{2\pi u}{\omega_n^2+u^2k^2} \\ F_2(r) &= \frac{1}{\beta\Omega}\sum_{\mathbf{q}}e^{i(kx-\omega_n\tau)}\frac{-i2\pi\omega_n/k}{\omega_n^2+u^2k^2}\end{aligned} \tag{C.22}$$

The correlation functions are given by

$$\begin{aligned}\langle[\phi(r)-\phi(0)]^2\rangle &= KF_1(r) \\ \langle[\theta(r)-\theta(0)]^2\rangle &= K^{-1}F_1(r) \\ \langle\phi(r)\theta(0)\rangle &= \frac{1}{2}F_2(r)\end{aligned} \tag{C.23}$$

Note that the integrals over momentum would diverge at large k. It is thus necessary to impose a momentum cutoff. A simple way to do this analytically it to add in the integral $e^{-\alpha|k|}$, which mimics a finite bandwidth. At finite temperature the summation over ω_n is performed in the standard way (Mahan, 1981) by introducing a function whose poles are ω_n. Since ω_n are even frequencies this function is the Bose function $f_B(z) = \frac{1}{e^{\beta z}-1}$ (see Mahan, 1981, where the method is well explained). This gives

$$\begin{aligned}F_1(r) &= \int_0^\infty dk\frac{e^{-\alpha k}f_B(uk)2(1-\cos(kx)\cosh(\tau uk))}{k} \\ &\quad + \int_0^\infty dk\frac{e^{-\alpha k}(1-\cos(kx)e^{-|\tau|uk})}{k} \\ F_2(r) &= -i\int_0^\infty\frac{dk}{k}e^{-\alpha k}\left[\sin(k\tilde{x})e^{-\tilde{\tau}uk} - 2f_B(uk)\sin(k\tilde{x})\sinh(\tilde{\tau}uk)\right]\end{aligned} \tag{C.24}$$

where $\tilde{x} = x\,\mathrm{Sign}(\tau)$, $\tilde{\tau} = \tau\,\mathrm{Sign}(\tau)$, and f_B is the Bose occupation factor.

Let us first take $\beta = \infty$. In that limit

$$\begin{aligned}F_1(r) &= \int_0^\infty\frac{dk}{k}e^{-\alpha k}[1-e^{-u|\tau|k}\cos(kx)] \\ F_2(r) &= -i\int_0^\infty\frac{dk}{k}e^{-\alpha k}e^{-u\tilde{\tau}k}\sin(p\tilde{x})\end{aligned} \tag{C.25}$$

which gives

$$
\begin{aligned}
F_1(r) &= \frac{1}{2}\log\left[\frac{x^2+(u|\tau|+\alpha)^2}{\alpha^2}\right] \\
F_2^{\text{naive}}(r) &= -i\text{Sign}(\tau)\arctan\left[\frac{x}{u|\tau|+\alpha}\right] \\
F_2^{\text{correct}}(r) &= -i\text{Arg}\left[y_\alpha + ix\right]
\end{aligned}
\tag{C.26}
$$

where y_α is defined in (A.3). One can of course directly recover this result by replacing the sum over frequencies ω_n by an integral in (C.22)

$$
\frac{1}{\beta}\sum_n \to \int \frac{d\omega}{2\pi} \tag{C.27}
$$

In (C.26), the 'naive' answer corresponds simply to computing (C.25). For F_2 this needs in fact to be corrected in a way that I will explain later, giving the 'correct' expression, which is the one one should use. At finite temperature the integrals can be evaluated if $(x, u\tau) \gg \alpha$. They give

$$
\begin{aligned}
F_1(r) &= \frac{1}{2}\log\left[\frac{\beta^2u^2}{\pi^2\alpha^2}\left(\sinh^2(\frac{\pi x}{\beta u})+\sin^2(\frac{\pi\tau}{\beta})\right)\right] \\
F_2^{\text{naive}}(r) &= -i\ \arctan\left[\frac{\tanh(\pi\tilde{x}/\beta u)}{\tan(\pi\tilde{\tau}/\beta)}\right] \\
F_2^{\text{correct}}(r) &= -i\ \text{Arg}\left[\tan(\frac{\pi y_\alpha}{\beta u})+i\ \tanh(\frac{\pi x}{\beta u})\right]
\end{aligned}
\tag{C.28}
$$

Quite remarkably, correlation functions of the exponential of the fields are as easy to compute. Let us compute correlation functions such as

$$
I = \langle\prod_j e^{i(A_j\phi(r_j)+B_j\theta(r_j))}\rangle \tag{C.29}
$$

where $r_j = (x_j, u\tau_j)$ and A and B are some coefficients. One immediately sees that *only* the correlation functions (C.29) for which $\sum_i A_i = 0$ and $\sum_i B_i = 0$ are *non-zero*. Indeed, the action is identical for a configuration with ϕ and $\phi + \pi/(\sum_i A_i)$ (or a similar transformation for θ). Upon this transformation the correlation function (C.29) is changed in

$$
\langle\cdots\rangle \to e^{i\pi}\langle\cdots\rangle \tag{C.30}
$$

Since in the path integral one has to sum over all configurations these two contributions sum up to zero. Let us now compute the full correlation. The term in the exponential can be rewritten in Fourier space as

$$
\sum_j A_j\phi(r_j) + B_j\theta(r_j) = \frac{1}{\beta\Omega}\sum_{\mathbf{q}}[A(\mathbf{q})\phi(-\mathbf{q}) + B(\mathbf{q})\theta(-\mathbf{q})] \tag{C.31}
$$

where

$$A(\mathbf{q}) = \sum_j A_j e^{-i(kx_j - \omega_n \tau_j)} \tag{C.32}$$

and a similar formula for B. The correlation can thus be written as

$$\langle \prod_j e^{i(A_j\phi(r_j)+B_j\theta(r_j))} \rangle = \frac{1}{Z} \int \mathcal{D}\phi\mathcal{D}\theta$$
$$e^{-\frac{1}{2}\frac{1}{\beta\Omega}\sum_{\mathbf{q}}\left[(\theta_{-\mathbf{q}},\phi_{-\mathbf{q}})M^{-1}\begin{pmatrix}\theta_{\mathbf{q}}\\ \phi_{\mathbf{q}}\end{pmatrix} - i[(B(-\mathbf{q}),A(-\mathbf{q}))\begin{pmatrix}\theta_{\mathbf{q}}\\ \phi_{\mathbf{q}}\end{pmatrix} + (\theta_{-\mathbf{q}},\phi_{-\mathbf{q}})\begin{pmatrix}B(\mathbf{q})\\ A(\mathbf{q})\end{pmatrix}]\right]} \tag{C.33}$$

where M is matrix (C.19). One can then use (C.5) (or simply complete the square in the exponential) to get

$$\langle \prod_j e^{i(A_j\phi(r_j)+B_j\theta(r_j))} \rangle = e^{-\frac{1}{2}\frac{1}{\beta\Omega}\sum_{\mathbf{q}}(B(-\mathbf{q}),A(-\mathbf{q}))M\begin{pmatrix}B(\mathbf{q})\\ A(\mathbf{q})\end{pmatrix}} \tag{C.34}$$

where matrix M is given by (C.19). In (C.34), let us write, for example, the terms proportional to AA. They are

$$-\frac{1}{2}\frac{1}{\beta\Omega}\sum_{i,j}\sum_{\mathbf{q}} A_i A_j e^{i\mathbf{q}(r_i - r_j)} \frac{uK\pi}{\omega_n^2 + u^2k^2}$$
$$= -\frac{1}{2\beta\Omega}\sum_{i,j}\sum_{\mathbf{q}} A_i A_j \cos(\mathbf{q}(r_i - r_j)) \frac{uK\pi}{\omega_n^2 + u^2k^2} \tag{C.35}$$

This integral is divergent at small $\mathbf{q}$ because the cosine goes to 1 and the denominator is $||\mathbf{q}||^2$. It is thus useful to make F_1 appear

$$\frac{1}{2\beta\Omega}\sum_{i,j}\sum_{\mathbf{q}} A_i A_j \cos(\mathbf{q}(r_i - r_j)) \frac{uK\pi}{\omega_n^2 + u^2k^2} = \frac{1}{2\beta\Omega}\sum_{i,j}\sum_{\mathbf{q}} A_i A_j$$
$$[\cos(\mathbf{q}(r_i - r_j)) - 1]\frac{uK\pi}{\omega_n^2 + u^2k^2} + \frac{1}{2\beta\Omega}\sum_{i,j} A_i A_j \sum_{\mathbf{q}} \frac{uK\pi}{\omega_n^2 + u^2k^2}$$
$$= \frac{-1}{4}\sum_{i,j} A_i A_j K F_1(r_i - r_j) + (\sum_i A_i)^2 \frac{1}{2\beta\Omega}\sum_{\mathbf{q}} \frac{uK\pi}{\omega_n^2 + u^2k^2} \tag{C.36}$$

The first term is finite and the integral in the second term is divergent and thus the second term is infinite. Since it appears inside the exponential with a minus sign (see (C.34)), the correlation is zero *unless* $\sum_i A_i = 0$. One thus recovers explicitly that the only non-zero correlations are the ones that correspond to

'neutral' coefficients A. Keeping only these neutral configurations the final result for the AA term can be written as

$$\frac{1}{2}K\sum_{i<j}A_iA_jF_1(r_i-r_j) \tag{C.37}$$

The terms that contains B_iB_j give exactly the same result (with K replaced by $1/K$), and also impose $\sum_i B_i = 0$. If these two conditions are fulfilled the correlation is thus

$$e^{-\frac{1}{2}\sum_{i<j}\left[[-A_iA_jK-B_iB_jK^{-1}]F_1(r_i-r_j)+[A_iB_j+B_iA_j]F_2(r_i-r_j)\right]} \tag{C.38}$$

This is the most general correlation function that we will encounter. Note that the fact that for such correlation one simply completes the square in the functional integral proves the quite general relation (Debye–Waller)

$$\langle T_\tau e^{\sum_j i(A_j\phi(r_j)+B_j\theta(r_j))}\rangle = e^{-\frac{1}{2}\langle T_\tau\left[\sum_j(A_j\phi(r_j)+B_j\theta(r_j))\right]^2\rangle} \tag{C.39}$$

I have put back the time ordering to emphasize that this relation is valid for operators. This relation can be shown also directly at the operator level (Emery, 1979), but is much more easy to prove using the functional integral. The results we obtained with the functional integral are of course identical with the ones that one would obtain by using the boson representation of the fields ϕ and θ and using (C.39) (see Chapter 3 for the operator derivation).

Finally, let us correct the expression for F_2. If we had to compute the single-particle Green's function

$$\langle T_\tau^F\tilde{\psi}_R(r)\tilde{\psi}_R^\dagger(0)\rangle \tag{C.40}$$

we would have to use the *fermionic* time-ordered product T_τ^F (see (A.27)). Instead, all calculations we have done for the correlations of ϕ and θ assume a *bosonic* time-ordered product. Thus, instead of

$$Y(\tau)\langle\tilde{\psi}_R(x,\tau)\tilde{\psi}_R^\dagger(0)\rangle - Y(-\tau)\langle\tilde{\psi}_R^\dagger(0)\tilde{\psi}_R(x,\tau)\rangle \tag{C.41}$$

The corresponding correlation function in bosons

$$\langle T_\tau^B e^{-i(\phi(r)-\theta(r))}e^{i(\phi(0)-\theta(0))}\rangle = e^{-[\frac{K+K^{-1}}{2}F_1(r)+F_2(r)]} \tag{C.42}$$

corresponds to (C.41) but with a plus sign for the second term. To correct it we have to put a minus sign if $\tau < 0$. This can be achieved by multiplying the result by

$$e^{\pm i\pi Y(-\tau)} \tag{C.43}$$

If we take the convenient choice

$$e^{i\pi Y(-\tau)\,\mathrm{Sign}(x)} \tag{C.44}$$

this amount into replacing in F_2 the arctangent by

$$\mathrm{Sign}(\tau)\ \arctan\left[\frac{x}{u|\tau|+\alpha}\right]+\pi Y(-\tau)\ \mathrm{Sign}(x) \tag{C.45}$$

which is nothing but the argument of the complex number $y_\alpha + ix$ ($y_\alpha = u\tau + \alpha\ \mathrm{Sign}(\tau)$). We can thus absorb the phase factor simply by changing in the definition of F_2 ((C.26) and (C.28)) the arctangent by the argument. The argument is defined with a cut on the negative real axis. It is easy to see that this modification takes care of *all* phase factors even in more complicated objects. Indeed, in an operator that contains a number n of fermionic operators either θ disappears (as in the density operator) or occurs with a coefficient n. Given formula (C.38) the extra phase of π only appears if n is odd, which corresponds indeed to a fermion-like operator for which the time-ordered product should be taken with a minus sign. For n even a term $e^{in\pi}$ appears, which leaves the results unchanged.

Finally, let us rewrite (C.14) using the chiral fields

$$\begin{aligned}\phi_R &= K\theta - \phi\\ \phi_L &= K\theta + \phi\end{aligned} \tag{C.46}$$

which are the fields only containing right (resp. left) movers (see Section 3.2). In the functional integral the chiral fields decouple and have the action

$$S = \frac{1}{4\pi K}\frac{1}{\beta\Omega}\sum_{k,\omega_n}(\phi^*_{R,q},\phi^*_{L,q})\begin{pmatrix} k(uk-i\omega_n) & 0\\ 0 & k(uk+i\omega_n)\end{pmatrix}\begin{pmatrix}\phi_{R,q}\\ \phi_{L,q}\end{pmatrix} \tag{C.47}$$

The correlation functions of these fields are easily obtained and give

$$\begin{aligned}\langle\phi^*_{R,q}\phi_{R,q}\rangle &= \frac{2\pi K}{k(uk-i\omega_n)}\\ \langle\phi^*_{L,q}\phi_{L,q}\rangle &= \frac{2\pi K}{k(uk+i\omega_n)}\end{aligned} \tag{C.48}$$

Of course, one can also recover the correlation functions between the fields ϕ and θ using (C.46) and (C.48).

C.3 Analytic continuation

The functional integral allows to obtain the time-ordered correlation function. In order to compute physical quantities we need the retarded one obtained by making the analytical continuation (A.37). In standard many-body problems one usually takes the Fourier transform of the time-ordered Green's functions $G(i\omega_n)$ the analytical continuation is then simple since one replaces $i\omega_n \to \omega + i\delta$. In one dimension the correlation functions are usually power laws with a non-integer exponent. They are easily obtained in real time and getting their Fourier transform in imaginary time is a little bit painful. It is thus simpler to follow another route to get the retarded correlation functions. The physical answer is

quite simple though. Since the correlation function in imaginary time is a power law it is also a power law of the Matsubara frequency. The analytical continuation of a power law with non-integer exponents is the same power law.

In order to perform the complete analytical continuation it is simpler to obtain first the ordered correlation function in *real* time. Let us define the ordered correlation function (in real time)

$$\chi^T_{BA}(t) = -[Y(t)\langle B(t)A(0)\rangle \pm Y(-t)\langle A(0)B(t)\rangle] \tag{C.49}$$

the plus sign is for boson-like operators, whereas the minus sign would be for fermion-like operators, as usual. $A(t)$ denotes the standard Heisenberg evolution (A.24) of operator A. The retarded correlation function is given by

$$\chi^R_{BA}(t) = -iY(t)[\langle B(t)A(0)\rangle \mp \langle A(0)B(t)\rangle] \tag{C.50}$$

where again the upper sign is for bosons. The retarded correlation function can thus be written as

$$\chi^R_{BA}(t) = iY(t)[\chi^T_{BA}(t) - (\chi^T_{A^\dagger B^\dagger}(-t))^*] \tag{C.51}$$

It is thus enough to obtain the time-ordered correlation functions in real time to get the retarded correlation function. These can be directly obtained from the time-ordered function in imaginary time by doing the Wick rotation (Negele and Orland, 1988)

$$\tau = it + \epsilon\ \mathrm{Sign}(t) \tag{C.52}$$

where $\epsilon = 0^+$.

Let me illustrate the procedure on the exponential of the field ϕ, which enters in many correlation functions (e.g. in the $2k_F$ part of the density–density correlation function)

$$\chi(x,\tau) = -\langle T_\tau e^{i2\phi(x,\tau)} e^{-i2\phi(0,0)}\rangle \tag{C.53}$$

Using (C.38), (C.28), and the standard trigonometric identities one has for $r \gg \alpha$ (compare with (3.102))

$$\chi(x,\tau) = -\frac{(\frac{\pi\alpha}{\beta u})^{2K}}{\left(\sinh(\frac{\pi}{\beta}(\frac{x}{u}+i\tau))\sinh(\frac{\pi}{\beta}(\frac{x}{u}-i\tau))\right)^K} \tag{C.54}$$

The real time correlation function is thus

$$\chi^T(x,t) = -\frac{(\frac{\pi\alpha}{\beta u})^{2K}}{\left(\sinh(\frac{\pi}{\beta}(\frac{x}{u}-t+i\epsilon\mathrm{Sign}(t)))\sinh(\frac{\pi}{\beta}(\frac{x}{u}+t-i\epsilon\mathrm{Sign}(t)))\right)^K} \tag{C.55}$$

Since for this correlation function $\chi_{A^\dagger B^\dagger}(\tau) = \chi_{AB}(\tau)$ one has

$$\chi^R(t) = -Y(t)[2 \text{ Im } \chi^T(x,t)] \tag{C.56}$$

One can rewrite the power law in the denominator as

$$e^{-K \log(A)} \tag{C.57}$$

where

$$\begin{aligned} A &= \sinh\left(\frac{\pi}{\beta}\left(\frac{x}{u} + (t - i\epsilon)\right)\right) \sinh\left(\frac{\pi}{\beta}\left(\frac{x}{u} - (t - i\epsilon)\right)\right) \\ &= \sinh\left(\frac{\pi}{\beta}\left(\frac{x}{u} + t\right)\right) \sinh\left(\frac{\pi}{\beta}\left(\frac{x}{u} - t\right)\right) + i\epsilon\frac{\pi}{\beta}\sinh\left(\frac{2\pi t}{\beta}\right) \end{aligned} \tag{C.58}$$

Since $t > 0$, A has a small positive imaginary part. Putting a cut on the logarithm in (C.57) along the negative real axis (Mahan, 1981), we see that (C.57) has an imaginary part only if the first term in (C.58) is negative. Since

$$\begin{aligned} &\sinh\left(\frac{\pi}{\beta}\left(\frac{x}{u} + t\right)\right) \sinh\left(\frac{\pi}{\beta}\left(\frac{x}{u} - t\right)\right) > 0, \quad \text{if} \quad |x| > ut \\ &\sinh\left(\frac{\pi}{\beta}\left(\frac{x}{u} + t\right)\right) \sinh\left(\frac{\pi}{\beta}\left(\frac{x}{u} - t\right)\right) < 0, \quad \text{if} \quad |x| < ut \end{aligned} \tag{C.59}$$

one has

$$e^{-K \log(A)} = e^{-K \log(|\sinh(\frac{\pi}{\beta}(\frac{x}{u}+t))\sinh(\frac{\pi}{\beta}(\frac{x}{u}-t))|)} e^{-iK\pi Y(ut-x)Y(ut+x)} \tag{C.60}$$

This gives for the retarded correlation function

$$\begin{aligned} \chi_R(t) = -Y(t)Y(ut-x)Y(ut+x)&(\frac{\pi\alpha}{\beta u})^{2K} 2\sin(\pi K) \\ &\left|\sinh\left(\frac{\pi}{\beta}\left(\frac{x}{u} + t\right)\right) \sinh\left(\frac{\pi}{\beta}\left(\frac{x}{u} - t\right)\right)\right|^{-K} \end{aligned} \tag{C.61}$$

C.4 Fourier transform of the retarded correlation function

Formula (C.61) gives the retarded correlation function in real space and time. Performing the Fourier transform is now easy. Let us note $\xi_+ = ut + x$ and $\xi_- = ut - x$. The Fourier transform of (C.61) is

$$\begin{aligned} \chi_R(k,\omega) &= \int_{-\infty}^{\infty} dt \int dx\, e^{i(\omega t - kx)} \chi_R(t,x) \\ &= -\int_0^{\infty} dt \int_{-ut}^{+ut} dx \left(\frac{\pi\alpha}{\beta u}\right)^{2K} 2\sin(\pi K) e^{i(\omega t - kx)} \\ &\quad \times \left|\sinh\left(\frac{\pi\xi_+}{\beta u}\right) \sinh\left(\frac{\pi\xi_-}{\beta u}\right)\right|^{-K} \end{aligned} \tag{C.62}$$

where ω is to be understood as $\omega + i\epsilon$. One can make the change of variables, to go to the light-cone variables ξ_+ and ξ_-:

$$\int_0^\infty dt \int_{-ut}^{+ut} dx = \frac{1}{2u} \int_0^\infty d\xi_+ \int_0^\infty d\xi_- \tag{C.63}$$

Thus,

$$\chi_R(k,\omega) = -\frac{1}{u}\left(\frac{\pi\alpha}{\beta u}\right)^{2K} \sin(\pi K) \left[\int_0^\infty d\xi_+ e^{i\frac{\xi_+}{2}(\frac{\omega}{u}-k)} \sinh\left(\frac{\pi\xi_+}{\beta u}\right)^{-K}\right] \left[\int_0^\infty d\xi_- e^{i\frac{\xi_-}{2}(\frac{\omega}{u}+k)} \sinh\left(\frac{\pi\xi_-}{\beta u}\right)^{-K}\right] \tag{C.64}$$

The integrals can be evaluated as

$$\int_0^\infty d\xi\, e^{i\xi q}\left(\sinh\left(\frac{\pi\xi}{\beta u}\right)\right)^{-K} = 2^K \frac{\beta u}{2\pi} B\left(-i\frac{\beta u q}{2\pi} + \frac{K}{2}, 1-K\right) \tag{C.65}$$

where the function $B(x,y)$ is defined as

$$B(x,y) = \frac{\Gamma(x)\Gamma(y)}{\Gamma(x+y)} \tag{C.66}$$

and $\Gamma(x)$ is the standard gamma function

$$\begin{aligned} \Gamma(x) &= \int_0^\infty dt\, e^{-t} t^{x-1} \\ \Gamma(n) &= (n-1)! \end{aligned} \tag{C.67}$$

One has thus the final formula

$$\chi_R(k,\omega) = -\frac{\sin(\pi K)\,\alpha^2}{u}\left(\frac{2\pi\alpha}{\beta u}\right)^{2K-2} B\left(-i\frac{\beta(\omega-uk)}{4\pi} + \frac{K}{2}, 1-K\right) B\left(-i\frac{\beta(\omega+uk)}{4\pi} + \frac{K}{2}, 1-K\right) \tag{C.68}$$

APPENDIX D

BOSONIZATION DICTIONARY

This is a summary of most of the useful abelian bosonization formulas.

D.1 Spinless fermions

The single fermion operator and the density for a model with strictly linear relation are given by

$$\begin{aligned} \psi(x) &= \psi_R(x) + \psi_L(x) \\ \rho(x) &= \rho_R(x) + \rho_L(x) + (\psi_R^\dagger(x)\psi_L(x) + \text{h.c.}) \end{aligned} \tag{D.1}$$

where $\rho_r = \psi_r^\dagger(x)\psi_r(x)$ and where the right and left going fermions are

$$\psi_r(x) = U_r \lim_{\alpha\to 0} \frac{1}{\sqrt{2\pi\alpha}} e^{i(rk_F - \frac{\pi}{L})x} e^{-i(r\phi(x)-\theta(x))} \tag{D.2}$$

The operators U_r are operators that commute with the bosons. U_r of different species anticommute and U_r of the same species commute. To determine the *sign* of correlations containing the ψ operators the U_r can be replaced by Majorana (real) fermion operators. The fields ϕ and θ obey

$$[\phi(x), \frac{1}{\pi}\nabla\theta(x')] = i\delta(x - x') \tag{D.3}$$

thus the canonically conjugate momentum $\Pi(x)$ is

$$\Pi(x) = \frac{1}{\pi}\nabla\theta(x) \tag{D.4}$$

The fields are related to the densities by

$$\begin{aligned} \nabla\phi(x) &= -\pi[\rho_R(x) + \rho_L(x)] \\ \nabla\theta(x) &= \pi[\rho_R(x) - \rho_L(x)] \end{aligned} \tag{D.5}$$

The fields obey the Hamiltonian

$$H = \frac{1}{2\pi}\int dx\, uK(\pi\Pi(x))^2 + \frac{u}{K}(\nabla\phi(x))^2 \tag{D.6}$$

where u is a velocity and K a dimensionless parameter. For non-interacting fermions $u = v_F$ and $K = 1$. Quite generally $K < 1$ for repulsive interactions and

$K > 1$ for attractive ones. In terms of the standard bosonic variables $[b_q, b_{q'}^\dagger] = \delta_{q,q'}$ one has

$$\begin{aligned}
\phi(x) &= -(N_R + N_L)\frac{\pi x}{L} - \frac{i\pi}{L}\sum_{p\neq 0}\left(\frac{L|p|}{2\pi}\right)^{1/2}\frac{1}{p}e^{-\alpha|p|/2-ipx}(b_p^\dagger + b_{-p}) \\
\theta(x) &= (N_R - N_L)\frac{\pi x}{L} + \frac{i\pi}{L}\sum_{p\neq 0}\left(\frac{L|p|}{2\pi}\right)^{1/2}\frac{1}{|p|}e^{-\alpha|p|/2-ipx}(b_p^\dagger - b_{-p}) \\
H &= \sum_{p\neq 0} v_F|p|b_p^\dagger b_p + \frac{\pi v_F}{L}\sum_r N_r^2
\end{aligned} \tag{D.7}$$

The parts containing the N can be dropped in the thermodynamic limit. For a quite general model, including higher harmonics gives for the density and single-particle operators

$$\begin{aligned}
\rho(x) &= \rho_0 - \frac{1}{\pi}\nabla\phi(x) + \rho_0\sum_{p\neq 0} e^{i2p(\pi\rho_0 x - \phi(x))} \\
\psi_B^\dagger(x) &= \rho_0^{1/2}\sum_p e^{i2p(\pi\rho_0 x-\phi(x))}e^{-i\theta(x)} \\
\psi_F^\dagger(x) &= U_r^\dagger\rho_0^{1/2}\sum_p e^{i(2p+1)(\pi\rho_0 x-\phi(x))}e^{-i\theta}
\end{aligned} \tag{D.8}$$

where p is an integer, B stands for a bosonic single-particle operator, and F for a fermionic one. The amplitude between the various terms in the above formula are non-universal and depend on the ultraviolet cutoff of the theory. For example for a fermionic model with a strictly linear dispersions only the term with $p = 1$ for the density and $p = 0$ for the single-particle operator exists.

With Hamiltonian (D.6) the compressibility and charge stiffness are given by

$$\begin{aligned}
\kappa &= \frac{K}{u\pi} \\
\mathcal{D} &= uK
\end{aligned} \tag{D.9}$$

D.2 Spin chains

Spins in the absence of magnetization have the bosonic expression

$$\begin{aligned}
S^+(x) &= \frac{e^{-i\theta(x)}}{\sqrt{2\pi\alpha}}[(-1)^x + \cos(2\phi(x))] \\
S_z(x) &= -\frac{1}{\pi}\nabla\phi(x) + \frac{(-1)^x}{\pi\alpha}\cos(2\phi(x))
\end{aligned} \tag{D.10}$$

For a finite magnetization the field ϕ in the above expressions is changed into

$$\phi \to \phi + \pi m x \tag{D.11}$$

The Hamiltonian in the Luttinger phase is (D.6). At the Heisenberg point $K = 1/2$.

D.3 Fermions with spins

For system with spins one introduces a boson for charge and for spin using

$$\begin{aligned}\phi_\rho &= \frac{\phi_\uparrow + \phi_\downarrow}{\sqrt{2}} \\ \phi_\sigma &= \frac{\phi_\uparrow - \phi_\downarrow}{\sqrt{2}}\end{aligned} \tag{D.12}$$

The basic formula for the fermion operator becomes (see (D.2))

$$\psi_{r,\sigma}(x) = \frac{1}{\sqrt{2\pi\alpha}} U_{r,\sigma} e^{irk_F x} e^{-\frac{i}{\sqrt{2}}[r\phi_\rho(x) - \theta_\rho(x) + \sigma(r\phi_\sigma(x) - \theta_\sigma(x))]} \tag{D.13}$$

The effective Hamiltonian in the Luttinger phase is of the form

$$H = H_\rho + H_\sigma \tag{D.14}$$

where each fixed Hamiltonian is identical to (D.6) with Luttinger parameters u_ρ, K_ρ and u_σ, K_σ or there is a gap in the corresponding sector. The compressibility, κ_ρ, spin susceptibility, κ_σ, charge, and spin stiffness are given by

$$\begin{aligned}\kappa_\rho &= \frac{2K_\rho}{\pi u_\rho} \\ \mathcal{D}_\rho &= 2u_\rho K_\rho \\ \kappa_\sigma &= \frac{K_\sigma}{2\pi u_\sigma} \\ \mathcal{D}_\sigma &= u_\sigma K_\sigma/2\end{aligned} \tag{D.15}$$

Due to the presence of the operator $\cos\sqrt{8}\phi_\sigma$ in the spin part of the Hamiltonian an expression for the density operator is (taking into account higher harmonics)

$$\begin{aligned}\rho(x) = \rho_0 - \frac{\sqrt{2}}{\pi}\nabla\phi_\rho(x) + \rho_0[e^{i(2k_F x - \sqrt{2}\phi_\rho(x))}\cos(\sqrt{2}\phi_\sigma(x)) + \text{h.c.}] \\ + \rho_0[e^{i(4k_F x - 2\sqrt{2}\phi_\rho(x))} + \text{h.c.}]\end{aligned} \tag{D.16}$$

D.4 Averages

With Hamiltonian (D.6) the correlation function

$$I = \langle \prod_j e^{i(A_j\phi(r_j) + B_j\theta(r_j))} \rangle \tag{D.17}$$

where $r_j = (x_j, u\tau_j)$ and A and B are some coefficients, is non-zero only if $\sum_i A_i = 0$ and $\sum_i B_i = 0$. Its value is

$$I = e^{-\frac{1}{2}\sum_{i<j}\left[[-A_iA_jK - B_iB_jK^{-1}]F_1(r_i - r_j) + [A_iB_j + B_iA_j]F_2(r_i - r_j)\right]} \tag{D.18}$$

where the full expressions for F_1 and F_2 are given in Appendix C. For a cutoff in momentum of the form $e^{-\alpha|p|}$ expressions at $T=0$ of F_1 and F_2 are

$$\begin{aligned} F_1(r) &= \frac{1}{2}\log\left[\frac{x^2+(u|\tau|+\alpha)^2}{\alpha^2}\right] \\ F_2(r) &= -i\ \mathrm{Arg}\left[y_\alpha + ix\right] \end{aligned} \tag{D.19}$$

with (A.3)

$$y_\alpha = u\tau + \alpha\ \mathrm{Sign}(\tau) \tag{D.20}$$

At finite temperature one gets (for $r \gg \alpha$)

$$\begin{aligned} F_1(r) &= \frac{1}{2}\log\left[\frac{\beta^2u^2}{\pi^2\alpha^2}\left(\sinh^2\left(\frac{\pi x}{\beta u}\right)+\sin^2\left(\frac{\pi\tau}{\beta}\right)\right)\right] \\ F_2(r) &= -i\mathrm{Arg}\left[\tan\left(\frac{\pi y_\alpha}{\beta u}\right)+i\tanh\left(\frac{\pi x}{\beta u}\right)\right] \end{aligned} \tag{D.21}$$

Similarly one has

$$\begin{aligned} \langle[\phi(r)-\phi(0)]^2\rangle &= KF_1(r) \\ \langle[\theta(r)-\theta(0)]^2\rangle &= K^{-1}F_1(r) \\ \langle\phi(r)\theta(0)\rangle &= \frac{1}{2}F_2(r) \end{aligned} \tag{D.22}$$

D.5 Babel tower

Bosonization is a technique, which like electric and telephone plugs would clearly benefit from an international normalization. Since one can rescale the fields at will, there are as many notations as there are authors. It is relatively easy to go from one notation to the other. The trick is to identify some physical operators (e.g. density or current) in the two notations. This fixes the fields ϕ and θ. Then one plugs this transformation in the Hamiltonian to identify the equivalent of the two Luttinger parameters u and K. It is impossible to give a list of all notations, but here are some equivalences with other some notations in the literature.

Notation used in Gogolin *et al.* (1999). The Hamiltonian is of the form

$$H_{\mathrm{GNT}} = \frac{u_{\mathrm{GNT}}}{2}\int dx\frac{1}{K_c}(\partial_x\Phi_{\mathrm{GNT}})^2 + K_c(\partial_x\Theta_{\mathrm{GNT}})^2] \tag{D.23}$$

The equivalence is

$$\begin{aligned} \Phi_{\mathrm{GNT}} &= -\phi/\sqrt{\pi} \\ \Theta_{\mathrm{GNT}} &= -\theta/\sqrt{\pi} \\ u_{\mathrm{GNT}} &= u \\ K_c &= K \end{aligned} \tag{D.24}$$

Notation used in Eggert and Affleck (1995). The Hamiltonian is of the form

$$H_{\mathrm{EA}} = \frac{v_{\mathrm{EA}}}{2} \int dx (\Pi_{\mathrm{EA}})^2 + (\partial_x \phi_{\mathrm{EA}})^2] \tag{D.25}$$

The equivalence is

$$\begin{aligned} \phi_{\mathrm{EA}} &= 2R\phi \\ \tilde{\phi}_{\mathrm{EA}} &= -\theta/(2\pi R) \\ v_{\mathrm{EA}} &= \pi u \\ R &= 1/(2\sqrt{\pi K}) \end{aligned} \tag{D.26}$$

(with $\nabla \tilde{\phi}_{\mathrm{EA}} = \Pi_{\mathrm{EA}}$).

Notation used in Kane and Fisher (1992*a*). The action is

$$H_{\mathrm{KF}} = \frac{v_{\mathrm{KF}}}{2g_{\mathrm{KF}}} \int dx\, d\tau\, [(\partial_x \theta_{\mathrm{KF}})^2 + \frac{1}{v_{\mathrm{KF}}^2} (\partial_\tau \theta_{\mathrm{KF}})^2] \tag{D.27}$$

The equivalence is

$$\begin{aligned} \phi_{\mathrm{KF}} &= -\theta/\pi \\ \theta_{\mathrm{KF}} &= -\phi/\pi \\ v_{\mathrm{KF}} &= u \\ g_{\mathrm{KF}} &= K \end{aligned} \tag{D.28}$$

APPENDIX E

SINE-GORDON

E.1 Renormalization

Let me give an alternative way to renormalize the sine-Gordon Hamiltonian. This method is more Wilson-like than the one using the correlation functions. We start from the action deriving from (4.17) (see also (3.26) for the quadratic part)

$$S = \frac{1}{2\pi K}\int dx\, d\tau\, [\frac{1}{u}(\partial_\tau\phi)^2 + u(\partial_x\phi)^2] + \frac{2g}{(2\pi\alpha)^2}\int dx\, d\tau\, \cos(\sqrt{8}\phi(x,\tau)) \quad \text{(E.1)}$$

The field $\phi(x,\tau)$ can be written in terms of the Fourier modes

$$\phi(x,\tau) = \frac{1}{\beta\Omega}\sum_{k,\omega_n} e^{i(kx-\omega_n\tau)}\phi(k,\omega_n) \quad \text{(E.2)}$$

For simplicity, I assume here $\beta = \infty$. Let me impose a sharp momentum cutoff Λ to start with. If one varies the cutoff between Λ and Λ' one can decompose ϕ in fast and slow Fourier modes ($r = (x, u\tau)$ and $\mathbf{q} = (k, \omega_n/u)$):

$$\phi(r) = \phi^>(r) + \phi^<(r) \quad \text{(E.3)}$$

where

$$\begin{aligned}\phi^>(r) &= \frac{1}{\beta\Omega}\sum_{\Lambda'<||\mathbf{q}||<\Lambda} e^{i\mathbf{q}\cdot r}\phi(q)\\ \phi^<(r) &= \frac{1}{\beta\Omega}\sum_{||\mathbf{q}||<\Lambda'} e^{i\mathbf{q}\cdot r}\phi(q)\end{aligned} \quad \text{(E.4)}$$

with the notation (A.5). The quadratic part of the action

$$S_0 = \frac{1}{2\pi K}\frac{1}{\beta\Omega}\sum_{\mathbf{q}}[\omega_n^2/u + uk^2]\phi(\mathbf{q})^*\phi(\mathbf{q}) \quad \text{(E.5)}$$

can obviously be written as

$$S_0 = S_0^> + S_0^< \quad \text{(E.6)}$$

The partition function can be expanded in powers of the cosine term, which gives up to second order (Z_0 is the partition function for $g = 0$)

$$\frac{Z}{Z_0} = \frac{1}{Z_0}\int \mathcal{D}\phi e^{-S_0^> - S_0^<}\left[1 - \frac{2g}{(2\pi\alpha)^2 u}\int d^2r\ \cos(\sqrt{8}(\phi^>(r) + \phi^<(r)))\right.$$
$$\left. + \frac{2g^2}{(2\pi\alpha)^4 u^2}\int d^2r_1 \int d^2r_2\ \cos(\sqrt{8}(\phi^>(r_1)+\phi^<(r_1)))\cos(\sqrt{8}(\phi^>(r_2)+\phi^<(r_2)))\right] \tag{E.7}$$

One can make the average over the fast modes in order to get an effective action for the slow modes. This gives

$$\frac{Z}{Z_0} = \frac{1}{Z_0^<}\int \mathcal{D}\phi\, e^{-S^<}\left[1 - \frac{2g}{(2\pi\alpha)^2 u}\int d^2r\ \cos(\sqrt{8}\phi^<(r))e^{-4\langle(\phi^>(r))^2\rangle_>}\right]$$
$$\left. + \frac{g^2}{(2\pi\alpha)^4 u^2}\sum_{\epsilon=\pm}\int d^2r_1 \int d^2r_2\ \cos(\sqrt{8}(\phi^<(r_1)+\epsilon\phi^<(r_2)))e^{-4\langle(\phi^>(r_1)+\epsilon\phi^>(r_2))^2\rangle_>}\right] \tag{E.8}$$

In order to get an effective action one can reexponentiate this expression. This is equivalent to the standard cumulant expansion. One obtains

$$\frac{Z}{Z_0} = \frac{1}{Z_0^<}\int \mathcal{D}\phi\, e^{-S^< - \frac{2g}{(2\pi\alpha)^2 u}\int d^2r \cos(\sqrt{8}\phi^<(r))e^{-4\langle\phi^>(r)\rangle_>}}$$
$$e^{\frac{g^2}{(2\pi\alpha)^4 u^2}\int d^2r_1\int d^2r_2[\sum_{\epsilon=\pm}\cos(\sqrt{8}(\phi^<(r_1)+\epsilon\phi^<(r_2)))e^{-4\langle(\phi^>(r_1)+\epsilon\phi^>(r_2))^2\rangle_>}]}$$
$$e^{-\frac{2g^2}{(2\pi\alpha)^4 u^2}\int d^2r_1\int d^2r_2 \cos(\sqrt{8}\phi^<(r_1))e^{-4\langle\phi^>(r_1)\rangle_>}\cos(\sqrt{8}\phi^<(r_2))e^{-4\langle\phi^>(r_2)\rangle_>} \tag{E.9}$$

The first term is like the original cosine but for the slow fields only, that is, with a smaller cutoff Λ'. To get back to an action identical to the original one has to rescale distance and time to bring back the cutoff to its original value. This can be done by defining

$$dk = \frac{\Lambda'}{\Lambda}dk' \tag{E.10}$$

and the same transformation for ω. This ensures that the new variables have the old cutoff Λ. In real space this means that one should rescale space and time according to

$$dx = \frac{\Lambda}{\Lambda'}dx', \quad d\tau = \frac{\Lambda}{\Lambda'}d\tau' \tag{E.11}$$

After this rescaling one recovers a theory that is exactly identical to the original one but with a new coupling constant

$$g(\Lambda') = \left(\frac{\Lambda}{\Lambda'}\right)^2 g(\Lambda)e^{-4\langle(\phi^>(r))^2\rangle_>} = \left(\frac{\Lambda}{\Lambda'}\right)^2 g(\Lambda)e^{-\frac{4}{\beta\Omega}\sum_{\Lambda'<||\mathbf{q}||<\Lambda}\frac{\pi K u}{\omega_n^2+u^2k^2}} \tag{E.12}$$

For $\beta \to \infty$ and $L \to \infty$ the sum can be converted to a two-dimensional integral

$$\begin{aligned} g(\Lambda') &= \left(\frac{\Lambda}{\Lambda'}\right)^2 g(\Lambda) e^{-2\int_{\Lambda'<||q||<\Lambda} dq \frac{K}{q}} \\ &= \left(\frac{\Lambda}{\Lambda'}\right)^2 g(\Lambda) e^{-2K\int_{\Lambda'}^{\Lambda} \frac{dq}{q}} = \left(\frac{\Lambda}{\Lambda'}\right)^2 g(\Lambda) e^{-2K\log(\Lambda/\Lambda')} \end{aligned} \tag{E.13}$$

If one parametrizes the cutoff as usual by $\Lambda(l) = \Lambda_0 e^{-l}$ where Λ_0 is the bare cutoff, and one makes the infinitesimal change $\Lambda' = \Lambda_0 e^{-l-dl}$, one gets

$$g(l+dl) = g(l)e^{(2-2K)dl} \tag{E.14}$$

which gives the renormalization equation

$$\frac{dg(l)}{dl} = g(l)(2-2K(l)) \tag{E.15}$$

This is identical to (2.134) obtained by a direct renormalization of the correlation functions.

In the term of order g^2 in (E.9) the last term is there to cancel the disconnected parts (that is, the parts for which the points r_1 and r_2 are very far from each other). The main contribution thus comes from the region where the two points r_1 and r_2 are close. There are thus two main contributions depending on the sign of ϵ. If $\epsilon = +1$ the term $\cos(\sqrt{8}(\phi_1+\phi_2))$ is essentially a term $\cos(2\sqrt{8}\phi(r))$ since we want the two points to be close $r_1 \sim r_2 \sim r$. This term is a new cosine term with an argument that is twice that of the original cosine. We can thus expect this new term to be less relevant than the original cosine since its coupling constant will renormalize with an equation similar to (E.15) but with $8K$ instead of $2K$. Close to the point where the original cosine becomes relevant, $K \sim 1$, one can throw away this contribution. We can thus only retain the contribution with $\epsilon = -1$. One can rewrite this part as

$$\begin{aligned} \delta I = \frac{g^2}{(2\pi\alpha)^4 u^2} \int d^2r_1 \int d^2r_2 \cos(\sqrt{8}(\phi^<(r_1) - \phi^<(r_2))) \\ [e^{-4\langle(\phi^>(r_1)-\phi^>(r_2))^2\rangle_>} - e^{-8\langle(\phi^>)^2\rangle_>}] \end{aligned} \tag{E.16}$$

This can be rewritten

$$\begin{aligned} \delta I =& \frac{g^2}{(2\pi\alpha)^4 u^2} \int d^2r_1 \int d^2r_2 \cos(\sqrt{8}(\phi^<(r_1) - \phi^<(r_2))) \\ & \left[e^{-\frac{4}{\beta\Omega}\sum_{\Lambda'<||\mathbf{q}||<\Lambda}[2-2\cos(\mathbf{q}r)]\frac{\pi K u}{\omega_n^2+u^2k^2}} - e^{-\frac{4}{\beta\Omega}\sum_{\Lambda'<||\mathbf{q}||<\Lambda}[2]\frac{\pi K u}{\omega_n^2+u^2k^2}} \right] \\ =& \frac{g^2}{(2\pi\alpha)^4 u^2} \int d^2r_1 \int d^2r_2 \cos(\sqrt{8}(\phi^<(r_1) - \phi^<(r_2))) \\ & e^{-\frac{4}{\beta\Omega}\sum_{\Lambda'<||\mathbf{q}||<\Lambda}[2-2\cos(\mathbf{q}r)]\frac{\pi K u}{\omega_n^2+u^2k^2}} \left(1 - e^{-\frac{4}{\beta\Omega}\sum_{\Lambda'<||\mathbf{q}||<\Lambda}[2\cos(\mathbf{q}r)]\frac{\pi K u}{\omega_n^2+u^2k^2}}\right) \end{aligned} \tag{E.17}$$

where $r = r_1 - r_2$. Since the integral over $\mathbf{q}$ is only for values of the order of the cutoff this constrains r to be of the order of $1/\Lambda$. One can thus: (i) make an expansion of the cosine in powers of r were we introduce the center of mass $R = (r_1 + r_2)/2$ and relative coordinates $r = r_1 - r_2$; (ii) expand the exponential in the last term. Because the last term in (E.17) is proportional to dl all rescaling terms and terms that depend on Λ/Λ' can be replaced by 1. There is one problem however: the fluctuations of the field ϕ are unbounded ($\langle\phi^2\rangle = \infty$) thus one cannot expand the cosine directly (Nozieres and Gallet, 1987). To do it safely one needs to normal order the cosine. This can be done using

$$\cos(\phi) =: \cos(\phi) : e^{-\frac{1}{2}\langle\phi^2\rangle} \tag{E.18}$$

The normal ordered cosine can be expanded safely. Thus,

$$\cos(\sqrt{8}(\phi^<(r_1) - \phi^<(r_2))) \simeq 4(r \cdot \nabla_R \phi(R))^2 e^{-\frac{4}{\beta\Omega}\sum_{||\mathbf{q}||<\Lambda'}[2-2\cos(\mathbf{q}r)]\frac{\pi K u}{\omega_n^2 + u^2 k^2}} \tag{E.19}$$

The exponential term in (E.19) exactly combines with the corresponding exponential term in (E.17). Using

$$\frac{4}{\beta\Omega}\sum_{\Lambda'<||\mathbf{q}||<\Lambda}[2\cos(\mathbf{q}r)]\frac{\pi K u}{\omega_n^2 + u^2 k^2} = 4K\int_{\Lambda'}^{\Lambda}\frac{dq}{q}J_0(qr) \tag{E.20}$$

one thus has

$$\begin{aligned}\delta I =& \frac{g^2 16 K dl}{(2\pi\alpha)^4 u^2}\int d^2R \int d^2r (r\cdot\nabla_R\phi(R))^2 e^{-4KF_{1,\Lambda}(r)}J_0(\Lambda r)\\ =& dl\frac{g^2 8K}{(2\pi\alpha)^4 u^2}\int d^2R\left[(\partial_X\phi)^2 + (\partial_Y\phi)^2\right]\left[\int d^2r r^2 e^{-4KF_{1,\Lambda}(r)}J_0(\Lambda r)\right]\end{aligned} \tag{E.21}$$

where we have expanded the last term in (E.17) and

$$F_{1,\Lambda}(r) = \frac{1}{\beta\Omega}\sum_{||\mathbf{q}||<\Lambda}[2 - 2\cos(\mathbf{q}r)]\frac{\pi u}{\omega_n^2 + u^2 k^2} = \int_0^{\Lambda}\frac{dq}{q}[1 - J_0(qr)] \tag{E.22}$$

The term δI is thus a correction to the coefficient $1/(2\pi K)$ in the quadratic action. The velocity u is not renormalized, which is a consequence of the Lorentz invariance of the action. This leads to the renormalization equation

$$\frac{dK^{-1}(l)}{dl} = \frac{g^2 8K(l)}{(2\pi)^2(\Lambda\alpha)^4 u^2}\Lambda^4\int_0^{\infty} dr\, r^3 e^{-4KF_{1,\Lambda}(r)}J_0(\Lambda r) \tag{E.23}$$

one can simply rescale the integral in (E.23) to make the Λ dependence disappear. The RG equation thus becomes

$$\frac{dK^{-1}(l)}{dl} = \frac{g^2 2K(l)}{(\pi u)^2(\Lambda\alpha)^4}\mathrm{C} \tag{E.24}$$

where

$$C = \int_0^\infty dz\, z^3 e^{-4KF_1(z)} J_0(z) \tag{E.25}$$

Equation (E.24) is essentially identical to (2.134). The difference between (E.24) and (2.134) in the precise determination of the dimensionless coupling constant for the renormalization equation of K comes from the fact that different cutoff procedures have been used in the two cases. Here we have used a hard cutoff in momentum space, whereas a hard cutoff in real space was imposed in (2.134). Clearly, C and hence the RG equations depend on the precise cutoff procedure used. Of course, the physical quantities are independent of this cutoff procedure. With a generalization of the procedure exposed in this appendix it is possible to derive the RG equations for an arbitrary cutoff (Nozieres and Gallet, 1987).

E.2 Variational calculation

Let us now examine another method, which can be useful even in the absence of a small parameter in the Hamiltonian. It is less powerful than the RG to give the critical properties of the system,[41] but is extremely useful to have the physics of the massive phases, for which the RG would stupidly flow to strong coupling. This is the standard variational method (Feynman, 1972).

Quite generally one can write

$$Z = \int \mathcal{D}\phi e^{-S} = \int \mathcal{D}\phi e^{-S_0} e^{-(S-S_0)} = Z_0 \langle e^{-(S-S_0)}\rangle_0 \tag{E.26}$$

where the index 0 denoted the partition function and the averages with respect of an action S_0. Here, S_0 can be any action. Thus, the free energy satisfies

$$F = F_0 - T\log[\langle e^{-(S-S_0)}\rangle_0] \tag{E.27}$$

Given the convexity of the exponential (see, e.g. Feynman 1972) it is easy to check that one has always

$$\langle e^{-(S-S_0)}\rangle > e^{-\langle (S-S_0)\rangle} \tag{E.28}$$

and thus

$$F \leq F_{\mathrm{var}} = F_0 + T\langle S - S_0\rangle_0 \tag{E.29}$$

The 'best' S_0 is obviously S, that is, the one for which the variational free energy F_{var} is the exact one, that is, minimum. The idea is to take a simple enough S_0 so that one can compute (e.g. a quadratic one), and to optimize it to try to get as close as possible of the physics of the original system.

[41] Nothing can beat the RG for that.

Let us take an example. We start from our favorite sine-Gordon action (see Section 2.3.2).

$$S = \frac{1}{2\pi K}\int dx\, d\tau\, [\frac{1}{u}(\partial_\tau\phi)^2 + u(\partial_x\phi)^2] - \frac{2g}{(2\pi\alpha)^2}\int dx\, d\tau\, \cos(\sqrt{8}\phi) \quad \text{(E.30)}$$

Given the cosine term, the optimal classical configuration (that is, the one giving the minimum of the action) would correspond to $\phi = 0$. One can thus reasonably expect that an approximation where one takes into account harmonic oscillations around this equilibrium position is a good one. Let us thus take for S_0

$$S_0 = \frac{1}{2\beta\Omega}\sum_{\mathbf{q}} G^{-1}(\mathbf{q})\phi^*(\mathbf{q})\phi(\mathbf{q}) \quad \text{(E.31)}$$

and try to optimize by finding the best Green's function $G(q)$. Here, we have *a priori* an infinite number of variational parameters (one for each q). The variational energy is

$$F_{\text{var}} = -T\sum_{q>0}\log[G(q)] + \frac{T}{2\pi K}\sum_q[\frac{1}{u}\omega_n^2 + uk^2]G(q) - T\frac{2g}{(2\pi\alpha)^2}\beta\Omega e^{-\frac{4}{\beta\Omega}\sum_{\mathbf{q}}G(\mathbf{q})} \quad \text{(E.32)}$$

I did not write the term $\langle S_0\rangle_{S_0}$, which gives a simple constant and does not contribute to the variational equations. The optimal $G(q)$ obeys

$$\frac{\partial F_{\text{var}}}{\partial G(q)} = 0 \quad \text{(E.33)}$$

This leads to

$$G^{-1}(q) = \frac{1}{\pi K}[\frac{1}{u}\omega_n^2 + uk^2] + \frac{16g}{(2\pi\alpha)^2}e^{-\frac{4}{\beta\Omega}\sum_{\mathbf{q}}G(\mathbf{q})} \quad \text{(E.34)}$$

which is a self-consistent equation for $G(q)$. Obviously, one can write

$$G^{-1}(\mathbf{q}) = \frac{1}{\pi K}[\frac{1}{u}\omega_n^2 + uk^2 + \frac{\Delta^2}{u}] \quad \text{(E.35)}$$

where the gap Δ satisfies

$$\frac{\Delta^2}{\pi K u} = \frac{16g}{(2\pi\alpha)^2}e^{-\frac{4}{\beta\Omega}\sum_{\mathbf{q}}\frac{\pi K u}{\omega_n^2+u^2k^2+\Delta^2}} \quad \text{(E.36)}$$

Let us look at the zero temperature limit $\beta \to \infty$ and the thermodynamic limit. We transform as usual the sum into a two-dimensional integral. To avoid an unphysical ultraviolet divergence one has again to put a large momentum cutoff

Λ. In the absence of the gap Δ the integral would be divergent at small q (infrared divergence).

$$\frac{4}{(2\pi)^2}\int d\mathbf{q}\frac{\pi K u}{\omega^2+u^2k^2+\Delta^2} = 2K\int_0^\Lambda q\,dq\,\frac{1}{q^2+(\Delta/u)^2}$$
$$\simeq 2K\log[u\Lambda/\Delta] \tag{E.37}$$

assuming that $\Delta \ll u\Lambda$. One has thus the selfconsistent equation

$$\Delta^2 = \frac{4Ku^2y}{\alpha^2}\left(\frac{\Delta}{u\Lambda}\right)^{2K} \tag{E.38}$$

It is easy to see that for $K > 1$ this equation has only $\Delta = 0$ for solution. The sine-Gordon system behaves as a free theory and the cosine potential is irrelevant. If, on the other hand, $K < 1$ a non-zero solution appears for Δ

$$\Delta = u\Lambda\left(\frac{4Ky}{(\alpha\Lambda)^2}\right)^{\frac{1}{2-2K}} \tag{E.39}$$

One essentially recovers the value of the gap (2.158) that we had obtained deep in the massive phase. The physics of the massive phase as given by the variational approach is essentially the one we had discussed from physical arguments. The field ϕ is trapped in one of the minima and makes small oscillations around this minima. Such a method is thus very useful to compute physical properties in the massive phases.

Two warnings in using this variational method. First, it obviously missed the correct critical properties. The way the gap goes to zero at the transition is not correct. It is as if the variational method was replacing the correct RG flow by a purely vertical flow. This is not a very serious drawback since any approximate method is not expected to capture critical behaviors. A more serious caveat is that the variational approach can only capture the small oscillations around the minima. It misses other excitations such as solitons where the field ϕ goes from one of the minima to the other. These excitations can be very important so caution should be exerted to check that the variational approach did not miss the essential physics for the problem at hand. Despite these two caveats this is a very useful approach.

E.3 Semiclassical approximations

I just briefly recall some results obtained for the sine-Gordon model. A complete description of these results is given in Rajaraman (1982). I take the model

$$H = \frac{1}{2\pi}\int dx\, uK(\pi\Pi(x))^2 + \frac{u}{K}(\nabla\phi(x))^2 + \bar{g}\int dx[1-\cos(\sqrt{8}\phi(x))] \tag{E.40}$$

so that the minimum of energy corresponds to $\phi = 0$.

To help you make the connection between the notation of Rajaraman and the ones of this book here is a dictionary (I denote with a suffix R the quantities in Rajaraman's book)

$$\begin{aligned} \lambda_{\mathrm{R}} &= 64\bar{g}K^2\pi^2 u \\ m_{\mathrm{R}} &= 2\sqrt{2\pi u\bar{g}K} \\ x_{\mathrm{R}} &= x/u \end{aligned} \tag{E.41}$$

Note that in many of Rajaraman's formulas the light velocity c has been taken to be one so his time is in fact $t \to ct$.

For $K > 1$ the cosine is irrelevant. For $K < 1$ the cosine is relevant and opens a gap in the spectrum. Hamiltonian (E.40) has various excitations. The first one is the soliton that takes ϕ from one minimum of the cosine to the next. For a soliton (see also Section 10.2)

$$\phi_S(x) = \sqrt{2}\arctan\left[e^{2\sqrt{\frac{2\pi\bar{g}K}{u}}x}\right] \tag{E.42}$$

which takes ϕ from 0 to 2π. The opposite solution is an anti-soliton. The minimum energy (mass) of the soliton is

$$M_S = 2\sqrt{\frac{2\bar{g}u}{\pi K}} \tag{E.43}$$

For $K > 1/2$ the soliton is the excitation of lowest energy. At higher energies one can of course make multi-solitons and antisolitons solutions, whose energy is at least M_S times the number of solitons and antisolitons (solitons and antisolitons repel). For $K < 1/2$ solitons and antisolitons attract. They can form bound states called breathers. There are N breathers solutions with $1 \leq N < \frac{1-K}{K}$. The mass of a breather is

$$M_{B,N} = 4\sqrt{\frac{2\bar{g}u}{\pi K}}\sin\left[\frac{\pi K N}{2(1-K)}\right] \tag{E.44}$$

The top (maximum N) breather is made of a bound soliton antisoliton. Its mass is slightly lower than twice the soliton mass, a sign of the attraction between solitons and anti-solitons. For small K the energy of the lowest ($N = 1$) breather is

$$M_P = \sqrt{2\pi\bar{g}uK} \tag{E.45}$$

One recovers exactly the mass of the phonon excitation (2.153). One can thus identify the lower breather with the oscillations around one minimum of the cosine (phonons).

The solitons and antisolitons correspond to the spinless fermions of the mapping of the sine-Gordon model to the massive Thiring model (see Section 4.2.2). On the Luther–Emery line $K = 1/2$ these particles do not interact, while they repel for $K > 1/2$ and attract for $K < 1/2$. Quite generally by rescaling the field ϕ one can check that if the cosine term is relevant at K_c then the Luther–Emery line occurs for $K_c/2$.

APPENDIX F

NUMERICAL SOLUTION

This is a fortran program finding the LL parameters u and K for a spin chain from the Bethe-ansatz equations (see Chapter 5). It is written in the *simplest* possible fashion, and much more sophisticated versions can easily be implemented. Nevertheless this most stupid implementation shows that very low computer skills are enough to get the exponents with very good accuracy, an illustration of the power of this combination of analytical and numerical techniques to tackle one-dimensional problems.

```
      program luttinger

      integer n,l
      real*8 pi,temp
      real*8 u,phi
      real*8 ener
      real*8 ener0,delphi,stiff
      real*8 enerp2,enerm2
      real*8 uoverk,utimesk

      pi = acos(-1.0d0)
C
C Number of sites
C
      l = 102
C
C N is the number of particles; Half filling is N = L/2
C N = 51 in this example
C u is the interaction of a spinless fermion model
C
      print *,'n ; u/t = ?'
      read *,n,u
C
C With the BA for a spin chain t=1 means Jxy = 2
C In the BA equations one needs Delta = Jz/Jxy
C If one measures energy in units of t u should be
C divided by two
C
      u = u/2.0d0
```

```
C
C Zero external flux for compressibility
C
      phi = 0.0d0
C
C Calculation of compressibility
C
      call energy(l,n,u,phi,ener0)
      print *,'E0 = ',ener0
      call energy(l,n+2,u,phi,enerp2)
      call energy(l,n-2,u,phi,enerm2)

      uoverk = enerp2+enerm2 - 2.0d0*ener0
      uoverk = dfloat(l) * uoverk / 2.0d0
      uoverk = uoverk/(2.0d0*pi)
      print *,'u/K = ',uoverk
C
C Calculation of chemical potential
C
      temp   = enerp2-enerm2
      temp   = temp/4.0d0
      print *,'mu = ',temp

C
C Calculation of the stiffness
C
C
C Let us pick a flux of 0.01 hopping it is small enough
C
      delphi = 0.01d0
      call energy(l,n,u,delphi,ener)
      stiff = (ener-ener0)/(delphi**2)
      stiff = 2.0d0*pi*dfloat(l)*stiff
      utimesk = stiff
      print *,'u K = ',utimesk

      print *,'u = ', sqrt(uoverk*utimesk)
      print *,'K = ', sqrt(utimesk/uoverk)
      print *,u,sqrt(uoverk*utimesk),sqrt(utimesk/uoverk)

      end

      subroutine energy(l,n,u,phi,ener)
C
```

```
C Computes the energy of the ground
C state for a spinless fermions (a.k.a. spin chain)
C l = number of sites
C n = number of particles
C constraint n <= l
C ener is the energy of the ground state
C
C to describe spinless fermions one takes Jxy = -2
C which ensures t = + 1
C one should take delta = -u in BA equations
C

      integer nn,n,l
      parameter(nn=100000)
      real*8 psi(nn),phi,p(nn)
      real*8 int(nn),pi,temp
      real*8 u,ener,enero
      integer i,j,k,iter

      do i=1,n
       psi(i) = 0.0d0
      enddo

      do i=1,n
       int(i) = dfloat(i) - dfloat(n+1)/2.0d0
      enddo
C
C Initializations
C
      pi = acos(-1.0d0)
      iter = 10000
      enero = 0.0d0

      do k=1,iter
       do i=1,n
        p(i) = (2.0d0*pi*int(i) + phi)
        do j=1,n
         temp = u* sin((psi(i)-psi(j))/2.0d0)
         temp = temp/(cos((psi(i)+psi(j))/2.0d0) + u *
     1                cos((psi(i)-psi(j))/2.0d0))
         p(i) = p(i) + 2.0d0*Atan(temp)
        enddo
        p(i) = p(i)/dfloat(l)
       enddo
```

```
      do i=1,n
       psi(i) = p(i)
      enddo
      ener = 0.0d0
      do i=1,n
       ener = ener - 2.0d0*(u + Cos(p(i)))
      enddo
      ener = ener + u*dfloat(l)/2.0d0
C     print *,ener
      if (ener.eq.enero) return
      enero = ener
     enddo
     print *,'problem: more than 100000 iterations'
     return
     end
```

REFERENCES

Abrahams, E., Anderson, P. W., Licciardello, D. C., and Ramakrishnan, T. V. (1979). *Phys. Rev. Lett.*, **42**, 673.

Abrahams, E., Kravchenko, S. V., and Sarachik, M. P. (2001). *Rev. Mod. Phys.*, **73**, 251.

Abrikosov, A. A., Gorkov, L. P., and Dzyaloshinski, I. E. (1963). *Methods of Quantum Field Theory in Statistical Physics.* Dover, New York.

Abrikosov, A. A. and Rhyzkin, J. A. (1978). *Adv. Phys.*, **27**, 147.

Affleck, I. (1966). *Nucl. Phys. B*, **265**, 448.

Affleck, I. (1988). In *Fields, Strings and Critical Phenomena* (ed. E. Brezin and J. Zinn-Justin), Amsterdam, pp. 563. Elsevier Science.

Affleck, I. (1995). *Acta. Phys. Pol. B*, **26**, 1869.

Affleck, I., Gepner, D., Schulz, H. J., and Ziman, T. (1989). *J. Phys. A*, **22**, 511.

Affleck, I. and Ludwig, A. W. W. (1991). *Nucl. Phys. B*, **360**, 641.

Affleck, I. and Ludwig, A. W. W. (1994). *J. Phys. A*, **27**, 5375.

Affleck, I. and Marston, J. B. (1988). *Phys. Rev. B*, **37**, 3774.

Altshuler, B. L. and Aronov, A. G. (1985). In *Electron–electron interactions in disordered systems* (ed. A. L. Efros and M. Pollak), Amsterdam. North-Holland.

Anderson, P. W. (1958). *Phys. Rev.*, **109**, 1492.

Anderson, P. W. (1967). *Phys. Rev. Lett.*, **18**, 1049.

Anderson, P. W. (1970). *J. Phys. C*, **3**, 2346.

Anderson, P. W. (1997). *The Theory of Superconductivity in the High-T_c Cuprate Superconductors.* Princeton University Press, Princeton, NJ.

Anderson, P. W., Yuval, G., and Hamann, D. R. (1970). *Phys. Rev. B*, **1**, 4464.

Andrei, N. (1994). Lectures of the Trieste Summer School 1992, cond-mat/9408101.

Andrei, N., Furuya, K., and Lowenstein, J. H. (1983). *Rev. Mod. Phys.*, **55**, 331.

Andrei, N. and Lowenstein, J. H. (1979). *Phys. Rev. Lett.*, **43**, 1698.

Anglin, J. R. and Ketterle, W. (2002). *Nature*, **416**, 211.

Apel, W. (1982). *J. Phys. C*, **15**, 1973.

Apel, W. and Rice, T. M. (1982*a*). *Phys. Rev. B*, **26**, 7063.

Apel, W. and Rice, T. M. (1982*b*). *J. Phys. C*, **16**, L271.

Aristov, D. N. and Luther, A. (2002). *Phys. Rev. B*, **65**, 165412.

Arrigoni, E. (1996). *Phys. Lett. A*, **215**, 91.

Augier, D., Poilblanc, D., Sorensen, E., and Affleck, I. (1999). *Phys. Rev. B*, **58**, 9110.

Auslaender, O. M., Yacoby, A., de Picciotto, R., Baldwin, K. W., Pfeiffer, L. N.,

and West, K. W. (2002). *Science*, **295**, 825.

Azuma, M., Hiroi, Z., Takano, M., Ishida, K., and Kitaoka, Y. (1994). *Phys. Rev. Lett.*, **73**, 3463.

Balents, L. and Fisher, M. P. A. (1996). *Phys. Rev. B*, **53**, 12133.

Bares, P. A., Blatter, G., and Ogata, M. (1991). *Phys. Rev. B*, **44**, 130.

Baxter, R. J. (1982). *Exactly Solved Models of Statistical Mechanics.* Academic Press, New York.

Belavin, A. A. (1979). *Phys. Lett. B*, **87**, 117.

Belavin, A. A., Polyakov, A. M., and Zamolodchikov, A. B. (1984). *Nucl. Phys. B*, **241**, 333.

Berezinskii, V. L. (1971). *Sov. Phys. JETP*, **32**, 493.

Berezinskii, V. L. (1974). *Sov. Phys. JETP*, **38**, 620.

Berkovits, R. and Avishai, Y. (1995). *Europhys. Lett.*, **29**, 475.

Biermann, S., Georges, A., Giamarchi, T., and Lichtenstein, A. (2002). In *Strongly Correlated Fermions and Bosons in Low Dimensional Disordered Systems* (ed. I. V. Lerner *et al.*), Dordrecht, pp. 81. Kluwer Academic Publishers. cond-mat/0201542.

Binder, K. (ed.) (1984). *Applications of the Monte-Carlo Method in Statistical Physics.* Springer-Verlag, Berlin.

Blatter, G., Feigel'man, M. V., Geshkenbein, V. B., Larkin, A. I, and Vinokur, V. M. (1994). *Rev. Mod. Phys.*, **66**, 1125.

Bockrath, M., Cobden, D.H., Lu, J., Rinzler, A.G., Smalley, R.E., Balents, L., and McEuen, P.L. (1999). *Nature*, **397**, 598.

Bocquet, M., Essler, F. H. L., Tsvelik, A. M., and Gogolin, A. O. (2001). *Phys. Rev. B*, **64**, 094425.

Boies, D., Bourbonnais, C., and Tremblay, A.-M. S. (1995). *Phys. Rev. Lett.*, **74**, 968.

Bonner, J. C. and Fisher, M. E. (1964). *Phys. Rev.*, **135A**, 640.

Bonner, J. C., Friedberg, S. A., Kobayashi, H., Meier, D. L., and Blöte, H. W. J. (1983). *Phys. Rev. B*, **27**, 248.

Bourbonnais, C. (1993). *J. Phys. I France*, **3**, 143.

Bourbonnais, C. and Caron, L. G. (1986). *Physica*, **143B**, 450.

Bourbonnais, C. and Caron, L. G. (1991). *Int. J. Mod. Phys. B*, **5**, 1033.

Bourbonnais, C., Creuzet, F., Jérome, D., Bechgaard, K., and Moradpour, A. (1984). *J. Phys. (Paris) Lett.*, **45**, L755.

Bourbonnais, C. and Dumoulin, B. (1996). *J. Phys. I France*, **67**, 1727.

Bourbonnais, C. and Jérome, D. (1999). In *Advances in Synthetic Metals, Twenty years of Progress in Science and Technology* (ed. P. Bernier, S. Lefrant, and G. Bidan), New York, pp. 206. Elsevier. preprint cond-mat/9903101.

Bouzerar, G., Poilblanc, D., and Montambaux, G. (1994). *Phys. Rev. B*, **49**, 8258.

Bradley, R. M. and Doniach, S. (1984). *Phys. Rev. B*, **30**, 1138.

Brazovskii, S. and Yakovenko, V. (1985). *J. Phys. (Paris) Lett.*, **46**, L111.

Bychkov, Yu. A., Gorkov, L. P., and Dzyaloshinskii, I. E. (1966). *Sov. Phys.*

JETP, **23**, 489.

Cabra, D. C., Honecker, A., and Pujol, P. (1998). *Phys. Rev. B*, **58**, 6241.

Caldeira, A. O. and Leggett, A. J. (1983). *Ann. Phys.*, **149**, 374.

Calleja, J. M., Goñi, A. R., Dennis, B. S., Weiner, J. S., Pinczuk, A., Schmitt-Rink, S., Pfeiffer, L. N., West, K. W., Müller, J. F., and Ruckenstein, A. E. (1991). *Solid State Commun.*, **79**, 911.

Capponi, S., Poilblanc, D., and Giamarchi, T. (2002). *Phys. Rev. B*, **61**, 13410.

Cardy, J. (1996). *Scaling and Renormalization in Statistical Physics*. Cambridge University Press, Cambridge.

Carmelo, J. M. P., Peres, N. M. R., and Sacramento, P. D. (2000). *Phys. Rev. Lett.*, **84**, 4673.

Carpentier, D., Peca, C., and Balents, L. (2002). *Phys. Rev. B*, **66**, 153304.

Cazalilla, M. A. (2002). *Europhys. Lett.*, **59**, 793.

Ceperley, D. (1995). *Rev. Mod. Phys.*, **67**, 279.

Chaboussant, G., Crowell, P., Lévy, L. P., Poivesana, O., Madouri, A., and Mailly, D. (1997). *Phys. Rev. B*, **55**, 3046.

Chaboussant, G., Julien, M.-H., Fagot-Revurat, Y., Hanson, M. E., Lévy, L. P., Berthier, C., Horvatić, M., and Piovesana, O. (1998). *Eur. Phys. J. B*, **6**, 167.

Chiari, B., Piovesana, O., Tarantelli, T., and Zanazzi, P. F. (1990). *Inorg. Chem.*, **29**, 1172.

Chitov, G. Y. and Bourbonnais, C. (2002). preprint, cond-mat/0212493.

Chitra, R. and Giamarchi, T. (1997). *Phys. Rev. B*, **55**, 5816.

Chitra, R., Pati, S., Krishnamurthy, H. R., Sen, D., and Ramasesha, S. (1995). *Phys. Rev. B*, **52**, 6581.

Chui, S. T. and Lee, P. A. (1975). *Phys. Rev. Lett.*, **35**, 315.

Citro, R. and Orignac, E. (2002). *Phys. Rev. B*, **65**, 134413.

Clarke, D. G., Giamarchi, T., and Shraiman, B. I. (1993). *Phys. Rev. B*, **48**, 7070.

Coleman, S. (1977). *Phys. Rev. D*, **15**, 2929.

Controzzi, D., Essler, F. H. L., and Tsvelik, A. M. (2001). *Phys. Rev. Lett.*, **86**, 680.

Cox, D. L. and Zawadowski, A. (1998). *Adv. Phys.*, **47**, 599.

Cross, M. C. and Fisher, D. S. (1979). *Phys. Rev. B*, **19**, 402.

Dagotto, E. (1999). *Rep. Prog. Phys.*, **62**, 1525.

Dagotto, E. and Rice, T. M. (1996). *Science*, **271**, 618. and references therein.

Dagotto, E., Riera, J., and Scalapino, D. (1992). *Phys. Rev. B*, **45**, 5744.

Damle, K. and Huse, D. A. (2002). *Phys. Rev. Lett.*, **89**, 277203.

Dardel, B., Malterre, D., Grioni, M., Weibel, P., Baer, Y., Voit, J., and Jérôme, D. (1993). *Europhys. Lett.*, **24**, 687.

Davidson, E. R. (1993). *Computers in Physics*, **7**, 519.

de Picciotto, R., Stormer, H. L., Pfeiffer, L. N., Baldwin, K. W., and West, K. W. (2001). *Nature*, **411**, 51.

de Picciotto, R., Stormer, H. L., Yacoby, A., Pfeiffer, L. N., Baldwin, K. W., and West, K. W. (2000). *Phys. Rev. Lett.*, **85**, 1730.

Dender, D.C., Hammar, P. R., Reich, D. H., Broholm, C., and Aeppli, G. (1997). *Phys. Rev. Lett.*, **79**, 1750.

Denlinger, J. D., Gweon1, G.-H., Allen, J. W., Olson, C. G., Marcus, J., Schlenker, C., and Hsu, L.-S. (1999). *Phys. Rev. Lett.*, **82**, 2540.

Di Francesco, P., Mathieu, P., and Senechal, D. (1997). *Conformal Field Theory.* Springer-Verlag, Berlin.

Donohue, P. and Giamarchi, T. (2001). *Phys. Rev. B*, **63**, 180508(R).

Donohue, P., Tsuchiizu, M., Giamarchi, T., and Suzumura, Y. (2001). *Phys. Rev. B*, **63**, 045121. and references therein.

Douçot, B. and Zinn-Justin, J. (ed.) (1995). Elsevier, Amsterdam.

Dressel, M., Schwartz, A., Grüner, G., and Degiorgi, L. (1996). *Phys. Rev. Lett.*, **77**, 398.

Dresselhaus, M. S., Dresselhaus, G., and Eklund, P. C. (1995). *Science of Fullerenes and Carbon Nanotubes.* Academic Press, San Diego, CA.

Dzyaloshinskii, I. E. and Larkin, A. I. (1972). *Sov. Phys. JETP*, **34**, 422.

Dzyaloshinskii, I. E. and Larkin, A. I. (1974). *Sov. Phys. JETP*, **38**, 202.

Edwards, S. F. and Anderson, P. W. (1975). *J. Phys. F*, **5**, 965.

Efetov, K. B. (1983). *Adv. Phys.*, **32**, 53.

Efetov, K. B., Larkin, A. I., and Khmel'nitskii, D. E. (1980). *Sov. Phys. JETP*, **52**, 568.

Egger, R. and Gogolin, A. O. (1997). *Phys. Rev. Lett.*, **79**, 5082.

Eggert, S. and Affleck, I. (1992). *Phys. Rev. B*, **46**, 10866.

Eggert, S. and Affleck, I. (1995). *Phys. Rev. Lett.*, **75**, 934.

Eggert, S., Affleck, I., and Takahashi, M. (1994). *Phys. Rev. Lett.*, **73**, 332.

Eggert, S., Gustafsson, D. P., and Rommer, S. (2001). *Phys. Rev. Lett.*, **86**, 516.

Emery, V. J. (1979). New York and London, pp. 247. Plenum Press.

Emery, V. J. and Kivelson, S. A. (1992). *Phys. Rev. B*, **46**, 10812.

Essler, F. H. L. and Tsvelik, A. M. (1999). *Phys. Rev. B*, **57**, 10592.

Essler, F. H. L. and Tsvelik, A. M. (2002). *Phys. Rev. Lett.*, **88**, 096403.

Fabrizio, M. (1993). *Phys. Rev. B*, **48**, 15838.

Fabrizio, M. and Gogolin, A. O. (1995). *Phys. Rev. B*, **51**, 17827.

Fabrizio, M., Gogolin, A. O., and Scheidl, S. (1994). *Phys. Rev. Lett.*, **72**, 2235.

Fazio, R. and van der Zant, H. (2001). *Phys. Rep.*, **355**, 235.

Feigelmann, M. V. and Vinokur, V. M. (1981). *Phys. Lett. A*, **87**, 53.

Fendley, P., Ludwig, A. W. W., and Saleur, H. (1995*a*). *Phys. Rev. Lett.*, **74**, 3005.

Fendley, P., Ludwig, A. W. W., and Saleur, H. (1995*b*). *Phys. Rev. Lett.*, **74**, 3005.

Feynman, R. P. (1972). *Statistical Mechanics.* Benjamin, Reading, MA.

Finkelstein, A. M. (1984). *Z. Phys. B*, **56**, 189.

Finkelstein, A. M. and Larkin, A. I. (1993). *Phys. Rev. B*, **47**, 10461.

Fisher, D. S. (1994). *Phys. Rev. B*, **50**, 3799.

Fisher, M. P. A. and Glazman, L. I. (1997). In *Mesoscopic Electron Transport*

(ed. L. Kowenhoven *et al.*), Dordrecht. Kluwer Academic Publishers. cond-mat/9610037.

Fisher, M. P. A., Weichman, P. B., Grinstein, G., and Fisher, D. S. (1989). *Phys. Rev. B*, **40**, 546.

Fukuyama, H. and Lee, P. A. (1978). *Phys. Rev. B*, **17**, 535.

Furusaki, A. and Nagaosa, N. (1993*a*). *Phys. Rev. B*, **47**, 4631.

Furusaki, A. and Nagaosa, N. (1993*b*). *Phys. Rev. B*, **47**, 3827.

Furusaki, A. and Zhang, S. C. (1999). *Phys. Rev. B*, **60**, 1175.

Gambetti-Cesare, E., Weinmann, D., Jalabert, R. A., and Brune, P. (2002). *Europhys. Lett.*, **60**, 120.

Garst, M. and Rosch, A. (2001). *Europhys. Lett.*, **55**, 66.

Gaudin, M. (1967). *Phys. Lett. A*, **24**, 55.

Gaudin, M. (1983). *La fonction d'onde de Bethe.* Masson, Paris.

Georges, A., Giamarchi, T., and Sandler, N. (2000). *Phys. Rev. B*, **61**, 16393.

Georges, A., Kotliar, G., Krauth, W., and Rozenberg, M. J. (1996). *Rev. Mod. Phys.*, **68**, 13.

Gerbier, F., Thywissen, J. H., Richard, S., Hugbart, M., Bouyer, P., and Aspect, A. (2002). preprint, cond-mat/0211094.

Giamarchi, T. (1991). *Phys. Rev. B*, **44**, 2905.

Giamarchi, T. (1992). *Phys. Rev. B*, **46**, 342.

Giamarchi, T. (1997). *Physica B*, **230-232**, 975.

Giamarchi, T. and Bhattacharya, S. (2002). In *High Magnetic Fields: Applications in Condensed Matter Physics and Spectroscopy* (ed. C. Berthier *et al.*), Berlin, pp. 314. Springer-Verlag. cond-mat/0111052.

Giamarchi, T. and Le Doussal, P. (1995). *Phys. Rev. B*, **52**, 1242.

Giamarchi, T. and Le Doussal, P. (1996). *Phys. Rev. B*, **53**, 15206.

Giamarchi, T., Le Doussal, P., and Orignac, E. (2001). *Phys. Rev. B*, **64**, 245119.

Giamarchi, T. and Maurey, H. (1996). In *Correlated Fermions and Transport in Mesoscopic Systems* (ed. T. Martin, G. Montambaux, and J. Tran Thanh Van), Gif sur Yvette, France. Editions Frontières. cond-mat/9608006.

Giamarchi, T. and Millis, A. J. (1992). *Phys. Rev. B*, **46**, 9325.

Giamarchi, T. and Orignac, E. (2003). In *Theoretical Methods for Strongly Correlated Electrons* (ed. D. Sénechal *et al.*), CRM Series in Mathematical Physics, New York. Springer. cond-mat/0005220.

Giamarchi, T. and Schulz, H. J. (1987). *Europhys. Lett.*, **3**, 1287.

Giamarchi, T. and Schulz, H. J. (1988*a*). *J. Phys. (Paris)*, **49**, 819.

Giamarchi, T. and Schulz, H. J. (1988*b*). *Phys. Rev. B*, **37**, 325.

Giamarchi, T. and Schulz, H. J. (1989). *Phys. Rev. B*, **39**, 4620.

Giamarchi, T. and Shastry, B. S. (1995). *Phys. Rev. B*, **51**, 10915.

Giamarchi, T. and Tsvelik, A. M. (1999). *Phys. Rev. B*, **59**, 11398.

Giamarchi, T., Varma, C. M., Ruckenstein, A. E., and Nozieres, P. (1993). *Phys. Rev. Lett.*, **70**, 3967.

Glattli, C. (2002). In *High Magnetic Fields: Applications in Condensed Matter*

Physics and Spectroscopy (ed. C. Berthier *et al.*), Berlin, pp. 1. Springer-Verlag.

Glazman, L. I. and Larkin, A. I. (1997). *Phys. Rev. Lett.*, **79**, 3736.

Glazman, L. I. and Raikh, M. E. (1988). *JETP Lett.*, **47**, 452.

Glazman, L. I., Ruzin, I. M., and Shklovskii, B. I. (1992). *Phys. Rev. B*, **45**, 8454.

Gogolin, A. O., Nersesyan, A. A., and Tsvelik, A. M. (1999). *Bosonization and Strongly Correlated Systems.* Cambridge University Press, Cambridge.

Gold, A. and Ghazali, A. (1990). *Phys. Rev. B*, **41**, 7626.

Goñi, A. R., Pinczuk, A., Weiner, J. S., Calleja, J. M., Dennis, B. S., Pfeiffer, L. N., and West, K. W. (1991). *Phys. Rev. Lett.*, **67**, 3298.

Gorkov, L. P. (1997). *Physica B*, **230-232**, 970.

Gorkov, L. P. and Dzyaloshinski, I. E. (1973). *JETP Lett.*, **18**, 401.

Görlitz, A., Vogels, J. M., Leanhardt, A. E., Raman, C., Gustavson, T. L., Abo-Shaeer, J. R., Chikkatur, A. P., Gupta, S., Inouye, S., Rosenband, T., and Ketterle, W. (2001). *Phys. Rev. Lett.*, **87**, 130402.

Götze, W. and Wölfle, P. (1972). *Phys. Rev. B*, **6**, 1226.

Greiner, M., Mandel, O., Esslinger, T., Hansch, T. W., and Bloch, I. (2002). *Nature*, **415**, 39.

Grotendorst, J., Marx, D., and Muramatsu, A. (ed.) (2002). *Quantum Simulations of Complex Many-Body Systems: From Theory to Algorithms.* J. von Neumann Institut fur computing, Juelich. http://www.fz-juelich.de/nic-series/volume10/volume10.html.

Grüner, G. (1988). *Rev. Mod. Phys.*, **60**, 1129.

Haldane, F. D. M. (1980). *Phys. Rev. Lett.*, **45**, 1358.

Haldane, F. D. M. (1981*a*). *J. Phys. C*, **14**, 2585.

Haldane, F. D. M. (1981*b*). *Phys. Rev. Lett.*, **47**, 1840.

Haldane, F. D. M. (1982*a*). *Phys. Rev. B*, **25**, 4925.

Haldane, F. D. M. (1982*b*). *Phys. Rev. B*, **26**, 5257.

Haldane, F. D. M. (1983). *Phys. Rev. Lett.*, **50**, 1153.

Haldane, F. D. M. (1988). *Phys. Rev. Lett.*, **60**, 635.

Haldane, F. D. M., Bak, P., and Bohr, T. (1983). *Phys. Rev. B*, **28**, 2743.

Hallberg, K. A., Horsch, P., and Martínez, G. (1995). *Phys. Rev. B*, **52**, R719.

Hammar, P. H., Reich, D. H., Broholm, C., and Trouw, F. (1998). *Phys. Rev. B*, **57**, 7846.

Hayward, C. A. and Poilblanc, D. (1996). *Phys. Rev. B*, **53**, 11721.

Heidenreich, R., Seiler, R., and Uhlenbrock, D. A. (1980). *J. Stat. Phys.*, **22**, 27.

Henderson, W., Vescoli, V., Tran, P., Degiorgi, L., and Grüner, G. (1999). *Eur. Phys. J. B*, **11**, 365.

Hida, K. (2001). *Phys. Rev. Lett.*, **86**, 1331.

Hirsch, J. E. (1985). *Phys. Rev. Lett.*, **54**, 1317.

Hirsch, J. E. and Fye, R. M. (1986). *Phys. Rev. Lett.*, **56**, 2521.

Horowitz, B., Bohr, T., Kosterlitz, J.M., and Schulz, H. J. (1983). *Phys. Rev.*

B, **28**, 6596.
Houghton, A., Kwon, H. J., and Marston, J. B. (2000). *Adv. Phys.*, **49**, 141.
Hwang, S. W., Tsui, D. C., and Shayegan, M. (1994). *Phys. Rev. B*, **49**, 16441.
Imada, M., Fujimori, A., and Tokura, Y. (1998). *Rev. Mod. Phys.*, **70**, 1039.
Imry, Y. (1997). *Introduction to Mesoscopic Physics.* Clarendon, Oxford.
Imry, Y. and Ma, S. K. (1975). *Phys. Rev. Lett.*, **35**, 1399.
Japaridze, G. I. and Nersesyan, A. A. (1978). *JETP Lett.*, **27**, 334.
Jeckelmann, E., Gebhard, F., and Essler, F. H. L. (2000). *Phys. Rev. Lett.*, **85**, 3910.
Jérome, D. (1994). Organic superconductors: From $(TMTSF)_2PF_6$ to fullerenes. New York, pp. 405. Marcel Dekker.
Jérome, D. and Schulz, H. J. (1982). *Adv. Phys.*, **31**, 299.
José, J. V., Kadanoff, L. P., Kirkpatrick, S., and Nelson, D. R. (1977). *Phys. Rev. B*, **16**, 1217.
Kalos, M. H. (ed.) (1982). *Monte-Carlo Methods in Quantum Problems.* Reidel publishing company, Dordrecht.
Kamenev, A. (2002). In *Strongly correlated Fermions and Bosons in low dimensional disordered systems* (ed. I. V. Lerner *et al.*), Dordrecht, pp. 313. Kluwer Academic Publishers.
Kane, C., Balents, L., and Fisher, M. P. A. (1997). *Phys. Rev. Lett.*, **78**, 5086.
Kane, C. and Fisher, M. P. A. (1992*a*). *Phys. Rev. B*, **46**, 15233.
Kane, C. and Fisher, M. P. A. (1992*b*). *Phys. Rev. Lett.*, **68**, 1220.
Kawakami, N. and Yang, S. K. (1991). *Phys. Rev. B*, **44**, 7844.
Kim, E. H. and Solyom, J. (1999). *Phys. Rev. B*, **60**, 15230.
Kimura, T., Kuroki, K., and Aoki, Hideo (1996*a*). *Phys. Rev. B*, **53**, 9572.
Kimura, T., Kuroki, K., and Aoki, H. (1996*b*). *Phys. Rev. B*, **54**, R9608.
Kishine, J. and Fukuyama, H. (1997). *J. Phys. Soc. Jpn.*, **66**, 26.
Kivelson, S. A., Fradkin, E., and Emery, V. J. (1998). *Nature*, **393**, 550.
Kociak, M., Kasumov, A. Yu., Gueron, S., Reulet, B., Vaccarini, L., Khodos, I. I., Gorbatov, Yu. B., Volkov, V.T., and Bouchiat, H. (2000). Superconductivity in ropes of single-walled carbon nanotubes.
Kohn, W. (1964). *Phys. Rev.*, **133**, A171.
Kojima, K., Keren, A., Luke, G. M., Nachumi, B., Wu, W. D., Uemura, Y. J., Azuma, M., and Takano, M. (1995). *Phys. Rev. Lett.*, **74**, 2812.
Kolomeisky, E. (1993). *Phys. Rev. B*, **47**, 6193.
Konik, R. M. and Fendley, P. (2002). *Phys. Rev. B*, **66**, 144416.
Korepin, V. E., Izergin, A. G., and Bogoliubov, N. M. (1993). *Quantum Inverse Scattering Method and Correlation Functions.* Cambridge University Press, Cambridge.
Kosterlitz, J. M. (1974). *J. Phys. C*, **7**, 1046.
Kosterlitz, J. M. and Thouless, D. J. (1973). *J. Phys. C*, **6**, 1181.
Kotliar, G. (1988). *Phys. Rev. B*, **37**, 3664.
Kouwenhoven, L. and Markus, C. (1998). *Physics World*, **11**, 35.
Kühner, T. D., White, S. R., and Monien, H. (2000). *Phys. Rev. B*, **61**, 12474.

Kveschenko, D. V. and Rice, T. M. (1994). *Phys. Rev. B*, **50**, 252.
Lanczos, C. (1950). *J. Res. Natl. Bur. Stand.*, **45**, 255.
Landau, D. and Binder, K. (2000). *A Guide to Monte Carlo Simulations in Statistical Physics.* Cambridge University Press, Cambridge.
Landau, L. D. (1957*a*). *Sov. Phys. JETP*, **3**, 920.
Landau, L. D. (1957*b*). *Sov. Phys. JETP*, **5**, 101.
Landau, L. D. (1958). *Sov. Phys. JETP*, **8**, 70.
Landau, L. D. and Lifshitz, I. M. (1986). *Statistical Physics.* 3rd edition. Pergamon Press, Oxford.
Landauer, R. (1970). *Phil. Mag. B*, **21**, 863.
Larkin, A. I. (1970). *Sov. Phys. JETP*, **31**, 784.
Larkin, A. I. and Ovchinnikov, Y. N. (1979). *J. Low Temp. Phys*, **34**, 409.
Larkin, A. I. and Sak, J. (1977). *Phys. Rev. Lett.*, **39**, 1025.
Laughlin, R. B. (1983). *Phys. Rev. Lett.*, **50**, 1395.
Le Hur, K. (2001). *Phys. Rev. B*, **63**, 165110.
Lecheminant, P., Gogolin, A. O., and Nersesyan, A. A. (2002). *Nucl. Phys. B*, **639**, 502.
Ledermann, U. and Le Hur, K. (2000). *Phys. Rev. B*, **61**, 2497.
Lee, P. A. and Larkin, A. I. (1978). *Phys. Rev. B*, **17**, 1596.
Lee, P. A. and Ramakhrishnan, T. V. (1985). *Rev. Mod. Phys.*, **57**, 287.
Lieb, E. H. and Liniger, W. (1963). *Phys. Rev.*, **130**, 1605.
Lin, H., Balents, L., and Fisher, M. P. A. (1997). *Phys. Rev. B*, **56**, 6569.
Lin, H., Balents, L., and Fisher, M. P. A. (1998). *Phys. Rev. B*, **58**, 1794.
Lukyanov, S. (1998). *Nucl. Phys. B*, **522**, 533.
Lukyanov, S. (1999). *Phys. Rev. B*, **59**, 11163.
Luther, A. and Emery, V. J. (1974). *Phys. Rev. Lett.*, **33**, 589.
Luther, A. and Peschel, I. (1974). *Phys. Rev. Lett.*, **32**, 992.
Luther, A. and Peschel, I. (1975). *Phys. Rev. B*, **12**, 3908.
Luther, A. and Timonen, J. (1985). *J. Phys. C*, **18**, 1439.
Magishi, K., Matsumoto, S., Kitaoka, Y., Ishida, K., Asayama, K., Uehara, M., Nagata, T., and Akimitsu, J. (1998). *Phys. Rev. B*, **57**, 11533.
Mahan, G. D. (1981). *Many Particle Physics.* Plenum, New York.
Manaka, H. and Yamada, I. (2001). *J. Phys. Soc. Jpn.*, **70**, 1808.
Marston, J. B., Fjaerestad, J. O., and Sudbo, A. (2002). *Phys. Rev. Lett.*, **89**, 056404.
Maslov, D. and Stone, M. (1995). *Phys. Rev. B*, **52**, R5539.
Mattis, D. C. (1974). *J. Math. Phys.*, **15**, 609.
Maurey, H. and Giamarchi, T. (1995). *Phys. Rev. B*, **51**, 10833.
Maurey, H. and Giamarchi, T. (1997). *Europhys. Lett.*, **38**, 681.
Meden, V. and Schönhammer, K. (1992). *Phys. Rev. B*, **46**, 15753.
Meirav, U., Kastner, M. A., and Wind, S. J. (1990). *Phys. Rev. Lett.*, **65**, 771.
Metzner, W., Castellani, C., and Di Castro, C. (1998). *Adv. Phys.*, **47**, 317.
Mikeska, H. J. and Schmidt, H. (1970). *J. Low Temp. Phys*, **2**, 371.
Mila, F. (1998). *Eur. Phys. J. B*, **6**, 201.

Mila, F. and Zotos, X. (1993). *Europhys. Lett.*, **24**, 133.
Milliken, F. P., Umbach, C. P., and Webb, R. A. (1996). *Solid State Commun.*, **97**, 309.
Mironov, A. D. and Zabrodin, A. V. (1991). *Phys. Rev. Lett.*, **66**, 534.
Monthus, C., Golinelli, O., and Jolicoeur, T. (1998). *Phys. Rev. B*, **58**, 805.
Moon, K., Yi, H., Kane, C. L., Girvin, S. M., and Fisher, M. P. A. (1993). *Phys. Rev. Lett.*, **71**, 4381.
Mori, M., Fukuyama, H., and Imada, M. (1994). *J. Phys. Soc. Jpn.*, **63**, 1639.
Moroz, A. V., Samokhin, K. V., and Barnes, C. H. W. (2000). *Phys. Rev. B*, **62**, 16900.
Moser, J., Gabay, M., Aubin-Senzier, P., Jérome, D., Bechgaard, K., and Fabre, J.M. (1998). *Eur. Phys. J. B*, **1**, 39.
Mott, N. F. (1949). *Proc. Phys. Soc. Sect. A*, **62**, 416.
Mott, N. F. (1990). *Metal–Insulator Transitions.* Taylor and Francis, London.
Mott, N. F. and Twose, W. D. (1961). *Adv. Phys.*, **10**, 107.
Nagaosa, N. (1995). *Solid State Commun.*, **94**, 495.
Nagata, T., Uehara, M., Goto1, J., Akimitsu, J., Motoyama, N., Eisaki, H., Uchida, S., Takahashi, H., Nakanishi, T., and Môri, N. (1998). *Phys. Rev. Lett.*, **81**, 1090.
Nakamura, M. (1999). *J. Phys. Soc. Jpn.*, **68**, 3123.
Nattermann, T., Giamarchi, T., and Le Doussal, P. (2003). *Phys. Rev. Lett.*, **91**, 056603.
Nattermann, T. and Scheidl, S. (2000). *Adv. Phys.*, **49**, 607.
Negele, J. W. and Orland, H. (1988). *Quantum Many–Particle Systems.* Frontiers in Physics. Addison–Wesley, Reading, MA.
Nelson, D. R. and Vinokur, V. M. (1993). *Phys. Rev. B*, **48**, 13060.
Nersesyan, A., Luther, A., and Kusmartsev, F. (1993). *Phys. Lett. A*, **176**, 363.
Nersesyan, A. A., Gogolin, A. O., and Essler, F. H. L. (1998). *Phys. Rev. B*, **81**, 910.
Noack, R., White, S., and Scalapino, D. (1994). *Phys. Rev. Lett.*, **73**, 882.
Nozieres, P. (1961). *Theory of Interacting Fermi Systems.* Benjamin, New York.
Nozieres, P. (1974). *J. Low Temp. Phys*, **17**, 31.
Nozieres, P. and Blandin, A. (1980). *J. Phys. (Paris)*, **41**, 193.
Nozieres, P. and de Dominicis, C. T. (1969). *Phys. Rev.*, **178**, 1097.
Nozieres, P. and Gallet, F. (1987). *J. Phys. (Paris)*, **48**, 353.
Odom, T. W., Huang, J. L., Kim, P., and Lieber, C. M. (1998). *Nature*, **391**, 62.
Ogata, M. and Fukuyama, H. (1994). *Phys. Rev. Lett.*, **73**, 468.
Ogata, M., Luchini, M. U., Sorella, S., and Assaad, F. F. (1991). *Phys. Rev. Lett.*, **66**, 2388.
Ogata, M. and Shiba, H. (1990). *Phys. Rev. B*, **41**, 2326.
Oitmaa, J. and Betts, D. D. (1978). *Can. J. Phys.*, **56**, 897.
Orignac, E. and Giamarchi, T. (1997). *Phys. Rev. B*, **56**, 7167.
Orignac, E. and Giamarchi, T. (1998*a*). *Phys. Rev. B*, **57**, 5812.

Orignac, E. and Giamarchi, T. (1998*b*). *Phys. Rev. B*, **57**, 11713.
Orignac, E. and Giamarchi, T. (2001). *Phys. Rev. B*, **64**, 144515.
Oshikawa, M. and Affleck, I. (1999). *Phys. Rev. B*, **60**, 1038.
Oshikawa, M. and Affleck, I. (2002). *Phys. Rev. B*, **65**, 134410.
Papa, E. and Tsvelik, A. M. (2001). *Phys. Rev. B*, **63**, 085109.
Penc, K., Hallberg, K., Mila, F., and Shiba, H. (1996). *Phys. Rev. Lett.*, **77**, 1390.
Penc, K. and Sólyom, J. (1991). *Phys. Rev. B*, **44**, 12690.
Penc, K. and Sólyom, J. (1993). *Phys. Rev. B*, **47**, 6273.
Peschel, I., Wang, X., Kaulke, M., and Hallberg, K. (ed.) (1998). *Density Matrix Renormalization.* Springer-Verlag, Berlin.
Pham, K. V., Gabay, M., and Lederer, P. (2000). *Phys. Rev. B*, **61**, 16397.
Pines, D. and Nozières, P. (1966). *The Theory of Quantum Liquids.* Benjamin, New York.
Poilblanc, D., Tsunetsugu, H., and Rice, T. M. (1994). *Phys. Rev. B*, **50**, 6511.
Pokrovsky, V. L. and Talapov, A. L. (1979). *Phys. Rev. Lett.*, **42**, 65.
Pollock, E. L. and Ceperley, D. M. (1987). *Phys. Rev. B*, **36**, 8343.
Pouget, J. P. (2001). *Eur. Phys. J. B*, **20**, 321.
Rajaraman, R. (1982). *Solitons and Instantons: An Introduction to solitons and Instantons in Quantum Field Theory.* North Holland, Amsterdam.
Rommer, S. and Eggert, S. (2000). *Phys. Rev. B*, **62**, 4370.
Rosch, A. and Andrei, N. (2000). *Phys. Rev. Lett.*, **85**, 1092.
Sachdev, S. (1994). *Phys. Rev. B*, **50**, 13006.
Sachdev, S. (1998). *Quantum Phase Transitions.* Cambridge University Press, Cambridge.
Safi, I. and Schulz, H. J. (1995). *Phys. Rev. B*, **52**, R17040.
Sassetti, M., Napoli, F., and Weiss, U. (1995). *Phys. Rev. B*, **52**, 11213.
Scalapino, D. J., White, S. R., and Zhang, S. C. (1992). *Phys. Rev. Lett.*, **68**, 2830.
Scalettar, R. T., Batrouni, G. G., and Zimányi, G. T. (1991). *Phys. Rev. Lett.*, **66**, 3144.
Schlottmann, P. (1978). *J. Phys. (Paris)*, **C6**, 1486.
Schlottmann, P. (1987). *Phys. Rev. B*, **36**, 5177.
Schmid, A. (1983). *Phys. Rev. Lett.*, **51**, 1506.
Schmitteckert, P., Schulze, T., Schuster, C., Schwab, P., and Eckern, U. (1998). *Phys. Rev. Lett.*, **80**, 560.
Schon, G. and Zaikin, A. D. (1990). *Phys. Rep.*, **198**, 237.
Schönhammer, K. (2002). *J. Phys. C*, **14**, 12783.
Schotte, K. D. and Schotte, U. (1969). *Phys. Rev.*, **182**, 479.
Schreck, F., Khaykovich, L., Corwin, K. L., Ferrari, G., Bourdel, T., Cubizolles, J., and Salomon, C. (2001). *Phys. Rev. Lett.*, **87**, 080403.
Schulz, H. J. (1980). *Phys. Rev. B*, **22**, 5274.
Schulz, H. J. (1983). *J. Phys. C*, **16**, 6769.
Schulz, H. J. (1986). *Phys. Rev. B*, **34**, 6372.

Schulz, H. J. (1990). *Phys. Rev. Lett.*, **64**, 2831.
Schulz, H. J. (1993). *Phys. Rev. Lett.*, **71**, 1864.
Schulz, H. J. (1994). In *Strongly Correlated Electronic Materials: The Los Alamos Symposium 1993* (ed. K. S. Bedell *et al.*), Reading, MA, pp. 187. Addison–Wesley.
Schulz, H. J. (1995). Fermi liquids and non–fermi liquids. In *Mesoscopic Quantum Physics, Les Houches LXI* (ed. E. Akkermans, G. Montambaux, J. L. Pichard, and J. Zinn-Justin), Amsterdam, pp. 533. Elsevier.
Schulz, H. J. (1996*a*). *Phys. Rev. B*, **53**, R2959.
Schulz, H. J. (1996*b*). Coupled luttinger liquids. In *Correlated Fermions and Transport in Mesoscopic Systems* (ed. T. Martin, G. Montambaux, and J. Tran Thanh Van), Gif sur Yvette, France, pp. 81. Editions frontières.
Schulz, H. J. (1998). *Phys. Rev. Lett.*, **77**, 2790.
Schulz, H. J. (1999). *Phys. Rev. B*, **59**, R2471.
Schulz, H. J. and Shastry, B. S. (1998). *Phys. Rev. Lett.*, **80**, 1924.
Schwartz, A., Dressel, M., Grüner, G., Vescoli, V., Degiorgi, L., and Giamarchi, T. (1998). *Phys. Rev. B*, **58**, 1261.
Scott-Thomas, J. H. F., Field, S. B., Kastner, M. A., Smith, H. I., and Antoniadis, D. A. (1989). *Phys. Rev. Lett.*, **62**, 583.
Senechal, D. (2003). In *Theoretical Methods for Strongly Correlated Electrons* (ed. D. Sénechal *et al.*), CRM Series in Mathematical Physics, New York. Springer. cond-mat/9908262.
Sengupta, A. and Georges, A. (1994). *Phys. Rev. B*, **49**, R10020.
Shankar, R. (1990). *Int. J. Mod. Phys. B*, **4**, 2371.
Shankar, R. (1994). *Rev. Mod. Phys.*, **66**, 129.
Shankar, R. (2002). In *High Magnetic Fields: Applications in Condensed Matter Physics and Spectroscopy* (ed. C. Berthier *et al.*), Berlin, pp. 47. Springer-Verlag.
Shastry, B. S. (1988). *Phys. Rev. Lett.*, **60**, 639.
Shastry, B. S. and Sutherland, B. (1990). *Phys. Rev. Lett.*, **65**, 243.
Shelton, D. G., Nersesyan, A. A., and Tsvelik, A. M. (1996). *Phys. Rev. B*, **53**, 8521.
Shelton, D. G. and Tsvelik, A. M. (1996). *Phys. Rev. B*, **53**, 14036.
Sólyom, J. (1973). *J. Low Temp. Phys*, **12**, 547.
Sólyom, J. (1979). *Adv. Phys.*, **28**, 209.
Sólyom, J. and Zawadowski, A. (1974). *J. Phys. F*, **4**, 80.
Stone, M. B., Chen, Y., Rittner, J., Yardimci, H., Reich, D. H., Broholm, C., Ferraris, D. V., and Lectka, T. (2002). *Phys. Rev. B*, **65**, 064423.
Stormer, H. L. (1999). *Rev. Mod. Phys.*, **71**, 298.
Strong, S. P. and Millis, A. J. (1992). *Phys. Rev. Lett.*, **69**, 2419.
Strong, S. P. and Millis, A. J. (1994). *Phys. Rev. B*, **50**, 9911.
Sutherland, B. (1975). *Phys. Rev. B*, **12**, 3795.
Suzumura, Y. and Fukuyama, H. (1983). *J. Phys. Soc. Jpn.*, **52**, 2870.
Takahashi, M. (1999). *Thermodynamics of One-Dimensional Solvable Models.*

Cambridge University Press, Cambridge.
Takano, M., Hiroi, Z., Azuma, M., and Bando, Y. (1991). *J. Solid State Chem.*, **95**, 230.
Tarucha, S., Honda, T., and Saku, T. (1995). *Solid State Commun.*, **94**, 413.
Tarucha, S., Saku, T., Tokura, Y., and Hirayama, Y. (1993). *Phys. Rev. B*, **47**, 4064.
Tennant, D. A., Cowley, R. A., Nagler, S. E., and Tsvelik, A. M. (1995). *Phys. Rev. B*, **52**, 13368.
Thacker, H. (1982). *Rev. Mod. Phys.*, **53**, 253.
Thornton, T. J., Pepper, M., Ahmed, H., Andrews, D., and Davies, G. J. (1986). *Phys. Rev. Lett.*, **56**, 1198.
Tinkham, M. (1975). *Introduction to Superconductivity.* McGraw Hill, New York.
Toulouse, G. (1969). *C. R. Acad. Sci. B*, **268**, 1200.
Tserkovnyak, Y., Halperin, B. I., Auslaender, O. M., and Yacoby, A. (2002). *Phys. Rev. Lett.*, **89**, 136805.
Tsuchiizu, M., Donohue, P., Suzumura, Y., and Giamarchi, T. (2001). *Eur. Phys. J. B*, **19**, 185.
Tsuchiizu, M. and Furusaki, A. (2002). *Phys. Rev. Lett.*, **88**, 056402.
Tsuchiizu, M. and Suzumura, Y. (1999). *Phys. Rev. B*, **59**, 12326.
Tsui, D. C., Stormer, H. L., and Gossard, A. C. (1983). *Phys. Rev. Lett.*, **48**, 1559.
Tsunetsugu, H., Troyer, M., and Rice, T. M. (1994). *Phys. Rev. B*, **49**, 16078.
Tsutsui, K., Poilblanc, D., and Capponi, S. (2001). *Phys. Rev. B*, **89**, 020406.
Tsvelick, A. M. and Wiegmann, P. B. (1983). *Adv. Phys.*, **32**, 453.
Tsvelik, A. M. (1992). *Phys. Rev. B*, **45**, 486.
Uchara, M., Nagata, T., Akimitsu, J., Takahashi, H., Môri, N., and Kinoshita, K. (1996). *J. Phys. Soc. Jpn.*, **65**, 2764.
Uhrig, G. S. and Schulz, H. J. (1996). *Phys. Rev. B*, **54**, R9624.
van Oudenaarden, A. and Mooij, J. E. (1996). *Phys. Rev. Lett.*, **76**, 4947.
Varma, C. M., Z, Z. Nussinov, and van Saarloos, W. (2002). *Phys. Rep.*, **361**, 267.
Varma, C. M. and Zawadowski, A. (1985). *Phys. Rev. B*, **32**, 7399.
Vescoli, V., Degiorgi, L., Henderson, W., Grüner, G., Starkey, K. P., and Montgomery, L. K. (1998). *Science*, **281**, 1191.
Vescoli, V., Zwick, F., Henderson, W., DeGiorgi, L., Grioni, M., Gruner, G., and Montgomery, L. K. (2000). *Eur. Phys. J. B*, **13**, 503.
Vidal, J., Mouhanna, D., and Giamarchi, T. (1999). *Phys. Rev. Lett.*, **83**, 3908.
Voit, J. (1988). *J. Phys. C*, **21**, L1141.
Voit, J. (1993). *Phys. Rev. B*, **47**, 6740.
Voit, J. (1995). *Rep. Prog. Phys.*, **58**, 977.
Voit, J. (1998). *Eur. Phys. J. B*, **5**, 505.
von Delft, J. and Schoeller, H. (1998). *Ann. Phys.*, **7**, 225.
von Klitzing, K., Dorda, G., and Pepper, M. (1980). *Phys. Rev. Lett.*, **45**, 494.

Wegner, F. (1979). *Z. Phys. B*, **35**, 207.
Wen, X. G. (1990*a*). *Phys. Rev. B*, **42**, 6623.
Wen, X. G. (1990*b*). *Phys. Rev. B*, **41**, 12838.
Wen, X. G. (1995). *Adv. Phys.*, **44**, 405.
White, S. R. (1993). *Phys. Rev. B*, **48**, 10345.
White, S. R., Affleck, I., and Scalapino, D. J. (2002). *Phys. Rev. B*, **65**, 165122.
Wiegmann, P. B. and Finkelshtein, A. M. (1978). *Sov. Phys. JETP*, **48**, 102.
Wigner, E. (1934). *Phys. Rev.*, **46**, 1002.
Wilson, K. G. (1975). *Rev. Mod. Phys.*, **47**, 773.
Yacoby, A., Stormer, H. L., Wingreen, N. S., Pfeiffer, L. N., Baldwin, K. W., and West, K. W. (1996). *Phys. Rev. Lett.*, **77**, 4612.
Yakovenko, V. M. (1992). *JETP Lett.*, **56**, 510.
Yang, C. N. (1967). *Phys. Rev. Lett.*, **19**, 1312.
Yao, Z., Postma, H. W. C., Balents, L., and Dekker, C. (1999). *Nature*, **402**, 273.
Ziman, J. M. (1972). *Principles of the Theory of Solids.* Cambridge University Press, Cambridge.
Zotos, X. (1999). *Phys. Rev. Lett.*, **82**, 1764.
Zotos, X. and Prelovsek, P. (1996). *Phys. Rev. B*, **53**, 983.

INDEX

$4k_F$ component, 80, 104, 108, 165, 251, 296
F_1 and F_2 expressions, 43, 383
U–V model, 215
Π field, 36
ϕ and θ fields
  boundary, 305
  commutator, 36, 73
  correlations, 43, 77, 103, 381
  definition, 35
  finite temperature, 98
  Hamiltonian, 37, 39
  Mott-δ, 120
  pairing operator, 46, 55
  relation to charge of excitations, 81, 211
  relation to densities, 36, 54, 72
  semiclassical interpretation, 82, 84
  single-particle operator, 35, 37, 51, 73
  spins, 167
  umklapp process, 108
t–J model, 213

adiabatic limit, 178
Ahronov–Bohm flux, 93, 148, 224
amplitudes, 78
analytic continuation, 375, 387
Anderson localization, 270

BA equations, 146
Bechgaard salts, 262
Bethe-ansatz, 137, 167, 171, 185, 209, 213, 234, 237, 332
BKT transition, 60, 91, 111, 171
bond ordering, 203, 217
bonding–antibonding bands, 241
Bose condensates, 345
Bose glass, 342
Bose–Hubbard Hamiltonian, 334, 344
boson representation
  creation and destruction operators, 33
  Hamiltonian, 35
bosonization, 14, 29, 70, 391
bosons, 333
boundary condition, 99, 303, 355
boundary exponent, 307

canonical transformation, 349
capacitance, 320, 323, 343
central charge, 99
charge density wave, 11, 47, 65, 104, 203, 217, 246, 251, 280, 282, 294, 318
charge stiffness, 224
chemical potential, 41, 108
chiral fields, 86, 304, 331, 376, 387
classical crystal, 86, 105, 115, 280
collective excitations, 4, 5, 30, 103
collective pinning, 275
commensurability, 110, 218
commensurate-incommensurate transition, 115
compressibility
  definition, 41
  fermions with spin, 53
  Mott-δ, 121
  spinless fermions, 42
conductace
  edge states, 330
conductance, 219, 227
  single impurity, 309, 312
conductance quantization, 301
conductivity, 219
  disordered fermions, 278, 288, 295
  Mott insulator, 232, 265
  umklapp process, 228
conformal transformation, 94, 355
contractions, 81, 133, 291
Coulomb blockade, 321
Coulomb gas, 58, 93, 317
Coulomb interaction, 100
$Cu_2(C_5H_{12}N_2)_2Cl_4$, 194
current, 83, 220

d wave symmetry, 245
deconfinement transition, 262
density operator
  bond ordering, 203
  classical crystal, 89
  commutator, 32
  correlations
    bosons, 335
    fermions with spin, 55, 65, 81
    Hubbard model, 203
    long-range interactions, 104
    spinless fermions, 44, 78
  Hubbard model, 202
  Luttinger liquid, 16
  relation to ϕ and θ, 36, 42, 54, 72
  semiclassical representation, 82

spinful fermion ladder, 249
spinless fermion ladder, 244
diamagnetic term, 221
dimensional crossover, 256
dimerization, 178
DMRG method, 157
doping, 108
dynamical exponent, 112, 121, 342
Dzyaloshinskii–Larkin solution, 15, 352

edge states, 328
Emery-Kivelson line, 366
exact diagonalizations, 154

Fermi liquid, 1, 205, 357
ferromagnet, 167
finite range interaction, 44
flux phases, 245
form factors, 234
forward and backward scattering, 277
Fourier conventions, 372
Fourier transforms, 389
free electron gas, 1
Friedel oscillations, 7, 217
frustration, 175
Fukuyama-Lee length, 283

g-ology, 17, 125
gaussian disorder, 275

Haldane's 'conjecture', 189
Hamiltonian
t–J model, 213
bosons, 334
dimerized spin chain, 180
disordered bosons, 340
disordered fermions, 276, 279
fermions with spin, 52
function of ϕ and θ, 37
Hubbard model, 9, 200, 201
Kondo model, 355, 359
Luttinger liquid, 75
magnetic anisotropies, 126
single impurity, 307, 311
spin ladder, 191
spin-Peierls, 177
spinful fermion ladder, 248
spinless fermions, 162
spinless fermions ladder, 239, 242
Tomonaga–Luttinger, 15, 29
two impurities, 318
two-channel Kondo, 364, 366
X-ray edge, 347, 348
XXZ model, 138, 160, 166
XY model, 91
hard core bosons, 162, 208
Heisenberg model, 148, 160
Hirsh–Fye algorithm, 156
holes in BA equations, 149
holon, 84, 114, 206, 211
Hopfield rule, 351
Hubbard bands, 114
Hubbard model, 156, 200

impurities
many, 276, 323
one, 307, 323
two, 318
instanton, 66, 314
interchain hopping, 240, 256

Jordan–Wigner transformation, 73, 162
Josephson coupling, 258, 344
Josephson junction arrays, 343

$KCuF_3$, 184
Klein factors, 35, 129, 202, 362, 376
Kondo model, 138, 355
Kondo temperature, 357
Korringa law, 205

labelling field, 71, 88
ladder
spinless fermions, 239
ladders
spin ladders, 189
Landau parameters, 3
lifetime, 3, 5, 278
linear response, 374
localization length, 271, 285, 287, 292
logarithmic corrections, 62, 131, 169, 232, 360
long-range interaction, 100, 327
Luther–Emery line, 112, 233
Luther–Emery liquid, 65, 294
Luttinger liquid, 6, 44, 70, 76
Hamiltonian, 39, 52, 75
parameters
U–V model, 216, 219
t–J model, 214
fermions with spin, 52
Hubbard model, 202, 209
long-range interaction, 101
spin ladder, 192
spinful fermion ladder, 248
spinless fermions ladder, 242
Tomonaga–Luttinger, 39
XXZ model, 166, 171
relation with Bethe-ansatz, 147, 404
spin gap, 67
Luttinger theorem, 3, 49

magnetic anisotropies, 124, 240
magnetic field, 121, 170
magnetic monopoles, 93
magnon, 140, 153
Majorana fermions, 129, 194, 367
many-body formalism, 371
massive phase, 63, 65, 112
massive Thiring model, 113, 138
massless regime, 62
mean field, 9, 197, 260
Meissner fraction, 226
memory function formalism, 229
Mermin–Wagner theorem, 67
miniband, 300
Monte-Carlo, 155
Mott insulator, 217, 263
Mott transition, 90, 106, 170, 208, 218, 337
Mott-U/Mott-δ, 111

nanotubes, 325
nesting property, 7, 11
neutron scattering, 185
NMR, 173, 204
normal ordering, 31, 216, 399

occupation factor, 48, 375
operator product expansion, 81
orbital antiferromagnet, 245
organic conductors, 187, 262
orthogonality catastrophe, 354

pairing operator
  correlations
    fermions with spin, 65
  fermions with spin, 55
  relation to ϕ and θ, 46
  spinful fermion ladder, 249
  spinless fermion ladder, 244
  spinless fermions, 45
parquet approximation, 12, 23
particle–hole excitations, 2, 12, 29, 355
particle–hole symmetry, 163, 203
path integral, 380
persistent currents, 225, 297
phase breaking process, 235
phase diagram
  U–V model, 219
  t–J model, 214
  bosons, 336, 337
  disordered fermions, 286, 294
  fermions with spin, 68
  Mott insulator, 111
  single impurity, 312
  spinful fermion ladder, 251
  spinless fermion ladder, 245
  spinless fermions, 47
  XXZ model, 161
phase separation, 215
phase shift, 352
plasmon, 103
point splitting, 166
Poisson summation formula, 72

quantification of conductance, 227
quantum fluctuations, 68, 87, 105, 150, 183, 198, 280
quantum Hall effect, 328
quantum phase transition, 66, 87, 108, 195
quantum wire, 101, 299
quasiparticles, 2–4
  Luttinger liquid, 14

random antiferromagnet, 292, 299
rapidities, 148
refermionization, 113, 118, 193
renormalization group
  C–IC transition, 115
  correlation functions, 27, 62, 132
  disordered bosons, 341
  disordered fermions, 286, 291
  fermions with spin, 26
  interchain hopping, 256, 260
  Kondo model, 356, 361
  magnetic anisotropies, 126
  method, 23
  sine-Gordon, 56, 396
  single impurity, 308, 311
  spinless fermions, 24
replica method, 272
resonant level model, 362
right and left goers, 15, 29, 85, 86, 119, 329, 348
roots in BA equations, 149
RPA approximation, 11, 19, 198, 353

scaling dimension, 60, 311
Schlottmann transformation, 361
sine-Gordon
  gap, 63
  Hamiltonian, 53
  phonons, 63, 403
  renormalization, 56
  solitons, 63, 114, 211, 403
single-particle density of states, 49, 206, 267, 327
single-particle operator
  bosons, 335
  boundary, 306
  fermions with spin, 51
  function of right and left movers, 38

Hubbard model, 205
Kondo model, 363
Luttinger liquid, 16
relation to ϕ and θ, 73
spinless fermions, 35, 37, 47
X-ray edge, 351
SO(4) symmetry, 201
specific heat, 40
spectral function, 1
Fermi liquid, 4
from Green's function, 5, 375
Luttinger liquid, 206
two-channel Kondo, 367
spin chain, 138
spin density wave, 11, 54, 65, 203, 244, 263
spin gap, 246
spin operator
correlations
Hubbard model, 203
XXZ model, 168, 172
spin rotation, 127
spin–orbit coupling, 124
spin-charge separation, 53, 54
spin-Peierls, 177, 263
spinful fermion ladder, 246, 247
spinon, 84, 152, 175, 177, 186, 206, 212
$Sr_{14}Cu_{24}O_{41}$, 253
$SrCu_2O_3$, 194
SU(2) symmetry, 201
superexchange, 259
susceptibility, 375
coupled spin chains, 198
Fermi liquid, 6, 9
fermions with spin, 53
in spin systems, 174
Kondo problem, 360, 368
Luttinger liquid, 27, 46, 53, 123, 204
singularity, 122

thermal length, 98, 235, 301
Tomonaga–Luttinger model, 15, 29, 75
topological excitations, 74
torus, 96
Toulouse limit, 361
tunneling, 311, 313
two body hopping, 258
two-channel Kondo, 364

umklapp process, 107–109, 202

variational method, 400
velocities (charge and spin), 21
vortex, 91, 344

warping of Fermi surface, 255
Wigner crystal, 105
Wilson RG, 396

X-ray edge problem, 347
XXZ model, 138, 160
XY model, 60, 91, 93